EPA/635/R-09/013

WWW.EPA.GOV/IRIS

TOXICOLOGICAL REVIEW OF METHANOL

(CAS No. 67-56-1)

In Support of Summary Information on the Integrated Risk Information System (IRIS)

October 2009

NOTICE

This document is an Interagency Science Consultation draft**.** This information is distributed solely for the purpose of pre-dissemination peer review under applicable information quality guidelines. It has not been formally disseminated by EPA. It does not represent and should not be construed to represent any Agency determination or policy. It is being circulated for review of its technical accuracy and science policy implications.

U.S. Environmental Protection Agency
Washington, DC

DISCLAIMER

This document is a preliminary draft for review purposes only. This information is distributed solely for the purpose of pre-dissemination peer review under applicable information quality guidelines. It has not been formally disseminated by EPA. It does not represent and should not be construed to represent any Agency determination or policy. Mention of trade names or commercial products does not constitute endorsement or recommendation for use.

CONTENTS TOXICOLOGICAL REVIEW OF METHANOL
(CAS NO. 67-56-1)

1. INTRODUCTION 1-26

2. CHEMICAL AND PHYSICAL INFORMATION 2-1

3. TOXICOKINETICS 3-1

3.1. Overview 3-1
3.2. Key Studies 3-5
3.3. Human Variability In Methanol Metabolism 3-10
3.4. Physiologically Based Toxicokinetic Models 3-15
3.4.1. Model Requirements for EPA Purposes 3-15
3.4.1.1. MOA and Selection of a Dose Metric 3-15
3.4.1.2. Criteria for the Development of Methanol PBPK Models 3-17
3.4.2. Methanol PBPK Models 3-18
3.4.2.1. Ward et al. (1997) 3-19
3.4.2.2. Bouchard et al. (2001) 3-19
3.4.2.3. Gentry et al. (2003, 2002) and Clewell et al. (2001) 3-20
3.4.3. Selected Modeling Approach 3-21
3.4.3.1. Available PK Data 3-22
3.4.3.2. Model Structure 3-23
3.4.3.3. Model Parameters 3-25
3.4.4. Mouse Model Calibration and Sensitivity Analysis 3-26
3.4.5. Rat Model Calibration 3-31
3.4.6. Human Model Calibration 3-35
3.4.6.1. Inhalation Route 3-35
3.4.6.2. Oral Route 3-41
3.4.7. Monkey PK Data and Analysis 3-42
3.4.7.1. PK Model Analysis for Monkeys 3-44
3.4.8. Summary and Conclusions 3-47

4. HAZARD IDENTIFICATION 4-1

4.1. Studies in Humans – Case Reports, Occupational and Controlled Studies 4-1
4.1.1. Case Reports 4-1
4.1.2. Occupational Studies 4-9
4.1.3. Controlled Studies 4-11
4.2. Acute, Subchronic and Chronic Studies and Cancer Bioassays in Animals—Oral and Inhalation 4-13
4.2.1. Oral Studies 4-13
4.2.1.1. Acute Toxicity 4-13
4.2.1.2. Subchronic Toxicity 4-13
4.2.1.3. Chronic Toxicity 4-14
4.2.2. Inhalation Studies 4-20
4.2.2.1. Acute Toxicity 4-20
4.2.2.2. Subchronic Toxicity 4-21
4.2.2.3. Chronic Toxicity 4-24
4.3. Reproductive AND Developmental Studies–Oral and Inhalation 4-32
4.3.1. Oral Studies 4-32
4.3.2. Inhalation Studies 4-34

4.3.3. Other Reproductive and Developmental Toxicity Studies 4-46
4.4. Neurotoxicity 4-50
4.4.1. Oral Studies 4-51
4.4.2. Inhalation Studies 4-53
4.4.3. Studies Employing In Vitro, S.C. and I.P. Exposures 4-60
4.5. Immunotoxicity 4-64
4.6. Mechanistic Data and Other Studies in Support of the MOA 4-69
4.6.1. Role of Methanol and Metabolites in the Developmental Toxicity of Methanol 4-69
4.6.2. Role of Folate Deficiency in the Developmental Toxicity of Methanol 4-74
4.6.3. Methanol-Induced Formation of Free Radicals, Lipid Peroxidation, and Protein Modifications 4-75
4.6.4. Exogenous Formate Dehydrogenase as a Means of Detoxifying the Formic Acid that Results from Methanol Exposure 4-78
4.6.5. Mechanistic Data Related to the Potential Carcinogenicity of Methanol 4-78
4.6.5.1. Genotoxicity 4-78
4.6.5.2. Lymphoma Responses Reported in ERF Life span Bioassays of Compounds Related to Methanol, Including an Analogue (Ethanol), Precursors (Aspartame and Methyl Tertiary Butyl Ether), and a Metabolite (Formaldehyde) 4-81
4.6.5.2.1. Ethanol. 4-83
4.6.5.2.2. Aspartame. 4-84
4.6.5.2.3. MTBE. 4-89
4.6.5.2.4. Formaldehyde. 4-90
4.7. Synthesis of Major Noncancer Effects 4-92
4.7.1. Summary of Key Studies in Methanol Toxicity 4-92
4.7.1.1. Oral 4-95
4.7.1.2. Inhalation 4-96
4.8. NONCANCER MOA Information 4-99
4.9. Evaluation of Carcinogenicity 4-102
4.9.1. Summary of Overall Weight-of-Evidence 4-102
4.9.2. Synthesis of Human, Animal, and Other Supporting Evidence 4-103
4.9.3. MOA Information 4-109
4.10. Susceptible Populations and Life Stages 4-110
4.10.1. Possible Childhood Susceptibility 4-110
4.10.2. Possible Gender Differences 4-111
4.10.3. Genetic Susceptibility 4-112

5. DOSE-RESPONSE ASSESSMENT AND CHARACTERIZATION 5-1

5.1. Inhalation RfC for Effects Other than Cancer 5-1
5.1.1. Choice of Principal Study and Critical Effect(s) 5-1
5.1.1.1. Key Inhalation Studies 5-1
5.1.1.2. Selection of Critical Effect(s) 5-2
5.1.2. Methods of Analysis for the POD—Application of PBPK and BMD Models 5-6
5.1.2.1. Application of the BMD/BMDL Approach 5-7
5.1.2.2. BMD Approach Applied to Brain Weight Data in Rats 5-9
5.1.3. RfC Derivation – Including Application of Uncertainty Factors 5-13
5.1.3.1. Comparison Between Endpoints and BMDL Modeling Approaches 5-13
5.1.3.2. Application of UFs 5-15
5.1.3.2.1. Interindividual Variation UF_H 5-15
5.1.3.2.2. Animal-to-Human Extrapolation UF_A. 5-17

5.1.3.2.3. Database UF_D. 5-17
5.1.3.2.4. Extrapolation from Subchronic to Chronic and LOAEL-to NOAEL Extrapolation UFs. 5-18
5.1.4. Previous RfC Assessment 5-18
5.2. Oral RfD 5-18
5.2.1. Choice of Principal Study and Critical Effect–with Rationale and Justification 5-19
5.2.1.1. Expansion of the Oral Database by Route-to-Route Extrapolation 5-20
5.2.2. RfD Derivation–Including Application of UFs 5-21
5.2.1.2. Consideration of Inhalation Data 5-21
5.2.1.3. Selection of Critical Effect(s) from Inhalation Data 5-21
5.2.1.4. Selection of the POD 5-22
5.2.2. RfD Derivation–Application of UFs 5-22
5.2.3. Previous RfD Assessment 5-22
5.3. Uncertanties in the Inhalation RfC and Oral RfD 5-23
5.3.1. Choice of Endpoint 5-24
5.3.2. Choice of Dose Metric 5-25
5.3.3. Choice of Model for BMDL Derivations 5-26
5.3.4. Choice of Animal-to-Human Extrapolation Method 5-27
5.3.5. Route-to-Route Extrapolation 5-27
5.3.6. Statistical Uncertainty at the POD 5-28
5.3.7. Choice of Bioassay 5-28
5.3.8. Choice of Species/Gender 5-28
5.3.9. Human Population Variability 5-28
5.4. 5.4. Cancer Assessment 5-29
5.4.1. Oral Exposure 5-29
5.4.1.1. Choice of Study/Data—with Rationale and Justification 5-29
5.4.1.2. Dose-Response Data 5-29
5.4.1.3. Dose Adjustments and Extrapolation Method 5-30
5.4.1.4. Oral Slope Factor 5-33
5.4.2. Inhalation Exposure 5-33
5.4.2.1. Choice of Study/Data–with Rationale and Justification 5-33
5.4.2.2. Dose-Response Data 5-34
5.4.2.3. Dose Adjustments and Extrapolation Method 5-35
5.4.2.4. IUR 5-36
5.4.3. Uncertainties in Cancer Risk Assessment 5-36
5.4.3.1. Quality of Studies that are the Basis for the PODs 5-37
5.4.3.2. Interpretation of Results of the Studies that are the Basis for the PODs 5-40
5.4.3.3. Consistency across Chronic Bioassays for Methanol 5-43
5.4.3.4. Choice of Endpoint for POD Derivation 5-45
5.4.3.5. Choice of Species/Gender 5-45
5.4.3.6. Choice of Model for POD Derivation 5-45
5.4.3.7. Choice of Dose Metric 5-46
5.4.3.8. Choice of Animal-to-Human Extrapolation Method 5-47
5.4.3.9. Human Relevance of Cancer Responses Observed in Rats and Mice 5-48
6. MAJOR CONCLUSIONS IN THE CHARACTERIZATION OF HAZARD AND DOSE RESPONSE 6-1
6.1. Human Hazard Potential 6-1
6.2. Dose Response 6-3

6.2.1. Noncancer/Inhalation 6-3
6.2.2. Noncancer/Oral 6-5
6.2.3. Cancer/Oral and Inhalation 6-6

7. REFERENCES 7-1

APPENDIX A. SUMMARY OF EXTERNAL PEER REVIEW AND PUBLIC COMMENTS AND DISPOSITION A-1

APPENDIX B. DEVELOPMENT, CALIBRATION AND APPLICATION OF A METHANOL PBPK MODEL B-1

APPENDIX C. RFC DERIVATION OPTIONS C-1

APPENDIX D. RFC DERIVATION – COMPARISON OF DOSE METRICS D-1

APPENDIX E. EVALUATION OF THE CANCER POTENCY OF METHANOL E-1

LIST OF TABLES

Table 2-1. Relevant physical and chemical properties of methanol 2-1
Table 3-1. Background blood methanol and formate levels in humans 3-11
Table 3-2. Human blood methanol and formate levels following methanol exposure 3-12
Table 3-3. Monkey blood methanol and formate levels following methanol exposure 3-13
Table 3-4. Mouse blood methanol and formate levels following methanol exposure 3-13
Table 3-5. Rat blood methanol and formate levels following methanol exposure 3-14
Table 3-6. Plasma formate concentrations in monkeys 3-15
Table 3-7. Serum folate concentrations in monkeys 3-15
Table 3-8. Routes of exposure optimized in models – optimized against blood concentration data3-20
Table 3-9. Key methanol kinetic studies for model validation 3-22
Table 3-10. Parameters used in the mouse, rat and human PBPK models 3-25
Table 3-11. Primate K_ms reported in the literature 3-38
Table 3-12. Parameter estimate results obtained using acslXtreme to fit all human data using either saturable or first-order metabolism 3-38
Table 3-13. Comparison of LLFs for Michaelis-Menten and first-order metabolism 3-40
Table 3-14. Monkey group exposure characteristics 3-47
Table 4–1. Mortality rate for subjects exposed to methanol-tainted whiskey in relation to their level of acidosis[a] 4-2
Table 4-2. Incidence of carcinogenic responses in Sprague-Dawley rats exposed to methanol in drinking water for up to 2 years 4-18
Table 4-3. Incidence of malignant lymphoma responses in Swiss mice exposed to methanol in drinking water for life 4-20
Table 4-4. Histopathological changes in tissues of B6C3F1 mice exposed to methanol via inhalation for 18 months 4-28
Table 4-5. Histopathological changes in lung and adrenal tissues of F344 rats exposed to methanol via inhalation for 24 months 4-31
Table 4-6. Reproductive and developmental toxicity in pregnant Sprague-Dawley rats exposed to methanol via inhalation during gestation 4-36
Table 4-7. Reproductive parameters in Sprague-Dawley dams exposed to methanol during pregnancy then allowed to deliver their pups 4-37
Table 4-8. Developmental effects in mice after methanol inhalation 4-39
Table 4-9. Benchmark doses at two added risk levels 4-40
Table 4-10. Reproductive parameters in monkeys exposed via inhalation to methanol during prebreeding, breeding, and pregnancy 4-42
Table 4-11. Mean serum levels of testosterone, luteinizing hormone, and corticosterone (± S.D.) in male Sprague-Dawley rats after inhalation of methanol, ethanol, n-propanol or n-butanol at threshold limit values 4-43
Table 4-12. Maternal and litter parameters when pregnant female C57BL/6J mice were injected i.p. with methanol 4-46
Table 4-13. Reported thresholds concentrations (and author-estimated ranges) for the onset of embryotoxic effects when rat and mouse conceptuses were incubated in vitro with methanol, formaldehyde, and formate 4-49
Table 4-14. Brain weights of rats exposed to methanol vapors during gestation and lactation 4-58
Table 4-15. Effect of methanol on Wistar rat acetylcholinesterase activities 4-61
Table 4-16. Effect of methanol on neutrophil functions in in vitro and in vivo studies in male Wistar rats 4-65

Table 4-17. Effect of intraperitoneally injected methanol on total and differential leukocyte counts and neutrophil function tests in male Wistar rats 4-66
Table 4-18. Effect of methanol exposure on animal weight/organ weight ratios and on cell counts in primary and secondary lymphoid organs of male Wistar rats 4-68
Table 4-19. The effect of methanol on serum cytokine levels in male Wistar rats 4-69
Table 4-20. Developmental outcome on GD10 following a 6-hour 10,000 ppm (13,104 mg/m^3) methanol inhalation by CD-mice or formate gavage (750 mg/kg) on GD8 4-70
Table 4-21. Summary of ontogeny of relevant enzymes in CD-1 mice and humans 4-71
Table 4-22. Dysmorphogenic effect of methanol and formate in neurulating CD-1 mouse embryos in culture (GD8) 4-72
Table 4-23. Time-dependent effects of methanol administration on serum liver and kidney function, serum ALT, AST, BUN, and creatinine in control and experimental groups of male Wistar rats 4-77
Table 4-24. Effect of methanol administration on male Wistar rats on malondialdehyde concentration in the lymphoid organs of experimental and control groups and the effect of methanol on antioxidants in spleen 4-77
Table 4-25. Summary of genotoxicity studies of methanol 4-80
Table 4-26. Incidence of carcinogenic responses in Sprague-Dawley rats exposed to ethanol in drinking water for up to 2 years 4-84
Table 4-27. Incidence of lymphomas and leukemias in Sprague-Dawley rats exposed to aspartame via the diet 4-85
Table 4-28. Incidence of combined dysplastic hyperplasias, papillomas and carcinomas of the pelvis and ureter and of malignant schwannomas in peripheral nerve in Sprague-Dawley rats exposed to aspartame via the diet 4-86
Table 4-29. Incidence of tumors in Sprague-Dawley rats exposed to aspartame from GD12 to natural death 4-87
Table 4-30. Comparison of the incidence of combined lymphomas and leukemias in female Sprague-Dawley rats exposed to aspartame in feed for a lifetime, either pre- and postnatally or postnatally only 4-88
Table 4-31. Incidence of Leydig cell testicular tumors and combined lymphomas and leukemias in Sprague-Dawley rats exposed to MTBE via gavage for 104 weeks 4-90
Table 4-32. Incidence of hemolymphoreticular neoplasms on Sprague-Dawley rats exposed to formaldehyde in drinking water for 104 weeks 4-91
Table 4-33. Incidence of leukemias in breeder and offspring Sprague-Dawley rats exposed to formaldehyde in drinking water for 104 weeks (Test BT 7005) 4-92
Table 4-34. Summary of studies of methanol toxicity in experimental animals (oral) 4-92
Table 4-35. Summary of studies of methanol toxicity in experimental animals (inhalation exposure) 4-93
Table 5-1. Summary of studies considered most appropriate for use in derivation of an RfC 5-5
Table 5-2. The EPA PBPK model estimates of methanol blood levels (AUC) in rats following inhalation exposures 5-10
Table 5-3. Comparison of benchmark dose modeling results for decreased brain weight in male rats at 6 weeks of age using modeled AUC of methanol as a dose metric 5-11
Table 5-4. Summary of PODs for critical endpoints, application of UFs and conversion to HEC values using BMD and PBPK modeling 5-14
Table 5-5. Summary of uncertainties in methanol noncancer risk assessment 5-23
Table 5-6. Incidence data for lymphoma, lympho-immunoblastic, and all lymphomas in male and female Sprague-Dawley rats 5-30
Table 5-7. BMD results and oral CSF using all lymphoma in male rats 5-33

Table 5-8. Incidence data for tumor responses in male and female F344 rats..... 5-34
Table 5-9. BMD results and IUR using pheochromocytoma in female rats..... 5-36
Table 5-10. Summary of uncertainty in the methanol cancer risk assessment 5-37
Table B-1. Parameters used in the mouse and human PBPK models.....B-5
Table B-2. Primate kms reported in the literature.....B-29
Table B-3. Parameter estimate results obtained using acslXtreme to fit all human data using either saturable or first-order metabolism B-31
Table B-4. Comparison of LLF for Michaelis-Menten and first-order metabolism.....B-32
Table B-5. PBPK model predicted C_{max} and 24-hour AUC for mice and humans exposed to MeOH.....B-35
Table B-6. Mouse total MeOH metabolic clearance/metabolites produced following inhalation exposures.....B-90
Table B-7. Human total MeOH metabolic clearance/metabolites produced from inhalation exposures.....B-91
Table B-8. Human total MeOH metabolic clearance/metabolites produced following oral exposures.....B-91
Table B-9. Repeated daily oral dosing of humans with MeOH.....B-93
Table C-1. EPA's PBPK model estimates of methanol blood levels (AUC) in rats following inhalation exposures.....C-3
Table C-2. Comparison of BMD_{1SD} results for decreased brain weight in male rats at 6 weeks of age using modeled AUC of methanol as a dose metric.....C-4
Table C-3. Comparison of BMD_{05} results for decreased brain weight in male rats at 6 weeks of age using modeled AUC of methanol as a dose metric.....C-9
Table C-4. EPA's PBPK model estimates of methanol blood levels (C_{max}) in rats following inhalation exposures.....C-13
Table C-5. Comparison of BMD_{1SD} results for decreased brain weight in male rats at 8 weeks of age using modeled C_{max} of methanol as a dose metric.....C-14
Table C-6. Comparison of BMD_{05} modeling results for decreased brain weight in male rats at 8 weeks of age using modeled C_{max} of methanol as a common dose metric C-20
Table C-7. EPA's PBPK model estimates of methanol blood levels (C_{max}) in mice following inhalation exposures.....C-24
Table C-8. Comparison of BMD modeling results for cervical rib incidence in mice using modeled C_{max} of methanol as a common dose metric C-25
Table C-9. Comparison of BMD modeling results for cervical rib incidence in mice using modeled C_{max} of methanol as a common dose metric C-33
Table C-10. Comparison of BMD modeling results for VDR in female monkeys using AUC blood methanol as the dose metric C-42
Table E-1. Calculation of mg/kg-day doses.....E-12
Table E-2. Incidence for neoplasms considered for dose-response modeling.....E-12
Table E-3. Results from multistage (1º) quantal modeling rat data using mg/kg-day exposures and default HED derivation method.....E-13
Table E-4. Results from time-to-tumor modeling data using mg/kg-day exposures and default HED derivation method.....E-13
Table E-5. PBPK model estimated dose-metrics for doses E-14
Table E-6a. Results from time-to-tumor modeling of data using PBPK dose metrics.....E-14
Table E-6b. HEDs from time-to-tumor modeling of data using PBPK dose metrics.....E-14
Table E-7. Results of Multistage (1º) quantal modeling of data using PBPK dose metrics.....E-15
Table E-8. Application of human PBPK model to derive HEDs from results of multistage (1º) quantal modeling of data using PBPK dose metrics E-15

Table E-9. Incidence for neoplasms considered for dose-response modeling E-16
Table E-10. PBPK dose metrics for doses E-16
Table E-11. Benchmark results from multistage quantal dose-response modeling data using PBPK dose-metrics E-17
Table E-12. Application of human PBPK model to derive HECs from $BMDL_{10}$ estimates in Table E-11 using multistage quantal modeling E-17
Table E-13. Incidence for malignant lymphoma (Apaja, 1980) E-17
Table E-14. PBPK dose metrics for doses in Apaja (1980) E-18
Table E-15. Benchmark results from Multistage-cancer dose-response modeling data for malignant lymphoma in Swiss Webster mice (Apaja, 1980) using PBPK dose-metrics E-18
Table E-16. Application of human PBPK model to derive HEDs from $BMDL_{10}$ estimates of Table E-15, Multistage (1º) modeling of malignant lymphoma in Swiss mice (Apaja, 1980) using PBPK dose metrics E-19
Table E-17. Benchmark results for all tumor types using BMDS 2.1 multistage "background dose" models and PBPK dose-metrics E-19

LIST OF FIGURES

Figure 3-1. Methanol metabolism and key metabolic enzymes in primates and rodents. 3-3
Figure 3-2. Folate-dependent formate metabolism. Tetrahydrofolate (THF)-mediated one carbon metabolism is required for the synthesis of purines, thymidylate, and methionine. ... 3-4
Figure 3-3. Plot of fetal (amniotic) versus maternal methanol concentrations in GD20 rats. 3-7
Figure 3-4. Schematic of the PBPK model used to describe the inhalation, oral, and i.v. route pharmacokinetics of methanol..... 3-24
Figure 3-5. Model fits to data sets from GD6, GD7, and GD10 mice for 6- to 7-hour inhalation exposures to 1,000–15,000 ppm methanol. 3-27
Figure 3-6. Simulation of inhalation exposures to methanol in NP mice from Perkins et al. (1995a) (8-hour exposures) and GD8 mice from Dorman et al. (1995)(6-hour exposures)..... 3-28
Figure 3-7. Conceptus versus maternal blood AUC values for rats and mice plotted (A) on a log-linear scale, as in Figure 8 of Ward et al. (1997), and (B) on a linear-linear scale... 3-30
Figure 3-8. NP rat i.v. route methanol blood kinetics..... 3-33
Figure 3-9. Model fits to data sets from inhalation exposures to 200 (triangles), 1,200 (diamonds), or 2,000 (squares) ppm methanol in male F-344 rats..... 3-33
Figure 3-10. Model fits to datasets from oral exposures to 100 and 2,500 mg/kg methanol in female Sprague-Dawley rats. 3-35
Figure 3-11. Urinary methanol elimination concentration (upper panel) and cumulative amount (lower panel) following inhalation exposures to methanol in human volunteers. 3-37
Figure 3-12. Data showing the visual quality of the fit using optimized first-order or Michaelis-Menten kinetics to describe the metabolism of methanol in humans..... 3-39
Figure 3-13. Inhalation exposures to methanol in human volunteers..... 3-41
Figure 3-14. Blood methanol concentration data from NP and pregnant monkeys..... 3-44
Figure 3-15. Chamber concentration profiles for monkey methanol exposures..... 3-46
Figure 4-1. Hemolymphoreticular neoplasms in male and female Sprague-Dawley rats in formaldehyde..... 4-110
Figure 5-1. Hill model BMD plot of decreased brain weight in male rats at 6 weeks age using modeled AUC of methanol in blood as the dose metric, 1 control mean S.D..... 5-12
Figure 5-2. PODs (in mg/m^3) for selected endpoints with corresponding applied UFs 5-15
Figure 5-3. All lymphomas versus methanol metabolized (mg/day) for female and male rats. 5-31
Figure 5-4. All lymphomas versus C_{max} (mg/L) for female and male rats. 5-31
Figure 5-5. All lymphomas versus AUC (hr x mg/L) for male and female rats..... 5-31
Figure 5-6. Lympho-immunoblastic Lymphoma minus “lung-only” response in rats of Soffritti et al. (2002a) methanol study versus methanol metabolized (mg/day)..... 5-42
Figure 5-7. Total amount metabolized per day (after periodicity is reached) in a 420 g rat 5-47
Figure B-1. Schematic of the PBPK model used to describe the inhalation, oral, and i.v. route pharmacokinetics of MeOH. B-3
Figure B-2. Model fits to data sets from GD6, GD7, and GD10 mice for 7-hour inhalation exposures to 1,000–15,000 ppm MeOH.....B-7
Figure B-3. Simulation of inhalation exposures to MeOH in NP mice from Perkins et al. (1995a) (8-hour exposures) and Dorman et al. (1995), (6-hour exposures). B-8
Figure B-4. Oral exposures to MeOH in pregnant mice on GD8 (Dorman et al., 1995) or NP and GD18. .....B-10
Figure B-5. Mouse intravenous route MeOH blood kinetics.....B-11
Figure B-6. Mouse model inhalation route sensitivity coefficients for metabolic parameters. B-15

Figure B-7. Mouse model inhalation route sensitivity coefficients for flow rates (QCC: cardiac output; QPC: alveolar ventilation), and partitioning to the body (PR) compartment are reported for blood MeOH AUC. B-15
Figure B-8. Mouse model sensitivity coefficients for oral exposures to MeOH. B-16
Figure B-9. Mouse daily drinking water ingestion pattern (A) and resulting predicted blood concentration for a 6 d/wk exposure (B). B-17
Figure B-10. NP rat i.v.-route methanol blood kinetics....B-19
Figure B-11. Model fits to data sets from inhalation exposures to 200 (triangles), 1,200 (diamonds), or 2,000 (squares) ppm MeOH in male F-344 rats. B-20
Figure B-12. Model fits to data sets from oral exposures to 100 (squares) or 2,500 (diamonds) mg/kg MeOH in female Sprague-Dawley rat....B-22
Figure B-13. Simulated Sprague-Dawley rat inhalation exposures to 500, 1,000, or 2,000 ppm MeOH. B-24
Figure B-14. Simulated rat oral exposures of Sprague-Dawley rats to 65.9, 624.2, or 2,177 mg MeOH/kg/day. B-25
Figure B-15. Rat daily drinking water ingestion pattern (A) and resulting predicted blood concentration for a 2-day exposure (B). B-26
Figure B-16. Urinary MeOH elimination concentration (upper panel) and cumulative amount (lower panel), following inhalation exposures to MeOH in human volunteers. B-28
Figure B-17. Control (nonexposed) blood methanol concentrations....B-30
Figure B-18. Data showing the visual quality of the fit using optimized first-order or Michaelis-Menten kinetics to describe the metabolism of MeOH in humans. B-31
Figure B-19. Inhalation exposures to MeOH in human volunteers. B-33
Figure B-20. Predicted 24-hour AUC (upper left), Cmax (upper right), and amount metabolized (lower) for MeOH inhalation exposures in the mouse (average over a 10-day exposure at 7 hours/day) and humans (steady-state values for a continuous exposure)....B-36
Figure B-21. Fit of the model to i.v. data using different clearance and uptake parameter optimizations. B-41
Figure B-22. Fit of the model to oral data using different clearance and uptake parameter optimizations. B-42
Figure B-23. Fit of the model to inhalation data using different clearance and uptake parameter optimizations. B-42
Figure B-24. Simulated human oral exposures to 0.1 mg MeOH/kg/-day comparing the first few days for four exposure scenarios B-92
Figure C-1. Hill model, BMR of 1 Control Mean S.D. - Decreased Brain weight in male rats at 6 weeks age versus AUC, F1 Generation inhalational study C-7
Figure C-2. Hill model, BMR of 0.05 relative risk - Decreased Brain weight in male rats at 6 weeks age versus AUC, F_1 Generation inhalational study. C-12
Figure C-3. Hill model, BMR of 1 Control Mean S.D. - Decreased Brain weight in male rats at 8 weeks age versus C_{max}, Gestation only inhalational study. C-18
Figure C-4. Exponential4 model, BMR of 0.05 relative risk - Decreased Brain weight in male rats at 8 weeks age versus C_{max}, Gestation only inhalational study. C-23
Figure C-5. Nested Logistic Model, 0.1 Extra Risk - Incidence of Cervical Rib in Mice versus C_{max} Methanol, GD 6-15 inhalational study....C-32
Figure C-6. Nested Logistic Model, 0.05 Extra Risk - Incidence of Cervical Rib in Mice versus C_{max} Methanol, GD 6-15 inhalational study....C-39
Figure C-7. 3rd Degree Polynomial Model, BMR of 1 Control Mean S.D. - VDR in female monkeys using AUC blood methanol as the dose metric....C-44

Figure D-1. Exposure-response data for methanol-induced CR plus SNR malformations in mice at various concentration-time combinations..... D-2
Figure D-2. Internal dose-response relationships for methanol-induced CR plus SNR malformations in mice at various concentration-time combinations for three dose metrics. D-3
Figure E-1. Female rat survival. E-20
Figure E-2. Male rats survival. E-20
Figure E-3. Female – Lymphomas lympho-immunoblastic – Multistage Weibull Model – Approach 1. .....E-21
Figure E-4. Female – All lymphomas – Multistage Weibull Model – Approach 1.....E-21
Figure E-5. Male – Hepatocellular carcinoma – Multistage Weibull Model – Approach 1.....E-22
Figure E-6. Male – Lymphomas lympho-immunoblastic – Multistage Weibull Model – Approach 1. .....E-22
Figure E-7. Male – All lymphomas – Multistage Weibull Model – Approach 1. .....E-23
Figure E-8. Female rats –All lymphomas time-to-tumor model fit and Kaplan Meier curves. E-23
Figure E-9. Male rats –All lymphomas time-to-tumor model fit and Kaplan Meier curves. ...E-24
Figure E-10. Male rats- All lymphomas; dose = amount metabolized (mg/day); 1º multistage model. E-24
Figure E-11. Female rat survival. E-25
Figure E-12. Male rat survival. E-25
Figure E-13. Female rats- pheochromocytomas; dose = amount metabolized (mg/d); 3º multistage model. E-26
Figure E-14. Plots for female (top; p= 0.55) and male (bottom; p= 0.21) mice – malignant lymphoma; dose=amount metabolized (mg/d); 2º multistage model.....E-26

LIST OF ACRONYMS

ACGIH	American Conference of Governmental and Industrial Hygienists
ADH	alcohol dehydrogenase
ADH1	alcohol dehydrogenase-1
ADH3	formaldehyde dehydrogenase-3
AIC	Akaike Information Criterion
ALD	aldehyde dehydrogenase
ALDH2	mitochondrial aldehyde dehydrogenase-2
ALT	alanine aminotransferase
ANOVA	analysis of variance
AP	alkaline phosphatase
AST	aspartate aminotransferase
ATP	adenosine triphosphate
ATSDR	Agency for Toxic Substances and Disease Registry
AUC	area under the curve, representing the cumulative product of time and concentration for a substance in the blood
β-NAG	N-acetyl-beta-D-glucosaminidase
BAA	butoxyacetic acid
BAL	butoxyacetaldehyde
BMC	benchmark concentration
BMCL	benchmark concentration, 95% lower bound
BMD	benchmark dose(s)
BMD_{1SD}	BMD for response one standard deviation from control mean
BMDL	95% lower bound confidence limit on BMD (benchmark dose)
$BMDL_{1SD}$	BMDL for response one standard deviation from control mean
BMDS	benchmark dose software
BMR	benchmark response
BSO	butathione sulfoximine
BUN	blood urea nitrogen
BW, bw	body weight
C_1 pool	one carbon pool
C_{max}	peak concentration of a substance in the blood during the exposure period
C-section	Cesarean section
CA	chromosomal aberrations
CAR	conditioned avoidance response
CASRN	Chemical Abstracts Service Registry Number
CAT	catalase
CERHR	Center for the Evaluation of Risks to Human Reproduction
CH_3OH	methanol
CHL	Chinese hamster lung (cells)

CHR	contact hypersensitivity response
CI	confidence interval
Cl_S	clearance rate
CNS	central nervous system
CO_2	carbon dioxide
con-A	concanavalin-A
CR	crown-rump length
CSF	Cancer slope factor
CT	computed tomography
CYP450	cytochrome P450
d, δ, Δ	delta, difference, change
D_2	dopamine receptor
DA	dopamine
DIPE	diisopropylether
DMDC	dimethyl dicarbonate
DNA	deoxyribonucleic acid
DNT	developmental neurotoxicity test(ing)
DOPAC	dihydroxyphenyl acetic acid
DPC	days past conception
DTH	delayed-type hypersensitivity
EFSA	European Food Safety Authority
EKG	electrocardiogram
EO	Executive Order
EPA	U.S. Environmental Protection Agency
ERF	European Ramazzini Foundation
EtOH	ethanol
F	fractional bioavailability
F_0	parental generation
F_1	first generation
F_2	second generation
F344	Fisher 344 rat strain
FAD	folic acid deficient
FAS	folic acid sufficient
FD	formate dehydrogenase
FP	folate paire
FR	folate reduced
FRACIN	fraction inhaled
FS	folate sufficient
FSH	follicular stimulating hormone
γ-GT	gamma glutamyl transferase

g	gravity
g, kg, mg, µg	gram, kilogram, milligram, microgram
G6PD	glucose-6-phosphate dehydrogenase
GAP43	growth-associated protein (neuronal growth cone)
GD	gestation day
GFR	glomerular filtration rate
GI	gastrointestinal track
GLM	generalized linear model
GLP	good laboratory practice
GSH	glutathione
HAP	hazardous air pollutant
Hb	hemoglobin
HCHO	formaldehyde
HCOO	formate
Hct	hematocrit
HEC	human equivalent concentration
HED	human equivalent dose
HEI	Health Effects Institute
HH	hereditary hemochromatosis
5_HIAA	5-hydroxyindolacetic acid
HMGSH	S-hydroxymethylglutathione
Hp	haptoglobin
HPA	hypothalamus-pituitary-adrenal (axis)
HPLC	high-performance liquid chromatography
HSDB	Hazardous Substances Databank
HSP70	biomarker of cellular stress
5-HT	serotonin
IL	interleukins
i.p.	intraperitoneal
IPCS	International Programme on Chemical Safety
IQ	intelligence quotient
IRIS	Integrated Risk Information System
IUR	inhalation unit risk
i.v.	intravenous
K_1	first order rate loss
K1C	first order clearance of methanol from the blood to the bladder for urinary elimination
KAI	first order uptake from the intestine
KAS	first order methanol oral absorption rate from stomach
KBL	rate constant for urinary excretion from bladder
KIA	first order uptake from intestine

KLH	keyhole limpet hemocyanin
KLL	alternate first order rate constant
K_m	substrate concentration at half the enzyme maximum velocity (V_{max})
K_m2	Michaelis-Menten rate constant for low affinity metabolic clearance of methanol
KSI	first order transfer between stomach and intestine
L, dL, mL	liter, deciliter, milliliter
LD_{50}	median lethal dose
LDH	lactate dehydrogenase
LH	luteinizing hormone
LLF	(maximum) log likelihood function
LMI	leukocyte migration inhibition (assay)
LOAEL	lowest-observed-adverse-effect level
M, mM, µM	molar, millimolar, micromolar
MAA	2-methoxyacetic acid
MCH	mean corpuscular hemoglobin
MCHC	mean corpuscular hemoglobin concentration
MCV	mean cell volume
MeOH	methanol
MLE	maximum likelihood estimate
M-M	Michaelis-Menten
MN	micronuclei
MOA	mode of action
4-MP	4-methylpyrazale messenger RNA
MRI	magnetic resonance imaging
MTBE	methyl tertiary butyl ether
MTX	methotrexate
N_2O/O_2	nitrous oxide
NAD^+	nicotinamide adenine dinucleotide
NADH	reduced form of nicotinamide adenine dinucleotide
NBT	nitroblue tetrazolium (test)
NCEA	National Center for Environmental Assessment
ND	not determined
NEDO	New Energy Development Organization (of Japan)
NIEHS	National Institute of Environmental Health Sciences
NIOSH	National Institute of Occupational Safety and Health
NK	natural killer
nmol	nanomole
NOAEL	no-observed-adverse-effect level
NOEL	no-observed-effect level

NP	nonpregnant
NR	not reported
NRC	National Research Council
NS	not specified
NTB	nitroblue tetra zolium
NTP	National Toxicology Program
NZW	New Zealand white (rabbit)
8-OHdG	8-hydroxydeoxyguanosine
OR	osmotic resistance
OSF	oral slope factor
OU	ocular uterque (each eye)
OXA	oxazolone
P, p	probability
PBPK	physiologically based pharmacokinetic
PEG	polyethylene glycol
PFC	plaque-forming cell
PK	pharmacokinetic
PMN	polymorphonuclear leucocytes
PND	postnatal day
POD	point of departure
ppb, ppb	parts per billion, parts per million
PWG	Pathology Working Group of the NTP of NIEHS
Q wave	the initial deflection of the QRS complex when such deflection is
QCC	cardiac output
QPC	pulmonary (alveolar) ventilation scaling coefficient
QRS	portion of electrocardiogram corresponding to the depolarization of ventricular cardiac cells.
R^2	square of the correlation coefficient, a measure of the reliability of a linear relationship.
RBC	red blood cell
RfC	reference concentration
RfD	reference dose
RNA	ribonucleic acid
ROS	reactive oxygen species
S9	microsomal fraction from liver
SAP	serum alkaline phosphatase
s.c.	subcutaneous
SCE	sister chromatid exchange
S.D.	standard deviation
S.E.	standard error
SEM	standard error of mean

SGPT	serum glutamate pyruvate transaminase
SHE	Syrian hamster embryo
SOD	superoxide dismutase
SOP	standard operating procedure(s)
t	time
$T_{½}$, $t_{½}$	half-life
T wave	the next deflection in the electrocardiogram after the QRS complex; represents ventricular repolarization
TAME	tertiary amyl methyl ether
TAS	total antioxidant status
Tau	taurine
THF	tetrahydrofolate
TLV	threshold limit value
TNFα	tumor necrosis factor-alpha
TNP-LPS	trinitrophenyl-lipopolysaccharide
TRI	Toxic Release Inventory
U83836E	vitamin E derivative
UF(s)	uncertainty factor(s)
UF_A	UF associated with interspecies (animal to human) extrapolation
UF_D	UF associated with deficiencies in the toxicity database
UF_H	UF associated with variation in sensitivity within the human population
UF_S	UF associated with subchronic to chronic exposure
V_d	volume of distribution
V_{max}	maximum enzyme velocity
$V_{max}C$	maximum velocity of the high-affinity/low-capacity pathway
v/v	volume/volume
VDR	visually directed reaching test
VitC	vitamin C
VYS	visceral yolk sac
WBC	white blood cell
WOE	weight of evidence
w/v	weight/volume
χ^2	chi square

FOREWORD

The purpose of this Toxicological Review is to provide scientific support and rationale for the hazard and dose-response assessment in IRIS pertaining to chronic exposure to methanol. It is not intended to be a comprehensive treatise on the chemical or toxicological nature of methanol.

The intent of Section 6, *Major Conclusions in the Characterization of Hazard and Dose Response*, is to present the major conclusions reached in the derivation of the reference dose, reference concentration and cancer assessment, where applicable, and to characterize the overall confidence in the quantitative and qualitative aspects of hazard and dose response by addressing the quality of data and related uncertainties. The discussion is intended to convey the limitations of the assessment and to aid and guide the risk assessor in the ensuing steps of the risk assessment process.

For other general information about this assessment or other questions relating to IRIS, the reader is referred to EPA's IRIS Hotline at (202) 566-1676 (phone), (202) 566-1749 (fax), or hotline.iris@epa.gov.

AUTHORS, CONTRIBUTORS, AND REVIEWERS

CHEMICAL MANAGER

Jeffrey Gift, Ph.D.
National Center for Environmental Assessment
U.S Environmental Protection Agency
Research Triangle Park, NC

AUTHORS

Stanley Barone, Ph.D.
National Center for Environmental Assessment
U.S. Environmental Protection Agency
Washington, DC

Allen Davis, MSPH
National Center for Environmental Assessment
U.S. Environmental Protection Agency
Research Triangle Park, NC

Jeffrey Gift, Ph.D.
National Center for Environmental Assessment
U.S. Environmental Protection Agency
Research Triangle Park, NC

Annette Iannucci, M.S.
Sciences International (first draft)
2200 Wilson Boulevard
Arlington, VA

Paul Schlosser, Ph.D.
National Center for Environmental Assessment
U.S. Environmental Protection Agency
Washington, DC

CONTRIBUTORS

Bruce Allen, Ph.D.
Bruce Allen Consulting
101 Corbin Hill Circle
Chapel Hill, SC

Hugh Barton, Ph.D.
National Center for Computational Toxicology
U.S. Environmental Protection Agency
Research Triangle Park, NC

J. Michael Davis, Ph.D.
National Center for Environmental Assessment
U.S. Environmental Protection Agency
Research Triangle Park, NC

Robinan Gentry, M.S.
ENVIRON International
650 Poydras Street
New Orleans, LA

Susan Goldhaber, M.S.
Alpha-Gamma Technologies, Inc.
3301 Benson Drive
Raleigh, NC

Mark Greenberg, Ph.D.
Senior Environmental Employee Program
U.S. Environmental Protection Agency
Research Triangle Park, NC

George Holdsworth, Ph.D.
Oak Ridge Institute for Science and Education (second draft)
Badger Road
Oak Ridge, TN

Angela Howard, Ph.D.
National Center for Environmental Assessment
U.S. Environmental Protection Agency
Research Triangle Park, NC

Connie Meacham, M.S.
National Center for Environmental Assessment
U.S. Environmental Protection Agency
Research Triangle Park, NC

Greg Miller
Office of Policy, Economics & Innovation
U.S. Environmental Protection Agency
Washington, DC

Sharon Oxendine, Ph.D.
Office of Policy, Economics & Innovation
U.S. Environmental Protection Agency
Washington, DC

Torka Poet, Ph.D.
Battelle, Pacific Northwest National Laboratories (Appendix B)
902 Battelle Boulevard
Richland, WA

John Rogers, Ph.D.
National Health & Environmental Effects Research laboratory
U.S. Environmental Protection Agency
Research Triangle Park, NC

Reeder Sams, II, Ph.D.
National Center for Environmental Assessment
U.S. Environmental Protection Agency
Research Triangle Park, NC

Roy Smith, Ph.D.
Air Quality Planning & Standards
U.S. Environmental Protection Agency
Research Triangle Park, NC

Frank Stack
Alpha-Gamma Technologies, Inc.
3301 Benson Drive
Raleigh, NC

Justin TeeGuarden, Ph.D.
Battelle, Pacific Northwest National Laboratories
902 Battelle Boulevard
Richland, WA

Chad Thompson, Ph.D., MBA
National Center for Environmental Assessment
U.S. Environmental Protection Agency
Washington, DC

Cynthia VanLandingham, M.S.
ENVIRON International (Appendix E)
650 Poydras Street
New Orleans, LA

Deborah Wales
National Center for Environmental Assessment
U.S. Environmental Protection Agency
Research Triangle Park, NC

Lutz Weber, Ph.D., DABT
Oak Ridge Institute for Science and Education
Badger Road
Oak Ridge, TN

Errol Zeiger, Ph.D.
Alpha-Gamma Technologies, Inc.
3301 Benson Drive
Raleigh, NC

REVIEWERS

This document has been reviewed by EPA scientists, interagency reviewers from other federal agencies and White House offices.

INTERNAL EPA REVIEWERS

Jane Caldwell, Ph.D.
National Center for Environmental Assessment
U.S Environmental Protection Agency
Washington, DC

Ila Cote, Ph.D., DABT
National Center for Environmental Assessment
U.S Environmental Protection Agency
Washington, DC

Robert Dewoskin Ph.D., DABT
National Center for Environmental Assessment
U.S Environmental Protection Agency
Research Triangle Park, NC

Joyce Donahue, Ph.D.
Office of Water
U.S. Environmental Protection Agency
Washington, DC

Marina Evans, Ph.D.
National Health and Environmental Effects Research Laboratory
U.S Environmental Protection Agency
Research Triangle Park, NC

Lynn Flowers, Ph.D., DABT
National Center for Environmental Assessment
U.S Environmental Protection Agency
Research Triangle Park, NC

Brenda Foos, M.S.
Office of Children's Health Protection and Environmental Education
U.S Environmental Protection Agency
Washington, DC

Jennifer Jinot, Ph.D.
National Center for Environmental Assessment

U.S Environmental Protection Agency
Washington, DC

Eva McLanahan, Ph.D.
National Center for Environmental Assessment
U.S Environmental Protection Agency
Research Triangle Park, NC

John Vandenberg, Ph.D.
National Center for Environmental Assessment
U.S Environmental Protection Agency
Research Triangle Park, NC

Debra Walsh, M.S.
National Center for Environmental Assessment
U.S Environmental Protection Agency
Research Triangle Park, NC

1. INTRODUCTION

This document presents background information and justification for the Integrated Risk Information System (IRIS) Summary of the hazard and dose-response assessment of methanol. IRIS Summaries may include oral reference dose (RfD) and inhalation reference concentration (RfC) values for chronic and other exposure durations, and a carcinogenicity assessment.

The RfD and RfC, if derived, provide quantitative information for use in risk assessments for health effects known or assumed to be produced through a nonlinear (presumed threshold) mode of action (MOA). The RfD (expressed in units of milligrams per kilogram per day [mg/kg-day]) is defined as an estimate (with uncertainty spanning perhaps an order of magnitude) of a daily exposure to the human population (including sensitive subgroups) that is likely to be without an appreciable risk of deleterious effects during a lifetime. The inhalation RfC (expressed in units of milligrams per cubic meter [mg/m^3]) is analogous to the oral RfD but provides a continuous inhalation exposure estimate. The inhalation RfC considers toxic effects for both the respiratory system (portal-of-entry) and for effects peripheral to the respiratory system (extrarespiratory or systemic effects). Reference values are generally derived for chronic exposures (up to a lifetime), but may also be derived for acute ($\leq$24 hours), short-term (>24 hours up to 30 days), and subchronic (>30 days up to 10% of lifetime) exposure durations, all of which are derived based on an assumption of continuous exposure throughout the duration specified. Unless specified otherwise, the RfD and RfC are derived for chronic exposure duration.

The carcinogenicity assessment provides information on the carcinogenic hazard potential of the substance in question, and quantitative estimates of risk from oral and inhalation exposure may be derived. The information includes a weight-of-evidence (WOE) judgment of the likelihood that the agent is a human carcinogen and the conditions under which the carcinogenic effects may be expressed. Quantitative risk estimates may be derived from the application of a low-dose extrapolation procedure. If derived, the oral slope factor is a plausible upper bound on the estimate of risk per mg/kg-day of oral exposure. Similarly, an inhalation unit risk (IUR) is a plausible upper bound on the estimate of risk per microgram per cubic meter ($\mu g/m^3$) air breathed.

Development of these hazard identification and dose-response assessments for methanol has followed the general guidelines for risk assessment as set forth by the National Research Council (NRC) (1983). EPA Guidelines and Risk Assessment Forum Technical Panel Reports that may have been used in the development of this assessment include the following: *Guidelines for the Health Risk Assessment of Chemical Mixtures* (U.S. EPA, 1986a), *Guidelines for Mutagenicity Risk Assessment* (U.S. EPA, 1986b), *Recommendations for and Documentation of Biological Values for Use in Risk Assessment* (U.S. EPA, 1988), *Guidelines for Developmental Toxicity Risk Assessment* (U.S. EPA, 1991), *Interim Policy for Particle Size and Limit*

Concentration Issues in Inhalation Toxicity Studies (U.S. EPA, 1994a), *Methods for Derivation of Inhalation Reference Concentrations and Application of Inhalation Dosimetry* (U.S. EPA, 1994b), *Use of the Benchmark Dose Approach in Health Risk Assessment* (U.S. EPA, 1995), *Guidelines for Reproductive Toxicity Risk Assessment* (U.S. EPA, 1996), *Guidelines for Neurotoxicity Risk Assessment* (U.S. EPA, 1998), *Science Policy Council Handbook*: *Risk Characterization* (U.S. EPA, 2000a), *Benchmark Dose Technical Guidance Document* (U.S. EPA, 2000b), *Supplementary Guidance for Conducting Health Risk Assessment of Chemical Mixtures* (U.S. EPA, 2000c), *A Review of the Reference Dose and Reference Concentration Processes* (U.S. EPA, 2002a), *Guidelines for Carcinogen Risk Assessment* (U.S. EPA, 2005a), *Supplemental Guidance for Assessing Susceptibility from Early-Life Exposure to Carcinogens* (U.S. EPA, 2005b), *Science Policy Council Handbook: Peer Review* (U.S. EPA, 2006a), and *A Framework for Assessing Health Risks of Environmental Exposures to Children* (U.S. EPA, 2006b).

The literature search strategy employed for this compound was based on the Chemical Abstracts Service Registry Number (CASRN) and at least one common name. Any pertinent scientific information submitted by the public to the IRIS Submission Desk was also considered in the development of this document. The relevant literature was reviewed through January, 2009.

2. CHEMICAL AND PHYSICAL INFORMATION

Methanol is also known as methyl alcohol, wood alcohol; Carbinol; Methylol; colonial spirit; columbian spirit; methyl hydroxide; monohydroxymethane; pyroxylic spirit; wood naphtha; and wood spirit (Chemfinder, 2002). Some relevant physical and chemical properties are listed below (Hazardous Substances Data Bank [HSDB], 2002, International Programme on Chemical Safety [IPCS], 1997).

Table 2-1. Relevant physical and chemical properties of methanol

CASRN:	67-56-1
Empirical formula:	CH_3OH
Molecular weight:	32.04
Vapor pressure:	160 mmHg at 30 ^oC
Vapor Density:	1.11
Specific gravity:	0.7866 g/mL (25 ^oC)
Boiling point:	64.7 ^oC
Melting point:	-98 ^oC
Water solubility:	Miscible
Log octanol-water partition coefficient:	-0.82 to -0.68
Conversion factor (in air):	1 ppm = 1.31 mg/m^3; 1 mg/m^3 = 0.763 ppm

Methanol is a clear, colorless liquid that has an alcoholic odor (IPCS, 1997). Endogenous levels of methanol are present in the human body as a result of both metabolism[1] and dietary sources such as fruit, fruit juices, vegetables and alcoholic beverages,[2] and can be measured in exhaled breath and body fluids (Turner et al., 2006; CERHR 2004; IPCS 1997). Dietary exposure to methanol also occurs through the intake of some food additives. The artificial sweetener aspartame and the beverage yeast inhibitor dimethyl dicarbonate (DMDC) release methanol as they are metabolized (Stegink et al., 1989). In general, aspartame exposure does not contribute significantly to the background body burden of methanol (Butchko, 2002). Oral, dermal, or inhalation exposure to methanol in the environment, consumer products, or workplace also occur.

Methanol is a high production volume chemical with many commercial uses and it is a basic building block for numerous chemicals. Many of its derivatives are used in the

[1] Methanol is generated metabolically through enzymatic pathways such as the methyltransferase system (Fisher et al., 2000).

[2] Fruits and vegetables contain methanol. Further, ripe fruits and vegetables contain natural pectin, which is degraded to methanol in the body by bacteria present in the colon (Siragusa et al., 1988). Increased levels of methanol in blood and exhaled breath have also been observed after the consumption of ethanol (Fisher et al., 2000).

construction, housing or automotive industries, with its use as a transportation fuel accounting for ~20% of its demand (Methanol Institute, 2006). Consumer products that contain methanol include varnishes, shellacs, paints, windshield washer fluid, antifreeze, adhesives, de-icers, and Sterno heaters. Methanol is used to produce other chemicals and is among the highest production volume chemicals in the EPA's Toxic Release Inventory (TRI), which reported that 183,000 pounds of methanol was released or disposed of in the United States in 2003, making methanol among the top 10 chemicals on the list entitled "On-site and Off-site Reported Disposed of or Otherwise Released (in pounds), for Facilities in All Industries, for All Chemicals" (U.S. EPA, 2006c). Natural gas is the primary feedstock for methanol and as such, the major portion of its production cost. Due to the high cost of natural gas in North America, North America methanol production capacity is down from 9 million metric tons at the turn of the century to less than 3 million metric tons at the end of 2005 and is expected to be nonexistent by 2010 (Methanol Institute, 2006). While production has switched to other regions of the world, demand for methanol is growing steadily in almost all end uses. A large reason for the increase in demand is its use in the production of biodiesel, a low-sulfur, high-lubricity fuel source that is gaining favor in nearly every major region of the world. Starting from less than 100,000 metric tons in 2005, global demand for methanol into biodiesel is expected to reach as much as 1.5 million metric tons by the year 2010. Power generation and fuel cells could also be large end users of methanol in the near future (Methanol Institute, 2006).

3. TOXICOKINETICS

3.1. OVERVIEW

As has been noted, methanol occurs naturally in the human body as a product of metabolism and through intake of fruits, vegetables, and alcoholic beverages (Turner et al., 2006; CERHR 2004; IPCS 1997). Table 3-1 summarizes background blood methanol levels in healthy humans which were found to range from 0.25–4.7 mg/L. One study reported a higher background blood methanol level in females versus males (Batterman and Franzblau, 1997), but most studies did not evaluate gender differences. Formate, a metabolite of methanol, also occurs naturally in the human body (IPCS 1997). Table 3-1 outlines background levels of formate in human blood. In most cases, methanol and formate blood levels were measured in healthy adults following restriction of methanol-producing foods from the diet.[3]

The absorption, excretion, and metabolism of methanol are well known and have been consistently summarized in reviews such as CERHR (2004), IPCS (1997), U.S. EPA (1996), Kavet and Nauss (1990), HEI (1987), and Tephly and McMartin (1984). Therefore, the major portion of this toxicokinetics overview is based upon those reviews.

Studies conducted in humans and animals demonstrate rapid absorption of methanol by inhalation, oral, and dermal routes of exposure. Table 3-2 outlines increases in human blood methanol levels following various exposure scenarios. Blood levels of methanol following various exposure conditions have also been measured in monkeys, mice, and rats, and are summarized in Tables 3-3, 3-4, and 3-5, respectively. Once absorbed, methanol pharmacokinetic (PK) data and physiologically based pharmacokinetic (PBPK) model predictions indicate rapid distribution to all organs and tissues according to water content, as an aqueous-soluble alcohol. Tissue:blood concentration ratios for methanol are predicted to be similar through different exposure routes, though the kinetics will vary depending on exposure route and timing (e.g., bolus oral exposure versus longer-term inhalation). Because smaller species generally have faster respiration rates relative to body weight than larger species, they are predicted to have a higher rate of increase of methanol concentrations in the body when exposed to the same concentration in air.

At doses that do not saturate metabolic pathways, a small percentage of methanol is excreted directly in urine. Because of the high blood:air partition coefficient for methanol and rapid metabolism in all species studied, the bulk of clearance therefore occurs by metabolism, though exhalation and urinary clearance will become more significant when doses or exposures are sufficiently high to saturate metabolism. Metabolic saturation and the corresponding clearance shift have not been observed in humans and nonhuman primates because doses used

[3] In general, background levels among people who are on normal/non-restricted diets will be higher than those reported.

were limited to the linear range, but the enzymes involved in primate metabolism are also saturable.

The primary route of methanol elimination in mammals is through a series of oxidation reactions that form formaldehyde, formate, and carbon dioxide (Figure 3-1). As noted in Figure 3-1, methanol is converted to formaldehyde by alcohol dehydrogenase-1 (ADH1) in primates and by catalase (CAT) and ADH1 in rodents. Although the first step of metabolism occurs through different pathways in rodents and nonhuman primates, Kavet and Nauss (1990) report that the reaction proceeds at similar rates (V_{max} = 30 and 48 mg/h/kg in rats and nonhuman primates, respectively). In addition to enzymatic clearance, methanol can react with hydroxyl radicals to spontaneously yield formaldehyde (Harris et al., 2003). Mannering et al. (1969) also reported a similar rate of methanol metabolism in rats and monkeys, with 10 and 14% of a 1 g/kg dose oxidized in 4 hours, respectively; the rate of oxidation by mice was about twice as fast, 25% in 4 hours. In an HEI study by Pollack and Brouwer (1996), the metabolism of methanol was 2 times as fast in mice versus rats, with a V_{max} for elimination of 117 and 60.7 mg/h/kg, respectively. Despite the faster elimination rate of methanol in mice versus rats, mice consistently exhibited higher blood methanol levels than rats when inhaling equivalent methanol concentrations (See Tables 3-4 and 3-5). Possible explanations for the higher methanol accumulation in mice include faster respiration (inhalation rate/body weight) and increased fraction of absorption by the mouse (Perkins et al., 1995a). Because smaller species generally have faster breathing rates than larger species, humans would be expected to absorb methanol via inhalation more slowly than rats or mice inhaling equivalent concentrations. If humans eliminate methanol at a comparable rate to rats and mice, then humans would also be expected to accumulate less methanol than those smaller species. However, if humans eliminate methanol more slowly than rats and mice, such that the ratio of absorption to elimination stays the same, then humans would be expected to accumulate methanol to the same internal concentration but to take longer to reach that concentration.

In all species, formaldehyde is rapidly converted to formate, with the half-life for formaldehyde being ~1 minute. Formaldehyde is oxidized to formate by two metabolic pathways (Teng et al., 2001). The first pathway (not shown in Figure 3-1) involves conversion of free formaldehyde to formate by the so-called low-affinity pathway (affinity = $1/K_m$ = 0.002/μM) mitochondrial aldehyde dehydrogenase-2 (ALDH2). The second pathway (Figure 3-1) involves a two-enzyme system that converts glutathione-conjugated formaldehyde (*S*-hydroxymethylglutathione [HMGSH]) to the intermediate *S*-formylglutathione, which is subsequently metabolized to formate and glutathione (GSH) by *S*-formylglutathione hydrolase.[4] The first enzyme in this pathway, formaldehyde dehydrogenase-3 (ADH3), is rate limiting, and the affinity of HMGSH for ADH3 (affinity = $1/K_m$ = 0.15/μM) is about a 100-fold higher than

[4] Other enzymatic pathways for the oxidation of formaldehyde have been identified in other organisms, but this is the pathway that is recognized as being present in humans (Caspi et al., 2006; http://metacyc.org)

that of free formaldehyde for ALDH2. In addition to the requirement of GSH for ADH3 activity, oxidation by ADH3 is nicotinamide adenine dinucleotide- (NAD^+-)dependent. Under normal physiological conditions NAD^+ levels are about two orders of magnitude higher than NADH, and intracellular GSH levels (mM range) are often high enough to rapidly scavenge formaldehyde (Svensson et al., 1999; Meister and Adnerson, 1983); thus, the oxidation of HMGSH is favorable. In addition, genetic ablation of ADH3 results in increased formaldehyde toxicity (Deltour et al., 1999). These data indicate that ADH3 is likely to be the predominant enzyme responsible for formaldehyde oxidation at physiologically relevant concentrations, whereas ALDHs likely contribute to formaldehyde clearance at higher concentrations (Dicker and Cederbaum, 1986).

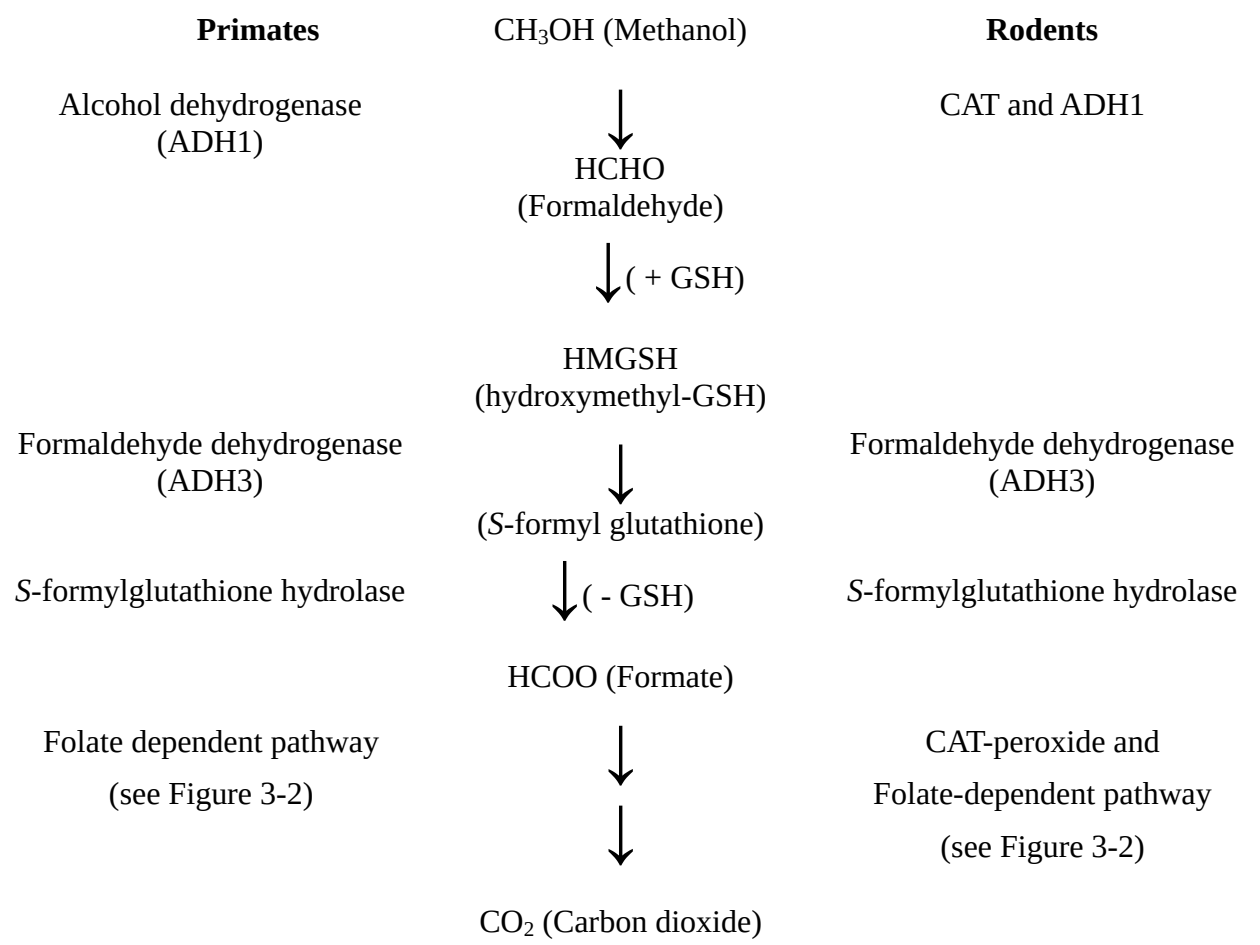

Figure 3-1. Methanol metabolism and key metabolic enzymes in primates and rodents.

Source: IPCS (1997).

Rodents convert formate to carbon dioxide (CO_2) through a folate-dependent enzyme system and a CAT-peroxide system (Dikalova et al., 2001). Formate can undergo adenosine triphosphate- (ATP-) dependent addition to tetrahydrofolate (THF), which can carry either one or two one-carbon groups. Formate can conjugate with THF to form N^{10}-formyl-THF and its

isomer N^5-formyl-THF, both of which can be converted to N^5, N^{10}-methenyl-THF and subsequently to other derivatives that are ultimately incorporated into DNA and proteins via biosynthetic pathways (Figure 3-2). There is also evidence that formate generates CO_2^- radicals, and can be metabolized to CO_2 via CAT and via the oxidation of N^{10}-formyl-THF (Dikalova et al., 2001).

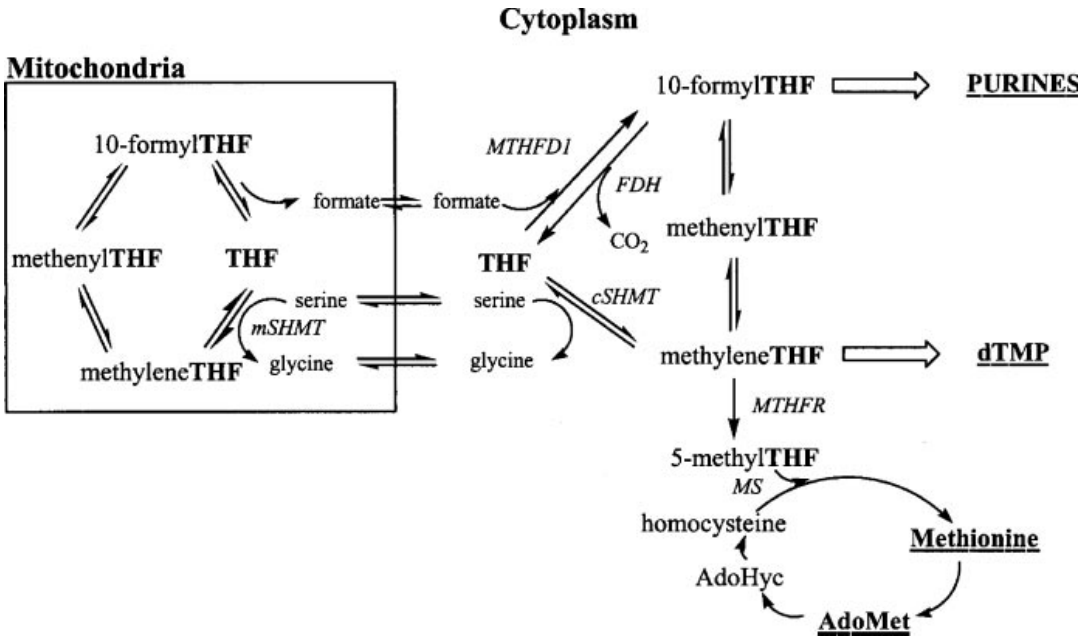

Figure 3-2. Folate-dependent formate metabolism. Tetrahydrofolate (THF)-mediated one carbon metabolism is required for the synthesis of purines, thymidylate, and methionine.

Source: Montserrat et al. (2006).

Unlike rodents, formate metabolism in primates occurs solely through a folate-dependent pathway. Black et al. (1985) reported that hepatic THF levels in monkeys are 60% of that in rats, and that primates are far less efficient in clearing formate than are rats and dogs. Studies involving [^{14}C]formate suggest that ~80% is exhaled as $^{14}CO_2$, 2-7% is excreted in the urine, and ~10% undergoes metabolic incorporation (Hanzlik et al., 2005, and references therein). Mice deficient in formyl-THF dehydrogenase exhibit no change in LD_{50} (via intraperitoneal [i.p.]) for methanol or in oxidation of high doses of formate. Thus it has been suggested that rodents efficiently clear formate via folate-dependent pathways, peroxidation by CAT, and by an unknown third pathway; conversely, primates do not appear to exhibit such capacity and are more sensitive to metabolic acidosis following methanol poisoning (Cook et al., 2001).

Blood methanol and formate levels measured in humans under various exposure scenarios are reported in Table 3-2. As noted in Table 3-2, 75-minute to 6-hour exposures of healthy humans to 200 parts per million (ppm) methanol vapors, the American Council of

Governmental Industrial Hygienists (ACGIH) threshold limit value (TLV) for occupational exposure (ACGIH, 2000), results in increased levels of blood methanol but not formate. A limited number of monitoring studies indicate that levels of methanol in outdoor air are orders of magnitude lower than the TLV (IPCS, 1997). Table 3-3 indicates that exposure of monkeys to 600 ppm methanol vapors for 2.5 hours increased blood methanol but not blood formate levels. Normal dietary exposure to aspartame, which releases 10% methanol during metabolism, is unlikely to significantly increase blood methanol or formate levels (Butchko et al., 2002). Data in Table 3-2 suggest that exposure to high concentrations of aspartame is unlikely to increase blood formate levels; no increase in blood formate levels were observed in adults ingesting "abusive doses" (100–200 mg/kg) of aspartame (Stegink et al., 1981). Kerns et al. (2002) studied the kinetics of formate in 11 methanol-poisoned patients (mean initial methanol level of 57.2 mmol/L or 1.83 g/L) and determined an elimination half-life of 3.4 hours for formate. Kavet and Nauss (1990) estimated that a methanol dose of 11 mM or 210 mg/kg is needed to saturate folate-dependent metabolic pathways in humans. There are no data on blood methanol and formate levels following methanol exposure of humans with reduced ADH activity or marginal folate tissue levels, a possible concern regarding sensitive populations. As discussed in greater detail in Section 3.2, a limited study in folate-deficient monkeys demonstrated no increase in blood formate levels following exposure to 900 ppm methanol vapors for 2 hours. In conclusion, limited available data suggest that typical occupational, environmental, and dietary exposures are likely to increase baseline blood methanol but not formate levels in most humans.

3.2. KEY STUDIES

Some recent toxicokinetic and metabolism studies (Burbacher et al., 2004a, 1999b; Medinsky et al., 1997; Pollack and Brouwer, 1996; Dorman et al., 1994) provide key information on interspecies differences, methanol metabolism during gestation, metabolism in the nonhuman primate, and the impact of folate deficiency on the accumulation of formate.

As part of an effort to develop a physiologically based toxicokinetic model for methanol distribution in pregnancy, Pollack and Brouwer (1996) conducted a large study that compared toxicokinetic differences in pregnant and nonpregnant (NP) rats and mice. Methanol disposition[5] was studied in Sprague-Dawley rats and CD-1 mice that were exposed to 100–2,500 mg/kg of body weight pesticide-grade methanol in saline by intravenous (i.v.) or oral routes. Exposures were conducted in NP rats and mice, pregnant rats on gestation days (GD)7, GD14, and GD20, and pregnant mice on GD9 and GD18. Disposition was also studied in pregnant rats and mice exposed to 1,000–20,000 ppm methanol vapors for 8 hours. Three to five animals were examined at each dose and exposure condition.

[5] Methanol concentrations in whole blood and urine were determined by gas chromatography with flame ionization detection (Pollack and Kawagoe, 1991)

Based on the fit of various kinetic models to methanol measurements taken from all routes of exposure, the authors concluded that high exposure conditions resulted in nonlinear disposition of methanol in mice and rats.[6] Both linear and nonlinear pathways were observed with the relative contribution of each pathway dependent on concentration. At oral doses of 100–500 mg/kg of body weight, methanol was metabolized to formaldehyde and then formic acid through the saturable nonlinear pathway. A parallel, linear route characteristic of passive-diffusion accounted for an increased fraction of total elimination at higher concentrations. Nearly 90% of methanol elimination occurred through the linear route at the highest oral dose of 2,500 mg/kg of body weight.

Oral exposure resulted in rapid and essentially complete absorption of methanol. No significant change in blood area under the curve (AUC) methanol was seen between NP and GD7, GD14 and GD20 rats exposed to single oral gavage doses of 100 and 2,500 mg/kg, nor between NP and GD9 and GD18 mice at 2,500 mg/kg. The data as a whole suggested that the distribution of orally and i.v. administered methanol was similar in rats versus mice and in pregnant rodents versus NP rodents with the following exceptions:

- There was a statistically significant increase in the ratio of apparent volume of distribution (V_d) to fractional bioavailability (F) by ~20% (while F decreased but not significantly), between NP and GD20 rats exposed to 100 mg/kg orally. However, this trend was not seen in rats or mice exposed to 2,500 mg/kg, and the result in rats at 100 mg/kg could well be a statistical artifact since both V_d and F were being estimated from the same data, making the model effectively over-parameterized.
- There were statistically significant decreases in the fraction of methanol absorbed by the fast process (resulting in a slower rise to peak blood concentrations, though the peak is unchanged) and V_{max} for clearance between NP and GD18 mice. No such differences were observed between NP and GD9 mice.
- The authors estimated a twofold higher V_{max} for methanol elimination in mice versus rats following oral administration of 2,500 mg/kg methanol, suggesting that similar oral doses would result in lower methanol concentrations in the mouse versus rat.

Methanol penetration from maternal blood to the fetal compartment was examined in GD20 rats by microdialysis.[7] A plot of the amniotic concentration versus maternal blood concentration (calculated from digitization of Figure 17 of Pollack and Brouwer [1996] report) is shown in Figure 3-3. The ratio is slightly less than 1:1 (dashed line in plot) and appears to be reduced with increasing methanol concentrations, possibly due to decreased blood flow to the

[6] A model incorporating parallel linear and nonlinear routes of methanol clearance was required to fit the data from the highest exposure groups.

[7] Microdialysis was conducted by exposing the uterus (midline incision), selecting a single fetus in the middle of the uterine horn and inserting a microdialysis probe through a small puncture in the uterine wall proximal to the head of the fetus.

fetal compartment. Nevertheless, this is a very minor departure from linearity, consistent with a substrate such as methanol that penetrates cellular membranes readily and distributes throughout total body water.

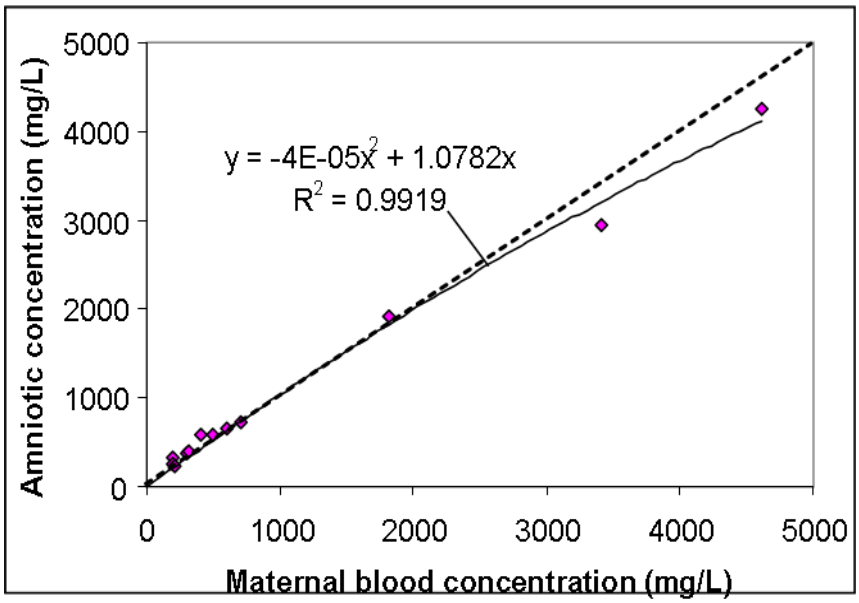

Figure 3-3. Plot of fetal (amniotic) versus maternal methanol concentrations in GD20 rats. Data extracted from Figure 17 by digitization, and amniotic concentration obtains as ("Fetal Amniotic Fluid/Maternal Blood Methanol")×("Maternal Methanol").

Source: Pollack and Brouwer (1996).

Inhalation exposure resulted in less absorption in both rats and mice as concentrations of methanol vapors increased, which was hypothesized to be due to decreased breathing rate and decreased absorption efficiency from the upper respiratory tract.[8] Based on blood methanol concentrations measured following 8-hour inhalation exposures to concentrations ranging from 1,000–20,000 ppm, the study authors (Pollack and Brown, 1996) concluded that methanol accumulation in the mouse occurred at a two- to threefold greater rate compared to the rat. They speculated that faster respiration rate and more complete absorption in the nasal cavity of mice may explain the higher methanol accumulation and greater sensitivity to developmental toxicity (see Section 4.3.2).

[8] Exposed mice spent some exposure time in an active state, characterized by a higher ventilation rate, and the remaining time in an inactive state, with lower (~½ of active) ventilation. The inactive ventilation rate was unchanged by methanol exposure, but the active ventilation showed a statistically significant methanol-concentration-related decline. There was also some decline in the fraction of time spent in the active state, but this too was not statistically significant.

The Pollack and Brouwer (1996) study was useful for comparing effects in pregnant and NP rodents exposed to high doses, but the implication of these results for humans exposed to ambient levels of methanol is not clear (CERHR, 2004).

Burbacher et al. (2004b, 1999a) examined toxicokinetics in *Macaca fascicularis* monkeys prior to and during pregnancy. The study objectives were to assess the effects of repeated methanol exposure on disposition kinetics, determine whether repeated methanol exposures result in formate accumulation, and examine the effects of pregnancy on methanol disposition and metabolism. Reproductive and developmental toxicity associated with this study were also examined and are discussed in Sections 4.3.2 and 4.4.2. In a 2-cohort design, 48 adult females (6 animals/dose/group/cohort) were exposed to 0, 200, 600, or 1,800 ppm methanol vapors (99.9% purity) for 2.5 hours/day, 7 days/week for 4 months prior to breeding and during the entire breeding and gestation periods. Six-hour methanol clearance studies were conducted prior to and during pregnancy. Burbacher et al. (2004b, 1999a) reported that:

- At no point during pregnancy was there a significant change in endogenous methanol blood levels, which ranged from 2.2–2.4 mg/L throughout.
- PK studies were performed initially (Study 1), after 90 days of pre-exposure and prior to mating (Study 2), between GD66 and GD72 (Study 3), and again between GD126 and GD132 (Study 4). These studies were analyzed using classical PK (one-compartment) models.
- Disproportionate mean, dose-normalized, and net blood methanol dose-time profiles in the 600 and 1,800 ppm groups suggested saturation of the metabolism-dependent pathway. Data from the 600 ppm group fit a linear model, while data from the 1,800 ppm group fit a Michaelis-Menten model.
- Methanol clearance rates modestly increased between Study 1 and Study 2 (90 days prior to mating). This change was attributed to enzyme induction from the subchronic exposure.
- Blood methanol levels were measured every 2 weeks throughout pregnancy, and while there was measurement-to-measurement variation, there was no significant change or trend over the course of pregnancy. There appears to be an upward trend in elimination half-life and corresponding downward trend in blood methanol clearance between Studies 2, 3, and 4. However, the changes are not statistically significant and the time-courses for blood methanol concentration (elimination phase) appear fairly similar.
- Significant differences between pre-breeding and gestational blood plasma formate levels were observed but were not dose dependent (Table 3-6).
- Significant differences in serum folate levels in periods prior to and during pregnancy were not dose dependent (Table 3-7).

An HEI review committee (Burbacher et al., 1999a) noted that this was a quality study using a relevant species. Although the study can be used to predict effects in adequately nourished individuals, the study may not be relevant to persons who are folate deficient.

A series of studies by Medinsky et al. (1997) and Dorman et al. (1994) examined metabolism and pharmacokinetics of [^{14}C]methanol and [^{14}C]formate in normal and folate-deficient cynomolgus, *M. fascicularis* monkeys that were exposed to environmentally relevant concentrations of [^{14}C]methanol through an endotracheal tube while anesthetized. In the first stage of the study, 4 normal 12-year-old cynomolgus monkeys were each exposed to 10, 45, 200, and 900 ppm [^{14}C]methanol vapors (>98% purity) for 2 hours. Each exposure was separated by at least 2 months. After the first stage of the study was completed, monkeys were given a folate-deficient diet supplemented with 1% succinylsulfathiozole (an antibacterial sulfonamide used to inhibit folic acid biosynthesis from intestinal bacteria) for 6–8 weeks in order to obtain folate concentrations of <3 ng/mL serum and <120 ng/mL erythrocytes. Folate deficiency did not alter hematocrit level, red blood cell count, mean corpuscular volume, or mean corpuscular hemoglobin level. The folate-deficient monkeys were exposed to 900 ppm [^{14}C]methanol for 2 hours. The results of the Medinsky et al. (1997) and Dorman et al. (1994) studies showed:

- Dose-dependent changes in toxicokinetics and metabolism did not occur as indicated by a linear relationship between inhaled [^{14}C]methanol concentration and end-of-exposure blood [^{14}C]methanol level, [^{14}C]methanol AUC and total amounts of exhaled [^{14}C]methanol and [^{14}C]carbon dioxide.
- Methanol concentration had no effect on elimination half-life (<1 hour) and percent urinary [^{14}C]methanol excretion (<0.01%) at all doses.
- Following exposure to 900 ppm methanol, urinary excretion or exhalation of [^{14}C]methanol did not differ significantly between monkeys in the folate sufficient and deficient state. There was no significant [^{14}C] formate accumulation at any dose.
- Peak blood [^{14}C]formate levels were significantly higher in folate-deficient monkeys, but did not exceed endogenous blood levels reported by the authors to be between 0.1 and 0.2 mmol/L (4.6 to 9.2 mg/L).

An HEI review committee (Medinsky et al., 1997) noted that absolute values in this study cannot be extrapolated to humans because the use of an endotracheal tube in anesthetized animals results in an exposure scenario that is not relevant to humans. However, the data in this study suggest that a single exposure to an environmentally relevant concentration of methanol is unlikely to result in a hazardous elevation in formate levels, even in individuals with moderate folate deficiency.

3.3. HUMAN VARIABILITY IN METHANOL METABOLISM

The ability to metabolize methanol may vary among individuals as a result of genetic, age, and environmental factors. Reviews by Agarwal (2001), Burnell et al. (1989), Bosron and Li (1986), and Pietruszko (1980), discuss genetic polymorphisms for ADH. Class I ADH, the primary ADH in human liver, is a hetero- or homodimer composed of randomly associated polypeptide units encoded by three separate gene loci (ADH1A, ADH1B, and ADH1C). Polymorphisms have been found to occur at the ADH1B (ADH1B*2, ADH1B*3) and ADH1C (ADH1C*2) gene loci; however, no human allelic polymorphism has been found in ADH1A. The ADH1B*2 phenotype is estimated to occur in ~15% of Caucasians of European descent, 85% of Asians, and <5% of African Americans. Fifteen percent of African Americans have the ADH1B*3 phenotype, while it is found in <5% of Caucasian Europeans and Asians. To date, there are two reports of polymorphisms in ADH3 (Cichoz-Lach et al., 2007; Hedberg et al., 2001), yet the functional consequence(s) for these polymorphisms remains unclear.

Although racial and ethnical differences in the frequency of the occurrence of ADH alleles in different populations have been reported, ADH enzyme kinetics (V_{max} and K_m) have not been reported for methanol. There is an abundance of information pertaining to the kinetic characteristics of the ADH dimers to metabolize ethanol in vitro; however, the functional and biological significance is not well understood due to the lack of data documenting metabolism and disposition of methanol or ethanol in individuals of known genotype. While potentially significant, the contribution of ethnic and genetic polymorphisms of ADH to the interindividual variability in methanol disposition and metabolism can not be reliably quantified at this time.

Because children generally have higher baseline breathing rates and are more active, they may receive higher methanol doses than adults exposed to equivalent concentrations of any air pollutant (CERHR, 2004). There is evidence that children under 5 years of age have reduced ADH activity. A study by Pikkarainen and Raiha (1967) measured liver ADH activity using ethanol as a substrate and found that 2-month-old fetal livers have ~3–4% of adult ADH liver activity. ADH activity in 4–5 month old fetuses is ~10% of adult activity, and an infant's activity is ~20% of adult activity. ADH continues to increase in children with age and reaches a level that is within adult ranges at 5 years of age. Adults were found to have great variation in ADH activity (1,625–6,530/g liver wet weight or 2,030–5,430 mU/100 mg soluble protein). Smith et al. (1971) also compared liver ADH activity in 56 fetuses (9–22 weeks gestation), 37 infants (premature to <1 year old), and 129 adults (>20 years old) using ethanol as a substrate. ADH activity was 30% of adult activity in fetuses and 50% of adult activity in infants. There is evidence that some human infants are able to efficiently eliminate methanol at high exposure levels, however, possibly via CAT (Tran et al., 2007).

ADH3 exhibits little or no activity toward small alcohols, thus the previous studies provide no information about the ontogeny of formaldehyde clearance. While such data on

ADH3 activity does not exist, ADH3 mRNA is abundantly expressed in the mouse fetus (Ang et al., 1996) and is detectible in human fetal tissues (third trimester), neonates and children (Hines et al., 2002; Estonius et al., 1996).

As noted earlier in this section, folate-dependent reactions are important in the metabolism of formate. Individuals who are commonly folate deficient include those who are pregnant or lactating, have gastrointestinal (GI) disorders, have nutritionally inadequate diets, are alcoholics, smoke, have psychiatric disorders, have pernicious anemia, or are taking folic acid antagonist medications such as some antiepileptic drugs (CERHR, 2004; IPCS, 1997). Groups which are known to have increased incidence of folate deficiencies include Hispanic and African American women, low-income elderly, and mentally ill elderly (CERHR, 2004). A polymorphism in methylene tetrahydrofolate reductase reduces folate activity and is found in 21% of Hispanics in California and 12% of Caucasians in the United States. Genetic variations in folic acid metabolic enzymes and folate receptor activity are theoretical causes of folate deficiencies.

Table 3-1. Background blood methanol and formate levels in humans

Description of human subjects	Methanol (mg/L) mean ± S.D. (Range)	Formate (mg/L) mean ± S.D. (Range)	Reference
12 males on restricted diet (no methanol-containing or methanol-producing foods) for 12 hr	0.570 ± 0.305 (0.25–1.4)	3.8 ± 1.1 (2.2–6.6)	Cook et al. (1991)
22 adults on restricted diet (no methanol-containing or methanol-producing foods) for 24 hr	1.8 ± 2.6 (No range data)	11.2 ± 9.1 (No range data)	Osterloh et al. (1996); Chuwers et al. (1995)
3 males who ate a breakfast with no aspartame-containing cereals and no juice	1.82 ± 1.21 (0.57–3.57)	9.08 ± 1.26 (7.31–10.57)	Lee et al. (1992)
5 males who ate a breakfast with no aspartame-containing cereals and no juice (second experiment)	1.93 ± 0.93 (0.54–3.15)	8.78 ± 1.82 (5.36–10.83)	Lee et al. (1992)
Adults who drank no alcohol for 24 hr	1.8 ± 0.7 (No range data)	No data	Batterman et al. (1998)
12 adults who drank no alcohol for 24 hr	1.7 ± 0.9 (0.4–4.7)	No data	Batterman and Franzblau (1997)
4 adult males who fasted for 8 hr, drank no alcohol for 24 hr, and took in no fruits, vegetables, or juices for 18 hr	No mean data (1.4–2.6)	No data	Davoli et al. (1986)
30 fasted adults	<4 (No range data)	19.1 (No range data)	Stegink et al. (1981)
24 fasted infants	<3.5 (No range data)	No data	Stegink et al. (1983)

Source: CERHR (2004).

Table 3-2. Human blood methanol and formate levels following methanol exposure

Human subjects; type of sample collected [b,c]	Exposure route	Exposure duration or method	Methanol exposure concentration	Blood methanol mean or range (mg/L)	Blood formate mean or range (mg/L)	Reference
Adult males and females administered aspartame; peak methanol level and range of formate levels up to 24 hr after dosing	Oral	1 dose in juice	0		19.1	Stegink et al. (1981)
			3.4 mg/kg bw[a]	<4	No data	
			10 mg/kg bw[a]	12.7	No data	
			15 mg/kg bw[a]	21.4	No data	
			20 mg/kg bw[a]	25.8	8.4–22.8	
Infants administered aspartame; peak exposure level	Oral	1 dose in beverage	0		No data	Stegink et al. (1983)
			3.4 mg/kg bw[a]	<3.5		
			5 mg/kg bw[a]	3.0		
			10 mg/kg bw[a]	10.2		
Adult males administered aspartame; range of peak serum methanol levels in all subjects	Oral	1 dose in water	0	1.4–2.6	No data	Davoli et al. (1986)
			0.6 – 0.87 mg/kg bw[a]	2.4–3.6		
Males; postexposure samples	Inhalation	75 min	0	0.570	3.8	Cook et al. (1991)
			191 ppm	1.881	3.6	
Males and females; postexposure serum levels	Inhalation	4 hr	0	1.8	11.2	Osterloh et al. (1996)
			200 ppm	6.5	14.3	
Males without exercise; postexposure blood methanol and plasma formate	Inhalation	6 hr	0	1.82	9.08	Lee et al. (1992)
			200 ppm	6.97	8.70	
Males with exercise; postexposure blood methanol and plasma formate	Inhalation	6 hr	0	1.93	8.78	
			200 ppm	8.13	9.52	
Females; postexposure samples	Inhalation	8 hr	0	1.8	No data	Batterman et al.(1998)
			800 ppm	30.7		

[a]Methanol doses resulting from intake of aspartame.
[b]Unless otherwise specified, it is assumed that whole blood was used for measurements.
[c]Information about dietary restrictions is included in Table 3-1.

Source: CERHR (2004).

Table 3-3. Monkey blood methanol and formate levels following methanol exposure

Strain-sex	Exposure route	Exposure duration	Methanol exposure concentration	Blood methanol mean in mg/L	Blood formate mean in mg/L	Reference
Monkey; Cynomolgus; female; mean blood methanol and range of plasma formate at 30 min post daily exposure during premating, mating, and pregnancy	Inhalation	2.5 hr/day, 7days/wk during premating, mating, and gestation (348 days)	0 200 ppm 600 ppm 1,800 ppm	2.4 5 11 35	8.7 8.7 8.7 10	Burbacher et al. (2004b, 1999a)
Monkey; Rhesus male; postexposure blood level	Inhalation	6 hr	200 ppm 1,200 ppm 2,000 ppm	3.9 37.6 64.4	5.4–13.2 at all doses	Horton et al. (1992)

Source: CERHR (2004).

Table 3-4. Mouse blood methanol and formate levels following methanol exposure

Species/strain/sex	Exposure route	Exposure duration	Methanol exposure concentration	Blood methanol mean (mg/L)	Blood formate mean (mg/L)	Reference
Mouse;CD-1;female; postexposure plasma methanol and peak formate level	Inhalation	6 hr on GD8	10,000 ppm 10,000 ppm + 4-MP 15,000 ppm	2,080 2,400 7,140	28.5 23 34.5	Dorman et al. (1995)
Mouse;CD-1;female; postexposure blood methanol level	Inhalation	8 hr	2,500 ppm 5,000 ppm 10,000 ppm 15,000 ppm	1,883 3,580 6,028 11,165	No data	Pollack and Brouwer (1996); Perkins et al. (1995a)
Mouse;CD-1;female; mean postexposure plasma methanol level	Inhalation	7 hr/day on GD6–GD15	0 1,000 ppm 2,000 ppm 5,000 ppm 7,500 ppm 10,000 ppm 15,000 ppm	1.6 97 537 1,650 3,178 4,204 7,330	No data	Rogers et al. (1993a)
Mouse;CD-1;female; plasma level 1 hr postdosing	Oral-Gavage	GD6–GD15	4,000 mg/kg bw	3,856	No data	
Mouse;CD-1;female; peak plasma level	Oral-Gavage	GD8	1,500 mg/kg bw 1,500 mg/kg bw + 4-MP	1,610 1,450	35 43	Dorman et al. (1995)

4-MP=4-methylpyrazole

Source: CERHR (2004).

Table 3-5. Rat blood methanol and formate levels following methanol exposure

Species;strain/sex: type of sample collected	Exposure route	Exposure duration	Methanol exposure concentration	Blood methanol level in mg/L	Blood formate level in mg/L	Reference
Rat;Sprague-Dawley; female; postexposure blood methanol level on 3 days	Inhalation	7 hr/day for 19 days	5,000 ppm 10,000 ppm 20,000 ppm	1,000–2,170 1,840–2,240 5,250–8,650	No data	Nelson et al. (1985)
Rat;Sprague-Dawley; female; postexposure blood methanol level	Inhalation	8 hr	1,000 ppm 5,000 ppm 10,000 ppm 15,000 ppm 20,000 ppm	83 1,047 1,656 2,667 3,916	No data	Pollack and Brouwer (1996); Perkins et al. (1995a)
Rat;LongEvans;female; postexposure plasma level on GD7– GD12	Inhalation	7 hr/day on GD7– GD 19	0 15,000 ppm	2.7–1.8 3,826–3,169	No data	Stanton et al. (1995)
Rat;LongEvans;female; 1 hr postexposure blood level	Inhalation	6 hr/day on GD6– PND 21	4,500 ppm	555	No data	Weiss et al. (1996)
Rat;Long-Evans;male and female; 1 hr postexposure blood level in pups	Inhalation	6 hr/day on PND1– PND 21	4,500 ppm	1,260	No data	
Rat/Fischer-344/male; postexposure blood level	Inhalation	6 hr	200 ppm 1,200 ppm 2,000 ppm	3.1 26.6 79.7	5.4–13.2 at all doses	Horton et al. (1992)
Rat;Long-Evans;male; post- exposure serum level	Inhalation	6 hr	200 ppm 5,000 ppm 10,000 ppm	7.4 680–873 1,468	No data	Cooper et al. (1992)
Rat;Long-Evans;male; peak blood formate level	Inhalation	6 hr	0 FS 0 FS 1,200 ppm–FS 1,200 ppm–FR 2,000 ppm–FS 2,000 ppm–FR	No data	8.3 10.1 8.3 46 8.3 83	Lee et al. (1994)
Rat;Long-Evans;male; peak blood methanol and formate	Oral-gavage	Single dose	3,500 mg/kg bw–FS 3,500 mg/kg bw–FP 3,500 mg/kg bw–FR 3,000 mg/kg bw/day–FS 3,000 mg/kg bw/day FR 2,000 mg/kg bw/day FS 2,000 mg/kg bw/day FR	4,800 4,800 4,800 No data	Baseline level 382 860 9.2 718 9.2 538	

FS = Folate sufficient; FR = Folate reduced; FP = Folate paire

Source: CERHR (2004).

Table 3-6. Plasma formate concentrations in monkeys

Exposure group	Mean plasma formate level (mg/L) during each exposure period			
	Baseline	Pre-breeding	Breeding	Pregnancy
Control	8.3	7.8	10	8.3
200 ppm	7.4	8.3	9.7	7.8
600 ppm	6.9	7.8	9.2	8.7
1800 ppm	6.4	8.7	11	10

Source: Burbacher et al. (1999a).

Table 3-7. Serum folate concentrations in monkeys

Exposure group	Mean serum folate level (µg/L) during each exposure period				
	Baseline	Day 70 Pre-pregnancy[a]	Day 98 Pre-pregnancy[a]	Day 55 Pregnancy[a]	Day 113 Pregnancy[a]
Control	14.4	14.0	13.4	16.0	15.6
200 ppm	11.9	13.2	12.9	15.5	13.4
600 ppm	12.5	15.4	13.4	14.8	16.4
1800 ppm	12.6	14.8	15.3	15.9	15.7

[a]Number of days exposed to methanol

Source: Burbacher et al. (1999a).

3.4. PHYSIOLOGICALLY BASED TOXICOKINETIC MODELS

In accordance with the needs of this human health risk assessment, particularly the derivation of human health effect benchmarks from studies of the developmental effects of methanol inhalation exposure in mice (Rogers et al., 1993a) and rats (NEDO, 1987) and carcinogenic effects of methanol in rats exposed via drinking water (Soffritti et al., 2002a) and inhalation (NEDO, 1987, 1985/2008b), mouse and rat models were developed to allow for the estimation of mouse and rat internal dose metrics. A human model was developed to extrapolate those internal metrics to inhalation and oral exposure concentrations that would result in the same internal dose in humans (human equivalent concentrations [HECs] and human equivalent doses [HEDs]). The procedures used for the development, calibration and use of these models are summarized in this section, with further details provided in Appendix B, "Development, Calibration and Application of a Methanol PBPK Model."

3.4.1. Model Requirements for EPA Purposes

3.4.1.1. MOA and Selection of a Dose Metric

Dose metrics closely associated with one or more key events that lead to the selected critical effect are preferred for dose-response analyses compared to metrics not clearly correlated. For instance, internal (e.g., blood, target tissue) measures of dose are preferred over external measures of dose (e.g., atmospheric or drinking water concentrations), especially when, as with methanol, blood methanol concentrations increase disproportionally with dose (Rogers

et al., 1993a). This is likely due to the saturable metabolism of methanol in rodents. In addition, respiratory and GI absorption may vary between and within species. Mode of action (MOA) considerations can also influence whether to model the parent compound with or without its metabolites for selection of the most adequate dose metric.

As discussed in Section 4, developmental effects following methanol exposures have been noted in both rats and mice, but are not as evident or clear in primate exposure studies (Burbacher et al., 2004a; Clary, 2003; Rogers et al., 1993a, 1993b; Andrews et al., 1987; Nelson et al., 1985), and carcinogenic effects have been observed in a drinking water study of Sprague-Dawley rats (Soffritti et al., 2002a) and an inhalation study of F344 rats (NEDO, 1985/2008b). The report of the New Energy Development Organization (NEDO, 1987) of Japan, which investigated developmental effects of methanol in rats, indicated that there is a potential that developing rat brain weight is reduced following maternal and neonatal exposures. These exposures included both in utero and postnatal exposures. The methanol PBPK models developed for this assessment do not explicitly describe these exposure routes. Mathematical modeling efforts have focused on the estimation of human equivalent external exposures that would lead to internal blood levels of methanol or its metabolites presumed to be associated with developmental effects as reported in rats (NEDO, 1987) and mice (Rogers et al., 1993a), and carcinogenic effects as reported in rats by Soffritti et al. (2002a).

In a recent review of the reproductive and developmental toxicity of methanol, a panel of experts concluded that methanol, not formate, is likely to be the proximate teratogen and determined that blood methanol level is a useful biomarker of exposure (CERHR, 2004; Dorman et al., 1995). The CERHR Expert Panel based their assessment of potential methanol toxicity on an assessment of circulating blood levels (CERHR, 2004). While recent in vitro evidence indicates that formaldehyde is more embryotoxic than methanol and formate (Harris et al., 2004, 2003), the high reactivity of formaldehyde would limit its unbound and unaltered transport as free formaldehyde from maternal to fetal blood (Thrasher and Kilburn, 2001), and the capacity for the metabolism of methanol to formaldehyde is likely lower in the fetus and neonate versus adults (see discussion in Section 3.3). Thus, even if formaldehyde is ultimately identified as the proximate teratogen, methanol would likely play a prominent role, at least in terms of transport to the target tissue. Further discussions of methanol metabolism, dose metric selection, and MOA issues are covered in Sections 3.3, 4.6, 4.8 and 4.9.2.

It has been suggested that the lymphomas observed in Sprague-Dawley rats following methanol exposure are associated with formaldehyde because formaldehyde and other compounds that metabolize to formaldehyde have been reported to cause lymphomas in Sprague-Dawley rats (Soffritti et al., 2005). Given the reactivity of formaldehyde, models that predict levels of formaldehyde in the blood are difficult to validate. However, production of formaldehyde or formate following exposure to methanol can be estimated by summing the total

amount of methanol cleared by metabolic processes.[9] This metric of formaldehyde or formate dose has limited value since it ignores important processes that may differ between species, such as clearance of these two metabolites, but it can be roughly be equated to the total amount of metabolites produced and may be the more relevant dose metric if formaldehyde is found to be the proximate toxic moiety. Thus, both blood methanol and total metabolism metrics are considered to be important components of the PBPK models. Dose metric selection and MOA issues are discussed further in Sections 3.3, 4.6, 4.8 and 4.9.2.

3.4.1.2. *Criteria for the Development of Methanol PBPK Models*

The development of methanol PBPK models that would meet the needs of this assessment was organized around a set of criteria that reflect: 1) the MOA(s) being considered for methanol; 2) absorption, distribution, metabolism, and elimination characteristics; 3) dose routes necessary for interpreting toxicity studies or estimating HECs; and 4) general parameters needed for the development of predictive PK models.

The criteria with a brief justification are provided below:

1) Must simulate blood methanol concentrations and total methanol metabolic clearance. Blood methanol is the recommended dose metric for developmental effects, but total metabolic clearance may be a useful metric, particularly for cancer endpoints.
2) Must be capable of simulating experimental blood methanol and total metabolic clearance (mg/day) data for the inhalation route of exposure in mice and rats (a) and humans (b), and the oral route in rats (c) and humans (d). These routes are important for determining dose metrics in the most sensitive test species under the conditions of the toxicity study and in the relevant exposure routes in humans.
3) The model code should easily allow designation of respiration rates during inhalation exposures. A standard variable in inhalation route risk assessments is ventilation rate. Blood methanol concentrations will depend strongly on ventilation rate, which varies significantly between species.
4) Must address the potential for saturable metabolism of methanol. Saturable metabolism has the potential to bring nonlinearities into the exposure:tissue dose relationship.
5) Model complexity should be consistent with modeling needs and limitations of the available data. Model should adequately describe the biological mechanisms that determine the internal dose metrics (blood methanol and metabolic clearance) to assure that it can be reliably used to predict those metrics in exposure conditions and scenarios where data are lacking. Compartments or processes should not be added that cannot be adequately characterized by the available data.

[9] This assumption is more likely to be appropriate for formaldehyde than formate as formaldehyde is a direct metabolite of methanol.

Although the rat and mouse models are useful for the evaluation of the dose metrics associated with methanol's developmental effects and the relevant toxicity studies, including gestational exposures, no pregnancy-specific PBPK model exists for methanol, and inadequate data exists for the development and validation of a fetal/gestational/conceptus compartment. However, EPA determined that nonpregnancy models for the appropriate species and routes of exposure could prove to be valuable because levels of methanol in NP, pregnant and fetal blood are expected to be similar following the same oral or inhalation exposure. Pollack and Brouwer (1996) determined that methanol distribution in rats and mice following repeated oral and i.v. exposures up to day 20 of gestation is "virtually unaffected by pregnancy, with the possible exception of the immediate perinatal period." The critical window for methanol induction of cervical rib malformations in CD-1 mice has been identified as occurring between GD6 and GD7 (Rogers and Mole, 1997; Rogers et al., 1993b), a developmental period roughly equivalent to week 3 of human development (Chernoff and Rogers, 2004). Methanol blood kinetics measured during and after inhalation exposure in NP and pregnant mice on GD6–GD10 and GD6–GD15 (Perkins et al., 1996, 1995a; Dorman et al., 1995; Rogers et al., 1993a) are also similar. Further, the available data indicate that the maternal blood:fetal partition coefficient is approximately 1 at dose levels most relevant to this assessment (Ward et al., 1997; Horton et al., 1992). The same has been found in rat (Zorzano et al., 1989; Guerri and Sanchis, 1985) and sheep (Brien et al., 1985; Cumming et al., 1984) studies of ethanol, a structurally related chemical that also penetrates cellular membranes readily and distributes throughout total body water. Consequently, fetal methanol concentrations are expected to be roughly equivalent to that in the mother's blood. Thus, pharmacokinetics and blood dose metrics for NP mice and humans are expected to provide reasonable approximations of pregnancy levels and fetal exposure, particularly during early gestation, that improve upon default estimations from external exposure concentrations.

3.4.2. Methanol PBPK Models

As has been discussed, methanol is well absorbed by both inhalation and oral routes and is readily metabolized to formaldehyde, which is rapidly converted to formate in both rodents and humans. As was discussed in Section 3.1, the enzymes responsible for metabolizing methanol are different in rodents and humans. Several rat, mouse and human PBPK models which attempt to account for these species differences have been published (Fisher et al., 2000; Ward et al., 1997; Perkins et al., 1995a; Horton et al., 1992). In addition, a gestational model for a similar water soluble compound, isopropanol, with the potential to be adapted to methanol pharmacokinetics, was of interest (Gentry et al., 2003, 2002; Clewell et al., 2001). Three PK models (Gentry et al., 2002; Bouchard et al., 2001; Ward et al., 1997) were identified as potentially appropriate for use in animal-to-human extrapolation of methanol metabolic rates and blood concentrations. An additional methanol PBPK model by Fisher et al. (2000) was

considered principally because it had an important feature – pulmonary compartmentalization (see below for details) – worth adopting in the final model.

3.4.2.1. *Ward et al. (1997)*

The PBPK model of Ward et al. (1997) describes inhalation, oral and i.v. routes of exposure and is parameterized for both NP and pregnant mice and rats (Table 3-8). The model has not been parameterized for humans.

Respiratory uptake of methanol is described as a constant infusion into arterial blood at a rate equal to the minute ventilation times the inhaled concentration and includes a parameter for respiratory bioavailability, which for methanol is <100%. This simple approach is nonstandard for volatile compounds but is expected to be appropriate for a compound like methanol, for which there is little clearance from the blood via exhalation. Oral absorption is described as a biphasic process, dependent on a rapid and a slow first-order rate constant. This is conceptually similar to the isopropanol model discussed below (Gentry et al., 2002; Clewell et al., 2001), which also employs slow and fast absorption processes but functionally separates them into stomach and duodenal compartments.

Methanol elimination in the Ward et al. (1997) model is primarily via saturable hepatic metabolism. The parameters describing this metabolism come from the literature, primarily previous work by Ward and Pollack (1996) and Pollack et al. (1993). A first-order elimination of methanol from the kidney compartment includes a lumped metabolic term that accounts for both renal and pulmonary excretion.

The model adequately fits the experimental blood kinetics of methanol in rat and mice and is therefore suitable for simulating blood dosimetry in the relevant test species and routes of exposure (oral and i.v.). The Ward et al. (1997) model meets criteria 1, 2a, 2c, 3, 4, and 5. The most significant limitation is the absence of parameters for the oral and inhalation routes in the human. A modified version of this model that includes human parameters and a standard PBPK lung compartment might be suitable for the purposes of this assessment.

3.4.2.2. *Bouchard et al. (2001)*

The Bouchard et al. (2001) model is not actually a PBPK model but is an elaborate classical PK model, since the transfer rates are not determined from blood flows, ventilation, partition coefficients, and the like. The Bouchard et al. (2001) model uses a single compartment for methanol: a central compartment represented by a volume of distribution where the concentration is assumed to equal that in blood. The model was developed for inhalation and i.v. kinetics only. Methanol is primarily eliminated via saturable metabolism. The model adequately simulates blood kinetics in NP rats and humans following inhalation exposure and in NP rats following i.v. exposure; there is no description for oral absorption. Because methanol distributes with total body water (Ward et al., 1997; Horton et al., 1992), this simple model structure is sufficient for predicting blood concentrations of methanol following inhalation and i.v. dosing.

The Bouchard et al. (2001) model has the advantage of simplicity, reflecting the minimum number of compartments necessary for representing blood methanol pharmacokinetics. Because volume of distribution can be easily and directly estimated for water-soluble compounds like methanol or fit directly to experimental kinetics data, concern over the scalability of this parameter is absent. The model has been parameterized for a required human exposure route, inhalation (Table 3-8). The model meets criteria 1, 2b, 3, 4, and 5 described in Section 3.4.1.2. However, the Bouchard model has specific and significant limitations. The model has neither been parameterized for the mouse, a test species of concern (Table 3-8), nor for the oral route in humans. As such, the model cannot be used to conduct the necessary interspecies extrapolation.

Table 3-8. Routes of exposure optimized in models – optimized against blood concentration data

	Ward et al.			Bouchard et al.		
Route	**Mouse**	**Rat**	**Human**	**Mouse**	**Rat**	**Human**
i.v.	P/NP	P/NP	--	--	NP	--
Inhalation	P/NP	--	--	--	NP	NP
Oral	P/NP	NP	--	--	--	--

P = Pregnant
NP = Nonpregnant

Source: Bouchard et al. (2001); Ward et al. (1997).

3.4.2.3. *Gentry et al. (2003, 2002) and Clewell et al. (2001)*

The model described in these three papers is for isopropanol, not methanol, and therefore lacks any immediately useful parameterization for the purposes of a methanol risk assessment. Although the overall model structure, the description of kinetics for both parent compound and primary metabolite, gestational compartments, lactational transfer, oral and i.v. routes, etc., are attractive for application to methanol, this model is not ideal. In particular, the model structure is more elaborate than necessary; because methanol partition coefficients are near 1 for all tissues except fat, there is no need to individually represent these tissues. Similarly, a fetal compartment may not be necessary because methanol kinetics in the fetus (conceptus) is expected to parallel maternal blood concentrations in the rodent. However, even if a fetal model was considered necessary, other than the partition coefficient, there are insufficient data to identify conceptus compartment parameters for methanol. This model would require the most modification and parameterization to be useful for methanol risk assessment since parameters would have to be estimated for all relevant species (at least mouse and humans) and for several routes of exposure. Therefore the isopropanol model was not considered further.

3.4.3. Selected Modeling Approach

As discussed earlier regarding model criteria, fetal methanol concentrations can reasonably be assumed to equal maternal blood concentration. Thus, as discussed in Section 3.4.2.3, methanol pharmacokinetics and blood dose metrics for NP mice and humans are expected to improve upon default extrapolations from external exposures as estimates of fetal exposure during early gestation. The same level of confidence cannot be placed on the whole-body rate of metabolism, in particular as a surrogate for formaldehyde dose. Because of formaldehyde's reactivity and the limited fetal metabolic (ADH) activity (see Sections 3.3 and 4.10.1), fetal formaldehyde concentration increases (from methanol) will probably not equal maternal increases in formaldehyde concentration. But since there is no model that explicitly describes formaldehyde concentration in the adult, let alone the fetus, the metabolism metric is the closest one can come to predicting fetal formaldehyde dose. This metric is expected to be a better predictor of formaldehyde dose than applied methanol dose or even methanol blood levels, which do not account for species differences in conversion of methanol to formaldehyde.

Most of the published rodent kinetic models for methanol describe the metabolism of methanol to formaldehyde as a saturable process but differ in the description of metabolism to and excretion of formate (Bouchard et al., 2001; Fisher et al., 2000; Ward et al., 1997). The model of Ward et al. (1997) used one saturable and one first-order pathway to describe methanol elimination in mice. The saturable pathway described in Ward et al. (1997) can specifically be ascribed to metabolic formation of formaldehyde in the liver, while the renal first-order elimination described in the model represents nonspecific clearance of methanol (e.g., metabolism, excretion, or exhalation). The model of Ward et al. (1997) does not describe kinetics of formaldehyde subsequent to its formation and does not include any description of formate.

Bouchard et al. (2001) employed a metabolic pathway for conversion of methanol to formaldehyde and a second pathway described as urinary elimination of methanol in rats and humans. They then explicitly describe two pathways of formaldehyde transformation, one to formate and the other to "other, unobserved formaldehyde byproducts." Finally, formate removal is described by two pathways, one to urinary elimination and one via metabolism to CO_2 (which is exhaled). All of these metabolic and elimination steps are described as first-order processes, but the explicit descriptions of formaldehyde and formate kinetics significantly distinguish the model of Bouchard et al. (2001) from that of Ward et al. (1997), which only describes methanol.

There are two other important distinctions between the Ward et al. (1997) and Bouchard et al. (2001) models. The former is currently capable of simulating blood data for all exposure routes in mice but not humans, while the latter is capable of simulating human inhalation route blood pharmacokinetics but not those in mice. The Ward et al. (1997) model has more

compartments than is necessary to adequately represent methanol disposition but has been fit to PK data in pregnant and NP mice for all routes of exposure (i.v., oral, and inhalation). The Ward et al. (1997) model has also been fit to i.v. and oral route PK data in rats. Based primarily on the extensive amount of fitting that has already been demonstrated for this model, it was determined that a modified Ward et al. (1997) model, with the addition of a lung compartment as described by Fisher et al. (2000), should be used for the purposes of this assessment. See Appendix B for a more complete discussion of the selected modeling approach and modeling considerations.

3.4.3.1. *Available PK Data*

Although limited human data are available, several studies exist that contain PK and metabolic data in mice, rats, and nonhuman primates for model parameterization. Table 3-9 contains references that were used to verify the model fits as reported in Ward et al. (1997).

Table 3-9. Key methanol kinetic studies for model validation

Reference	i.v. dose (mg/kg)	Inhalation (ppm)	Oral/dermal/ IP	Species	Samples	Digitized figures[a]
Batterman et al., 1998			Dermal	Human Male/female	Blood	Figure 1
Batterman & Franzblau 1997		800 (8 hr)			Blood, urine, exhaled	
Burbacher, 2004a, 2004b		0-1,800 (2.5 hr, 4 mo)		Monkeys Cynomolgus Pregnant, NP	Blood	
Osterloh et al., 1996; Chuwers et al., 1995; D'Alessandro et al., 1994		200 (4 hr)		Human Male/female	Blood, urine	Figure 1, Osterloh et al., 1996
Medinsky et al., 1997; Dorman et al., 1994		10-900 (2 hr)		Monkeys Cynomolgus Folate deficient	Blood, urine, exhaled	
Gonzalez-Quevedo et al., 2002			IP: 2 mg/kg-day, 2 wk	Rat	Blood	
Horton et al., 1992	100 (rats only)	50-2,000 (6 hr)		Rat & Monkey Rhesus	Blood, urine, exhaled	Figure 7
Perkins et al., 1996, 1995a, 1995b		1,000-20,000 (8 hr)		Mouse and Rat	Blood, urine	
Pollack and Brouwer, 1996; Pollack et al., 1993	100-2,500	1,000-20,000 (8 hr)	Oral: 100-2,500 mg/kg	Rat: Sprague-Dawley, & Mouse; CD-1 Pregnant, NP	Blood	
Rogers and Mole, 1997; Rogers et al., 1993a;		1,000-15,000 (7 hr, 10 days)		Mouse Pregnant	Blood	
Sedivec et al., 1981		78-231 (8 hr)		Human	Urine, blood	Figures 2, 3, 6, 7, 8
Ward et al., 1997; Ward and Pollack, 1996	100, 500 (Rat), 2,500 (Mouse)		Oral: 2,500 mg/kg	GD18 Mouse, GD14 & GD20 Rats	Blood, conceptus	

[a]data obtained from the reported figure

3.4.3.2. *Model Structure*

A model was developed which includes compartments for alveolar air/blood methanol exchange, liver, fat, bladder (human simulations) and the rest of the body (Figure 3-4). This model is a revision of the model reported by Ward et al. (1997), reflecting significant simplifications (removal of compartments for placenta, embryo/fetus, and extraembrionic fluid) and three elaborations (addition of an intestine lumen compartment to the existing stomach lumen compartment, use of a saturable rate of absorption from the stomach (but not intestine), and addition of a bladder compartment which impacts simulations for human urinary excretion), while maintaining the ability to describe methanol blood kinetics in mice, rats, and humans. A fat compartment was included because it is the only tissue with a tissue:blood partitioning coefficient appreciably different than 1, and the liver is included because it is the primary site of metabolism. A bladder compartment was also added for use in simulating human urinary excretion to capture the difference in kinetics between changes in blood methanol concentration and urinary methanol concentration. The model code describes inhalation, oral, and i.v. dose routes, and data exist (Table 3-9) that were used to fit parameters and evaluate model predictions for all three of those routes in both mice and rats. In humans, inhalation exposure data were available for model calibration and validation but not oral or i.v. data. However, oral exposures were simulated in humans, assuming a continuous, zero-order ingestion rate, thereby obviating the need for oral uptake parameters.

PK data from exposure routes other than inhalation and oral were used to test or further refine the parameters for methanol clearance. Monkey data were evaluated for insight into primate kinetics. Data from Osterloh et al. (1996) and Sedivec et al. (1981) were used to validate the modified Ward et al. (1997) model parameterization for humans. The fact that optimized human parameters were similar to those predicted in monkeys was important to the validation process (Bourchard et al., 2001)(see section 3.4.7 and Appendix B). Blood levels of methanol have been reported following i.v., oral, and inhalation exposure in rats and mice and inhalation exposure in nonhuman primates and humans.

The metabolic clearance of methanol was represented in mice, rats, and humans by specifying separate rate constants for the species-specific enzymes: two saturable processes for mice and rats[10] and one for humans. The requirement for two saturable processes in the mouse and rat models may reflect saturation of CAT and ADH1. Simulated methanol clearance by these metabolic processes is not linked to production of formaldehyde or formate; it is simply cleared from the methanol mass balance leaving the system. Metabolism of formaldehyde is not explicitly simulated by the model, and this model tracks neither formate nor formaldehyde. Since the metabolic conversion of formaldehyde to formate is rapid (<1 minute) in all species

[10] The need for two saturable metabolic pathways in the mouse model was confirmed through simulation and optimization. High exposure (>2,000 ppm methanol) and low exposure (1,000 ppm methanol) blood data could not be fit visually, or by more formal optimization, without the second saturable metabolic pathway.

(Kavet and Nauss, 1990), the methanol clearance rate may approximate a formate production rate, though this has not been verified.

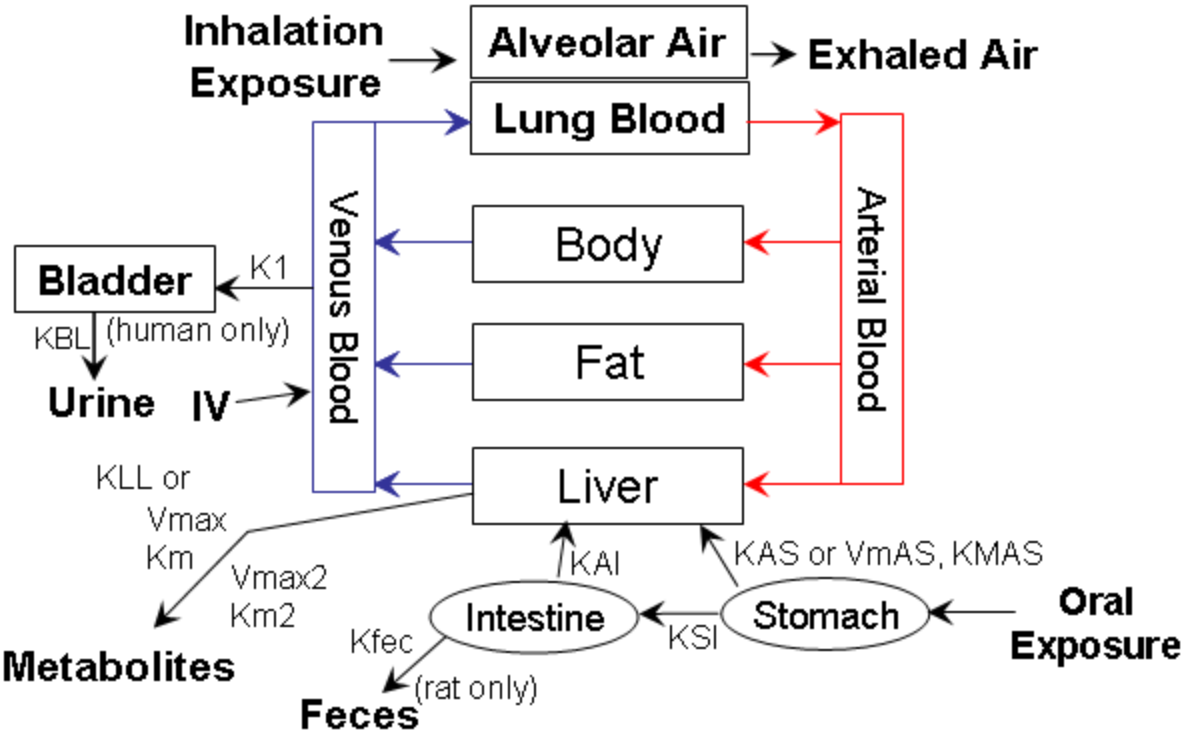

Figure 3-4. Schematic of the PBPK model used to describe the inhalation, oral, and i.v. route pharmacokinetics of methanol. KAS, first-order oral absorption rate from stomach; VmAS and KMAS, Michaelis-Menten rate constants for saturable absorption from stomach; KAI, first-order uptake from the intestine; KSI, first-order transfer between stomach and intestine; V_{max} and K_m and $V_{max}2$ and K_m2, Michaelis-Menten rate constants for high affinity/low capacity and low affinity/high capacity metabolic clearance of methanol; KLL, alternate first-order rate constant; KBL, rate constant for urinary excretion from bladder. Both metabolic pathways were used to describe methanol clearance in the mouse, while a single metabolic pathway describes clearance in the human.

The primary purpose of this assessment is for the determination of noncancer and cancer risk associated with increases in the levels of methanol or its metabolites (e.g., formate, formaldehyde). Thus, the focus of model development is on obtaining accurate predictions of increased body burdens over background. The PBPK models do not describe or account for background levels of methanol, formaldehyde or formate, and background levels were subtracted from the reported data before use in model fitting or validation (if not already subtracted by study authors), as described below. This approach is not expected to have a significant impact on PBPK model parameter estimates as background levels of methanol and its metabolites are low

relative to exposure levels used in methanol bioassays. Further, while it is possible that background levels of methanol or its metabolites contribute to background responses for some adverse effects, the results of dose-response modeling of cancer endpoints using "background dose" models suggest that this contribution is relatively small (see discussion in Appendix E, Section E.4).

3.4.3.3. *Model Parameters*

The EPA methanol model uses a consistent set of physiological parameters obtained predominantly from the open literature (Table 3-10); the Ward et al. (1997) model employed a number of data-set specific parameters.[11] Parameters for blood flow, ventilation, and metabolic capacity were scaled as a function of body weight raised to the 0.75 power, according to the methods of Ramsey and Andersen (1984).

Table 3-10. Parameters used in the mouse, rat and human PBPK models

	Mouse	Rat SD | F344		Human		Source
Body weight (kg)	0.03[a]	0.275[b]		70		Measured/estimated
Tissue volume (% body weight)						
Liver	5.5	3.7		2.6		Brown et al. 1997
Blood arterial	1.23	1.85		1.98		
venous	3.68	4.43		5.93		
Fat	7.0	7.0		21.4		
Lung	0.73	0.50		0.8		
Rest of body	72.9	73.9		58.3		Calculated[c]
Flows (L/hr/kg$^{0.75}$)						
Alveolar ventillation[d]	25.4	16.4		16.5		Perkins et al. 1995a; Brown et al. 1997; U.S. EPA, 2004
Cardiac output	25.4	16.4		24.0		
Percentage of cardiac output						
Liver	25.0	25.0		22.7		Brown et al. 1997
Fat	5.0	7.0		5.2		
Rest of body	70.0	68		72.1		Calculated
Biochemical constants[e]				**1st order**	**saturable**	
$V_{max}C$ (mg/hr/kg$^{0.75}$)	19	5.0	0	NA	33.1	Fitted
Km (mg/L)	5.2	6.3	NA	NA	23.7	
$V_{max}2C$ (mg/hr/kg$^{0.75}$)	3.2	8.4	22.3	NA		
Km2 (mg/L)	660	65	100	NA		
K1C (BW$^{0.25}$/hr)	NA	NA		0.0373	0.0342	

[11] Some data sets provided in the Ward et al., (1997) model code were corrected to be consistent with figures in the published literature describing the experimental data.

	Mouse	Rat SD | F344	Human		Source
KLLC ($BW^{0.25}$/hr)[f]	NA	NA	95.7	NA	
Oral absorption					
VmASC (mg/hr/$kg^{0.75}$)	1830	5570	377		Mouse and rat fitted (mouse and human KMASC assumed = rat); other human values are those for ethanol from Sultatos et al. (2004), with VmASC set so that for a 70-kg person VmAS/KMAS = the first-order constant of Sultatos et al.
KMASC (mg/kg)	620	620	620		
KSI (hr^{-1})	2.2	7.4	3.17		
KAI (hr^{-1})	0.33	0.051	3.28		
Kfec (hr^{-1})	0	0.029	0		
Partition coefficients					
Liver:Blood	1.06	1.06	0.583[h]		Ward et al., 1997; Fiserova-Bergerova and Diaz, 1986
Fat:Blood	0.083	0.083	0.142		
Blood:Air	1350[i]	1350	1626		Horton et al., 1992; Fiserova-Bergerova and Diaz, 1986
Body:Blood	0.66	0.66	0.805		Rodent: estimated; human: Fiserova-Bergerova and Diaz, 1986 (human "body" assumed = muscle)
Lung:Blood	1	1	1.07		
KBL (hr^{-1}), bladder time-constant [j]	NA		0.564	0.612	Fitted (human)
FRACIN (%), nhalation fractional availability	0.665	0.20	0.866[k]		Rodent: fitted; human Ernstgard et al., 2005

NA - Not applicable for that species
[a]Both sources of mouse data report body weights of approximately 30 g
[b]The midpoints of rat weights reported for each study was used and ranged from 0.22 to 0.33 kg
[c]The volume of the other tissues was subtracted from 91% (whole body minus a bone volume of approximately 9%) to get the volume of the remaining tissues
[d]Minute ventilation was measured and reported for much of the data from Perkins et al. (1996) and the average alveolar ventilation (estimated as 2/3 minute ventilation) for each exposure concentration was used in the model. When ventilation rates were not available, a mouse QPC (Alveolar Ventilation/$BW^{0.75}$) of 25.4 was used (average from Perkins et al., 1995). The QPC used to fit the human data was obtained from U.S. EPA (2004). This QPC was somewhat higher than calculated from Brown et al. (1997) (~13 L/hr/$kg^{0.75}$)
[e]V_{max}, Km, and $V_{max}2$, Km2 represent the two saturable metabolic clearance processes assumed to occur solely in the liver. The V_{max} used in the model = $V_{max}C$ (mg/$kg^{0.75}$·hr)×$BW^{0.75}$. K1C is the first-order loss from the blood for human simulations that represents urinary elimination. Allometric scaling for first-order clearance processes was done as previously described (Teeguarden et al., 2005); The K1 used in the model= K1C / $BW^{0.25}$
[f]KLLC – alternate human first-order metabolism rate (used only when $V_{max}C = V_{max}2C = 0$)
[g]Human oral simulations used a zero order dose rate equal to the mg/kg-day dose
[h]Human liver:blood estimated from correlation to (measured) fat:blood, based on data from 28 other solvents
[I]Rat partition coefficient used for mice as done by Ward et al. (1997)
[j]KBL – a first-order rate constant for clearance from the bladder compartment, used to account for the difference between blood kinetics and urinary excretion data as observed in humans
[k]For human exposures, the fractional availability was from Šedivec et al. (1981), corrected for the fact that alveolar ventilation is 2/3 of total respiration rate

3.4.4. Mouse Model Calibration and Sensitivity Analysis

The process by which the mouse, rat, and human inhalation and oral models were calibrated is discussed in more detail in Appendix B, "Development, Calibration and Application of a Methanol PBPK Model." The calibrated mouse inhalation model predicted blood methanol blood concentration time-course agreed well with measured values in adult mice in the critical

inhalation studies of Rogers and Mole (1997) (Figure 3-5), Perkins et al. (1995a, 1995b), and Rogers et al. (1993a), as well as in NP and early gestation (GD8) mice of Dorman et al. (1995) (Figure 3-6). Parameter values used in the calibrated model are given in Table 3-10.

The mouse model was also calibrated for the oral route by fitting all but one of the rate constants for oral uptake of methanol to the oral-route blood methanol kinetics of Ward et al. (1997, 1995). The best model fit to the mouse oral route blood methanol PK data was obtained using a two-compartment GI tract model, as depicted in Figure 3-4. Because the oral data in rats led to the conclusion that a saturable rate of uptake from the stomach lumen was necessary (see section 3.4.5), the same equation was used for uptake in the mouse. But attempts to identify the uptake saturation constant, KMASC, from the mouse data were unsuccessful; therefore KMASC for the mouse was set equal to the value obtained for rats. Adjusting the other mouse oral uptake parameters gave an adequate fit to those data. This calibration allows inhalation to oral dose-route extrapolations in the mouse, which can then be extrapolated to identify human oral route exposures equivalent to mouse inhalation exposures (if equivalent human exposures exist).

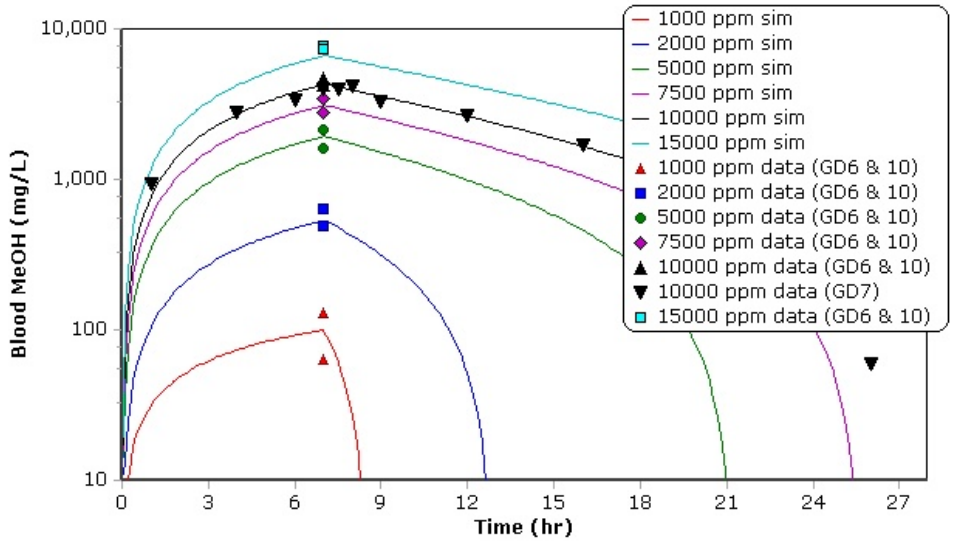

Figure 3-5. Model fits to data sets from GD6, GD7, and GD10 mice for 6- to 7-hour inhalation exposures to 1,000–15,000 ppm methanol. Maximum concentrations are from Table 2 in Rogers et al. (1993a). The dataset for GD7 mice exposed to 10,000 ppm is from Rogers and Mole (1997) and personal communication. Symbols are concentration ± SEM of a minimum of N=4 mice/concentration. Default ventilation rates (Table 3-10) were used to simulate these data.

Source: Rogers and Mole (1997); Rogers et al. (1993a)

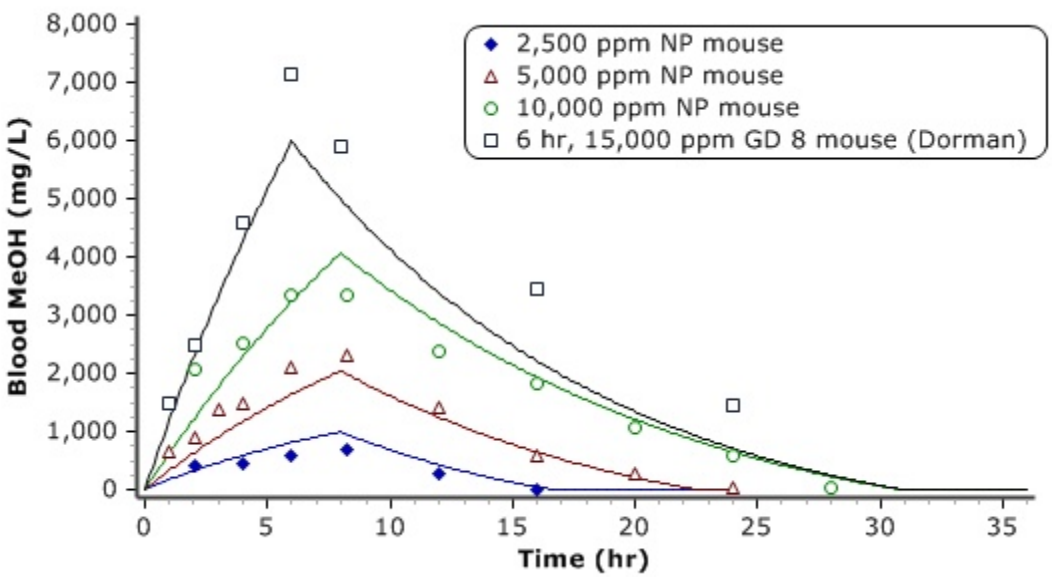

Figure 3-6. Simulation of inhalation exposures to methanol in NP mice from Perkins et al. (1995a) (8-hour exposures) and GD8 mice from Dorman et al. (1995)(6-hour exposures). Data points are measured blood methanol levels and lines represent PBPK model simulations. DigitizIt (SharIt! Inc., Greensburg, PA) was used to digitize data from Figure 2 of Perkins et al. (1995a) and Figure 2 from Dorman et al. (1995). Default ventilation rates (Table 3-10) were used to simulate the Dorman data. The alveolar ventilation rate for each data set from Perkins et al. (1995a) was set equal to the measured value reported in that manuscript. For the 2,500, 5,000, and 10,000 ppm exposure groups, the alveolar ventilation rates were 29, 24, and 21 (L/hours/kg$^{0.75}$), respectively. The cardiac output for these simulations was set equal to the alveolar ventilation rate.

Source: Dorman et al. (1995); Perkins et al. (1995a).

The parameterization of methanol clearance (high-and low-affinity metabolic pathways) was also verified by simulation of datasets describing the pharmacokinetics of methanol following i.v. administration. The results of this calibration of the methanol PBPK model are described in Appendix B and were generally consistent with both the available inhalation and oral-route data. Up to 20 hours postexposure, blood methanol kinetics appears similar for NP and pregnant mice. However, some data suggests that clearance in GD18 mice is slower than in NP and earlier in gestation (GD10 and less), particularly beyond 20 hours postexposure (see the i.v. and oral data of Ward et al. [1997] in Appendix B).

Intravenous-route blood methanol kinetic data in NP mice were only available for a single i.v. dose of 2,500 mg/kg, but were available for GD18 mice following administration of a broader range of doses: 100, 500, and 2,500 mg/kg. The i.v. maternal PK data in GD18 mice appeared to show an unexpected dose-dependent nonlinearity in initial blood concentrations. Before discussing the nonlinearity, it is first noted that data values used here were obtained from a computational “command file” provided by Ward et al. (1997). These values appear to be

consistent with the plots in their publication but are *inconsistent* with some of the values in their Table 6 (Ward et al., 1997). In particular, the initial maternal blood concentration (i.e., the C_{max}) after the 2,500 mg/kg i.v. is listed as 4,250 mg/L in their command file but as 3,251 mg/L in their published table. The corresponding data point in their Figure 5A is distinctly centered above 4,000 mg/L (digitizing yields 4,213 mg/L), and so must be 4,250 rather than 3,251 mg/L. Therefore the data values listed in the command file were used in the subsequent analysis, rather than those in the published table.

After i.v. dosing the ratio of the administered doses to the first concentrations measured by Ward et al. (1997) (5-minute time points) were 0.588 L/kg, 0.585 L/kg, and 0.397 L/kg at doses of 2,500, 500, and 100 mg/kg, respectively. The discrepancy between the first two values and the third value suggests either a dose dependence in the V_d or some source of experimental variability.[12] It may be that V_d, which is not impacted by any other PBPK parameters and is only determined by the biochemical partitioning properties of methanol, is 1.5-fold lower at 100 mg/kg than at the higher concentrations, while the V_d at 500 and 2,500 mg/kg are exactly as predicted by the PBPK model without adjustment. However, it was found that the PBPK model, obtained with measured partition coefficients and otherwise calibrated to inhalation data, could adequately fit the data at the nominal dose of 100 mg/kg without other parameter adjustment simply by simulating a dose of 200 mg/kg, as shown in Figure B-5. The fact that the alternate dose (200 mg/kg) differs by a factor of 2 from the nominal dose suggests that the data could also be the result of a simple dilution error in dose preparation. If the first two of the dose/concentration values were *not* virtually identical (0.588 and 0.585 L/kg), but instead the 500 mg/kg value was more intermediate between those for 2,500 and 100 mg/kg, then a regular dose dependence in V_d would seem more likely. However, based on these values, the U.S. EPA has concluded that the apparent dose dependency is probably the result of a dosing error and therefore, that dose-dependent parameter changes (e.g., in the partition coefficients) should not be introduced in an attempt to otherwise better fit these data.

Further, the nominal "nonlinearity" between the maternal blood and conceptus shown in Figure 8 of Ward et al. (1997) is the result of those data being plotted on a log-y/linear-x scale. Replotting the data from Tables 5 and 6 (using the value of 4,250 mg/L from the command file as the GD18 maternal C_{max} for the 2,500 mg/kg) shows the results to be linear, especially in the low-dose region which is of the most concern (Figure 3-7). Therefore, the current model uses a consistent set of parameters that are not varied by dose and fit the 2,500 and 500 mg/kg i.v. data adequately, although they do not fit the 100 mg/kg i.v. data unless, as noted above, a presumed i.v. dose of 200 mg/kg is employed. With that exception, both the single set of parameters used herein and the assumption that maternal blood methanol is a good metric of fetal exposure are well supported by the data.

[12] It is possible that Ward et al., (1997) were unaware of that discrepancy because they plotted the results for each dose in separate figures, and it only becomes obvious when all the data and simulations are plotted together.

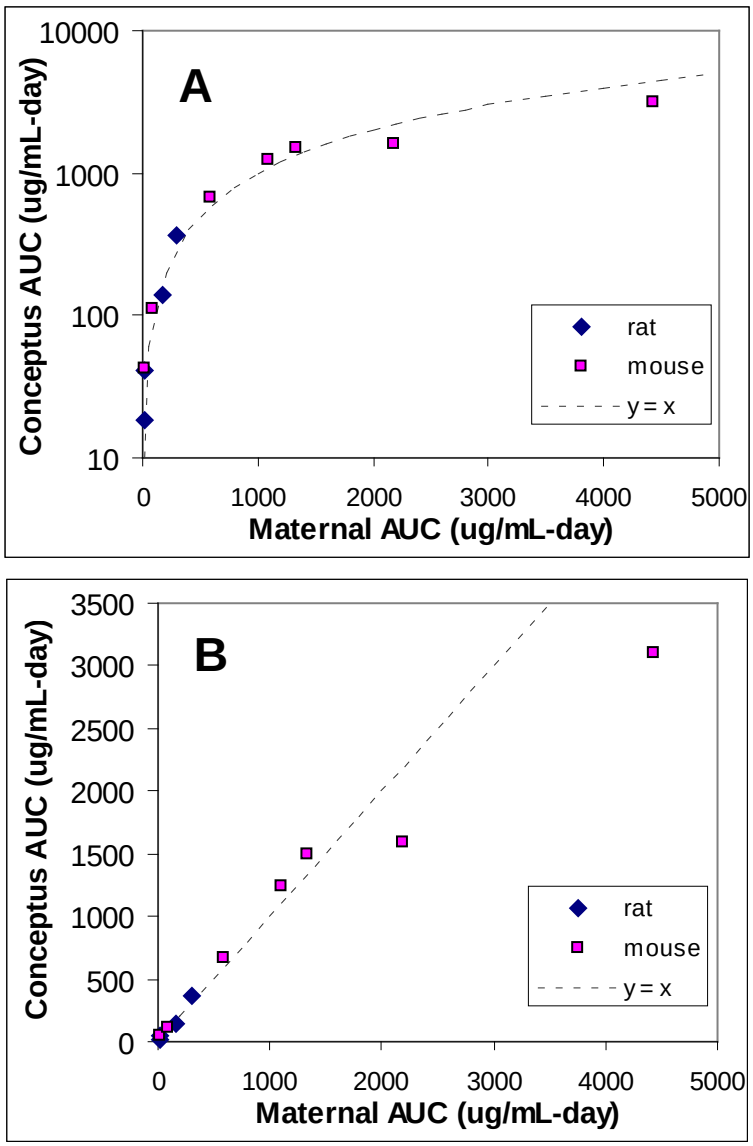

Figure 3-7. Conceptus versus maternal blood AUC values for rats and mice plotted (A) on a log-linear scale, as in Figure 8 of Ward et al. (1997), and (B) on a linear-linear scale. In both panels the line y = x is plotted (dashed line) for comparison. Thus the apparent "nonlinear" relationship indicated by Ward et al. (1997) is seen to be primarily a simple artifact of the choice of axes. However, as evident in panel B, there appears to be some nonlinearity at the two highest doses in the mouse (results of 2,500 mg/kg i.v. in GD18 mice and 15,000 ppm exposure to GD8 mice), where distribution from the dam to the conceptus is below 1:1.

Source: Ward et al. (1997).

To summarize the mouse model calibration: using the single set of parameters listed for the mouse in Table 3-10, the PBPK model has been shown to adequately fit or reproduce methanol PK data from a variety of laboratories and publications, including both NP mice and pregnant mice up to GD10. Two saturable metabolic pathways are thus described by the model

and supported by the data. Also, it is thereby demonstrated that a model based on NP mouse physiology adequately describes (predicts) dosimetry in the pregnant mouse dam through GD10. Finally, as illustrated in Figure 3-7b, methanol PK in the conceptus and dam of both mice (including lower doses at GD18) and rats (GD14 and GD20) are virtually identical, except for the very highest doses in mice. Thus the existing model appears to be adequate for predicting internal methanol doses, including fetal exposures, at bioassay conditions.

An evaluation of the importance of selected parameters on mouse model estimates of blood methanol AUC was performed by conducting a sensitivity analysis using the subroutines within acslXtreme v2.3 (Aegis Technologies, Huntsville, Alabama). The analysis was conducted by measuring the change in model output corresponding to a 1% change in a given model parameter when all other parameters were held fixed. Sensitivity analyses were conducted for the inhalation and oral routes. The inhalation route analysis was conducted under the exposure conditions of Rogers and Mole (1997) and Rogers et al. (1993a): 7-hour inhalation exposures at the no-observed-effect level (NOEL) concentration of 1,000 ppm. The oral route sensitivity analysis was conducted for an oral dose of 1,000 mg/kg.

The parameters with the largest sensitivity coefficients for the inhalation route at 1,000 ppm (absolute values >1) were pulmonary ventilation scaling coefficient (QPC) and maximum velocity of the high-affinity/low-capacity pathway ($V_{max}C$). The sensitivity coefficient for QPC increases during the exposure period as metabolism begins to saturate. Following oral exposure, mouse blood methanol AUC was sensitive to the rate constants for oral uptake. Blood AUC was most sensitive to the maximum and saturation rate constants for uptake from the stomach (VmASC and KMASC). The sensitivity coefficient for VmASC decreased during the first hours after exposure from 1 to less than 0.1 at the end of exposure. Blood methanol AUC was also modestly sensitive to first-order uptake from the intestine (KAI), and first-order transfer between stomach and intestine (KSI), the rate constants for uptake from the intestine and transfer rates between compartments, respectively. For a more complete description of this sensitivity analysis for the mouse methanol PBPK model see Appendix B.

3.4.5. Rat Model Calibration

The rat model was calibrated to fit data from i.v., inhalation, and oral exposures in rats, using data provided in the command file of Ward et al. (1997) and obtained from figures in Horton et al. (1992) using DigitizIt. Holding other parameters constant, the rat PBPK model was initially calibrated against the entire set of i.v.-route blood PK data (Figure 3-7) by fitting Michaelis-Menten constants for one high-affinity/low-capacity and one low-affinity/high-capacity enzyme to both the Ward et al. (1997) data for Sprague-Dawley (SD) rats and the Horton et al. (1992) data for Fischer 344 (F344) rats, assuming that any difference between the two data sets (100 mg/kg data) were from experimental variability and that a single set of parameters could be fit to data for both strains of rat. However when the resulting parameters

were then used to simulate the F344 inhalation uptake data of Horton et al. (with the fractional absorption for inhalation, FRACIN, adjusted to fit those data), it was found that the clearance rate predicted after the end of inhalation exposure was much more rapid than shown by the data. More careful examination of the i.v. data then revealed that there too the clearance for F344 rats was slower than for SD rats, and that the metabolic parameters obtained from fitting the combined i.v. data best represented the SD rat data. It was concluded that the combined data set indicated a true strain difference in metabolic parameters. The metabolic parameters for SD rats were then obtained by fitting only the Ward et al. (1997) i.v. data (both doses).

The 100 mg/kg i.v. data of Horton et al. (1992) were combined with their inhalation data and a simultaneous optimization of the metabolic parameters and FRACIN for F344 rats was attempted over that data set. For this data set, however, the optimization either converged with the metabolic Vmax for the high affinity (low Km) pathway at zero, or with that Km value increasing to be statistically indistinguishable from the high Km value. Therefore the Vmax for the high affinity pathway was allowed to be zero, the Km for that pathway was not estimated, and only a single Vmax and low affinity (high Km) were fit to those data, with a simultaneous identification of FRACIN. Since there are no inhalation data for SD rats, this value of FRACIN was assumed to apply for both strains. The optimized parameters for both strains of rats are given in Table 3-10.

When the model was calibrated using the available inhalation and i.v. data for F344 rats (Horton et al., 1992), a low fractional absorption of 20% was optimized to best fit the data, vs. 66.5% for the mouse. This lower fractional absorption is consistent with values presented by Perkins et al. (1995), who also found that the fractional absorption of methanol from inhalation studies was lower in rats than in mice.

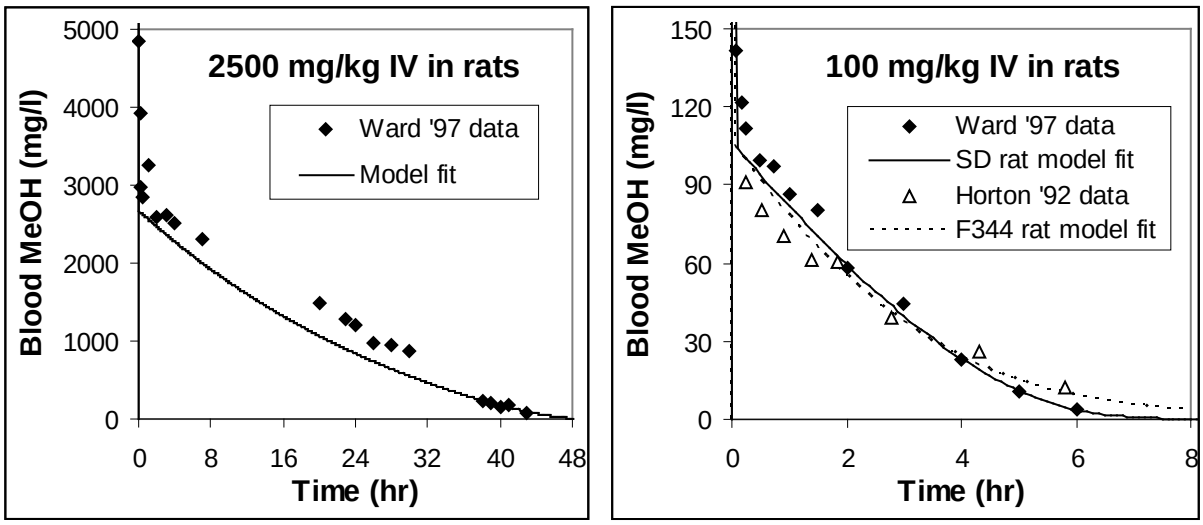

Figure 3-8. NP rat i.v. route methanol blood kinetics. Methanol (MeOH) was infused into: female Sprague-Dawley rats (275 g; solid diamonds and lines) at target doses of 100 or 2,500 mg/kg (Ward et al., 1997); or male F-344 rats (220 g; open triangles and dashed line) at target doses of 100 mg/kg (Horton et al., 1992). Data points represent measured blood concentrations and lines represent PBPK model simulations.

Source: Ward et al. (1997); Horton et al. (1992).

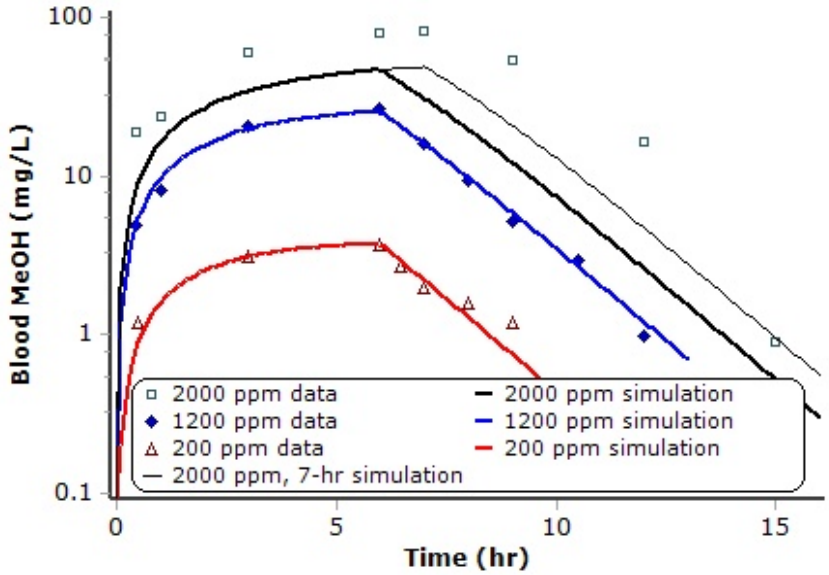

Figure 3-9. Model fits to data sets from inhalation exposures to 200 (triangles), 1,200 (diamonds), or 2,000 (squares) ppm methanol in male F-344 rats. The model was calibrated against all three sets of concentration data, though it converged to parameter values that only fit the lower two data sets well. Symbols are concentrations obtained from Horton et al. (1992) using DigitizIt! Lines represent PBPK model fits. Since the 2000 ppm data peak occurred at 7 hr, a 7-hr simulated exposure is also shown for comparison.

Source: Horton et al. (1992).

Finally, oral absorption parameters were optimized to the oral absorption data reported by Ward et al. (1997), also using the optimization routines in acslXtreme v2.5.0.6 (Aegis Technologies, Huntsville, Alabama) (Table 3-10: Figure 3-9). While the two-compartment GI model (Figure 3-4) allows for both slow and fast absorption modes, it was not possible to fit both the 100 mg/kg data and the first several hours of the 2500 mg/kg data with that model structure using linear absorption and inter-compartment transfer rates. In particular the shorter-time data for 2500 mg/kg indicate a much slower rate of increase in blood levels than the linear-absorption model (top, thick line in upper panel of Figure 3-10), but the 100 mg/kg data (lower panel of Figure 3-10) are indeed consistent with a linear model, showing a rapid rise to a fairly narrow peak, then dropping rapidly. As long as linear rate equations were used, the shape of the absorption curve at 2500 mg/kg would mirror that at 100 mg/kg, but the data show a clear difference. It was concluded that the rate of absorption must at least partly saturate at the higher dose, and hence that Michaelis-Menten kinetics should be used.

Even with the addition of saturable absorprtion from the stomach, it was also found that the 2500 mg/kg model simulations over-predicted all of those data (result not shown) and it was hypothesized that fecal elimination might become significant at such a high exposure level, so a term for fecal elimination from the intestine compartment was added. When that fecal rate constant and the saturable absorption from the stomach compartment were both used, the resulting fit to the data (thin, dashed line in upper panel) was considerably improved with an almost identical (excellent) fit to the 100 mg/kg data (saturable curve can be distinguished from the linear curve just after the peak is reached in the lower panel of Figure 3-4). For the purpose of scaling across individuals, strains, and species, the Km for absorption from the stomach (KMAS) was assumed to scale in proportion to the stomach (lumen) volume; i.e., with BW^{1}. The Vmax (VmAS) was assumed to scale as $BW^{0.75}$, with the result that for low doses the effective linear rate constant (VmAS/KMAS) scales as $BW^{-0.25}$, which is a standard assumption for linear rates. Since the quantity on which the rate depends is the total amount in the stomach (mg methanol), the resulting scaling constant for the Km, KMASC, conveniently has units of mg/kg BW; i.e., the standard units for oral dosing.

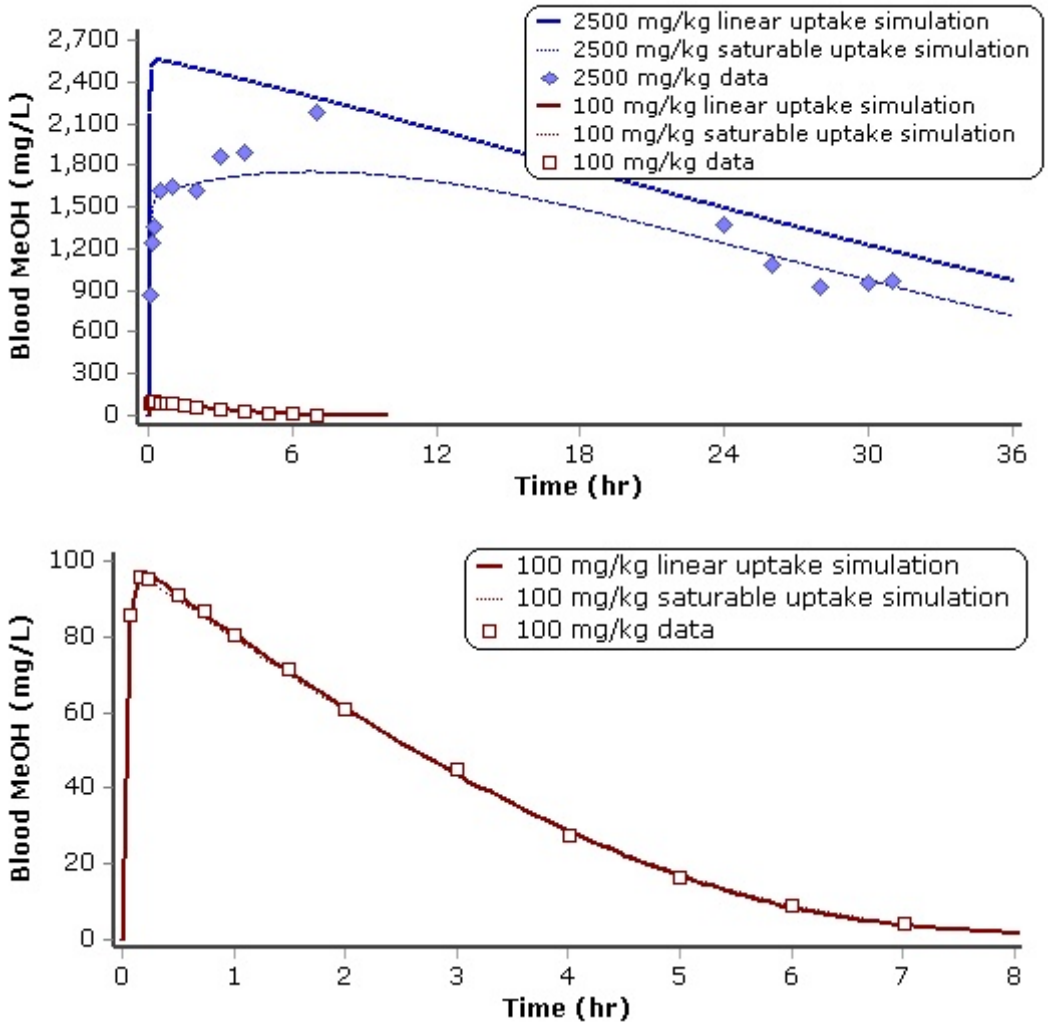

Figure 3-10. Model fits to datasets from oral exposures to 100 and 2,500 mg/kg methanol in female Sprague-Dawley rats. Symbols are concentration data obtained from the command file. Lines represent PBPK model fits.

Source: Ward et al. (1997).

3.4.6. Human Model Calibration

3.4.6.1. *Inhalation Route*

The mouse model was scaled to humans by setting either a standard human body weight (70 kg) or study-specific body weights and using human tissue compartment volumes and blood flows, and then calibrated to fit the human inhalation exposure data available from the open literature, which comprised data from four publications (Ernstgard et al., 2005; Batterman et al., 1998; Osterloh et al., 1996; Sedivec et al., 1981).

Since the human data included time-course data for urinary elimination, a first-order rate of loss of methanol from the blood (K1) was used to provide an estimate of methanol elimination to the bladder compartment in humans, and the rate of elimination from that compartment then

characterized by a second constant (KBL). Note that the total amount eliminated by this route depends only on K1, while KBL affects the rate at which the material cleared from the blood then appears in the urine. Inhalation-route urinary methanol kinetic data described by Sedivec et al. (1981) (Figure 3-11) was used in the model calibration to inform this rate constant. Without use of the bladder compartment and rate constant, the fit of the model predictions to the data in Figure 3-11 is quite poor (results not shown), and a statistical test on the improvement of fit obtained by introducing the additional parameter (KBL) is significant ($p < 0.0001$). Conversion between the PBPK-model-predicted rate of urinary excretion (mg/hours) or cumulative urinary excretion (mg) and the urine methanol concentration data reported by the authors was achieved by assuming 0.5 mL/hours/kg body weight total urinary output (Horton et al., 1992). The resulting values of K1C and KBL, shown in Table 3-10, differ somewhat depending on whether first-order or saturable liver metabolism is used. These are only calibrated against a small dataset and should be considered an estimate. Urinary elimination is a minor route of methanol clearance with little impact on blood methanol kinetics.

Although the high doses used in the mouse studies clearly warrant the use of a second metabolic pathway with a high K_m, the human exposure data all represent lower concentrations and may not require or allow for accurate calibration of a second metabolic pathway. Horton et al. (1992) employed two sets of metabolic rate constants to describe human methanol disposition, similar to the description used for rats and mice, but in vitro studies using monkey tissues with nonmethanol substrates were used as justification for this approach. Although Bouchard et al. (2001) described their metabolism using Michaelis-Menten metabolism, Starr and Festa (2003) reduced that to an effective first-order equation and showed adequate fits. Perkins et al. (1995a) estimated a K_m of 320 ± 1273 mg/L (mean ± S.E.) by fitting a one-compartment model to data from a single estimated oral dose. In addition to the extremely high standard error, the large standard error for the associated V_{max} (93 ± 87 mg/kg/hours) indicates that the set of Michaelis-Menten constants was not uniquely identifiable using this data. Other Michaelis-Menten constants have been used to describe methanol metabolism in various models for primates (Table 3-11).

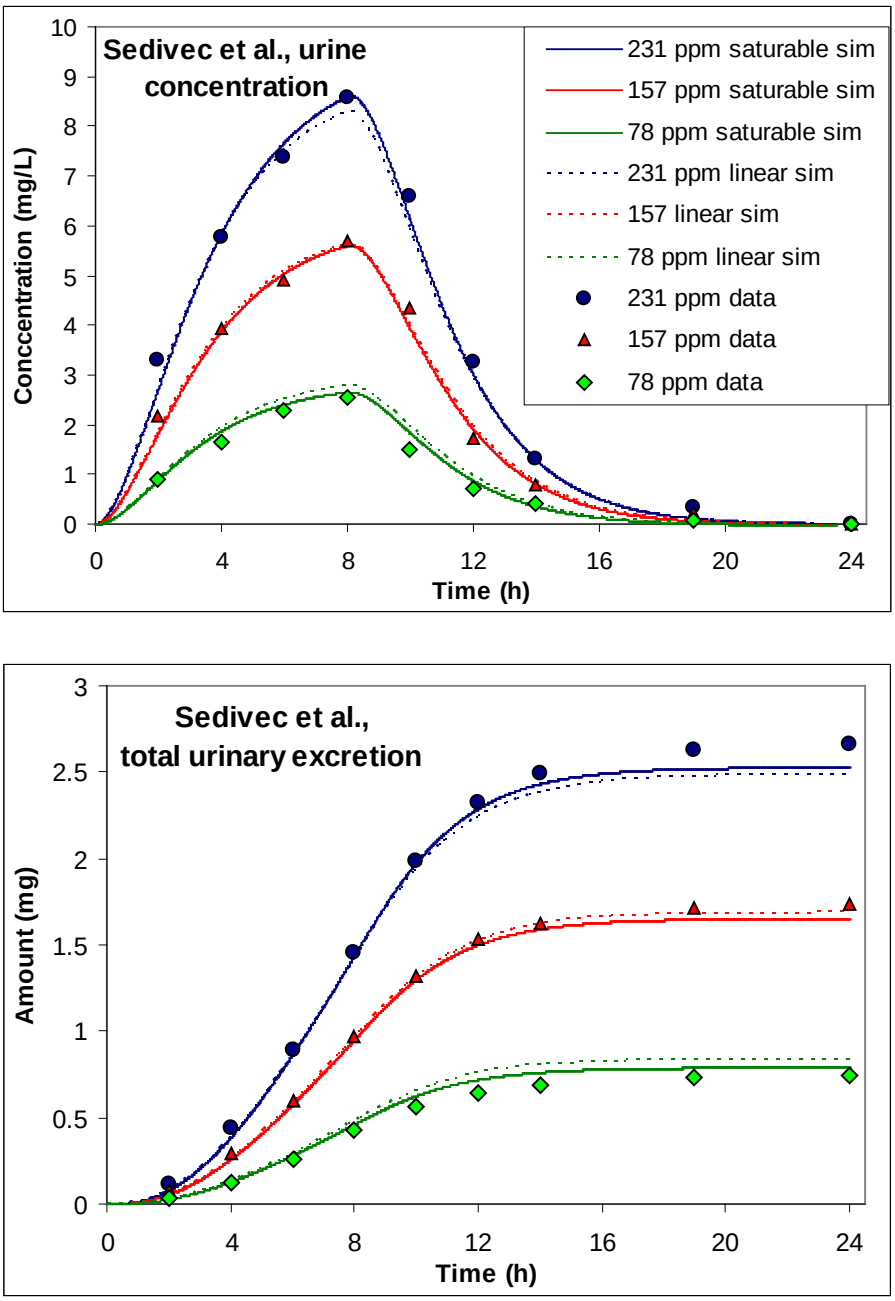

Figure 3-11. Urinary methanol elimination concentration (upper panel) and cumulative amount (lower panel) following inhalation exposures to methanol in human volunteers. Data points in lower panel represent estimated total urinary methanol elimination from humans exposed to 78 (diamonds), 157 (triangles), and 231 (circles) ppm methanol for 8 hours, and lines represent PBPK model simulations.

Source: Sedivec et al. (1981).

Table 3-11. Primate K_ms reported in the literature

K_m (mg/L)	Reference	Note
320 ±1273[a]	Jacobsen et al., 1988	Human: oral poisoning, estimated dose
716 ± 489[a]	Noker et al., 1980	Cynomolgus Monkey: 2 g/kg dose
278	Makar et al., 1968	Rhesus Monkey: 0.05-1 mg/kg dose
252 ± 116[a]	Eells et al., 1983	Cynomolgus Monkey: 1 g/kg dose
33.9	Horton et al., 1992	PBPK model: adapted from rat K_m
0.66	Fisher et al., 2000	PBPK model, Cynomolgus Monkey:10-900 ppm
23.7 ± 8.7[a,b]	(This analysis.)	PBPK model, human: 100-800 ppm

[a]The values reported are mean ± S.D.
[b]This K_m was optimized while varying V_{max}, K1C, and KBL, from all of the at-rest human inhalation data as a part of this project. The S.D. given for this analysis is based on the Optimize function of acslXtreme, which assumes all data points are discrete and not from sets of data obtained over time; therefore a true S.D. would be higher. The final value reported in Table B-1 (21 mg/L) was obtained by sequentially rounding and fixing these parameters, then re-optimizing the remaining ones.

Source: Perkins et al. (1995b).

Table 3-12. Parameter estimate results obtained using acslXtreme to fit all human data using either saturable or first-order metabolism

Parameters	Optimized value	S.D.	Correlation coefficient	LLF
Michaelis-Menten (optimized)			-0.994	-24.1
K_m	23.7	8.9		
$V_{max}C$	33.1	10.1		
First order			NA	-31.0
KLLC	95.7	5.4		

Note. The S.D.s are based on the Optimize function of acslXtreme v2.3, which assumes all data points are discrete and not from sets of data obtained over time. Therefore a true S.D. would be a higher value.

To estimate both Michaelis-Menten and first-order rates, all human data under nonworking conditions (Batterman et al., 1998; Osterloh et al., 1996; Sedivec et al., 1981) were used (Table 3-12). The metabolic (first-order or saturable) and urinary elimination constants were numerically fit to the human datasets, while holding the value for FRACIN at 0.8655 (estimated from the results of Sedivec et al. [1981]) and holding the ventilation rate constant at 16.5 L/hours/kg$^{0.75}$ and QPC at 24 L/hours/kg$^{0.75}$ (values used by EPA [2000d] for modeling the inhalation-route kinetics of vinyl chloride). Other human-specific physiological parameters were used,as reported in Table 3-10. Final fitted parameters that have been used in the saturable

model are given in Table 3-10. The resulting fits of two different possible parameterizations (first-order ["linear"] or optimized K_m/V_{max}) are shown in Figures 3-11 and 3-12.

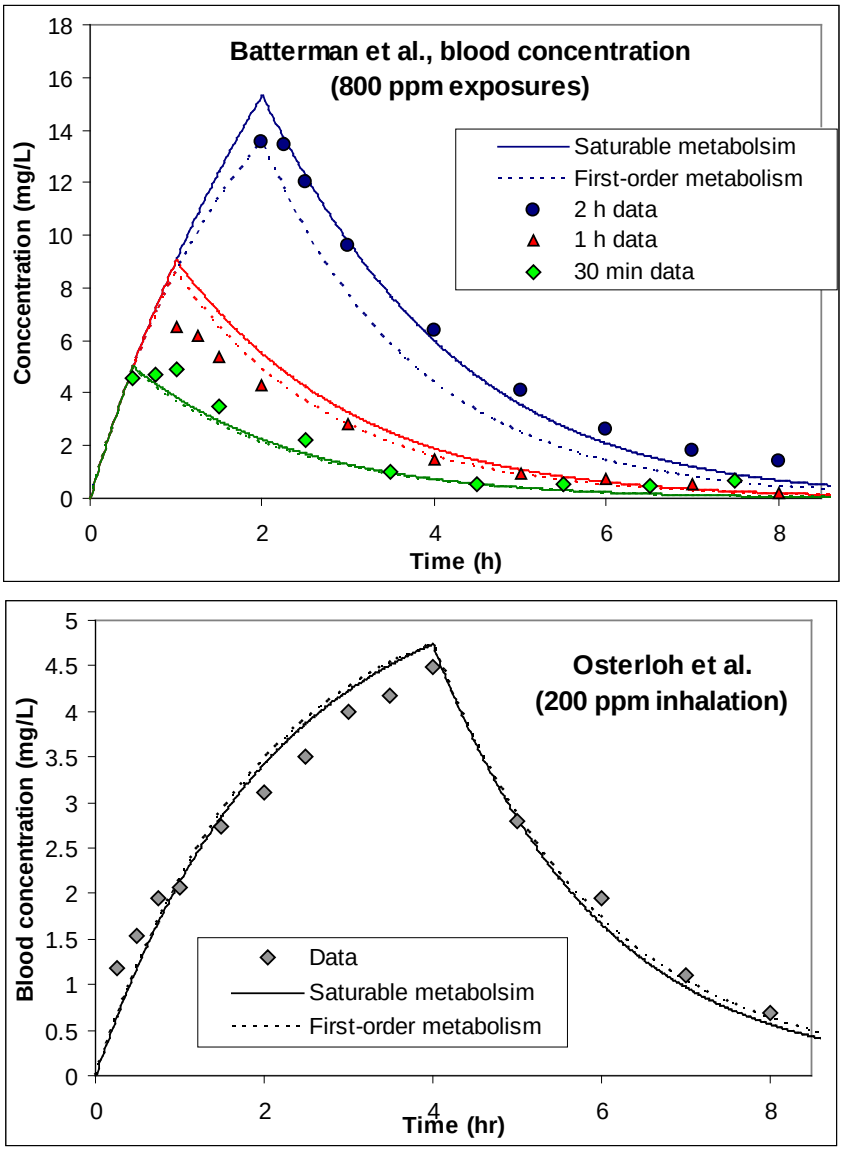

Figure 3-12. Data showing the visual quality of the fit using optimized first-order or Michaelis-Menten kinetics to describe the metabolism of methanol in humans. Rate constants used for each simulation are given in Table 3-12.

Source: Batterman et al. (1998: top); Osterloh et al. (1996: bottom).

Use of a first-order rate has the advantage of resulting in a simpler (one fewer variable) model, while providing an adequate fit to the data; however, the saturable model clearly fits some of the data better. To discriminate the goodness-of-fit resulting of the inclusion of an additional variable necessary to describe saturable metabolism versus using a single first-order

rate, a likelihood ratio test was performed.[13] The hypothesis that one metabolic description is better than another is calculated using the likelihood functions evaluated at the maximum likelihood estimates. Since the parameters are optimized in the model using the maximum log likelihood function (LLF), the resultant LLF is used for the statistical comparison of the models. The equation states that two times the log of the likelihood ratio follows a chi square (χ^2) distribution with *r* degrees of freedom:

$$-2[\log(\lambda(\text{model}1)/\lambda(\text{model}2))] = -2[\log\lambda(\text{model}1) - \log\lambda(\text{model}2)] \cong \chi_r^2$$

The likelihood ratio test states that if the two times the difference between the maximum LLFs of the two different descriptions of metabolism is greater than the χ^2 distribution then the model fit has been improved (Devore, 1995; Steiner et al., 1990) .

At greater than a 99.95% confidence level, using two metabolic rate constants (K_m and $V_{max}C$) is preferred over using a single rate constant (Table 3-13). Forcing the model to use the K_m calculated by Perkins et al. (1995b) would result in model fits indistinguishable from the first-order case (results not shown). While the correlation coefficients (Table 3-12) indicate that $V_{max}C$, and K_m are highly correlated, that is not unexpected, and the S.D.s (Table B-3) indicate that each is reasonably bounded. If the data were indistinguishable from a linear system, K_m in particular would not be so bounded from above since the Michaels-Menten model becomes indistinguishable from a linear model as $V_{max}C$ and K_m tend to infinity. Further, the internal dose candidate points of departure (PODs), for example the $BMDL_{10}$ for the inhalation-induced brain-weight changes from NEDO (1987) with methanol blood AUC as the metric, is 90.9 mg-hr/L, which corresponds to an average blood concentration of 3.8 mg/L. Therefore, the Michaelis-Menten metabolism rate equation appears to be sufficiently supported by the existing data with values in a concentration range in which the nonlinearity has an impact.

Table 3-13. Comparison of LLFs for Michaelis-Menten and first-order metabolism

LLF (logλ) for M-M	LLF (logλ) for 1st order	LLF 1st versus M-M[a]	χ_r^2 (99% confidence)[b]	χ_r^2 (99.95% confidence)[b]
-24.1	-31.0	34.1	13.8	12.22

Note. Models were optimized for all human datasets under non working conditions. M-M: Michaelis-Menten
[a]obtained using this equation: $-2[\log\lambda(\text{model}1) - \log\lambda(\text{model}2)]$
[b]significance level at *r*=1 degree of freedom.

While the use of Michaelis-Menten kinetics might allow predictions across a wide exposure range (into the nonlinear region), extrapolation above 1,000 ppm is not suggested since the highest human exposure data are for 800 ppm. Extrapolation to higher concentrations is

[13] Models are considered to be nested when the model structures are identical except for the addition of complexity, such as the added metabolic rate. Under these conditions, the likelihood ratio can be used to compare the relative ability of the two models to describe the data, as described in "Reference Guide for Simusolv" (Steiner et al., 1990).

potentially misleading since the nonlinearity in the exposure-internal-dose relationship for humans is uncertain above this point. The use of a BMD or internally applied uncertainty factors (UFs) should place the exposure concentrations well within the linear range of the model.

The data from Ernstgard et al. (2005) were used to assess the use of the first-order metabolic rate constant to a dataset collected under conditions of light work. Historical measures of QPC (52.6 L/hours/kg$^{0.75}$) and QCC (26 L/hours/kg$^{0.75}$) for individuals exposed under conditions of 50 watts of work from that laboratory (52.6 L/hours/kg$^{0.75}$) (Ernstgard, 2005; Corley et al., 1994; Johanson et al., 1986) were used for the 2-hour exposure period (Figure. 3-12). Otherwise, there were no changes in the model parameters (no fitting to these data). The results are remarkably good, given the lack of parameter adjustment to data collected in a different laboratory and using different human subjects than those to which the model was calibrated.

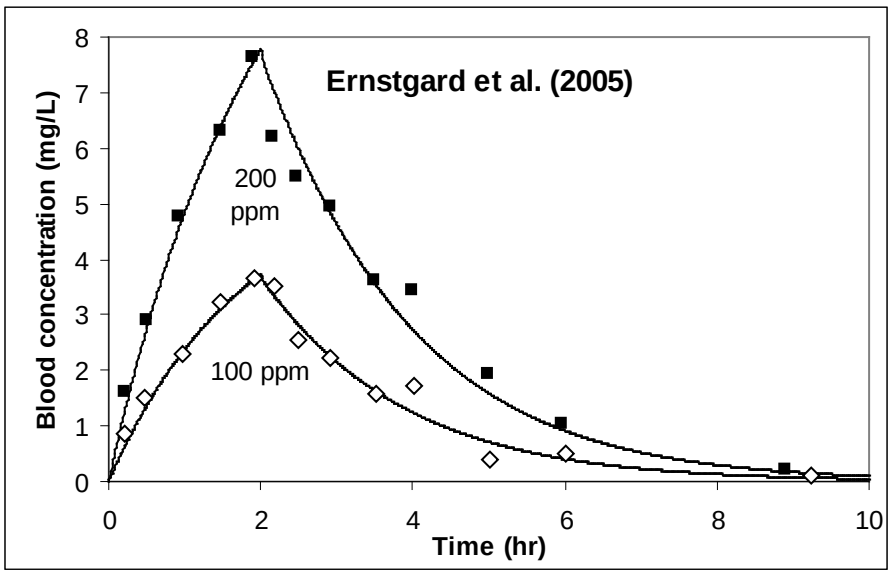

Figure 3-13. Inhalation exposures to methanol in human volunteers. Data points represent measured blood methanol concentrations from humans (4 males and 4 females) exposed to 100 ppm (open symbols) or 200 ppm (filled symbols) for 2 hours during light physical activity. Solid lines represent PBPK model simulations with no fitting of model parameters. For the first 2 hours, a QPC of 52.6 L/hours/kg$^{0.75}$ (Johansen et al., 1986), and a QCC of 26 L/hours/kg$^{0.75}$ (Corley et al., 1994) was used by the model.

Source: Ernstgard et al. (2005).

3.4.6.2. *Oral Route*

There were no methanol human data available for calibration or validation of the oral route for the human model. In the absence of methanol data to estimate rate constants for oral uptake, human oral absorption parameters reported values for ethanol (Sultatos et al., 2004) are

set in the code, except that saturable absorption from the stomach was retained with the KMASC equal to the mouse value. The maximum rate of absorption form the stomach, VMASC, was then set such that for a 70-kg person, VMAS/KM (the effective first-order rate constant at low doses) matched the first-order absorption rate from Sultatos et al. (0.21 hr^{-1}). Also, while Sultatos et al. included a rate of metabolism for ethanol in the stomach, the corresponding fecal elimination rate was set to zero here, effectively assuming 100% absorption of methanol for humans. However, human oral dosimetry was described as zero-order uptake, in which continuous infusion at a constant rate into the stomach equal to the daily dose/24 hours was assumed and human internal doses were computed at steady state. Since absorption is 100% for the human model, at steady state the net rate of absorption must equal the rate of infusion to the stomach, irrespective of the other parameter values. (Changes in the absorption constants simply cause the amount of methanol in each GI compartment at steady state to change until the net rate of absorption from the somtach and intestine equals the rate of infusion.) Thus the human absorption constants were set to what is considered a reasonable estimate, given the lack of human oral PK data, but the simulations are conducted in a way that makes the result insensitive to their values; having human values set does allow for simulations of non-constant infusion, should such be desired. Since the AUC was computed for a continuous oral exposure, its value is just 24 hours times the steady-state blood concentration at a given oral uptake rate.

3.4.7. Monkey PK Data and Analysis

In order to estimate internal doses (blood AUCs) for the monkey health-effects study of Burbacher et al. (1999b) and further elucidate the potential differences in methanol pharmacokinetics between NP and pregnant individuals (2nd and 3rd trimester), a focused reanalysis of the data of Burbacher et al. (1999a) was performed. Individual blood concentration measurements prior to and following exposure are shown in scatter plots in Appendix B of Burbacher et al. (1999a). More specifically, the monkeys in the study were exposed for 2.5 hours/day, with the methanol concentration raised to approximately the target concentration for the first 2 hours of each exposure and the last 30 minutes providing a chamber "wash-out" period, when the exposure chamber concentration was allowed to drop to 0. Blood samples were taken and analyzed for methanol concentration at 30 minutes, 1, 2, 3, 4, and 6 hours after removal from the chamber (or 1, 1.5, 2.5, 3.5, 4.5, and 6.5 hours after the end of active exposure). These data were analyzed to compare the PK in NP versus pregnant animals, and fitted with a simple PK model to estimate 24-hour blood AUC values for each exposure level. Dr. Burbacher graciously provided the original data, which were used in this analysis.

Two cohorts of monkeys were examined, but the data (plots) did not indicate a systematic difference between the two, so the data from the two cohorts were combined. The data from the scatter plots of Burbacher et al. (1999a) for the NP (pre-pregnancy), first pregnancy (2nd trimester), and second pregnancy (3rd trimester) studies are compared in Figure 3-13, along with

model simulations (explained below). Since the pregnancy time points were from animals that had been previously exposed for 87 days *plus* the duration of pregnancy to that time point, the pre-exposed NP animals were used for comparison, rather than naïve animals, with the expectation that effects due to changes in enzyme expression (i.e., induction) from the subchronic exposure would not be a distinguishing factor. Note that each exposure group included a pre-exposure baseline or background measurement, also shown. To aid in distinguishing the data visually, the NP data are plotted at times 5 minutes prior to the actual blood draws and the 3rd trimester at 5 minutes after each blood draw.

Overall there appears to be no significant or systematic difference among the NP and pregnant groups. The solid lines are model simulations calibrated to only the 2nd trimester data (details below), but they just as adequately represent average concentrations for the NP and 3rd trimester data. Likewise, a PK model calibrated to the NP PK data adequately predicted the maternal methanol concentrations in the pregnant monkeys (results not shown). Since any maternal:fetal methanol differences are expected to be similar in experimental animals and humans (with the maternal:fetal ratio being close to one due to methanol's high aqueous solubility and relatively limited metabolism by the fetus), the predicted levels for the 2nd trimester maternal blood are used in place of measured or predicted fetal concentrations.

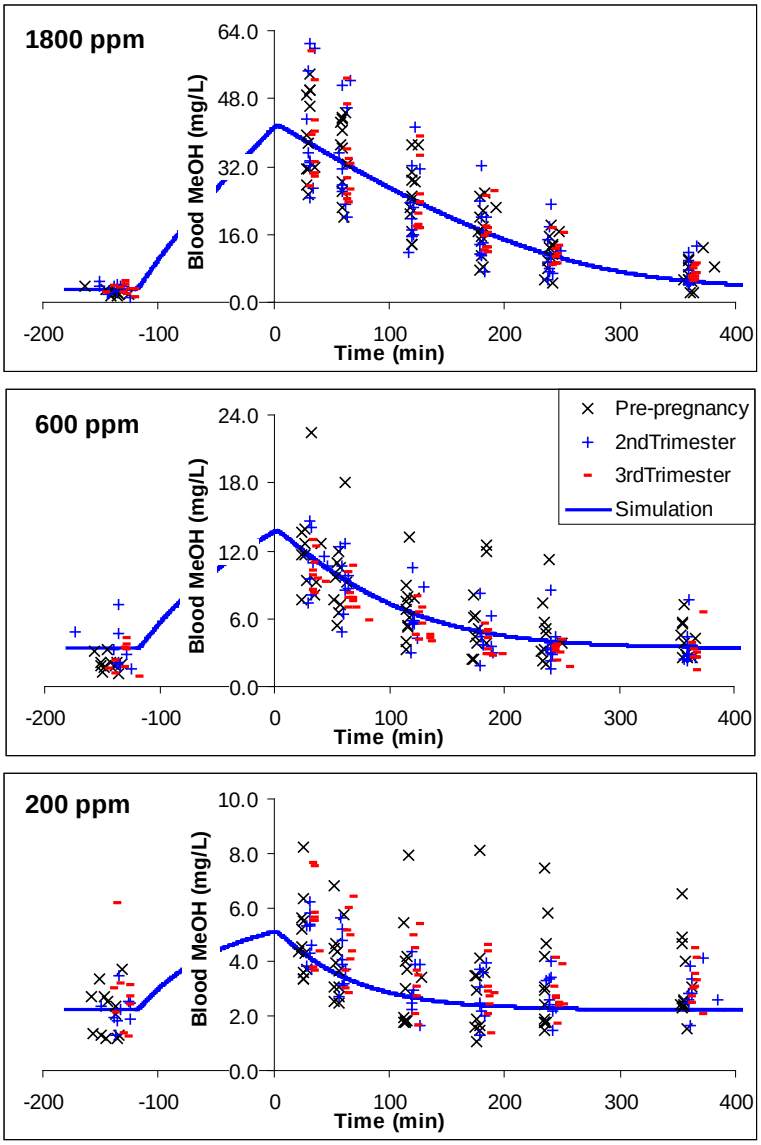

Figure 3-14. Blood methanol concentration data from NP and pregnant monkeys. NP and 3rd trimester data are plotted, respectively, at 5 minutes before and after actual collection times to facilitate comparison. Solid line is from simple PK model, fit to 2nd trimester data only.

Source: Burbacher et al. (1999a; Figure B-4).

3.4.7.1. *PK Model Analysis for Monkeys*

To analyze and integrate the PK data of Burbacher et al. (1999a), the one-compartment model for Michaelis-Menten kinetics used by Burbacher et al. (1999a, 1999b) was extended by the addition of a chamber compartment to capture the kinetics of concentration change in the exposure chamber, as shown in Figure 3-14. The data in Figure 3-14 (digitized from Figure 5 of Burbacher et al., 1999a, 1999b) show an exponential rise to and fall from the approximate target concentration during the exposure period. The use of a single-compartment model for the

chamber allows this dynamic to be captured, so that the full concentration-time course is used in simulating the monkey internal concentration rather than an approximate step function (i.e. rather than assuming an instantaneous rise and fall). The pair of equations representing the time-course in the chamber and monkey are as follows (bolded parameters are fit to data):

$$\text{Chamber: } dC_{ch}/dt = [(C_{CM} \cdot S - C_{ch}) \cdot F_{ch} - R_{inh}]/V_{ch}$$

$$\text{Monkey: } dC_{mk}/dt = [R_{inh} - V_{max} \cdot C_{mk}/(K_m + C_{mk})]/(V_{mk} \cdot BW)$$

$$\text{with } R_{inh} = C_{ch} \cdot R_C \cdot (1000 \cdot BW)^{0.74} \cdot F \text{ and } C_{net} = C_{mk} + C_{bg}.$$

d: delta, change

C_{ch}: instantaneous chamber concentration (mg/L)

t: time (hour)

C_{CM}: chamber in-flow methanol concentration (mg/L), which was set to the concentrations corresponding to those reported in Table 2 of Burbacher et al. (1999a), using the "Breeding" column for the NP (87 days pre-exposed; values in Table 3-14)

S: exposure switch, set to 1 when exposure is on (first 2 hours) and 0 when off

F_{ch}:chamber air-flow, 25,200 L/hours, as specified by Burbacher et al. (1999a,1999b)

R_{inh}: net rate of methanol inhalation by the monkeys (mg/hr)

V_{ch} (1,220 L): chamber volume, initially set to 1,380 L ("accessible volume" stated by Burbacher et al. [1999a, 1999b]), but allowed to vary below that value to account for volume taken by equipment, monkey, and to allow for imperfect mixing

C_{mk}: instantaneous inhalation-induced monkey blood methanol concentration (mg/L); this is added to the measured background/endogenous concentration before comparison to data

V_{max} (39.3 mg/hr): fitted (nonscaled) Michaelis-Menten maximum elimination rate

K_m (14.6 mg/L): fitted (nonscaled) Michaelis-Menten saturation constant

V_{mk} (0.75 L/kg): fitted volume of distribution for monkey

BW: monkey body weight (kg); for NP monkeys set to group average values in data of Burbacher et al. (1999a, 1999b; personal communication)

R_c: allometric scaling factor for total monkey respiration (0.12 L/hours/$g^{0.74}$ = 2 mL/minute/$g^{0.74}$), as used by Burbacher et al. (1999a, 1999b)(note that scaling is to BW in g, not kg)

F: fractional absorption of inhaled methanol, set to 0.6 (60%), the (rounded) value measured in humans by Sedivec et al. (1981); F and V_{mk} cannot be uniquely identified, given the model structure, so F was set to the (approximate) human value to obtain a realistic estimate of V_{mk}

C_{net}: net blood concentration, equal to sum of the inhalation-induced concentration (C_{mk}) and the background blood level (C_{bg}) (mg/L)

C_{bg}: background (endogenous) methanol concentration, set to the pre-exposure group-specific mean from the data of Burbacher et al. (1999a, 1999b; personal communication)

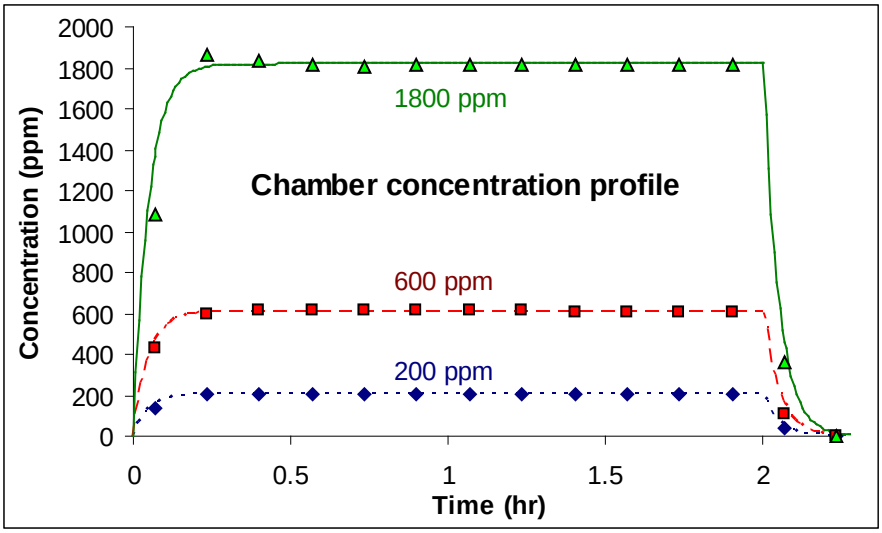

Figure 3-15. Chamber concentration profiles for monkey methanol exposures. Lines are model simulations. Indicated concentrations are target concentrations; measured concentrations differed slightly (see Table 3-14).

Source: Burbacher et al. (1999a).

The model was specifically fit to the 2nd trimester monkey data, assuming that the parameters were the same for all the exposure groups and concentrations. While the discussion above and data show little difference between the NP and two pregnancy groups, the 2nd trimester group was presumed to be most representative of the average internal dosimetry over the entire pregnancy. Further, the results of Mooney and Miller (2001) show that developmental effects on the monkey brain stem following ethanol exposure are essentially identical for monkeys exposed only during early pregnancy versus full-term, indicating that early pregnancy is a primary window of vulnerability.

Model simulation results are the lines shown in Figures 3-13 and 3-14. The model provides a good fit to the monkey blood and chamber air concentration data. While the chamber volume was treated as a fitted parameter, which was not done by Burbacher et al. (1999a), the chamber concentration data support this estimate. The model does an adequate job of fitting the data for all exposure groups without group-specific parameters. In particular, the data for all exposure levels can be adequately fit using a single value for the volume of distribution (V_{mk}) as well as each of the metabolic parameters. While one may be able to show statistically distinct parameters for different groups or exposure levels (by fitting the model separately to each), as was done by Burbacher et al. (1999a), it is unlikely that such differences are biologically significant, given the fairly large number of data points and the large variability evident in the blood concentration data. Thus, the single set of parameters listed with the parameter descriptions above will be used to estimate internal blood concentrations for the dose-response

analysis. The chamber concentrations for "pregnancy" exposures recorded by Burbacher et al. (1999a; Table 2) and average body weights for each exposure group at the 2nd trimester time point were used along with the model to calculate 24-hour blood methanol AUCs (Table 3-14).

Table 3-14. Monkey group exposure characteristics

Exposure concentration (ppm)[a]	Group average BW (kg)[b]	24-hr blood methanol AUC (mg-hr/L)[c]
206	3.46	6.73
610	4.08	28.28
1,822	3.83	138.11

[a]From Burbacher et al. (1999a,1999b), Table 2, "pregnancy" exposure.
[b]From Burbacher, original data (personal communication).
[c]Calculated using the two-compartment PK model as described above.

3.4.8. Summary and Conclusions

Mouse, rat, and human versions of a methanol PBPK model have been developed and calibrated to data available in the open literature. The model simplifies the structure used by Ward et al. (1997), while adding specific refinements such as a standard lung compartment employed by Fisher et al. (2000) and a two-compartment GI tract.

Although the endpoints of concern are developmental effects which occur during in utero and (to a lesser extent) lactational exposure, no pregnancy-specific PBPK model exists for methanol and inadequate data exists for the development and validation of a fetal/gestational/conceptus compartment. The fact that the unique physiology of pregnancy and the fetus/conceptus are not represented in a methanol model would be important if methanol pharmacokinetics differed significantly during pregnancy or if the observed partitioning of methanol into the fetus/conceptus versus the mother showed a concentration ratio significantly greater than or less than 1. Methanol pharmacokinetics during GD6–GD10 in the mouse are not different from NP mice (Pollack and Brouwer, 1996), and the maternal blood:fetus/conceptus partition coefficient is reported to be near 1 (Ward et al., 1997; Horton et al., 1992). At GD18 in the mouse, maternal blood levels are only modestly different from those in NP animals (see Figures B-4 and B-5 [Appendix B] for examples), and in general the PBPK model simulations for the NP animal match the pregnancy data as well as the nonpregnancy data. Likewise, maternal blood kinetics in monkeys differs little from those in NP animals (see Section 3.4.7 for details). Further, in both mice and monkeys, to the extent that late-pregnancy blood levels differ from NP for a given exposure, they are higher; i.e., the difference between model predictions and actual concentrations is in the same direction. These data support the assumption that the ratio of actual target-tissue methanol concentration to (predicted) NP maternal blood concentrations will be about the same across species, and hence, that using NP maternal blood levels in place of fetal concentrations will not lead to a systematic error when extrapolating risks.

The findings in the mouse (similar blood methanol kinetics between NP and pregnant animals prior to GD18 and a maternal blood:fetal partition coefficient close to 1) are assumed to be applicable to the rat. However, the critical gestational window for the reduced brain weight effect observed in the NEDO (1987) rat study is broader than for the mouse cervical rib effect. In addition, NEDO (1987) rats were exposed not only to methanol gestationally but also lactationally and via inhalation after parturition. The additional routes of exposure presented to the pups in this study present uncertainties and suggest that average blood levels in pups might be greater than those of the dam.

Methanol is transported directly from the maternal circulation to fetal circulation via the placenta, but transfer via lactation involves distribution to the breast tissue, then milk, then uptake from the pup's GI tract. Therefore blood or target-tissue levels in the breast-feeding infant or pup are likely to differ more from maternal levels than do fetal levels. In addition, the health-effects data indicate that most of the effects of concern are due to fetal exposure, with a relatively small influence due to postbirth exposures. Further, it would be extremely difficult to distinguish the contribution of postbirth exposure from pre birth exposure to a given effect in a way that would allow the risk to be estimated from estimates of both exposure levels, even if one had a lactation/child PBPK model that allowed for prediction of blood (or target-tissue) levels in the offspring. Finally, one would still expect the target-tissue concentrations in the offspring to be closely related to maternal blood levels (which depend on ambient exposure and determine the amount delivered through breast milk), with the relationship between maternal levels and those in the offspring being similar across species. Further, as discussed to a greater extent in Sections 5.1.2 and 5.3, it is likely that the difference in blood levels between rat pups and dams would be similar to the difference between mothers and human offspring. Therefore, it is assumed that the potential differences between pup and dam blood methanol levels do not have a significant impact on this risk assessment and the estimation of HECs. The use of the full intrahuman UF of 10 is also expected to account for PK differences between children and adults.

Therefore, the development of a lactation/child PBPK model appears not to be necessary, given the minimal change that is likely to result in risk extrapolations, and use of (NP) maternal blood levels as a measure of risk in the offspring is considered preferable over use of default extrapolation methods. In particular, the existing human data allow for predictions of maternal blood levels, which depend strongly on the rate of maternal methanol clearance. Since bottle-fed infants do *not* receive methanol from their mothers, they are expected to have lower or, at most, similar overall exposures for a given ambient concentration than the breast-fed infant, so that use of maternal blood levels for risk estimation should also be adequately protective for that group.

The model fits to the mouse oral-route methanol kinetic data, using a consistent set of parameters (Figure B-4 in Appendix B), are fairly good for doses of 1,500 mg/kg but underpredict blood levels by 30% or more after a dose of 2,500 mg/kg. In particular, the oral mouse model consistently underpredicts the amount of blood methanol reported in two studies

(Ward et al., 1997, 1995). Ward et al. (1997) utilized a different V_{max} for each oral absorption dataset; the GD18 and the GD8 data from Dorman et al. (1995) were both fit using a V_{max} of ~80 mg/kg/hours (body weights were not listed; the model assumed that GD8 and GD18 mice were both 30 g; Ward et al. [1997] did not scale by body weight). Additionally, lower partition coefficients for placenta (1.63 versus 3.28) and embryonic fluid (0.0037 versus 0.77) were used for GD8 and GD18. The current refined model adequately fits the oral PK data using a single set of parameters that is not varied by dose or source of data.

The rat models were able to adequately predict the limited inhalation, oral and i.v. datasets available. Low-dose exposures were emphasized in model optimization due to their greater relevance to risk assessment. Based on a rat inhalation exposure to 500 ppm, the HEC would be 281 ppm (by applying an AUC of 201.3 [Figure B-12] to Equation 1 of Appendix B).

The final mouse, rat, and human methanol PBPK models fit multiple datasets for inhalation, oral, and i.v., from multiple research groups using consistent parameters that are representative of each species but are not varied within species or by dose or source of data. Also, a simple PK model calibrated to NP monkey data, which were shown to be essentially indistinguishable from pregnant monkey PK data, was used to estimate blood methanol AUC values (internal doses) in that species. In Section 5, the models and these results are used to estimate chronic human exposure concentrations from internal dose metrics.

4. HAZARD IDENTIFICATION

4.1. STUDIES IN HUMANS – CASE REPORTS, OCCUPATIONAL AND CONTROLLED STUDIES

4.1.1. Case Reports

An extensive library of case reports has documented the consequences of acute accidental/intentional methanol poisoning. Nearly all have involved ingestion, but a few have involved percutaneous and/or inhalation exposure. As many of the case reports demonstrate, the association of Parkinson-like symptoms with methanol poisoning is related to the observation that lesions in the putamen are a common feature both in Parkinson's disease and methanol overexposure. These lesions are commonly identified using computed tomography (CT) or by Magnetic Resonance Imaging (MRI). Other areas of the brain (e.g., the cerebrum, cerebellum, and corpus callosum) also have been shown to be adversely affected by methanol overexposure. Various therapeutic procedures (e.g., ethanol infusion, sodium bicarbonate or folic acid administration, and hemodialysis) have been used in many of these methanol overexposures, and the reader is referred to the specific case reports for details in this regard. The reader also is referred to Kraut and Kurtz (2008) and Barceloux et al. (2002) for a more in-depth discussion of the treatments in relation to clinical features of methanol toxicity. A brief discussion of the terms cited in case report literature follows.

Basal ganglia, a group of interconnected subcortical nuclei in each cerebral hemisphere, refers to various structures in the grey matter of the brain that are intimately involved, for example, in coordinating motor function, maintaining ocular and respiratory function, and consciousness. The connectivity within the basal ganglia involves both excitatory and inhibitory neurotransmitters such as dopamine (associated with Parkinson's disease when production is deficient).

The structures comprising the basal ganglia include but are not limited to: the putamen and the globus pallidus (together termed the lentiform nuclei), the pontine tegmentum, and the caudate nuclei. Dystonia or involuntary muscle contraction can result from lesions in the putamina; if there are concomitant lesions in the globus pallidus, Parkinsonism can result (Bhatia and Marsden, 1994). Bhatia and Marsden (1994) have discussed the various behavioral and motor consequences of focal lesions of the basal ganglia from 240 case-study reports. Lesions in the subcortical white matter adjacent to the basal ganglia often occur as well (Airas et al., 2008; Rubinstein et al., 1995; Bhatia and Marsden, 1994). In the case reports of Patankar et al. (1999), it was noted that the severity and extent of necrosis in the lenticular nuclei do not necessarily correlate with clinical outcome.

In one of the earliest reviews of methanol overexposure, Bennett et al. (1953) described a mass accidental poisoning when 323 persons, ranging in age from 10 to 78 years, in Atlanta, Georgia, consumed "whisky" adulterated with as much as 35–40% methanol. In all, 41 people died. Of the 323 individuals, 115 were determined to be acidotic with symptoms (visual impairment, headache [affecting ~62%], dizziness [affecting ~30%], nausea, abdominal pain and others) beginning around 24 hours postexposure. Visual impairment was mostly characterized by blurred or indistinct vision; some who were not acidotic experienced transient visual disturbances. The cardiovascular parameters were unremarkable. The importance of acidosis to outcome is shown in Table 4-1. Among the key pathological features were cerebral edema, lung congestion, gastritis, pancreatic necrosis, fatty liver, epicardial hemorrhages, and congestion of abdominal viscera.

In another early investigation of methanol poisoning (involving 320 individuals), Benton and Calhoun (1952) reported on methanol's visual disturbances.

Table 4–1. Mortality rate for subjects exposed to methanol-tainted whiskey in relation to their level of acidosis[a]

Subjects	Number	Percent deaths
All patients	323	6.2
Acidotic (CO_2 <20 mEq)	115	19
Acidotic (CO_2 <10 mEq)	30	50

[a]These data do not include those who died outside the hospital or who were moribund on arrival.

Source: Bennett et al. (1953).

Riegel and Wolf (1966), in a case report involving a 60-year-old woman who ingested methanol, noted that nausea and dizziness occurred within 30 minutes of ingestion. She subsequently passed out and remained unconscious for 3 days. Upon awakening she had paralysis of the vocal cords and was clinically blind in one eye after 4 months. Some aspects of Parkinson-like symptoms were evident. There was a pronounced hypokinesia with a mask-like face resembling a severe state of Parkinson's disease. The patient had difficulty walking and could only make right turns with difficulty. There was no memory loss.

Treatment of a 13-year-old girl who ingested an unspecified amount of a windshield-washer solution containing 60% methanol was described by Guggenheim et al. (1971). She displayed profound acidosis; her vital signs, once she was treated for acidosis, were normal by 36 hours after hospital admission. During the ensuing 6 months after discharge from the hospital, visual acuity (20/400, both eyes) worsened, and she experienced muscle tremors, arm pain, and difficulty in walking. A regimen of levadopa treatment greatly improved her ability to function normally.

Ley and Gali (1983) also noted symptoms that are Parkinson like following methanol intoxication. In this case report respiratory support was needed; the woman was in a coma. Once stabilized, she exhibited symptoms similar to those noted in other case study reports, such as blurred vision, movement difficulty, and tremors. Computerized Axial Tomography scan findings highlighted the central nervous system (CNS) as an important site for methanol poisoning.

Rubinstein et al. (1995) presented evidence that a methanol blood level of 36 mg/dL (360 mg/L) is associated with a suite of CNS and ocular deficits that led to a 36-year-old man (who subsequently died) becoming comatose. CT scans at 1–2 days following ingestion were normal. However, MRI scans at day 4 revealed lesions in the putamen and peripheral white matter of the cerebral and cerebellar hemispheres. Bilateral cerebellar cortical lesions had been reported in an earlier case of methanol poisoning by Chen et al. (1991).

Finkelstein and Vardi (2002) reported that long-term inhalation exposure of a woman scientist to methanol without acute intoxication resulted in a suite of delayed neurotoxic symptoms (e.g., hand tremor, dystonia, bradykinesia, and other decrements in body movement). Despite treatment with levadopa, an increase in the frequency and severity of effects occurred. Exposure to bromine fumes was concomitant with exposure to methanol.

Hantson et al. (1997a) found, in four cases, that MRI and brain CT scans were important tools in revealing specific brain lesions (e.g., in the putamina and white matter). The first subject was a 57-year-old woman who complained of blurred vision, diplopia, and weakness 24 hours after ingesting 250 mL of a methanolic antifreeze solution. Upon hospital admission she was comatose and in severe metabolic acidosis. An MRI scan at 9 days indicated abnormal hyperintense foci in the putamina (decreased in size by day 23) and subtle lesions (no change by day 23) in the white matter. Upon her discharge, bilateral deficits in visual acuity and color discrimination persisted.

Similar deficits (metabolic acidosis, visual acuity, and color discrimination) were seen in a man who ingested 300 mL of 75% methanol solution. His blood methanol level was 163 mg/dL (1,630 mg/L). An MRI administered 24 hours after hospital admission revealed abnormal hyperintense foci in the putamina, with less intense lesions in the white matter. Like the first subject, a subsequent MRI indicated the foci decreased in size over time, but visual impairments persisted.

The third individual, a male, ingested an unspecified amount of a methanolic solution. His blood methanol level was 1,290 mg/dL (12,900 mg/L), and he was in a coma upon hospital admission. An MRI revealed lesions in the putamina and occipital subcortical white matter. A follow-up CT scan was performed after 1 year and showed regression of the putaminal lesions

but no change in the occipital lesions. Upon his discharge, severe visual impairment remained but no extrapyramidal signs were observed.

The last case was a man who became comatose 12 hours after ingesting 100 mL methanol. His blood methanol level at that time was 60 mg/dL (600 mg/L). An MRI revealed lesions in the putamina; at 3 weeks these lesions were observed to have decreased in size. Upon his discharge, the neurological signs had improved but optic neuropathy (in visual evoked potential) was observed.

In a separate publication, Hantson et al. (1997b) reported a case of a 26-year-old woman who had ingested 250–500 mL methanol during the 38th week of pregnancy. Her initial blood methanol level was 230 mg/dL (2,300 mg/L) (formate was 33.6 mg/dL or 336 mg/L), yet only a mild metabolic acidosis was indicated. No distress to the fetus was observed upon gynecologic examination. Six days after therapy was initiated (methanol was not present in blood), she gave birth. No further complications with either the mother or newborn were noted.

There have been several case reports involving infant or toddler exposures to methanol (De Brabander et al., 2005; Wu et al., 1995; Brent et al., 1991; Kahn and Blum, 1979). The report by Wu et al. (1995) involved a 5-week-old infant with moderate metabolic acidosis and a serum methanol level of 1,148 mg/dL (11,480 mg/L), a level that is ordinarily fatal. However, this infant exhibited no toxic signs and survived without any apparent permanent problems. De Brabander et al. (2005) reported the case of a 3-year-old boy who ingested an unknown amount of pure methanol; at 3 hours after ingestion, the blood methanol level was almost 30 mg/dL (300 mg/L). Ethanol infusion as a therapeutic measure was not well tolerated; at 8 hours after ingestion, fomepizole was administered, and blood methanol levels stabilized below 20 mg/dL (200 mg/L), a level above which is considered to be toxic by the American Academy of Clinical Toxicology (Barceloux et al., 2002). Neither metabolic acidosis nor visual impairment was observed in this individual. Hantson et al. (1997a), in their review, touted the efficacy of fomepizole over ethanol in the treatment of methanol poisoning

Bilateral putaminal lesions, suggestive of nonhemorrhagic necrosis in the brain of a man who accidentally ingested methanol, were reported by Arora et al. (2005). Approximately 10 hours after MRI examination, he developed blurred vision and motor dysfunction. After 5 months, visual deficits persisted along with extrapyramidal symptoms. Persistent visual dysfunction was also reported in another methanol poisoning case (Arora et al., 2007); the vision problems developed ~46 hours subsequent to the incident.

Vara-Castrodeza et al. (2007) applied diffusion-weighted MRI on a methanol-induced comatose woman. Diffusion-weighted MRI provides an image contrast distinct from standard imaging in that contrast is dependent on the molecular motion of water (Schaefer et al., 2000). The neuroradiological findings were suggestive of bilateral putaminal hemorrhagic necrosis,

cerebral and intraventricular hemorrhage, diffuse cerebral edema, and cerebellar necrosis. Diffusion-weighted MRI allows for differentiation of restricted diffusion which is indicative of nonviable tissue. In this case, treatment for acidosis (blood methanol levels had risen to 1,000 mg/L) was unsuccessful and the patient died.

Emergency treatment was unable to save the life of a 38-year-old man who presented with abdominal pain and convulsions after methanol intoxication (Henderson and Brubacher, 2002). A review of a head CT scan performed before the individual went into respiratory arrest revealed bilateral globus pallidus ischemia.

Discrete lesions of the putamen, cerebral white matter, and corpus callosum were observed upon MRI (8 days post ingestion) in a man exposed to methanol (blood level 370 mg/L) complaining of vision loss (Keles et al., 2007). Standard treatments corrected the acidosis (pH 6.8), and at 1-month follow-up, his cognitive function improved but blindness and bilateral optic atrophy were described as permanent. The follow-up MRI showed persistent putaminal lesions with cortical involvement.

Fontenot and Pelak (2002) described a case of a woman who presented with persistent blurred vision and a worsening mental status 36 hours after ingestion of an unspecified amount of methanol. The initial CT scan revealed mild cerebral edema. The blood methanol level at this time was 86 mg/dL (860 mg/L). A repeat CT scan 48 hours after presentation showed hypodensities in the putamen and peripheral white matter. One month after discharge, cognitive function improved, and the patient experienced only a mild lower-extremity tremor.

Putaminal necrosis and edema of the deep white matter (the corpus callosum was not affected) was found upon MRI examination of a 50-year-old woman who apparently ingested an unknown amount of what was believed to be pure laboratory methanol (Kuteifan et al., 1998). Her blood methanol level was 39.7 mM (127 mg/dL; 1,272 mg/L) upon hospital admission and dropped to 102 mg/dL (1,020 mg/L) at 10 hours and to 71 mg/dL (710 mg/L) at 34 hours. The woman, a chronic alcoholic, was in a vegetative state when found and did not improved over the course of a year.

MRI and CT scans performed on a 51-year-old man with generalized seizures who had a blood methanol level of 95 mM (304 mg/dL; 3,044 mg/L) revealed bilateral hemorrhagic necrosis of the putamen and caudate nuclei (Gaul et al., 1995). In addition, there was extensive subcortical necrosis and bilateral necrosis of the pontine tegmentum and optic nerve. The patient died several hours after the scans were performed.

The relation of methanol overexposure to brain hemorrhage was a focus of the report by Phang et al. (1988), which followed the treatment of 7 individuals, 5 of whom died within 72 hours after hospital admission. In two of the deceased individuals, CT scans and autopsy revealed putaminal hemorrhagic necrosis. The investigators postulated that the association of

methanol with hemorrhagic necrosis may be complicated by the use of heparin during hemodialysis treatment for acidosis

Treatment of two men who had drunk a solution containing 58% methanol and presented with impaired vision, coma, and seizures was discussed in a case report by Bessell-Browne and Bynevelt (2007). A CT scan on one individual revealed bilateral putaminal and cerebral lesions. Blood methanol levels were 21 mg/L. This individual, despite standard treatments, never regained consciousness. The second individual, upon MRI, showed scattered hemorrhage at the grey-white interface of the cerebral hemispheres.

There have been two case reports (Adanir et al., 2005; Downie et al., 1992) that involved percutaneous and inhalation exposure. Use of a methanol-containing emollient by a woman with chronic pain led to vision loss, hyperventilation and finally, coma (Adanir et al., 2005). Subsequent to standard treatment followed by hospital discharge, some visual impairment and CNS decrements remained. The methanol blood threshold for ocular damage and acidosis appeared to be ~20 mg/L. Dutkiewicz et al. (1980) have determined the skin absorption rate to be 0.192 mg/cm^2/minute. In the case report of Aufderheide et al. (1993), two firefighters were transiently exposed to methanol by inhalation and the percutaneous route. Both only complained of a mild headache and had blood methanol levels of 23 and 16 mg/dL (230 and 160 mg/L), respectively.

Bebarta et al. (2006) conducted a prospective observational study of seven men who had purposefully inhaled a methanol-containing product. Four had a blood methanol level upon hospital presentation of >24 mg/dL (240 mg/L); the mean formic acid level was 71 µg/dL. One individual had a blood methanol level of 86 mg/dL (860 mg/L) and a blood formic acid level of 250 µg/mL upon hospital admission. This latter individual was treated with fomepizole. No patient had an abnormal ophthalmologic examination. All seven stabilized quickly and acidosis was normalized in 4 hours.

Numerous other case reports documenting putaminal necrosis/hemorrhage and/or blindness have been reported (Blanco et al., 2006; Feany et al., 2001; Hsu et al., 1997; Pelletier et al., 1992; Chen et al., 1991).

Hovda et al. (2005) presented a combined prospective and retrospective case series study of 51 individuals in Norway (39 males and 12 females, many of whom were alcoholics) who were hospitalized after consuming tainted spirits containing 20% methanol and 80% ethanol. In general, serum methanol concentrations were highest among those most severely affected. The poor outcome was closely correlated with the degree of metabolic acidosis. It was noted by the investigators that the concomitant consumption of ethanol prevented more serious sequelae in 2/5 individuals who presented with detectable ethanol levels and were not acidotic despite 2 having the highest blood methanol levels. However, others with detectable levels of ethanol

along with severe metabolic acidosis (two of whom died) presumably had subtherapeutic levels of ethanol in their system.

In a later report, Hovda et al. (2007) focused on formate kinetics in a 63-year-old male who died 6 days after being admitted to the hospital with headache, vomiting, reduced vision, and dizziness. The investigators speculated that the prolonged metabolic acidosis observed ($T^{1/2}$ for formic acid was 77 hours before dialysis, compared to a typical normal range of 2.5–12 hours) may have been related to retarded formate elimination.

Hovda and colleagues (Hunderi et al., 2006) found a strong correlation between blood methanol concentration and the osmolal gap ($R^2 = 0.92$) among 17 patients undergoing dialysis after consuming methanol-contaminated spirits. They concluded that the osmolal gap could be taken as a priori indication of methanol poisoning and be used to guide initiation and duration of dialysis. As they indicated, many hours of dialysis could be safely dispensed with. The osmolal gap pertains to the effect that methanol (and other alcohols) has on the depression of the freezing point of blood in the presence of normal solutes. Braden et al. (1993) demonstrated in case studies that the disappearance of the osmolal gap correlates with the correction of acidosis; they cautioned that methanol and ethanol should not be assumed to be the main factors in causing osmolal gap as glycerol and acetone and its metabolites can as well. A more detailed discussion of the anion and osmolal gap has been provided by Henderson and Brubacher (2002).

Hassanian-Moghaddam et al. (2007) compiled data on the prognostic factor relating to outcome in methanol-poisoning cases in Iran. They examined 25 patients, 12 of whom died; 3 of the survivors were rendered blind. There was a significant difference in mean pH of the first arterial blood gas measurements of those who subsequently died compared with survivors. It was concluded that poor prognosis was associated with pH <7, coma upon admission, and >24-hours delay from intake to admission.

The use of blood methanol levels as predictors of outcome is generally not recommended (Barceloux et al., 2002). These investigators cited differences in sampling time, ingestion of ethanol, and levels of toxic (e.g., formic acid) metabolites among the complicating factors. As an illustration, the case report by Prabhakaran et al. (1993) cites two women who ingested a methanol solution (photocopying diluent) at about the same time, were admitted to the hospital about the same time (25–26 hours after ingestion) and had identical plasma methanol concentrations (83 mg/dL; 830 mg/L) upon admission, but different outcomes. Patient #1 was in metabolic acidosis and had an unstable conscious state even after treatment. Upon discharge at day 6, there were no apparent sequelae. Patient #2 had severe metabolic acidosis, fixed and dilated pupils, and no brain stem reflexes. This patient died at day 3 even though therapeutic measures had been administered.

In a discussion of 3 fatal methanol-overexposure cases, Andresen et al. (2008) found antemortem blood methanol levels of 540 and 740 mg/dL (5,400 and 7,400 mg/L) in 2 individuals. At autopsy brain stem blood levels were 738 and 1,008 mg/dL (7,380 and 10,080 mg/L), respectively. These brain levels were much higher than blood levels postmortem. Autopsy revealed brain and pulmonary edema in all three individuals; in the two who had the longer survival times, there was hemorrhagic necrosis of the putamen and hemorrhages of the tissue surrounding the optic nerve. In their study of 26 chronic users of methylated spirits, Meyer et al. (2000) found that the best predictor of death or a poor outcome in chronic abusers was a pH <7.0; there was no correlation between blood methanol levels and outcome. Mahieu et al. (1989) considered a latency period before treatment exceeding 10 hours and a blood formate level >50 mg/dL (500 mg/L) as predictive of possible permanent sequelae. Liu et al. (1998) in their examination of medical records of 50 patients treated for methanol poisoning over a 10-year period found that 1) deceased patients had a higher mean blood methanol level than survivors; and 2) initial arterial pH levels <7.0 (i.e., severe metabolic acidosis). Coma or seizure was also associated with higher mortality upon hospital admission.

Numerous cases of methanol poisoning have been documented in a variety of countries. In Tunisia, 16 cases of methanol poisoning were discussed by Brahmi et al. (2007). Irreversible blindness occurred in two individuals, with others reporting CNS symptoms, GI effects, visual disturbances, and acidosis. Putaminal necrosis was also described in case reports from Iran (Sefidbakht et al., 2007). Of 634 forensic autopsies carried out in Turkey during 1992–2003, 18 appeared to be related to methanol poisoning (Azmak, 2006). Brain edema and focal necrosis of the optic nerve were among various sequelae noted. Dethlefs and colleagues (Naraqi et al., 1979; Dethlefs and Naraqi, 1978) described permanent ocular damage in 8/24 males who ingested methanol in Papua New Guinea.

In summary, most cases of accidental/intentional methanol poisoning reveal a common set of symptoms, many of which are likely to be presented upon hospital admission. These include:

- blurred vision and bilateral or unilateral blindness
- convulsions, tremors, and coma
- nausea, headache, and dizziness
- abdominal pain
- diminished motor skills
- acidosis
- dyspnea
- behavioral and/or emotional deficits
- speech impediments

Acute symptoms generally are nausea, dizziness, and headache. In the case reports cited above, the onset of symptom sets as well as their severity varies depending upon how much methanol was ingested, whether or not and when appropriate treatment was administered, and individual variability. A longer time between exposure and treatment, with few exceptions, results in more severe outcomes (e.g., convulsions, coma, blindness, and death). The diminution of some acute and/or delayed symptoms may reflect concomitant ingestion of ethanol or how quickly therapeutic measures (one of which includes ethanol infusion) were administered in the hospital setting.

Those individuals who are in a metabolic acidotic state (e.g., pH <7.0) are typically the individuals who manifest the more severe symptoms. Many case reports stress that, unlike blood pH levels <7.0, blood levels of methanol are not particularly good predictors of health outcome. According to a publication of the American Academy of Clinical Toxicology (Barceloux et al., 2002), "the degree of acidosis at presentation most consistently correlates with severity and outcome."

As the case reports demonstrate, those individuals who present with more severe symptoms (e.g., coma, seizures, severe acidosis) generally exhibit higher mortality (even after treatment) than those without such symptoms. In survivors of poisoning, persistence or permanence of vision decrements and particularly blindness often have been observed

Correlation of symptomatology with blood levels of methanol has been shown to vary appreciably between individuals. Blood methanol levels in the case reports involving ingestion ranged from values of 30 to over 1,000 mg/dL (300 to over 10,000 mg/L). The lowest value (20 mg/dL; 200 mg/L) reported (Adanir et al., 2005) involved a case of percutaneous absorption (with perhaps associated inhalation exposure) that led to vision and CNS deficits after hospital discharge. In one case report (Rubinstein et al., 1995) involving ingestion, coma and subsequent death were associated with an initial blood methanol level of 36 mg/dL (360 mg/L).

Upon MRI and CT scans, the more seriously affected individuals typically have focal necrosis in both brain white matter and more commonly, in the putamen. Bilateral hemorrhagic and nonhemorrhagic necrosis of the putamen is considered by many radiologists as the most well-known sequelae of methanol overexposure.

4.1.2. Occupational Studies

Occupational health studies have been carried out to investigate the potential effects of chronic exposure to lower levels of methanol than those seen in acute poisoning cases such as those described above. For example, Frederick et al. (1984) conducted a health hazard evaluation on behalf of the National Institute for Occupational Safety and Health (NIOSH) to

determine if vapor from duplicating fluid (which contains 99% methanol) used in mimeograph duplicating machines caused adverse health effects in exposed persons. A group of 84 teacher's aides were selected for study, 66 of whom responded with a completed medical questionnaire. A group of 297 teachers (who were not exposed to methanol vapors to the same extent as the teacher's aides) completed questionnaires as a control group. A 15-minute breathing zone sample was taken from 21 duplicators, 15 of which were greater than the NIOSH-recommended short term ceiling concentration of 800 ppm (1048 mg/m^3). The highest breathing zone concentrations were in the vicinity of duplicators for which no exhaust ventilation had been provided (3,080 ppm [4,036 mg/m^3] was the highest value recorded). Upon comparison of the self-described symptoms of the 66 teacher's aides with those of 66 age-matched teachers chosen from the 297 who responded, the number of symptoms potentially related to methanol were significantly higher in the teacher's aides. These included blurred vision (22.7 versus 1.5%), headache (34.8 versus 18.1%), dizziness (30.3 versus 1.5%), and nausea (18 versus 6%). By contrast, symptoms that are not usually associated with methanol exposure (painful urination, diarrhea, poor appetite, and jaundice) were similar in incidence among the groups.

To further investigate these disparities, NIOSH physicians (not involved in the study) defined a hypothetical case of methanol toxicity by any of the following four symptom aggregations: 1) visual changes; 2) one acute symptom (headache, dizziness, numbness, giddiness, nausea or vomiting) combined with one chronic symptom (unusual fatigue, muscle weakness, trouble sleeping, irritability, or poor memory); 3) two acute symptoms; or 4) three chronic symptoms. By these criteria, 45% of the teacher's aides were classified as being adversely affected by methanol exposure compared to 24% of teachers ($p < 0.025$). Those teacher's aides and teachers who spent a greater amount of time using the duplicators were affected at a higher rate than those who used the machines for a lower percentage of their work day.

Tanner (1992) reviewed the occupational and environmental causes of Parkinsonism, spotlighting the potential etiological significance of manganese, carbon monoxide, repeated head trauma (such as suffered by boxers), and exposure to solvents. Among the latter, Tanner (1992) discussed the effects of methanol and n-hexane on the nervous system. Acute methanol intoxication resulted in inebriation, followed within hours by GI pain, delirium, and coma. Tanner (1992) pinpointed the formation of formic acid, with consequent inhibition of cytochrome oxidase, impaired mitochondrial function, and decreased ATP formation as relevant biochemical and physiological changes for methanol exposure. Nervous system injury usually includes blindness, Parkinson-like symptoms, dystonia, and cognitive impairment, with injury to putaminal neurons most likely underlying the neurological responses.

Kawai et al. (1991) carried out a biomarker study in which 33 occupationally exposed workers in a factory making methanol fuel were exposed to concentrations of methanol of up to 3,577 ppm (4,687 mg/m^3), as measured by personal samplers of breathing zone air. Breathing zone exposure samples were correlated with the concentrations of methanol in urine at the end of the shift in 38 exposed individuals and 30 controls (r = 0.82). Eleven of 22 individuals who experienced high exposure to methanol (geometric mean of 459 ppm [601 mg/m^3]) complained of dimmed vision during work while 32% of this group of workers experienced nasal irritation. These incidences were statistically significant compared to those of persons who worked in low-exposure conditions (geometric mean of 31 ppm [41 mg/m^3]). One 38-year-old female worker who had worked at the factory for only 4 months reported that her visual acuity had undergone a gradual impairment. She also displayed a delayed light reflex.

Lorente et al. (2000) carried out a case control study of 100 mothers whose babies had been born with cleft palates. Since all of the mothers had worked during the first trimester, Lorente et al. (2000) examined the occupational information for each subject in comparison to 751 mothers whose babies were healthy. Industrial hygienists analyzed the work histories of all subjects to determine what, if any, chemicals the affected mothers may have been exposed to during pregnancy. Multivariate analysis was used to calculate odds ratios, with adjustments made for center of recruitment, maternal age, urbanization, socioeconomic status, and country of origin. Occupations with positive outcomes for cleft palate in the progeny were hairdressing (OR = 5.1, with a 95% confidence interval [CI] of 1.0–26) and housekeeping (OR = 2.8, with a 95% CI of 1.1–7.2). Odds ratios for cleft palate only and cleft lip with or without cleft palate were calculated for 96 chemicals. There seemed to be no consistent pattern of association for any chemical or group of chemicals with these impairments, and possible exposure to methanol was negative for both outcomes.

4.1.3. Controlled Studies

Two controlled studies have evaluated humans for neurobehavioral function following exposure to ~200 ppm (262 mg/m^3) methanol vapors in a controlled setting. The occupational TLV established by the American Conference of Governmental Industrial Hygienists (ACGIH, 2000) is 200 ppm (262 mg/m^3). In a pilot study by Cook et al. (1991), 12 healthy young men (22–32 years of age) served as their own controls and were tested for neurobehavioral function following a random acute exposure to air or 191 ppm (250 mg/m^3) methanol vapors for 75 minutes. The majority of results in a battery of neurobehavioral endpoints were negative. However, statistical significance was obtained for results in the P-200 and N1-P2 component of event-related potentials (brain wave patterns following light flashes and sounds), the Sternberg memory task, and subjective evaluations of concentration and fatigue. As noted by the Cook et

al. (1991), effects were mild and within normal ranges. Cook et al. (1991) acknowledged limitations in their study design, such as small sample size, exposure to only one concentration for a single duration time, and difficulties in masking the methanol odor from experimental personnel and study subjects.

In a randomized double-blind study, neurobehavioral testing was conducted on 15 men and 11 women (healthy, aged 26–51 years) following exposure to 200 ppm (262 mg/m^3) methanol or water vapors for 4 hours (Chuwers et al., 1995); subjects served as their own controls in this study. Exposure resulted in elevated blood and urine methanol levels (up to peak levels of 6.5 mg/L and 0.9 mg/L, respectively) but not formate concentrations. The majority of study results were negative. No significant findings were noted for visual, neurophysiological, or neurobehavioral tests except for slight effects ($p < 0.05$) on P-300 amplitude (brain waves following exposure to sensory stimuli) and Symbol Digit testing (ability to process information and psychomotor skills). Neurobehavioral performance was minimally affected by methanol exposure at this level. Limitations noted by Chuwers et al. (1995) are that studies of alcohol's affect on P-300 amplitude suggest that this endpoint may be biased by unknown factors and some experimenters and subjects correctly guessed if methanol was used.

Although the slight changes in P-200 and P-300 amplitude noted in both the Chuwers et al. (1995) and Cook et al. (1991) studies may be an indication of moderate alterations in cognitive function, the results of these studies are generally consistent and suggest that the exposure concentrations employed were below the threshold for substantial neurological effects. This is consistent with the data from acute poisoning events which have pointed to a serum methanol threshold of 200 mg/L for the instigation of acidosis, visual impairment, and CNS deficits.

Mann et al. (2002) studied the effects of methanol exposure on human respiratory epithelium as manifested by local irritation, ciliary function, and immunological factors. Twelve healthy men (average age 26.8 years) were exposed to 20 and 200 ppm (26.2 and 262 mg/m^3, respectively) methanol for 4 hours at each concentration; exposures were separated by 1-week intervals. The 20 ppm (26.2 mg/m^3) concentration was considered to be the control exposure since previous studies had demonstrated that subjects can detect methanol concentrations of 20 ppm (26.2 mg/m^3) and greater. Following each single exposure, subclinical inflammation was assessed by measuring concentrations of interleukins (IL-8, IL-1β, and IL-6) and prostaglandin E2 in nasal secretions. Mucociliary clearance was evaluated by conducting a saccharin transport time test and measuring ciliary beat frequency. Interleukin and prostaglandin data were evaluated by a 1-tailed Wilcoxon test, and ciliary function data were assessed by a 2-tailed Wilcoxon test. Exposure to 200 (262 mg/m^3) versus 20 ppm (26.2 mg/m^3) methanol resulted in a statistically-significant increase in IL-1β (median of 21.4 versus 8.3 pg/mL) and IL-8 (median of

424 versus 356 pg/mL). There were no significant effects on IL-6 and prostaglandin E2 concentration, ciliary function, or on the self-reported incidence of subjective symptoms of irritation. The authors concluded that exposure to 200 ppm (262 mg/m^3) methanol resulted in a subclinical inflammatory response.

In summary, adult human subjects acutely exposed to 200 ppm (262 mg/m^3) methanol have experienced slight neurological (Chuwers et al., 1995) and immunological effects (increased subclinical biomarkers for inflammation) with no self-reported symptoms of irritation (Mann et al., 2002). These exposure levels were associated with peak methanol blood levels of 6.5 mg/L (Chuwers et al., 1995), which is approximately threefold higher than background methanol blood levels reported for adult human subjects on methanol-restrictive diets (Table 3-1). Nasal irritation effects have been reported by adult workers exposed to 459 ppm (601 mg/m^3) methanol (Kawai et al., 1991). Frank effects such as blurred vision, bilateral or unilateral blindness, coma, convulsions/tremors, nausea, headache, abdominal pain, diminished motor skills, acidosis, and dyspnea begin to occur as blood levels approach 200 mg methanol/L, while 800 mg/L appears to be the threshold for lethality. Data for subchronic, chronic or in utero human exposures are very limited and inconclusive.

4.2. ACUTE, SUBCHRONIC AND CHRONIC STUDIES AND CANCER BIOASSAYS IN ANIMALS—ORAL AND INHALATION

A number of studies in animals have investigated the acute, subchronic, and chronic toxicity of methanol. Most are via the inhalation route. Presented below are summaries of these investigations.

4.2.1. Oral Studies

4.2.1.1. *Acute Toxicity*

Although there are few studies that have examined the short-term toxic effects of methanol via the oral route, a number of median lethal dose (LD_{50}) values have been published for the compound. As listed in Lewis (1992), these include 5,628 mg/kg in rats, 7,300 mg/kg in mice, and 7,000 mg/kg in monkeys.

4.2.1.2. *Subchronic Toxicity*

An oral repeat dose study was conducted by the EPA (1986c) in rats. Sprague-Dawley rats (30/sex/dose) were gavaged with 0, 100, 500, or 2,500 mg/kg-day of methanol. Six weeks after dosing, 10 rats/sex/dose group were subjected to interim sacrifice, while the remaining rats continued on the dosing regimen until the final sacrifice (90 days). This study generated data on weekly body weights and food consumption, clinical signs of toxicity, ophthalmologic evaluations, mortality, blood and urine chemistry (from a comprehensive set of hematology,

serum chemistry, and urinalysis tests), and gross and microscopic evaluations for all test animals. Complete histopathologic examinations of over 30 organ tissues were done on the control and high-dose rats. Histopathologic examinations of livers, hearts, and kidneys and all gross lesions seen at necropsy were done on low-dose and mid-dose rats. There were no differences between dosed animals and controls in body weight gain, food consumption, or upon gross or microscopic evaluations. Elevated levels ($p \leq 0.05$ in males) of serum alanine transaminase (ALT)[14] and serum alkaline phosphatase (SAP), and increased (but not statistically significant) liver weights in both male and female rats suggest possible treatment-related effects in rats bolus dosed with 2,500 mg methanol/kg-day despite the absence of supportive histopathologic lesions in the liver. Brain weights of high-dose group (2,500 mg/kg-day) males and females were significantly less than those of the control group at terminal sacrifice. Based on these findings, 500 mg/kg-day of methanol is considered an NOEL from this rat study.

4.2.1.3. *Chronic Toxicity*

A report by Soffritti et al. (2002a) summarized a European Ramazzini Foundation (ERF) chronic duration experimental study of methanol[15] in which the compound was provided to 100 Sprague-Dawley rats/sex/group ad libitum in drinking water at concentrations of 0, 500, 5,000, and 20,000 ppm (v/v). The animals were 8 weeks old at the beginning of the study. In general, ERF does not randomly assign animals to treatment groups, but assigns all animals from a given litter to the same treatment group (Bucher, 2002). All rats were exposed for up to 104 weeks, then maintained until they died naturally. Rats were housed in groups of 5 in Makrolon cages (41 × 25 × 15 cm) in a room that was maintained at 23 ± 2°C and 50–60% relative humidity. The in-life portion of the experiment ended at 153 weeks with the death of the last animal. Mean daily drinking water, food consumption, and body weights were monitored weekly for the first 13 weeks, every 2 weeks thereafter for 104 weeks, then every 8 weeks until the end of the experiment. Clinical signs were monitored 3 times/day, and the occurrence of gross changes was evaluated every 2 weeks. All rats were necropsied at death then underwent histopathologic examination of organs and tissues.[16]

---

[14] Also known as serum glutamate pyruvate transaminase (SGPT)

[15] Soffritti et al. (2002a) report that methanol was obtained from J.T. Baker, Deventer, Holland, purity grade 99.8%.

[16] Histopathology was performed on the following organs and tissues: skin and subcutaneous tissue, brain, pituitary gland, Zymbal glands, parotid glands, submaxillary glands, Harderian glands, cranium (with oral and nasal cavities and external and internal ear ducts) (5 sections of head), tongue, thyroid and parathyroid, pharynx, larynx, thymus and mediastinal lymph nodes, trachea, lung and mainstem bronchi, heart, diaphragm, liver, spleen, pancreas, kidneys, adrenal glands, esophagus, stomach (fore and glandular), intestine (four levels), urinary bladder, prostate, gonads, interscapular fat pad, subcutaneous and mesenteric lymph nodes, and any other organs or tissues with pathologic lesions.

Soffritti et al. (2002a) reported no substantial dose-related differences in survival, but no data were provided. Using individual animal data available from the ERF website,[17] Cruzan (2009) reports that male rats treated with methanol generally survived better than controls, with 50% survival occurring at day 629, 686, 639 and 701 in the 0, 500, 5,000, and 20, 000 mg/L groups, respectively. There were no significant differences in survival between female control and treatment groups, with 50% survival occurring at day 717, 691, 678 and 708 in the 0, 500, 5,000, and 20, 000 mg/L groups, respectively. Body weight and water and food consumption were monitored in the study, but the data were not documented in the published report. However, based on data available from the ERF website, average doses of 0, 53.2, 524, and 1,780 mg/kg-day in males and 0, 66.0, 624.1, and 2,177 mg/kg-day in females could be calculated (see Appendix E) from drinking water concentrations of 0, 500, 5,000, and 20,000 ppm.

Soffritti et al. (2002a) reported that water consumption in high-dose females was reduced compared to controls between 8 and 56 weeks and that the mean body weight in high-dose males tended to be higher than that of control males. Overall, there was no pattern of compound-related clinical signs of toxicity, and the available data did not provide any indication that the control group was not concurrent with the treated group (Cruzan, 2009). Soffritti et al. (2002a) further reported that there were no compound-related signs of gross pathology or histopathologic lesions indicative of noncancer toxicological effects in response to methanol.

Soffritti et al. (2002a) reported a number of oncogenic responses to methanol (Table 4-2), principally hemolymphoreticular neoplasms, the majority of which were reported to be lympho-immunoblastic lymphomas. In ERF bioassays, including this methanol study, hemolymphoreticular neoplasms are generally divided into specific histological types (lymphoblastic lymphoma, lymphoblastic leukemia, lymphocytic lymphoma, lympho-immunoblastic lymphoma, myeloid leukemia, histocytic sarcoma, and monocytic leukemia) for identification purposes. According to Soffritti et al. (2007), the overall incidence of hemolymphoreticular tumors (lymphomas/leukemias) in ERF studies is 13.3% (range, 4.0–25.0%) in female historical controls (2,274 rats) and 20.6% (range, 8.0–30.9%) in male historical controls (2,265 rats). The high-dose responses, shown in Table 4-2, of 28% and 40% for females and males, respectively, are above their corresponding historical ranges.[18]

The National Toxicology Program (NTP) does not routinely subdivide lymphomas into specific histological types as was done by the ERF. In 2004, a Pathology Working Group (PWG) of National Institute of Environmental Health Sciences (NIEHS) performed a limited review of about 75 slides provided by ERF as representive of lesions in Sprague-Dawley rats

[17] http://www.ramazzini.it/fondazione/foundation.asp.

[18] While historical control data can be informative, for reasonably well-conducted studies, it should not take precedence over concurrent controls or appropriate statistical dose-response trend tests.

associated with aspartame exposure (EFSA, 2006; Hailey, 2004). The primary objective of this review was to "provide a second opinion for this set of lesions by a group of pathologists experienced in Toxicologic Pathology."[19] Eleven of the slides reviewed by the PWG were related to lymphomas, and three of these had been classified by ERF as lympho-immunoblastic. The PWG concluded that "The diagnoses of lymphatic and histocytic neoplasms in the cases reviewed were generally confirmed" (Hailey, 2004). In particular, the PWG accepted the more specific diagnoses of ERF when the lesions were considered to be consistent with a neoplasm of lymphocytic, histocytic, monocytic, and/or myeloid origin. The PWG noted, however, that while lymphoblastic lymphomas, lymphocytic lymphomas, lympho-immunoblastic lymphomas, and lymphoblastic leukemias as malignant lymphomas can be combined, myeloid leukemias, histocytic sarcomas, and monocytic leukemia should be treated as separate malignancies and not combined with the other lymphomas since they are of different cellular origin (Hailey, 2004). McConnell et al. (1986) and Cruzan (2009) have also noted that myeloid leukemia, histocytic sarcoma, and monocytic leukemia are of a different cell line and are not typically combined with other lymphomas for statistical significance or dose-response modeling. Consistent with these judgments, EPA has not included the myeloid leukemia, histocytic sarcoma, and monocytic leukemia in combination with lymphoblastic lymphoma, lymphoblastic leukemia, lymphocytic lymphoma, and lympho-immunoblastic lymphoma in its consideration of tumorgenic responses reported by ERF (see Section 5.4.1; Table 5-6). Thus, EPA's analysis of this tumorogenic response differs from the lymphoreticular tumor response shown in Table 4-2 and reported by Soffriti et al. (2002a). As described in Section 5.4.1.1, EPA's reassessment indicates a significant increase in tumor response at the two highest doses for males and across all doses for females (Fisher's exact, $p < 0.05$), as well as a significant dose-response trend (Cochran Armitage trend test; $p < 0.05$).

Schoeb et al. (2009) have suggested that the interpretation of lesions in ERF studies, including the Soffritti et al. (2002a) methanol study, may have been confounded by a respiratory infection referred to as *Mycoplasma pulmonis (M. pulmonis)* disease and that lesions of this disease were interpreted as lymphoma. They noted that lympho-immunoblastic lymphoma is not listed as a lymphoma type in rats in available reference sources and that the cellular morphology of the lung lympho-immunoblastic lymphomas reported by ERF for aspartame (Soffritti et al., 2005) and MTBE (Belpoggi et al., 1999) studies are more consistent with *M. pulmonis* disease. As noted above, an NIEHS PWG (Hailey, 2004) has confirmed the ERF diagnosis of the several lymphomas, including three lymphomas from the lung, thymus and medullary lymph node and mesenteric lymph node that were characterized by ERF as "lympho-immunoblastic." Hailey

[19] This review was not considered a "peer review" of the pathology data from this study. As noted by Hailey (2004), "a peer review would necessitate a review of the study data by a second party, and selection and examination of lesions based upon that data review."

(2004) reports that the PWG "accepted their [ERF's] more specific diagnosis if the lesion was considered to be consistent with a neoplasm of lymphocytic, histocytic, monocytic, and/or myeloid origin." The concerns of Schoeb et al. (2009) regarding the possibility of infection confounding the interpretation of lung lesions in the ERF study are not unfounded. Chronic inflammatory changes are apparently a common finding in ERF studies (Caldwell et al., 2008), probably caused by the ERF bioassay design that does not employ specific pathogen-free (SPF) rats (EFSA, 2006) and allows the rats to live out their "natural life span" in the absence of disease barriers (e.g., fully enclosed cages). However, an infection of the ERF colony with *M. pulmonis* has not been confirmed (Caldwell et al., 2008) and, without confirmation, cannot be used to discount an existing dose-related trend (U.S. EPA, 2005). Further, even if the rats of the ERF methanol study were suffering from a respiratory infection that confounded the interpretation of lung lesions, 60% of reported lymphoma incidences involved other organ systems, and the dose-response for lymphomas in other organ systems is not remarkably different than for all lymphomas (see analysis in Section 5.4.3.2).

Another cancer response, reported by Soffritti et al. (2002a), that is considered to be potentially related to methanol exposure was an increase in rare hepatocellular carcinomas in male rats. Although the increase was not statistically increased compared to concurrent controls, EPA has analyzed historical data for this tumor type in this species and determined that the incidence in all dose groups was significantly elevated relative to historical controls (Fisher's exact $p < 0.05$ for all doses and $p < 0.01$ for the high-dose group). The historical control group (n = 407) used was the combined control groups from ERF studies for which individual animal pathology data have been made available via the ERF website[20] and include data for methanol, formaldehyde, aspartame, MTBE, and TAME.

As noted in Table 4-2, increased incidences of carcinomas of the ear ducts and osteosarcomas of the head were reported for both female and male rats, with a statistically significant increase in only the high-dose male ear duct carcinomas. Ear duct carcinomas are a rare finding in Charles River rats and NTP historical databases of Sprague-Dawley rats (Cruzan, 2009). In their limited review of pathology slides from the ERF aspartame bioassay (Soffritti et al., 2006, 2005), NTP pathologists interpreted a majority of such head pathologies, including in the ear duct, as being hyperplastic in nature, not carcinogenic (EFSA, 2006; Hailey, 2004). Soffritti et al. (2002a) also noted an increased incidence of testicular hyperplasia in high-dose males and uterine sarcomas in high-dose females compared to controls. However, these increases were not statistically significant and were within historical control ranges for this species and strain (NTP, 2007, 1999; Haseman et al., 1998). The group-specific total number of malignant tumors was also shown to increase with dose in both sexes of rats.

[20] http://www.ramazzini.it/fondazione/foundation.asp.

Table 4-2. Incidence of carcinogenic responses in Sprague-Dawley rats exposed to methanol in drinking water for up to 2 years

Tissues/affected sites	Dose (mg/kg-day)							
	Males				Females			
	0	53.2	524	1780	0	66.0	624.1	2177
Ear duct (carcinomas)	9/100	13/100	17/100	24/100[b]	9/100	8/100	16/100	19/100
Head (osteosarcomas)	6/100	6/100	13/100	11/100	1/100	4/100	3/100	6/100
Hemolymphoreticular tumors	28/100	35/100	36/100	40/100	13/100	24/100	24/100	28/100[a]
Liver (hepatocarcinomas)	0/100	2/100	2/100	3/100	0/100	0/100	1/100	0/100
Testis (interstitial cell adenomas)	12/100	9/100	13/100	17/100				
Total malignant tumors	50/100	55/100	64/100	70/100[b]	43/100	48/100	48/100	63/100[b]

[a]$p < 0.05$ using the χ^2 test.
[b]$p < 0.01$ using the χ^2 test.

Source: Soffritti et al. (2002a).

Apaja (1980) performed dermal and drinking water chronic bioassays in which male and female Eppley Swiss Webster mice (25/sex/dose group; 8 weeks old at study initiation) were exposed 6 days per week until natural death to various concentrations of malonaldehyde and methanol. The stated purpose of the study was to determine the carcinogenicity of malonaldehyde, a product of oxidative lipid deterioration in rancid beef and other food products in advanced stages of degradation. However, due to its instability, malonaldehyde was obtained from the more stable malonaldehyde bis(dimethyacetal), which was hydrolyzed to malonaldehyde and methanol in dilute aqueous solutions in the presence of a strong mineral acid. In the drinking water portion of this study, mice were exposed to 3 different concentrations of the malonaldehyde/methanol solution and three different control solutions of methanol alone, 0.222%, 0.444% and 0.889% methanol in drinking water (222, 444 and 889 ppm, assuming a density of 1 g/ml), corresponding to the stoichiometric amount of methanol liberated by hydrolysis of the acetal in the three test solutions. The methanol was described as Mallinckrodt analytical grade. No unexposed control groups were included in these studies. However, the author provided pathology data from historical records of untreated Swiss mice of the Eppley colony used in two separate chronic studies, one involving 100 untreated males and 100 untreated females (Toth et al., 1977) and the other involving 100 untreated females histopathological analyzed by Apaja (Apaja, 1980).

Mice in the Apaja (1980) study were housed five/plastic cage and fed Wayne Lab-Blox pelleted diet. Water was available ad libitum throughout life. Liquid consumption per animal was measured 3 times/week. The methanol dose in the dermal study (females only) was 21.3 mg (532 mg/kg-day using an average weight of 0.04 kg as approximated from Figure 4 of the study), three times/week. The methanol doses in the drinking water study were reported as 22.6, 40.8

and 84.5 mg/day (560, 1000 and 2100 mg/kg-day using an average weight of 0.04 kg as approximated from Figures 14-16 of the study) for females, and 24.6, 43.5 and 82.7 mg/day (550, 970, and 1800 mg/kg-day using an average weight of 0.045 kg as approximated from Figures 14-16 of the study) for males, 6 days/week. The animals were checked daily and body weights were monitored weekly. The in-life portion of the experiment ended at 120 weeks with the death of the last animal. Like the Soffritti et al. (2002a) study, test animals were sacrificed and necropsied when moribund.[21]

The authors reported that survival of the methanol exposed females of the drinking water study was lower than untreated historical controls ($p < 0.05$), but no significant differences in survival was noted for males. An increase in liver parenchymal cell necrosis was reported in the male and female high-dose groups, with the incidence in females (8%) being significant ($p < 0.01$) relative to untreated historical controls. Incidence of acute pancreatitis was higher in high-dose males ($p <0.001$), but did not appear to be dose-related in females, increasing at the mid- ($p <0.0001$) and low-doses ($p <0.01$) when compared to historical controls but not appearing at all in the high-dose females. Significant increases relative to untreated historical controls were noted in amyloidosis of the spleen, nephropathy and pneumonia, but the increases did not appear to be dose related.

The author reported incidences of malignant lymphoma in females of 15%, 16%, 36%, and 40% for 532 mg/kg-day (dermal), 560, 1,000, and 2,100 mg/kg-day (drinking water), respectively. Males from the drinking water study had incidences of malignant lymphoma of 4, 24, and 16% for 550, 970, and 1,800 mg/kg-day. The lymphomas were classified according to Rappaport's classification (Rappaport, 1966), but location of the lymphoma (organ system) was not reported. The distributions of lymphomas according to subclasses reported by the author are shown in Table 4-3 for historical untreated and methanol exposed mice in the drinking water studies. The author indicates that the incidences in both males and females were "within the normal range of occurrence of malignant lymphomas in Eppley Swiss mice," but provides no references or supporting data for this statement and reports elsewhere that the response in high-dose females and mid-dose males were significantly different from unexposed mice from "historical data of untreated controls (Table 9)" of Toth et al. (1977) ($p < 0.05$). Though not statistically significant (Fishers exact $p = 0.06$), the malignant lymphoma response in the mid-dose females was also more than double that of untreated controls from another study (18/100) for which the histopathology was also performed by Apaja (Apaja, 1980).

[21] The following tisues were fixed in 10% formalin (pH 7.5), embedded in paraffin, sectioned, stained routinely with hematoxylineosin (special stains used as needed) and histologically evaluated: skin, lungs, liver spleen, pancreas, kidneys, adrenal glands, esophagus, stomach, small and large intestines, rectum, urinary bladder, uterus and ovaries or testes, prostate glands and tumors or other gross pathological lesions.

Table 4-3. Incidence of malignant lymphoma responses in Swiss mice exposed to methanol in drinking water for life

Malignant Lymphoma	Dose (mg/kg-day)								
	Males (%)				Females (%)				
	0[a] n=100	550 n=25	970 n=25	1800 n=24	0[a] n=100	0[b] n=100	560 n=25	1000 n=25	2100 n=25
Lymphocytic, well diff.						8		4	12
Lymphocytic moderately diff.			4			3		4	4
Lymphocytic, poorly diff.			4	8.3		7	4	4	4
Mixed cell type			4				4	4	8
Histocytic type		4	4	4.2			12	12	8
Unclassified			8	4.2				8	4
Total	8	4	24[c]	17	20	18	16	36[d]	40[c]

[a]Toth et al. (1977); [b] Hinderer et al. (1979)
[c]$p < 0.05$ as reported by author compared with Toth et al. (1977); Female response is also significant ($p < 0.05$; Fishers exact test) versus untreated controls from Hinderer et al. (1979) and combined controls from both studies.
[d]$p = 0.06$ by Fishers exact test versus untreated controls from Hinderer et al. (1979) and combined controls from both studies.

4.2.2. Inhalation Studies

4.2.2.1. *Acute Toxicity*

Lewis (1992) reported a 4-hour median lethal concentration (LC_{50}) for methanol in rats of 64,000 ppm (83,867 mg/m^3).

Japan's NEDO sponsored a series of toxicological tests on monkeys (*M. fascicularis*), rats, and mice, using inhalation exposure.[22] A short-term exposure study evaluated monkeys (sex unspecified) exposed to 3,000 ppm (3,931 mg/m^3), 21 hours/day for 20 days (1 animal), 5,000 ppm (6,552 mg/m^3) for 5 days (1 animal), 5,000 ppm (6,552 mg/m^3) for 14 days (2 animals), and 7,000 and 10,000 ppm (9,173 and 13,104 mg/m^3, respectively) for up to 6 days (1 animal at each exposure level) (NEDO, 1987, unpublished report). Most of the experimental findings were discussed descriptively in the report, without specifying the extent of change for any of the effects in comparison to seven concurrent controls. However, the available data indicate that clinical signs of toxicity were apparent in animals exposed to 5,000 ppm (all exposure durations) or higher concentrations of methanol. These included reduced movement, crouching, weak knees, involuntary movements of hands, dyspnea, and vomiting. In the

[22] In their bioassays, NEDO (1987) used inbred rats of the F344 or Sprague-Dawley strain, inbred mice of the B6C3F1 strain and wild-caught *M. fascicularis* monkeys imported from Indonesia. The possibility of disease among wild-caught animals is a concern, but NEDO (1987) state that the monkeys were initially quarantined for 9 weeks and measures were taken throughout the studies against the transmission of pathogens for infectious diseases. The authors indicated that "no infectious disease was observed in monkeys" and that "subjects were healthy throughout the experiment."

discussion section of the summary report, the authors stated that there was a sharp increase in the blood levels of methanol and formic acid in monkey exposed to >3,000 ppm (3,931 mg/m^3) methanol. They reported that methanol and formic acid concentrations in the blood of monkeys exposed to 3,000 ppm or less were 80 mg/L and 30 mg/L, respectively.[23] In contrast, monkeys exposed to 5,000 ppm or higher concentrations of methanol had blood methanol and formic acid concentrations of 5,250 mg/L and 1,210 mg/L, respectively. Monkeys exposed to 7,000 ppm and 10,000 ppm became critically ill and had to be sacrificed prematurely. Food intake was said to be little affected at 3,000 ppm, but those exposed to 5,000 ppm or more showed a marked reduction. Clinically, the monkeys exposed to 5,000 ppm or more exhibited reduced movement, weak knees, and involuntary movement of upper extremities, eventually losing consciousness and dying.

There were no significant changes in growth, with the exception of animals exposed to the highest concentration, where body weight was reduced by 13%. There were few compound-related changes in hematological or clinical chemistry effects, although animals exposed to 7,000 and 10,000 ppm showed an increase in white blood cells. A marked change in blood pH values at the 7,000 ppm and 10,000 ppm levels (values not reported) was attributed to acidosis due to accumulation of formic acid. A range of histopathologic changes to the CNS was apparently related to treatment. Severity of the effects was increased with exposure concentration. Lesions included characteristic degeneration of the bilateral putamen, caudate nucleus, and claustrum, with associated edema in the cerebral white matter. Necrosis of the basal ganglia was noted following exposure to 5,000 ppm for 5 days (1 animal) and 14 days(1 animal). Exposure to 3,000 ppm was considered to be close to the threshold for these necrotic effects, as the monkeys exposed at this level experienced little more than minimal fibrosis of responsive stellate cells of the thalamus, hypothalamus and basal ganglion. The authors reported that no clinical or histopathological effects of the visual system were apparent, but that exposure to 3,000 ppm (3,931 mg/m^3) or more caused dose-dependent fatty degeneration of the liver, and exposure to 5,000 ppm (6,552 mg/m^3) or more caused vacuolar degeneration of the kidneys, centered on the proximal uniferous tubules.

4.2.2.2. *Subchronic Toxicity*

A number of experimental studies have examined the effects of subchronic exposure to methanol via inhalation. For example, Sayers et al. (1944) employed a protocol in which 2 male dogs were repeatedly exposed (8 times daily for 3 minutes/exposure) to 10,000 ppm (13,104 mg/m^3) methanol for 100 days. One of the dogs was observed for a further 5 days before sacrifice; the other dog was observed for 41 days postexposure. There were no clinical

[23] Note that Burbacher et al. (2004b, 1999a) measured blood levels of methanol and formic acid in control monkeys of 2.4 mg/L and 8.7 mg/L, respectively (see Table 3-3).

signs of toxicity, and both gained weight during the study period. Blood samples were drawn on a regular basis to monitor hematological parameters, but few if any compound-related changes were observed. Ophthalmoscopic examination showed no incipient anomalies at any point during the study period. Median blood concentrations of methanol were 65 mg/L (range 0–280 mg/L) for one dog, and 140 mg/L (70–320 mg/L) for the other.

White et al. (1983) exposed 4 male Sprague-Dawley rats/group, 6 hours/day, 5 days/week to 0, 200, 2,000, or 10,000 ppm (0, 262, 2,621, and 13,104 mg/m^3) methanol for periods of 1, 2, 4, and 6 weeks. Additional groups of 6-week-exposure animals were granted a 6-week postexposure recovery period prior to sacrifice. The lungs were excised intact and lavaged 6 times with known volumes of physiological saline. The lavage supernatant was then assayed for lactate dehydrogenase (LDH) and *N*-acetyl-*β*-*D*-glucosamidase (*β*-NAG) activities. Other parameters monitored in relation to methanol exposure included absolute and relative lung weights, lung DNA content, protein, acid RNase and acid protease, pulmonary surfactant, number of free cells in lavage/unit lung weight, surface protein, LDH, and *β*-NAG. As discussed by the authors, none of the monitored parameters showed significant changes in response to methanol exposure.

Andrews et al. (1987) carried out a study of methanol inhalation in 5 Sprague-Dawley rats/sex/group and 3 *M. fascicularis* monkeys/sex/group, 6 hours/day, 5 days/week, to 0, 500, 2,000, or, 5,000 ppm (0, 660, 2,620, and 6,552 mg/m^3) methanol for 4 weeks. Clinical signs were monitored twice daily, and all animals were given a physical examination once a week. Body weights were monitored weekly, and animals received an ophthalmoscopic examination before the start of the experiment and at term. Animals were sacrificed at term by exsanguination following i.v. barbiturate administration. A gross necropsy was performed, weights of the major organs were recorded, and tissues and organs taken for histopathologic examination. As described by the authors, all animals survived to term with no clinical signs of toxicity among the monkeys and only a few signs of irritation to the eyes and nose among the rats. In the latter case, instances of mucoid nasal discharges appeared to be dose related. There were no differences in body weight gain among the groups of either rats or monkeys, and overall, absolute and relative organ weights were similar to controls. The only exception to this was a decrease in the absolute adrenal weight of female high-concentration monkeys and an increase in the relative spleen weight of mid-concentration female rats. These changes were not considered by the authors to have biological significance. For both rats and monkeys, there were no compound-related changes in gross pathology, histopathology, or ophthalmoscopy. These data suggest a NOAEL of 5,000 ppm (6,600 mg/m^3) for Sprague-Dawley rats and monkeys under the conditions of the experiment.

Two studies by Poon et al. (1995, 1994) examined the effects of methanol on Sprague-Dawley rats when inhaled for 4 weeks. The effects of methanol were evaluated in comparison to those of toluene and toluene/methanol mixtures (Poon et al., 1994), and to gasoline and gasoline/methanol mixtures (Poon et al., 1995). In the first case (Poon et al., 1994), 10 Sprague-Dawley rats/sex/group were exposed via inhalation, 6 hours/day, 5 days/week to 0, 300, or 3,000 ppm (0, 393, 3,930 mg/m^3) methanol for 4 weeks. Clinical signs were monitored daily, and food consumption and body weight gain were monitored weekly. Blood was taken at term for hematological and clinical chemistry determinations. Weights of the major organs were recorded at necropsy, and histopathologic examinations were carried out. A 10,000 × g liver supernatant was prepared from each animal to measure aniline hydroxylase, aminoantipyrine N-demethylase, and ethoxyresorufin-O-deethylase activities. For the most part, the responses to methanol alone in this experiment were unremarkable. All animals survived to term, and there were no clinical signs of toxicity among the groups. Body weight gain and food consumption did not differ from controls, and there were no compound-related effects in hematological or clinical chemistry parameters or in hepatic mixed function oxidase activities. However, the authors described a reduction in the size of thyroid follicles that was more obvious in female than male rats. The authors considered this effect to possibly have been compound related, although the incidence of this feature for the 0, 300, and 3,000 ppm-receiving females was 0/6, 2/6, and 2/6, respectively.

The second experimental report by Poon et al. (1995) involved the exposure of 15 Sprague-Dawley rats/sex/group, 6 hours/day, 5 days/week for 4 weeks to 0 or 2,500 ppm (0 and 3,276 mg/m^3) to methanol as part of a study on the toxicological interactions of methanol and gasoline. Many of the toxicological parameters examined were the same as those described in Poon et al. (1994) study. However, in this study urinalysis featured the determination of ascorbic and hippuric acids. Additionally, at term, the lungs and tracheae were excised and aspirated with buffer to yield bronchoalveolar lavage fluid that was analyzed for ascorbic acid, protein, and the activities of gamma-glutamyl transferase (γ-GT), AP and LDH. Few if any of the monitored parameters showed any differences between controls and those animals exposed to methanol alone. However, two male rats had collapsed right eyes, and there was a reduction in relative spleen weight in females exposed to methanol. Histopathologic changes in methanol-receiving animals included mild panlobular vacuolation of the liver in females and some mild changes to the upper respiratory tract, including mucous cell metaplasia. The incidence of the latter effect, though higher, was not significantly different than controls in rats exposed to 2,500 ppm (3,267 mg/m^3) methanol. However, there were also signs of an increased severity of the effect in the presence of the solvent. No histopathologic changes were seen in the lungs or lower respiratory tract of rats exposed to methanol alone.

4.2.2.3. *Chronic Toxicity*

Information on the chronic toxicity of methanol has come from NEDO (1987, unpublished report) which includes the results of experiments on 1) monkeys exposed for up to 3 years, 2) rats and mice exposed for 12 months, 3) mice exposed for 18 months, and 4) rats exposed for 2 years.

In the monkeys, 8 animals (sex unspecified) were exposed to 10, 100, or 1,000 ppm (13, 131, and 1,310 mg/m^3) methanol, 21 hours/day, for 7 months (2 animals), 19 months, (3 animals), or 29 months (3 animals). There was no indication in the NEDO (1987) report that this study employed a concurrent control group. One of the 3 animals receiving 100 ppm methanol and scheduled for sacrifice at 29 months was terminated at 26 months. Clinical signs were monitored twice daily, body weight changes and food consumption were monitored weekly, and all animals were given a general examination under anesthetic once a month. Blood was collected for hematological and clinical chemistry tests at term, and all animals were subject to a histopathologic examination of the major organs and tissues.

While there were no clinical signs of toxicity in the low-concentration animals, there was some evidence of nasal exudate in monkeys in the mid-concentration group. High-concentration (1,000 ppm) animals also displayed this response and were observed to scratch themselves over their whole body and crouch for long periods. Food and water intake, body temperature, and body weight changes were the same among the groups. NEDO (1987) reported that there was no abnormality in the retina of any monkey. When animals were examined with an electrocardiogram, there were no abnormalities in the control or 10 ppm groups. However, in the 100 ppm group, one monkey showed a negative change in the T wave. All 3 monkeys exposed to 1,000 ppm (1,310 mg/m^3) displayed this feature, as well as a positive change in the Q wave. This effect was described as a slight myocardial disorder and suggests that 10 ppm (13.1 mg/m^3) is a NOAEL for chronic myocardial effects of methanol and mild respiratory irritation. There were no compound-related effects on hematological parameters. However, 1 monkey in the 100 ppm (131 mg/m^3) group had greater than normal amounts of total protein, neutral lipids, total and free cholesterol, and glucose, and displayed greater activities of ALT and aspartate transaminase (AST). The authors expressed doubts that these effects were related to methanol exposure and speculated that the animal suffered from liver disease.[24]

Histopathologically, no degeneration of the optical nerve, cerebral cortex, muscles, lungs, trachea, tongue, alimentary canal, stomach, small intestine, large intestine, thyroid gland, pancreas, spleen, heart, aorta, urinary bladder, ovary or uterus were reported (neuropathological findings are discussed below Section 4.4.2. Most of the internal organs showed no compound-

[24] Ordinarily, the potential for liver disease in test animals would be remote, but may be a possibility in this case given that these monkeys were captured in the wild.

related histopathologic lesions. However, there were signs of incipient fibrosis and round cell infiltration of the liver in monkeys exposed to 1,000 ppm (1,310 mg/m^3) for 29 months. NEDO (1987) indicated that this fibrosis occurred in 2/3 monkeys of the 1,000 ppm group to a "strictly limited extent." They also qualitatively reported a dose-dependent increase in "fat granules" in liver cells "centered mainly around the central veins" at all doses, but did not provide any response data. The authors state that 1,000 ppm (1,310 mg/m^3) represents a chronic lowest-observed-adverse-effect level (LOAEL) for hepatic effects of inhaled methanol, suggesting that the no effect level would be 100 ppm (131 mg/m^3). However, this is a tenuous determination given the lack of information on the pathological progression and significance of the appearance of liver cell fat granules at exposures below 1,000 ppm and the lack detail (e.g., time of sacrifice) for the control group.

Dose-dependent changes were observed in the kidney; NEDO (1987) described the appearance of Sudan-positive granules in the renal tubular epithelium at 100 ppm (131 mg/m^3) and 1,000 (1,310 mg/m^3) and hyalinization of the glomerulus and penetration of round cells into the renal tubule stroma of monkeys exposed to methanol at 1,000 (1,310 mg/m^3). The former effect was more marked at the higher concentration and was thought by the authors to be compound-related. This would indicate a no effect level at 10 ppm (13.1 mg/m^3) for the chronic renal effects of methanol. The authors observed atrophy of the tracheal epithelium in four monkeys. However, the incidence of these effects was unrelated to dose and therefore, could not be unequivocally ascribed to an effect of the solvent. No other histopathologic abnormalities were related to the effects of methanol. Confidence in these determinations is considerably weakened by concern over whether a concurrent control group was used in the chronic study.[25]

NEDO (1987) describes a 12-month inhalation study in which 20 F344 rats/sex/group were exposed to 0, 10, 100, or 1,000 ppm (0, 13.1, 131, and 1,310 mg/m^3) methanol, approximately 20 hours/day, for a year. Clinical signs of toxicity were monitored daily; body weights and food consumption were recorded weekly for the first 13 weeks, then monthly. Blood samples were drawn at term to measure hematological and clinical chemistry parameters. Weights of the major organs were monitored at term, and a histopathologic examination was carried out on all major organs and tissues. Survival was high among the groups; one high-concentration female died on day 337 and one low-concentration male died on day 340. As described by the authors, a number of procedural anomalies arose during this study. For example, male controls in two cages lost weight because of an interruption to the water supply. Another problem was that the brand of feed was changed during the study. Fluctuations in some clinical chemistry and hematological parameters were recorded. The authors considered the fluctuations to be minor and within the normal range. Likewise, a number of histopathologic

[25] All control group responses were reported in a single table in the section of the NEDO (1987) report that describes the acute monkey study, with no indication as to when the control group was sacrificed.

changes were observed, which, in every case, were considered to be unrelated to exposure level or due to aging.

A companion experiment featured the exposure of 30 B6C3F1 mice/sex/group for 1 year to the same concentrations as the F344 rats (NEDO, 1987). Broadly speaking, the same suite of toxicological parameters was monitored as described above, with the addition of urinalysis. 10 mice/sex/group were sacrificed at 6 months to provide interim data on the parameters under investigation. A slight atrophy in the external lacrimal gland was observed in both sexes and was significant in the 1,000 ppm male group compared with controls. An apparently dose-related increase in moderate fatty degeneration of hepatocytes was observed in males (1/20, 4/20, 6/20 and 8/20 in the 0, 10, 100, and 1,000 ppm dose groups, respectively) which was significantly increased over controls at the 1,000 ppm dose. However the incidence of moderate to severe fatty degeneration was observed in untreated animals maintained outside of the chamber. In addition, there was a clear correlation between fatty degeneration and body weight (a change which was not associated with treatment at 12 months); heavier animals tended to have more severe cases of fatty degeneration. The possibility of renal deficits due to methanol exposure was suggested by the appearance of protein in the urine. However, this effect was also seen in controls and did not display a dose-response effect. Therefore, it is unlikely to be a consequence of exposure to methanol. NEDO (1987) reported other histopathologic and biochemical (e.g., urinalysis and hematology) findings that do not appear to be related to treatment, including a number of what were considered to be spontaneous tumors in both control and exposure groups.

NEDO (1987, 1985/2008a, unpublished reports)[26] exposed 52 male and 53 female B6C3F1 mice/group for 18 months at the same concentrations of methanol (0, 10, 100 and 1,000 ppm) and with a similar experimental protocol to that described in the 12-month studies.[27] The fact that the duration of this study was only 18 months and not the more typical 2 years limits its ability to detect carcinogenic responses with relatively long latency periods. Animals were sacrificed at the end of the 18-month exposure period. NEDO (1985/2008a) reported that "there was no microbiological contamination that may have influenced the result of the study" and that the study included an assessment of general conditions, body weight change, food consumption rate, laboratory tests (urinalysis, hematological, and plasma biochemistry) and pathological tests (pathological autopsy,[28] organ weight check and histopathology[29]). As stated

[26] This study is described in a summary report (NEDO, 1987) and a more detailed, eight volume translation of the original chronic mouse study report (NEDO, 1985/2008a).

[27] The authors reported that "[t]he levels of methanol turned out to be ~4 ppm in low level exposure group (10 ppm) for ~11 weeks from week 43 of exposure due to the analyzer malfunction" and that "the average duration of methanol exposure was 19.1 hours/day for both male and female mice."

[28] Autopsy was performed on all cases to look for gross lesions in each organ.

in the summary report (NEDO, 1987), a few animals showed clinical signs of toxicity, but the incidence of these responses was not related to dose. Likewise, there were no compound-related changes in body weight increase, food consumption,[30] urinalysis, hematology, or clinical chemistry parameters. High-concentration males had lower testis weights compared to control males. Significant differences were detected for both absolute and relative testis weights. One animal in the high-dose group had severely atrophied testis weights, approximately 25% of that of the others in the dose group. Exclusion of this animal in the analysis still resulted in a significant difference in absolute testis weight compared to controls but resulted in no difference in relative testis weight. High-concentration females had higher absolute kidney and spleen weights compared to controls, but there was no significant difference in these organ weights relative to body weight. At necropsy, there were signs of swelling in spleen, preputial glands, and uterus in some animals. Some animals developed nodes in the liver and lung although, according to the authors, none of these changes were treatment-related. NEDO (1985/2008a) reported that all nonneoplastic changes were "nonspecific and naturally occurring changes that are often experienced by 18-month old B6C3F1 mice" and that fatty degeneration of liver that was suspected to occur dose-dependently in the 12-month NEDO (1987) study was not observed in this study. Similarly, though the study found various neoplastic changes across dose groups, there was no compound-related formation of tumors in any organ or tissue.

EPA reviewed the cancer findings documented in a recent translation of the original NEDO report on this chronic mouse study (NEDO, 1985/2008a) to identify possible compound-related effects. Hyperplastic and neoplastic histopathological findings have been tabulated and are as shown in Table 4-4.

---

[29] Complete histopathological examinations were performed for the control group and high-dose (1,000 ppm) groups. Only histopathological examinations of the liver were performed on the low- and medium-level exposure groups because no chemical-related changes were found in the high-level exposure group and because liver changes were noted in the 12-month mouse study (NEDO, 1987).

[30] NEDO (1985/2008a) reports sporadic reductions in food consumption of the 1,000 ppm group, but no associated weight loss or abnormal test results.

Table 4-4. Histopathological changes in tissues of B6C3F1 mice exposed to methanol via inhalation for 18 months

Tissues/tumor type	Exposure concentration (ppm)							
	0	10	100	1,000	0	10	100	1,000
	Number of animals affected/number examined							
	Males				Females			
Lung								
Adenomatosis	0/52	0/3	0/3	0/52	0/53	0/0	0/5	1/53
Pulmonary adenoma	4/52	0/3	0/3	7/52	3/53	0/0	0/0	2/53
Liver								
Hepatocellular adenoma	3/52	2/52	2/52	4/52	1/53	1/52	1/53	4/53
Hepatocellular carcinoma	2/52	4/52	0/52	1/52	3/53	0/52	3/53	2/53
Neoplastic nodule	16/52	13/52	16/52	20/52	1/53	0/52	0/53	1/53

Source: NEDO (1985/2008a).

There is no clear evidence for treatment-related carcinogenic effects in the mice in this study. However, the fact that the study duration was limited to 18 months rather than the traditional 2-year bioassay makes it difficult to draw a definitive conclusion, particularly regarding pulmonary adenomas, which were marginally increased in high-dose male mice of this study and were also increased in male rats of the NEDO chronic rat study (NEDO, 1987, 1985/2008b, unpublished reports). In this study, the lack of adenomatosis in control or treated male mice supports the conclusion of the authors that the observed tumors were probably unrelated to methanol exposure. There was no apparent relationship to treatment in any neoplastic findings in the liver. Of relevance to the findings of treatment-related lymphomas and leukemias in Sprague-Dawley rats receiving methanol in drinking water in the Soffritti et al. (2002a) study, few lymphomas and leukemias were identified in the NEDO (1987, 1985/2008b) study reports, with no sign of a dose-related trend.

Another study reported in (NEDO (1987, 1985/2008b)[31] was a 24-month carcinogenicity bioassay in which 52 F344 rats/sex/group were kept in whole body inhalation chambers containing 0, 10, 100, or 1,000 ppm (0, 13.1, 131, and 1,310 mg/m^3) methanol vapor. Animals were maintained in the exposure chambers for approximately 19.5 hours/day for a total of 733–736 days (males) and 740–743 days (females). Animals were monitored once a day for clinical signs of toxicity, body weights were recorded once a week, and food consumption was measured weekly in a 24-animal subset from each group. Urinalysis was carried out on the day prior to sacrifice for each animal, the samples being monitored for pH, protein, glucose, ketones, bilirubin, occult blood, and urobilinogen. Routine clinical chemistry and hematological

[31] This study is described in a summary report (NEDO, 1987) and a more detailed, eight-volume translation of the original chronic rat study report (NEDO, 1985/2008b).

measurements were carried out and all animals were subject to necropsy at term, with a comprehensive histopathological examination of tissues and organs.[32]

There was some fluctuation in survival rates among the groups in the rat study, though apparently unrelated to exposure concentration.[33] In all groups, at least 60% of the animals survived to term. A number of toxicological responses were described by the authors, including atrophy of the testis, cataract formation, exophthalmia, small eye ball, alopecia, and paralysis of the hind leg. However, according to the authors, the incidence of these effects were unrelated to dose and more likely represented effects of aging. NEDO (1985/2000b) reported a mild, nonsignificant (4%) body weight suppression among 1,000 ppm females between 51 and 72 weeks, but that body weight gain was largely similar among the groups for the duration of the experiment. Food consumption was significantly lower than controls in high-concentration male rats during the day 210–365 time interval, but no corresponding weight loss was observed. Among hematological parameters, mid- and high-concentration females had a significantly ($p > 0.05$) higher differential leukocyte count than controls, but dose dependency was not observed. Serum total cholesterol, triglyceride, free fatty acid, and phospholipid concentrations were significantly ($p > 0.05$) lower in high-concentration females compared to controls. Likewise, serum sodium concentrations were significantly ($p > 0.05$) lower in mid- and high-concentration males compared to controls. High-concentration females had significantly lower ($p > 0.05$) serum concentrations of inorganic phosphorus but significantly ($p > 0.05$) higher concentrations of potassium compared to controls. Glucose levels were elevated in the urine of high-concentration male rats relative to controls, and female rats had lower pH values and higher bilirubin levels in mid- and high-concentration groups relative to controls. In general, NEDO (1987, 1985/2008b) reported that these variations in urinary, hematology, and clinical chemistry parameters were not related to chemical exposure.

NEDO (1987) reported that there was little change in absolute or relative weights of the major organs or tissues. When the animals were examined grossly at necropsy, there were some signs of swelling in the pituitary and thyroid, but these effects were judged to be unrelated to treatment. The most predominant effect was the dose-dependent formation of nodes in the lung of males (2/52, 4/52, 5/52, and 10/52 [$p < 0.01$] for control, low-, mid-, and high-concentration groups, respectively). Histopathologic examination pointed to a possible association of these nodes with the appearance of pulmonary adenoma (1/52, 5/52, 2/52, and 6/52 for control, low-, mid- and high-concentration groups, respectively) and a single pulmonary adenocarcinoma in the

[32] Complete histopathological examinations were performed on the cases killed on schedule (week 104) among the control and high-exposure groups, and the cases that were found dead/ killed in extremis of all the groups. Because effects were observed in male and female kidneys, male lungs as well as female adrenal glands of the high-level exposure group, these organs were histopathologically examined in the low- and mid-exposure groups.

[33] Survival at the time of exposure termination (24 months) was 69%, 65%, 81%, and 65% for males and 60%, 63%, 60% and 67% for females of the control, low-, mid- and high-exposure groups, respectively.

high-dose group (1/52). Other examples of tumor formation that were increased in high-concentration animals versus controls included an increased incidence of pituitary adenomas in high-concentration males (17/52 compared to 12/52 controls), hyperplastic change in the testis in high-concentration males (10/52 compared to 4/52 controls), and chromaffinoma (pheochromocytomas)[34] in the adrenals of high-concentration females (7/52 compared to 2/52 controls). Individually, these changes did not achieve statistical significance, and in general, the authors concluded that few if any of the observed changes were effects of methanol.

EPA reviewed the cancer findings of this study that are documented in a recent translation of the original NEDO (1985/2008b) report to identify possible compound-related effects. High-dose incidences of pituitary adenomas (17/52; 33%) and hyperplastic change in testes (10/52; 19%) mentioned above were within historical incidences for this rat strain.[35] However, the observed incidence rate for pulmonary adenoma/adenocarcinoma in high-dose males of 13.5% (7/52) was significantly elevated (Fisher's exact test $p < 0.05$) over the concurrent control rate of 2% (1/52) and historical control rates of 2.5% ± 2.6% (n = 1054) and 3.84% ± 2.94% (n = 1199) reported by NTP for the pre-1995 control F344 male rats fed NIH-07 diet (NTP, 1999) and post-1994 control F344 male rats fed NTP-2000 diet (NTP, 2007), respectively. Also, the incidence of pulmonary adenoma/adenocarcinoma in male rats exhibited a dose-response trend (Cochrane-Armitage $p < 0.05$). While the observed incidence rate for pheochromocytomas in high-dose females of 13.7% (7/51) was not significantly elevated over the concurrent control rate of 4% (2/50), it was significantly elevated (Fisher's exact test $p < 0.05$) over NTP historical control rates for total (benign, complex and malignant) pheochromocytomas of 2.5% ± 2.6% (n = 1054) and 3.84% ± 2.94% (n = 1199) reported by NTP for pre-1995 control F344 female rats fed NIH-07 diet (NTP, 1999) and post-1994 control F344 female rats fed NTP-2000 diet (NTP, 2007), respectively.[36] Also, the incidence of pheochromocytomas in female rats exhibited a dose-response trend (Cochrane-Armitage $p < 0.05$). The histopathological incidences for pulmonary and adrenal effects reported by NEDO (1987, 1985/2008b) are shown in Table 4-5.

[34] There were some differences in nomenclature used in the NEDO (1985/2008b) report translation versus those used in the older summary report (NEDO, 1987). For example, it is probable that the adrenal chromaffinoma referred to in NEDO (1987) are the same lesions as the pheochromocytoma referred to in NEDO (1985/2008b).

[35] NTP reports high incidences in historical control male F344 rats of pituitary gland adenomas, ranging from 45.4% ± 20.19% (NTP, 2007) to 63.4% ± 18.3% (NTP, 1999). While control incidences for testicular hyperplasia are not reported, historical incidences of testicular ademoma ranged from 70.1% ±11.2% (NTP, 1999) to 86.32% ±9.34% (NTP, 2007) in this rat strain.

[36] NEDO (1987, 1985/2008b) does not categorize reported chromoffinoma (pheochromocytomas) as benign, complex or malignant. The historical rates for complex and malignant tumors are much lower, ranging from 0.1% to 0.7 % for female F344 rats (NTP, 2007; NTP, 1999; Haseman et al., 1998).

Table 4-5. Histopathological changes in lung and adrenal tissues of F344 rats exposed to methanol via inhalation for 24 months

Tissues/ tumor type	Exposure concentration (ppm)							
	0	10	100	1000	0	10	100	1000
	Number of animals affected/number examined							
	Males				Females			
Lung								
Pulmonary adenoma	1/52	5/50	2/52	6/52	2/52	0/19	0/20	0/52
Pulmonary adenocarcinoma	0/52	0/50	0/52	1/52	0/52	0/19	0/20	0/52
Combined pulmonary adenoma/adenocarcinoma	1/52	5/50	2/52	7/52 [a,b]	2/52	0/19	0/20	0/52
Adenomatosis	4/52	1/50	5/52	4/52	3/52	2/19	1/20	1/52
Epithelial swelling	3/52	2/50	1/52	1/52	0/52	0/19	0/20	0/52
Adrenal glands								
Pheochromocytoma	7/52	2/16	2/10	4/51	2/50	3/51	2/49	7/51 [b,c]
Medullary hyperplasia	0/52	0/16	0/10	2/51	2/50	3/51	7/49	2/51

[a] $p < 0.05$ over concurrent controls using the Fisher's Exact test.
[b] $p < 0.05$ for Cochrane-Armitage test of overall dose-response trend.
[c] $p < 0.05$ over NTP historical controls for total (benign, complex and malignant) pheochromocytomas using the Fisher's Exact test

Source: NEDO (1987, 1985/2008b).

In contrast to the conclusions of the NEDO (1987) summary report that there were no compound-related changes in F344 rats exposed to methanol via inhalation, EPA identifies potential treatment-related changes in the lungs of male rats and the adrenal medulla of female rats in the more detailed translation of the original report (NEDO, 1985/2008b). The NEDO (1987) summary report did not report the statistically significant combined pulmonary adenoma and adenocarcinoma finding in the high-dose group of male rats. Table 6 (page 146) of the NEDO (1987) summary reports only "Tumural changes occurring at a rate of over 5%." The lung response of the male rats as shown in Table 4-5 suggests a proliferative change in cells of the alveolar epithelium involving a progression towards adenoma and adenocarcinoma that appears to be more pronounced with increasing methanol exposure and considerably elevated over historical controls. Similarly, for female rats, the observed increase in medullary hyperplasia in the 100 ppm dose group, in conjunction with a higher incidence of pheochromocytoma in the adrenal gland is suggestive of a methanol-induced progressive change leading to a carcinogenic response.

4.3. REPRODUCTIVE AND DEVELOPMENTAL STUDIES–ORAL AND INHALATION

Many studies have been conducted to investigate the reproductive and developmental toxicity of methanol. The purpose of these studies was principally to determine if methanol has a similar toxicology profile to another widely studied teratogen, ethanol.

4.3.1. Oral Studies

Three studies were identified that investigated the reproductive and developmental effects of methanol in rodents via the oral route (Fu et al., 1996; Sakanashi et al., 1996; Rogers et al., 1993a). Two of these studies also investigated the influence of folic acid-deficient (FAD) diets on the effects of methanol exposures (Fu et al., 1996; Sakanashi et al., 1996).

Rogers et al. (1993a) conducted a developmental toxicity study in which methanol in water was administered to pregnant female CD-1 mice via gavage on GD6–GD15. Eight test animals received 4 g/kg-day methanol given in 2 daily doses of 2g/kg; 4 controls received distilled water. By analogy to the protocol of an inhalation study of methanol that was described in the same report, it is assumed that dams were sacrificed on GD17, at which point implantation sites, live and dead fetuses, resorptions/litter, and the incidences of external and skeletal anomalies and malformations were determined. In the brief summary of the findings provided by the authors, it appears that cleft palate (43.5% per litter versus 0% in controls) and exencephaly (29% per litter versus 0% in controls) were the prominent external defects following maternal methanol exposure by gavage. Likewise, an increase in totally resorbed litters and a decrease in the number of live fetuses per litter were evident. However, it is possible that these effects may have been caused or exacerbated by the high bolus dosing regimen employed. It is also possible that effects were not observed due to the limited study size. The small number of animals in the control group relative to the test group limits the power of this study to detect treatment-related responses.

Sakanashi et al. (1996) tested the influence of dietary folic acid intake on various reproductive and developmental effects observed in CD-1 mice exposed to methanol. Starting 5 weeks prior to breeding and continuing for the remainder of the study, female CD-1 mice were fed folic acid free diets supplemented with 400 (low), 600 (marginal) or 1,200 (sufficient) nmol folic acid/kg. After 5 weeks on their respective diets, females were bred with CD-1 male mice. On GD6–GD15, pregnant mice in each of the diet groups were given twice-daily gavage doses of 2.0 or 2.5 g/kg-day methanol (total dosage of 4.0 or 5.0 g/kg-day). On GD18, mice were weighed and killed, and the liver, kidneys and gravid uteri removed and weighed. Maternal liver and plasma folate levels were measured, and implantation sites, live and dead fetuses, and resorptions were counted. Fetuses were weighed individually and examined for cleft palate and exencephaly. One third of the fetuses in each litter were examined for skeletal morphology.

They observed an approximate 50% reduction in liver and plasma folate levels in the mice fed low versus sufficient folic acid diets in both the methanol exposed and unexposed groups. Similar to Rogers et al. (1993a), Sakanashi et al. (1996) observed that an oral dose of 4–5 g/kg-day methanol during GD6–GD15 resulted in an increase in cleft palate in mice fed sufficient folic acid diets, as well as an increase in resorptions and a decrease in live fetuses per litter. They did not observe an increase in exencephaly in the FAS group at these doses, and the authors suggest that this may be due to diet and the source of CD-1 mice differing between the two studies.

In the case of the animals fed the folate deficient diet, there was a 50% reduction in maternal liver folate concentration and a threefold increase in the percentage of litters affected by cleft palate (86.2% versus 34.5% in mice fed sufficient folic acid) and a 10-fold increase in the percentage of litters affected by exencephaly (34.5% versus 3.4% in mice fed sufficient folic acid) at the 5 g/kg methanol dose. Sakanashi et al. (1996) speculate that the increased methanol effect from the FAD diet could have been due to an increase in tissue formate levels (not measured) or to a critical reduction in conceptus folate concentration following the methanol exposure. Plasma and liver folate levels at GD18 within each dietary group were not significantly different between exposed versus unexposed mice. However, these measurements were taken 3 days after methanol exposure. Dorman et al. (1995) observed a transient decrease in maternal red blood cells (RBCs) and conceptus folate levels within 2 hours following inhalation exposure to 15,000 ppm methanol on GD8. Thus, it is possible that short-term reductions in available folate during GD6–GD15 may have affected fetal development.

Fu et al. (1996) also tested the influence of dietary folic acid intake on reproductive and developmental effects observed in CD-1 mice exposed to methanol. This study was performed by the same laboratory and used a similar study design and dosing regimen as Sakanashi et al. (1996), but exposed the pregnant mice to only the higher 2.5 g/kg-day methanol (total dosage of 5.0 g/kg-day) on GD6–GD10. Like Sakanashi et al. (1996), Fu et al. (1996) measured maternal liver and plasma folate levels on GD18 and observed similar, significant reductions in these levels for the FAD versus FAS mice. However, Fu et al. (1996) also measured fetal liver folate levels at GD18. This measurement does not address the question of whether methanol exposure caused short-term reductions in fetal liver folate because it was taken 8 days after the GD6–GD10 exposure period. However, it did provide evidence regarding the extent to which a maternal FAD diet can impact fetal liver folate levels in this species and strain. Significantly, the maternal FAD diet had a greater impact on fetal liver folate than maternal liver folate levels. Relative to the FAS groups, fetal liver folate levels in the FAD groups were reduced 2.7-fold for mice not exposed to methanol (1.86 ± 0.15 nmol/g in the FAD group versus 5.04 ± 0.22 nmol/g in the FAS group) and 3.5-fold for mice exposed to methanol (1.69 ± 0.12 nmol/g in the FAD

group versus 5.89 ± 0.39 nmol/g in the FAS group). Maternal folate levels in the FAD groups were only reduced twofold both for mice not exposed (4.65 ± 0.37 versus 9.54 ± 0.50 nmol/g) and exposed (4.55 ± 0.19 versus 9.26 ± 0.42 nmol/g). Another key finding of the Fu et al. (1996) study is that methanol exposure during GD6–GD10 appeared to have similar fetotoxic effects, including cleft palate, exencephaly, resorptions, and decrease in live fetuses, as the same level of methanol exposure administered during GD6–GD15 (Sakanashi et al., 1996; Rogers et al., 1993a). This is consistent with the hypothesis made by Rogers et al. (1993b) that the critical period for methanol-induced cleft palate and exencephaly in CD-1 mice is within GD6–GD10. As in the studies of Sakanashi et al. (1996) and Rogers et al. (1993a), Fu et al. (1996) reported a higher incidence of cleft palate than exencephaly.

4.3.2. Inhalation Studies

Nelson et al. (1985) exposed 15 pregnant Sprague-Dawley rats/group to 0, 5,000, 10,000, or 20,000 ppm (0, 6,552, 13,104, and 26,209 mg/m^3) methanol (99.1% purity) for 7 hours/day. Exposures were conducted on GD1–GD19 in the two lower concentration groups and GD7–GD15 in the highest concentration group, apparently on separate days. Two groups of 15 control rats were exposed to air only. Day 1 blood methanol levels measured 5 minutes after the termination of exposure in NP rats that had received the same concentrations of methanol as those animals in the main part of the experiment were 1.00 ± 0.21, 2.24 ± 0.20, and 8.65 ± 0.40 mg/mL for those exposed to 5,000, 10,000 and 20,000 ppm methanol, respectively. Evidence of maternal toxicity included a slightly unsteady gait in the 20,000 ppm group during the first few days of exposure. Maternal bodyweight gain and food intake were unaffected by methanol. Dams were sacrificed on GD20, and 13–30 litters/group were evaluated. No effect was observed on the number of corpora lutea or implantations or the percentage of dead or resorbed fetuses. Statistical evaluations included analysis of variance (ANOVA) for body weight effect, Kruskal-Wallis test for endpoints such as litter size and viability and Fisher's exact test for malformations. Fetal body weight was significantly reduced at concentrations of 10,000 and 20,000 ppm by 7% and 12–16%, respectively, compared to controls. An increased number of litters with skeletal and visceral malformations were observed at ≥10,000 ppm, with statistical significance obtained at 20,000 ppm. Numbers of litters with visceral malformations were 0/15, 5/15, and 10/15 and with skeletal malformations were 0/15, 2/15, and 14/15 at 0, 10,000, and 20,000 ppm, respectively. Visceral malformations included exencephaly and encephaloceles. The most frequently observed skeletal malformations were rudimentary and extra cervical ribs. The developmental and maternal NOAELs for this study were identified as 5,000 ppm (6,552 mg/m^3) and 10,000 ppm (13,104 mg/m^3), respectively.

NEDO (1987) sponsored a teratology study in Sprague-Dawley rats that included an evaluation of postnatal effects in addition to standard prenatal endpoints. Thirty-six pregnant females/group were exposed to 0, 200, 1,000, or 5,000 ppm (0, 262, 1,310, and 6,552 mg/m^3) methanol vapors (reagent grade) on GD7–GD17 for 22.7 hours/day. Statistical significance of results was evaluated by t-test, Mann-Whitney U test, Fisher's exact test, and/or Armitage's χ^2 test.

Contrary to the Nelson et al. (1985) report of a 10,000 ppm NOAEL for this rat strain, in the prenatal portion of the NEDO (1987) study, reduced body weight gain and food and water intake during the first 7 days of exposure were reported for dams in the 5,000 ppm group. However, it was not specified if these results were statistically significant. One dam in the 5,000 ppm group died on GD19, and one dam was sacrificed on GD18 in moribund condition. On GD20, 19–24 dams/group were sacrificed to evaluate the incidence of reproductive deficits and such developmental parameters as fetal viability, weight, sex, and the occurrence of malformations. As summarized in Table 4-6, adverse reproductive and fetal effects were limited to the 5,000 ppm group and included an increase in late-term resorptions, decreased live fetuses, reduced fetal weight, and increased frequency of litters with fetal malformations, variations, and delayed ossifications. Malformations or variations included defects in ventricular septum, thymus, vertebrae, and ribs.

Postnatal effects of methanol inhalation were evaluated in the remaining 12 dams/group that were permitted to deliver and nurse their litters. Effects were only observed in the 5,000 ppm group, and included a 1-day prolongation of the gestation period and reduced post-implantation survival, number of live pups/litter, and survival on PND4 (Table 4-7). When the delay in parturition was considered, methanol treatment had no effect on attainment of developmental milestones such as eyelid opening, auricle development, incisor eruption, testes descent, or vaginal opening. There were no adverse body weight effects in offspring from methanol treated groups. The weights of some organs (brain, thyroid, thymus, and testes) were reduced in 8-week-old offspring exposed to 5000 ppm methanol during prenatal development.

Table 4-6. Reproductive and developmental toxicity in pregnant Sprague-Dawley rats exposed to methanol via inhalation during gestation

Effect	Exposure concentration (ppm)			
	0	200	1,000	5,000
Reproductive effects				
Number of pregnant females examined	19	24	22	20
Number of corpora lutea	17.0 ± 2.6	17.2 ± 2.7	16.4 ± 1.9	16.5 ± 2.4
Number of implantations	15.7 ± 1.6	15.0 ± 3.0	15.5 ± 1.2	14.5 ± 3.3
Number of resorptions	0.79 ± 0.85	0.71 ± 1.23	0.95 ± 0.65	1.67 ± 2.03
Number of live fetuses	14.95 ± 1.61	14.25 ± 3.54	14.55 ± 1.1	12.86 ± 4.04[a]
Sex ratio (M/F)	144/140	177/165	164/156	134/136
Fetal weight (male)	3.70 ± 0.24	3.88 ± 0.23	3.82 ± 0.29	3.02 ± 0.27[c]
Fetal weight (female)	3.51 ± 0.19	3.60 ± 0.25	3.60 ± 0.30	2.83 ± 0.26[c]
Total resorption rate (%)	11.2 ± 9.0	15.6 ± 21.3	10.6 ± 8.4	23.3 ± 22.7[a]
Soft tissue malformations				
Number of fetuses examined	136	165	154	131
Abnormality at base of right subclavian	0.7 ± 2.87 (1)	0	0	0
Excessive left subclavian	0	0	0	3.5 ± 9.08 (3)
Ventricular septal defect	0	0.6 ± 2.96 (1)	0	47.6 ± 36.51 (16)[b]
Residual thymus	2.9 ± 5.91 (4)	2.4 ± 5.44 (4)	2.6 ± 5.73 (4)	53.3 ± 28.6 (20)[b]
Serpengious urinary tract	43.0 ± 24.64 (18)	35.2 ± 31.62 (19)	41.8 ± 38.45 (15)	22.1 ± 22.91 (13)
Skeletal abnormalities				
Number of fetuses examined	148	177	165	138
Atresia of foramen costotransversarium	23.5 ± 5.47 (3)	7.7 ± 1.3 (8)	3.5 ± 8.88 (4)	45.2 ± 25.18 (20)[b]
Patency of foramen costotransversium	0	0	0.6 ± 2.67 (1)	13.7 ± 20.58 (7)
Cleft sternum	0	0	0	5.6 ± 14.14 (3)
Split sternum	0	0	0	7.0 ± 14.01 (5)
Bifurcated vertebral center	0.8 ± 3.28 (1)	1.6 ± 5.61 (2)	3.0 ± 8.16 (3)	14.5 ± 16.69 (11)[b]
Cervical rib	0	0	0	65.2 ± 25.95 (19)[b]
Excessive sublingual neuropore	0	0	0	49.9 ± 27.31 (19)
Curved scapula	0	0	0	0.7 ± 3.19 (1)
Waved rib	0	0	0	6.1 ± 11.84 (5)
Abnormal formation of lumbar vertebrae	0	0	0	0.7 ± 3.19 (1)

[a]$p < 0.05$, [b]$p < 0.01$, [c]$p < 0.001$, as calculated by the authors.
Values are means ± S.D. Values in parentheses are the numbers of litters.

Source: NEDO (1987).

Table 4-7. Reproductive parameters in Sprague-Dawley dams exposed to methanol during pregnancy then allowed to deliver their pups

Effect	Exposure concentration (ppm)			
	0	200	1,000	5,000
Number of dams	12	12	12	12
Duration of gestation (days)	21.9 ± 0.3	21.9 ± 0.3	21.9 ± 0.3	22.6 ± 0.5[c]
Number of implantations	15.8 ± 1.6	14.8 ± 1.2	15.3 ± 1.3	14.6 ± 1.1[a]
Number of pups	15.2 ± 1.6	14.4 ± 1.3	14.5 ± 1.4	13.1 ± 2.2[a]
Number of live pups	15.2 ± 1.6	14.1 ± 1.4	14.3 ± 1.4	12.6 ± 2.5[b]
Number of live pups on PND4	15.0 ± 1.7 (2)	13.8 ± 1.5 (3)	14.2 ± 1.6 (1)	10.3 ± 2.8 (9)[c]
Sex ratio (M/F)	88/94	87/85	103/70[a]	75/81
Postimplantation embryo survival rate	96.3 ± 4.2	94.9 ± 5.1	93.6 ± 6.1	86.2 ±16.2[a]

[a]$p < 0.05$, [b]$p < 0.01$, [c]$p < 0.001$, as calculated by the authors.
Values are means ± S.D. Values in parentheses are the numbers of litters.

Source: NEDO (1987).

NEDO (1987) contains an account of a two-generation reproductive study that evaluated the effects of pre- and postnatal methanol (reagent grade) exposure (20 hours/day) on reproductive and other organ systems of Sprague-Dawley rats. The F_0 generation (30 males and 30 females per exposure group)[37] was exposed to 0, 10, 100, and 1,000 ppm (0, 13.1, 131, and 1,310 mg/m^3) from 8 weeks old to the end of mating (males) or to the end of lactation period (females). The F_1 generation was exposed to the same concentrations from birth to the end of mating (males) or to weaning of F_2 pups 21 days after delivery (females). Males and females of the F_2 generation were exposed from birth to 21 days old (one animal/sex/litter was exposed to 8 weeks of age). NEDO (1987) noted reduced brain, pituitary, and thymus weights, and early testicular descent in the offspring of F_0 and F_1 rats exposed to 1,000 ppm methanol. The early testicular descent is believed to be an indication of earlier fetal development as indicated by the fact that it was correlated with increased pup body weight. However, no histopathologic effects of methanol were observed. As discussed in the report, NEDO (1987) sought to confirm the possible compound-related effect of methanol on the brain by carrying out an additional study in which Sprague-Dawley rats were exposed to 0, 500, 1,000, and 2,000 ppm (0, 655, 1,310, and 2,620 mg/m^3) methanol from the first day of gestation through the F_1 generation (see Section 4.4.2).

[37] A second control group of 30 animals/sex was maintained in a separate room to "confirm that environmental conditions inside the chambers were not unacceptable to the animals."

Rogers et al. (1993a) evaluated development toxicity in pregnant female CD-1 mice exposed to air or 1,000, 2,000, 5,000, 7,500, 10,000, or 15,000 ppm (0, 1,310, 2,620, 6,552, 9,894, 13,104, and 19,656 mg/m^3) methanol vapors (≥ 99.9% purity) in a chamber for 7 hours/day on GD6–GD15 in a 3-block design experiment. The numbers of mice exposed at each dose were 114, 40, 80, 79, 30, 30, and 44, respectively. During chamber exposures to air or methanol, the mice had access to water but not food. In order to determine the effects of the chamber exposure conditions, an additional 88 control mice were not handled and remained in their cages; 30 control mice were not handled but were food deprived for 7 hours/day on GD6–GD15. Effects in dams and litters were statistically analyzed using the General Linear Models procedure and multiple *t*-test of least squares means for continuous variables and the Fisher's exact test for dichotomous variables. An analysis of plasma methanol levels in 3 pregnant mice/block/treatment group on GD6, GD10, and GD15 revealed a dose-related increase in plasma methanol concentration that did not seem to reach saturation levels, and methanol plasma levels were not affected by gestation stage or number of previous exposure days. Across all 3 days, the mean plasma methanol concentrations in pregnant mice were approximately 97, 537, 1,650, 3,178, 4,204, and 7,330 µg/mL in the 1,000, 2,000, 5,000, 7,500, 10,000, and 15,000 ppm exposure groups, respectively.

The dams exposed to air or methanol in chambers gained significantly less weight than control dams that remained in cages and were not handled. There were no methanol-related reductions in maternal body weight gain or overt signs of toxicity. Dams were sacrificed on GD17 for a comparison of developmental toxicity in methanol-treated groups versus the chamber air-exposed control group. Fetuses in all exposure groups were weighed, assessed for viability, and examined for external malformations. Fetuses in the control, 1,000, 2,000, 5,000, and 15,000 ppm groups were also examined for skeletal and visceral defects. Incidence of developmental effects is listed in Table 4-8. A statistically significant increase in cervical ribs/litter was observed at concentrations of 2,000, 5,000, and 15,000 ppm. At doses of ≥5,000 ppm the incidences of cleft palates/litter and exencephaly/litter were increased with statistical significance achieved at all concentrations with the exception of exencephaly which increased but not significantly at 7,500 ppm.[38] A significant reduction in live pups/litter was noted at ≥7,500 ppm, with a significant increase in fully resorbed litters occurring at ≥10,000 ppm. Fetal weight was significantly reduced at ≥10,000 ppm. Rogers et al. (1993a) identified a developmental NOAEL and LOAEL of 1,000 ppm and 2,000 ppm, respectively. They also provide BMD maximum likelihood estimates (benchmark concentration [BMC]; referred to by the authors as MLE) and estimates of the lower 95% confidence limit on the BMC

[38] Due to the serious nature of this response and the relative lack of a response in controls, all incidence of exenceaphaly reported in this study at 5,000 ppm or higher are considered biologically significant.

(benchmark concentration, 95% lower bound [BMCL]; referred to as benchmark dose [BMD] by Rogers et al. (1993a) for 5% and 1% added risk, by applying a log-logistic dose-response model to the mean percent/litter data for cleft palate, exencephaly and resorption. The BMC_{05} and $BMCL_{05}$ values for added risk estimated by Rogers et al. (1993a) are listed in Table 4-9. From this analysis, the most sensitive indicator of developmental toxicity was an increase in the proportion of fetuses per litter with cervical rib anomalies. The most sensitive BMCL and BMC from this effect for 5% added risk were 305 ppm (400 mg/m^3) and 824 ppm (1,080 mg/m^3), respectively.[39]

Table 4-8. Developmental effects in mice after methanol inhalation

Endpoint	Exposure concentration (ppm)						
	0	**1,000**	**2,000**	**5,000**	**7,500**	**10,000**	**15,000**
No. live pups/litter	9.9	9.5	12.0	9.2	8.6[b]	7.3[c]	2.2[c]
No. fully resorbed litters	0	0	0	0	3	5[a]	14[c]
Fetus weight (g)	1.20	1.19	1.15	1.15	1.17	1.04[c]	0.70[c]
Cleft palate/ litter (%)	0.21	0.65	0.17	8.8[b]	46.6[c]	52.7[c]	48.3[c]
Exencephaly/litter (%)	0	0	0.88	6.9[a]	6.8	27.4[c]	43.3[c]
Anomalies							
Cervical ribs/litter (%)	28	33.6	49.6[b]	74.4[c]	ND	ND	60.0[a]
Sternebral defects/litter (%)	6.4	7.9	3.5	20.2[c]	ND	ND	100[c]
Xiphoid defects/litter (%)	6.4	3.8	4.1	10.9	ND	ND	73.3[c]
Vertebral arch defects/litter (%)	0.3	ND	ND	1.5	ND	ND	33.3[c]
Extra lumbar ribs/litter (%)	8.7	2.5	9.6	15.6	ND	ND	40.0[c]
Ossifications (values are means of litter means)							
Sternal	5.96	5.99	5.94	5.81	ND	ND	5.07[c]
Caudal	5.93	6.26	5.71[a]	5.42	ND	ND	3.20[a]
Metacarpal	7.96	7.92	7.96	7.93	ND	ND	7.60[b]
Proximal phalanges	7.02	7.04	7.04	6.12	ND	ND	3.33[c]
Metatarsals	9.87	9.90	9.87	9.82	ND	ND	8.13[c]
Proximal phalanges	7.18	7.69	6.91	5.47	ND	ND	0[c]
Distal phalanges	9.64	9.59	9.57	8.46[b]	ND	ND	4.27[c]
Supraoccipital score+	1.40	1.65	1.57	1.48	ND	ND	3.20[c]

ND = Not determined. + = on a scale of 1–4, where 1 is fully ossified and 4 is unossified.
Statistical significance: [a]$p < 0.05$, [b]$p < 0.01$, [c]$p < 0.001$, as calculated by the authors.

Source: Rogers et al. (1993a).

[39] The BMD analysis of the data described in Section 5 was performed similarly using, among others, a similar nested logistic model. However, the Rogers et al. (1993a) analysis was performed using added risk and external exposure concentrations, whereas the analyses in Section 5 used extra risk and internal dose metrics that were then converted to human equivalent exposure concentrations.

Table 4-9. Benchmark doses at two added risk levels

Endpoint	BMC_{05} (ppm)	$BMCL_{05}$ (ppm)	BMC_{01} (ppm)	$BMCL_{01}$ (ppm)
Cleft Palate (CP)	4,314	3,398	2,717	1,798
Exencephaly (EX)	5,169	3,760	2,122	784
CP and EX	3,713	3,142	2,381	1,816
Resorptions (RES)	5,650	4,865	3,749	2,949
CP, EX, and RES	3,667	3,078	2,484	1,915
Cervical ribs	824	305	302	58

Source: Rogers et al. (1993a).

Rogers and Mole (1997) investigated the critical period of sensitivity to the developmental toxicity of inhaled methanol in the CD-1 mouse by exposing 12–17 pregnant females to 0 or 10,000 ppm (0 and 13,104 mg/m^3), 7 hours/day on 2 consecutive days during GD6–GD13, or to a single exposure to the same methanol concentration during GD5–GD9. Another group of mice received a single 7-hour exposure to methanol at 10,000 ppm. The latter animals were sacrificed at various time intervals up to 28 hours after exposure. Blood samples were taken from these animals to measure the concentration of methanol in the serum. Serum methanol concentrations peaked at ~4 mg/mL 8 hours after the onset of exposure. Methanol concentrations in serum had declined to pre-exposure levels after 24 hours. All mice in the main body of the experiment were sacrificed on GD17, and their uteri removed. The live, dead, and resorbed fetuses were counted, and all live fetuses were weighed, examined externally for cleft palate, and then preserved. Skeletal abnormalities were determined after the carcasses had been cleaned and eviscerated. Cleft palate, exencephaly, and skeletal defects were observed in the fetuses of exposed dams. For example, cleft palate was observed following 2-day exposures to methanol on GD6–GD7 through GD11–GD12. These effects also were apparent in mice receiving a single exposure to methanol on GD5–GD9. This effect peaked when the dams were exposed on GD7. Exencephaly showed a similar pattern of development in response to methanol exposure. However, the data indicated that cleft palate and exencephaly might be competing malformations, since only one fetus displayed both features. Skeletal malformations included exoccipital anomalies, atlas and axis defects, the appearance of an extra rudimentary rib on cervical vertebra No.7, and supernumerary lumbar ribs. In each case, the maximum time point for the induction of these defects appeared to be when the dams were exposed to methanol on or near GD7. When dams were exposed to methanol on GD5, there was also an increased incidence of fetuses with 25 presacral vertebrae (26 is normal). However, an increased incidence of fetuses with 27 presacral vertebrae was evident when dams were exposed on GD7. These results indicate that gastrulation and early organogenesis is a period of increased embryonic sensitivity to methanol.

Burbacher et al. (1999a, 1999b) carried out toxicokinetic and reproductive/developmental studies of methanol in *M. fascicularis* monkeys that were published by the Health Effects Institute (HEI) in a two-part monograph. Some of the data were subsequently published in the open scientific literature (Burbacher et al., 2004a, 2004b). The experimental protocol featured exposure to 2 cohorts of 12 monkeys/group to low exposure levels (relative to the previously discussed rodent studies) of 0, 200, 600, or 1,800 ppm (0, 262, 786, and 2,359 mg/m^3) methanol vapors (99.9% purity), 2.5 hours/day, 7 days/week, during a premating period and mating period (–180 days combined) and throughout the entire gestation period (–168 days). The monkeys were 5.5–13 years old and were a mixture of feral-born and colony-bred animals. The study included an evaluation of maternal reproductive performance and tests to assess infant postnatal growth and newborn health, reflexes, behavior, and development of visual, sensorimotor, cognitive, and social behavioral function (see Section 4.4.2 for a review of the developmental neurotoxicity findings from this study). Blood methanol levels, clearance, and the appearance of formate were also examined and are discussed in Section 3.2.

With regard to reproductive parameters, there was a statistically significant decrease ($p = 0.03$) in length of pregnancy in all treatment groups, as shown in Table 4-10. Maternal menstrual cycles, conception rate, and live birth index were all unaffected by exposure. There were also no signs of an effect on maternal weight gain or clinical toxicity among the dams. The decrease in pregnancy length was largely due to complications of pregnancy requiring Cesarean section (C-section) deliveries in the methanol exposure groups. The C-section deliveries were performed in response to signs of difficulty in the pregnancy and thus may serve as supporting evidence of reproductive dysfunction in the methanol-exposed females.

While pregnancy duration was virtually the same in all exposure groups, there were some indications of increased pregnancy duress only in methanol-exposed monkeys. C-sections were done in 2 monkeys from the 200 ppm group and 2 from the 600 ppm group due to vaginal bleeding, presumed, but not verified, to be from placental detachment.[40] A monkey in the 1,800 ppm group also received a C-section after experiencing nonproductive labor for 3 nights. In addition, signs of prematurity were observed in 1 infant from the 1,800 ppm group that was born after a 150-day gestation period. The authors speculated that the shortened gestation length could be due to a direct effect of methanol on the fetal hypothalamus-pituitary-adrenal (HPA) axis or an indirect effect of methanol on the maternal uterine environment. Other fetal parameters such as crown-rump length and head circumference were unchanged among the groups. Infant growth and tooth eruption were unaffected by prenatal methanol exposure.

[40] Burbacher et al. (2004a, 2004b) note, however, that in studies of pregnancy complication in alcohol- exposed human subjects, an increased incidence of uterine bleeding and abrutio placenta has been reported.

Table 4-10. Reproductive parameters in monkeys exposed via inhalation to methanol during prebreeding, breeding, and pregnancy

Exposure (ppm)	Conception rate	Weight gain (kg)	Pregnancy duration (days)[a]	Live born delivery rate
0	9/11	1.67 ± 0.07	168 ± 2	8/9
200	9/12	1.27 ± 0.14	160 ± 2[b]	9/9
600	9/11	1.78 ± 0.25	162 ± 2[b]	8/9
1,800	10/12	1.54 ± 0.20	162 ± 2[b]	9/10

Values are means ± SE.;
[a]Live-born offspring only; [b]$p < 0.05$, as calculated by the authors.

Source: Burbacher et al. (2004a).

In later life, 2 females out of the total of 9 offspring in the 1,800 ppm group experienced a wasting syndrome at 12 and 17 months of age. Food intake was normal and no cause of the syndrome could be determined in tests for viruses, hematology, blood chemistry, and liver, kidney, thyroid, and pancreas function. Necropsies revealed gastroenteritis and severe malnourishment. No infectious agent or other pathogenic factor could be identified. Thus, it appears that a highly significant toxicological effect on postnatal growth can be attributed to prenatal methanol exposure at 1,800 ppm (2,300 mg/m^3).

In summary, the Burbacher et al. (2004a, 2004b, 1999b) studies suggest that methanol exposure can cause reproductive effects, manifested as a shortened mean gestational period due to pregnancy complications that precipitated delivery via a C-section, and developmental neurobehavioral effects which may be related to the shortened gestational period (see Section 4.4.2). The low exposure of 200 ppm may signify a LOAEL for reproductive effects. However, the decrease in gestational length was marginally significant and largely the result of human intervention (C-section) for reasons (presumably pregnancy complications) that were not objectively confirmed with clinical procedures (e.g., placental ultrasound). Also, this effect did not appear to be dose related, the greatest gestational period decrease having occurred at the lowest (200 ppm) exposure level. Thus, a clear NOAEL or LOAEL cannot be determined from this study.

In a study of the testicular effects of methanol, Cameron et al. (1984) exposed 5 male Sprague-Dawley rats/group to methanol vapor, 8 hours/day, 5 days/week for 1, 2, 4, and 6 weeks at 0, 200, 2,000, or 10,000 ppm (0, 262, 2,620, and 13,104 mg/m^3). The authors examined the possible effects of methanol on testicular function by measuring blood levels of testosterone, luteinizing hormone (LH), and follicular stimulating hormone (FSH) using radioimmunoassay. When the authors tabulated their results as a percentage of the control value for each duration series, the most significant changes were in blood testosterone levels of animals exposed to 200 ppm methanol, the lowest concentration evaluated. At this exposure level, animals exposed for 6 weeks had testosterone levels that were 32% of those seen in controls. However, higher

concentrations of methanol were associated with testosterone levels that were closer to those of controls. However, the lack of a clear dose-response is not necessarily an indication that the effect is not related to methanol. The higher concentrations of methanol could be causing other effects (e.g., liver toxicity) which can influence the results. Male rats exposed to 10,000 ppm methanol for 6 weeks displayed blood levels of LH that were about 3 times higher (mean ± S.D.) than those exposed to air (311 ± 107% versus 100 ± 23%). In discussing their results, the authors placed the greater emphasis on the fact that an exposure level equal to the ACGIH TLV (200 ppm) had caused a significant depression in testosterone formation in male rats.

A follow-up study report by the same research group (Cameron et al., 1985) described the exposure of 5 male Sprague-Dawley rats/group, 6 hours/day for either 1 day or 1 week, to methanol, ethanol, n-propanol, or n-butanol at their respective TLVs. Groups of animals were sacrificed immediately after exposure or after an 18-hour recovery period, and the levels of testosterone, LH, and corticosterone measured in serum. As shown in Table 4-11, the data were consistent with the ability of these aliphatic alcohols to cause a transient reduction in the formation of testosterone. Except in the case of n-butanol, rapid recovery from these deficits can be inferred from the 18-hour postexposure data.

Table 4-11. Mean serum levels of testosterone, luteinizing hormone, and corticosterone (± S.D.) in male Sprague-Dawley rats after inhalation of methanol, ethanol, n-propanol or n-butanol at threshold limit values

Testosterone (as a percentage of control)					
Condition	**TLV (ppm)**	**Single-day exposure**		**One-week exposure**	
		End of exposure	**18 hr postexposure**	**End of exposure**	**18 hr postexposure**
Control		100 ± 17	100 ± 20	100 ± 26	100 ± 17
Methanol	200	41 ± 16[a]	98 ± 18	81 ± 22	82 ± 27
Ethanol	1,000	64 ± 12[a]	86 ± 16	88 ± 14	101 ± 13
n-Propanol	200	58 ± 15[a]	81 ± 13	106 ± 28	89 ± 17
n-Butanol	50	37 ± 8[a]	52 ± 22[a]	73 ± 34	83 ± 18
Luteinizing hormone					
Control		100 ± 30	100 ± 35	100 ± 28	100 ± 36
Methanol	200	86 ± 32	110 ± 40	78 ± 13	70 ± 14
Ethanol	1,000	110 ± 22	119 ± 54	62 ± 26	81 ± 17
n-Propanol	200	117 ± 59	119 ± 83	68 ± 22	96 ± 28
n-Butanol	50	124 ± 37	115 ± 28	78 ± 26	98 ± 23

Testosterone (as a percentage of control)					
Condition	**TLV (ppm)**	**Single-day exposure**		**One-week exposure**	
		End of exposure	**18 hr postexposure**	**End of exposure**	**18 hr postexposure**
Corticosterone					
Control		100 ± 20	ND	100 ± 21	ND
Methanol	200	115 ± 18	ND	74 ± 26	ND
Ethanol	1,000	111 ± 32	ND	60 ± 25	ND
n-Propanol	200	112 ± 21	ND	79 ± 14	ND
n-Butanol	50	143 ± 11[a]	ND	85 ± 26	ND

ND = No data.;
[a]$p < 0.05$, as calculated by the authors.

Source: Cameron et al. (1985).

In a series of studies that are relevant to the reproductive toxicity of methanol in males, Lee et al. (1991) exposed 8-week-old male Sprague-Dawley rats (9–10/group) to 0 or 200 ppm (0 and 262 mg/m^3) methanol, 8 hours/day, 5 days/week, for 1, 2, 4, or 6 weeks to measure the possible treatment effects on testosterone production. Study results were evaluated by one factor ANOVA followed by Student's *t*-test. In the treated rats, there was no effect on serum testosterone levels, gross structure of reproductive organs, or weight of testes and seminal vesicles. Lee et al. (1991) also studied the in vitro effect of methanol on testosterone production from isolated testes, but saw no effect on testosterone formation either with or without the addition of human chorionic gonadotropin hormone.

In a third experiment from the same report, Lee et al. (1991) examined testicular histopathology to determine if methanol exposure produced lesions indicative of changing testosterone levels; the effects of age and folate status were also assessed. This is relevant to the potential toxicity of methanol because folate is the coenzyme of tetrahydrofolate synthetase, an enzyme that is rate limiting in the removal of formate. Folate deficiency would be expected to cause potentially toxic levels of methanol, formaldehyde, and formate to be retained. The same authors examined the relevance of folate levels, and by implication, the overall status of formate formation and clearance in mediating the testicular functions of Long-Evans rats. Groups of 4-week-old male Long-Evans rats were given diets containing either adequate or reduced folate levels plus 1% succinylsulfathiazole, an antibiotic that, among other activities, [41] would tend to reduce the folate body burden. At least 9 rats/dietary group/dose were exposed to 0, 50, 200, or 800 ppm (0, 66, 262, and 1,048 mg/m^3) methanol vapors starting at 7 months of age while 8–12 rats/dietary group/dose were exposed to 0 or 800 ppm methanol vapors at 15 months of age.

[41] Succinylsulfathiazone antibiotic may have a direct impact on the effects being measured, the extent of which was not addressed by the authors of this study.

The methanol exposures were conducted continuously for 20 hours/day for 13 weeks. Without providing details, the study authors reported that visual toxicity and acidosis developed in rats fed the low folate diet and exposed to methanol. No methanol-related testicular lesions or changes in testes or body weight occurred in rats that were fed either the folate sufficient or deficient diets and were 10 months old at the end of treatment. Likewise, no methanol-lesions were observed in 18-month-old rats that were fed diets with adequate folate. However, the incidence but not severity of age-related testicular lesions was increased in the 18-month-old rats fed folate-deficient diets. Subcapsular vacuoles in germinal epithelium were noted in 3/12 control rats and 8/13 rats in the 800 ppm group. One rat in the 800 ppm group had atrophied seminiferous tubules and another had Leydig cell hyperplasia. These effects, as well as the transient decrease in testosterone levels observed by Cameron et al. (1985, 1984), could be the result of chemically-related strain on the rat system as it attempts to maintain hormone homeostasis.

Dorman et al. (1995) conducted a series of in vitro and in vivo studies of developmental toxicity in ICR BR (CD-1) mice associated with methanol and formate exposure. The studies used HPLC grade methanol and appropriate controls. PK and developmental toxicity parameters were measured in mice exposed to a 6-hour methanol inhalation (10,000 or 15,000 ppm), methanol gavage (1.5 g/kg) or sodium formate (750 mg/kg by gavage) on GD8. In the in vivo inhalation study, 12–14 dams/group were exposed to 10,000 ppm methanol for 6 hours on GD8,[42] with and without the administration of fomepizole (4-methylpyrazole) to inhibit the metabolism of methanol by ADH1. Dams were sacrificed on GD10, and folate levels in maternal RBC and conceptus (decidual swelling) were measured, as well as fetal neural tube patency (an early indicator of methanol-induced dysmorphogenic response). The effects observed included a transient decrease in maternal RBC and conceptus folate levels within 2 hours following exposure and a significant ($p < 0.05$) increase in the incidence of fetuses with open neural tubes (9.65% in treated versus 0 in control). These responses were not observed following sodium formate administration, despite peak formate levels in plasma and decidual swellings being similar to those observed following the 6-hour methanol inhalation of 15,000 ppm. This suggests that these methanol-induced effects are not related to the accumulation of formate. As this study provides information relevant to the identification of the proximate teratogen associated with developmental toxicity in rodents, it is discussed more extensively in Section 4.6.1.

[42] Dorman et al. (1985) state that GD8 was chosen because it encompasses the period of murine neurulation and the time of greatest vulnerability to methanol-induced neural tube defects.

4.3.3. Other Reproductive and Developmental Toxicity Studies

Additional information relevant to the possible effects of methanol on reproductive and developmental parameters has been provided by experimental studies that have exposed experimental animals to methanol during pregnancy via i.p. injections (Rogers et al., 2004). Relevant to the developmental impacts of the chemical, a number of studies also have examined the effects of methanol when included in whole-embryo culture (Hansen et al., 2005; Harris et al., 2003; Andrews et al., 1998, 1995, 1993).

Pregnant female C57BL/6J mice received 2 i.p. injections of methanol on GD7 (Rogers et al., 2004). The injections were given 4 hours apart to provide a total dosage of 0, 3.4, and 4.9 g/kg. Animals were sacrificed on GD17 and the litters were examined for live, dead, and resorbed fetuses. Rogers et al. (2004) monitored fetal weight and examined the fetuses for external abnormalities and skeletal malformations. Methanol-related deficits in maternal and litter parameters observed by Rogers et al. (2004) are summarized in Table 4-12.

Table 4-12. Maternal and litter parameters when pregnant female C57BL/6J mice were injected i.p. with methanol

Parameter	Methanol dose (g/kg)		
	0	**3.4**	**4.9**
No. pregnant at term	43	13	24
Wt gain GD7–GD8 (g)	0.33 ± 0.10	0.37 ± 0.15	-0.24 ± 0.14[a]
Wt gain GD7–GD10 (g)	1.63 ± 0.18	2.20 ± 0.20	1.50 ± 0.20
Live fetuses/litter	7.5 ± 0.30	6.3 ± 0.5[a]	3.7 ± 0.4[a]
Resorbed fetuses/litter	0.4 ± 0.1	1.3 ± 0.4[a]	4.4 ± 0.4[a]
Dead fetuses/litter	0.1 ± 0.1	0	0.1 ± 0.1
Fetal weight (g)	0.83 ± 0.02	0.82 ± 0.03	0.70 ± 0.02[a]

Values are means ± SEM.
[a]$p < 0.05$, as calculated by the authors.

Source: Rogers et al. (2004).

Rogers et al. (2004) used a number of sophisticated imaging techniques, such as confocal laser scanning and fluorescence microscopy, to examine the morphology of fetuses excised at GD7, GD8, and GD9. They identified a number of external craniofacial abnormalities, the incidence of which was, in all cases, significantly increased in the high-dose group compared to controls. For some responses, such as microanophthalmia and malformed maxilla, the incidence was also significantly increased in animals receiving the lower dose. Fifteen compound-related skeletal malformations were tabulated in the report. In most cases, a dose-response effect was evident, resulting in statistically significant incidences in affected fetuses and litters, when compared to controls. Apparent effects of methanol on the embryonic forebrain included a

narrowing of the anterior neural plate, missing optical vesicles, and holoprosencephaly (failure of the embryonic forebrain to divide). The authors noted that there was no sign of incipient cleft palate or exencephaly, as had been observed in CD-1 mice exposed to methanol via the oral and inhalation routes (Rogers et al., 1993a).

In order to collect additional information on cell proliferation and histological changes in methanol-treated fetuses, Degitz et al. (2004a) used an identical experimental protocol to that of Rogers et al. (2004) by administering 0, 3.4, or 4.9 g methanol/kg in distilled water i.p. (split doses, 4 hours apart) to C57BL/6J mice on GD7. Embryos were collected at various times on GD8 and GD10. Embryos from dams exposed to 4.9 g/kg and examined on GD8 exhibited reductions in the anterior mesenchyme, the mesenchyme subjacent to the mesencephalon and the base of the prosencephalon (embryonic forebrain), and in the forebrain epithelium. The optic pits were often lacking; where present their epithelium was thin and there were fewer neural crest cells in the mid- and hindbrain regions.

At GD9, there was extensive cell death in areas populated by the neural crest, including the forming cranial ganglia. Dose-related abnormalities in the development of the cranial nerves and ganglia were seen on GD7. In accordance with an arbitrary dichotomous scale devised by the authors, scores for ganglia V, VIII, and IX were significantly (not otherwise specified) reduced at all dose levels, and ganglia VII and X were reduced only at the highest dose. At the highest dose (4.9 g/kg), the brain and face were poorly developed and the brachial arches were reduced in size or virtually absent. Flow cytometry of the head regions of the embryos from the highest dose at GD8 did not show an effect on the proportion of cells in S-phase.

Cell growth and development were compared in C57BL/6J and CD-1 mouse embryos cultured in methanol (Degitz, et al., 2004b). GD8 embryos, with 5–7 somites, were cultured in 0, 1, 2, 3, 4, or 6 mg methanol/mL for 24 hours and evaluated for morphological development. Cell death was increased in both strains in a developmental stage- and region-specific manner at 4 and 6 mg/mL after 8 hours of exposure. The proportions of cranial region cells in S-phase were significantly ($p < 0.05$) decreased at 6 mg/mL following 8- and 18-hour exposures to methanol. After 24 hours of exposure, C57BL/6J embryos had significantly ($p < 0.05$) decreased total protein at 4 and 6 mg/kg. Significant ($p < 0.05$) developmental effects were seen at 3, 4, and 6 mg/kg, with eye dysmorphology being the most sensitive endpoint. CD-1 embryos had significantly decreased total protein at 3, 4, and 6 mg/kg, but developmental effects were seen only at 6 mg/kg. It was concluded that the C57BL/6J embryos were more severely affected by methanol in culture than the CD-1 embryos.

Andrews et al. (1993) carried out a comparative study of the developmental toxicity of methanol in whole Sprague-Dawley rat or CD-1 mouse embryos. Nine-day rat embryos were explanted and cultured in rat serum containing 0, 2, 4, 8, 12, or 16 mg/mL methanol for 24 hours

then transferred to rat serum alone for a further 24 hours. Eight-day mouse embryos were cultured in 0, 2, 4, 6, or 8 mg/mL methanol in culture medium for 24 hours. At the end of the culture period, embryos were examined for growth, development and dysmorphogenesis. For the rats, doses of 8 mg/mL and above resulted in a concentration-related decrease in somite number, head length, and developmental score. Some lethality was seen in embryos incubated at 12 mg/mL methanol. For the mouse embryos, incubation concentrations of 4 mg/mL methanol and above resulted in a significant decrease in developmental score and crown-rump length. The high concentration (8 mg/mL) was associated with embryo lethality. These data suggest that mouse embryos are more sensitive than rat embryos to the developmental effects of methanol. Using a similar experimental system to examine the developmental toxicity of formate and formic acid in comparison to methanol, Andrews et al. (1995) showed that the formates are embryotoxic at doses that are four times lower than equimolar doses of methanol. Andrews et al. (1998) showed that exposure to combinations of methanol and formate was less embryotoxic than would be expected based on simple toxicity additivity, suggesting that the embryotoxicity observed following low-level exposure to methanol is mechanistically different from that observed following exposure to formate.

A study by Hansen et al. (2005) determined the comparative toxicity of methanol and its metabolites, formaldehyde and sodium formate, in GD8 mouse (CD-1) and GD10 rat (Sprague-Dawley) conceptuses. Incubation of whole embryos was for 24 hours in chemical-containing media (mouse: 4–12 mg/mL methanol, 1–6 µg/mL formaldehyde, 0.5–4 mg/mL sodium formate; rat: 8–20 mg/mL, 1–8 µg/mL, 0.5–8 mg/mL). Subsequently, the visceral yolk sac (VYS) was removed and frozen for future protein and DNA determination. The embryos were examined morphologically to determine growth and developmental parameters such as viability, flexure and rotation, crown-rump length, and neuropore closure. In other experiments, the chemicals were injected directly into the amniotic space. For each response, Table 4-13 provides a comparison of the concentrations or amounts of methanol, formaldehyde, and formate that resulted in statistically significant changes in developmental abnormalities compared to controls.

For a first approximation, these concentrations or amounts may be taken as threshold-dose ranges for the specific responses under the operative experimental conditions. The data show consistently lower threshold values for the effects of formaldehyde compared to those of formate and methanol. The mouse embryos were more sensitive towards methanol toxicity than rat embryos, consistent with in vivo findings, whereas the difference in sensitivity disappeared when formaldehyde was administered. Hansen et al. (2005) hypothesized that, while the MOA for the initiation of the organogenic defects is unknown, the relatively low threshold levels of formaldehyde for most measured effects suggest formaldehyde involvement in the embryotoxic effects of methanol. By contrast, formate, the putative toxicant for the acute effects of methanol

poisoning (acidosis, neurological deficits), did not appear to reproduce the methanol-induced teratogenicity in these whole embryo culture experiments.

Table 4-13. Reported thresholds concentrations (and author-estimated ranges) for the onset of embryotoxic effects when rat and mouse conceptuses were incubated in vitro with methanol, formaldehyde, and formate

Parameter	Mouse			Rat		
	Methanol	Formaldehyde	Formate	Methanol	Formaldehyde	Formate
	In vitro incubation (mg/mL)					
Viability (%)	8.0	0.004	NS	16.0	0.006	2.0
Normal rotation (%)	4.0	0.003	0.5	8.0	0.003	4.0
CR[a] length	No change	No change	No change	No change	No change	No change
Neural tube closure (%)	8.0	0.001	2.0	12.0	No change	No change
Reduced embryo protein	8.0	0.003	4.0	8.0	0.004	2.0
Reduced VYS[b] protein	10.0	0.004	4.0	12.0	0.004	NR
Reduced embryo DNA	8.0	0.003	No change	12.0	0.003	NR
Reduced VYS DNA	4.0	0.001	0.5	12.0	0.003	NR
Microinjection (author-estimated dose ranges in µg)						
Viability (%)	46–89	0.003–0.5	1.01–1.5	46–89	1.01–1.5	1.51–4.0
Normal rotation (%)	1–45	0.003–0.5	0.03–0.5	46–89	1.01–1.5	0.51–1.0
CR[a] length	No change	No change	No change	No change	No change	No change
Neural tube closure (%)	1–45	0.003–0.5	1.01–1.5	No change	No change	1.01–1.5
Reduced embryo protein	1–45	0.501–1.0	No change	No change	1.51–2.0	0.51–1.0
Reduced VYS[b] protein	135–178	1.01–1.5	No change	No change	No change	1.01–1.5
Reduced embryo DNA	46–89	0.501–1.0	No change	No change	No change	0.51–1.0
Reduced VYS[b] DNA	1–45	0.003–0.5	0.03–0.5	No change	No change	0.51–1.0

[a]CR = crown-rump length,
[b]VYS = visceral yolk sac.
NR = not reported

Source: Hansen et al. (2005); Harris et al. (2004) (adapted).

Harris et al. (2003) provided biochemical evidence consistent with the concept that formaldehyde might be the ultimate embryotoxicant of methanol by measuring the activities of enzymes that are involved in methanol metabolism in mouse (CD-1) and rat (Sprague-Dawley) whole embryos at different stages of development. Specific activities of the enzymes ADH1, ADH3, and CAT, were determined in rat and mouse conceptuses during the organogenesis period of 8–25 somites. Activities were measured in heads, hearts, trunks, and VYS from early- and late-stage mouse and rat embryos. While CAT activities were similar between rat and mouse embryos, mouse ADH1 activities in the VYS were significantly lower throughout organogenesis when compared to the rat VYS or embryos of either species. ADH1 activities of heads, hearts, and trunks from mouse embryos were significantly lower than those from rats at the 7–12 somite

stage. However, these interspecies differences were not evident in embryos of 20–22 somites. ADH3 activities were lower in mouse versus rat VYS, irrespective of the stage of development. However, while ADH3 activities in mouse embryos were markedly lower than those of rats in the early stages of development, the levels of activity were similar to at the 14–16 somite stage and beyond. A lower capacity to transform formaldehyde to formate might explain the increased susceptibility of mouse versus rat embryos to the toxic effects of methanol. The hypothesis that formaldehyde is the ultimate embryotoxicant of methanol is supported by the demonstration of diminished ADH3 activity in mouse versus rat embryos and by the demonstration by Hansen et al. (2005) that formaldehyde has a far greater embryotoxicity than either formate or methanol itself.

That formate can induce similar developmental lesions in whole rat and mouse conceptuses was demonstrated by Andrews et al. (1995), who evaluated the developmental effects of sodium formate and formic acid in rodent whole embryo cultures in vitro. Day 9 rat (Sprague-Dawley) embryos were cultured for 24 or 48 hours and day 8 mouse (CD-1) cultures were incubated for 24 hours. As tabulated by the authors, embryos of either species showed trends towards increasing lethality and incidence of abnormalities with exposure concentration. Among the anomalies observed were open anterior and posterior neuropores, plus rotational defects, tail anomalies, enlarged pericardium, and delayed heart development.

4.4. NEUROTOXICITY

A substantial body of information exists on the toxicological consequences to humans who consume or are exposed to large amounts of methanol. As discussed in Section 4.1, neurological consequences of acute methanol intoxication in humans include Parkinson-like responses, visual impairment, confusion, headache, and numerous subjective symptoms. The occurrence of these symptoms has been shown to be associated with necrosis of the putamen when neuroimaging techniques have been applied (Salzman, 2006). Such profound changes have been linked to tissue acidosis that arises when methanol is metabolized to formaldehyde and formic acid through the actions of ADH1 and ADH3. However, the well-documented impact of the substantial amounts of formate that are formed when humans and animals are exposed to large amounts of methanol may obscure the potentially harmful effects that may arise when humans and animals exposed to smaller amounts. Human acute exposure studies (Chuwers et al., 1995; Cook et al., 1991) (See Section 4.1.3) at TLV levels of 200 ppm would indicate that some measures of neurological function (e.g., sensory evoked potentials, memory testing and psychomotor testing) were impaired in the absence of measureable formate production.

4.4.1. Oral Studies

Two rodent studies investigated the neurological effects of developmental methanol exposure via the oral route (Aziz et al., 2002; Infurna and Weiss, 1986). One of these studies also investigated the influence of FAD diets on the effects of methanol exposures (Aziz et al., 2002). In the first, Infurna and Weiss (1986) exposed 10 pregnant female Long-Evans rats/dose to 2% methanol (purity not specified) in drinking water on either GD15–GD17 or GD17–GD19. Daily methanol intake was calculated at 2,500 mg/kg-day by the study authors. Dams were allowed to litter and nurse their pups. Data were analyzed by ANOVA with the litter as the statistical unit. Results of the study were equivalent for both exposure periods. Treatment had no effect on gestational length or maternal bodyweight. Methanol had no effect on maternal behavior as assessed by the time it took dams to retrieve pups after they were returned to the cage following weighing. Litter size, pup birth weight, pup postnatal weight gain, postnatal mortality, and day of eye opening did not differ from controls in the methanol treated groups. Two neurobehavioral tests were conducted in offspring. Suckling ability was tested in 3–5 pups/treatment group on PND1. An increase in the mean latency for nipple attachment was observed in pups from the methanol treatment group, but the percentage of pups that successfully attached to nipples did not differ significantly between treatment groups. Homing behavior, the ability to detect home nesting material within a cage containing one square of shavings from the pup's home cage and four squares of clean shavings, was evaluated in 8 pups/group on PND10. Pups from both of the methanol exposure groups took about twice as long to locate the home material and took less direct paths than the control pups. Group-specific values differed significantly from controls. This study suggests that developmental toxicity can occur at this drinking water dose without readily apparent signs of maternal toxicity.

Aziz et al. (2002) investigated the role of developmental deficiency in folic acid and methanol-induced developmental neurotoxicity in PND45 rat pups. Wistar albino female rats (80/group) were fed FAD[43] and FAS diets separately. Following 14–16 weeks on the diets, liver folate levels were estimated and females exhibiting a significantly low folic acid level were mated. Throughout their lactation period, dams of both the FAD and the FAS group were given 0, 1, 2, or 4% v/v methanol via drinking water, equivalent to approximately 480, 960 and 1,920 mg/kg-day.[44] Pups were exposed to methanol via lactation from PND1–PND21. Litter size was culled to 8 with equal male/female ratios maintained as much as possible. Liver folate levels were determined at PND21 and neurobehavioral parameters (motor performance using the

[43] Along with the FAD diet, 1% succinylsulphathiazole was also given to inhibit folic acid biosynthesis from intestinal bacteria.

[44] Assuming that Wistar rat drinking water consumption is 60 mL/kg-day (Rogers et al., 2002), 1% methanol in drinking water would be equivalent to 1% x 0.8 g/mL x 60 mL/kg-day = 0.48 g/kg-day = 480 mg/kg-day.

spontaneous locomotor activity test and cognitive performance using the conditioned avoidance response [CAR] test), and neurochemical parameters (dopaminergic and cholinergic receptor binding and dopamine levels) were measured at PND45. The expression of growth-associated protein (GAP 43), a neuro-specific protein in the hippocampus that is primarily localized in growth cone membranes and is expressed during developmental regenerative neurite outgrowth, was examined using immunohistochemistry and western blot analysis.

A loss in body weight gain was observed at PND7, PND14, and PND21 in animals exposed to 2% (11, 15 and 19% weight gain reduction) and 4% (17, 24 and 29% weight gain reduction) methanol in the FAD group and only at 4% (9, 14 and 17% weight gain reduction) methanol in the FAS group. No significant differences in food and water intake were observed among the different treatment groups. Liver folate levels in the FAD group were decreased by 63% in rats prior to mating and 67% in pups on PND21.

Based on reports of Parkinson-like symptoms in survivors of severe methanol poisoning (see Section 4.1), Aziz et al. (2002) hypothesized that methanol may cause a depletion in dopamine levels and degeneration of the dopaminergic nigrostriatal pathway.[45] Consistent with this hypothesis, they found dopamine levels were significantly decreased (32% and 51%) in the striatum of rats in the FAD group treated with 2% and 4% methanol, respectively. In the FAS group, a significant decrease (32%) was observed in the 4% methanol-exposed group.

Methanol treatment at 2% and 4% was associated with significant increases in activity, in the form of distance traveled in a spontaneous locomotor activity test, in the FAS group (13% and 39%, respectively) and more notably, in the FAD group (33% and 66%, respectively) when compared to their respective controls. Aziz et al. (2002) suggest that these alterations in locomotor activity may be caused by a significant alteration in dopamine receptors and disruption in neurotransmitter availability. Dopamine receptor ($D_{2)}$ binding in the hippocampus of the FAD group was significantly increased (34%) at 1% methanol, but was significantly decreased at 2% and 4% methanol exposure by 20% and 42%, respectively. In the FAS group, D_2 binding was significantly increased by 22% and 54% in the 2% and 4% methanol-exposed groups.

At PND45, the CAR in FAD rats exposed to 2% and 4% methanol was significantly decreased by 48% and 52%, respectively, relative to nonexposed controls. In the FAS group, the CAR was only significantly decreased in the 4% methanol-exposed animals and only by 22% as compared to their respective controls. Aziz et al. (2002) suggest that the impairment in CAR of the methanol-exposed FAD pups may be due to alterations in the number of cholinergic (muscarinic) receptor proteins in the hippocampal region of the brain. Muscarinic receptor

[45] The nigrostriatal pathway is one of four major dopamine pathways in the brain that are particularly involved in the production of movement. Loss of dopamine neurons in the substantia nigra is one of the pathological features of Parkinson's disease (Kim et al., 2003),

binding was significantly increased in the 2% (20%) and 4% (42%) methanol-exposed group in FAD animals, while FAS group animals had a significant increase in cholinergic binding only in the 4% methanol exposed group (21%). High concentrations of methanol may saturate the body's ability to remove toxic metabolites, including formaldehyde and formate, and this may be exacerbated in FAD pups having a low store of folate.

Immunohistochemistry showed an increase in the expression of GAP-43 protein in the dentate granular and pyramidal cells of the hippocampus in 2% and 4% methanol-exposed animals in the FAD group. The FAS group showed increased expression only in the 4% methanol-exposed group. The Western blot analysis also confirmed a higher expression of GAP-43 in the 2% and 4% methanol-exposed FAD group rats. Aziz et al. (2002) suggested that up-regulation of GAP-43 in the hippocampal region may be associated with axonal growth or protection of the nervous system from methanol toxicity.

The Aziz et al. (2002) study provides evidence that hepatic tetrahydrofolate is an important contributing factor in methanol-induced developmental neurotoxicity in rodents. The immature blood-brain barrier and inefficient drug-metabolizing enzyme system make the developing brain a particularly sensitive target organ to the effects of methanol exposure.

4.4.2. Inhalation Studies

A review by Carson et al. (1981) has summarized a number of older reports of studies on the toxicological consequences of methanol exposure. In one example relevant to neurotoxicity, the review cites a research report of Chen-Tsi (1959) who exposed 10 albino rats/group (sex and strain unstated) to 1.77 and 50 mg/m^3 (1.44 and 40.7 ppm) methanol vapor, 12 hours/day, for 3 months. Deformation of dendrites, especially the dendrites of pyramidal cells, in the cerebral cortex was included in the description of histopathological changes observed in adult animals following exposure to 50 mg/m^3 (40.7 ppm) methanol vapor. One out of ten animals exposed to the lower methanol concentration also displayed this feature.

Information on the neurotoxicity of methanol inhalation exposure in adult monkeys (*M. fascicularis*) has come from NEDO (1987) which describes the results of a number of experiments. The study included an acute study, a chronic study monkeys, and a repeated exposure experiment (of variable duration depending upon exposure level), followed by recovery period (1–6 months), and an experiment looking at chronic formaldehyde exposure (1 or 5 ppm), a combustion product of methanol. This last experiment was apparently only a pilot and included only one monkey per exposure condition.

In the chronic experiment 8 monkeys were included per exposure level (control, 10, 100, 1,000 ppm or 13, 131, and 1,310 mg/m^3, respectively, for 21 hours/day); however, animals were serially sacrificed at 3 time points: 7 months, 19 months, or >26 months. This design reduced

the number of monkeys at each exposure level to 2 subjects at 7 months and 3 subjects at the subsequent time points (see Section 4.2.2). One of the 3 animals receiving 100 ppm methanol and scheduled for sacrifice at 29 months was terminated at 26 months.

Histopathologically, no overt degeneration of the retina, optical nerve, cerebral cortex, or other potential target organs (liver and kidney) was reported in the chronic experiment. Regarding the peripheral nervous system, 1/3 monkeys exposed to 100 ppm (131 mg/m^3) and 2/3 exposed to 1,000 ppm (1,310 mg/m^3) for 29 months showed slight but clear changes in the peroneal nerves. There was limited evidence of CNS degeneration inside the nucleus of the thalamus of the brain at exposure to 100 ppm (131 mg/m^3) or 1,000 ppm (1,310 mg/m^3) for 7 months or longer. Abnormal appearance of stellate cells (presumed astroglia) within the cerebral white matter was also observed in a high proportion (7/8 in both mid- and high-exposure groups) of monkeys exposed to 100 ppm and 1,000 ppm for 7 months or more. All monkeys that had degeneration of the inside nucleus of the thalamus also had degeneration of the cerebral white matter. According to NEDO (1987), the stellate cell response was transient and "not characteristic of degeneration." The authors also noted that the stellate cell response was "nearly absent in normal monkeys in the control group" and "in the groups exposed to a large quantity of methanol or for a long time their presence tended to become permanent, so a relation to the long term over which the methanol was inhaled is suspected." However, all control group responses are reported in a single table in the section of the NEDO (1987) report that describes the acute monkey study, with no indication as to when the control group was sacrificed.

In the recovery experiment, monkeys were exposed to 1,000, 2,000, 3,000, or 5,000 ppm methanol, followed by recovery periods of various duration. Monkeys exposed to 3,000 ppm for 20 days followed by a 6-month recovery period experienced relatively severe fibrosis of responsive stellate cells and lucidation of the medullary sheath. However, resolution of some of the glial responses was noted in the longer duration at lower exposure levels, with no effects observed on the cerebral white matter in monkeys exposed for 7 months to 1,000 ppm methanol followed by a 6-month recovery period. In general, the results from the recovery experiment corroborated results observed in the chronic experiment. NEDO (1987) interpreted the lack of glial effects after a 6-month recovery as an indication of a transient effect. The authors failed to recognize that glial responses to neural damage do not necessarily persist following resolution of neurodegeneration (Aschner and Kimmelberg, 1996).

The limited information available from the NEDO (1987) summary report suggests that 100 ppm (131 mg/m^3) may be an effect level following continuous, chronic exposure to methanol. However, the current report does not indicate a robust dose response for the neurodegenerative changes in the thalamus and glial changes in the white matter. The number of animals at each exposure level for each serial sacrifice also limits statistical power (2–3 monkeys/time point/exposure level). Confidence in this study is also weakened by the lack of documentation for a concurrent control group.

Weiss et al. (1996) exposed 4 cohorts of pregnant Long-Evans rats (10–12 dams/ treatment group/cohort) to 0 or 4,500 ppm (0 and 5,897 mg/m^3) methanol vapor (high-performance liquid chromatography [HPLC] grade), 6 hours/day, from GD6 to PND21. Pups were exposed together with the dams during the postnatal period. Average blood methanol levels in pups on PND7 and PND14 were about twice the level observed in dams. However, methanol exposure had no effect on maternal gestational weight gain, litter size, or postnatal pup weight gain up to PND18[46]. Neurobehavioral tests were conducted in neonatal and adult offspring; the data generated from those tests were evaluated by repeated measures ANOVA. Three neurobehavioral tests conducted in 13–26 neonates/group included a suckling test, conditioned olfactory aversion test, and motor activity test. In contrast to earlier test results reported by Infurna and Weiss (1986), methanol exposure had no effect on suckling and olfactory aversion tests conducted on PND5 and PND10, respectively. Results of motor activity tests in the methanol group were inconsistent, with decreased activity on PND18 and increased activity on PND25. Tests that measured motor function, operant behavior, and cognitive function were conducted in 8–13 adult offspring/group. Some small performance differences were observed between control and treated adult rats in the fixed wheel running test only when findings were evaluated separately by sex and cohort. The test requires the adult rats to run in a wheel and rotate it a certain amount of times in order to receive a food reward. A stochastic spatial discrimination test examined the rats' ability to learn patterns of sequential responses. Methanol exposure had no effect on their ability to learn the first pattern of sequential responses, but methanol-treated rats did not perform as well on the reversal test. The result indicated possible subtle cognitive deficits as a result of methanol exposure. A morphological examination of offspring brains conducted on PND1 and PND21 indicated that methanol exposure had no effect on neuronal migration, numbers of apoptotic cells in the cortex or germinal zones, or myelination. However, neural cell adhesion molecule (NCAM) 140 and NCAM 180 gene expression in treated rats was reduced on PND4 but not 15 months after the last exposure. NCAMs are glycoproteins required for neuron migration, axonal outgrowth, and establishing mature neuronal function patterns.

Stanton et al. (1995) exposed 6–7 pregnant female Long-Evans rats/group to 0 or 15,000 ppm (0 and 19,656 mg/m^3) methanol vapors (≥ 99.9% purity) for 7 hours/day on GD7–GD19. Mean serum methanol levels at the end of the 1st, 4th, 8th, and 12th days of exposure were, 3,836, 3,764, 3,563, and 3,169 µg/mL, respectively. As calculated by authors, dams received an estimated methanol dose of 6,100 mg/kg-day. A lower body weight on the first

[46] The fact that this level of exposure caused effects in the Sprague-Dawley rats of the NEDO (1987) study but did not cause a readily apparent maternal effect in Long-Evans rats of this study could be due to diffences in strain susceptibility.

2 days of exposure was the only maternal effect; there was no increase in postimplantation loss. Dams were allowed to deliver and nurse litters. Parameters evaluated in pups included mortality, growth, pubertal development, and neurobehavioral function. Examinations of pups revealed that two pups from the same methanol-exposed litter were missing one eye; aberrant visually evoked potentials were observed in those pups. A modest but significant reduction in body weight gain on PND1, PND21, and PND35 was noted in pups from the methanol group. For example, by PND35, male pups of dams exposed to methanol had a mean body weight of 129 grams versus 139 grams in controls ($p < 0.01$). However, postnatal mortality was unaffected by exposure to methanol. The study authors did not consider a 1.7-day delay in vaginal opening in the methanol group to be an adverse effect. Preputial separation was not affected by prenatal methanol exposure. Neurobehavioral status was evaluated using 8 different tests on specific days up to PND160. Tests included motor activity on PND13–PND21, PND30, and PND60, olfactory learning and retention on PND18 and PND25, behavioral thermoregulation on PND20-21, T-maze delayed alternation learning on PND23–PND24, acoustic startle reflex on PND24, reflex modification audiometry on PND61–PND63, passive avoidance on PND73, and visual evoked potentials on PND160. A single pup/sex/litter was examined in most tests, and some animals were subjected to multiple tests. The statistical significance of neurobehavioral testing was assessed by one-way ANOVA, using the litter as the statistical unit. Results of the neurobehavioral testing indicated that methanol exposure had no effect on the sensory, motor, or cognitive function of offspring under the conditions of the experiment. However, given the comparatively small number of animals tested for each response, it is uncertain whether the statistical design had sufficient power to detect small compound-related changes.

NEDO (1987, unpublished report) sponsored a teratology study that included an evaluation of postnatal effects in addition to standard prenatal endpoints in Sprague-Dawley rats. Thirty-six pregnant females/group were exposed to 0, 200, 1,000, or 5,000 ppm (0, 262, 1,310, and 6,552 mg/m^3) methanol vapors (reagent grade) on GD7–GD17 for 22.7 hours/day. Statistical significance of results was evaluated by t-test, Mann-Whitney U test, Fisher's exact test, and/or Armitage's χ^2 test.

Postnatal effects of methanol inhalation were evaluated in the remaining 12 dams/group that were permitted to deliver and nurse their litters. Effects were only observed in the 5,000 ppm. There were no adverse effects on offspring body weight from methanol exposure. However, the weights of some organs (brain, thyroid, thymus, and testes) were reduced in 8-week-old offspring following prenatal-only exposure to 5,000 ppm methanol. An unspecified number of offspring were subjected to neurobehavioral testing or necropsy, but results were incompletely reported.

NEDO (1987, unpublished report) also contains an account of a two-generation reproductive study that evaluated the effects of pre- and postnatal methanol (reagent grade) exposure (20 hours/day) on reproductive and other organ systems of Sprague-Dawley rats and in particular the brain. The F_0 generation (30 males and 30 females per exposure group)[47] was exposed to 0, 10, 100, and 1,000 ppm (0, 13.1, 131, and 1,310 mg/m^3) from 8 weeks old to the end of mating (males) or to the end of lactation period (females). The F_1 generation was exposed to the same concentrations from birth to the end of mating (males) or to weaning of F_2 pups 21 days after delivery (females). Males and females of the F_2 generation were exposed from birth to 21 days old (1 animal/sex/litter was exposed to 8 weeks of age). NEDO (1987) noted reduced brain, pituitary, and thymus weights, in the offspring of F_0 and F_1 rats exposed to 1,000 ppm methanol. As discussed in the report, NEDO (1987) sought to confirm the possible compound-related effect of methanol on the brain by carrying out an additional study in which Sprague-Dawley rats were exposed to 0, 500, 1,000, and 2,000 ppm (0, 655, 1,310, and 2,620 mg/m^3) methanol from the first day of gestation through the F_1 generation. Brain weights were measured in 10–14 offspring/sex/group at 3, 6, and 8 weeks of age. As illustrated in Table 4-14, brain weights were significantly reduced in 3-week-old males and females exposed to ≥ 1,000 ppm. At 6 and 8 weeks of age, brain weights were significantly reduced in males exposed to ≥ 1,000 ppm and females exposed to 2,000 ppm. Due to the toxicological significance of this postnatal effect and the fact that it has not been measured or reported elsewhere in the peer-reviewed methanol literature, the brain weight changes observed by NEDO (1987) following gestational and postnatal exposures and following gestation-only exposure (in the teratology study discussed above) are evaluated quantitatively and discussed in more detail in Section 5 of this review.

[47] A second control group of 30 animals/sex was maintained in a separate room to "confirm that environmental conditions inside the chambers were not unacceptable to the animals."

Table 4-14. Brain weights of rats exposed to methanol vapors during gestation and lactation

Offspring age	Sex	Brain weight (g) (% control) at each exposure level					
		0 ppm	200 ppm	500 ppm	1,000 ppm	2,000 ppm	5,000 ppm
3 wk	Male	1.45 ± 0.06	--	1.46 ± 0.08 (101%)	1.39 ± 0.05[c] (96%)	1.27 ± 0.06[e] (88%)	--
	Female	1.41 ± 0.06	--	1.41 ± 0.07 (100%)	1.33 ± 0.07[d] (94%)	1.26 ± 0.09[e] (89%)	--
6 wk	Male	1.78 ± 0.07	--	1.74 ± 0.09 (98%)	1.69 ± 0.06[d] (95%)	1.52 ± 0.07[e] (85%)	--
	Female	1.68 ± 0.08	--	1.71 ± 0.08 (102%)	1.62 ± 0.07 (96%)	1.55 ± 0.05[e] (92%)	--
8 wk[a]	Male	1.99 ± 0.06	--	1.98 ± 0.09 (99%)	1.88 ± 0.08[d] (94%)	1.74 ± 0.05[e] (87%)	--
	Female	1.85 ± 0.05	--	1.83 ± 0.07 (99%)	1.80 ± 0.08 (97%)	1.67 ± 0.06[e] (90%)	--
8 wk[b]	Male	2.00 ± 0.05	2.01 ± 0.08 (100%)	--	1.99 ± 0.07 (100%)	--	1.81 ± 0.16[d] (91%)
	Female	1.86 ± 0.08	1.91 ± 0.06 (103%)	--	1.90 ± 0.08 (102%)	--	1.76 ± 1.09 (95%)

[a]Exposed throughout gestation and F_1 generation.
[b]Exposed on gestational days 7-17 only.
[c]$p < 0.05$, [d]$p < 0.01$, [e]$p < 0.001$, as calculated by the authors.
Values are means ± S.D.

Source: NEDO (1987).

Burbacher et al. (1999a,1999b) carried out toxicokinetic, reproductive, developmental and postnatal neurological and neurobehavioral studies of methanol in *M. fascicularis* monkeys that were published by HEI in a two-part monograph. Some of the data were subsequently published in the open scientific literature (Burbacher et al., 2004a, 2004b). The experimental protocol featured exposure to 2 cohorts of 12 monkeys/group to low-exposure levels (relative to the previously discussed rodent studies) of 0, 200, 600, or 1,800 ppm (0, 262, 786, and 2,359 mg/m^3) methanol vapors (99.9% purity), 2.5 hours/day, 7 days/week, during a premating period and mating period (–180 days combined) and throughout the entire gestation period (–168 days). The monkeys were 5.5–13 years old and were a mixture of feral-born and colony-bred animals. The outcome study included an evaluation of maternal reproductive performance (discussed in Section 4.3.2) and tests to assess infant postnatal growth and newborn health, neurological outcomes included reflexes, behavior, and development of visual, sensorimotor, cognitive, and social behavioral function. Blood methanol levels, clearance, and the appearance of formate were also examined and are discussed in Section 3.2. The effects observed were in the absence of appreciable increases in maternal blood formate levels.

Neurobehavioral function was assessed in 8–9 infants/group during the first 9 months of life (Burbacher et al., 2004a, 1999b). Although results in 7/9 tests were negative, 2 effects were possibly related to methanol exposure. The Visually Directed Reaching (VDR) test is a measure of sensorimotor development and assessed the infants' ability to grasp for a brightly colored object containing an applesauce-covered nipple. Beginning at 2 weeks after birth, infants were tested 5 times/day, 4 days/week. Performance on this test, measured as age from birth at achievement of test criterion (successful object retrieval on 8/10 consecutive trials over 2 testing sessions), was reduced in all treated male infants. The times (days after birth) to achieve the criteria for the VDR test were 23.7 ± 4.8 (n = 3), 32.4 ± 4.1 (n = 5), 42.7 ± 8.0 (n = 3), and 40.5 ± 12.5 (n = 2) days for males and 34.2 ± 1.8 (n = 5), 33.0 ± 2.9 (n = 4), 27.6 ± 2.7 (n = 5), and 40.0 ± 4.0 (n = 7) days for females in the control to 1,800 ppm groups, respectively. Statistical significance was obtained in the 1,800 ppm group when males and females were evaluated together ($p = 0.04$) and in the 600 ppm ($p = 0.007$) for males only. However, there was no significant difference between responses and/or variances among the dose levels for males and females combined ($p = 0.244$), for males only ($p = 0.321$) and for males only, excluding the high-dose group ($p = 0.182$). Yet there was a significant dose-response trend for females only ($p = 0.0265$). The extent to which VDR delays were due to a direct effect of methanol on neurological development or a secondary effect due to the methanol-induced decrease in length of pregnancy and subsequent prematurity is not clear. Studies of reaching behavior have shown that early motor development in pre-term human infants without major developmental disorders differs from that of full-term infants (Fallang et al., 2003). Clinical studies have indicated that the quality of reaching and grasping behavior in pre-term infants is generally less than that in full-term infants (Fallang et al., 2003; Plantinga et al., 1997). For this reason, measures of human infant development generally involve adjustment of a child's "test age" if he or she had a gestational age of fewer than 38 weeks, often by subtracting weeks premature from the age measured from birth (Wilson and Cradock, 2004). When this type of adjustment is made to the Burbacher et al. (2004a, 1999b) VDR data, the dose-response trend for males only becomes worse ($p = 0.448$) and the dose-response trend for the females only is improved ($p = 0.009$), though the variance in the data could not be modeled adequately. Thus, only the unadjusted VDR response for females only exhibited a dose response that could be adequately modeled for the purposes of this assessment (see Appendix C).

At 190–210 days of age, the Fagan Test of infant intelligence was conducted. The paradigm makes use of the infant's proclivity to direct more visual attention to novel stimuli rather than familiar stimuli. The test measures the time infants spend looking at familiar versus novel items. Deficits in the Fagan task can qualitatively predict deficits in intelligence quotient (IQ) measurements assessed in children at later ages (Fagan and Singer, 1983). Control monkey

infants in the Burbacher et al. (2004a, 1999b) study spent more than 62% ± 4% (mean for both cohorts) of their time looking at novel versus familiar monkey faces, while none of the treated monkeys displayed a preference for the novel faces (59% ± 2%, 54% ± 2% and 59% ± 2% in 200, 600 and 1,800 ppm groups, respectively). Unlike the VDR results discussed previously, results of this test did not appear to be gender specific and were neither statistically significant (ANOVA $p = 0.38$) nor related to exposure concentration. The findings indicated a cohort effect which appeared to reduce the statistical power of this analysis. The authors' exploratory analysis of differences in outcomes between the 2 cohorts indicated an effect of exposure in the second cohort and not the first cohort due to higher mean performance in controls of cohort 2 (70% ± 5% versus 55% ± 4% for cohort 1). In addition, this latter finding could reflect the inherent constraints of this endpoint. If the control group performs at the 60% level and the most impaired subjects perform at approximately the 50% chance level (worse than chance performance would not be expected), the range over which a concentration-response relationship can be expressed is limited. Because of the longer latency between assessment and birth, these results would not be confounded with the postulated methanol-induced decrease in gestation length of the exposed groups of this study. Negative results were obtained for the remaining seven tests that evaluated early reflexes, gross motor development, spatial and concept learning and memory, and social behavior. Infant growth and tooth eruption were unaffected by methanol exposure.

4.4.3. Studies Employing In Vitro, S.C. and I.P. Exposures

There is some experimental evidence that the presence of methanol can affect the activity of acetylcholinesterase (Tsakiris, et al., 2006). Although these experiments were carried out on erythrocyte membranes in vitro, the apparent compound-related changes may have implications for possible impacts of methanol and/or its metabolites on acetylcholinesterase at other centers, such as the brain. Tsakiris et al. (2006) prepared erythrocyte ghosts from blood samples of healthy human volunteers by repeated freezing-thawing. The ghosts were incubated for 1 hour at 37°C in 0, 0.07, 0.14, 0.6 or 0.8 mmol/L methanol and the specific activities of acetylcholinesterase monitored. Respective values (in change of optical density units/minute-mg protein) were 3.11 ± 0.15, 2.90 ± 0.10, 2.41 ± 0.10 ($p < 0.05$), 2.05 ± 0.11 ($p < 0.01$), and 1.81 ± 0.09 ($p < 0.001$). More recently, Simintzi et al. (2007) carried out an in vitro experiment to investigate the effects of aspartame metabolites, including methanol, on 1) a pure preparation of acetylcholinesterase, and 2) the same activity in homogenates of frontal cortex prepared from the brains of (both sexes of) Wistar rats. The activities were measured after incubations with 0, 0.14, 0.60, or 0.8 mmoles/L (0, 4.5, 19.2, and 25.6 mg/L) methanol, and with methanol mixed with the other components of aspartame metabolism, phenylalanine and aspartic acid. After incubation at

37°C for 1 hour, the activity of acetylcholinesterase was measured spectrophotometrically. As shown in Table 4-15, the activities of the acetylcholinesterase preparations were reduced dose dependently after incubation in methanol. Similar results were also obtained with the other aspartame metabolites, aspartic acid, and phenylalanine, both individually or as a mixture with methanol. While the implications of this result to the acute neurotoxicity of methanol are uncertain, the authors speculated that methanol may bring about these changes through either interactions with the lipids of rat frontal cortex or perturbation of proteinaceous components.

Table 4-15. Effect of methanol on Wistar rat acetylcholinesterase activities

Methanol concentration (mmol/L)	Acetylcholinesterase activity (ΔOD/min-mg)	
	Frontal cortex	Pure enzyme
Control	0.269 ± 0.010	1.23 ± 0.04
0.14	0.234 ± 0.007[a]	1.18 ± 0.06
0.60	0.223 ± 0.009[b]	1.05 ± 0.04[b]
0.80	0.204 ± 0.008[b]	0.98 ± 0.05[b]

Values are means ± S.D. for four experiments. The average value of each experiment was derived from three determinations of each enzyme activity.
[a]$p < 0.01$.
[b]$p < 0.001$.

Source: Simintzi et al. (2007).

In another experiment of relevance to neurotoxicity, the impact of repeat methanol exposure on amino acid and neurotransmitter expression in the retina, optic nerve, and brain was examined by Gonzalez-Quevedo et al. (2002). The goal of the study was to determine whether a sustained increase in formate levels, at concentrations below those known to produce toxic effects from acute exposures, can induce biochemical changes in the retina, optical nerve, or certain regions of the brain. Male Sprague-Dawley rats (5–7/group; 100–150 g) were divided into 6 groups and treated for 4 weeks according to the following plan. Four groups of animals received tap water ad libitum as drinking water for 1 week. During the second week, groups 1 and 2 (control and methanol respectively) received saline subcutaneously, (s.c.) and groups 3 and 4 (methotrexate[48] [MTX] and methotrexate-methanol [MTX-methanol], respectively) received MTX s.c. (0.2 mg/kg-day). During the 3rd week, MTX was reduced to 0.1 mg/kg and 20% methanol (2g/kg-day) was given i.p. to groups 2 (methanol) and 4 (MTX-methanol). Groups 1 (control) and 3 (MTX) received equivalent volumes of saline administered i.p. The treatment was continued until the end of the fourth week. Groups 5, (taurine[49] [Tau]) and 6, (Tau-MTX-

[48] Methotrexate depletes folate stores (resulting in an increase in the formate levels of methanol exposed animals) by interfering with tetrahydrofolate(THF) regeneration (Dorman et al., 1994).
[49] Taurine plays and important role in the CNS, especially in the retina and optical nerve, and was administered here to explore its possible protective effect (Gonzalez-Quevedo et al., 2002)

methanol) received 2% Tau in their drinking water ad libitum during the first 4 weeks, after which they were treated in the same manner as groups 1 and 4, respectively. Weights were documented weekly on all animals. Blood for formate and amino acid determinations and biopsy samples of retina, optic nerve, hippocampus, and posterior cortex of each animal were collected at the end of the experiment. Formate levels were not affected by Tau alone or MTX alone. While methanol alone increased blood formate levels, MTX-methanol, and Tau-MTX-methanol produced a threefold increase in blood formate levels as compared to controls and a twofold increase as compared to methanol alone. The amino acids aspartate, glutamate, asparagine, serine, histidine, glutamine, threonine, glycine, arginine, alanine, hypotaurine, gamma-aminobutyric acid (which is also a neurotransmitter), and tyrosine were measured in blood, brain, and retinal regions.

None of the amino acids measured were altered in the blood of methanol-, MTX-, or MTX-methanol-treated animals. Tau was increased in the blood of animals treated with taurine in the drinking water (Tau and Tau-MTX-methanol) and histidine was increased in the Tau group but not in the Tau-MTX-methanol group.

The levels of aspartate, Tau, glutamine, and glutamate were found to be altered by treatment in various areas of the brain. Aspartate was increased in the optic nerve of animals treated with MTX-methanol and Tau-MTX-methanol, indicating a possible relation to formate accumulation. The authors note that L-aspartate is a major excitatory amino acid in the brain and that increased levels of excitatory amino acids can trigger neuronal cell damage and death (Albin and Greenamyre, 1992). Aspartate, glutamine and Tau were found to be increased with respect to controls in the hippocampus of the three groups receiving methanol. Glutamate was significantly increased in the hippocampus in the methanol and the Tau-MTX-methanol groups with respect to controls, but no statistically significant difference was found in the MTX-methanol group when compared to controls, methanol alone, or the Tau-MTX-methanol groups. The authors suggest that increased levels of aspartate and glutamine in the hippocampus could provide an explanation for some of the CNS symptoms observed in methanol poisonings on the basis of their observed impact on cerebral arteries (Huang et al., 1994). The fact that these increases resulted primarily from methanol without MTX is significant in that it indicates methanol can cause excitotoxic effects without formate mediation. The treatments used did not produce any significant changes in amino acid levels in the posterior cortex.

The neurotransmitters serotonin (5-HT) and dopamine (DA) and their respective metabolites, 5-hydroxyindolacetic acid (5-HIAA) and dihydroxyphenylacetic acid (DOPAC), were measured in the brain regions described. The levels of these monoamines were not affected by formate accumulation, as the only increases were observed for 5-HT and 5-HIAA following methanol-only exposure. 5-HT was increased in the retina and hippocampus of methanol-only

treated animals, and the metabolite 5-HIAA was increased in the hippocampus of methanol-only treated animals; DA and DOPAC levels were not altered by the treatments in any of the areas measured. The posterior cortex did not show any changes in monoamine levels for any treatment group.

Rajamani et al. (2006) examined several oxidative stress parameters in male Wistar rats following methotrexate-induced folate deficiency. Animals (6/group) were divided into 3e groups: saline controls, methotrexate (MTX) controls, and MTX-methanol treated animals. Animals in the MTX-only group were treated with 0.2 mg/kg-day MTX s.c. injection for 7 days and following confirmation of folate deficiency, received either saline for MTX control and saline controls or a single dose of 3 g/kg methanol (20% w/v in saline) i.p. on day 8. On the 9th day, all animals were sacrificed and blood and tissue samples were collected. The optic nerve, retina, and brain were collected and the brain was dissected into the following regions: cerebral cortex, cerebellum, mid-brain, pons medulla, hippocampus and hypothalamus. Each region was homogenized, then centrifuged at 300 × g for 15 minutes and the supernatant was examined for indicators of oxidative stress including the free radical scavengers superoxide dismutase (SOD), CAT, glutathione peroxidase, and reduced GSH levels. The levels of protein thiols, protein carbonyls, and amount of lipid peroxidation were also measured. Compared to controls the levels of SOD, CAT, GSH peroxidase, oxidized GSH, protein carbonyls and lipid peroxidation were elevated in all of the brain regions where it was measured, with greater increases observed in the MTX-methanol treated animals than in the MTX alone group. The level of GSH and protein thiols was decreased in all regions of the brain, with a greater decrease observed in the MTX-methanol-treated animals than MTX-treated animals. In addition, expression of HSP70, a biomarker of cellular stress, was increased in the hippocampus. Overall, these results suggest that methanol treatment of folate-deficient rats results in increased oxidative stress in the brain, retina and optic nerve.

To determine the effects of methanol intoxication on the HPA axis, a combination of oxidative stress, immune and neurobehavioral parameters were observed (Parthasarathy et al., 2006a). Adult male Wistar albino rats (6 animals/group) were treated with either 0 or 2.37g/kg-day methanol i.p. for 1, 15 or 30 days. Oxidative stress parameters examined included SOD, CAT, GSH peroxidase, GSH, and ascorbic acid (Vitamin C). Plasma corticosterone levels were measured, and lipid peroxidation was measured in the hypothalamus and the adrenal gland. An assay for DNA fragmentation was conducted in tissue from the hypothalamus, the adrenal gland and the spleen. Immune function tests conducted included the footpad thickness test for delayed type hypersensitivity (DTH), a leukocyte migration inhibition assay, the hemagglutination assay (measuring antibody titer), the neutrophil adherence test, phagocytosis index, and a nitroblue tetrazolium (NBT) reduction and adherence assay used to measure the killing ability of

polymorphonuclear leukocytes (PMNs). The open field behavior test was used to measure general locomotor and explorative activity during methanol treatment in the 30-day treatment group, with tests conducted on days 1, 4, 8, 12, 16, 20, 24, and 28. All enzymatic (SOD, CAT, and GSH peroxidase) and nonenzymatic antioxidants (GSH and Vitamin C) were significantly increased in the 1-day methanol-exposed group as compared to controls. However, with increasing time of treatment, all of the measured parameters were significantly decreased when compared with control animals. Lipid peroxidation was significantly increased in both the hypothalamus and the adrenal gland at 1, 15, and 30 days, with the 30-day treated animals also significantly increased when compared to the 15-day methanol-treated animals.

Leukocyte migration and antibody titer were both significantly increased over controls for all time points, while footpad thickness was significantly decreased in 15- and 30-day treated animals. Neutrophil adherence was significantly decreased after 1 and 30 days of exposure. A significant decrease in the NBT reduction and adherence was found when comparing PMNs from the 30-day treated animals with cells from the 15-day methanol-treated group.

The open field behavior tests showed a significant decrease in ambulation from the 4th day on and significant decreases in rearing and grooming from the 20th day on. A significant increase was observed in immobilization from the 8th day on and in fecal bolus from the 24th day on in methanol-exposed animals.

While corticosterone levels were significantly increased following 1 or 15 days of methanol treatment, they were significantly decreased after 30 days of treatment, as compared to controls. Following 30 days of methanol treatment, DNA from the hypothalamus, the adrenal gland, and the spleen showed significant fragmentation. The authors conclude that exposure to methanol-induced oxidative stress, disturbs HPA-axis function, altering corticosterone levels and producing effects in several nonspecific and specific immune responses.

4.5. IMMUNOTOXICITY

Parthasarathy et al. (2005a) provided data on the impact of methanol on neutrophil function in an experiment in which 6 male Wistar rats/group were given a single i.p. exposure of 2,370 mg/kg methanol mixed 1:1 in saline. Another group of 6 animals provided blood samples that were incubated with methanol in vitro at a methanol concentration equal to that observed in the in vivo-treated animals 30 and 60 minutes postexposure. Total and differential leukocyte counts were measured from these groups in comparison to in vivo and in vitro controls. Neutrophil adhesion was determined by comparing the neutrophil index in the untreated blood samples to those that had been passed down a nylon fiber column. The cells' phagocytic ability was evaluated by their ability to take up heat-killed *Candida albicans*. In another experiment, neutrophils were assessed for their killing potential by measuring their ability to take up then

convert NBT to formazan crystals.[50] One hundred neutrophils/slides were counted for their total and relative percent formazan-positive cells.

The blood methanol concentrations 30 and 60 minutes after dosing were 2,356 ± 162 and 2,233 ± 146 mg/L, respectively. The mean of these values was taken as the target concentration for the in vitro methanol incubation. In the in vitro studies, there were no differences in total and differential leukocyte counts, suggesting that no lysis of the cells had occurred at this methanol concentration. This finding contrasts with the marked difference in total leukocytes observed as a result of methanol incubation in vivo, in which, at 60 minutes after exposure, 16,000 ± 1,516 cells/mm^3 were observed versus 23,350 ± 941 in controls ($p < 0.001$). Some differences in neutrophil function were observed in blood samples treated with methanol in vitro and in vivo. These differences are illustrated for the 60-minute postexposure samples in Table 4-16.

Table 4-16. Effect of methanol on neutrophil functions in in vitro and in vivo studies in male Wistar rats

Parameter	In vitro studies (60 minutes)		In vivo studies (60 minutes)	
	Control	Methanol	Control	Methanol
Phagocytic index (%)	89.8 ± 3.07	81.6 ± 2.2[a]	66.0 ± 4.8	84.0 ± 7.0[b]
Avidity index	4.53 ± 0.6	4.47 ± 0.7	2.4 ± 0.1	3.4 ± 0.3[a]
NBT reduction (%)	31.6 ± 4.6	48.6 ± 4.3[b]	4.6 ± 1.2	27.0 ± 4.6[b]
Adherence (%)	50.2 ± 5.1	39.8 ± 2.4[a]	49.0 ± 4.8	34.6 ± 4.0[b]

Values are means ± S.D. for six animals.
[a]$p < 0.01$.
[b]$p < 0.001$.

Source: Parthasarathy et al. (2005a).

Parthasarathy et al. (2005a) observed differences in the neutrophil functions of cells exposed to methanol in vitro versus in vivo, most notably in the phagocytic index that was reduced in vitro but significantly increased in vivo. However, functions such as adherence and NBT reduction showed consistency in the in vitro and in vivo responses. The authors noted that, by and large, the in vivo effects of methanol on neutrophil function were more marked than those in cells exposed in vitro.

Another study by Parthasarathy et al. (2005b) also exposed 6 male Wistar rats/group i.p. to methanol at approximately 1/4 the LD_{50} (2.4 g/kg). The goal was to further monitor possible methanol-induced alterations in the activity of isolated neutrophils and other immunological parameters. The exposure protocol featured daily injections of methanol for up to 30 days in the presence or absence of sheep RBCs. Blood samples were assessed for total and differential leukocytes, and isolated neutrophils were monitored for changes in phagocytic and avidity

[50] Absence of NBT reduction indicates a defect in some of the metabolic pathways involved in intracellular microbial killing.

indices, NBT reduction, and adherence. In the latter test, blood samples were incubated on a nylon fiber column, then eluted from the column and rechecked for total and differential leukocytes. Phagocytosis was monitored by incubating isolated buffy coats from the blood samples with heat-killed *C. albicans*. NBT reduction capacity examined the conversion of the dye to formazan crystals within the cytoplasm. The relative percentage of formazan-positive cells in each blood specimen gave a measure of methanol's capacity to bring about cell death. As tabulated by the authors, there was a dose-dependent reduction in lymphoid organ weights (spleen, thymus, and lymph node) in rats exposed to methanol for 15 and 30 days via i.p. injection, irrespective of the presence of sheep RBCs. Methanol also appeared to result in a reduction in the total or differential neutrophil count. These and potentially related changes to neutrophil function are shown in Table 4-17.

Table 4-17. Effect of intraperitoneally injected methanol on total and differential leukocyte counts and neutrophil function tests in male Wistar rats

Parameter	Without sheep red blood cell treatment			With sheep red blood cell treatment		
	Control	15-day methanol	30-day methanol	Control	15-day methanol	30-day methanol
Organ weights (mg)						
Spleen	1223 ± 54	910 ± 63[a]	696 ± 83[a,b]	1381 ± 27	1032 ± 39[a]	839 ± 35[a,b]
Thymus	232 ± 12	171 ± 7[a]	121 ± 10[a,b]	260 ± 9	172 ± 10[a]	130 ± 24[a,b]
Lymph node	32 ± 2	24 ± 3[a]	16 ± 2[a,b]	39 ± 2	28 ± 1[a]	23 ± 1[a,b]
Leukocyte counts						
Total leukocytes	23,367 ± 946	16,592 ± 1219[a]	13,283 ± 2553[a,b]	18,633 ± 2057	16,675 ± 1908	14,067 ± 930[a,b]
% neutrophils	24 ± 8	21 ± 3	16 ± 3[a]	8 ± 3	23 ± 4[a]	15 ± 5[a,b]
% Lymphocytes	71 ± 7	76 ± 3	79 ± 5	89 ± 4	78.5 ± 4[a]	82 ± 6
Neutrophil function tests						
Phagocytic index (%)	91.0 ± 2.0	80.0 ± 4.0[a]	79.0 ± 2.0[a]	87.0 ± 4.0	68.0 ± 3.0[a]	63.0 ± 4.0[a]
Avidity index	2.6 ± 0.3	3.2± 0.5[a]	3.2 ± 0.1[a]	4.1 ± 0.1	2.6 ± 0.3[a]	2.1 ± 0.3[a]
NBT reduction (%)	6.3 ± 2.0	18.2 ± 2.0[a]	15.0 ± 1.0[a,b]	32.0 ± 3.3	22.0 ± 3.0[a]	19.0 ± 2.4[a]
Adherence (%)	49.0 ± 5.0	44.0 ± 5.0	29.5 ± 5.0[a,b]	78.0 ± 9.2	52.0 ± 9.0[a]	30.0 ± 4.3[a,b]

Values are means ± S.D. (n = 6).
[a]$p < 0.05$ from respective control.
[b]$p < 0.05$ between 15-and 30-day treatment groups.

Source: Parthasarathy et al. (2005b).

The study provided data that showed altered neutrophil functions following repeated daily exposures of rats to methanol for periods up to 30 days. This finding is indicative of a possible effect of methanol on the immunocompetence of an exposed host.

Parthasarathy et al. (2006a) reported on additional immune system indicators as part of a study to determine the effects of methanol intoxication on the HPA axis. As described in Section 4.4.3. immune function tests conducted included the footpad thickness test for DTH, a leukocyte migration inhibition assay, the hemagglutination assay (measuring antibody titer), the neutrophil adherence test, phagocytosis index, and a NBT reduction and adherence assay used to measure the killing ability of PMNs.

Leukocyte migration and antibody titer were both significantly increased over controls for all time points, while footpad thickness was significantly deceased in 15- and 30-day treated animals. Neutrophil adherence was significantly decreased after 1 and 30 days of exposure. A significant decrease in the NBT reduction and adherence was found when comparing PMNs from the 30-day treated animals with cells from the 15-day methanol-treated group.

Parthasarathy et al. (2007) reported the effects of methanol on a number of specific immune functions. As before, 6 male Wistar rats/group were treated with 2,370 mg/kg methanol in a 1:1 mixture in saline administered intraperitoneally for 15 or 30 days. Animals scheduled/designated for termination on day 15 were immunized intraperitoneally with 5×10^9 sheep RBCs on the 10th day. Animals scheduled for day 30 termination were immunized on the 25th day. Controls were animals that were not exposed to methanol but immunized with sheep RBCs as described above. Blood samples were obtained from all animals at sacrifice and lymphoid organs including the adrenals, spleen, thymus, lymph nodes, and bone marrow were removed. Cell suspensions were counted and adjusted to 1×10^8 cells/mL. Cell-mediated immune responses were assessed using a footpad thickness assay and a leucocyte migration inhibition (LMI) test, while humoral immune responses were determined by a hemagglutination assay, and by monitoring cell counts in spleen, thymus, lymph nodes, femoral bone marrow, and in splenic lymphocyte subsets. Plasma levels of corticosterone were measured along with levels of such cytokines as TNF-α, IFN-γ, IL-2, and IL-4. DNA damage in splenocytes and thymocytes was also monitored using the Comet assay.

Table 4-18 shows decreases in the animal weight/organ weight ratios for spleen, thymus, lymph nodes and adrenal gland as a result of methanol exposure. However, the splenocyte, thymocyte, lymph node, and bone marrow cell counts were time-dependently lower in methanol-treated animals.

Table 4-18. Effect of methanol exposure on animal weight/organ weight ratios and on cell counts in primary and secondary lymphoid organs of male Wistar rats.

Organ	Immunized		
	Control	15 days	30 days
Animal weight/organ weight ratio			
Spleen	3.88 ± 0.55	2.85 ± 0.36[a]	2.58 ± 0.45[a]
Thymus	1.35 ± 0.29	0.61 ± 0.06[a]	0.63 ±0.04[a]
Lymph node	0.10 ± 0.01	0.08 ± 0.01[a]	0.06 ± 0.02[a]
Adrenal	0.14 ± 0.01	0.15 ± 0.01	0.12 ± 0.01[a, b]
Cell counts			
Splenocytes (× 10^8)	5.08 ± 0.06	3.65 ±0.07[a]	3.71 ± 0.06[a]
Thymocytes (× 10^8)	2.66 ± 0.09	1.95 ± 0.03[a]	1.86 ± 0.09[a]
Lymph node (× 10^7)	3.03 ± 0.04	2.77 ± 0.07[a]	2.20 ± 0.06[a, b]
Bone marrow (× 10^7)	4.67 ± 0.03	3.04 ± 0.09[a]	2.11 ± 0.05[a,b]

Values are means ± six animals.
[a]$p < 0.05$ versus control groups.
[b]$p < 0.05$ versus 15-day treated group.

Source: Parthasarathy et al. (2007).

Parthasarathy et al. (2007) also documented their results on the cell-mediated and humoral immunity induced by methanol. Leucocyte migration was significantly increased compared to control animals, an LMI of 0.82 ± 0.06 being reported in rats exposed to methanol for 30 days. This compares to an LMI of 0.73 ± 0.02 in rats exposed for 15 days and 0.41 ± 0.10 in controls. By contrast, footpad thickness and antibody titer were decreased significantly in methanol-exposed animals compared to controls (18.32 ± 1.08, 19.73 ± 1.24, and 26.24 ± 1.68% for footpad thickness; and 6.66 ± 1.21, 6.83 ± 0.40, and 10.83 ± 0.40 for antibody titer in 30-day, 15-day exposed rats, and controls, respectively).

Parthasarathy et al. (2007) also provided data in a histogram that showed a significant decrease in the absolute numbers of Pan T cells, CD4, macrophage, major histocompatibility complex (MHC) class II molecule expressing cells, and B cells of the methanol-treated group compared to controls. The numbers of CD8 cells were unaffected. Additionally, as illustrated in the report, DNA single strand breakage was increased in immunized splenocytes and thymocytes exposed to methanol versus controls. Although some fluctuations were seen in corticosterone levels, the apparently statistically significant change versus controls in 15-day exposed rats was offset by a decrease in 30-day exposed animals. Parthasarathy et al. (2007) also tabulated the impacts of methanol exposure on cytokine levels; these values are shown in Table 4-19.

Table 4-19. The effect of methanol on serum cytokine levels in male Wistar rats

Cytokines (pg/mL)	Immunized		
	Control	15 days	30 days
IL-2	1810 ± 63.2	1303.3 ± 57.1[a]	1088.3 ± 68.8[a,b]
IL-4	44.8 ± 2.0	74.0 ± 5.1[a]	78.8 ± 4.4[a]
TNF-α	975 ± 32.7	578.3 ± 42.6[a]	585 ± 45[a]
IFN-γ	1380 ± 55.1	961 6 ± 72.7[a]	950 ± 59.6[a]

Values are means ± six animals.
[a]$p < 0.05$ versus control groups.
[b]$p < 0.05$ versus 15-day treated group.

Source: Parthasarathy et al. (2007).

Drawing on the results of DNA single strand breakage in this experiment, the authors speculated that methanol-induced apoptosis could suppress specific immune functions such as those examined in this research report. Methanol appeared to suppress both humoral and cell-mediated immune responses in exposed Wistar rats.

4.6. MECHANISTIC DATA AND OTHER STUDIES IN SUPPORT OF THE MOA

While the role of the methanol metabolite, formate, in inducing the toxic consequences of acute exposure to methanol, including ocular toxicity and metabolic acidosis, is well established in humans (see Section 4.1), there is controversy over the possible roles of the parent compound, metabolites, and folate deficiency (potentially associated with methanol metabolism) in the developmental neurotoxicity of methanol. Experiments that have attempted to address these issues are reviewed in the following paragraphs.

4.6.1. Role of Methanol and Metabolites in the Developmental Toxicity of Methanol

Dorman et al. (1995) conducted a series of in vitro and in vivo studies that provide information for identifying the proximate teratogen associated with developmental toxicity in CD-1 mice. The studies used CD-1 ICR BR (CD-1) mice, HPLC grade methanol, and appropriate controls. PK and developmental toxicity parameters were measured in mice exposed to sodium formate (750 mg/kg by gavage), a 6-hour methanol inhalation (10,000 or 15,000 ppm), or methanol gavage (1.5 g/kg). In the in vivo inhalation study, 12–14 dams/ group were exposed to 10,000 ppm methanol for 6 hours on GD8,[51] with and without the administration of fomepizole (4-methylpyrazole) to inhibit the metabolism of methanol by ADH1. Dams were sacrificed on GD10, and fetuses were examined for neural tube patency. As shown in Table 4-20, the incidence of fetuses with open neural tubes was significantly increased in the

[51] Dorman et al. (1995) state that GD8 was chosen because it encompasses the period of murine neurulation and the time of greatest vulnerability to methanol-induced neural tube defects.

methanol group (9.65% in treated versus 0 in control) and numerically but not significantly increased in the group treated with methanol and fomepizole (7.21% in treated versus 0 in controls). These data should not be interpreted to suggest that a decrease in methanol metabolism is protective. As discussed in Section 3.1, rodents metabolize methanol via both ADH1 and CAT. This fact and the Dorman et al. (1995) observation that maternal formate levels in blood and decidual swellings (swelling of the uterine lining) did not differ in dams exposed to methanol alone or methanol and fomepizole suggest that the role of ADH1 relative to CAT and nonenzymatic methanol clearance is not of great significance in adult rodents.

Table 4-20. Developmental outcome on GD10 following a 6-hour 10,000 ppm (13,104 mg/m^3) methanol inhalation by CD-mice or formate gavage (750 mg/kg) on GD8

Treatment	No. of litters	Open neural tubes (%)	Head length (mm)	Body length (mm)
Air	14	2.29 ± 1.01	3.15 ± 0.03	5.89 ± 0.07
Air/fomepizole	14	2.69 ± 1.19	3.20 ± 0.05	5.95 ± 0.09
Methanol	12	9.65 ± 3.13[a]	3.05 ± 0.07	5.69 ± 0.13
Methanol/fomepizole	12	7.21 ± 2.65	3.01 ± 0.05	5.61 ± 0.11
Water	10	0	3.01 ± 0.07	5.64 ± 0.11
Formate	14	2.02 ± 1.08	2.91 ± 0.08	5.49 ± 0.12

Values are means ± S.D.
[a]$p < 0.05$, as calculated by the authors.

Source: Dorman et al. (1995) (adapted).

The data in Table 4-20 suggest that the formate metabolite is not responsible for the observed increase in open neural tubes in CD-1 mice following methanol exposure. Formate administered by gavage (750 mg/kg) did not increase this effect despite the fact that this formate dose produced the same toxicokinetic profile as a 6-hour exposure to 10,000 ppm methanol vapors (1.05 mM formate in maternal blood and 2.0 mmol formate/kg in decidual swellings). However, the data are consistent with the hypotheses that the formaldehyde metabolite of methanol may play a role. Both CAT and ADH1 activity are immature at days past conception (DPC)8 (Table 4-21). If fetal ADH1 is more mature than fetal CAT, it is conceivable that the decrease in the open neural tube response observed for methanol combined with fomepizole (Table 4-20) may be due to fomepizole having a greater effect on the metabolism of fetal methanol to formaldehyde than is observed in adult rats. Unfortunately, the toxicity studies were carried out during a period of development where ADH1 expression and activity are just starting to develop (Table 4-21); therefore, it is uncertain whether any ADH1 was present in the fetus to be inhibited by fomepizole.

Table 4-21. Summary of ontogeny of relevant enzymes in CD-1 mice and humans

	CD-1 Mouse						Human		
	Days Past Conception (DPC)						Trimesters		
	6.5	7.5		8.5		9.5	1	2	3
Somites			(8–12)		(13–20)	(21–29)			
CAT							N/A	N/A	N/A
mRNA									
activity[a]									
embryo			1		10	20			
VYS			10		15	20			
ADH1									
mRNA	–	–		–		+	+	+	+
activity									
embryo			320		460	450			
VYS			240		280	290			
ADH3									
mRNA	+	+		+		+	–	–	+
activity									
embryo			300		490	550			
VYS			500		500	550			

[a]Activity of CAT and ADH1 are expressed as nmol/minute/mg and pmol/minute/mg, respectively.

Source: Harris et al. (2003).

Dorman et al. (1995) provide additional support for their hypothesis that methanol's developmental effects in CD-1 mice are not caused by formate in an in vitro study involving the incubation of GD8 whole CD-1 mouse embryos with increasing concentrations of methanol or formate. Developmental anomalies were observed on GD9, including cephalic dysraphism, asymmetry and hypoplasia of the prosencephalon, reductions of brachial arches I and II, scoliosis, vesicles on the walls of the mesencephalon, and hydropericardium (Table 4-22). The concentrations of methanol used for embryo incubation (0–375 mM) were chosen to be broadly equivalent to the peak methanol levels in plasma that have been observed (approximately 100 mM) after a single 6-hour inhalation exposure to 10,000 ppm (13,104 mg/m^3). As discussed above, these exposure conditions induced an increased incidence of open neural tubes on GD10 embryos when pregnant female CD-1 mice were exposed on GD8. (Table 4-20). Embryonic lesions such as cephalic dysraphism, prosencephalic lesions, and brachial arch hypoplasia were observed with 250 mM (8,000 mg/L) methanol and 40 mM (1,840 mg/L) formate. The study authors noted that a formate concentration of 40 mM (1,840 mg/L) greatly exceeds blood formate levels in mice inhaling 15,000 ppm methanol (0.75 mM = 35 mg/L), a teratogenic dose.

Table 4-22. Dysmorphogenic effect of methanol and formate in neurulating CD-1 mouse embryos in culture (GD8)

Treatment	Concentration (mM)	Live embryos		Cephalic dysraphism			Prosencephalic lesions			Brachial arch hypoplasia
		Total	No. abnormal	Severe	Moderate	Total	Hypoplasia	Asymmetry	Total	
Vehicle		20	3	0	2	2	2	0	2	0
Methanol	62	13	1	0	0	0	1	0	1	0
	125	14	5	1	0	2	2	2	4	1
	187	13	7	2	4	6	3	1	4	1
	250	15	7	2	5	7	7[a]	1	8	6[a]
	375	12	7	6[a]	5	11[a]	9[a]	1	10[a]	8[a]
Formate	4	12	2	0	0	0	2	0	2	1
	8	13	5	1	5	6	4	2	6	0
	12	9	5	0	5	5	1	2	3	0
	20	16	7	2	5	7	2	1	3	1
	40	16	14[a]	10[a]	4	14[a]	3	5[a]	8	13[a]

[a]$p < 0.05$, as calculated by the authors.

Source: Dorman et al. (1995) (adapted).

As discussed in Section 4.3.3, a series of studies by Harris et al. (2004, 2003) also provide evidence as to the moieties that may be responsible for methanol-induced developmental toxicity. Harris et al. (2004) have shown that among methanol and its metabolites, viability of cultured rodent embryos is most affected by formate. In contrast, teratogenic endpoints (of interest to this risk assessment) in cultured rodent embryos are more sensitive to methanol and formaldehyde than formate. Data from these studies indicate that developmental toxicity may be more related to formaldehyde than methanol, as formaldehyde-induced teratogenicity occurs at several orders of magnitude lower than methanol (Table 4-14) (Hansen et al., 2005; Harris et al., 2004). It should also be noted that CAT, ADH1, and ADH3 activities are present in both the rat embryo and VYS at stages as early as 6–12 somites (Harris et al., 2003); thus, it is presumable that in these ex vivo studies methanol is metabolized to formaldehyde and formaldehyde is subsequently metabolized to S-formylglutathione.

Studies involving GSH also lend support that formaldehyde may be a key proximal teratogen. Inhibition of GSH synthesis with butathione sulfoximine (BSO) has little effect on developmental toxicity endpoints, yet treatment with BSO and methanol or formaldehyde increases developmental toxicity (Harris et al., 2004). Among the enzymes involved in methanol clearance, only ADH3-mediated metabolism of formaldehyde is GSH dependent. This hypothesis that ADH3-mediated metabolism of formaldehyde is important for the amelioration of methanol's developmental toxicity is also supported by the diminished ADH3 activity in the mouse versus rat embryos, which is consistent with the greater sensitivity of the mouse to

methanol developmental toxicity (Harris et al., 2003) (Section 4.3.3). Similarly reasonable explanations for this greater mouse sensitivity are not readily apparent for the two MOAs described below that attribute methanol toxicity to methanol metabolism per se, either through the depletion of folate (Section 4.6.2) or the generation of reactive oxidant species (Section 4.6.3). Mouse livers actually have considerably higher hepatic tetrahydrofolate and total folate than rat or monkey liver. Harris et al. (2003) and Johlin et al. (1987) have shown that CAT activity in the embryo and VYS of rats and mice appear similar..

Without positive identification of the actual moiety responsible for methanol-induced teratogenicity, MOA remains unclear. If the moiety is methanol, then it is possible that generation of NADH during methanol oxidation creates an imbalance in other enzymatic reactions. Studies have shown that ethanol intake leads to a >100-fold increase in cellular NADH, presumably due to ADH1-mediated reduction of the cofactor NAD^+ to NADH (Cronholm, 1987; Smith and Newman, 1959). This is of potential importance because, for example, ethanol intake has been shown to increase the in vivo and in vitro enzymatic reduction of other endogenous compounds (e.g., serotonin) in humans (Svensson et al., 1999; Davis et al., 1967). In rodents, CAT-mediated methanol metabolism may obviate this effect; in humans, however, methanol is primarily metabolized by ADH1.

If the teratogenic moiety of methanol is formaldehyde, then reactivity with protein sulfhydryls and nonprotein sulfhydryls (e.g., GSH) or DNA protein cross-links may be involved. Metabolic roles ascribed to ADH3, particularly regulation of S-nitrosothiol biology (Foster and Stamler, 2004), could also be involved in the MOA. Recently, Staab et al. (2008) have shown that formaldehyde alters other ADH3-mediated reactions through cofactor recycling and that formaldehyde alters levels of cellular S-nitrosothiol, which plays a key role in cellular signaling and many cellular functions and pathways (Hess et al., 2005).

Studies such as those by Harris et al. (2004, 2003) and Dorman et al. (1995, 1994) suggest that formate is not the metabolite responsible for methanol's teratogenic effects. The former researchers suggest that formaldehyde is the proximate teratogen, and provide evidence in support of that hypothesis. However, questions remain. Researchers in this area have not yet reported using a sufficient array of enzyme inhibitors to conclusively identify formaldehyde as the proximate teratogen. Studies involving other inhibitors or toxicity studies carried out in genetically engineered mice, while not devoid of confounders, might further inform regarding the methanol MOA for developmental toxicity. Even if formaldehyde is ultimately identified as the proximate teratogen, methanol would likely play a prominent role, at least in terms of transport to the target tissue. The high reactivity of formaldehyde would limit its unbound and unaltered transport as free formaldehyde from maternal to fetal blood (Thrasher and Kilburn,

2001), and, as has been discussed, the capacity for the metabolism of methanol to formaldehyde is likely lower in the fetus and neonate versus adults (Section 3.3).

4.6.2. Role of Folate Deficiency in the Developmental Toxicity of Methanol

As discussed in Sections 3.1 and 4.1, humans and other primates are susceptible to the effects of methanol exposure associated with formate accumulation because they have lower levels of hepatic tetrahydrofolate-dependent enzymes that help in formate oxidation. Tetrahydofolate-dependent enzymes and critical pathways that depend on folate, such as purine and pyrimidine synthesis, may also play a role in the developmental toxicity of methanol. Studies of rats and mice fed folate-deficient diets have identified adverse effects on reproductive performance, implantation, fetal growth and developmental defects, and the inhibition of folate cellular transport has been associated with several developmental abnormalities, ranging from neural tube defects to neurocristopathies such as cleft-lip and cleft-palate, cardiacseptal defects, and eye defects (Antony, 2007). Folate deficiency has been shown to exacerbate some aspects of the developmental toxicity of methanol in mice (see discussion of Fu et al., 1996, and Sakanashi et al., 1996, in Section 4.3.1) and rats (see discussion of Aziz et al., 2002, in Section 4.4.1).

The studies in mice focused on the influence of FAD on the reproductive and skeletal malformation effects of methanol. Sakanashi et al. (1996) showed that dams exposed to 5 g/kg-day methanol on GD6–GD15 experienced a threefold increase in the percentage of litters affected by cleft palate and a 10-fold increase in the percentage of litters affected by exencephaly when fed a FAD (resulting in a 50% decrease in liver folate) versus a FAS diet. They speculated that the increased methanol effect from FAD diet could have been due to an increase in tissue formate or a critical reduction in conceptus folate concentration immediately following the methanol exposure. The latter appears more likely, given the high levels of formate needed to cause embryotoxicity (Section 4.3.3) and the decrease in conceptus folate that is observed within 2 hours of GD8 methanol exposure (Dorman et al., 1995). Fu et al. (1996) confirmed the findings of Sakanashi et al. (1996) and also determined that the maternal FAD diet had a much greater impact on fetal liver folate than maternal liver folate levels.

The rat study of Aziz et al. (2002) focused on the influence of FAD on the developmental neurotoxicity of methanol. Experiments by Aziz et al. (2002) involving Wistar rat dams and pups exposed to methanol during lactation provide evidence that methanol exposure during this postnatal period affects the developing brain. These effects (increased spontaneous locomotor activity, decreased conditioned avoidance response, disturbances in dopaminergic and cholinergic receptors and increased expression of GAP-43 in the hippocampal region) were more pronounced in FAD as compared to FAS rats. This suggests that folic acid may play a role in methanol-induced neurotoxicity. These results do not implicate any particular proximate

teratogen, as folate deficiency can increase levels of both methanol, formaldehyde and formate (Medinsky et al., 1997). Further, folic acid is used in a number of critical pathways such as purine and pyrimidine synthesis. Thus, alterations in available folic acid, particularly to the conceptus, could have significant impacts on the developing fetus apart from the influence it is presumed to have on formate removal.

4.6.3. Methanol-Induced Formation of Free Radicals, Lipid Peroxidation, and Protein Modifications

Oxidative stress in mother and offspring has been suggested to be part of the teratogenic mechanism of a related alcohol, ethanol. Certain reproductive and developmental effects (e.g., resorptions and malformation rates) observed in Sprague-Dawley rats following ethanol exposure were reported to be ameliorated by antioxidant (Vitamin E) treatment (Wentzel et al., 2006; Wentzel and Eriksson, 2006). A number of studies have examined markers of oxidative stress associated with methanol exposure.

Skrzydlewska et al. (2005) provided inferential evidence for the effects of methanol on free radical formation, lipid peroxidation, and protein modifications, by studying the protective effects of N-acetyl cysteine and the Vitamin E derivative, U83836E, in the liver of male Wistar rats exposed to the compound via gavage. Forty-two rats/group received a single oral gavage dose of either saline or 50% methanol. This provided a dose of approximately 6,000 mg/kg, as calculated by the authors. Other groups of rats received the same concentration of methanol, but were also injected intraperitoneally with either N-acetylcysteine or U-83836E. N-acetylcysteine and U-83836E controls were also included in the study design. Animals in each group were sacrificed after 6, 14, and 24 hours or after 2, 5, or 7 days. Livers were rapidly excised for electron spin resonance (ESR) analysis, and 10,000 × g supernatants were used to measure GSH, malondialdehyde, a range of protein parameters, including free amino and sulfhydryl groups, protein carbonyls, tryptophan, tyrosine, and bityrosine, and the activity of cathepsin B.

Skrzydlewska et al. (2005) provided data that showed an increase in an ESR signal at g = 2.003 in livers harvested 6 and 12 hours after methanol exposure. The signal, thought to be indicative of free radical formation, was opposed by N-acetylcysteine and U83836E. Other compound-related changes included: 1) a significant decrease in GSH levels that was most evident in rats sacrificed 12 and 24 hours after exposure; 2) increased concentrations in the lipid peroxidation product, malondialdehyde (by a maximum of 44% in the livers of animals sacrificed 2 days after exposure); 3) increased specific concentrations of protein carbonyl groups and bityrosine; but 4) reductions in the specific level of tryptophan. Given the ability of N-acetylcysteine and U83836E to oppose these changes, at least in part, the authors speculated that a number of potentially harmful changes may have occurred as a result of methanol exposure.

These include free radical formation, lipid peroxidation, and disturbances in protein structure. However, it is unclear whether or not the metabolites of methanol, formaldehyde, and/or formate, were involved in any of these changes.

Rajamani et al. (2006) examined several oxidative stress parameters in male Wistar rats following methotrexate-induced folate deficiency. Compared to controls, the levels of free radical scavengers SOD, CAT, GSH peroxidase, oxidized GSH, protein carbonyls, and lipid peroxidation were elevated in several regions of the brain, with greater increases observed in the MTX-methanol-treated animals than in the MTX-alone group. The level of GSH and protein thiols was decreased in all regions of the brain, with a greater decrease observed in the MTX-methanol-treated animals than MTX-treated animals.

Dudka (2006) measured the total antioxidant status (TAS) in the brain of male Wistar rats exposed to a single oral gavage dose of methanol at 3 g/kg. The animals were kept in a nitrous oxide atmosphere (N_2O/O_2) throughout the experiment to reduce intrinsic folate levels, and various levels of ethanol and/or fomepizole (as ADH antidotes) were administered i.p. after 4 hours. Animals were sacrificed after 16 hours, the brains homogenized, and the TAS determined spectrophotometrically. As illustrated graphically by the author, methanol administration reduced TAS in brain irrespective of the presence of ADH antidotes. The author speculated that, while most methanol is metabolized in the liver, some may also reach the brain. Metabolism to formate might then alter the $NADH/NAD^+$ ratio resulting in an increase in xanthine oxidase activity and the formation of the superoxide anion.

Parthasarathy et al. (2006b) investigated the extent of methanol-induced oxidative stress in rat lymphoid organs. Six male Wistar rats/group received 2,370 mg/kg methanol (mixed 1:1 with saline) injected i.p. for 1, 15 or 30 days. A control group received a daily i.p. injection of saline for 30 days. At term, lymphoid organs such as the spleen, thymus, lymph nodes, and bone marrow were excised, perfused with saline, then homogenized to obtain supernatants in which such indices of lipid peroxidation as malondialdehyde, and the activities of CAT, SOD, and GSH peroxidase were measured. Parthasarathy et al. (2006b) also measured the concentrations of GSH and ascorbic acid (nonenzymatic antioxidants) and the serum concentrations of a number of indicators of liver and kidney function, such as ALT, AST, blood urea nitrogen (BUN), and creatinine.

Table 4-23 shows the time-dependent changes in serum liver and kidney function indicators that resulted from methanol administration. Treatment with methanol for increasing durations resulted in increased serum ALT and AST activities and the concentrations of BUN and creatinine.

Table 4-23. Time-dependent effects of methanol administration on serum liver and kidney function, serum ALT, AST, BUN, and creatinine in control and experimental groups of male Wistar rats

Parameters	Methanol administration (2,370 mg/kg)			
	Control	Single dose	15 days	30 days
ALT (µmoles/min-mg)	29.0 ± 2.5	31.4 ± 3.3	53.1 ± 2.3[a]	60.4 ± 2.8[a]
AST (µmoles/min-mg)	5.8 ± 0.4	6.4 ± 0.3	9.0 ± 1.2[a]	13.7 ± 1.2[a]
BUN (mg/L)	301 ± 36	332 ± 29	436 ± 35[a]	513 ± 32[a]
Creatinine (mg/L)	4.6 ± 0.3	4.8 ± 0.3	5.6 ± 0.2[a]	7.0 ± 0.4[a]

Values are means ± S.D. of 6 animals.
[a]$p < 0.05$ versus controls.

Source: Parthasarathy et al. (2006b) (adapted).

Table 4-24. Effect of methanol administration on male Wistar rats on malondialdehyde concentration in the lymphoid organs of experimental and control groups and the effect of methanol on antioxidants in spleen

Parameters	Methanol administration (2,370 mg/kg)			
	Control	Single dose	15 days	30 days
Malondialdehyde in lymphoid organs				
Spleen	2.62 ± 0.19	4.14 ± 0.25[a]	7.22 ± 0.31[a]	9.72 ± 0.52[a]
Thymus	3.58 ± 0.35	5.76 ± 0.36[a]	9.23 ± 0.57[a]	11.6 ± 0.33[a]
Lymph nodes	3.15 ± 0.25	5.08 ± 0.24[a]	8.77 ± 0.57[a]	9.17 ± 0.67[a]
Bone marrow	3.14 ± 0.33	4.47 ± 0.18[a]	7.20 ± 0.42[a]	9.75 ± 0.56[a]
Antioxidant levels in spleen				
SOD (units/mg protein)	2.40 ± 0.16	4.06 ± 0.19[a]	1.76 ± 0.09[a]	1.00 ± 0.07[a]
CAT (µmoles H_2O_2 consumed/min-mg protein	35.8 ± 2.77	52.5 ± 3.86[a]	19.1 ± 1.55[a]	10.8 ± 1.10[a]
GPx (µg GSH consumed/min-mg protein)	11.2 ± 0.60	20.0 ± 1.0[a]	7.07 ± 0.83[a]	5.18 ± 0.45[a]
GSH (µg/mg protein)	2.11 ± 0.11	3.75 ± 0.15[a]	1.66 ± 0.09[a]	0.89 ± 0.04[a]
Vit C (µg/mg protein)	0.45 ± 0.04	0.73 ± 0.05[a]	0.34 ± 0.18[a]	0.11 ± 0.03[a]

Values are means ± S.D. of six animals.
[a] $p < 0.05$, versus controls.

Source: Parthasarathy et al. (2006b) (adapted).

Table 4-24 gives the concentration of malondialdehyde in the lymphoid organs of control and experimental groups, and, as an example of all tissue sites examined, the levels of enzymatic and nonenzymatic antioxidants in spleen. The results show that malondialdehyde concentrations were time-dependently increased at each tissue site and that, in spleen as an example of all the lymphoid tissues examined, increasing methanol administration resulted in lower levels of all antioxidants examined compared to controls. Parthasarathy et al. (2006b) concluded that

exposure to methanol may cause oxidative stress by altering the oxidant/antioxidant balance in lymphoid organs in the rat.

4.6.4. Exogenous Formate Dehydrogenase as a Means of Detoxifying the Formic Acid that Results from Methanol Exposure

In companion reports, Muthuvel et al. (2006a, 2006b) used 6 male Wistar rats/group to test the ability of exogenously-administered formate dehydrogenase (FD) to reduce the serum levels of formate that were formed when 3 g/kg methanol was administered i.p. to rats in saline. In the first experiment, purified FD (from *Candida boitinii*) was administered by i.v. conjugated to the N-hydroxysuccinimidyl ester of monomethoxy polyethylene glycol propionic acid (PEG-FD) (Muthuvel et al., 2006a). In the second, rats were administered FD-loaded erythrocytes (Muthuvel et al., 2006b). In the former case, some groups of rats were made folate deficient by means of a folate-depleted diet; in the latter, folate deficiency was brought about by i.p. administration of methotrexate. In some groups, the rats received an infusion of an equimolar mixture of carbonate and bicarbonate (each at 0.33 mol/L) to correct the formate-induced acidosis. As illustrated by the authors, methanol-exposed rats receiving a folate-deficient diet showed significantly higher levels of serum formate than those receiving a folate-sufficient diet. However, administration of native or PEG-FD reduced serum formate in methanol-receiving folate-deficient rats to levels seen in animals receiving methanol and the folate-sufficient diet.

In the second report, Muthuvel et al. (2006b) carried out some preliminary experiments to show that hematological parameters of normal, reconstituted but unloaded, and reconstituted and FD-loaded erythrocytes, were similar. In addition, they showed that formate levels of serum were reduced in vitro in the presence of FD-loaded erythrocytes. Expressing blood formate concentration in mmol/L at the 1-hour time point after carbonate/bicarbonate and enzyme-loaded erythrocyte infusion via the tail vein, the concentration was reduced from 10.63 ± 1.3 (mean ± S.D.) in methanol and methotrexate-receiving controls to 5.83 ± 0.97 (n = 6). This difference was statistically significant at the $p < 0.05$ level. However, FD-loaded erythrocytes were less efficient at removing formate in the absence of carbonate/bicarbonate. Effective elimination of formate appears to require an optimum pH for the FD activity in the enzyme-loaded erythrocytes.

4.6.5. Mechanistic Data Related to the Potential Carcinogenicity of Methanol

4.6.5.1. *Genotoxicity*

The genotoxicity/mutagenicity of methanol has not been extensively studied, but the results of those studies that have thus far have been mostly negative. For example, in a survey of

the capacity of 71 drinking water contaminants to induce gene reversion in the Ames test, Simmon et al. (1977) listed methanol as one of 45 chemicals that gave negative results with *Salmonella typhimurium* strains TA 98, 100, 1535, 1537, and 1538, irrespective of the presence or absence of metabolic activation (an S9 microsomal fraction). This result was confirmed by DeFlora et al. (1984) and in NEDO (1987) for the same strains of Salmonella. DeFlora et al. (1984) also found methanol to be negative for induction of DNA repair in *E. coli* strains WP2, WP2 (*uvrA*$^-$, *polA*$^-$), and CM871 (*uvrA*$^-$, *recA*$^-$, *lexA*$^-$), again irrespectively of the presence or absence of S9.

Abbondandolo et al. (1980) used a *ade6-60/rad10-198,h*$^-$ strain of *Schizosaccharomyces pombe* (P1 strain) to determine the capacity of methanol and other solvents to induce forward mutations. Negative results were obtained for methanol, irrespective of metabolic activation status. In other genotoxicity/mutagenicity studies of methanol using fungi, Griffiths (1981) reported methanol to be negative for the induction of aneuploidy in *Neurospora crassa*. By contrast, weakly positive results for the compound were obtained by Crebelli et al. (1989) for the induction of chromosomal malsegregation in the diploid strain P1 of *Aspergillus nidulans*.

In an extensive review of the capacity of a wide range of compounds to induce transformation in mammalian cell lines, Heidelberger et al. (1983) reported methanol to be negative in Syrian hamster embryo (SHE) cells. It also did not enhance the transformation of SHE cells by Simian adenovirus. However, McGregor et al. (1985) reported in an abstract that a statistically significant increase in forward mutations in the mouse lymphoma L5178Y tk$^+$/tk$^-$ cell line occurred at a concentration of 7.9 mg/mL methanol in the presence of S9.

The capacity of methanol to bring about genetic changes in human cell lines was examined by Ohno et al. (2005), who developed a system in which the chemical activation of the *p53R2* gene was assessed by the incorporation of a *p53R2*-dependent luciferase reporter gene into two human cell lines, MCF-7 and HepG2. Methanol, among 80 chemicals tested in this system, gave negative results. NEDO (1987) used Chinese hamster lung (CHL) cells to monitor methanol's capacity to induce 1) forward mutations to azaguanine, 6-thioguanine, and ouabain resistance, and 2) chromosomal aberrations (CA) though with negative results throughout. However, methanol did display some capacity to induce sister chromatid exchanges (SCE) in CHL cells, since the incidence of these lesions at the highest concentration (28.5 mg/mL) was significantly greater than in controls (9.41 ± 0.416 versus 6.42 ± 0.227 [mean ± SE per 100 cells]).

In an in vivo experiment examining the genotoxicity/mutagenicity of methanol, Campbell et al. (1991) exposed 10 male C57BL/6J mice/group to 0, 800, or 4,000 ppm (0, 1,048, and 5,242 mg/m^3) methanol, 6 hours/day, for 5 days. At sacrifice, blood cells were examined for the formation of micronuclei (MN). Excised lung cells for SCE, CA and MN, and excised testicular

germ cells were examined for evidence of synaptonemal damage, in each case with negative results.

There was no evidence of methanol-induced formation of MN in the blood of fetuses or pregnant CD-mice when the latter were gavaged twice daily with 2,500 mg/kg methanol on GD6–GD10 (Fu et al., 1996). The presence of marginal or adequate amounts of folic acid in the diet of the dams did not affect MN formation. NEDO (1987) carried out an in vivo MN test in 6 male SPF mice/group who received a single gavage dose of 1,050, 2,110, 4,210, and 8,410 mg/kg methanol. Twenty-four hours later, 1,000 cells were counted for MN in bone marrow smears. No compound-related effects on MN incidence were observed. Table 4-25 provides a summary of the genotoxicity/mutagenicity studies of methanol.

Table 4-25. Summary of genotoxicity studies of methanol

Test system	Cell/strain	Result	Reference	Comments
In vitro tests				
Gene reversion/ *S. typhimurium*	TA98; TA100; TA1535, TA1537, TA1538	- (+S9); - (-S9)	Simmon et al. (1977)	
	TA98; TA100; TA1535, TA1537, TA1538	- (+S9); - (-S9)	De Flora et al. (1984)	
	TA98; TA100; TA1535, TA1537, TA1538	- (+S9); - (-S9)	NEDO (1987)	
DNA repair/*E. coli*	WP2, WP2 *(uvrA$^-$, polA$^-$)*,CM871*(uvrA$^-$, recA$^-$, lexA$^-$)*	- (+S9), - (-S9)	DeFlora et al. (1984)	
Forward mutations/ *S. pombe*	P1 (*ade6-60/rad10-198,h$^-$*)	- (+S10), - (-S10)	Abbondandolo et al. (1980)	Molecular activation used a 10,000 × g (S10) supernatant from liver of induced Swiss mice
Aneuploidy/ *N. crassa*	*(arg-1, ad-3A, ad-3B, nic-2, tol, C/c, D/d, E/e)*	- (S9 status not reported)	Griffiths (1981)	
Chromosomal malsegregation/ *A. nidulans*	P1 (diploid)	+ (S9 status not reported)	Crebelli et al. (1989)	
Forward mutations/Mouse lymphoma cells	L5178Y tk$^+$/tk$^-$	+ (+S9), ND (-S9)	McGregor et al. (1985)	Results reported in an abstract
Forward mutations/Chinese hamster lung cells	to azaguanine, 6-thioguanine and ouabain resistance	- (-S9), ND (+S9)	NEDO (1987)	
Chromosomal aberrations/Chinese hamster lung cells		- (-S9), ND (+S9)	NEDO (1987)	
Sister chromatid exchanges/Chinese hamster lung cells		+ (-S9), ND (+S9)	NEDO (1987)	

Test system	Cell/strain	Result	Reference	Comments
Genetic activation/ human cell lines	MCF-7 and HepG2 containing a *p53R2*-dependent luciferase reporter gene	- (-S9), ND (+S9)	Ohno et al. (2005)	
Cell transformation/ Syrian hamster embryo cells	with/without transformation by Simian adenovirus	- (-S9), ND (+S9) - (-S9), ND (+S9)	Heidelberger et al. (1983)	Review
In vivo tests				
Mouse/MN formation	C57BL/6J (Blood cells)	–	Campbell et al. (1991)	Molecular activation not applicable
	C57BL/6J (Lung cells)	–	Campbell et al. (1991)	Molecular activation not applicable
Mouse/SCEs	C57BL/6J (Lung cells)	–	Campbell et al. (1991)	Molecular activation not applicable
Mice/CA	C57BL/6J (Lung cells)	–	Campbell et al. (1991)	Molecular activation not applicable
Mouse/synaptonemal damage	C57BL/6J (Testicular germ cells)	–	Campbell et al. (1991)	Molecular activation not applicable
Mouse/MN formation	CD-1 (Blood cells)	–	Fu et al. (1996)	Molecular activation not applicable
	SPF (Bone marrow cells)	–	NEDO (1987)	Molecular activation not applicable

ND = not determined.

4.6.5.2. *Lymphoma Responses Reported in ERF Life span Bioassays of Compounds Related to Methanol, Including an Analogue (Ethanol), Precursors (Aspartame and Methyl Tertiary Butyl Ether), and a Metabolite (Formaldehyde)*

The ERF or the European Foundation of Oncology and Environmental Sciences have conducted nearly 400 experimental bioassays on over 200 compounds/agents, using some 148,000 animals over nearly 4 decades. Of the over 200 compounds tested by ERF,[52] 8 have been associated with an increased incidence of hemolymphoreticular tumors in Sprague-Dawley rats, suggesting that it may be a rare and potentially species/strain-specific finding. These eight chemicals are: methanol, formaldehyde, aspartame, MTBE, DIPE, TAME, mancozeb, and toluene. Methanol, formaldehyde, aspartame, and MTBE share a common metabolite, formaldehyde, and DIPE, TAME, methanol and MTBE are all gasoline-oxygenate additives (Caldwell et al., 2008).

With the exception of a positive study for malignant lymphomas in Swiss Webster mice exposed to methanol (Apaja, 1989), lymphoma responses have not been reported by other institutions performing long-term testing of these chemicals in various strains of rats, including

[52] While ERF has tested over 200 chemicals in 398 long-term ERF bioassays, only 112 of their bioassays have been published to date (Caldwell, et al., 2008). The extent to which the unpublished studies are documented varies.

formaldehyde inhalation studies in F344 (Kerns et al., 1983; Kamata et al., 1987)[53] and Sprague-Dawley (Albert et al., 1982; Sellakumar et al., 1985) rats, formaldehyde oral studies in Wistar rats (Til et al., 1989; Tobe et al., 1989), toluene oral studies in F344 rats (NTP, 1990), MTBE inhalation studies in F344 rats (Chun et al., 1992), aspartame oral studies in Wistar (Ishii et al., 1981) and Sprague-Dawley (Molinary, 1984) rats, and methanol inhalation studies in F344 rats (NEDO, 1987, 1985/2008b). Several differences in study design may contribute to the differences in responses observed across institutions, particularly study duration and test animal strain. Fischer-344 rats have a high background of mononuclear cell leukemia (20% in control females)[54] and a very low background rate of ''lymphoma'' (0% in control females) at 104 weeks (NTP, 2006). In contrast, Sprague-Dawley rats from NTP studies exhibit a low background rate of "leukemias" (0.8% in control females) and a higher background rate of "lymphomas" (1.08% in control females) at 104 weeks (NTP, 2006). Similarly, Chandra et al. (1992) report a background level of 1.6% for malignant lymphocytic lymphomas in female control Sprague-Dawley rats for 17 2-year carcinogenicity studies.

In lifetime studies of Sprague-Dawley rats at ERF, the overall incidence of lymphomas/leukemias has been reported to be 13.3% (range, 4.0–25.0%) in female historical controls (2,274 rats) and 20.6% (range, 8.0–30.9%) in male historical controls (2,265 rats) (Soffritti et al., 2007). The difference in background rates reported by ERF versus other labs for this tumor type could be due to differences in study duration, differences in tumor classification systems, and/or misdiagnoses due to confounding effects (see discussion in Section 4.2.1.3). A high background incidence can increase the difficulty of detecting chemically related responses (Melnick et al., 2007), and the background rate reported by ERF for this tumor type is considered to be high relative to other tumor types and relative to the background rate for this tumor type in Sprague-Dawley rats from other laboratories (EFSA, 2006; Cruzan, 2009).[55] However, it is in a range that can be considered reasonable for studies that employ a large number of animals (Leakey et al., 2003; Caldwell et al., 2009).

Thus, with respect to the identification of hemolymphoreticular carcinogenic responses, life span studies of Sprague-Dawley rats performed by ERF may be more sensitive than the 2-year studies of Fischer 344 (F344) strain of rats used by NTP (1990) and NEDO (1987,

[53] Though Kerns et al. (1983) did not report a positive response for lymphoma, a survival-adjusted analysis of the data from this study indicates a statistically significant trend in female rat mononuclear cell leukemia ($p = 0.0056$) and a nearly significant increase in female mouse lymphoma ($p = 0.06$). In the Kamata et al., (1987) study, only a small percentage of the original 32 rats/group survived to the end of the study (28 months) due largely to interim sacrifices (5/group) at 12, 18 and 24 months.

[54] Due to this and other health concerns, NTP transitioned to the use of Wistar rats in 2008, and more recently has adopted Sprague-Dawley rats as the rat model for NTP studies due to the reproductive capability and size of Wistar rats (http://ntp.niehs.nih.gov/go/29502).

[55] Cruzan (2009) reports that the incidences of total cancers derived from bloodforming cells, designated as hemolymphoreticular tumors by Ramazzini pathologists, is consistently about four times higher than the incidences of such tumors in SD rats recorded in the Charles River Laboratory historical database (CRL database).

1985/2008b). The results of ERF studies of the carcinogenic potential of methanol, MTBE, and formaldehyde and related chemicals, ethanol and aspartame, are summarized in this section.

4.6.5.2.1. *Ethanol.* In a study that was reported in the same article that described the carcinogenic responses of Sprague-Dawley rats to methanol, Soffritti et al. (2002a) exposed 110 Sprague-Dawley rats/sex/group to ethanol in drinking water at concentrations of 0 or 10% (v/v) beginning at 39 weeks of age and ending at natural death, and including a single breeding cycle. Various numbers of the offspring (30 male controls, 39 female controls, 49 exposed males, and 55 exposed females) were exposed to ethanol in drinking water at the same concentrations as their parents. The experiment concluded with the death of the last offspring at 179 weeks of age. Animals were examined for the same toxicological parameters as those described for methanol, and organs and tissues were grossly and histopathologically examined at necropsy. Soffritti et al. (2002a) reported that food and drinking water intake were lower in exposed animals compared to controls but that body weight changes were similar among the groups.[56] There were no compound-related clinical signs of toxicity and no differences in survival rates among the groups. While there were apparently no nononcogenic pathological changes evident on gross inspection or histopathologic examination, a number of benign and malignant tumors were considered by the authors to be compound-related. Compared to controls, these included increased incidences of: 1) total malignant tumors in male and female breeders (145/220 versus 99/220) and offspring (49/69 versus 54/104); 2) total malignant tumors per 100 animals in female breeders (130 versus 60.9) and offspring (164.1 versus 96.4); 3) carcinomas of the head and neck, especially to the oral cavity, lips and tongue in male and female breeders (27/220 versus 5/220) and offspring (26/69 versus 5/104); 4) squamous cell carcinomas of the forestomach in male and female breeders (5/220 versus 0/220) and offspring (2/69 versus 0/104); 5) interstitial cell adenomas of the testis in male breeders (23/110 versus 9/110) and offspring (4/30 versus 4/49); 6) Sertoli-Leydig cell tumors in ovaries of female offspring (3/39 versus 1/55); 7) adenocarcinomas of the uterus in female breeders (9/110 versus 2/110) and offspring (8/39 versus 6/55); 8) pheochromoblastomas in male and female breeders (13/220 versus 4/220) and offspring (4/69 versus 2/104); and 9) osteosarcomas in male and female breeders ([for the head] 14/220 versus 4/220) and offspring ([for the head] 10/69 versus 7/104). Notably, Soffritti et al. (2002a) did not observe increases in any of the lymphoma responses reported in their methanol bioassay. Incidence data for these responses and their statistical significance compared to controls are shown in Table 4-26.

[56] Test animals were likely receiving calories from ethanol exposure.

Table 4-26. Incidence of carcinogenic responses in Sprague-Dawley rats exposed to ethanol in drinking water for up to 2 years

Tissues/affected sites	Concentration in percent (v/v)							
	Male (breeders)		Female (breeders)		Male (offspring)		Female (offspring)	
	0	10	0	10	0	10	0	10
Total malignant tumors	51/110	66/110	48/110	79/110[b]	23/49	23/30[a]	31/55	26/39
Oral cavity (carcinomas)	3/110	15/110[b]	2/110	12/110	2/49	10/30[b]	3/55	16/39[b]
Forestomach (squamous cell carcinomas)	0/110	2/110	0/110	3/110	0/49	1/30	0/55	1/39
Testis (interstitial cell adenomas)	9/110	23/110[d]			4/49	4/30		
Sertoli-Leydig cell tumors (ovary)			1/110	2/110			0/55	3/39
Uterus (adenocarcinomas)			2/110	9/110[c]			6/55	8/39
Head (osteosarcomas)	0/110	8/110	4/110	6/110	4/49	6/30	3/55	4/39
Adrenal gland (pheochromoblastomas)	3/110	9/110	1/110	4/110	1/49	4/30	1/55	0/39
Total malignant tumors per 100 animals	61.8	89.1[b]	60.9	130[b]	61.2	136.7[b]	96.4	164.1[b]

[a]$p < 0.05$ using the χ^2 test, as calculated by the authors.
[b]$p < 0.01$ using the χ^2 test, as calculated by the authors.
[c]$p < 0.05$ using Fisher's exact test, as calculated by the reviewers.
[d]$p < 0.01$ using Fisher's exact test, as calculated by the reviewers.

Source: Soffritti et al. (2002a).

4.6.5.2.2. *Aspartame.* Soffritti et al. (2006, 2005) reported the results of a cancer bioassay on the artificial sweetener aspartame. The study has potential relevance to the carcinogenicity of methanol because aspartame has been shown to be metabolized to aspartic acid, phenylalanine, and methanol in the GI tract prior to absorption into systemic circulation. In the study, aspartame (>98% purity) was given to 100 or 150 Sprague-Dawley rats/sex/group in feed at dietary concentrations of 0, 80, 400, 2,000, 10,000, 50,000, and 100,000 ppm. The authors reported these concentrations to be equivalent to approximate daily doses of 0, 4, 20, 100, 500, 2,500, and 5,000 mg/kg-day, respectively, under the conditions of the study. Animals were maintained until their "natural death," with the in-life phase of the experiment concluding with the death of the last animal at 151 weeks. All animals were monitored for body weight, food and water consumption. At death, animals were examined grossly and given a complete histopathological examination.

Soffritti et al. (2006, 2005) reported that there were no differences among the groups in mean body weight, survival, or daily water consumption. However, there appeared to be a dose-related reduction in food consumption in both male and female rats.

The principal histopathological finding was an increased incidence of lymphomas and leukemias in female rats, a response reported by the authors to be statistically significant compared to concurrently exposed controls (Table 4-27) and greater than the range of overall incidence of lymphomas and leukemias in historical controls at the ERF (13.4% [range, 7.0–18.4] in females and 21.8% [range, 8.0–30.9] in males). Among the hemolymphoreticular neoplasms observed, the most frequent type observed was lympho-immunoblastic lymphoma. The authors concluded that aspartame causes a "dose-related statistically significant increase in lymphomas and leukemias in females at dose levels very near those to which humans can be exposed." They postulated that an increase in the incidence of lymphomas and leukemias could be associated with the formation of either methanol or formaldehyde. Other potentially compound-related effects of aspartame were (1) an increase in combined dysplastic hyperplasias, papillomas, and carcinomas of the renal pelvis and ureter, and (2) an increasing trend in the formation of malignant schwannomas in peripheral nerves (Table 4-28).

The European Commission asked the European Food Safety Authority (EFSA) to assess the study and review all ERF findings related to aspartame. An EFSA review panel assessed the study and considered additional unpublished data provided to it by the ERF. In their report, EFSA (2006) concluded that the Soffritti et al. (2005, 2006) study had flaws that brought into question the reported findings. The review panel noted the high background of chronic inflammatory changes in the lung and other vital organs. These background inflammatory changes were thought to contribute significant uncertainty to the interpretations of the study. In fact, the review panel concluded that most of the documented changes, in particular, the apparent compound-related increase in lymphomas and leukemias, may have been incidental findings and, therefore, unrelated to aspartame.

Table 4-27. Incidence of lymphomas and leukemias in Sprague-Dawley rats exposed to aspartame via the diet

Group	ppm in feed	Dose (mg/kg-day)	Lymphomas/leukemias (incidence and %)	
			Male	Female
I	0	0	31/150 (21)	13/150 (9)
II	80	4	23/150 (15)	22/150 (15)
III	400	20	25/150 (17)	30/150[b] (20)
IV	2,000	100	33/150 (22)	28/150[a] (19)
V	10,000	500	15/100 (15)	19/100[a] (19)
VI	50,000	2,500	20/100 (20)	25/100[b] (25)
VII	100,000	5,000	29/100 (29)	25/100[b] (25)

[a]$p < 0.05$ using the poly-k test.
[b]$p < 0.01$ using the poly-k test.

Source: Soffritti et al. (2006, 2005).

Table 4-28. Incidence of combined dysplastic hyperplasias, papillomas and carcinomas of the pelvis and ureter and of malignant schwannomas in peripheral nerve in Sprague-Dawley rats exposed to aspartame via the diet

Group	ppm in feed	Dose (mg/kg-day)	Incidence and %			
			Combined hyperplasias, papillomas and carcinomas of the pelvis and ureter		Peripheral nerve malignant schwannomas	
			Male	Female	Male	Female
I	0	0	1/150 (0.7)	2/150[c] (1.3)	1/150[c] (0.7)	0/150 (0)
II	80	4	3/149 (2)	6/150 (4)	1/150 (0.7)	2/150 (1.3)
III	400	20	5/149 (3)	9/150[a] (6)	3/150 (2)	0/150 (0)
IV	2,000	100	5/150 (3)	10/150[a] (7)	2/150 (1.3)	3/150 (2)
V	10,000	500	3/100 (3)	10/100[b] (10)	2/100 (2)	1/100 (1)
VI	50,000	2,500	3/100 (3)	10/99[b] (10)	3/100 (3)	1/100 (1)
VII	100,000	5,000	4/100 (4)	15/100[b] (15)	4/100 (4)	2/100 (2)

[a]$p < 0.05$ using the poly-k test.
[b]$p < 0.01$ using the poly-k test.
[c]$p < 0.05$ using the Cochran-Armitage test for trend.

Source: Soffritti et al. (2006).

In their conclusions, the EFSA review panel took note of negative results of 2-year carcinogenic studies of aspartame (Ishii et et al., 1981; Ishii, 1981; NTP, 2003) and of the findings of a recent epidemiological study carried out by the US National Cancer Institute (NCI, 2006).

In an effort to further clarify these issues, Soffritti et al. (2007) reported the results of another lifetime study of aspartame in which 95 controls and 70 Sprague-Dawley rats/sex/group were exposed, first in utero, then via the diet, to aspartame at concentrations of 0, 400, or 2,000 ppm (mg/kg) of feed. The authors assumed an average food consumption of 20 g/day and an average body weight (males and females) of 400 g, thereby deriving average target doses of 0, 40, and 200 mg/kg-day. Soffritti et al. (2007) began administering the aspartame-supplemented feed to the dams on GD12; and offspring received feed containing aspartame at the appropriate concentration from weaning until natural death. Animals were observed three times daily Monday–Friday, and twice daily on Saturdays, Sundays, and holidays. This regimen was both to monitor clinical signs and to reduce the possibility of decedents undergoing autolysis before discovery. As described by the authors, all deceased animals were refrigerated, then necropsied no more than 19 hours after discovery.

Food and drinking water consumption was monitored once/day. Beginning at 6 weeks of age, individual body weights were recorded once a week for 13 weeks, then every 2 weeks until natural death. All animals were examined grossly every 2 weeks. After necropsy, tissues and organs were sampled for histopathological processing and microscopic examination (including

skin and subcutaneous tissue, mammary gland, brain, pituitary, Zymbal's gland, salivary gland, Harderian gland, cranium, tongue, thyroid, parathyroid, pharynx, larynx, thymus and mediastinal lymph nodes, trachea, lung and main stem bronchi, heart, diaphragm, liver, spleen, pancreas, kidney, adrenal gland, esophagus, stomach, intestine, urinary bladder, prostate, vagina, gonads, interscapular brown fat pads, subcutaneous and mesenteric lymph nodes), as were all pathological lesions identified on gross necropsy.

There were no differences in food and water consumption or in body weights among the dose groups. As illustrated graphically by the authors, there was little change in overall survival rates. Discussion of the histopathological findings focused exclusively on the cancer outcomes. The incidence of total malignant tumors was increased significantly in high-dose males compared to controls ($p < 0.01$). The slight increase in the incidence of total malignant tumors in females was not statistically significant (Table 4-29). With regard to the incidence of type- or site-specific neoplasms, Soffritti et al. (2007) reported statistically significant increases (calculated using the Cox regression model) in combined lymphomas and leukemias in both sexes of Sprague-Dawley rats. In males, the most frequently observed histiotypes were lymphoblastic lymphomas involving the lung and mediastinal peripheral nodes, while in females, the most commonly observed lesions were lymphocytic lymphomas and lympho-immunoblastic lymphomas involving the thymus, spleen, lung and peripheral nodes. There was also an increase in the incidence of mammary gland carcinomas in female Sprague-Dawley rats. The incidences of total malignant, mammary, and lymphocytic and leukocytic tumors, in comparison to concurrent and the range of historical controls for combined lymphomas and leukemias and mammary gland tumors observed at the ERF, are shown in Table 4-29.

Table 4-29. Incidence of tumors in Sprague-Dawley rats exposed to aspartame from GD12 to natural death

Dose (mg/kg-day)	Malignant tumors		Lymphomas/leukemias	Mammary carcinomas
	Tumor-bearing animals (percent)	Tumors/100 animals	Tumor-bearing animals (percent)	Tumor-bearing animals (percent)
Males				
0	23/95 (24.2)	27.4	9/95 (9.5)	0/95 (0)
20	18/70 (25.7)	27.1	11/70 (15.7)	0/70 (0)
100	28/70 (40.0)[a]	44.3	12/70 (17.1)[b]	2/70 (2.9)
Historical controls	ND	ND	8–31%	NR
Females				
0	42/95 (44.2)	50.5	12/95 (12.6)	5/95 (5.3)
20	31/70 (44.3)	62.9	12/70 (17.1)	5/70 (7.1)
100	37/70 (52.9)	85.7	22/70 (33.4)[a]	11/70 (15.7)[b]
Historical controls	ND	ND	7-18%	4–14%

Dose (mg/kg-day)	Malignant tumors		Lymphomas/leukemias	Mammary carcinomas
	Tumor-bearing animals (percent)	Tumors/100 animals	Tumor-bearing animals (percent)	Tumor-bearing animals (percent)

[a]$p < 0.01$ versus concurrent controls, as calculated by the authors using the Cox regression model.
[b]$p < 0.05$ versus concurrent controls, as calculated by the authors using the Cox regression model.
ND = no data.; NR = not reported.

Source: Soffritti et al. (2007).

With regard to target organs and tissues susceptible to aspartame carcinogenicity, Soffritti et al. (2007) drew attention to the similar outcome of these results to those reported by Soffritti et al. (2006, 2005). The authors suggested that the increased incidence in combined lymphomas and leukemias in female Sprague-Dawley rats as compared to the earlier study was likely due to the earlier exposure to aspartame experienced by the animals in the Soffritti et al. (2007) study (prenatal and postnatal versus postnatal only). The authors provided a direct comparison of the incidence of lymphomas/leukemias between the studies, as summarized in Table 4-30.

Table 4-30. Comparison of the incidence of combined lymphomas and leukemias in female Sprague-Dawley rats exposed to aspartame in feed for a lifetime, either pre- and postnatally or postnatally only

Dose (mg/kg-day)	Percent with lymphomas/leukemias	
	Pre-and postnatal exposure[a]	Postnatal exposure only[b]
0	12.6	8.7
20	17.1	20.0
100	31.4	18.7

Source: [a] Soffritti et al. (2007); [b] Soffritti et al. (2006, 2005).

An EFSA (2009) review of the Sofftitti et al. (2007) study notes that the ratio between the incidence in the low-dose group and the incidence in the concurrent control in Table 4-30 is considerably lower in the animals exposed prenatally (1.4:1) compared to those exposed postnatally (2.3:1). The ratio in the groups exposed to 100 mg/kg bw/day relative to the respective concurrent controls is only slightly higher in animals exposed prenatally (2.5:1) compared to those exposed postnatally (2.2:1). EFSA also notes that the incidence of lymphomas and leukemias in aspartame-receiving males of the Soffritti et al. (2007) study was within the range of historical controls for these responses in Sprague-Dawley rats at the ERF. For example, the percent incidence of combined lymphomas and leukemias in males exposed pre- and postnatally to 100 mg/kg-day aspartame (17.1%) was within the range of historical controls for this response (8–31%, with an overall mean of 20.6%). Soffritti et al. (2007) acknowledge this fact, but reason that comparisons of potentially compound-associated incidences of tumor formation to incidences in concurrent controls provide a more scientifically

valid indicator of the tumorigenic impact of a chemical under investigation than comparisons to historical control data.[57] Furthermore, the incidence of combined lymphomas and leukemias in the female rats in the high-dose group is well above the historical control range. Therefore, Soffritti et al. (2007) concluded that their second experiment confirmed the carcinogenic potential of aspartame in Sprague-Dawley rats observed in Soffritti et al. (2006, 2005). The high and variable incidence of this tumor type in ERF controls remains a concern. However, the results provide support for studies suggesting similar effects from methanol (Soffritti et al., 2002a) since methanol is one of the degradation products of aspartame and appears to have carcinogenic potential at some of the same target organs and tissues.

4.6.5.2.3. *MTBE.* In an experiment that also may be relevant to the carcinogenicity of methanol, scientists at the ERF carried out a cancer bioassay on MTBE, in which the compound was administered to 60 Sprague-Dawley rats/sex/group by gavage in olive oil at 0, 250, and 1,000 mg/kg-day, 4 days/week, for 104 weeks (Belpoggi et al., 1995). Doses adjusted to daily dose were 0, 143, and 571 mg/kg-day. This experiment and its findings may relate to the carcinogenicity of methanol, since methanol is one of several metabolites of MTBE (ATSDR, 1997). At the end of the exposure period, the animals were allowed to live out their "natural" life, the last animal dying 166 weeks after the start of the experiment (at 174 weeks of age).

Mean daily feed and drinking water consumption were determined weekly for the first 13 weeks of the experiment, then every 2 weeks until 112 weeks of age. Individual body weights were measured according to the same protocol, then every 8 weeks until the end of the experiment. All animals were examined for gross lesions weekly for the first 13 weeks, then every 2 weeks until term. All animals were examined grossly at death, then histopathologically examined for a full suite of organs and tissues.

As described by the authors, there were no differences among the groups in body weight and clinical signs of toxicity. Survival was dose-dependently reduced in female rats after 16 weeks of exposure. Paradoxically, survival was improved in high-dose males compared to controls after 80 weeks. Although there were no noncarcinogenic effects of MTBE reported, a number of benign and malignant tumors were identified, including tumor types that were not observed in the ERF methanol study such as an increased incidence of testicular Leydig tumors in high-dose males and as determined by the authors, as well as a dose-related statistically significant increase in lymphomas and leukemias in females. The incidences of these tumors compared to the initial number of animals exposed and compared to those at risk at the time of the first observed tumor formation are shown in Table 4-31.

[57] There are also potential problems with the use of historical control information from a colony that has been maintained for over three decades. Population sensitivity can and does change over time.

Table 4-31. Incidence of Leydig cell testicular tumors and combined lymphomas and leukemias in Sprague-Dawley rats exposed to MTBE via gavage for 104 weeks

Duration-adjusted dose	Leydig cell tumors			Combined lymphomas and leukemias					
	Number of males			Number of males			Number of females		
	Affected	Initial	At risk[c]	Affected	Initial	At Risk[d]	Affected	Initial	At Risk[e]
0	2	60	26	10	60	59	2	60	58
143	2	60	25	9	60	59	6[b]	60	51
571	11[a]	60	32	7	60	58	12[b]	60	47

[a]$p < 0.05$ using prevalence analysis
[b]$p < 0.01$ using a log-ranked test.
[c]Alive male rats at 96 weeks of age, when first Leydig cell tumor was observed.
[d] Alive male rats at 32 weeks of age, when first leukemia was observed.
[e] Alive female rats at 56 weeks of age, when first leukemia was observed.

Source: Belpoggi et al. (1995).

The possible contribution of the metabolite methanol to the reported responses cannot be quantified. It is also possible that the parent compound and/or one or more of MTBE's other metabolites (e.g., tertiary butanol or formaldehyde) may be etiologically linked to the formation of the identified neoplasms (Blancato et al., 2007).

4.6.5.2.4. *Formaldehyde.* Scientists at the ERF have carried out two long-term experiments on the potential carcinogenicity of formaldehyde, which is itself a metabolite of methanol, aspartame and MTBE. While the tumorigenic effects at the portal-of-entry (such as in the oral cavity and GI tract, for oral studies) may lack relevance to the possible effects of metabolites formed *in situ* following methanol exposure, systemic neoplasms such as lymphomas and leukemias have been described for formaldehyde as well (Soffritti et al., 2002b, 1989). This suggests that formaldehyde metabolized from methanol, aspartame and MTBE may be etiologically important in the formation of lymphomas and leukemias in animals exposed to these compounds.

In the first formaldehyde study (designated BT 7001; Soffritti et al., 1989), 50 Sprague-Dawley rats/sex/group (starting at 7 weeks of age) were exposed to formaldehyde in drinking water at concentrations of 10, 50, 500, 1,000, and 1,500 mg/L for 104 weeks. Another 50 Sprague-Dawley rats/sex received methanol in drinking water at 15 mg/L, and 100 rats/sex received water only, as controls. Body weight and water and food consumption were monitored weekly for the first 13 weeks, then every 2 weeks thereafter. All animals were allowed to live out their "natural" life, at which point they were subjected to necropsy and a complete histopathological examination.

The final results of the BT 7001 Soffritti et al. (1989) experiment were reported by Soffriti et al. (2002b). Water consumption was reduced compared to controls in high-dose males

and in females at the three highest doses. However, there appeared to be no evidence of compound-related body weight changes, clinical signs of toxicity among the groups, nor nononcogenic histopathological effects of formaldehyde. The authors noted statistically significant increases in the incidence of tumor-bearing males at 1500 ppm ($p<0.01$) and in total malignant tumors in females at 100, 1000 and 1500 ppm ($p<0.01$) and in males at 500 ppm ($p<0.05$) and 1500 ppm ($p<0.01$). They reported statistically significant increases in malignant mammary tumors in females at 100 ppm ($p<0.01$) and 1500 ppm ($p<0.05$), and in testicular interstitial cell adenomas in the 1000 ppm males ($p<0.05$). They also noted sporadic incidences in the treatment groups only (primarily at the highest dose) of leiomyosarcomas of the stomach and intestine considered to be very rare for the ERF rat colony. As for methanol and the other compounds discussed in this section, they reported increases in the number of hemolymphoreticular tumors for both sexes. The incidence of hemolymphoreticular neoplasms among the dose groups is shown in Table 4-32.

Table 4-32. Incidence of hemolymphoreticular neoplasms on Sprague-Dawley rats exposed to formaldehyde in drinking water for 104 weeks

Concentration in drinking water (mg/L)	Males	Females
0	8/100	7/100
0 (15 mg/L methanol)	10/50	5/50
10	4/50	5/50
50	10/50	7/50
100	13/50[b]	8/50
500	12/50[a]	7/50
1,000	11/50[a]	11/50[a]
1,500	23/50[b]	10/50[b]

[a]$p < 0.05$ using the χ^2 test; [b]$p < 0.01$ using the χ^2 test.
Source: Soffritti et al. (2002b).

Soffritti et al. (1989) also described the results of another experiment (BT 7005) in which approximately 20 Sprague-Dawley rats/sex/group were exposed to either regular drinking water or 2,500 mg/L formaldehyde, beginning at 25 weeks of age for 104 weeks. These animals were allowed to mate and approximately 40–60 of the F_0 pups were likewise exposed to 0 or 2,500 ppm formaldehyde in drinking water (after weaning) for 104 weeks. As before, parents and progeny lived out their normal life span but then were subjected to a complete histopathological examination. Incidence of leukemias in exposed breeders and offspring is shown in Table 4-33. The authors considered this data to indicate a “slight” increase in leukemias in breeders at 2,500 ppm, but the changes did not achieve statistical significance.

Table 4-33. Incidence of leukemias in breeder and offspring Sprague-Dawley rats exposed to formaldehyde in drinking water for 104 weeks (Test BT 7005)

Concentration (ppm)	Incidence of leukemias			
	Breeder		Offspring	
	Males	Females	Males	Females
0	0/20	1/20	3/59	3/49
2,500	2/18	2/18	4/36	0/37

Source: Soffritti et al. (1989).

4.7. SYNTHESIS OF MAJOR NONCANCER EFFECTS

4.7.1. Summary of Key Studies in Methanol Toxicity

A substantial body of information exists on the toxicological consequences to humans who consume or are acutely exposed to large amounts of methanol. Neurological and immunological effects have been noted in adult human subjects acutely exposed to as low as 200 ppm (262 mg/m^3) methanol (Mann et al., 2002; Chuwers et al., 1995). Nasal irritation effects have been reported by adult workers exposed to 459 ppm (601 mg/m^3) methanol. Frank effects such as blurred vision and bilateral or unilateral blindness, coma, convulsions/tremors, nausea, headache, abdominal pain, diminished motor skills, acidosis, and dyspnea begin to occur as blood levels approach 200 mg methanol/L, and 800 mg/L appears to be the threshold for lethality. Data for subchronic, chronic or in utero human exposures are very limited. Determinations regarding longer term effects of methanol are based primarily on animal studies.

An end-point-by-end-point survey of the primary effects of methanol in experimental animals is given in the following paragraphs. Tabular summaries of the principal toxicological studies that have examined the impacts of methanol when experimental animals were exposed to methanol via the oral or inhalation routes are provided in Tables 4-34 and 4-35. Most studies focused on developmental and reproductive effects. A large number of the available studies were performed by routes of exposure (e.g., i.p.) that are less relevant to the assessment. The data are summarized separate sections that address oral exposure (Section 4.7.1.1) and inhalation exposure (Section 4.7.1.2).

Table 4-34. Summary of studies of methanol toxicity in experimental animals (oral)

Species, strain, number/sex	Dose/duration	NOAEL (mg/kg-day)	LOAEL (mg/kg-day)	Effect	Reference
Rat Sprague-Dawley 30/sex/group	0, 100, 500, and 2,500 mg/kg-day for 13 wk	500	2,500	Reduction of brain weights, increase in the serum activity of ALT and AP. Increased liver weights	U.S. EPA (1986c)

Species, strain, number/sex	Dose/duration	NOAEL (mg/kg-day)	LOAEL (mg/kg-day)	Effect	Reference
Rat Sprague-Dawley 100/sex/group	0, 500, 5,000, or 20,000 ppm (v/v) in drinking water, for 104 wk. Doses were approx. 0, 46.6, 466, and 1,872 mg/kg-day (male) and 0, 52.9, 529, and 2101 mg/kg-day (female)	466–529	1,872–2,101	Increased incidence of ear duct[a] carcinomas, lymphoreticular tumors, and total malignant tumors. No noncancer effects	Soffritti et al. (2002a)
Mouse Swiss	560, 1000 and 2100 mg/kg/d (female) and 550, 970, and 1800 mg/kg/d (male), 6 days/wk for life	ND	1,800-2,100	Increased incidence of liver parenchymal cell necrosis and malignant lymphomas	Apaja (1980)
Reproductive/developmental toxicity studies					
Rat Long-Evans 10 pregnant females/group	0 and 2,500 mg/kg-day on either GD15–GD17 or GD17–GD19.	NA	2,500	Neurobehavioral deficits (such as homing behavior, suckling ability	Infurna and Weiss (1986)
Mouse CD-1 8 pregnant females and 4 controls	4 g/kg-day in 2 daily doses on GD6-GD15	NA	4,000	Increased incidence of totally resorbed litters, cleft palate and exencephaly. A decrease in the number of live fetuses/litter	Rogers, et al. (1993a)

NA = Not applicable; ND = Not determined; M= male, F=female.
[a]In an NTP evaluation of pathology slides from another bioassay from this laboratory in which a similar ear duct carcinoma finding was reported (Soffritti et al., 2006, 2005), NTP pathologists interpreted a majority of these ear duct responses as being hyperplastic, not carcinogenic, in nature (EFSA, 2006; Hailey, 2004).

Table 4-35. Summary of studies of methanol toxicity in experimental animals (inhalation exposure)

Species, strain, number/sex	Dose/duration	NOAEL (ppm)	LOAEL (ppm)	Effect	Reference
Monkey *M. fascicularis*, 1 or 2 animals/group	0, 3,000, 5,000, 7,000, or 10,000 ppm, 21 hr/day, for up to 14 days	ND	ND	Clinical signs of toxicity, CNS changes, including degeneration of the bilateral putamen, caudate nucleus, and claustrum. Edema of cerebral white matter.	NEDO (1987)
Dog (2)	10,000 ppm for 3 min, 8 times/day for 100 days	NA	NA	None	Sayers et al. (1944)
Rat Sprague-Dawley 5 males/ group	0, 200, 2000, or 10,000 ppm, 8 hr/day, 5 days/wk for up to 6 wk	NA	200	Transient reduction in plasma testosterone levels	Cameron et al. (1984)

Species, strain, number/sex	Dose/duration	NOAEL (ppm)	LOAEL (ppm)	Effect	Reference
Rat Sprague-Dawley 5 males/ group	0, or 200 ppm, 6 hr/day, for either 1 or 7 days	NA	200	Transient reduction in plasma testosterone levels	Cameron et al. (1985)
Rat Sprague-Dawley 5/sex/group	0, 500, 2,000, or 5,000 ppm, 5 days/wk for 4 wk	5,000	NA	No compound-related effects	Andrews et al. (1987)
Monkey *M. fascicularis* 3/sex/group	0, 500, 2,000, or 5,000 ppm, 5 days/wk for 4 wk	5,000	NA	No compound-related effects	
Rat Sprague-Dawley 10/sex/group	0, 300, or 3,000 ppm, 6 hr/day, 5 days/wk for 4 wk	NA	300	Reduction in size of thyroid follicles	Poon et al. (1994)
Rat Sprague-Dawley 15/sex/group	0 or 2,500 ppm, 6 hr/day, 5 days/wk for 4 wk	NA	2,500	Reduction of relative spleen weight in females, histopathologic changes to the liver, irritation of the upper respiratory tract	Poon et al. (1995)
Monkey *M. fascicularis* 2 or 3 animals/ group/time point	0, 10, 100, or 1,000 ppm, 21 hr/day for either 7, 19, or 29 mo	ND ND	ND ND	Limited fibrosis of the liver Possible myocardial and renal effects	NEDO (1987)
Rat F344 20/sex/group	0, 10, 100, or 1,000 ppm, 20 hr/day, for 12 mo	NA	NA	No compound-related effects	
Mouse B6C3F$_1$ 30/sex/group	0, 10, 100, or 1000 ppm, 20 hr/day, for 12 mo	NA	NA	No clear-cut compound-related effects	
Mouse B6C3F$_1$ 52–53/sex/group	0, 10, 100, or 1,000 ppm, 20 hr/day, for 12 mo	100	1,000	Increase in kidney weight, decrease in testis and spleen weights	
Rat F344 52/sex/group	0, 10, 100, or 1,000 ppm, ~20 hr/day for 2 yr	100	1,000	Fluctuations in a number of urinalysis, hematology, and clinical chemistry parameters. Development of pulmonary adenoma/adenocarcinoma (males), pheochromocytomas (females)	
Reproductive/developmental toxicity studies					
Rat Sprague-Dawley 15/pregnant females/group	0, 5,000, 10,000, or 20,000 ppm, 7 hr/day on either GD1–GD19 or GD7–GD15.	5,000	10,000	Reduced fetal body weight, increased incidence of visceral and skeletal abnormalities, including rudimentary and extra cervical ribs	Nelson et al. (1985)
Rat Sprague-Dawley 36/pregnant females/group	0, 200, 1,000, or 5000 ppm, 22.7 hr/day, on GD7–GD17	1,000	5,000	Late-term resorptions, reduced fetal viability, increased frequency of fetal malformations, variations and delayed ossifications.	NEDO (1987)

Species, strain, number/sex	Dose/duration	NOAEL (ppm)	LOAEL (ppm)	Effect	Reference
Rat Sprague-Dawley F_1 and F_2 generations of a two-generation study	0, 10, 100, or 1000 ppm, 20 hr/day; F_1- birth to end of mating (M) or weaning (F); F2- birth to 8 wks	100	1,000	Reduced weight of brain, pituitary, and thymus at 8, 16 and 24 wk postnatal in F_1 and at 8 wk in F_2	
Rat Sprague-Dawley Follow-up study of brain weights in F_1 generation of 10–14/sex/group in F_1 generation	0, 500, 1,000, and 2,000 ppm; GD0 through F_1 generation	500	1,000	Reduced brain weight at 3 wk and 6 wk (males only). Reduced brain and cerebrum weight at 8 wk (males only)	
Mouse CD-1 30–114 pregnant females/group	0, 1,000, 2,000, 5,000, 7,500, 10,000, or 15,000 ppm, 7 hr/day on GD6–GD15.	1,000	2,000	Increased incidence of extra cervical ribs, cleft palate, exencephaly; reduced fetal weight and pup survival, Delayed ossification	Rogers et al. (1993a)
Mouse CD-1 12–17 pregnant females/group	0 and 10,000 ppm on two consecutive days during GD6–GD13 or on a single day during GD5–GD9	NA	10,000	Cleft palate, exencephaly, skeletal malformations	Rogers and Mole (1997)
Rat Long-Evans 6–7 pregnant females/group	0 or 15,000 ppm, 7 hr/day on GD7–GD19	NA	15,000	Reduced pup weight	Stanton et al. (1995)
Rat Long-Evans 10–12 pregnant females/group	0 or 4,500 ppm from GD10 to PND21.	NA	4,500	Subtle cognitive deficits	Weiss et al. (1996)
Monkey *M. fascicularis* 12 monkeys/group	0, 200, 600, or 1800 ppm, 2.5 hr/day, 7 days/wk, during premating, mating and gestation	ND	ND[a]	Shortened period of gestation; may be related to exposure (no dose-response), neurotoxicological deficits including reduced performance in the VDR test; may be related to premature births.	Burbacher et al. (20004a, 2004b, 1999a, 1999b)

ND = Not determined due to study limitations such as small number of animals /time point/ exposure level
NA = Not applicable.
[a]Gestation resulted in a shorter period of gestation in dams exposed to as low as 200 ppm (263 mg/m^3). However, because of uncertainties associated with these results, including clinical intervention and the lack of a dose-response, EPA was not able to identify a definitive NOAEL or LOAEL from this study.

4.7.1.1. *Oral*

There have been very few subchronic, chronic, or in utero experimental studies of oral methanol toxicity. In one such experiment, an EPA-sponsored 90-day gavage study in Sprague-Dawley rats suggested a possible effect of the compound on the liver (U.S. EPA, 1986c). In the absence of gross or histopathologic evidence of toxicity, fluctuations on some clinical chemistry

markers of liver biochemistry and increases in liver weights at the highest administered dose (2,500 mg/kg-day) justify the selection of the mid-dose level (500 mg/kg-day) as a NOAEL for this effect under the operative experimental conditions. That the bolus effect may have been important in the induction of those few effects that were apparent in the subchronic study is suggested by the outcome of lifetime drinking water study of methanol that was carried out in Sprague-Dawley rats by Soffritti et al. (2002a). According to the authors, no noncancer toxicological effects of methanol were observed at drinking water concentrations of up to 20,000 ppm (v/v). Based on default assumptions on drinking water consumption and body weight gain assumptions, the high concentration was equivalent to a dose of 1,780 mg/kg-day in males and 2,177 mg/kg-day in females. In the stated absence of any changes to parameters reflective of liver toxicity in the Soffritti et al. (2002a) study, the slight impacts to the liver observed in the subchronic study at 2,500 mg/kg-day suggest the latter dose to be a minimal LOAEL. Logically, the true but unknown threshold would at the high end of the range from 500 (the default NOAEL) to 2,500 mg/kg-day for liver toxicity via oral gavage.

Two studies have pointed to the likelihood that oral exposure to methanol is associated with developmental neurotoxicity or developmental deficits. When Infurna and Weiss (1986) exposed pregnant Long-Evans rats to 2% methanol in drinking water (providing a dose of approximately 2,500 mg/kg-day), they observed no reproductive or developmental sequelae other than from 2 tests within a battery of fetal behavioral tests (deficits in suckling ability and homing behavior). In the oral section of the Rogers et al. (1993a) study, such teratological effects as cleft palate and exencephaly and skeletal malformations were observed in fetuses of pregnant female mice exposed to daily gavage doses of 4,000 mg/kg methanol during GD6–GD15. Likewise, an increase in totally resorbed litters and a decrease in the number of live fetuses/litter appear likely to have been an effect of the compound. Similar skeletal malformations were observed by Rogers and Mole (1997), Rogers et al. (1993a), and Nelson et al. (1985) following inhalation exposure.

4.7.1.2. *Inhalation*

Some clinical signs, gross pathology, and histopathological effects of methanol have been seen in experimental animals including adult nonhuman primates exposed to methanol vapor. Results from an unpublished study (NEDO, 1987) of *M. fascicularis* monkeys, chronically exposed to concentrations as low as 10 ppm for up to 29 months, resulted in histopathological effects in the liver, kidney, brain and peripheral nervous system. These results were generally reported as subtle and do not support a robust dose response over the range of exposure levels used. Confidence in the methanol-induced findings of effects in adult nonhuman primates is limited because this study utilized a small number (2–3) of animals/dose level/time of sacrifice and inadequately reporting of results (i.e., lack of clear documentation of a concurrent control

group). In addition, the monkeys used in this study were all wild-caught. All of these concerns limit the study's utility in derivation of an RfC.

A number of studies have examined the potential toxicity of methanol to the male reproductive system (Lee et al., 1991; Cameron et al., 1985, 1984). The data from Cameron et al. (1985, 1984) showed a transient but not necessarily dose-related decrease in serum testosterone levels of male Sprague-Dawley rats. Lee et al. (1991) reported the appearance of testicular lesions in 18-month-old male Long-Evans rats that were exposed to methanol for 13 weeks and maintained on folate-deficient diets. Taken together, the Lee et al. (1991) and Cameron et al. (1985, 1984) study results could indicate chemically-related strain on the rat system as it attempts to maintain hormone homeostasis. However, the available data are insufficient to definitively characterize methanol as a toxicant to the male reproductive system.

When Sprague-Dawley rats were exposed to methanol, 6 hours/day for 4 weeks, there were some signs of irritation to the eyes and nose. Mild changes to the upper respiratory tract were also described in Sprague-Dawley rats that were exposed for 4 weeks to up to 300 ppm methanol (Poon et al., 1995). Other possible effects of methanol in rats included a reduction in size of thyroid follicles (Poon et al., 1994), panlobular vacuolation of the liver, and a decrease in spleen weight (Poon et al., 1995). NEDO (1987) reported dose-related increases in moderate fatty degeneration in hepatocytes of male mice exposed via inhalation for 12 months, but this finding was not observed in the NEDO (1987) 18-month mouse inhalation study. Nodes reported in the liver of mice from the 18-month study may have been precancerous, but the 18-month study duration was not of sufficient duration to make a determination.

One of the most definitive and quantifiable toxicological impacts of methanol when administered to experimental animals via inhalation is related to the induction of developmental abnormalities in fetuses exposed to the compound in utero. Developmental effects have been demonstrated in a number of species, including monkeys, but particularly rats and mice. Most developmental teratological effects appear to be more severe in the latter species. For example, in the study of Rogers et al. (1993a) in which pregnant female CD-1 mice were exposed to methanol vapors on GD6–GD15 at a range of concentrations, reproductive and fetal effects included an increase in the number of resorbed litters, a reduction in the number of live pups, and increased incidence of exencephaly, cleft palate, and the number of cervical ribs. While the biological significance of the cervical rib effect has been the subject of much debate (See discussion of Chernoff and Rogers [2004] in Section 5), it appears to be the most sensitive indicator of developmental toxicity from this study, with a NOAEL of 1,000 ppm (1,310 mg/m^3). In rats, however, the most sensitive developmental effect, as reported in the NEDO (1987) two-generation inhalation studies, was a postnatal reduction in brain weight at 3, 6 and 8 weeks postnatally, which was significantly lower than controls when pups and their dams were exposed

to 1,000 ppm (1,310 mg/m^3) during gestation and throughout lactation. The NOAEL reported in this study was 500 ppm (655 mg/m^3).

Rogers and Mole (1997) addressed the question of which period of gestation was most critical for the adverse developmental effects of methanol in CD-1 rats. Such malformations and anomalies as cleft palate, exencephaly, and a range of skeletal defects, appeared to be induced with a greater incidence when the dams were exposed on or around GD6. These findings were taken to indicate that methanol is most toxic to embryos during gastrulation and in the early stages of organogenesis. However, NEDO (1987) gestation-only and two-generation studies showed that significant reductions in brain weight were observed at a lower exposure levels when pups and their dams were exposed during lactation as well as gestation, indicating that exposure during the later stages of organogenesis, including postnatal development, can significantly contribute to the severity of the effects in this late-developing organ system.

In comparing the toxicity (NOAELs and LOAELs) for the onset of developmental effects in mice and rats exposed in utero, there is suggestive evidence from the above studies that mice may be more susceptible to methanol than rats. Supporting evidence for this proposition has come from in vitro studies in which rat and mouse embryos were exposed to methanol in culture (Andrews et al., 1993). Further evidence for species-by-species variations in the susceptibility of experimental animals to methanol during organogenesis has come from experiments on monkeys (Burbacher et al., 2004a, 2004b, 1999a,1999b). In these studies, exposure of monkeys to methanol during premating, mating, and throughout gestation resulted in a shorter period of gestation in dams exposed to as low as 200 ppm (263 mg/m^3). The shortened gestation period was largely the result of C-sections performed in the methanol-exposure groups “in response to signs of possible difficulty in the maintenance of pregnancy,” including vaginal bleeding. Though statistically significant, the finding of a shortened gestation length may be of limited biological significance. Gestational age, birth weight and infant size observations in all exposure groups were within normal ranges for *M. fascicularis* monkeys, and vaginal bleeding 1–4 days prior to delivery of a healthy infant does not necessarily imply a risk to the fetus (as cited in CERHR, 2004). An ultrasound examination could have substantiated fetal or placental problems arising from presumptive pregnancy duress (see Section 4.3.2). As discussed in Section 4.4.2, there is also evidence from this study that methanol caused neurobehavioral effects in exposed monkey infants that may be related to the gestational exposure. However, the data are not conclusive,and a dose-response trend is not robust. There is insufficient evidence to determine if the primate fetus is more or less sensitive than rodents to methanol teratogenesis. Several other uncertainties contributed to decreased confidence in the use of this primate in quantitative estimates of risk. These included: a mixture of wild- and colony-derived monkey mothers used in the study; the use of a cohort design necessitated by the complexity of this study also

seemingly resulted in limitations in power to detect effects (e.g., Fagan test results for controls); and no apparent adjustment in statistical analysis for results from the neurobehavioral battery of tests employed leading to concern about inflation of type 1 error. Because of the uncertainties associated with these results, including the fact that the decrease in gestational length was not exacerbated with increasing methanol exposure, EPA was not able to identify a definitive NOAEL or LOAEL from this study. This study does support the weight of evidence for developmental neurotoxicity in the hazard characterization of low-level methanol exposure.

Weiss et al. (1996) and Stanton et al. (1995) evaluated the developmental and developmental neurotoxicological effects of methanol exposure on pregnant female Long-Evans rats and their progeny. In the former study, exposure of dams to 15,000 ppm (19,656 mg/m^3), 7 hours/day on GD7–GD19 resulted in reduced weight gain in pups, but produced little other evidence of adverse developmental effects. The authors subjected the pups to a number of neurobehavioral tests that gave little if any indication of compound-related changes. This study, while using high exposure levels, was limited in its power to detect effects due to the small number of animals used. In the Weiss et al. (1996) study, exposure of pregnant female Long-Evans rats to 0 or 4,500 (0 and 5,897 mg/m^3) methanol from GD6 to PND21 likewise provided fluctuating and inconsistent results in a number of neurobehavioral tests that did not necessarily indicate any compound-related impacts. The finding of this study indicated subtle cognitive defects not on the learning of an operant task but in the reversal learning. This study also reported exposure-related changes in neurodevelopmental markers of NCAMs on PND4. NCAMs are a family of glycoproteins that is needed for migration, axonal outgrowth, and establishment of the pattern for mature neuronal function.

Taking all of these findings into consideration reinforces the conclusion that the most appropriate endpoints for use in the derivation of an RfC for methanol are associated with developmental neurotoxicity and developmental toxicity. Among an array of findings indicating developmental neurotoxicity and developmental malformations and anomalies that have been observed in the fetuses and pups of exposed dams, an increase in the incidence of cervical ribs of gestationally exposed mice (Rogers et al., 1993a) and a decrease in the brain weights of gestationally and lactationally exposed rats (NEDO, 1987) appear to be the most robust and most sensitive effects.

4.8. NONCANCER MOA INFORMATION

A review by Jacobsen and McMartin (1986) has provided a comprehensive summary of the mechanism by which methanol brings about its acute toxic effects. Overwhelmingly, the evidence points to methanol poisoning being a consequence of formate accumulation. This compound is formed from formaldehyde under the action of ADH3. Formaldehyde itself is

formed from methanol under the action of ADH1. Evidence for the involvement of formate comes from the delay in the onset of harmful symptoms, detection of formate in the blood stream, and the profound acidosis that develops 12–24 hours after exposure to methanol. Treatments for methanol poisoning include the i.v. administration of buffer to correct the acidosis, hemodialysis to remove methanol from the blood stream, and i.v. administration of either ethanol or fomepizole to inhibit the activity of ADH1. Therapies to increase endogenous levels of folate may enhance the activity of THF synthetase, an enzyme that catalyzes the oxidation of formate to CO_2. Jacobsen and McMartin (1986) have drawn attention to the accumulation of lactate in advanced stages of severe methanol poisoning, a possible consequence of formate inhibition of mitochondrial respiration and tissue hypoxia. The additional decrease in blood pH is likely to enhance the nonionic diffusion of formic acid across cell membranes, with resulting CNS-depression, hypotension, and further lactate production.

Jacobsen and McMartin (1986) summarized a body of evidence that also points to the formate-related acidosis as the etiologically important factor in ocular damage. The hypothesis suggests that ocular toxicity is due to the inhibition of cytochrome oxidase in the optic nerve by formate. This would cause inhibition of ATP formation and consequent disruption of optic nerve function.

While it is well established that the toxic consequences of acute methanol poisoning arise from the action of formate, there is less certainty on how the toxicological impacts of longer-term exposure to lower levels of methanol are brought about. For example, since developmental effects in experimental animals appear to be significant adverse effects associated with in utero methanol exposure, it is important to determine potential MOAs for how these specific effects are brought about.

As described in Section 4.6.1, data from experiments carried out by Dorman et al. (1995), formate is not the probable proximate teratogen in pregnant CD-1 mice exposed to high concentrations of methanol vapor. This conclusion is based on the fact that there appeared to be little, if any, accumulation of formate in the blood of methanol-exposed mice, and exencephaly did not occur until formate levels were grossly elevated. Another line of argument is based on the observation that treatment of pregnant mice with a high oral dose of formate did not induce neural tube closure defects at media concentrations comparable to those observed in uterine decidual swelling after maternal exposure to methanol. Lastly, methanol- but not formate-induced neural tube closure defects in mouse embryos in vitro at media concentrations comparable to the levels of methanol detected in blood after a teratogenic exposure.

Harris et. al (Hansen et al., 2005; Harris et al., 2004, 2003) carried out a series of physiological and biochemical experiments on mouse and rat embryos exposed to methanol, formaldehyde and formate, concluding that the etiologically important substance for embryo

dysmorphogenesis and embryolethality was likely to be formaldehyde rather than the parent compound or formate. Specific activities for enzymes involved in methanol metabolism were determined in rat and mouse embryos during the organogenesis period of 8–25 somites (Harris et al., 2003). The experiment was based on the concept that differences in the metabolism of methanol to formaldehyde and formic acid by the enzymes ADH1, ADH3, and CAT may contribute to hypothesized differences in species sensitivity that were apparent in toxicological studies. A key finding was that the activity of ADH3 (converting formaldehyde to formate) was lower in mouse VYS than that of rats throughout organogenesis, consistent with the greater sensitivity of the mouse to the developmental effects of methanol exposure. Another study (Harris et al., 2004) which showed that the inhibition of GSH synthesis increases the developmental toxicity of methanol also lends support to this hypothesis because ADH3-mediated metabolism of formaldehyde is the only enzyme involved in methanol clearance that is GSH-dependent. These findings provide inferential evidence for the proposition that formaldehyde may be the ultimate teratogen through diminished ADH3 activity. This concept is further supported by the demonstration that the LOAELs for the embryotoxic effects of formaldehyde in rat and mouse embryos were much lower than those for formate and methanol (Hansen et al., 2005). Taking findings from both sets of experiments together, Harris et. al. (Hansen et al., 2005; Harris et al., 2004, 2003) concluded that the demonstrable lower capacity of mouse embryos to transform formaldehyde to formate (by ADH3) could explain the increased susceptibility of mouse versus rat embryos to the toxic effects of methanol.

While studies such as those by Harris et al. (2004, 2003) and Dorman et al. (1995, 1994) strongly suggest that formate is not the metabolite responsible for methanol's teratogenic effects, there are still questions regarding the relative involvement of methanol versus formaldehyde. In vitro evidence suggests that formaldehyde is the more embryotoxic moiety, but methanol would likely play a prominent role, at least in terms of transport to the target tissue. The high reactivity of formaldehyde would limit its unbound and unaltered transport as free formaldehyde from maternal to fetal blood (Thrasher and Kilburn, 2001), and the capacity for the metabolism of methanol to formaldehyde is likely lower in the fetus and neonate versus adults (see discussion in Section 3.3)

In humans, metabolism of methanol occurs primarily through ADH1, whereas in rodents methanol clearance involves primarily CAT, as well as ADH1. There are no known studies that compare enzyme activities of human ADH1 and rodent CAT. Assuming that relative expression and activity of ADH1 is comparable across species, rodents are expected to clear methanol more rapidly than humans due to involvement of CAT. In fact, even among rodents the metabolism of methanol may be quite different, as one study has demonstrated that the rate of methanol oxidation in mice is twice the rate in rats, as well as nonhuman primates (Mannering et al.,

1969). Despite a faster rate of methanol metabolism, mice have consistently shown higher blood methanol levels than rats following exposure to equivalent concentrations (Tables 3-4 and 3-5). A faster respiration rate and increased fraction of absorption by mice is thought to be the reason for the higher blood methanol levels compared to rats (Perkins et al., 1995a). Using the exposure conditions of Horton et al. (1992) for rats, when the respiration rate scaling coefficient (QPC) was increased from the rat value of 16.4 to the mouse value of 25.4 while holding all other parameters constant, peak blood concentrations were predicted by the PBPK model to increase by 1.4-fold at 200 ppm and 1.8-fold at 2,000 ppm (where metabolism is becoming saturated). Because smaller species generally have faster breathing rates than larger species (in the PBPK model, the respiration rate/BW is 3 times slower in humans versus rats and almost 10 times slower versus mice), humans would be expected to accumulate less methanol than rats or mice inhaling equivalent concentrations and given the same metabolism rate. However, Horton et al. (1992) measured a blood concentration in rats exposed to 200 ppm methanol of about 3.7 mg/L after 6 hours of exposure while Sedevic et al. (1981) measured around 5.5 mg/L in human volunteers after 6 hours of exposure to 231 ppm. Correcting for the higher exposure, human blood concentrations would be around 4.8 mg/L if exposed at 200 ppm. Simulations with the mouse model predict a blood level of 5.7 mg/L after 6 hours of exposure to 200 ppm, only 20% higher than this interpolated human value. Thus the slower inhalation rate in humans is offset by the slower metabolic rate, leading to equivalent blood concentrations. (If the same rate of metabolism/BW as mice is used, human blood concentrations are predicted to decrease by approximately fivefold.). These differences are considered in Section 5 for the characterization of human and rodent PBPK models used for the derivation of human equivalent concentrations (HECs).

4.9. EVALUATION OF CARCINOGENICITY

4.9.1. Summary of Overall Weight-of-Evidence

Under the current *Guidelines for Carcinogen Risk Assessment* (U.S. EPA 2005a, 2005b), methanol is *likely to be carcinogenic to humans* by all routes of exposure based on dose-dependent trends in multiple tumors in both sexes of two strains of rats, by inhalation and oral routes of exposure and increases in malignant lymphoma in both sexes of Swiss mice by oral exposure. Specifically, EPA's analysis of the Soffritti et al. (2002a) lifespan study of Sprague-Dawley rats exposed to methanol in drinking water for 104 weeks indicates a statistically significant increase in the incidence of lymphoma[58] in lung and other organs at the two highest

[58] Combining lymphoblastic lymphomas, lymphocytic lymphomas, lympho-immunoblastic lymphomas and/or lymphoblastic leukemias as malignant lymphomas but excluding myeloid leukemias, histocytic sarcomas and monocytic leukemia as tumors of different origin (Cruzan, 2009; Hailey, 2004; McConnell et al., 1986).

doses for males and across all doses for females (Fisher's exact, $p < 0.05$) and a statistically significant increase in relatively rare hepatocellular carcinomas in males compared to historical controls (n=407)[59] (Fisher's exact $p < 0.05$ for all doses and $p < 0.01$ for the high-dose group). Statistically significant increases in the incidence of malignant lymphomas relative to historical controls (Fisher's exact, $p < 0.05$) have also been observed in another rodent species, Swiss mice, following similar mg/kg-day exposures to methanol in drinking water for life (Apaja, 1980). The only available chronic inhalation studies of methanol (NEDO, 1985/2008a, 2008b) reported slight but statistically significant tumor responses in F344 rats at 24 months, and no evidence of carcinogenicity in $B6C3F_1$ mice at 18 months. EPA's analysis of the NEDO (1985/2008b) inhalation study of F344 rats indicates a dose-response trend (Cochrane-Armitage $p < 0.05$) and an increased incidence over concurrent controls at the high dose (Fisher's exact $p < 0.05$) of pulmonary adenomas/adenocarcinomas in male rats. This analysis also indicates a statistically significant dose-response trend (Cochrane-Armitage $p < 0.05$) and a statistically significant increased incidence over NTP historical controls at the high-dose (Fisher's exact $p < 0.05$) of pheochromocytomas in female rats.

This WOE conclusion is supported by the results of other studies performed by ERF that have shown tumorigenic responses similar to that of methanol in male and female Sprague-Dawley rats exposed to formaldehyde (via drinking water), a metabolite of methanol, and to aspartame (via feed) and MTBE (via olive oil gavage), substances that hydrolyze to release methanol and formaldehyde. Confidence in the designation of methanol as a likely human carcinogen is strengthened by the fact that methanol is metabolized to formaldehyde, a chemical that has been classified as carcinogenic to humans (group 1) (IARC, 2004). As discussed below and in Section 5.4.3, there are uncertainties in the interpretation of these findings. All of the key studies have design and reporting limitations. EPA has reanalyzed the reported data from both the ERF (Soffritti et al., 2002a) and NEDO (1987, 1985/2008a, 2008b) studies. In reassessing the ERF study data, EPA decided to combine only those lymphomas considered to have originated from the same cell type. In the case of the NEDO data, the significance of the tumor findings were incompletely reported in the original NEDO (1987) summary. Hence, EPA used translations of the original, detailed Japanese study reports provided by NEDO and the Methanol Institute (NEDO, 1985/2008a,2008b) and reanalyzed the individual animal data.

4.9.2. Synthesis of Human, Animal, and Other Supporting Evidence

Evidence of the carcinogenic potential of methanol arises from drinking water studies in Sprague-Dawley rats (Soffritti et al., 2002a) and in Eppley Swiss Webster mice (Apaja, 1980),

[59] Obtained by combining control data from ERF studies of methanol, formaldehyde, aspartame, MTBE, and TAME.available from the ERF website at http://www.ramazzini.it/fondazione/foundation.asp).

and an inhalation study in F344 rats (NEDO, 1985/2008b), with no information available in humans. As is described in Section 4.2.1.3 (Table 4-2), Soffritti et al. (2002a) reported a number of tumors in methanol-exposed Sprague-Dawley rats. EPA reanalyzed the tumor findings from this study using individual animal pathology available from the ERF website (see Section 5.4.1.1).[60] As indicated above, the increase in a relatively rare hepatocellular carcinoma in males compared to historical controls (Fisher's exact $p < 0.05$ for all doses and $p < 0.01$ for the high-dose group) is potentially related to methanol dosing. A significant increase in the incidence of ear duct carcinoma was also reported by Soffritti et al. (2002a). However, the high incidence for this tumor in controls of the Soffritti et al. (2002a) study relative to other studies of Sprague-Dawley rats (Cruzan, 2009) and the results of an NTP evaluation of pathology slides from another bioassay (EFSA, 2006; Hailey, 2004) raise questions about the ear duct pathological determinations of Soffritti et al. (2002a).[61]

As is described in Section 4.2.1.3 (Table 4-3), Apaja (1980) found an increase in malignant lymphomas in mid-dose ($p = 0.06$) and high-dose ($p < 0.05$) female and mid-dose ($p < 0.05$) male Eppley Swiss Webster mice exposed for life via drinking water. The lack of a concurrent unexposed control data limit the confidence that can be placed on the relevance of the increased lymphoma responses noted in this study. However, while controls were not concurrent, they were from proximate (within 3 years) generations of the same mouse colony, lymphomas were evaluated via the same classification criteria and, in the case of the Hinderer (1979) controls, the histopathological analysis was performed by the same author (Apaja, 1980). In addition, this is a late developing tumor, as noted by the author, suggesting the possibility of a higher tumor response in the females of all exposure groups had their survival not been significantly lower than untreated historical controls (see dose-response analysis in Appendix E). Further, additional support for these study results comes from the fact that, as described above, Soffritti et al. (2002a) subsequently reported an increase in lymphomas following similar levels of mg/kg-day methanol drinking water doses to Sprague-Dawley rats, another rodent species with a high spontaneous lymphoma rate.

Chronic inhalation bioassays have been conducted in monkeys, mice, and F344 rats (NEDO, 1987, 1985/2008a; 1985/2008b). No exposure-related carcinogenic responses were observed in the monkey or mouse studies. As is described in Section 4.2.2.3, individual tumor responses from the rat study were not significantly increased over concurrent controls, but the

[60] ERF provided the EPA with the detailed, individual animal data via reports available through their web portal (http://www.ramazzini.it/fondazione/foundation.asp). This allowed the EPA to combine lymphomas of similar histopathological origins and confirm the tumor incidences reported in the Soffriti et al. (2002a) paper.

[61] In an NTP evaluation of pathology slides from another bioassay from this laboratory in which a similar ear duct carcinoma finding was reported (Soffritti et al., 2006, 2005), NTP pathologists interpreted a majority of these ear duct responses as being hyperplastic, not carcinogenic, in nature (EFSA, 2006; Hailey, 2004).

response in the high-dose (1,000 ppm) group for pulmonary adenomas/adenocarcinomas in male rats was increased over concurrent controls (Fisher's exact $p < 0.05$), and the dose-response for both pulmonary adenomas/adenocarcinomas in male rats and pheochromocytomas in female rats represent increasing trends (Cochran-Armitage trend test $p < 05$). Further, the high-dose responses for both of these tumor types were elevated ($p < 0.05$) over historical control incidences within their respective sex and strain. As can be seen from Table 4-5, the severity and combined incidence of effects reported in the alveolar epithelium of male rat lungs (epithethial swelling, adenomatosis, pulmonary adenoma and pulmonary adenocarcinoma) and the adrenal glands of female rats (hyperplasia and pheochromocytoma) were increased over controls and lower exposure groups. This pathology and the appearance of a rare adenocarcinoma in the high-dose group are suggestive of a progressive effect associated with methanol exposure. The increased pheochromocytoma response in female rats is considered to be potentially treatment related because this is a historically rare tumor type for female F344 rats (NTP, 2007, 1999; Haseman et al., 1998)[62] and because, when viewed in conjunction with the increased medullary hyperplasia observed in the mid-exposure (100 ppm) group females, it is indicative of a proliferative change with increasing methanol exposure.

Additional support for the designation of methanol as a likely carcinogen is provided by the fact that methanol is metabolized to formaldehyde, which has been associated with increased incidences of lymphoma and leukemia in humans (IARC, 2004). Furthermore, lymphomas similar to those noted in Sprague-Dawley rats following exposure to methanol in drinking water and following a similar dose-response pattern were noted in a bioassay for formaldehyde in drinking water conducted by the same laboratory (Soffritti et al., 2002b, 1989) (Section 4.9.3). These shared endpoints suggests that the carcinogenic effects of methanol may result from its conversion to formaldehyde, though the moiety and MOA responsible for methanol-associated tumor formation have not been identified.

Significant increases in the incidence of lymphoreticular tumors have also been reported for other chemicals that convert in the body to methanol and/or formaldehyde including aspartame (Soffritti et al., 2007, 2006, 2005) and MTBE (Belpoggi et al., 1997, 1995). In contrast, no such tumors have been reported in a similar study conducted with a structurally similar alcohol, ethanol (Soffritti et al., 2002a). In addition, epidemiological studies have associated formaldehyde exposure with increases in the incidence of related lymphohematopoietic tumors. While lymphomas are a rare finding in chronic laboratory bioassays, NCI (Hauptmann et al., 2003) and NIOSH (Pinkerton et al., 2004) have reported increased lymphohematopoietic cancer risk, principally leukemia, in humans from occupational

[62] Haseman et al. (1998) report rates for spontaneous pheochromocytomas in 2-year NTP bioassays of 5.7% (benign) and 0.3% (malignant) in male F344 rats and 0.3% (benign) and 0.1% (malignant) in female (n = 1517) F344 rats.

exposure to formaldehyde.[63] The similarities in tumor response across these chemicals, as well as a similar shape in the dose-response curve, supports the hypothesis that the common carcinogenic moiety for these compounds is the generation or presence of formaldehyde. The dose-response analysis discussed in Section 5 provides additional evidence supporting a role for the formaldehyde metabolite of methanol. When "total metabolites in blood" predicted by a PBPK model was used as the dose metric, model fit to the dose-response data was significantly improved.

As discussed in Section 4.6.5.2, there are challenges relative to the interpretation of the observed lymphoreticular tumors because there is no indication that ERF used specific pathogen-free (SPF) rats (Schoeb et al., 2009), and the protocol for the studies conducted by the ERF (Soffritti et al., 2002c) is different from 2-year bioassays conducted by NTP and NEDO. A distinct characteristic of the protocol for long-term bioassays conducted by the ERF is to maintain animals until spontaneous death, rather than sacrificing them at the end of exposure at 104 weeks. This difference in protocol may have an impact on the tumors observed compared to a 2-year bioassay (Melnick et al., 2007). The ERF methanol and ethanol studies (Soffritti et al., 2002a), as well as the aspartame studies (Soffritti et al., 2007, 2006) described in Section 4.6.5.2, employed a large number of animals (100 or more per dose group) compared to a typical (e.g., NTP) cancer bioassay. In addition, the Sprague-Dawley rats used by ERF appear to have increased sensitivity to certain lymphoma responses relative to F344 rats that have been typically used in NTP studies (Caldwell et al., 2008).[64] According to Soffritti et al. (2007, 2006), the overall incidence of lymphomas/leukemias in ERF studies is 13.3% (range, 4.0–25.0%) in female historical controls (2,274 rats) and 20.6% (range, 8.0–30.9%) in male historical controls (2,265 rats). This background rate is considered to be high relative to other tumor types and relative to the background rate for this tumor type in Sprague-Dawley rats from other laboratories (Cruzan, 2009; EFSA, 2006),[65] However, it is in a range that can be considered reasonable for studies that employ a large number of animals (Caldwell et al., 2009; Leakey et al., 2003). These characteristics of ERF studies (i.e., lifetime observation, large number of animals, and test strain sensitive to endpoint but with a relatively low control background rate and mortality) may give them the sensitivity needed to detect a chemically related lymphoma response.

---

[63] IARC (2004) concluded that there was sufficient epidemiological evidence that formaldehyde causes nasopharyngeal cancer in humans but, also, that there was strong evidence for a causal association between formaldehyde and the development of leukemia in humans.

[64] F344 rats have a high mortality rate due to late-developing mononuclear cell leukemia, but the lymphoblastic and immunoblastic lymphomas reported in the Sprague-Dawley rat by ERF following methanol, MTBE, formaldehyde and aspartame administration are rarely diagnosed in the F344 rat (Caldwell et al., 2008).

[65] Cruzan (2009) reports that the incidences of total cancers derived from bloodforming cells, designated as hemolymphoreticular tumors by Ramazzini pathologists, is consistently about four times higher than the incidences of such tumors in SD rats recorded in the Charles River Laboratory historical database (CRL database).

Other aspects of ERF studies may impede their ability to reliably detect a chemically related response (EFSA, 2009, 2006). Chronic inflammatory responses have been reported in test animals of some ERF studies (EFSA, 2009, 2006), which may be the result of infections in test animals resulting from a bioassay design that does not employ SPF rats (Schoeb et al., 2009) and allows the rats to live out their "natural life span" in the absence of disease barriers (e.g., fully enclosed cages). In fact, the ERF has acknowledged that the primary cause of spontaneous death in their rats is respiratory infection (Caldwell et al., 2008; Ramazzini Foundation, 2006; Soffritti et al., 2006). Cruzan (2009) has suggested that respiratory infections in test animals of the Soffritti et al. (2002a) methanol study were not specific to older rats, as findings of lung pathology were reported as often in rats dying prior to 18 months as in rats dying at or after 24 months.[66]

In their reviews of the recently published ERF studies on aspartame (Soffritti et al., 2007, 2006), the European Food Safety Authority (EFSA) have suggested that the increased incidence of lymphomas/leukemias reported in treated rats was related to chronic respiratory disease in the rat colony (EFSA, 2009, 2006), which they suggest was caused by a *Mycoplasma pulmonis* (*M. pulmonis*) infection. EFSA felt that the increased incidence of these tumors was unrelated to aspartame, given the high background incidence of chronic inflammatory changes such as bronchopneumonia in the lungs of treated and untreated rats, and the concern that such tumors might arise as a result of abundant lymphoid hyperplasia in the lungs of rats suffering from chronic respiratory disease. The scientific evidence to support the EFSA opinion that lymphomas/leukemias can result from chronic infection is limited (Schoeb et al., 2009; Caldwell et al., 2008). Epithelial hyperplasias and lymphoid accumulations are commonly found in the larynx and trachea of rats infected with *M. pulmonis*, but induction of lymphoma has not been noted (Everitt and Richter, 1990; Lindsey et al., 1985). Further, the lung, not the larynx or trachea, has been reported as the site of respiratory tract hemolymphoreticular tumors in ERF studies of MTBE (Belpoggi et al., 1998, 1995) and methanol (Soffritti et al., 2002a).[67] In their review of the molecular biology and pathogenicity of *M. pulmonis*, Razin et al. (1998) note that further study is needed before any conclusion can be reached regarding a relationship between *M. pulmonis* and neoplasia. In addition, if the increased incidence of lymphoreticular tumors in the ERF methanol study was strictly the consequence of an incipient respiratory infection in the ERF rat colony, one would expect this to be a common finding across ERF studies. However, as discussed in Section 4.6.5.2, of the 200 compounds tested by ERF, only 8, which includes

[66] The infection rate did not have a significant impact on survival, however. The 2-year survival rate was 40–50% in the ERF methanol bioassay (see Appendix E, Figures E-1 and E-2), which is above the average 2-year NTP study survival rate of 41.5% for Sprague-Dawley rats (Caldwell et al., 2008).

[67] ERF provided EPA with the detailed, individual animal data for the Soffriti et al. (2000a) via reports available through their web portal (http://www.ramazzini.it/fondazione/foundation.asp).

methanol, have been associated with an increased incidence of hemolymphoreticular tumors. Further, the chemicals for which hemolymphoreticular tumors have been reported have chemical characteristics or physical properties in common,[68] consistent with the hypothesis that the increased response is chemical-related.

While evidence for a causal association between respiratory infections and lymphomas is limited, there is evidence that respiratory infections may have confounded the interpretation of lung lesions in the ERF studies. Schoeb et al. (2009) state that lymphomas illustrated in two ERF studies (Figure 10 of Soffritti et al., 2005 and Figures 1-5 of Belpoggi et al., 1999) do not demonstrate the lymphoma type, cellular morphology, and organ distribution typical of lymphoma in rats, but are consistent with "lymphocyte and plasma cell accumulation in the lung that is characteristic of *M. pulmonis* disease." They suggest that, because *M. pulmonis* disease can be exacerbated by chemical treatment, a plausible alternative explanation for the dose-related response reported in the MTBE, aspartame and methanol ERF bioassays is that the studies were confounded by *M. pulmonis* disease and that lesions of the disease were interpreted as lymphoma. However, several ERF lymphoma diagnoses in multiple rat organ systems, including the lung, have been confirmed by an independent panel of six NIEHS pathologists (Hailey, 2004). Further, 60% of the lymphoma incidences reported in the ERF methanol study involved organ systems other than the lungs (Schoeb et al., 2009). The incidence of "lung-only" lymphomas is evenly distributed across the control and dose groups of the methanol study such that removing "lung-only" lympho-immunoblastic lymphomas from consideration (i.e., using only lymphomas from other organ systems) does not significantly alter the dose-response for this lesion (see Section 5.4.3.2).

Based on the NEDO (1987) summary report, IPCS (1997) concluded that "no evidence of carcinogenicity was found in either species [F344 rats and $B6C3F_1$ mice]." This determination was made based on Fisher's exact test results which indicated that the reported high-dose pulmonary adenoma response in male rats and the high-dose pheochromocytoma response in female rats were not statistically significant. However, IPCS did not have translations of the original NEDO mouse and rat chronic studies (NEDO, 1985/2008a; 1985/2008b), which provided additional detail for EPA's analysis and reported combined lung adenoma and adenocarcinoma results for high-dose male rats. In addition, IPCS did not consider trend test results or historical tumor data for F344 rats, both of which indicate a positive result for lung adenoma/adenocarcinoma (males) and pheochromocytomas (females) from the NEDO rat study.

[68] Methanol, formaldehyde, aspartame, and MTBE, have common metabolites (e.g., formaldehyde); DIPE, TAME, methanol, and MTBE are all gasoline-oxygenate additives.

4.9.3. MOA Information

As discussed in Section 4.6.5.1, the results of genotoxicity/mutagenicity studies have been largely negative, irrespective of the presence or absence of metabolic activation (an S9 microsomal fraction). Studies that investigate the MOA for methanol, particularly with respect to its developmental effects, have been discussed extensively in Sections 4.6. and 4.8. Studies such as those by Harris et al. (2004, 2003) suggest that formaldehyde is the proximate teratogen and provide evidence in support of that hypothesis. It is reasonable to hypothesize that the highly reactive molecule, formaldehyde, has a role in the carcinogenicity of methanol, given the ability of formaldehyde to bind to proteins and DNA, induce DNA-protein cross-links, and possibly participate in reactions leading to free radical formation and the formation of lipid peroxidation products. As discussed in Section 4.6.3, evidence of oxidative stress following methanol exposure has been reported in several organ systems. Studies of Wistar rats suggest that methanol exposure can cause the production of free radical formation, lipid peroxidation, and protein modifications in the liver (Skrzydlewska et al., 2005) and brain (Rajamani et al., 2006), and adversely impact the oxidant/antioxidant balance in the brain (Dudka, 2006) and lymphoid organs (Parthasarathy et al., 2006b).

As discussed in Section 4.6.5.2, ERF studies of a number of compounds that have formaldehyde as a metabolic product have been reported to cause lymphomas in Sprague-Dawley rats. As described in Section 4.6.5.2.4, the ERF has conducted a formaldehyde drinking water study (Soffritti et al., 2002b, 1989) that is comparable in its design to the methanol drinking water study of Soffritti et al. (2002a). The mg/kg-day doses of metabolized methanol in Sprague-Dawley rats from the ERF methanol study estimated from the PBPK model described in Section 3.4 and mg/kg-day doses of formaldehyde reported in the ERF formaldehyde study were plotted together versus the hemolymphoreticular neoplasm incidences in their respective studies (Figure 4-1). Separate linear models were fit to the male and female rat data from these studies. The model fits shown in Figure 4-1 demonstrate that when metabolized methanol is used as the dose metric for the methanol study data, the dose-response data from these two studies can be adequately fit by two separate linear dose-response functions for the combined male ($R^2 = 0.6722$) and combined female ($R^2 = 0.779$) responses. Even if it is true that formaldehyde is the common moiety responsible for these tumors, one would not expect this approach to result in perfect dose-response alignment because the metabolized methanol estimate is not an accurate representation of formaldehyde distribution, and formaldehyde from methanol administration would not be expected to distribute the same as orally administered formaldehyde. However, the similarities in the dose-response data for male and female rats from these studies are consistent with the hypothesis that formaldehyde is key to methanol's carcinogenic MOA.

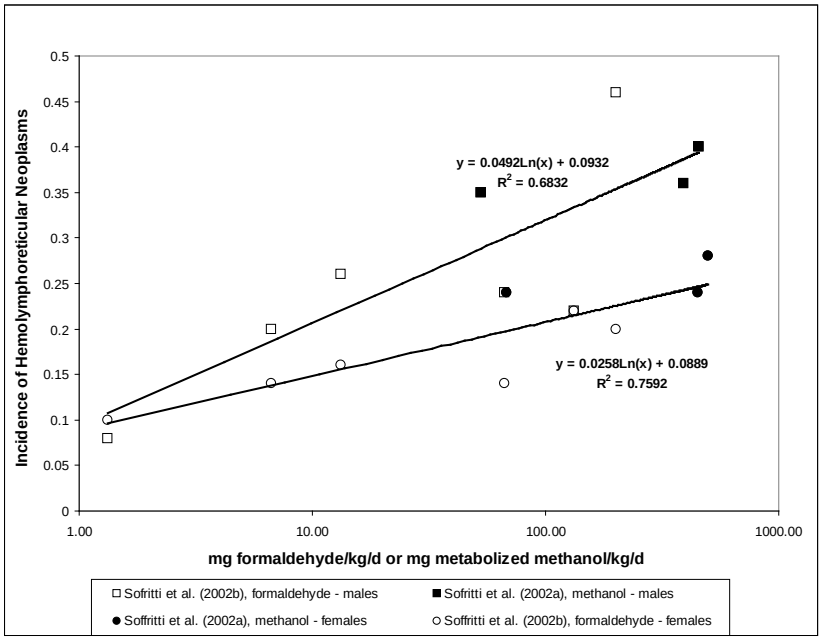

Figure 4-1. Hemolymphoreticular neoplasms in male and female Sprague-Dawley rats in formaldehyde and methanol drinking water studies versus mg formaldehyde/kg/day or mg metabolized methanol/kg/day (predicted by EPA PBPK model).

Source: Soffritti et al. (2002b).

As discussed above, methanol is metabolized to formaldehyde, which is deemed to be carcinogenic to humans (IARC, 2004) by both the oral and inhalation routes, and there are readily apparent similarities between the dose-response data from oral studies of rats exposed to formaldehyde and methanol. In addition, the dose-response model fit for the lymphoma response observed in the Soffritti et al. (2002a) study is improved when predicted total metabolites is used as the dose-metric (Section 5.4.1.2). However, the database of information available concerning methanol's carcinogenic MOA is limited, and the extent to which the parent or a metabolite such as formaldehyde is responsible for the carcinogenic effects observed in the studies conducted by Soffritti et al. (2002a) or NEDO (1987, 1985/2008b) is not clear.

4.10. SUSCEPTIBLE POPULATIONS AND LIFE STAGES

4.10.1. Possible Childhood Susceptibility

Studies in animals have identified the fetus as being more sensitive than adults to the toxic effects of methanol; the greatest susceptibility occurs during gastrulation and early organogenesis (CERHR, 2004). Table 4-21 summarizes some of the data regarding the relative ontogeny of CAT, ADH1, and ADH3 in humans and mice. Human fetuses have limited ability to metabolize methanol as ADH1 activity in 2-month-old and 4–5 month-old fetuses is 3–4% and

10% of adult activity, respectively (Pikkarainen and Raiha, 1967). ADH1 activity in 9–22 week old fetal livers was found to be 30% of adult activity (Smith et al., 1971). Likewise, ADH1 activity is ~20–50% of adult activity during infancy (Smith et al., 1971; Pikkarainen and Raiha, 1967). Activity continues to increase until reaching adult levels at 5 years of age (Pikkarainen and Raiha, 1967). However, no difference between blood methanol levels in 1-year-old infants and adults was observed following ingesting the same doses of aspartame, which releases 10% methanol by weight during metabolism (Stegink et al., 1983). Given that the exposure was aspartame as opposed to methanol, it is difficult to draw any conclusions from this study vis-à-vis ontogeny data and potential influences of age differences in aspartame disposition. With regard to inhalation exposure, increased breathing rates relative to adults may result in higher blood methanol levels in children compared to adults (CERHR, 2004). It is also possible that metabolic variations resulting in increased methanol blood levels in pregnant women could increase the fetus' risk from exposure to methanol. In all, unresolved issues regarding the identification of the toxic moiety increase the uncertainty with regards to the extent and pathologic basis for early life susceptibility to methanol exposure.

The prevalence of folic acid deficiency has decreased since the United States and Canada introduced a mandatory folic acid food fortification program in November 1998. However, folate deficiency is still a concern among pregnant and lactating women, and factors such as smoking, a poor quality diet, alcohol intake, and folic antagonist medications can enhance deficiency (CERHR, 2004). Folate deficiency could affect a pregnant woman's ability to clear formate, which has also been demonstrated to produce developmental toxicity in rodent in in vitro studies at high-doses (Dorman et al., 1995). It is not known if folate-deficient humans have higher levels of blood formate than individuals with adequate folate levels. A limited study in folate-deficient monkeys demonstrated no formate accumulation following an endotracheal exposure of anesthetized monkeys to 900 ppm methanol for 2 hours (Dorman et al., 1994). The situation is obscured by the fact that folic acid deficiency during pregnancy by itself is thought to contribute to the development of severe congenital malformations (Pitkin, 2007).

4.10.2. Possible Gender Differences

There is limited information on potential differences in susceptibility to the toxic effects of methanol according to gender. However, one study reported a higher background blood methanol level in human females versus males (Batterman and Franzblau, 1997). In rodents, fetuses exposed in utero were found to be the most sensitive subpopulation. One study suggested a possible increased sensitivity of male versus female rat fetuses and pups. When rats were exposed to methanol pre- and postnatally, 6- and 8-week-old male progeny had significantly lower brain weights at 1,000 ppm, compared to those in females that demonstrated the same

effect only at 2,000 ppm (NEDO, 1987). In general, there is little evidence for substantial disparity in the level or degree of toxic response to methanol in male versus female experimental animals or humans. However, it is possible that the compound-related deficits in fetal brain weight that were evident in the pups of F_1 generation Sprague-Dawley rats exposed to methanol in the NEDO (1987) study may reflect a threshold neurotoxicological response to methanol. It is currently unknown whether higher levels of exposure would result in brain sequelae comparable to those observed in acutely exposed humans.

4.10.3. Genetic Susceptibility

Polymorphisms in enzymes involved in methanol metabolism may affect the sensitivity of some individuals to methanol. For example, as discussed in Chapter 3, data summarized in reviews by Agarwal (2001), Burnell et al. (1989), Bosron and Li (1986), and Pietruszko (1980) discuss genetic polymorphisms for ADH. Class I ADH, the primary ADH in human liver, is a dimer composed of randomly associated polypeptide units encoded by three genetic loci (ADH1A, ADH1B, and ADH1C). Polymorphisms are observed at the ADH1B (ADH1B*2, ADH1B*3) and ADH1C (ADH1C*2) loci. The ADH1B*2 phenotype is estimated to occur in ~15% of Caucasians of European descent, 85% of Asians, and less that 5% of African Americans. Fifteen percent of African Americans have the ADH1B*3 phenotype, while it is found in less than 5% of Caucasian Europeans and Asians. The only reported polymorphisms in ADH3 occur in the promoter region, one of which reduces the transcriptional activity in vitro nearly twofold (Hedberg et al., 2001). While polymorphisms in ADH3 are described in more than one report (Cichoz-Lach et al., 2007; Hedberg et al., 2001), the functional consequence(s) for these polymorphisms remains unclear.

5. DOSE-RESPONSE ASSESSMENT AND CHARACTERIZATION

5.1. INHALATION RfC FOR EFFECTS OTHER THAN CANCER[69]

In general, the RfC is an estimate of a daily exposure of the human population (including susceptible subgroups) that is likely to be without an appreciable risk of adverse health effects over a lifetime. It is derived from a POD, generally the statistical lower confidence limit on the BMCL or BMDL, with uncertainty/variability factors applied to reflect limitations of the data used. The inhalation RfC considers toxic effects for both the respiratory system (portal-of-entry) effects and systems peripheral to the respiratory system (extra-respiratory or systemic effects). It is generally expressed in mg/m^3. EPA performed an IRIS assessment of methanol in 1991 and determined that the database was inadequate for derivation of an RfC. While some limitations still exist in the database (see Sections 5.1.3.2 and 5.3), the experimental toxicity database has expanded and newer methods and models have been developed to analyze the results. In this update, the PBPK model, described in Section 3.4, was developed by EPA and is used to estimate HECs and HEDs from inhalation study data for the derivation of both the RfC and RfD. In both cases, the use of a PBPK model replaces part of the UF adjustments traditionally used for species-to-species extrapolation.

Additionally, this assessment uses the BMD method in its derivation of the POD.[70] The suitability of these methods to derive a POD is dependent on the nature of the toxicity database for a specific chemical. Details of the BMD analyses are found in Appendix C. The use of the BMD approach for determining the POD improves the assessment by including consideration of shape of the dose-response curve, independence from experimental doses, and estimation of the uncertainty pertaining to the calculated dose response. However, the methanol database still has limitations and uncertainties associated with it, in particular, those uncertainties associated with human variability, animal-to-human differences, and limitations in the database influence derivation of the RfC.

5.1.1. Choice of Principal Study and Critical Effect(s)

5.1.1.1. *Key Inhalation Studies*

While a substantial body of information exists on the toxicological consequences to humans exposed to large amounts of methanol, no human studies exist that would allow for

[69] The RfC discussion precedes the RfD discussion in this assessment because the inhalation database ultimately serves as the basis for the RfD. The RfD development would be difficult to follow without prior discussion of inhalation database and PK models used for the route-to-route extrapolation.

[70] Use of BMD methods involves fitting mathematical models to dose-response data and using the results to select a POD that is associated with a predetermined benchmark response (BMR), such as a 10% increase in the incidence of a particular lesion or a 10% decrease in body weight gain (see Section 5.1.2.2).

quantification of subchronic, chronic, or in utero effects of methanol exposure. Table 4-35 summarizes available experimental animal inhalation studies of methanol. Several of these studies, including the monkey chronic (NEDO, 1987) and developmental (Burbacher et al., 2004a, 2004b, 1999a, 1999b) studies, the male rat reproductive studies (Lee et al., 1991; Cameron et al., 1985, 1984), and the 4-week rat studies (Poon et al., 1994), are lacking in key attributes (e.g., documented dose response, documented controls, and duration of exposure) necessary for their direct use in the quantification of a chronic RfC. These studies will be considered in this chapter for their contributions to the overall RfC uncertainty. Several inhalation reproductive or developmental studies were adequately documented and are of appropriate size and design for quantification and derivation of an RfC. These studies are considered for use in the derivation of an RfC and are summarized below.

5.1.1.2. *Selection of Critical Effect(s)*

Developmental effects have been assessed in a number of toxicological studies of monkeys, rats, and mice. The findings of Rogers and Mole (1997) indicate that methanol is toxic to mouse embryos in the early stages of organogenesis, on or around GD7. In the study of Rogers et al. (1993a), in which pregnant female CD-1 mice were exposed to methanol vapors (1,000, 2,000, and 5,000 ppm) on GD6–GD15, reproductive and fetal effects included an increase in the number of resorbed litters, a reduction in the number of live pups, and increased incidences of exencephaly, cleft palate, and the number of cervical ribs. They reported a NOAEL for cervical rib malformations at 1,000 ppm (1,310 mg/m^3) and a LOAEL of 2,000 ppm (2,620 mg/m^3, 49.6% per litter versus 28.0% per litter in the control group). Increased incidence of cervical ribs was also observed in the rat organogenesis study (NEDO, 1987) in the 5,000 ppm dose group (65.2% per litter versus 0% in the control group), indicating that the endpoint is significant across species.

The biological significance of the cervical rib endpoint within the regulatory arena has been the subject of much debate (Chernoff and Rogers, 2004). Previous studies have classified this endpoint as either a malformation (birth defect of major importance) or a variation (morphological alternation of minor significance). There is evidence that incidence of supernumerary ribs (including cervical ribs) is not just the addition of extraneous, single ribs but rather is related to a general alteration in the development and architecture of the axial skeleton as a whole. In CD-1 mice exposed during gestation to various types of stress, food and water deprivation, and the herbicide dinoseb, supernumerary ribs were consistently associated with increases in length of the 13th rib (Branch et al., 1996). This relationship was present in all fetal ages examined in the study. The authors concluded that these findings are consistent with supernumerary ribs being one manifestation of a basic alteration in the differentiation of the thoraco-lumbar border of the axial skeleton. The biological significance of this endpoint is further strengthened by the association of supernumerary ribs with adverse health effects in

humans. The most common effect produced by the presence of cervical ribs is thoracic outlet disease (Nguyen et al., 1997; Fernandez Noda et al., 1996; Henderson, 1914). Thoracic outlet disease is characterized by numbness and/or pain in the shoulder, arm, or hands. Vascular effects associated with this syndrome include cerebral and distal embolism (Bearn et al., 1993; Connell et al., 1980; Short, 1975), while neurological symptoms include extreme pain, migraine, and symptoms similar to Parkinson's (Evans, 1999; Saxton et al., 1999; Fernandez Noda et al., 1996). Schumacher et al. (1992) observed 242 rib anomalies in 218 children with tumors (21.8%) and 11 (5.5%) in children without malignancy, a statistically significant ($p < 0.001$) difference that indicates a strong association between the presence of cervical ribs and childhood cancers. Specific cancers associated with statistically significant increases in anomalous ribs included leukemia, brain, tumor, neuroblastoma, soft tissue sarcoma, and Wilm's tumor.

A number of rat studies have confirmed the toxicity of methanol to embryos during organogenesis (Weiss et al., 1996; NEDO, 1987; Nelson et al., 1985). NEDO (1987) reported reduced brain, pituitary, and thymus weights in F_1 and F_2 generation Sprague-Dawley rats at 1,000 ppm methanol. In a follow-up study of the F_1 generation brain weight effects, NEDO (1987) reported decreased brain, cerebellum, and cerebrum weights in F_1 males exposed at 1,000 ppm methanol from GD0 through the F_1 generation. The exposure levels used in these studies are difficult to interpret because dams were exposed prior to gestation, and dams and pups were exposed during gestation and lactation. However, it is clear that postnatal exposure increases the severity of brain weight reduction. In another experiment in which NEDO (1987) exposed rats only during organogenesis (GD7–GD17), the observed decreases in brain weights in offspring at 8 weeks of age were less severe than in the studies for which exposure was continued postnatally. This finding is not unexpected, given that the brain undergoes tremendous growth beginning early in gestation and continuing in the postnatal period. Rats are considered altricial (i.e., born at relatively underdeveloped stages), and many of their neurogenic events occur postnatally (Clancy et al., 2007). Brain effects from postnatal exposure are also relevant to humans given that, in humans, gross measures of brain growth increase for at least 2–3 years after birth, with the growth rate peaking approximately 4 months after birth (Rice and Barone, 2000).

A change in brain weight is considered to be a biologically significant effect (U.S. EPA, 1998). This is true regardless of changes in body weight because brain weight is generally protected during malnutrition or weight loss, unlike many other organs or tissues (U.S. EPA, 1998). Thus, change in absolute brain weight is an appropriate measure of effects on this critical organ system. Decreases in brain weight have been associated with simultaneous deficits in neurobehavioral and cognitive parameters in animals exposed during gestation to various solvents, including toluene and ethanol (Gibson, 2000; Coleman et al., 1999; Hass,

1995). NEDO (1987) reports that brain, cerebellum, and cerebrum weights decrease in a dose-dependant manner in male rats exposed to methanol throughout gestation and the F_1 generation.

Developmental neurobehavioral effects associated with methanol inhalation exposure have been investigated in monkeys. Burbacher et al. (2004a, 2004b, 1999a, 1999b) exposed *M. fascicularis* monkeys to 0, 262, 786, and 2,359 mg/m^3 methanol, 2.5 hours/day, 7 days/week during premating/mating and throughout gestation (approximately 168 days). In these studies, exposure of monkeys to up to 1,800 ppm (2,359 mg/m^3) methanol during premating, mating, and throughout gestation resulted in no changes in reproductive parameters other than a shorter period of gestation in all exposure groups that did not appear to be dose related. The shortened gestation period was largely the result of C-sections performed in the methanol exposure groups "in response to signs of possible difficulty in the maintenance of pregnancy," including vaginal bleeding. As discussed in Section 4.7.1.2, though statistically significant, the shortened gestation finding may be of limited biological significance given questions concerning its relation to the methanol exposure. Developmental parameters, such as fetal crown-rump length and head circumference, were unaffected, but there appeared to be neurotoxicological deficits in methanol-exposed pups. VDR was significantly reduced in the 786 mg/m^3 group for males and the 2,359 mg/m^3 group for both sexes. However, a dose-response trend for this endpoint was only exhibited for females. In fact, this is the only effect reported in the Burbacher et al. (2004a, 2004b, 1999a, 1999b) studies for which a significant dose-response trend is evident. As discussed in Section 4.4.2, confidence may have been increased by statistical analyses to adjust for multiple testing (CERHR, 2004). Yet it is worth noting that the dose-response trend for VDR in females remained significant with ($p = 0.009$) and without ($p = 0.0265$) an adjustment for the shortened gestational periods, and it is a measure of functional deficits in sensorimotor development that is consistent with early developmental CNS effects (brain weight changes discussed above) that have been observed in rats.

Another test, the Fagan test of infant intelligence, indicated small but not significant deficits of performance (time spent looking at novel faces versus familiar faces) in treated monkeys. Although not statistically significant and not quantifiable, the results of this test are also important when considered in conjunction with the brain weight changes noted in the NEDO (1987) rat study. As discussed in Section 4.7.1.2, the monkey data are not conclusive, and there is insufficient evidence to determine if the primate fetus is more or less sensitive than rodents to methanol teratogenesis. Taken together, however, the NEDO (1987) rat study and the Burbacher et al. (2004a, 2004b, 1999a, 1999b) monkey study suggest that prenatal exposure to methanol can result in adverse effects on developmental neurology pathology and function, which can be exacerbated by continued postnatal exposure.

A number of studies described in Section 4.3.2 and summarized in Section 4.7.1.2 have examined the potential toxicity of methanol to the male reproductive system (Lee et al., 1991;

Cameron et al., 1985, 1984). Some of the observed effects, including a transient decrease in testosterone levels, could be the result of chemically related strain on the rat system as it attempts to maintain hormone homeostasis. However, the data are insufficient to definitively characterize methanol as a toxicant to the male reproductive system.

The studies considered for use in the derivation of an RfC are summarized in Table 5-1. As discussed in Sections 5.1.3.1 and 5.3, there is uncertainty associated with the selection of an effect endpoint from the methanol database for use in the derivation of an RfC. Taking into account the limitations of the studies available for quantification purposes, decreased brain weight at 6 weeks in male Sprague-Dawley rats exposed throughout gestation and the postnatal period (NEDO, 1987) was chosen as the critical effect for the purposes of this dose-response assessment as it can be reliably quantified and represents both a sensitive organ system and a key period of development. RfC derivations utilizing alternative endpoints (e.g., cervical rib effects in mice and delayed sensorimotor development in monkeys) and alternative methods (e.g., use of different BMRLs) are summarized in Appendix C and in Section 5.1.3.1.

Table 5-1. Summary of studies considered most appropriate for use in derivation of an RfC

Reference	Species (strain)	Sex	Number/ dose group	Exposure Duration	Critical Effect	NOAEL (ppm)	LOAEL (ppm)
NEDO (1987) Two-generation study	Rat Sprague-Dawley	M,F	Not specified - F_1 and F_2 generation	F_1- Birth to end of mating (M) or weaning (F); F_2-birth to 8 wk	Reduced weight of brain, pituitary, and thymus at 8, 16, and 24 wk postnatal in F_1 and at 8 wk in F_2	100	1,000
NEDO (1987) Follow-up study of F_1 generation			10–14/ sex/ group- F_1 generation	GD0 through F_1 generation	Reduced brain weight at 3 wk and 6 wk (males only). Reduced brain and cerebrum weight at 8 wk (males only)	500	1,000
NEDO (1987) Teratology study	Rat Sprague-Dawley	M,F	10–12/sex/ group	GD7–GD17	Reduced brain, pituitary, thyroid, thymus, and testis weights at 8 wk postnatal.	1,000	5,000
Nelson et al. (1985)	Rat Sprague-Dawley	F	15 pregnant dams/group	GD1–GD19 or GD7–GD15	Reduced fetal body weight, increased incidence of visceral and skeletal abnormalities, including rudimentary and extra cervical ribs	5,000	10,000

Reference	Species (strain)	Sex	Number/ dose group	Exposure Duration	Critical Effect	NOAEL (ppm)	LOAEL (ppm)
Rogers et al. (1993a)	Mouse CD-1	F	30–114 pregnant dams/ group	GD6-15	Increased incidence of extra cervical ribs, cleft palate, exencephaly; reduced fetal weight and pup survival, delayed ossification	1,000	2,000
Burbacher et al. (20004a, 2004b, 1999a, 1999b)	*M. fascicularis*		12 pregnant monkeys/group	2.5 hr/day, 7 days/wk, during premating, mating and gestation	Shortened period of gestation; may be related to exposure (no dose response), neurotox. deficits including reduced performance in the VDR test	-	-[b]

[a]Animals were dosed 20–21 hr/day. NS = Not Specified
[b]Gestational exposure resulted in a shorter period of gestation in dams exposed to as low as 200 ppm (263 mg/m^3). However, because of uncertainties associated with these results, including clinical intervention and the lack of a dose-response, EPA was not able to identify a definitive NOAEL or LOAEL from this study.

5.1.2. Methods of Analysis for the POD—Application of PBPK and BMD Models

Potential PODs for the RfC derivation, described here and in Appendix C, have been calculated via the use of monkey, rat and mouse PBPK models, described in Section 3.4. First, the doses used in an experimental bioassay were converted to an internal dose metric that is most appropriate for the endpoint being assessed. The PBPK models are capable of calculating several measures of dose for methanol, including the following:

- C_{max} – The peak concentration of methanol in the blood during the exposure period;
- *AUC* – Area under the curve, which represents the cumulative product of concentration and time for methanol in the blood; and
- *Total metabolism* – The production of metabolites of methanol, namely formaldehyde and formate.

As described in Section 3.4, the focus of model development is on obtaining accurate predictions of increased body burdens over background. The PBPK models do not describe or account for background levels of methanol, formaldehyde or formate.

Although there remains uncertainty surrounding the identification of the proximate teratogen of importance (methanol, formaldehyde, or formate), the dose metric chosen for derivation of an RfC was based on blood methanol levels. This decision was primarily based on evidence that the toxic moiety is not likely to be the formate metabolite of methanol (CERHR, 2004) and evidence that levels of the formaldehyde metabolite following methanol maternal and/or neonate exposure would be much lower in the fetus and neonate than in adults. While recent in vitro evidence indicates that formaldehyde is more embryotoxic than methanol and formate, the high reactivity of formaldehyde would limit its unbound and unaltered transport as

free formaldehyde from maternal to fetal blood (Thrasher and Kilburn, 2001), and the capacity for the metabolism of methanol to formaldehyde is likely lower in the fetus and neonate versus adults (see discussion in Section 3.3). Thus, even if formaldehyde is identified as the proximate teratogen, methanol would likely play a prominent role, at least in terms of transport to the target tissue. Further discussions of methanol metabolism, dose metric selection, and MOA issues are covered in Sections 3.3, 4.6, 4.8 and 4.9.2.

A BMDL was then derived in terms of the internal dose metric utilized. Finally, the BMDL values were converted to HECs via the use of a PBPK model parameterized for humans. The next section describes the rationale for and application of the benchmark modeling methodology for the RfC derivation.

5.1.2.1. *Application of the BMD/BMDL Approach*

Several developments over the past few years impact the derivation of the RfC: 1) EPA has developed draft BMD assessment methods (U.S. EPA, 2000b, 1995) and supporting software (Appendix C) to improve upon the previous NOAEL/LOAEL approach; 2) MOA studies have been carried out that can give more insight into methanol toxicity; and 3) EPA has refined PBPK models for methanol on the basis of the work of Ward et al. (1997) (see Section 3.4. for description of the EPA model). The EPA PBPK model provides estimates of HECs from rodent exposures that are supported by pharmacokinetic information available for rodents and humans. The following sections describe how the BMD/BMDL approach, along with the EPA PBPK model, is used to obtain a POD for use in the derivation of an RfC for methanol in accordance with current draft BMD technical guidance (U.S. EPA, 2000b).

The BMD approach attempts to fit models to the dose-response data for a given endpoint. It has the advantage of taking more of the dose-response data into account when determining the POD, as well as estimating the dose for which an effect may have a specific probability of occurring. The BMD approach also accounts, in part, for the quality of the study (e.g., study size) by estimating a BMDL, the 95% lower bound confidence limit on the BMD. The BMDL is closer to the BMD (higher) for large studies and further away from the BMD (lower) for small studies. Because the BMDL approach will account, in part, for a study's power, dose spacing, and the steepness of the dose-response curve, it is generally preferred over the NOAEL approach.

When possible, all experimental data points are included in this assessment to ensure adequate fit of a BMD model and derivation of a BMDL. A summary of the POD values determined by BMD analysis for the critical endpoint (as well as other considered endpoints) (see Appendix C for modeling results), application of UFs, and conversion to HECs using the BMD and PBPK approach, is included in Section 5.1.3.1.

Use of the BMD approach has uncertainty associated with it. An element of the BMD approach is the use of several models to determine which best fits the data.[71] In the absence of an established MOA or a theoretical basis for why one model should be used over another, model selection is based on best fit to the experimental data selection. Model fit was determined by statistics (AIC and χ^2 residuals of individual dose groups) and visual inspection recommended by EPA (2000b)[72]

The PBPK model developed by EPA for methanol (described in Section 3.4) was applied for the estimation of methanol blood levels in the exposed dams (NEDO, 1987). When using PBPK models, it is very important to determine what estimate of internal dose (i.e., dose metric) can serve as the most appropriate dose metric for the health effects under consideration.

The results of NEDO (1987), shown in Table 4-8, indicate that there is not a cumulative effect of ongoing exposure on brain-weight decrements in rats exposed postnatally; i.e., the dose response in terms of percent of control is about the same at 3 weeks postnatal as at 8 weeks postnatal in rats exposed throughout gestation and the F_1 generation. However, there does appear to be a greater brain-weight effect in rats exposed postnatally versus rats exposed only during organogenesis (GD7–GD17). In male rats exposed during organogenesis only, there is no statistically significant decrease in brain weight at 8 weeks after birth at the 1,000 ppm exposure level. Conversely, in male rats exposed to the same level of methanol throughout gestation and the F_1 generation, there was an approximately 5% decrease in brain weights (statistically significant at the $p < 0.01$ level). The fact that male rats exposed to 5,000 ppm methanol only during organogenesis experienced a decrease in brain weight of 10% at 8 weeks postnatal indicates that postnatal exposure is not necessary for the observation of persistent postnatal effects. However, the fact that this decrease was less than the 13% decrease observed in male rats exposed to 2,000 ppm methanol throughout gestation and the 8 week postnatal period indicates that both exposure concentration and duration are important components of the ability of methanol to cause this effect. The extent to which the observation of the increased effect is due to a cumulative effect in rats exposed postnatally versus recovery in rats for which exposure was discontinued at birth is not clear.

The fact that brain weight is susceptible to both the level and duration of exposure suggests that a dose metric that incorporates a time component would be the most appropriate metric to use. For these reasons, and because it is more typically used in internal-dose-based

[71]USEPA's BMDS 2.1 was used for this assessment as it provides data management tools for running multiple models on the same dose-response data set. At this time, BMDS offers over 30 different models that are appropriate for the analysis of dichotomous, continuous, nested dichotomous and time-dependent toxicological data. Results from all models include a reiteration of the model formula and model run options chosen by the user, goodness-of-fit information, the BMD, and the estimate of the lower-bound confidence limit on the BMD (BMDL).

[72]Akaike's Information Criterion (AIC) (Akaike, 1973) is used for model selection and is defined as -2L + 2P where L is the log-likelihood at the maximum likelihood estimates for the parameters and P is the number of model degrees of freedom.

assessments and better reflects total exposure within a given day, daily AUC (measured for 22 hours exposure/day) was chosen as the most appropriate dose metric for modeling the effects of methanol exposure on brain weights in rats exposed throughout gestation and continuing into the F_1 generation.

Application of the EPA methanol PBPK model (described in Section 3.4) to the NEDO (1987) study, in which developing rats were exposed during gestation and the postnatal period, presents complications that need to be discussed. The neonatal rats in this study were exposed to methanol gestationally before parturition as well as lactationally and inhalationally after parturition. The PBPK model developed by EPA only estimates internal dose metrics for methanol exposure in NP adult mice and rats. Experimental data indicate that inhalation-route blood methanol kinetics in NP mice and pregnant mice on GD6–GD10 are similar (Dorman et al., 1995; Perkins et al., 1995a,1995b; Rogers et al., 1993a, 1993b). In addition, experimental data indicate that the maternal blood:fetal partition coefficient for mice is approximately 1 (see Section 3.4.1.2). Assuming that these findings apply for rats, the data indicate that PBPK estimates of PK and blood dose metrics for NP rats are better predictors of fetal exposure during gestation than would be obtained from default extrapolations from external exposure concentrations. However, as is discussed to a greater extent in Section 5.3, the additional routes of exposure presented to the pups in this study (lactation and inhalation) present uncertainties that suggest the average blood levels in pups in the NEDO (1987) report might be greater than those of the dam. The assumption made in this assessment is that, if such differences exist between human mothers and their offspring, they are not expected to be significantly greater than that which has been postulated for rats. Thus, the PBPK model-estimated adult blood methanol level is considered to be an appropriate dose metric for the purpose of this analysis and HEC derivation.

5.1.2.2. *BMD Approach Applied to Brain Weight Data in Rats*

The NEDO (1987) study reported decreases in brain weights in developing rats exposed during gestation only (GD7–GD17) or during gestation and the postnatal period, up to 8 weeks. Because of the biological significance of decreases in brain weight as an endpoint in the developing rat and because this endpoint was not evaluated in other peer-reviewed studies, BMD analysis was performed using these data. For the purposes of deriving an RfC for methanol from developmental endpoints using the BMD method and rat data, decreases in brain weight at 6 weeks of age in the more sensitive gender, males, exposed throughout gestation and continuing into the F_1 generation (both through lactation and inhalation routes) were utilized. Decreases in brain weight at 6 weeks (gestation and postnatal exposure), rather than those seen at 3 and 8 weeks, were chosen as the basis for the RfC derivation because they resulted in lower estimated BMDs and BMDLs. Decreased brain weights in male rats at 8 weeks age after gestation-only

exposure were not utilized because they were less severe at the same dose level (1,000 ppm) compared to gestation and postnatal exposure.

The first step in the current BMD analysis is to convert the inhalation doses, given as ppm values from the studies, to an internal dose metric using the EPA PBPK model (see Section 3.4). For decreased brain weight in male rats, AUC of methanol in blood (hr × mg/L) is chosen as the appropriate internal dose metric for the reasons discussed in Section 5.1.2.1. Predicted AUC values for methanol in the blood of rats are summarized in Table 5-2. These AUC values are then used as the dose metric for the BMD analysis of decreased brain weight in male rats.[73] The full details of this analysis are reported in Appendix C. More details concerning the PBPK modeling were presented in Section 3.4.

Table 5-2. The EPA PBPK model estimates of methanol blood levels (AUC) in rats following inhalation exposures

Exposure level (ppm)	Methanol in blood AUC (hr × mg/L)[a] in Rats
500	79.2
1,000	226.7
2,000	967.8

[a]AUC values were obtained by simulating 22 hr/day exposures for 5 days and calculated for the last 24 hours of that period.

The current draft BMD technical guidance (U.S. EPA, 2000b) suggests that, in the absence of knowledge as to what level of response to consider adverse, a change in the mean equal to one S.D. from the control mean can be used as a BMR for continuous endpoints. However, it has been suggested that other BMRs, such as 5% change relative to estimated control mean, are also appropriate when performing BMD analyses on fetal weight change as a developmental endpoint (Kavlock et al., 1995). Therefore, both a one S.D. change from the control mean and a 5% change relative to estimated control mean were considered (see Appendix C for RfC derivations using alternative BMRs). For this endpoint, a one S.D. change from the control mean returned the lowest BMDL estimates and was considered the most suitable BMR for use in the RfC derivation. All models were fit using restrictions and option settings suggested in the draft EPA BMD technical guidance document (U.S. EPA, 2000b).

A summary of the results most relevant to the development of a POD using the BMD approach (BMD, BMDL, and model fit statistics) for decreased brain weight at 6 weeks in male rats exposed to methanol throughout gestation and continuing into the F_1 generation is provided in Table 5-3. BMDL values in Table 5-3 represent the 95% lower-bound confidence limit on the AUC estimated to result in a mean that is one S.D. from the control mean. There is a 2.5-fold

[73]All BMD assessments in this review were performed using BMDS version 2.1. A copy of the BMDS can be obtained at: <http://www.epa.gov/ncea/bmds.htm>.

range of BMDL estimates from adequately fitting models, indicating considerable model dependence. In addition, the fit of the Hill and more complex Exponential models is better than the other models in the dose region of interest as indicated by a lower scaled residual at the dose group closest to the BMD (0.09 versus -0.67 or -0.77) and visual inspection. In accordance with draft EPA BMD Technical Guidance (EPA, 2000b), the BMDL from the Hill model (bolded), is selected as the most approriate basis for an RfC derivation because it results in the lowest BMDL from among a broad range of BMDLs and provides a superior fit in the low dose region nearest the BMD. The Hill model dose-response curve for decreased brain weight in male rats is presented in Figure 5-1, with response plotted against the chosen internal dose metric of AUC of methanol in rats. The $BMDL_{1SD}$ was determined to be 90.9 hr × mg/L using the 95% lower confidence limit of the dose-response curve expressed in terms of the AUC for methanol in blood.

Table 5-3. Comparison of benchmark dose modeling results for decreased brain weight in male rats at 6 weeks of age using modeled AUC of methanol as a dose metric

Model	BMD_{1SD} (AUC, hr × mg/L) [a]	$BMDL_{1SD}$ (AUC, hr × mg/L)[a]	*p*-value	AIC[c]	Scaled residual[d]
Linear	278.30	225.30	0.5376	-203.84	-0.77
2nd degree polynomial	278.30	225.30	0.5376	-203.84	-0.77
3rd degree polynomial	278.30	225.30	0.5376	-203.84	-0.77
Power	278.30	225.30	0.5376	-203.84	-0.77
Hill[b]	170.57	**90.93**	0.8366	-203.04	0.09
Exponential 2	260.94	209.10	0.612	-204.10	-0.67
Exponential 3	260.94	209.10	0.612	-204.10	-0.67
Exponential 4	172.08	96.93	0.8205	-203.10	0.09
Exponential 5	172.08	96.93	0.8205	-203.10	0.09

[a]The BMDL is the 95% lower confidence limit on the AUC estimated to decrease brain weight by 1 control mean S.D. using BMDS model options and restrictions suggested by EPA BMD technical guidance (U.S. EPA, 2000b).
[b]In accordance with draft EPA BMD Technical Guidance (EPA, 2000), the BMDL from the Hill model (bolded) is chosen for us in an RfC derivation because it is the lowest of a broad range of BMDL estimates from adequately fitting models and because the Hill model provides good fit in the dose region of interest as indicated by a relatively low scaled residual at the dose group closest to the BMD (0.09 versus -0.67 or -0.77).
[c]AIC = Akaike Information Criterion = -2L + 2P, where L is the log-likelihood at the maximum likelihood estimates for the parameters, and P is the number of modeled degrees of freedom (usually the number of parameters estimated).
[d]χ^2d residual (measure of how model-predicted responses deviate from the actual data) for the dose group closest to the BMD scaled by an estimate of its S.D. Provides a comparative measure of model fit near the BMD. Residuals that exceed 2.0 in absolute value should cause one to question model fit in this region.

Source: NEDO (1987).

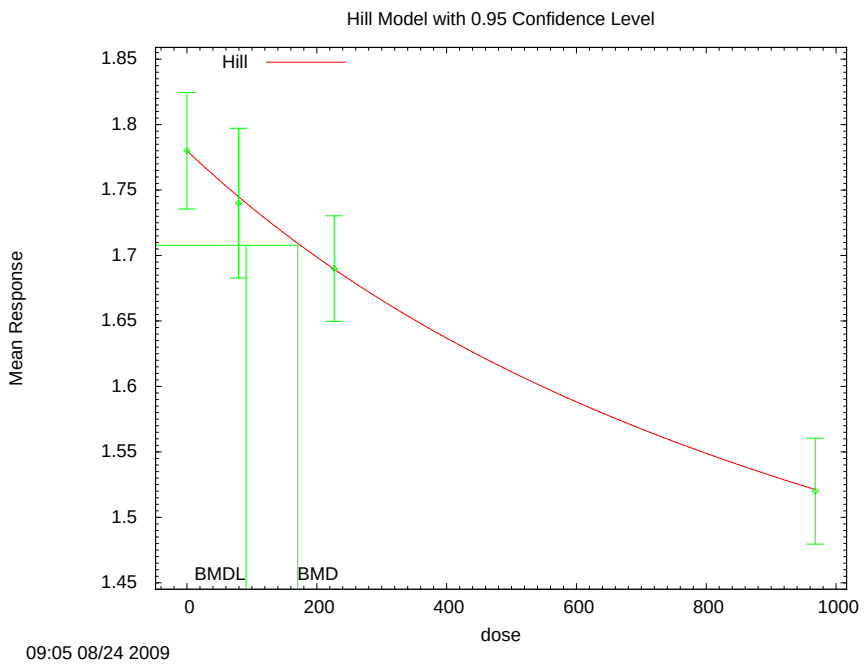

Figure 5-1. Hill model BMD plot of decreased brain weight in male rats at 6 weeks age using modeled AUC of methanol in blood as the dose metric, 1 control mean S.D.

Once the $BMDL_{1SD}$ was obtained in units of hr × mg/L, it was used to derive a chronic RfC. The first step is to calculate the HEC using the PBPK model described in Appendix B. An algebraic equation is provided (Equation 1 of Appendix B) that describes the relationship between predicted methanol AUC and the human equivalent inhalation exposure concentration (HEC) in ppm.

$$\text{BMDLHEC (ppm)} = 0.0224*\text{BMDL1SD}+(1334*\text{BMDL1SD})/(794+ \text{BMDL1SD})$$

$$BMDL_{HEC}\ (\text{ppm}) = 0.0224*90.9+(1334*90.9)/(794+ 90.9) = 139\ \text{ppm}$$

Next, because RfCs are typically expressed in units of mg/m^3, the HEC value in ppm was converted using the conversion factor specific to methanol of 1 ppm = 1.31 mg/m^3:

$$\text{HEC}\ (mg/m^3) = 1.31 \times 139\ \text{ppm} = 182\ mg/m^3$$

5.1.3. RfC Derivation – Including Application of Uncertainty Factors

5.1.3.1. *Comparison Between Endpoints and BMDL Modeling Approaches*

A summary of the PODs for the various developmental endpoints and BMD modeling approaches considered for the derivation of an RfC, along with the UFs applied[74] and the conversion to an HEC, are presented in Table 5-4 and graphically compared in Figure 5-2 (see Appendix C for details). Information is presented that compares the use of different endpoints (i.e., cervical rib, decreased brain weight, and increased latency of VDR) and different methods (i.e., different BMR levels) for estimating the POD. These comparisons are presented to inform the analysis of uncertainty surrounding these choices. Each approach considered for the determination of the POD has strengths and limitations, but when considered together for comparative purposes they allow for a more informed determination for the POD for the methanol RfC.

A 10% extra risk BMR is adequate for most traditional bioassays using 50 animals per dose group. A smaller BMR of 5% extra risk can sometimes be justified for developmental studies (e.g., Rogers et al., 1993a), because they generally involve a larger number of subjects. Reference values estimated for cervical rib incidence in mice using C_{max} as the dose metric were 13.6 and 10.4 mg/m^3 using $BMDL_{10}$ and $BMDL_{05}$ PODs, respectively (see Appendix D for discussion of choice of C_{max} as the appropriate dose metric for incidence of cervical rib in mice). The reference value estimated for alterations in sensorimotor development and performance as measured by the VDR test in female monkeys using AUC as the dose metric was 1.7 mg/m^3 using the $BMDL_{SD}$ as the POD. As discussed in Section 4.4.2, confidence in this endpoint is reduced by a marginal dose-response trend in one sex (females) and a limited sample size. Although the VDR test demonstrates that prenatal and continuing postnatal exposure to methanol can result in neurotoxicity, the use of such statistically borderline results is not warranted in the derivation of the RfC, given the availability of better dose-response data in other species. Decreases in brain weight at 6 weeks of age in male rats exposed during gestation and throughout the F_1 generation using AUC as the dose metric yield the reference values of 1.8 and 2.4 mg/m^3 for BMRs of one S.D. from the control mean and 5% change relative to control mean, respectively. Because decreases in brain weight in male rats at 6 weeks postbirth resulted in a clear dose response and returned RfC estimates lower than or approximate to the other endpoints considered, it was chosen as the critical endpoint. One S.D. from the control mean was chosen as the appropriate level of response (BMR) for the calculation of the RfC because it is the standard recommended by EPA's draft technical guidance (U.S. EPA, 2000b) and yields a lower BMDL than 5% relative deviance for this data set. Thus, the RfC is:

[74] The rationale for the selection of these UFs is discussed later in Section 5.1.3.

$$RfC = POD_{HEC} \div UF = 182\ mg/m^3 \div 100 = 2\ mg/m^3 \text{ (rounded to one significant figure)}$$

Table 5-4. Summary of PODs for critical endpoints, application of UFs and conversion to HEC values using BMD and PBPK modeling

	Rogers et al. (1993a)		Burbacher et al. (1999a,1999b)	NEDO (1987)	
	$BMDL_{10}$ mouse cervical rib C_{max}	**$BMDL_{05}$ mouse cervical rib C_{max}**	**$BMDL_{1SD}$ female monkey VDR[a] AUC**	**$BMDL_{05}$ rat brain wt.[b] AUC**	**$BMDL_{1SD}$ rat brain wt.[b] AUC**
BMDL	94.3 mg/L	44.7 mg/L	81.7 hr×mg/L	123.9 hr×mg/L	90.9 hr×mg/L
HEC (mg/m^3)[c]	1360	1036	165	240	182
UF_H[d]	10	10	10	10	10
UF_A[e]	3	3	3	3	3
UF_D	3	3	3	3	3
UF_S	1	1	1	1	1
UF_L	1	1	1	1	1
UF_{TOTAL}	100	100	100	100	100
RfC (mg/m^3)	13.6	10.4	1.7	2.4	1.8

[a]VDR = test of sensorimotor development as measured by age from birth at achievement of test criterion for grasping a brightly colored object.
[b]Brain weight at 6 weeks postbirth, multiple routes of exposure (whole gestation, lactation, inhalation)
[c]The PBPK model used for this HEC estimate is described in Appendix B. An algebraic equation (Equation 1 of Appendix B) describes the relationship between predicted methanol AUC and the human equivalent inhalation exposure concentration (HEC) in ppm. This equation can also be used to estimate model predictions for HECs from C_{max} values because C_{max} values and AUC values were estimated at steady-state for constant 24 hours exposures (i.e., AUC = 24 x C_{max}). The ppm HEC estimate is then converted to mg/m^3 by multiplying by 1.31.
[d]The rationale for the selection of these UFs is discussed in Section 5.1.3 below.
[e]These uncertainty factor (UF) acronyms are defined in Sections 5.1.2.1.1 to 5.1.2.1.4.

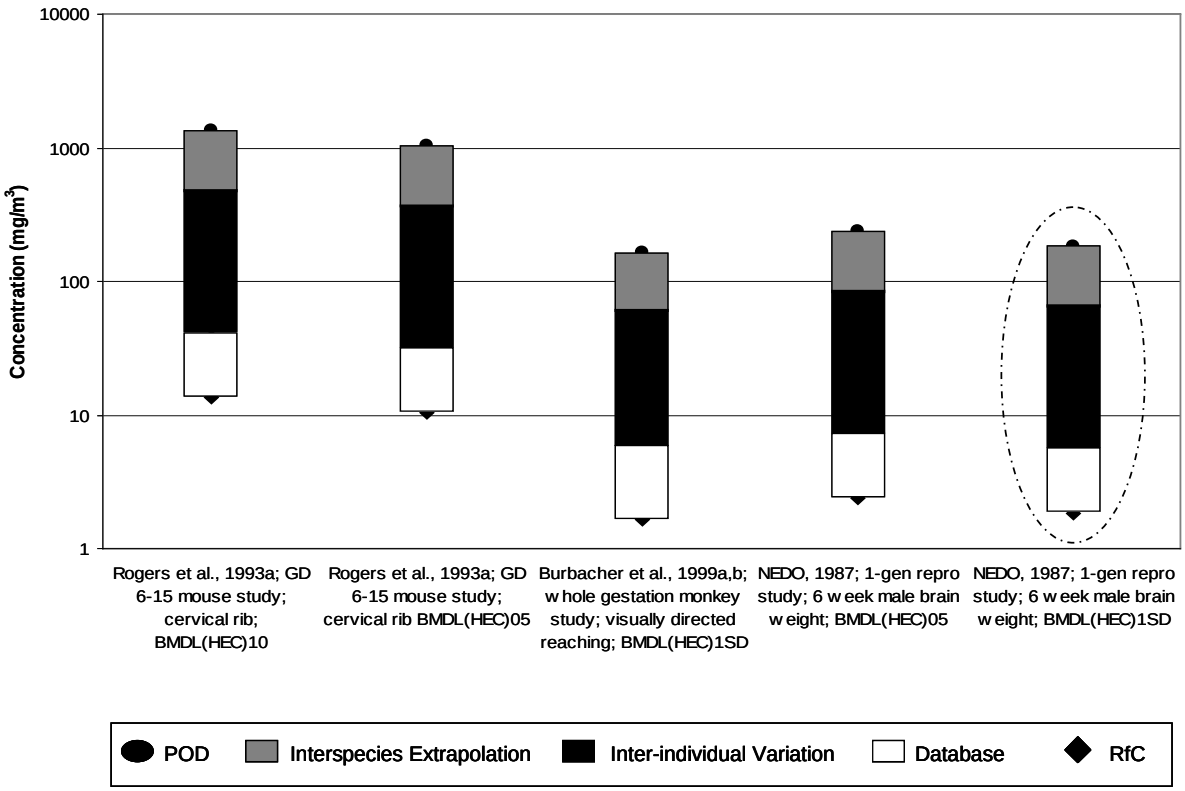

Figure 5-2. PODs (in mg/m^3) for selected endpoints with corresponding applied UFs (chosen RfC value is circled)

5.1.3.2. *Application of UFs*

UFs are applied to the POD, identified from the rodent data, to account for recognized uncertainties in extrapolation from experimental conditions to the assumed human scenario (i.e., chronic exposure over a lifetime). A composite UF of 100-fold (10-fold for interindividual variation, 3-fold for residual toxicodynamic differences associated with animal-to-human extrapolation, and 3-fold for database uncertainty) was applied to the POD for the derivation of the RfC, as described below.

5.1.3.2.1. *Interindividual Variation UF_H.* A factor of 10 was applied to account for variation in sensitivity within the human population (UF_H). The UF of 10 is commonly considered to be appropriate in the absence of convincing data to the contrary. The data from which to determine the potential extent of variation in how humans respond to chronic exposure to methanol are limited, given the complex nature of the developmental endpoint employed and uncertainties surrounding the importance of metabolism to the observed teratogenic effects. Susceptibility to methanol is likely to involve intrinsic and extrinsic factors. Some factors may include alteration of the body burden of methanol or its metabolites, sensitization of an individual to methanol

effects, or augmentation of underlying conditions or changes in processes that share common features with methanol effects. Additionally, inherent differences in an individual's genetic make-up, diet, gender, age, or disease state may affect the pharmacokinetics and pharmacodynamics of methanol, influencing susceptibility intrinsically. Co-exposure to a pollutant that alters metabolism or clearance or that adds to background levels of metabolites may also affect the pharmacokinetics and pharmacodynamics of methanol, influencing susceptibility extrinsically (see Section 4.9). The determination of the UF for human variation is supported by several types of information, including information concerning background levels of methanol in humans, variation in pharmacokinetics revealed through human studies and from PBPK modeling, variation of methanol metabolism in human tissues, and information on physiologic factors (including gender and age), or acquired factors (including diet and environment) that may affect methanol exposure and toxicity.

In using the AUC of methanol in blood as the dose metric for derivation of health benchmarks for methanol, the assumption is made that concentrations of methanol in blood over time are related to its toxicity, either through the actions of the parent or it subsequent metabolism. However, the formation of methanol's metabolites has been shown in humans to be carried out by enzymes that are inducible, highly variable in activity, polymorphic, and to also be involved in the metabolism of other drugs and environmental pollutants. Hence, differences in the metabolism of methanol that are specific for target tissue, gender, age, route of administration, and prior exposure to other environmental chemicals may give a different pattern of methanol toxicity if metabolism is required for that toxicity. Eighty-five percent of Asians carry an atypical phenotype of ADH that may affect their ability to metabolize methanol (Agarwal, 2001; Bosron and Li, 1986; Pietruszko, 1980). Also, polymorphisms in ADH3 occurring in the promoter region reduce the transcriptional activity in vitro nearly twofold, although no studies have reported differences in ADH3 enzyme activity in humans (Hedberg et al., 2001).

Although data on the specific potential for increased susceptibility to methanol are lacking, there is information on PK and pharmacodynamic factors suggesting that children may have differential susceptibility to methanol toxicity (see Section 4.10.1). Thus, there is uncertainty in children's responses to methanol that should be taken into consideration for derivation of the UF for human variation that is not available from either measured human data or PBPK modeling analyses. The enzyme primarily responsible for metabolism of methanol in humans, ADH, has been reported to be reduced in activity in newborns. Differences in pharmacokinetics include potentially greater pollutant intake due to greater ventilation rates, activity, and greater intake of liquids in children. In terms of differences in susceptibility to methanol due to pharmacodynamic considerations, the substantial anatomical, physiologic, and biochemical changes that occur during infancy, childhood, and puberty suggest that there are

developmental periods in which the endocrine, reproductive, immune, audiovisual, nervous, and other organ systems may be especially sensitive.

There are some limited data from short-term exposure studies in humans and animal experiments that suggest differential susceptibility to methanol on the basis of gender. Gender can provide not only different potential targets for methanol toxicity but also differences in methanol pharmacokinetics and pharmacodynamics. NEDO (1987) reported that in rats exposed to methanol pre- and postnatally, 6- and 8-week-old male progeny had significantly lower brain weights at 1,000 ppm, whereas females only showed decreases at 2,000 ppm. In general, gender-related differences in distribution and clearance of methanol may result from the greater muscle mass, larger body size, decreased body fat, and increased volumes of distribution in males compared to females.

5.1.3.2.2. *Animal-to-Human Extrapolation* UF_A. A factor of 3 was applied to account for uncertainties in extrapolating from rodents to humans. Application of a full UF of 10 would depend on two areas of uncertainty: toxicokinetic and toxicodynamic uncertainty. In this assessment, the toxicokinetic component is largely addressed by the determination of a HEC through the use of PBPK modeling. Given the chosen dose metric (AUC for methanol blood), uncertainties in the PBPK modeling of methanol are not expected to be greater for one species than another. The analysis of parameter uncertainty for the PBPK modeling performed for human, mouse, and rat data gave similar results as to how well the model fit the available data. Thus, the human and rodent PBPK model performed similarly using this dose metric for comparisons between species. As discussed in Section 5.3 below, uncertainty does exist regarding the relation of maternal blood levels estimated by the model to fetal and neonatal blood levels that would be obtained under the (gestational, postnatal and lactational) exposure scenario employed in the critical study. However, at environmentally relevant exposure levels, it is assumed that the ratio of the difference in blood concentrations between a human infant and mother would be similar to and not significantly greater than the difference between a rat dam and its fetus. Key parameters and factors which determine the ratio of fetal or neonatal human versus mother methanol blood levels either do not change significantly with age (partition coefficients, relative blood flows) or scale in a way that is common across species (allometrically). For this reason and because EPA has confidence in the ability of the PBPK model to accurately predict adult blood levels of methanol, the PK uncertainty is reduced and a value of 1 was applied. Rodent-to-human pharmacodynamic uncertainty is covered by a factor of 3, as is the practice for deriving RfCs (U.S. EPA, 1994b). Therefore, a factor of 3 is used for interspecies uncertainty.

5.1.3.2.3. *Database* UF_D. A database UF of 3 was applied to account for deficiencies in the toxicity database. The database for methanol toxicity is quite extensive: there are chronic and

developmental toxicity studies in rats, mice, and monkeys, a two-generation reproductive toxicity study in rats, and neurotoxicity and immunotoxicity studies. However, there is uncertainty regarding which test species is most relevant to humans. In addition, limitations of the developmental toxicity database employed in this assessment include gaps in testing and imperfect study design, reporting, and analyses. Developmental studies were conducted at levels inducing maternal toxicity, a full developmental neurotoxicity test (DNT) in rodents has not been performed and is warranted given the critical effect of decreased brain weight, there are no chronic oral studies in mice, and chronic and developmental studies in monkeys were generally inadequate for quantification purposes, for reasons discussed in Section 5.1.1.1. Problems of interpretation of developmental and reproductive studies also arise given the dose spacing between lowest and next highest level. For these reasons, an UF of 3 was applied to account for deficiencies in the database.

5.1.3.2.4. *Extrapolation from Subchronic to Chronic and LOAEL-to NOAEL Extrapolation UFs.* A UF was not necessary to account for extrapolation from less than chronic results because developmental toxicity (cervical rib and decreased brain weight) was used as the critical effect. The developmental period is recognized as a susceptible lifestage where exposure during certain time windows is more relevant to the induction of developmental effects than lifetime exposure (U.S. EPA, 1991).

A UF for LOAEL-to-NOAEL extrapolation was not applied because BMD analysis was used to determine the POD, and this factor was addressed as one of the considerations in selecting the BMR. In this case, a BMR of one S.D. from the control mean in the critical effect was selected based on the assumption that it represents a minimum biologically significant change.

5.1.4. Previous RfC Assessment

The health effects data for methanol were assessed for the IRIS database in 1991 and were determined to be inadequate for derivation of an RfC.

5.2. ORAL RfD

In general, the RfD is an estimate of a daily exposure to the human population (including susceptible subgroups) that is likely to be without an appreciable risk of adverse health effects over a lifetime. It is derived from a POD, generally the statistical lower confidence limit on the BMDL, with uncertainty/variability factors applied to reflect limitations of the data used. The RfD is expressed in terms of mg/kg-day of exposure to an agent and is derived by a similar methodology as is the RfC. Ideally, studies with the greatest duration of exposure and conducted via the oral route of exposure give the most confidence for derivation of an RfD. For methanol, the oral database is currently more limited than the inhalation database. With the development of

PBPK models for methanol, the inhalation database has been used to help bridge data gaps in the oral database to derive an RfD.

5.2.1. Choice of Principal Study and Critical Effect–with Rationale and Justification

No studies have been reported in which humans have been exposed subchronically or chronically to methanol by the oral route of exposure and thus, would be suitable for derivation of an oral RfD. Data exist regarding effects from oral exposure in experimental animals, but they are more limited than data from the inhalation route of exposure (see Sections 4.2, 4.3, and 4.4).

Only 2 oral studies of 90-days duration or longer in animals have been reported (Soffritti et al., 2002a; U.S. EPA, 1986c) for methanol. EPA (1986c) reported that there were no differences in body weight gain, food consumption, or gross or microscopic evaluations in Sprague-Dawley rats gavaged with 100, 500, or 2,500 mg/kg-day versus control animals. Liver weights in both male and female rats were increased, although not significantly, at the 2,500 mg/kg-day dose level, suggesting a treatment-related response despite the absence of histopathologic lesions in the liver. Brain weights of high-dose group males and females were significantly less than control animals at terminal (90 days) sacrifice. The data were not reported in adequate detail for dose-response modeling and BMD estimation. Based primarily on the qualitative findings presented in this study, the 500 mg/kg-day dose was deemed to be a NOAEL.[75]

The only lifetime oral study available was conducted by Soffiritti et al. (2002a) in Sprague-Dawley rats exposed to 0, 500, 5,000, 20,000 ppm (v/v) methanol, provided ad libitum in drinking water. Based on default, time-weighted average body weight estimates for Sprague-Dawley rats (U.S. EPA, 1988), average daily doses of 0, 46.6, 466, and 1,872 mg/kg-day for males and 0, 52.9, 529, 2,101 mg/kg-day for females were reported by the study authors. All rats were exposed for up to 104 weeks, and then maintained until natural death. The authors report no substantial changes in survival nor was there any pattern of compound-related clinical signs of toxicity. The authors did not report noncancer lesions, and there were no reported compound-related signs of gross pathology or histopathologic lesions indicative of noncancer toxicological effects in response to methanol.

Five oral studies investigated the reproductive and developmental effects of methanol in rodents (Aziz et al., 2002; Fu et al., 1996; Sakanashi et al., 1996; Rogers et al., 1993a; Infurna and Weiss, 1986), including three studies that investigated the influence of FAD diets on the effects of methanol exposures (Aziz et al., 2002; Fu et al., 1996; Sakanashi et al., 1996). Infurna and Weiss (1986) exposed pregnant Long-Evans rats to 2,500 mg/kg-day in drinking water on either GD15–GD17 or GD17–GD19. Litter size, pup birth weight, pup postnatal weight gain,

[75] EPA (1986c) did not report details required for a BMD analysis such as standard deviations for mean responses.

postnatal mortality, and day of eye opening were not different in treated animals versus controls. Mean latency for nipple attachment and homing behavior (ability to detect home nesting material) were different in both methanol treated groups. These differences were significantly different from controls. Rogers et al. (1993a) exposed pregnant CD-1 mice via gavage to 4 g/kg-day methanol, given in 2 equal daily doses. Incidence of cleft palate and exencephaly was increased following maternal exposure to methanol. Also, an increase in totally resorbed litters and a decrease in the number of live fetuses per litter were observed.

Aziz et al. (2002), Fu et al. (1996), and Sakanashi et al. (1996) investigated the role of folic acid in methanol-induced developmental neurotoxicity. Like Rogers et al. (1993a), the former 2 studies observed that an oral gavage dose of 4–5 g/kg-day during GD6–GD15 or GD6–GD10 resulted in an increase in cleft palate in mice fed sufficient folic acid diets, as well as an increase in resorptions and a decrease in live fetuses per litter. Fu et al. (1996) also observed an increase in exencephaly in the FAS group. Both studies found that an approximately 50% reduction in maternal liver folate concentration resulted in an increase in the percentage of litters affected by cleft palate (as much as threefold) and an increase in the percentage of litters affected by exencephaly (as much as 10-fold). Aziz et al. (2002) exposed rat dams throughout their lactation period to 0, 1, 2, or 4% v/v methanol via the drinking water, equivalent to approximately 480, 960 and 1,920 mg/kg-day.[76] Pups were exposed to methanol via lactation from PND1–PND21. Methanol treatment at 2% and 4% was associated with significant increases in activity (measured as distance traveled in a spontaneous locomotor activity test) in the FAS group (13 and 39%, respectively) and most notably, in the FAD group (33 and 66%, respectively) when compared to their respective controls. At PND45, the CAR in FAD rats exposed to 2% and 4% methanol was significantly decreased by 48% and 52%, respectively, relative to nonexposed controls. In the FAS group, the CAR was only significantly decreased in the 4% methanol-exposed animals and only by 22% as compared to their respective controls.

5.2.1.1. *Expansion of the Oral Database by Route-to-Route Extrapolation*

Given the oral database limitations, including the limited reporting of noncancer findings in the subchronic (U.S. EPA, 1986c) and chronic studies (Soffritti et al., 2002a) of rats and the high-dose levels used in the two rodent developmental studies, EPA has derived an RfD by using relevant inhalation data and route-to-route extrapolation with the aid of the EPA PBPK model (see Sections 3.4 and 5.1). Several other factors support use of route-to-route extrapolation for methanol. The limited data for oral administration indicate similar effects as reported via inhalation exposure (e.g., the brain and fetal skeletal system are targets of toxicity). Methanol has been shown to be rapidly and well-absorbed by both the oral and inhalation routes of

[76] Assuming that Wistar rat drinking water consumption is 60 mL/kg-day (Rogers et al., 2002), 1% methanol in drinking water would be equivalent to 1% x 0.8 g/mL x 60 mL/kg-day = 0.48 g/kg-day = 480 mg/kg-day.

exposure (CERHR, 2004; Kavet and Nauss, 1990). Once absorbed, methanol distributes rapidly to all organs and tissues according to water content, regardless of route of exposure.

As with the species-to-species extrapolation used in the development of the RfC, the dose metric used for species-to-species and route-to-route extrapolation of inhalation data to oral data is the AUC of methanol in blood. Simulations for human oral methanol exposure were conducted using the model parameters as previously described for human inhalation exposures, with human oral kinetic/absorption parameters from Sultatos et al. (2004) (i.e., KAS = 0.2, KSI = 3.17, and KAI = 3.28). Human oral exposures were assumed to occur during six drinking episodes during the day, at times 0, 3, 5, 8, 11, and 15 hours from the first ingestion of the day. For example, if first ingestion occurred at 7 am, these would be at 7 am, 10 am, 12 noon, 3 pm, 6 pm, and 10 pm. Each ingestion event was treated as occurring over 3 minutes, during which the corresponding fraction of the daily dose was infused into the stomach lumen compartment. The fraction of the total ingested methanol simulated at each of these times was 25%, 10%, 25%, 10%, 25%, and 5%, respectively. Six days of exposure were simulated to allow for any accumulation (visual inspection of plots showed this to be finished by the 2nd or 3rd day), and the results for the last 24 hours were used. Dividing the exposure into more and smaller episodes would decrease the estimated peak concentration but have little effect on AUC. This dose metric was used for dose-response modeling to derive the POD, expressed as a BMDL. The BMDL was then back-calculated using the EPA PBPK model to obtain an equivalent oral drinking water dose in terms of mg/kg-day.

5.2.2. RfD Derivation–Including Application of UFs

5.2.1.2. *Consideration of Inhalation Data*

Inhalation studies considered for derivation of the RfC are used to supplement the oral database using the route-to-route extrapolation, as previously described. BMD approaches were applied to the existing inhalation database, and the EPA PBPK model was used for species-to-species extrapolations. The rationale and approach for determining the RfC is described above (Section 5.1), and the data used to support the derivation of the RfC were extrapolated using the EPA PBPK model to provide an oral equivalent POD.

5.2.1.3. *Selection of Critical Effect(s) from Inhalation Data*

Methanol-induced effects on the brain in rats (weight decrease) and fetal axial skeletal system in mice (cervical ribs and cleft palate) were consistently observed at lower levels, than other targets, in the oral and inhalation databases. Analysis of inhalation developmental toxicity studies shows lower BMDLs for decreased male brain weight in rats exposed throughout gestation and the F_1 generation (NEDO, 1987) than BMDLs associated with the fetal axial skeletal system in mice. Therefore, as was noted in Section 5.1.3.1, the BMDL for decreases in

brain weight in male rats is chosen to serve as the basis for the route-to-route extrapolation and calculation of the RfD.

5.2.1.4. *Selection of the POD*

The BMDL chosen for the RfC is used to determine the POD for the RfD. This value is based on a developmental toxicity dataset that includes in utero and postnatal exposures and is below the range of estimates for other developmental datasets consisting of exposure only throughout organogenesis. The neonatal brain is the target organ chosen for derivation of the RfC. The BMDL for the RfC (AUC of 90.9 hr × mg/L methanol in blood) is converted using the EPA model to a human equivalent oral exposure of 38.5 mg/kg-day.[77]

5.2.2. RfD Derivation–Application of UFs

In an approach consistent with the RfC derivation, UFs are applied to the oral POD of 38.5 mg/kg-day to address interspecies extrapolation, intraspecies variability, and database uncertainties for the RfD. Because the same dataset, endpoint, and PBPK model used to derive the RfC were also used to calculate the oral POD, the total UF of 100 is applied to the BMDL of 38.5 mg/kg-day to yield an RfD of 1.12 mg/kg-day for methanol.

RfD = 38.5 mg/kg-day ÷ 100 = 0.4 mg/kg-day (rounded to one significant figure)

5.2.3. Previous RfD Assessment

The previous IRIS assessment for methanol included an RfD of 0.5 mg/kg-day that was derived from a EPA (1986c) subchronic oral study in which Sprague-Dawley rats (30/sex/dose) were gavaged daily with 0, 100, 500, or 2,500 mg/kg-day of methanol. There were no differences between dosed animals and controls in body weight gain, food consumption, gross or microscopic evaluations. Elevated levels of SGPT, serum alkaline phosphatase (SAP), and increased but not statistically significant liver weights in both male and female rats suggest possible treatment-related effects in rats dosed with 2,500 mg methanol/kg-day, despite the absence of supportive histopathologic lesions in the liver. Brain weights of both high-dose group males and females were significantly less than those of the control group. Based on these findings, 500 mg/kg-day of methanol was considered a NOAEL in this rat study. Application of a 1,000-fold UF (interspecies extrapolation, susceptible human subpopulations, and subchronic to chronic extrapolation) yielded an RfD of 0.5 mg/kg-day.

[77] The PBPK model used for this HEC estimate is described in Appendix B. An algebraic equation is provided (Equation 2) that describes the relationship between predicted methanol AUC and the HED in mg/kg-day.

5.3. UNCERTANTIES IN THE INHALATION RfC AND ORAL RfD

The following is a more extensive discussion of the uncertainties associated with the RfC and RfD for methanol beyond that which is addressed quantitatively in Sections 5.1.2, 5.1.3, and 5.2.2. A summary of these uncertainties is presented in Table 5-5.

Table 5-5. Summary of uncertainties in methanol noncancer risk assessment

Consideration	Potential Impact	Decision	Justification
Choice of endpoint	Use of other endpoint could ↑ RfC by up to ~5-fold (see Table 5-4 and Section 5.3.1)	RfC is based on the most sensitive and quantifiable endpoint, decreased brain weight in male rats exposed pre- and postnatally	Chosen endpoint is considered the most relevant due to its biological significance, and consistency across a developmental and a subchronic study in rats and with the observation of other developmental neurotoxicities reported in monkeys.
Choice of dose metric	Alternatives could ↑ or ↓ RfC/D (e.g., use of C_{max} increased RfC by ~20%)	AUC for methanol in arterial blood	AUC was selected as the most appropriate dose metric because it incorporates time (brain weight is sensitive to both the level and duration of exposure) and better reflects exposure within a given day.
Choice of model for BMDL derivation	Use of a linear model could ↑ RfC by ~2.5-fold (see Table 5-3)	Hill model used	Hill model gave lowest of a broad range of BMDL estimates from adequate models and provides good fit in low dose region.
Choice of animal-to-human extrapolation method	Alternatives could ↑ or ↓ RfC/D (e.g., use of standard dosimetry assumption would ↑ RfC by ~2-fold; see Section 5.3.4)	A PBPK model was used to extrapolate animal to human concentrations	Use of a PBPK model reduced uncertainty associated with the animal to human extrapolation. AUC blood levels of methanol is an appropriate dose metric and a peer-reviewed PBPK model that estimates this metric was verified by EPA using established (U.S. EPA, 2006a) methods and procedures
Statistical uncertainty at POD (sampling variability due to bioassay size)	POD would be ~90% higher if BMD were used	A BMDL was used as the POD	Lower bound is 95% CI of administered exposure
Choice of bioassay	Alternatives could ↑ RfC/D	NEDO (1987)	Alternative bioassays were available, but the chosen bioassay was adequately conducted and reported and resulted in the most sensitive and reliable BMDL for derivation of the RfC.
Choice of species/gender	RfC would be ↑ or ↓ if based on another species/gender	RfC is based on the most sensitive and quantifiable endpoint (↓ brain weight) in the most sensitive species and gender adequately evaluated (male rats).	Choice of female rats would have resulted in a higher RfC/D. Effects in mice also yield higher RfCs. Qualitative evidence from NEDO (1987) and Burbacher et al. (2004a, 2004b) suggest that monkeys may be a more sensitive species, but data are not as reliable for quantification.
Human population variability	RfC could ↓ or ↑ if another value of the UF was used	10-fold uncertainty factor applied to derive the RfC/RfD values	10-fold UF is applied because of limited data on human variability or potential susceptible subpopulations, particularly pregnant mothers and their neonates.

5.3.1. Choice of Endpoint

The impact of endpoint selection on the derivation of the RfC and RfD was discussed in Sections 5.1.3.1 and 5.2.2.2. Potential RfC values considered ranged from 1.7 to 13.6 mg/m^3, depending on whether neurobehavioral function in male monkeys, brain weight decrease in male rats, or cervical ribs incidence in mice was chosen as the critical effect for derivation of the POD, with the former endpoint representing the lower end of the RfC range. The use of other endpoints, particularly pre-term births identified in the Burbacher et al. (2004a, 2004b, 1999a, 1999b) monkey study, would potentially result in lower reference values, but significant uncertainties associated with those studies preclude their use as the basis for an RfC.

Burbacher et al. (2004a, 2004b, 1999a, 1999b) exposed *M. fascicularis* monkeys to 0, 262, 786, and 2,359 mg/m^3 methanol 2.5 hours/day, 7 days/week during premating/mating and throughout gestation (approximately 168 days). They observed a slight but statistically significant gestation period shortening in all exposure groups that was largely due to C-sections performed in the methanol exposure groups "in response to signs of possible difficulty in the maintenance of pregnancy," including vaginal bleeding. As discussed in Sections 4.3.2 and 5.1.1.2, there are questions concerning this effect and its relationship to methanol exposure. An ultrasound was not done to confirm the existence of real fetal or placental problems. Neurobehavioral function was assessed in infants during the first 9 months of life. Two tests out of nine, returned positive results possibly related to methanol exposure. VDR performance was reduced in all treated male infants, and was significantly reduced in the 2,359 mg/m^3 group for both sexes and the 786 mg/m^3 group for males. However, an overall dose-response trend for this endpoint was only observed in females. As discussed in Section 4.4.2, confidence in this endpoint may have been increased by statistical analyses to adjust for multiple testing (CERHR, 2004), but it is a measure of functional deficits in sensorimotor development that is consistent with early developmental CNS effects (brain weight changes discussed above) that have been observed in rats. The Fagan test of infant intelligence indicated small but not significant deficits of performance (time spent looking a novel faces versus familiar faces) in treated infants. Although these results indicate that prenatal and continuing postnatal exposure to methanol can result in neurotoxicity to the offspring, especially when considered in conjunction with the gross morphological effects noted in NEDO (1987), the use of such statistically borderline results is not warranted in the derivation of the RfC, given the availability of better dose-response data in other species.

NEDO (1987) also examined the chronic neurotoxicity of methanol in *M. fascicularis* monkeys exposed to 13.1, 131, or 1,310 mg/m^3 for up to 29 months. Multiple effects were noted at 131 mg/ m^3, including slight myocardial effects (negative changes in the T wave on an EKG), degeneration of the inside nucleus of the thalamus, and abnormal pathology within the cerebral white tissue in the brain. The results support the identification of 13.1 mg/m^3 as the NOAEL for

neurotoxic effects in monkeys exposed chronically to inhaled methanol. However, as discussed in Section 4.2.2.3, there exists significant uncertainty in the interpretation of these results and their utility in deriving an RfC for methanol. These uncertainties include lack of appropriate control group data, limited nature of the reporting of the neurotoxic effects observed, and use of wild-caught monkeys in the study. Thus, while the NEDO (1987) study suggests that monkeys may be a more sensitive species to the neurotoxic effects of chronic methanol exposure than rodents, the substantial deficits in the reporting of data preclude the quantification of data from this study for the derivation of an RfC.

The increased incidence of cervical ribs was identified as a biologically significant, potential co-critical effect based on the findings of Rogers et al. (1993a). Mice were exposed to 1,000, 2,000, or 5,000 ppm, and incidence of cervical ribs was statistically increased at 2,000 ppm. However, given that the reference values for the increased incidence of cervical ribs are estimated to be approximately five times higher than the reference values calculated using decreases in brain weight in male rats (NEDO, 1987), decreased brain weight was chosen as the basis for the derivation of the RfC.

5.3.2. Choice of Dose Metric

A recent review of the reproductive and developmental toxicity of methanol by a panel of experts concluded that methanol, not its metabolite formate, is likely to be the proximate teratogen and that blood methanol level is a useful biomarker of exposure (CERHR, 2002; Dorman et al., 1995). The CERHR Expert Panel based their assessment of potential methanol toxicity on an assessment of circulating blood levels (CERHR, 2002). In contrast to the conclusions of the NTP-CERHR panel, in vitro data from Harris et al. (2004, 2003) suggest that the etiologically important substance for embryo dysmorphogenesis and embryolethality was likely to be formaldehyde rather than the parent compound or formate. Although there remains uncertainty surrounding the identification of the proximate teratogen of importance (methanol, formaldehyde, or formate), the dose metric chosen for derivation of an RfC was based on blood methanol levels. This decision was primarily based on evidence that the toxic moiety is not likely to be the formate metabolite of methanol (CERHR, 2004), and evidence that levels of the formaldehyde metabolite following methanol maternal and/or neonate exposure would be lower in the fetus and neonate than in adults. While recent in vitro evidence indicates that formaldehyde is more embryotoxic than methanol and formate, the high reactivity of formaldehyde would limit its unbound and unaltered transport as free formaldehyde from maternal to fetal blood (Thrasher and Kilburn, 2001) (see discussion in Section 3.3). Thus, even if formaldehyde is ultimately identified as the proximate teratogen, methanol would likely play a prominent role, at least in terms of transport to the target tissue. Further discussions of methanol metabolism, dose metric selection, and MOA issues are in Sections 3.3, 4.6, 4.8 and 4.9.2.

There exists some concern in using the F_1 generation NEDO (1987) rat study as the basis from which to derive the RfC. This concern mainly arises from issues related to the low confidence that the PBPK model is accurately predicting dose metrics for neonates exposed through multiple and simultaneous routes. The PBPK model was structured to predict internal dose metrics for adult NP animals and was optimized using adult metabolic and physiological parameters. Young animals have very different metabolic and physiological profiles than adults (enzyme activities, respiration rates, etc.). This fact, coupled with multiple routes of exposure, make it likely that the PBPK did not accurately predict the internal dose metrics for the offspring. Stern et al. (1996) reported that when rat pups and dams were exposed together during lactation to 4,500 ppm methanol in air, methanol blood levels in pups from GD6–PND21 were approximately 2.25 times greater than those of dams. This discrepancy persisted until PND48, when postnatal exposure continued to PND52. It is logical to assume that similar differences in blood methanol levels would also be observed in the NEDO (1987) F_1 study, as the exposure scenario is similar to that of Stern et al. (1996). Differences between pup and dam blood methanol levels might be expected to be slightly greater than twofold in the NEDO (1987) F_1 study as the exposure was continuous (versus 6 hours/day in the Stern et al. [1996] paper) and lasted for a longer duration (~64 days versus 37). Under a similar scenario, human newborns may experience higher blood levels than their mothers as a result of breast feeding. As has been discussed in Chapter 3, children have a limited capacity to metabolize methanol via ADH; however, there is some evidence that human infants are able to efficiently eliminate methanol at high-exposure levels, possibly via CAT (Tran et al., 2007). At environmentally relevant exposure levels, it is assumed that the ratio of the difference in blood concentrations between infant and mother would not be significantly greater than the twofold difference that has been observed in rats.[78] For this reason and because EPA has confidence in the ability of the PBPK model to accurately predict adult blood levels of methanol, the maternal blood methanol levels for the estimation of HECs from the NEDO (1987) study were used as the dose metric.

5.3.3. Choice of Model for BMDL Derivations

The Hill model adequately fit the dataset (goodness-of-fit *p*-value = 0.84). Data points were well predicted near the BMD (scaled residual = 0.09) (see Figure 5-1). There is a 2.5-fold range of BMDL estimates from adequately fitting models, indicating considerable model dependence. The BMDL from the Hill model was selected, in accordance with EPA BMD Technical Guidance (EPA, 2000b), because it results in the lowest BMDL from among a broad range of BMDLs and provides a superior fit in the low dose region nearest the BMD.

[78] Key parameters and factors which determine the ratio of fetal or neonatal human versus mother methanol blood levels either do not change significantly with age (partition coefficients, relative blood flows) or scale in a way that is common across species (allometrically).

5.3.4. Choice of Animal-to-Human Extrapolation Method

A PBPK model developed by the EPA, adapted from Ward et al. (1997), was used to extrapolate animal-to-human concentrations. An AUC blood level of methanol (90.9 hr x mg/L) associated with a one S.D. change from the control mean for brain weights in rats was estimated using the rat PBPK model. Then the human PBPK model was used to convert back to a human equivalent exposure concentration or a $BMCL_{HEC/1SD}$ of 182 mg/m^3. If no PBPK models were available, a $BMCL_{HEC/1SD}$ of 424 mg/m^3 would have been derived by adjusting the 556.5 mg/m^3 $BMCL_{1SD}$ for external exposure concentration for duration and the animal-to-human standard adjustment factor for systemic effects (the ratio of animal and human blood:air partition coefficients). This value is approximately 2-fold higher than the value derived using the PBPK model. However, as discussed above, use of PBPK-estimated maternal blood methanol levels for the estimation of HECs allows for the use of data-derived extrapolations rather than standard methods for extrapolations from external exposure levels.

As discussed in Section 3.4, the PBPK models do not describe or account for background levels of methanol, formaldehyde or formate, and background levels were subtracted from the reported data before use in model fitting or validation (if not already subtracted by study authors), as described below. This approach was taken because the relationship between background doses and background responses is not known, because the primary purpose of this assessment is for the determination of noncancer and cancer risk associated with increases in the levels of methanol or its metabolites (e.g., formate, formaldehyde) over background, and because the subtraction of background levels is not expected to have a significant impact on PBPK model parameter estimates as background levels of methanol and its metabolites are low relative to exposure levels used in methanol bioassays.

5.3.5. Route-to-Route Extrapolation

To estimate an oral dose POD for decrease in brain weight in rats, a route-to-route extrapolation was performed on the inhalation exposure POD used to derive the RfC. One way to characterize the uncertainty associated with this approach is to compare risk levels (BMDL values) using the dose metric, AUC methanol, for developmental decreases in brain weight derived from 1) an existing oral subchronic study and 2) from a model estimating this metric from an existing inhalation subchronic study. There are currently no oral developmental studies investigating decreases in brain weight available to compare to the risk values estimated using the second procedure. However, the fact that the oral BMDL of 38.5 mg/kg-day estimated in this assessment from the NEDO (1987) inhalation study of neonate rats via a PBPK model is lower than the NOAEL of 500 mg/kg-day identified in EPA (1986c) methanol study of adult rats is consistent with other studies which suggest that fetal/neonatal organisms are a sensitive subpopulation.

5.3.6. Statistical Uncertainty at the POD

There is uncertainty in the selection of the BMR level. For decreased brain weight in rats, no established standard exists, so a BMR of one S.D. change from the control mean was used. Parameter uncertainty can be assessed through CIs. Each description of parameter uncertainty assumes that the underlying model and associated assumptions are valid. For the Hill model applied to the data for decreased brain weight in rats, there is a degree of uncertainty at the one S.D. level (the POD for derivation of the RfC), with the 95% one-sided lower confidence limit (BMDL) being ~50% below the maximum likelihood estimate of the BMD.

5.3.7. Choice of Bioassay

The NEDO (1987) study was used for development of the RfC and RfD because it resulted in the lowest BMDL. It was also a well-designed study, conducted in a relevant species with an adequate number of animals per dose group, and with examination of appropriate developmental toxicological endpoints. Developmental (Burbacher et al., 2004a, 2004b, 1999a, 1999b) and chronic studies (NEDO, 1987) of methanol have been performed in monkeys. As discussed above in Section 5.3.1 and other sections of this assessment, while the monkey may be a sensitive species for use in the determination of human risk, reporting deficits and study uncertainties preclude their use in the derivation of an RfC.

5.3.8. Choice of Species/Gender

The RfC and RfD were based on decreased brain weight at 6 weeks postbirth in male rats (the gender most sensitive to this effect) (NEDO, 1987). This decrease in brain weight also occurs in female rats; however, if the decreased brain weight in female rats had been used, higher RfC and RfD values would have been derived (approximately 66% higher than the male derived values).

5.3.9. Human Population Variability

The extent of interindividual variation of methanol metabolism in humans has not been well characterized. As discussed in Section 4.9, there are a number of issues that may lead to sensitive human subpopulations. Potentially sensitive subpopulations would include individuals with polymorphisms in the enzymes involved in the metabolism of methanol and individuals with significant folate deficiencies. Sensitive lifestages would include children and neonates, as they have increased respiration rates compared to adults, which may increase their methanol blood levels compared to adults. Also, children have been shown to have decreased ADH activity relative to adults, thus decreasing their ability to metabolize and eliminate methanol. As demonstrated by these examples, there exists considerable uncertainty pertaining to human

population variability in methanol metabolism, which provides justification for the 10-fold intraspecies UF used to derive the RfC and RfD.

5.4. 5.4. CANCER ASSESSMENT

5.4.1. Oral Exposure

5.4.1.1. *Choice of Study/Data—with Rationale and Justification*

No human data exist that would allow for quantification of the cancer risk of chronic methanol exposure. Table 4-34 summarizes the available experimental animal oral exposure studies of methanol. The Soffritti et al. (2002a) and Apaja (1980) oral studies report effects that show a statistically significant increase in incidence of cancer endpoints in the treated groups versus the control group (pair-wise comparison). As detailed in Section 4.2.1.3, Soffritti et al. (2002a) exposed Sprague-Dawley rats via drinking water to 500–20,000 ppm methanol for 104 weeks. Exposure ended at 104 weeks, but the animals were not euthanized and were followed until their natural death. Increased lymphoma responses in multiple organs of male and female rats were the only carcinogenic effects reported in the Soffritti et al. (2002a) methanol drinking water study that are considered dose related and quantifiable. Hepatocellular carcinomas observed in male rats are considered potentially dose related (relative to historical controls) but are not quantifiable due to the lack of a statistically significant dose-response trend. Significant increases reported for head and ear duct carcinomas in male rats were not used because NTP pathologists interpreted a majority of these ear duct responses as being hyperplastic, not carcinogenic, in nature (EFSA, 2006; Hailey, 2004). Apaja (1980) observed significant increases in malignant lymphomas relative to untreated, historical controls in Swiss mice exposed to methanol in drinking water for life. Due to the lack of a concurrent control, the Apaja (1980) study was not considered adequate for derivation of an oral slope factor, but a quantitative analysis of the dose-response data from this study is included in Appendix E for comparison purposes.

5.4.1.2. *Dose-Response Data*

The tumor incidence data selected for modeling were the lympho-immunoblastic lymphomas and the combined lympho-immunoblastic, lymphoblastic and lymphocytic lymphomas in both male and female rats of the Soffritti et al (2002a) study. These lymphomas were combined at the recommendation of NTP pathologists due to their similar histological origin. The incidence of histiocytic sarcomas and myeloid leukemias was not significantly increased in either sex, and the data for these tumors was not combined with the lymphoblastic lymphomas because they are of a different cell line and the combination is not typically evaluated either for statistical significance or dose-response modeling (Hailey, 2004; McConnell, et al., 1986). Table 5-6 gives the lymphoma incidence data from the study which differs slightly

from the data reported in Soffritti et al. (2002a) in the incidence of lympho-immunoblastic lymphomas in the male 5,000 ppm group.[79]

Table 5-6. Incidence data for lymphoma, lympho-immunoblastic, and all lymphomas in male and female Sprague-Dawley rats

Dose (ppm)	Dose (mg/kg-day)	Number of animals examined	Lymphoma lympho-immunoblastic	All lymphomas combined
Female rats				
0	0	100	9	9
500	66.0	100	17	19[a]
5,000	624.1	100	19[a]	20[a]
20,000	2,177	100	21[a]	22[b]
Male rats				
0	0	100	16	17
500	53.2	100	24	27
5,000	524	100	28[a]	29[a]
20,000	1,780	99	37[b]	38[b]

Statistically significant by Fisher's Exact test: [a]$p < 0.05$, [b]$p < 0.01$

Source: Soffritti et al. (2002a) and ERF web portal (http://www.ramazzini.it/fondazione/foundation.asp).

5.4.1.3. *Dose Adjustments and Extrapolation Method*

As with the extrapolations used in the development of the RfC and RfD, the PBPK model was used for species-to-species extrapolation of the doses to be used in the cancer dose-response analysis. Three dose metrics were considered for use in the dose-response analysis: total metabolized methanol; maximum blood concentration of the parent (C_{max}); and area under the blood concentration time curve (AUC) for the parent. Internal dose estimates (above background) corresponding to the administered doses from the animal bioassay were determined for each of these metrics with the PBPK model (see Appendix E, Table E-5). To help inform the selection of the most appropriate dose metric, dose-response analyses were performed using these PBPK model results to assess which dose metric best corresponded to the observed incidence data in Table 5-6 (see Appendix E, Tables E-6 and E-7). Figures 5-3, 5-4, and 5-5 show the fit of the multistage model to the all lymphoma incidence data for female and males, using each dose metric as the dose input.

[79] EPA obtained detailed, individual animal data via an interagency agreement with NIEHS which supported the development of reports made available through the Ramazzini Foundation (ERF) web portal (http://www.ramazzini.it/fondazione/foundation.asp). This allowed EPA to combine lymphomas of similar histopathological origin and confirm the tumor incidences reported in the Soffriti et al. (2000a) paper.

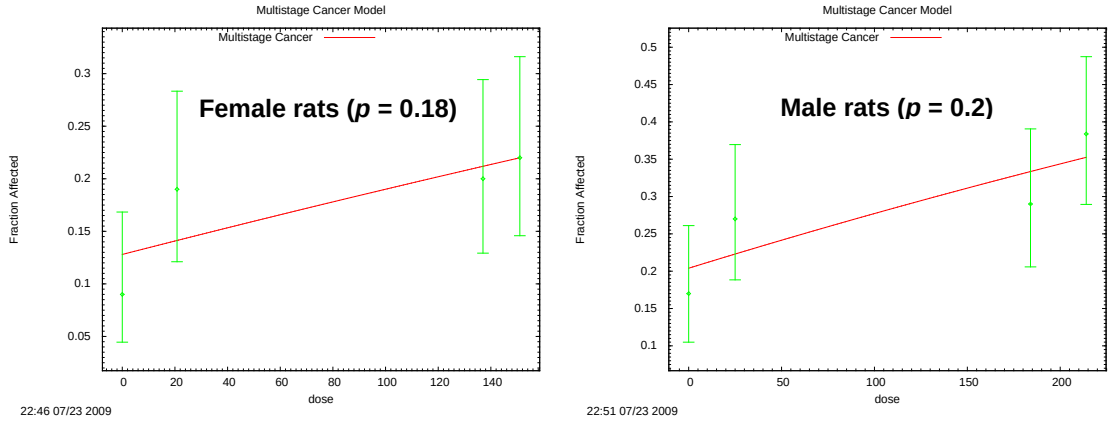

Figure 5-3. All lymphomas versus methanol metabolized (mg/day) for female and male rats

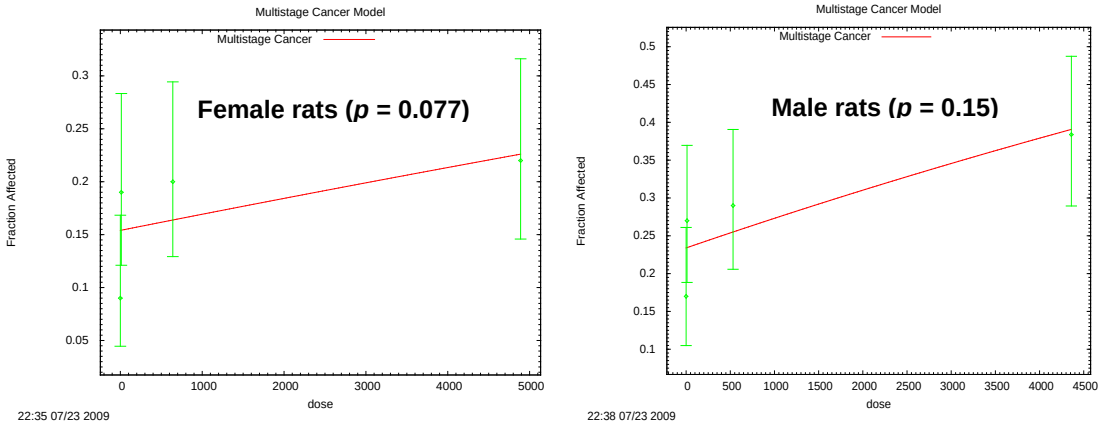

Figure 5-4. All lymphomas versus C_{max} (mg/L) for female and male rats.

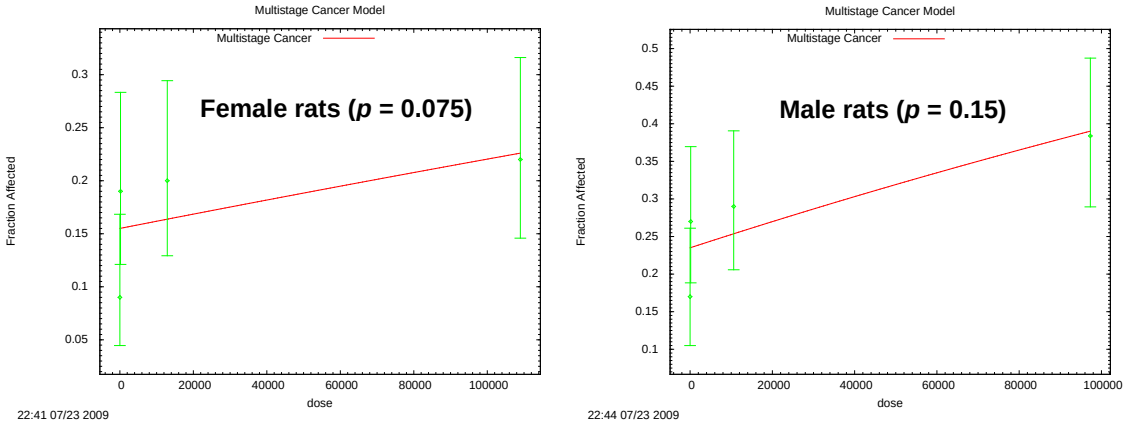

Figure 5-5. All lymphomas versus AUC (hr x mg/L) for male and female rats

The dose-response modeling suggests that total metabolized methanol is a better dose metric than the parent compound metrics as indicated by improved model fit to responses reported by Soffritti et al. (2002a) for both lympho-immunoblastic lymphoma (see Appendix E, Table E-7) and all lymphoma (see Figures 5-3 to 5-5 and Appendix E, Table E-7), and also for malignant lymphoma responses reported by Apaja (1989) (see Appendix E, Table E-17). Chi-square p values for the total metabolite dose metric ranged from 0.18 to 0.55 and were consistently higher than for the other dose metrics. This could be an indication of the importance of metabolite formation, which is likely to be more rapid at low doses, to the carcinogenic response. The total metabolized methanol dose metric was selected as the dose metric for use in the dose-response assessment to derive the POD because it provided the best fit to the response data. The estimated BMDL for the total methanol metabolized dose metric was then back-calculated using the EPA PBPK model to obtain a human equivalent oral drinking water dose in terms of mg/kg-day (see Appendix E, Table E-8).

Multistage and multistage Weibull time-to-tumor models were applied to the lymphoma data obtained from ERF for the Sofffritti et al. (2002a) drinking water study and considered for determining the POD to be used in the derivation of the oral cancer slope factor (see Appendix E, Table 3-8). Appendix E gives the details and justification for the various approaches used. As described in Appendix E, time-to-tumor modeling and multistage quantal modeling gave similar results, and the tumor responses modeled did not exhibit significant time dependence on dose. The EPA multistage cancer model fit the response data adequately and was used to derive the oral cancer slope factor (CSF) (see Appendix E, Tables E-7, E-8, and Figure E-10).

BMDs and BMDLs were estimated for the combined lymphomas in male and female rats. The BMR selected was the standard value of 10% extra risk recommended for dichotomous models (U.S. EPA, 2000b).[80] The 95% one-sided lower confidence limit defined the BMDL. The dose terms in the fitting were set equal to the estimated total metabolized doses derived using the PBPK model for methanol for each of the administered doses in the bioassay.

Application of the multistage model to the incidence data for all lymphomas in male rats (Table 5-6) resulted in the BMD and $BMDL_{10}$ values presented in Table 5-7. The results for the male rat were used in the derivation of the CSF because the female data for this endpoint yielded slightly higher values (see Appendix E, Tables E-7 and E-8). Assuming that metabolized methanol distributes in the body according to body weight to the ¾ power, the male rat mg-day $BMDL_{10}$ was converted to a human mg-day $BMDL_{10}$.[81] The human PBPK model (Appendix B) was then used to convert this human mg-day value for total methanol metabolized back to a

[80] The use of lower BMR values was determined not to have a significant impact on the CSF derivation.

[81] Male rat mg/day was converted to human mg/day by multiplying by $(BW_{human})^{3/4}/(BW_{rat})^{3/4} = (70\ kg)^{3/4}/(0.33\ kg)^{3/4} = 55.6$

human equivalent methanol oral dose HED($BMDL_{10}$) of 51.5 mg/kg-day for lymphomas in the male rat (see Appendix E, Table E-8).[82]

Table 5-7. BMD results and oral CSF using all lymphoma in male rats

Amount metabolized (mg/d)			Human equivalent $BMDL_{10}$ (mg/kg-day)	Oral CSF $(mg/kg\text{-}day)^{-1}$
BMD_{10} (mg/d)	Rat $BMDL_{10}$ (mg/d)	Estimated human $BMDL_{10}$ (mg/d)		
101.7	63.9	3,553	51.5	1.9E-03

Source: Soffritti et al. (2002a).

In the case of methanol, there is no information to inform the MOA for carcinogenicity. As recommended in the *Guidelines for Carcinogen Risk Assessment* (U.S. EPA, 2005a), "when the weight of evidence evaluation of all available data is insufficient to establish the MOA for a tumor site and when scientifically plausible based on the available data, linear extrapolation is used as a default approach." Accordingly, for the derivation of a quantitative estimate of cancer risk for ingested methanol, a linear extrapolation was performed to determine the CSF.

5.4.1.4. *Oral Slope Factor*

The oral slope factor was derived based on a linear extrapolation from this POD ($BMDL_{10/HED}$ of 55.4 mg/kg-day for lymphomas in the male rat) to the estimated background response level:

$$0.1/\ HED(BMDL_{10}) = 0.1/51.5\ mg/kg\text{-}day = 2E\text{-}03\ (mg/kg\text{-}day)^{-1}$$

(rounded to one significant figure)

5.4.2. Inhalation Exposure

5.4.2.1. *Choice of Study/Data–with Rationale and Justification*

No human data exist that would allow for quantification of the cancer risk associated with chronic methanol exposure. Table 4-35 summarizes the available experimental animal inhalation exposure studies of methanol. The NEDO (1987, 1985/2008b) 24-month rat study is the only inhalation bioassay available that reports an increase in incidence of any cancer endpoints (see Section 4.2.2.3). This NEDO (1987, 1985/2008b) study was of high quality and was based on standard OECD guidelines (OECD, 2007). F344 rats were exposed for 104 weeks to air concentrations of 0, 10, 100 and 1,000 ppm methanol. Rats were sacrificed and necropsied at the

[82] The following algebraic equation is provided in Appendix B (Equation 4) to describe the relationship between predicted human mg-day methanol cleared and the human equivalent oral dose (HED) in mg/kg-day:

HED = (3.3*3,553 mg/d)/(19,282.9 – 3, 553 mg/d) + (0.014287*3, 553 mg-d) = 51.5 mg/kg-d

end of the 104-week exposure period. The NEDO (1987, 1985/2008b) study reports increased pulmonary adenomas/adenocarcinomas and pheochromocytomas in high-dose (1,000 ppm) male and female rats, respectively. The combined incidence of pulmonary adenomas and adenocarcinomas was significantly increased in the high-dose males (see Tables 4-4 and 5-8), and both tumor types were considerably elevated at the high-dose over historical control incidences within their respective sex and strain (see discussion in Section 4.2.2.3). As shown in Table 4-5, the severity and combined incidence of potential precursor effects in the alveolar epithelium of male rat lungs (epithethial swelling, adenomatosis, pulmonary adenoma, and pulmonary adenocarcinoma) and the adrenal glands of female rats (hyperplasia and pheochromocytoma) were increased in the higher exposure groups compared with the controls and lower exposure groups. While the incidence of male rat pulmonary adenomas was also high in the lowest (10 ppm) exposure group, the appearance of a rare adenocarcinoma in the high-dose group is suggestive of a progressive effect associated with methanol exposure. While the increased pheochromocytoma response in female rats is not statistically increased over controls, it is considered to be potentially treatment related because this is a historically rare tumor type for female F344 rats (NTP, 2007, 1999; Haseman et al., 1998),[83] and when viewed in conjunction with the increased medullary hyperplasia observed in the mid-exposure (100 ppm) group females, it is suggestive of a proliferative change with increasing methanol exposure.

5.4.2.2. *Dose-Response Data*

The tumor incidence data selected for modeling are the NEDO (1987, 1985/2008b) reported incidences of adenoma/adenocarcinoma in male rats and pheochromocytoma in female rats. These data are presented in Table 5-8.

Table 5-8. Incidence data for tumor responses in male and female F344 rats

Dose (ppm)	Number of animals affected/number examined	
	Pheochromocytoma	**Pulmonary adenoma/adenocarcinoma**
	Female rats	
0	2/50	2/52
10	3/51	0/19
100	2/49	0/20
1000	7/51[a,b]	0/52
	Male rats	
0	7/52	1/52
10	2/16	5/50
100	2/10	2/52
1000	4/51	7/52[b,c]

[83] Haseman et al., (1998) report rates for spontaneous pheochromocytomas in 2-year NTP bioassays of 5.7% (benign) and 0.3% (malignant) in male F344 rats and 0.3% (benign) and 0.1% (malignant) in female (n=1517) F344 rats.

Dose (ppm)	Number of animals affected/number examined

[a]$p < 0.05$ over NTP historical controls for total (benign, complex and malignant) pheochromocytomas using the Fisher's Exact test
[b]$p < 0.05$ for Cochrane-Armitage test of overall dose-response trend.
[c]$p < 0.05$ over concurrent controls using the Fisher's Exact test.

Source: NEDO (1987, 1985/2008b).

5.4.2.3. *Dose Adjustments and Extrapolation Method*

As with the extrapolations used in the development of the RfC and RfD, the PBPK model was used for species-to-species extrapolation of the doses to be used in the cancer dose-response analysis. Three dose metrics were considered for use in the dose-response analysis: total metabolized methanol, maximum blood concentration of the parent (C_{max}), and area under the blood concentration time curve (AUC) for the parent. Each of the dose metrics corresponding to the administered dose from the animal bioassay was determined with the PBPK model (see Appendix E, Table E-10). To help inform the selection of the most appropriate dose metric, dose-response analyses were performed using these PBPK model results to assess which dose metric best corresponded to the observed incidence data in Table 5-8 (see Table E-11). All of the dose metrics resulted in similar fit to the incidence data for both endpoints, with the total metabolites metric providing a slightly improved fit to the female pheochromocytoma response data.

Unlike the oral data discussed in Section 5.4.1.2, dose-response modeling of the inhalation data from NEDO (1987, 1985/2008b) does not suggest the use of any one dose metric over the other. However, since the pheochromocytoma response likely involves systemically distributed, metabolized methanol, and to be consistent with the oral CSF, analysis the total methanol metabolized dose metric is selected as the dose metric for use in the dose-response assessment to derive the inhalation POD. The estimated BMDL for the methanol metabolized dose metric was then back-calculated using the EPA PBPK model to obtain a human equivalent air exposure concentration in terms of mg/m3 (see Table E-13).

The EPA multistage model was applied to the data in Table 5-8 obtained from the NEDO (1987, 1985/2008b) inhalation study and considered for determining POD to be used in the derivation of the inhalation cancer unit risk (Table E-11). Appendix E gives the details and justification for the various approaches used. As described in Appendix E, time-to-tumor and quantal modeling gave similar results, and the tumor responses modeled did not exhibit significant time dependence on dose. The EPA multistage cancer model fit the response data adequately and was used to derive the IUR (Tables E-11, E-12, and Figure E-13).

BMDs and BMDLs were estimated for tumor responses in male and female rats as shown in Table 5-8. The BMR selected was the standard value of 10% extra risk recommended for

quantal models (U.S. EPA, 2000b).[84] The 95% one-sided lower confidence limit defined the BMDL. The dose terms in the fitting were set equal to the estimated total metabolized doses derived using the PBPK model for methanol for each of the administered doses in the bioassay.

Application of the multistage model to the incidence data for pheochromocytomas in female rats (Table 5-8) resulted in the BMD and $BMDL_{10}$ values presented in Table 5-9. The results for the female rat were used because the female data for pheochromocytoma yielded slightly lower BMDL values (Tables E-11 and E-13). Assuming that metabolized methanol distributes in the body according to body weight to the ¾ power, the female rat mg-day $BMDL_{10}$ was converted to a human mg-day $BMDL_{10}$.[85] The human PBPK model (Appendix B) was then used to convert this human mg-day value for total methanol metabolized back to a human equivalent methanol inhalation concentration, $HEC(BMCL_{10})$, of 81.9 mg/m^3 or 81,900 $\mu g/m^3$ for pheochromocytomas in the female rat (see Appendix E, Table E-13).[86]

Table 5-9. BMD results and IUR using pheochromocytoma in female rats

Amount metabolized (mg/day)			Human equivalent $BMCL_{10}$ (mg/m^3)	IUR $(\mu g/m^3)^{-1}$
BMD_{10} (mg/day)	$BMDL_{10}$ (mg/day)	Estimated human $BMDL_{10}$ (mg/day)		
29.5	14.6	971	81.9	1.2E-06

Source: NEDO (1987, 1985/2008b).

5.4.2.4. *IUR*

The IUR in terms of $(\mu g/m^3)^{-1}$ was then derived based on a linear extrapolation from this POD to the estimated background response level:

$$0.1/\ HEC(BMCL_{10}) = 0.1/(81{,}900\ \mu g/m^3) = 1E\text{-}06\ (\mu g/m^3)^{-1}$$

(rounded to one significant figure)

5.4.3. Uncertainties in Cancer Risk Assessment

The following is a discussion of the uncertainties associated with the cancer potency estimate for methanol beyond that which can be addressed with the quantitative approach applied. A summary of these uncertainties is presented in Table 5-10.

[84] The use of lower BMR values was determined not to have a significant impact on the IUR derivation.

[85] Female rat mg/day is converted to human mg/day by multiplying by $(BW_{human})^{¾}/(BW_{rat})^{¾} = (70\ kg)^{¾}/(0.26\ kg)^{¾} = 66.5$

[86] The following algebraic equation is provided in Appendix B (Equation 3) to describe the relationship between predicted human mg-day methanol cleared and the human equivalent inhalation concentration (HEC) in mg/m^3:

$$HED = (14.69 \times 971\ mg/d)/(19282.9 - 971\ mg/d) + (0.063554 \times 971\ mg/d) = 81.9\ mg/\ m^3$$

Table 5-10. Summary of uncertainty in the methanol cancer risk assessment

Consideration	Potential impact	Decision	Justification
Quality of the studies relied upon for the determination of the PODs	Key chronic studies not always well reported; could lead to ↑ or ↓ of risks	Utilize re-analyses of the Soffritti et al. (2002a) and NEDO (1985/2008a, 2008b) chronic studies	Consideration of all available information resulted in the determination that the Soffritti et al. (2002a) and NEDO (1985/2008a, 2008b) chronic studies are adequate (see discussion of individual studies in Sections 4.2.1.3 and 4.2.2.3 and summaries in Sections 4.9.1 and 4.9.2).
Interpretation of results from study relied upon for the determination of the POD	Differences in tumor classification can lead to over or underestimate of risk	Derive POD based on incidence of combined lymphomas as suggested by NTP pathologists; Assume proper classification of lung and adrenal tumors by NEDO	Both NTP and EFSA recommend that only lymphomas of the same cellular origin be combined for dose-response analysis. With respect to lung and adrenal tumors, examination of concurrent alveolar and adrenal noncancer hyperplastic endpoints supports a proliferative change in these organ systems consistent with the appearance of carcinogenic responses.
Consistency of results across chronic studies	If effects not relevant to humans, risk is overestimated.	Derive PODs based on Soffritti et al. (2002a) and NEDO (1985/2008b).	Though tissue concordance across species, strains and routes of exposure is not assumed, lymphomas have been observed in more than one species by oral route. Also there is evidence that the observed lymphomas are relevant to humans (see discussions in Section 4.9. concerning human studies of methanol metabolite formaldehyde).
Choice of endpoint for POD derivation	Route-to-route extrapolation from Soffriti et al. (2002a) study would ↑ inhalation POD by about 4-fold	Derive oral CSF from lymphoma data and inhalation CSF from adrenal effects.	Oral POD was based on the only tumor type from Soffritti et al. (2002a) drinking water study significantly increased (all lymphomas); Inhalation POD based on most sensitive tumor response from NEDO (1985/2008b) study, increased pheochromocytoma in female rats.
Choice of species/gender	CSF and IUR would be ↓ if based on another gender	CSF and IUR are based on the most sensitive and reliably quantifiable species/gender	Choice of female rat lymphoma and male rat adenoma/adenocarcinoma would have resulted in lower CSF and IUR values, respectively. Use of the Apaja (1989) mouse data would have resulted in a higher, but less reliable CSF due to study problems, including a lack of concurrent controls
Choice of model for POD derivation	Use of other models could ↑ or ↓ POD, but not significantly	Derive cancer potency factor based on multistage model.	Use of the multistage model is consistent with EPA guidance (U.S. EPA, 2005a). The multistage model provides adequate fit to the data, which is not improved by a time-to-tumor modeling.
Choice of animal-to-human extrapolation method	Traditional method could ↑ the HEC($BMCL_{10}$) estimate by 4-fold.	A PBPK model was used to extrapolate animal–to-human concentrations.	Use of a PBPK model reduces uncertainty associated with the animal to human extrapolation. Total metabolites normalized by body weight is an appropriate dose metric and a verified PBPK model exists that estimates this metric.

5.4.3.1. *Quality of Studies that are the Basis for the PODs*

The protocols used at the laboratories that have performed cancer bioassays of methanol, particularly those of the ERF, differ from the more commonly used (e.g., NTP) protocols. The unique features of the ERF study design and their implications to a methanol cancer risk

assessment are discussed in Section 4.9.2. Separate from these experimental design issues are considerations relative to the quality of the cancer bioassays and any associate uncertainties.

The number of animals per dose group in ERF studies is often higher than the 50 animals per sex per dose group typically used in EPA and NTP studies, increasing the statistical power of the ERF cancer bioassay. However, ERF sometimes shares controls across concurrent studies (Cruzan, 2009; Belpoggi et al., 1995). In contrast, EPA requires (U.S. EPA, 1998) and NTP generally uses (Melnick et al., 2007) concurrent, matched controls for each carcinogen bioassay. The use shared controls does not necessarily compromise a study, but the use of a concurrent, matched control is generally preferred as a means of further avoiding confounding factors and increasing the reliability of a study regarding the interpretation of findings in treated animals.

The published report of the methanol bioassay (Soffritti et al., 2002a) indicates that the experiment was performed according to good laboratory practice (GLP) and standard operating procedures (SOP) of the ERF. Further, an independent review of ERF (Huff, 2002) suggests that quality control procedures associated with GLP were in place. However, questions have been raised about the quality of studies at the ERF by European Food Safety Authority (EFSA, 2006) in regards to the aspartame bioassays conducted by the ERF (Soffritti et al., 2006); by extension this EFSA report has raised issues for consideration in regards to methanol. EFSA (2006) has suggested that an inspection by the Italian GLP compliance monitoring authority (Ministry of Health) necessary to confirm GLP had not been conducted.[87] The EFSA (2006) report also identifies specific deviations from OECD guidelines (OECD, 2007), including a lack of a complete analysis of the test substance, no clear information on the stability of the substance, a lack of clinical observations or macroscopic changes, a lack of hematological assays, a lack of serology (e.g., to confirm the presence of infection) and limited histopathology reports. While these details may be recorded internally by the ERF as part of their standard protocol, because there is no documentation of these details available for consideration, there remains some uncertainty regarding the level at which they were performed. There is limited evidence, however, that these factors had a significant impact on the adequacy of the study for assessing carcinogenic potential (see Sections 4.2.1.3, 4.9.2 and 5.4.3.2).

EFSA (2006) also expresses concern over the possibility of compromised pathological diagnosis in the ERF aspartame study (Soffritti et al., 2006) due to extensive autolysis. ERF performs pathological examinations on “dying animals undergoing necropsy” (Soffritti et al., 2002a). This creates difficulties in pathological examinations associated with cell autolysis that can occur when pathology slides are prepared after natural death. The NTP (Hailey, 2004) commented on the increased prevalence of autolysis in slides from the ERF (Soffritti et al., 2006) aspartame study. EPA conducted a detailed analysis of the individual animal tissue data obtained

[87] Since the publication of the EFSA (2006) report, the EPA has confirmed through communication with the ERF laboratory (Knowles, 2008) that ERF is currently in the process of obtaining this certification.

from ERF for their chronic methanol, MTBE, formaldehyde, and aspartame studies, and determined that autolysis and other causes of tissue loss did not substantially impact tissue denominators. For most of the tissues evaluated there were more than 96 (individual animal) samples available for microscopic evaluation, and for all sites and dose groups, denominators were larger than for routine NTP bioassays (i.e., >50). Thus, missing tissues does not appear to have been a serious problem in the methanol study. While this analysis does not completely rule out the possibility that pathology slides and diagnoses were impacted by autolysis, it does indicate that this possibility would be offset by the large group size (response denominator) employed. Further, even if autolysis was a confounding factor, its presence would not negate positive cancer findings as autolysis would tend to decrease, not increase, the power to observe an effect.

There were no differences in survival among the methanol dose groups of the Soffritti et al. (2002a) study. However, Cruzan (2009) has suggested that "While the survival at 104 weeks was within the normal, but widespread, range for Sprague-Dawley rats, there was significant early mortality among all groups, including the controls" and that "the control group from an inhalation study (Cruzan et al., 1998) had much better survival through 104 weeks than seen in the RF methanol study." Yet, according to Table 12 of the Cruzan (2009) article, 104-week survival in male (~40%) and female (~50%) control rats of the Cruzan et al. (1998) study was not discernibly different from the 104 week survival of male (~40%) and female (~50%) control rats of the Soffritti et al. (2002a) methanol study (see Appendix E, Figures E-1 and E-2). Survival of male and female Sprague-Dawley rats in the Soffritti et al. (2002a) study at 104 weeks was greater than 40% in all but the female 5,000 ppm group. Further, at the NTP (NTP, 2006), the 104-week survival of 353 control female Sprague-Dawley rats was 41.5% (range of 28.3%–51% in 7 studies) using NTP's new diet and corn oil gavage, indicating that survival in the Soffritti et al. (2002a) methanol study was not low.

Studies such as the Soffritti et al. (2002a) methanol study that allow test animals to live a full life span can be difficult to interpret due to the need to distinguish between age-related and chemical-related effects. Full life-span studies may have advantages. Huff et al. (2009) note that "studies truncated after 2 years of exposure do not allow sufficient latency periods for late-developing tumors, such as the 80% of all human cancers that occur after 60 years of age." Several recent publications have noted deficiencies with the 2-year study design used at the NTP and have recommended extending the duration of rodent studies to increase the sensitivity of their bioassays (Huff et al., 2009; Huff et al., 2007; Maronpot et al., 2004; Bucher et al., 2002).

While arguments have been documented related to the possible confounding influence of infection and autolysis on the results obtained from the ERF, available evidence does not indicate that these factors significantly influenced the observed lymphoma/leukemia response in the methanol or other bioassays conducted at ERF. In addition, for the purposes of this assessment

and at the request of the EPA, the ERF and NEDO have provided additional study details beyond that which is normally available from published journal articles, including quality assurance reports and individual animal data. Based on a review of this information, consideration of the issues, and absent additional data to the contrary, EPA has determined that both studies were sufficient for use in the assessment of risk from methanol exposure.

5.4.3.2. *Interpretation of Results of the Studies that are the Basis for the PODs*

There are a number of uncertainties regarding the interpretation of both the lymphoma response in male Sprague-Dawley rats (Soffritti et al., 2002a) that forms the basis of the oral CSF and the pheochromocytoma response in F344 rats (NEDO, 1985/2008b) that forms the basis for the inhalation CSF.

There is also a wide range in the background incidence of hemolymphoreticular tumors reported in control groups of ERF studies. Between 1984 and 1997, incidence rates of hemolymphoreticular neoplasms in control rats at ERF increased by 38% among male rats and decreased by 12% among female rats (Caldwell et al., 2008). Soffritti et al. (2007, 2006) reports that among 2,265 untreated males and 2,274 untreated females the average incidence of lymphomas and leukemias is 20.6% (range, 8.0-30.9%) in males and 13.3% (range, 4.0-25%) in females. Caldwell et al. (2008) noted that for the incidences of these lesions for the ERF colony are relatively low and stable across studies. EFSA (2006) and Cruzan (2009) consider it to be high relative to other tumor types and relative to the background rate for this tumor type in Sprague-Dawley rats from other laboratories (see Section 4.9.2 for further discussion).

In the ERF bioassays, including methanol, hemolymphoreticular neoplasms were divided into specific histological types (lymphoblastic lymphoma, lymphoblastic leukemia, lymphocytic lymphoma, lympho-immunoblastic lymphoma, myeloid leukemia, histocytic sarcoma, and monocytic leukemia) for identification purposes. Upon examining slides from the aspartame study conducted by the ERF, a PWG of the NTP at the NIEHS (Hailey, 2004) found that "The diagnoses of lymphatic and histocytic neoplasms in the cases reviewed were generally confirmed. The NTP does not routinely subdivide lymphomas into specific histological types as was done by the ERF, however the PWG accepted their more specific diagnosis if the lesion was considered to be consistent with a neoplasm of lymphocytic, histocytic, monocytic, and/or myeloid origin." The NTP PWG also noted that while lymphoblastic lymphomas, lymphocytic lymphomas, lympho-immunoblastic lymphomas and lymphoblastic leukemias as malignant lymphomas can be combined, myeloid leukemias, histocytic sarcomas and monocytic leukemia should be treated as separate malignancies and not combined with the other lymphomas for statistical evaluation since they are of different cellular origin (Hailey, 2004). Other researchers have also noted this distinction between myeloid leukemias and histiocytic sarcomas and other lymphomas (McConnell et al., 1986). To decrease the uncertainty in the combination of tumors relied upon for dose-response modeling, the current dose-response modeling conducted for

methanol did not include myeloid leukemia, histocytic sarcoma, monocytic leukemia, alone or in combination with lymphoblastic lymphoma, lymphoblastic leukemia, lymphocytic lymphoma, and lympho-immunoblastic lymphoma.

As expressed by EFSA (2006) and others (Cruzan, 2009; Schoeb et al., 2009), there is concern that the lympho-immunoblastic lymphoma response in the ERF aspartame study (Soffritti et al., 2006, 2005) was caused by or confused with sequalae of a *M. pulmonis* infection. Infection of the ERF colony with *M. pulmonis* has not been confirmed (Caldwell et al., 2008) and, as discussed in Section 4.9.2, a link between *M. pulmonis* infection and induction of lymphoma in rats has not been established in the literature. As noted in Section 4.9.2, there is evidence suggesting that respiratory infections may have confounded the interpretation of lung lesions in ERF studies. Lymphoma illustrations in 2 ERF studies (Figure 10 of Soffritti et al. [2005] and Figures 1-5 of Belpoggi et al. [1999]), suggest that ERF MTBE and aspartame bioassays may have been confounded by a respiratory infection such as *M. pulmonis* and that lesions associated with this infection may have been interpreted as lymphoma (Schoeb et al., 2009). However, other ERF lymphoma diagnoses in multiple rat organ systems, including the lung, have been confirmed by an independent working group panel of six NIEHS pathologists (Hailey, 2004). In addition, the incidence of “lung-only” lympho-immunoblastic lymphomas was evenly distributed across the control and 0, 500 5000, 20,000 ppm dose groups for male (9, 10, 14 and 13) and female (3, 5, 6 and 7) rats of the Soffritti et al. (2002a) methanol study (Schoeb et al., 2009). Consequently, removing “lung-only” lympho-immunoblastic lymphomas from consideration and using only lymphomas from organ systems not likely to be confounded by a respiratory infection (i.e., subtracting the lung-only incidence from lympho-immunoblastic lymphomas reported in Table 5-6) still results in significant dose-response curves for this lesion with p values of 0.20 and 0.42 for males and females, respectively (see Figure 5-6). The $BMDL_{10}$ estimates of 99 (males) and 110 (females) mg metabolized methanol/day are about 50% higher than metabolized methanol $BMDL_{10}$ estimates for this endpoint when “lung-only” responses are included (Appendix E, Table E-7).

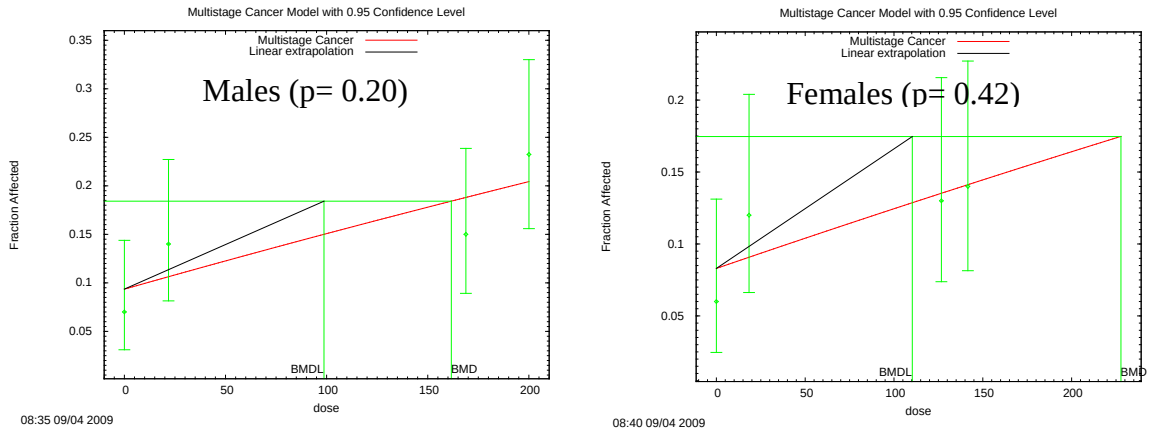

Figure 5-6. Lympho-immunoblastic Lymphoma minus "lung-only" response in rats of Soffritti et al. (2002a) methanol study versus methanol metabolized (mg/day).

For increases in 2 other tumor types (ear duct and head/oral cavity tumors) reported in the ERF methanol study (Table 4-2), an independent review of the 75 pathology slides from the ERF aspartame study has suggested differences in interpretation. After reviewing these slides, the NTP PWG noted that "about half" of hyperplastic and neoplastic lesions in the ear duct or oral cavity were more severely classified by ERF study pathologists, compared with diagnosis from the PWG (EFSA, 2006). Though a similar review has not been conducted of the Soffritti et al. (2002a) ERF methanol bioassay results, there is uncertainty regarding the ERF interpretation of these lesions. For this reason, these lesions were not considered in the derivation of the oral CSF.

Another uncertainty that confounds the interpretation of some ERF studies is the possibility of litter effects in ERF test groups. Bucher (2002) has reported that ERF does not randomize the assignment of animals to treatment groups, but generally "assigns all animals from a given litter to the same treatment group, recording which litter each animal came from." This approach would make it more difficult to distinguish the relative contributions of the chemical and genetics to the effect of concern. In response to an EPA query regarding this matter (Knowles, 2008), ERF has stated that "the assignment of test animals to dose groups will vary in ERF studies according to the experimental protocol and aims of the research" and "in the case of experiments in which exposure begins at 6-8 weeks of age (for example BT960, methanol), randomization is performed so as to have no more than one female and one male from each litter in each experimental group." For other experiments in which exposure begins during prenatal life, [88] "randomization is performed on the breeders," but the offspring are not randomized across dose groups in order to "..simulate as much as possible the human situation in which all descendents are part of a population."

[88] For some chemicals such as vinyl chloride (Maltoni and Cotti, 1988) and aspartame (Soffriti et al., 2006), ERF has started exposure as early as *in utero*, This early exposure study design can markedly increase the sensitivity of a cancer bioassay (Maltoni and Cotti, 1988; Soffriti et al., 2006; Melnick et al., 2007).

There is uncertainty regarding the pheochromocytoma response observed in the NEDO (1985/2008b) study with respect to both its relation to exposure and to its pathology. As discussed in Section 4.2.2.3, the incidence of pheochromocytomas in female rats exhibited a dose-response trend (Cochrane-Armitage $p < 0.05$). While the incidence of 13.7% (7/51) in the high-dose group was significantly elevated ($p < 0.05$) over NTP historical controls, it was not significantly elevated over the concurrent control rate of 4% (2/50). Much of the uncertainty is inherent in difficulties associated with the characterization of this lesion. According to NTP (2000), the primary criterion used to distinguish pheochromocytomas from nonneoplastic adrenal medullary hyperplasia, the presence of mild-to-moderate compression of the adjacent tissue, can be a difficult determination. Further, while NEDO (1985/2008b) reported adrenal effects as "hyperplasia of medullary cells" and "pheochromocytoma," NTP pathologists categorize pheochromocytomas into three types: benign, complex and malignant (NTP, 2007, 1999). This is an important distinction as complex and malignant pheochromocytomas are a rare tumor type, occurring spontaneously in female F344 rats at rates ranging from 0.1% to 0.7% (NTP, 2007, 1999; Haseman et al., 1998) and with cell proliferation activity that is much higher than benign pheochromocytomas (Pace et al., 2002). Thus, severity of the pheochromocytoma response reported by NEDO (1985/2008b) is uncertain, potentially ranging from mischaracterized hyperplasia to highly proliferative and potentially metastatic malignancies. Finally, the NEDO study was a two-year study, and these lesions, which include diffuse hyperplasia, nodular hyperplasia, and pheochromocytoma, progress with age. Thus, it is possible that a life-span study would have detected a more severe carcinogenic response (e.g., progression of the mid-dose group hyperplastic responses as reported in Table 4-5).

5.4.3.3. *Consistency across Chronic Bioassays for Methanol*

The observation of a lymphoma response in rats (Soffritti et al., 2002a) and mice (Apaja, 1980), along with reported associations between lymphomas and human exposure to methanol's metabolite, formaldehyde (see Section 4.9), contributes significantly to the cancer weight-of-evidence determination. This was the only carcinogenic response that was observed in more than one animal bioassay. However, tissue concordance across species, strains and routes of exposure is not assumed, and a lack of such concordance does not negate the validity of individual findings nor the potential relevance of such findings to humans.

Besides the Soffritti et al. (2002a) drinking water study of rats (2 years) reported by ERF, the only other chronic studies available are the Apaja (1980) lifespan drinking water study study in Swiss mice which did not include a concurrent untreated control group, and those reported in the Japanese NEDO (1987, 1985/2008a, 2008b) study of monkeys (7–29 months), mice (18 months), and F344 rats (2 years). None of the NEDO studies involved lifetime evaluations, and only the rat study can be said to cover a significant portion of the test species life span. The only organ system that exhibited an increase in effects in both inhalation and drinking water

studies was the testes. High-dose rats of the Soffritti et al. (2002a) methanol study exhibited an increase in testicular interstitial cell adenomas, and the incidence of testicular hyperplasia was increased in high-dose rats of the NEDO (1987, 1985/2008b) study. However, neither effect was statistically increased over controls, and both effects were well within their historical control ranges. An increase in lymphomas was the only carcinogenic effect reported in the Soffritti et al. (2002a) and Apaja (1980) drinking water studies that is considered dose related and quantifiable, and male pulmonary adenoma/adenocarcinoma and female pheochromocytoma were the only carcinogenic effects from the NEDO (1987, 1985/2008b) inhalation study that are considered exposure related and quantifiable.

As discussed in Section 4.9.2, there are several differences between the NEDO (1987, 1985/2008b) and Soffritti et al. (2002a) studies conducted in rats which limit their direct comparison and may explain some of the differences in response. These include route of exposure, lifetime evaluation period, and strain of species used. Pulmonary adenomas observed in the NEDO inhalation study could be portal-of-entry effects associated with the inhalation route of exposure. Differences in systemic effects observed in the two studies such as the pheochromocytoma response in the NEDO (1987, 1985/2008b) study and the lymphoma responses observed in the Soffritti et al. (2002a) study are systemic responses and differences would not be expected based on route of exposure. Differences in the evaluation period between the two studies may have contributed to the lack of endpoint concordance. In the Soffritti et al. (2002a) study, the animals were administered methanol for 104 weeks and then followed until the completion of their natural lifetime. The average life span for these animals was 94 and 96 weeks for males and females, respectively, with animals living as long as 153 weeks (female). However, this does not explain the difference in lymphoma response between the studies as many of the lympho-immunoblastic lymphomas (most common type observed) were observed prior to 104 weeks (control – 5/9; 500 ppm – 7/17; 5,000 ppm – 13/19; 20,000 ppm – 11/21). The NEDO (1987, 1985/2008b) study was conducted in F344 rats versus the Sprague-Dawley rats used in the Soffritti et al. (2002a) ERF study. More importantly, the background rates of selected types of lymphomas and leukemias are very different between the two strains of rats. In the F344 rat, there is a high background rate of mononuclear cell leukemia, while there is a much lower background rate of this leukemia type in the Sprague-Dawley rat (Caldwell et al., 2008). The types of lymphoma reported in the Sprague-Dawley rat by Soffritti et al. (2002a) following methanol administration are rarely diagnosed in the F344 rat. Thus, the strain difference between the two studies is a likely explanation for the fact that lymphomas were only increased in the Soffritti et al. (2002a) rat study. NTP (2007, 1999) reports do not suggest a significant difference between F344 and Sprague-Dawley rats with respect to pulmonary adenomas and pheochromocytomas. Another possible explanation for this difference includes a different profile of circulating metabolites associated with oral first-pass liver metabolism.

5.4.3.4. *Choice of Endpoint for POD Derivation*

Keeping in mind the aforementioned uncertainties associated with the interpretation of the Soffritti et al. (2002a) and NEDO (1985/2008b) study results, the choice of tumors to use for the derivation of the oral and inhalation CSFs was made on the basis of the appearance of a dose-related increase in response rates for the selected tumor categories. Analysis of lymphomas used a pair-wise statistical comparison (Fisher's Exact test) and a trend test (Cochran Armitage trend test) to determine whether the slope of that trend was statistically significantly greater than 0. The Fisher's Exact result for the male rat high-dose group and the results of the Cochran Armitage Trend Test were both $p < 0.01$. The decision not to include the liver tumors in the dose-response analysis was made based on a lack of dose response according to pair-wise and a trend test results versus concurrent controls This is not to say that the slight increase in the incidence of this tumor type observed in all dose groups of male rats was not related to methanol exposure (this is a relatively rare Sprague-Dawley rat tumor), only that the increase was not statistically significant and did not contribute significantly to the overall tumor response.

As discussed in Sections 4.2.2.3 and 4.9.2, the high-dose incidences for pulmonary adenomas/adenocarcinomas were increased over concurrent controls ($p < 0.05$). While the high-dose incidences of pheochromocytomas in the NEDO (1985/2008b) study were not statistically increased over concurrent controls, the dose-response for both tumor types represents increasing trends (Cochran Armitage trend test; $p < 0.05$), and in both cases, the high-dose response incidences were considerably elevated over historical control incidences ($p < 0.05$) within their respective sex and strain. Further, both tumor responses are accompanied by proliferative changes (e.g., hyperplastic responses) in their respective cell types that suggest tumor progression.

5.4.3.5. *Choice of Species/Gender*

The oral CSF was based on male rat lymphomas rather than female rat lymphomas. The inhalation IUR was based on female rat pheochromocytomas rather than male rat adenoma/carcinomas. In both cases, the gender that exhibited the steeper dose response and the higher risk estimate was chosen.

Both the CSF and IUR were based on rat studies. Use of the Apaja (1989) mouse data would have resulted in a 5-fold higher, but less reliable oral CSF due to a high level of uncertainty associated with the Apaja (1989) study, which contained limited experimental detail and did not include a concurrent control group (see Section 4.2.1.3).

5.4.3.6. *Choice of Model for POD Derivation*

The multistage-cancer model contained in EPA's BMDS version 2.1 was used to derive both the CSF and IUR estimates for methanol. When no biologically-based cancer model exists and evidence for a nonlinear cancer MOA is lacking, as is the case for methanol, the preference

within the EPA's IRIS program is for the use of a multistage model. There is uncertainty associated with whether the multistage model is the most appropriate choice, but in the absence of a biologically based model, dose-response modeling is largely a curve-fitting exercise, and the multistage model is sufficiently flexible for most cancer bioassay data. In the case of the oral CSF, individual animal response data was obtained from the authors of the principal study (Sofffritti et al., 2002a) and a multistage-Weibull time-to-tumor model was applied to determine whether the lifespan study design of the study had an appreciable impact on the dose-response analysis. As described in Appendix E, time-to-tumor modeling and multistage quantal modeling gave similar results, and the tumor responses modeled did not exhibit significant time dependence on dose.

5.4.3.7. *Choice of Dose Metric*

The total methanol metabolized was selected over AUC or the C_{max} as the most appropriate dose metric for derivation of the oral cancer slope factor and inhalation unit risk primarily because it provided the best fit to response data, particularly lymphoma incidence from Soffritti et al. (2002a) (see Figures 5-3 through 5-5 and Table E-7 of Appendix E) and Apaja (1989) (see Table E-17 of Appendix E). Also, lymphomas and respiratory effects have been observed in studies conducted with formaldehyde, and lymphomas have been observed in chronic bioassays conducted with other compounds that convert to formaldehyde (i.e., MTBE and aspartame). As discussed in Section 4.9.3, metabolites of methanol, particularly formaldehyde, may play a role in the MOA.

In considering the dose-response relationship for methanol-induced carcinogenesis, a key factor is the saturation of metabolism since metabolic transformation to formaldehyde and generation of oxidative stress are considered likely candidates in the mode of action. Cruzan (2009) indicates that saturation occurs at dose of "600 mg/kg," but saturation depends on the dose rate, not the total administered dose. For example, if 600 mg/kg is given in a single bolus, the internal concentration immediately following that bolus could well be high enough to saturate metabolism, while the same total dose ingested over the course of a day might not.

To aid in interpretation of the Soffretti et al. (2002a) bioassay, water ingestion in rats was assumed to shift between nocturnal (high activity) and diurnal (low activity) periods, each lasting 12 hours. Rats were assumed to consume 20% of their daily water ingestion during the diurnal period and 80% during the nocturnal period. Ingestion in each period was assumed to occur in "bouts" which were treated as periods of continuous (zero-order) infusion to the stomach. During the nocturnal period each bout was assumed to last 45 minutes, followed by 45 minutes without ingestion (overall period is 1.5 hours) and during the diurnal period the bout was assumed to last on 3 hours followed by 2.5 hours without ingestion (overall period is 3 hours).

Given this exposure pattern, the total amount metabolized per day (after periodicity is reached) in a 420 g rat (average weight in Soffretti et al., 2002a) was estimated using the PBPK model, with the results shown in Figure 5-7. The amount increases almost linearly with exposure until ~ 400 mg/kg/d, but continues to increase above that point, becoming almost completely saturated by 2,000 mg/kg/d. This pattern occurs in part because of the circadian ingestion pattern. The more rapid ingestion rate during the dark cycle leads to the highest internal concentrations and hence the initial metabolic saturation during that part of the day. But the lower ingestion (light) period, internal concentrations drop, allowing for an exposure range (400-1600 mg/kg/d) where nocturnal metabolism is saturated but diurnal metabolism is not.

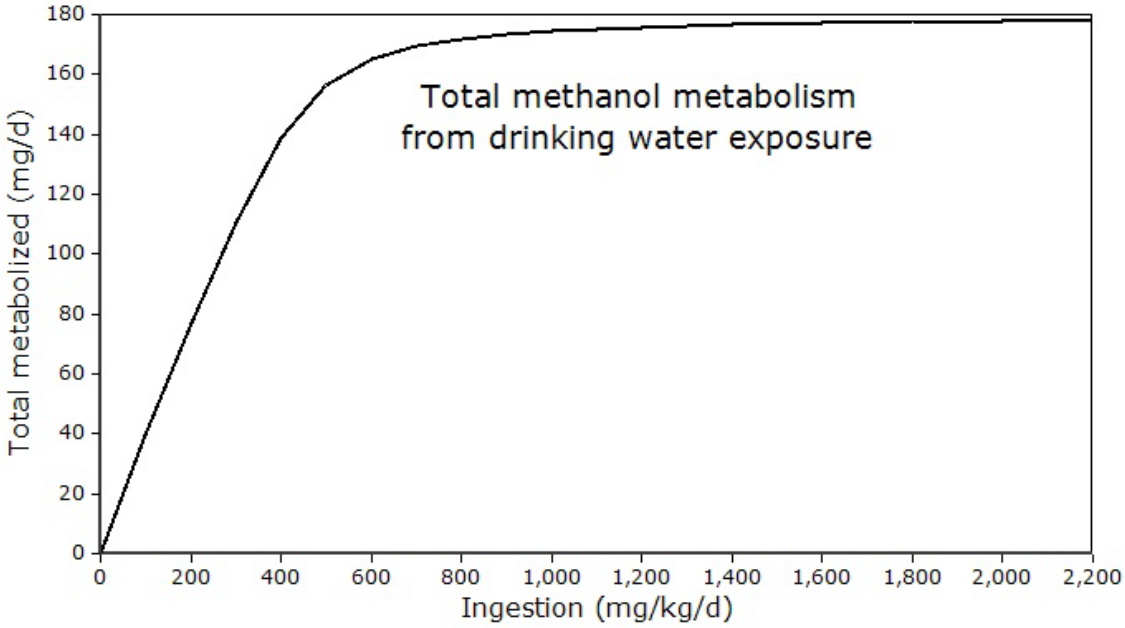

Figure 5-7. Total amount metabolized per day (after periodicity is reached) in a 420 g rat

While, based on this exposure-dose pattern, one might expect a similar exposure-response relationship, this pattern does not include detoxification mechanisms. If such mechanisms also saturate, then it is possible for the slower increase in total metabolism above 400 mg/kg/d to result in a significant increase in effect, though full metabolic saturation at ~2,000 mg/kg/d would still be expected to result in a maximal effect at that exposure level.

5.4.3.8. *Choice of Animal-to-Human Extrapolation Method*

A PBPK model was used to extrapolate animal-to-human concentrations. The estimated methanol metabolized for each dose administered to the animals in NEDO (1985/2008b) and Soffritti et al. (2002a) were determined using the animal PBPK model, and then the $BMDL_{10}$ determined by the methods described previously (Section 5.4.2.1). Assuming that metabolized methanol distributes in the body according to body weight to the ¾ power, the rat mg-day $BMDL_{10}$ was converted to a human mg-day $BMDL_{10}$. The human PBPK model (Appendix B)

was then used to convert this human mg-day values for total methanol metabolized back to a human equivalent methanol oral dose HED($BMDL_{10}$) of 51.5 mg/kg-day for lymphomas in the male rat, and a human equivalent methanol inhalation concentration HEC($BMCL_{10}$) of 81.9 mg/m^3 for pheochromocytomas in the female rat. If traditional dosimetry assumptions are used, the HED($BMDL_{10}$) and HEC($BMCL_{10}$) estimates would have been approximately 4-fold higher than the value derived using the PBPK model.

As discussed in Sections 3.4 and 5.3.4, the PBPK models do not describe or account for background levels of methanol, formaldehyde or formate, and background levels were subtracted from the reported data before use in model fitting or validation (if not already subtracted by study authors), as described below. This approach was taken because the relationship between background doses and background responses is not known, because the primary purpose of this assessment is for the determination of noncancer and cancer risk associated with increases in the levels of methanol or its metabolites (e.g., formate, formaldehyde) over background, and because the subtraction of background levels is not expected to have a significant impact on PBPK model parameter estimates as background levels of methanol and its metabolites are low relative to exposure levels used in methanol bioassays. Further, while it is possible that background levels of methanol or its metabolites contribute to background responses for some adverse effects, the results of dose-response modeling of cancer endpoints using "background dose" models suggest that this contribution is relatively small (see discussion in Appendix E, Section E.4).

5.4.3.9. *Human Relevance of Cancer Responses Observed in Rats and Mice*

As discussed in Sections 4.9.2, there is human evidence for the association of lymphomas with a metabolite of methanol, formaldehyde. However, there is no information available in the literature regarding the observation of cancer in humans following chronic administration of methanol. The only observations in animals were noted in the chronic studies of methanol conducted by Apaja (1980), Soffritti et al. (2002a) and NEDO (1985/2008b) and there is uncertainty associated with the interpretation of the tumor responses reported in these studies. As a consequence, the overall WOE, while convincing, is not strong.

6. MAJOR CONCLUSIONS IN THE CHARACTERIZATION OF HAZARD AND DOSE RESPONSE

6.1. HUMAN HAZARD POTENTIAL

Methanol is the smallest member of the family of aliphatic alcohols. Also known as methyl alcohol or wood alcohol, among other synonyms, it is a colorless, very volatile, and flammable liquid that is widely used as a solvent in many commercial and consumer products. It is freely miscible with water and other short-chain aliphatic alcohols but has little tendency to distribute into lipophilic media. Methanol can be formed in the mammalian organism as a metabolic byproduct and can be ingested with foodstuffs, such as fruits or vegetables. A potential for human exposure exists today in the form of the artificial sweetener, aspartame, which is a methyl ester of the dipeptide aspartyl-phenylalanine. Methanol is the major anti-freeze constituent of windshield washer fluid. Its use as a fuel additive for internal combustion engines is, as yet, limited by its corrosive properties.

Because of its very low oil:water partition coefficient, methanol is taken up efficiently by the lung or the intestinal tract and distributes freely in body water without any tendency to accumulate in fatty tissues. It can be metabolized completely to CO_2, but may also, as a regular byproduct of metabolism, enter the C_1-pool and become incorporated into biomolecules. Animal studies indicate that blood methanol levels increase with the breathing rate and that metabolism becomes saturated at high exposure levels. Because of its volatility it can also be excreted unchanged via urine or exhaled air.

The acute toxicity in laboratory animals in response to high levels of exposure results from CNS depression. NEDO (1987) reported that methanol blood levels around 5,000 mg/L were necessary to cause clinical signs and CNS changes in monkeys. In humans, however, acute toxicity is caused by metabolic acidosis that appears to affect predominantly the nervous system, with potentially lasting effects such as blindness, Parkinson-like symptoms, and cognitive impairment. These effects can be observed in humans when blood methanol levels exceed 200 mg/L. The species differences in toxicity from acute exposures appear to be the result of a limited ability of humans to metabolize formic acid.

Despite the existence of many case reports on acute human exposures, the knowledge base for long-term, low-level exposure of humans to methanol is limited. The current TLV for methanol is 200 ppm (262 mg/m^3) (ACGIH, 2000). Controlled experiments with human volunteers indicate that only minor neurobehavioral changes occur following 4-hour exposure to this concentration. A limited study on self-reported health effects in 66 persons exposed to methanol at levels that came close to or exceeded the NIOSH short-term ceiling of 800 ppm (1048 mg/m^3), in comparison with an age-matched group of 66 less or not exposed persons, suggested a statistically significant increase in the incidence of CNS-related symptoms, such as dizziness, nausea, headache, and blurred vision (Frederick et al., 1984). Impaired vision and

nasal irritation were observed in a study of 33 methanol-exposed workers (Kawai et al., 1991). None of the case reports or human studies have investigated cancer as a potential outcome of methanol exposure.

A number of reproductive, developmental, subchronic and chronic exposure duration studies have been conducted in mice, rats, and monkeys. This summary will focus primarily on reproductive and developmental toxicity, and cancer as the main endpoints of concern. Sections 4.7, 5.1.1 and 5.2.1 contain more extensive summaries that consider the dose-related effects that have been observed in other organ systems following subchronic or chronic exposure.

Although there is no evidence in humans, methanol has shown to be a reproductive and developmental toxicant in several animal studies. No studies have been reported in which humans have been exposed subchronically or chronically to methanol by the oral route of exposure, and thus would be suitable for derivation of an oral RfD. Data exist regarding effects from oral exposure in experimental animals, but they are more limited than data from the inhalation route of exposure (see Sections 4.2, 4.3, and 4.4). Two oral studies in rats (Soffritti et al., 2002a; U.S. EPA, 1986), one oral study in mice (Apaja, 1980) and several inhalation studies in monkeys, rats and mice (NEDO, 1987, 1985/2008a, 2008b) of 90-days duration or longer have been reported. While some noncancer effects of methanol exposure were noted in these studies, principally in the liver and brain, they were either not quantifiable due to study limitations or occurred at high doses relative to reproductive/developmental effects. As discussed below, the results of inhalation reproductive/developmental toxicity studies in rats (NEDO, 1987), mice (Rogers et al., 1993a), and monkeys (Burbacher et al., 2004a, 2004b, 1999a, 1999b) are the principal considerations for both the RfD and RfC values derived in this assessment.

A larger number of studies have used the inhalation route to assess the potential of reproductive or developmental toxicity of methanol in mice, rats, and monkeys, with concentrations ranging from 200 to 20,000 ppm (blood levels reaching as high as 8.65 mg/mL). To sum up the findings, rat dams survived even the highest doses without gross signs of toxicity, but their offspring were severely affected (Nelson et al., 1985). Two more inhalation studies, Rogers et al. (1993a,1993b) and Rogers and Mole (1997), confirmed that methanol causes exencephaly and cleft palate in mice, the most sensitive days being GD6 and GD7 (i.e., early organogenesis). These severe malformations were observed at exposure concentrations of 5,000 ppm or above. Nelson et al. (1985) and Rogers et al. (1993a) also observed an increased occurrence of ossification disturbances and skeletal anomalies at methanol concentrations $\geq$ 2,000 ppm, of which cervical ribs in mouse fetuses is considered the critical effect for toxicity value derivation in this review. A study conducted in pregnant cynomolgus monkeys that were exposed to 200–600 ppm methanol for 2.5 hours/day throughout premating, mating, and gestation showed no signs of maternal or fetal toxicity. The potential compound-related effects

noted were a shortening of the gestation period by less than 5% and developmental neurotoxicity, particularly delayed sensorimotor development (Burbacher et al., 2004a, 2004b, 1999a, 1999b).

While all of the above studies were conducted with exposure durations of 7 hours/day or less, NEDO (1987) conducted a series of developmental/reproductive studies in rats that used exposure times of 20 hours/day or more at concentrations between 500 and 5,000 ppm. A two-generation study by these researchers that exposed the dams throughout pregnancy and the pups through 8 weeks of age, demonstrated dose-dependent reductions in brain weights that forms the basis for the RfC derived in this review.

Carcinogenic effects following methanol exposure were observed in a chronic drinking water study in Eppley Swiss Webster mice (Apaja, 1980) and two chronic rat studies: a drinking water study of Sprague-Dawley rats (Soffritti et al., 2002a) and an inhalation study of F344 rats (NEDO, 1985/2008b). Following administration via drinking water, both Apaja (1980) and Soffritti et al. (2002a) observed positive dose-response trends for increases in the incidence of lymphomas in both test animal genders. Soffritti et al. (2002a) characterized the lymphomas in their study as lymphoreticular, principally lympho-immunoblastic. EPA re-analyzed the lymphoma data from the Soffritti et al. (2002a) study for quantification purposes, combining only tumors of the same cell type origin. There was a slight increase in hepatocellular carcinomas in male rats of all exposure groups of this study that was not statistically elevated over controls in any group, but potentially this tumor is related to methanol exposure given the low historical background rate for this tumor in this rat strain. As discussed in Section 5.4.1.1, the other tumor increases reported by Soffritti et al. (2002a) are not quantifiable or were considered hyperplastic rather than carcinogenic following a review by NTP pathologists (EFSA, 2006; Hailey, 2004). No tumor responses were significantly increased over controls in the chronic inhalation bioassays performed by NEDO (1987) in monkeys, and mice, but the high-dose incidences for pulmonary adenomas/adenocarcinomas in male rats was elevated over concurrent controls and pheochromocytomas in female rats were significantly elevated over historical control incidences for these tumor types within their respective sex and strain. The dose response for both of these tumor types represents increasing trends (Cochran Armitage trend test; $p < 0.05$). Further, both tumor responses are accompanied by proliferative changes (e.g., hyperplastic responses) in their respective cell types.

6.2. DOSE RESPONSE

6.2.1. Noncancer/Inhalation

Clearly defined toxic endpoints at moderate exposure levels have been observed only in reproductive and developmental toxicity studies. Three endpoints from developmental toxicity studies were considered for derivation of the RfC: formation of cervical ribs in CD-1 mice exposed to methanol during organogenesis (Rogers et al., 1993a), deficits in sensorimotor

development as measured by VDR tests administered to monkeys exposed to methanol (Burbacher et al., 2004a, 2004b, 1999a, 1999b), and reduced brain weights in rats exposed to methanol from early gestation through 8 weeks of postnatal life (NEDO, 1987). For the purpose of comparability and to better illustrate methodological uncertainty, reference values were derived for all of these endpoints using a BMD modeling approach which evaluated several models and various measures of risk. In the present review, mostly because of a paucity of adequate long-term or developmental oral studies and the existence of several inhalation studies that examined sensitive subpopulations (pregnant mothers, developing fetuses and neonates) in various species, it was decided to use the critical effect from an inhalation study to derive an RfD. Thus, the criteria and rationales on which the RfC assessment is based also form the basis for the RfD derivation.

The Rogers et al. (1993a) inhalation study is a multidose developmental study that was considered for use in the derivation of a reference value. The exposure concentrations in this study were 0, 1,000, 2,000, and 5,000 ppm administered for 7 hours/day on GD7–GD17. The BMD evaluation, based on the nested log-logistic model of BMDS version 2.1, produced BMD/BMDL values in terms of internal peak blood methanol (C_{max}). PBPK modeling was used to convert the internal animal dose metrics to HECs, and a UF of 100 was applied to yield RfCs of 10.4 mg/m^3 and 13.6 mg/m^3 for 5 and 10% extra risk, respectively.

Reproductive and developmental neurobehavioral effects observed in monkeys following methanol inhalation exposure (Burbacher et al., 2004a, 2004b, 1999a, 1999b) were also considered for use in the derivation of a reference value. *M. fascicularis* monkeys were exposed to 0, 262, 786, and 2,359 mg/m^3 methanol 2.5 hours/day, 7 days/week during premating/mating and throughout gestation (approximately 168 days). Delayed sensorimotor development as measured by a VDR test was the only effect in this study that exhibited a dose-response and is a measure of a functional deficit that is consistent with early developmental CNS effects (e.g., brain weight changes) that have been observed in rats (NEDO, 1987). Though there is uncertainty associated with this effect and its relation to methanol exposure, a BMD analysis was performed for comparative purposes. BMD/BMDL values for the VDR endpoint were estimated using AUCs derived from a monkey PBPK model of blood methanol data reported in the Burbacher et al. (1999a) study. A human methanol PBPK modeling was then used to convert the internal AUC BMDL to an HEC, and a UF of 100 was applied to yield a reference value estimate of 1.7 mg/m^3.

Reduced brain weight was evaluated based on the results of a two-generation study by NEDO (1987) in which fetal rats and their dams were exposed from the first day of gestation until 8 weeks of age, and brain weights were determined at 3, 6, and 8 weeks of age. To obtain reference value estimates from these studies, a rat PBPK model was used to predict PODs in terms of internal doses, which were divided by UFs and converted to HEC reference values via a

human PBPK model (see Table 5-4). BMD modeling was executed using two different BMRs, one S.D. (as is usual with continuous data) and 5% relative (to control response) risk. The resulting reference value estimates were 2.4 and 1.8 mg/m^3 (5% relative risk and 1 S.D., respectively) for reduced brain weight at 6 weeks of age following gestational and postnatal exposure.

Despite the variety of approaches, different critical effects, and different data sources, all reference value estimates fell within a narrow range. The reference value associated with the BMD estimate of the dose corresponding to a one S.D. decrease in brain weight in male rats at 6 weeks post-birth observed in the NEDO (1987) developmental toxicity study is considered most suitable for derivation of the methanol chronic RfC due to the relevance of the exposure scenario/study design (see Sections 5.1.2.2 and 5.3), and endpoint (see Section 5.3) to the potential for developmental effects in neonatal humans, the relative robustness of the dose-response data and because it resulted in one of the lowest reference values of the BMD derivations (see Table 5-4). Thus, the proposed chronic RfC for exposure to methanol is 2 mg/m^3, an evaluation that includes a UF_H of 10 for intraspecies variability, a UF_A of 3 to address the pharmacodynamic component of interspecies variability, and a UF_D of 3 for database uncertainty.

The confidence in this RfC is medium to high. Confidence in the NEDO (1987) developmental studies is medium to high. While there are issues with the lack of reporting detail, the critical effect (brain weight reduction) has been reproduced in an oral study of adult rats (U.S. EPA, 1986c), and the exposure regimen involving pre- and postnatal exposures addresses a potentially sensitive human subpopulation. Confidence in the database is medium. Despite the fact that skeletal and brain effects have been demonstrated and corroborated in multiple animal studies in rats, mice, and monkeys, some study results were not quantifiable, there is uncertainty regarding which is the most relevant test species, and there is limited data regarding reproductive or developmental toxicity of methanol in humans. There is also uncertainty regarding the potential active agent—the parent compound, methanol, formaldehyde, or formic acid. There are deficiencies in our knowledge of the metabolic pathways of methanol in the human fetus during early organogenesis, when the critical effects can be induced in animals. Thus, the medium-to-high confidence in the critical study and the medium confidence in the database together warrant an overall confidence descriptor of medium to high.

6.2.2. Noncancer/Oral

There is a paucity of scientific data regarding the outcomes of chronic oral exposure to methanol. No data exist for long-term methanol exposure of humans. A subchronic (90-day) oral study in Sprague-Dawley rats reported brain and liver weight changes, with some evidence for minor liver damage at 2,500 mg/kg-day that was not supported by histopathologic findings

(U.S. EPA, 1986c). Liver necrosis was reported in Eppley Swiss Webster mice that consumed approximately 2000 mg/kg-day (Apaja, 1980). In the only other study that administered methanol chronically to animals by the oral route, Soffritti et al. (2002a) reported that, overall, there was no pattern of compound-related clinical signs of toxicity in Sprague-Dawley rats exposed to up to approximately 2,000 mg/kg-day. The authors further reported that there were no compound-related signs of gross pathology nor histopathologic lesions indicative of noncancer toxicological effects in response to methanol; however, they did not provide any detailed data to illustrate these findings.

As discussed above and in Section 5.1.1, reproductive and developmental effects are considered the most sensitive and quantifiable effects reported in studies of methanol. Oral reproductive and developmental studies employed single doses that were too high to be of use. In the absence of suitable reproductive or developmental data from oral exposure studies, it was decided to conduct a route-to-route extrapolation and to use the critical effect from the inhalation study (brain weight) to derive an RfD. Thus, the POD (in terms of AUC methanol in blood) used for the derivation of the RfC was also used for the derivation of the RfD. This POD was divided by a UF of 100, and a human PBPK model was used to obtain an RfD value of 0.4 mg/kg-day. As for the RfC, the 100-fold UF includes a UF_H of 10 for intraspecies variability, a UF_A of 3 to address pharmacodynamic uncertainty, and a UF_D of 3 for database uncertainty.

The confidence in the RfD is medium to high. Despite the relatively high confidence in the critical studies, all limitations to confidence as presented for the RfC also apply to the RfD. Confidence in the RfD is slightly lower than for the RfC due to the lack of adequate oral studies for the RfD derivation, necessitating a route-to-route extrapolation.

6.2.3. Cancer/Oral and Inhalation

Under the current *Guidelines for Carcinogen Risk Assessment* (U.S. EPA 2005a, 2005b), methanol fulfils the criteria to be described as *likely to be a human carcinogen* by all routes of exposure. This descriptor is based principally on findings of dose-related, statistically significant increases in the incidence of: lymphoreticular tumors in lifetime studies of both sexes of Eppley Swiss Webster mice (Apaja, 1980) and both sexes of Sprague-Dawley rats (Soffritt et al., 2002a), a slight but significant (compared to historical controls) increase in relatively rare hepatocellular carcinomas in male Sprague-Dawley rats following oral exposure (Soffritti et al., 2002a), and dose-related occurrences of pulmonary adenomas/adenocarcinomas and pheochromocytomas in F344 rats by inhalation exposure (NEDO, 1985/2008b). This determination is supported by the results of other studies that have shown tumorigenic responses similar to those observed by Soffritti et al. (2002a) in rats exposed to formaldehyde, a metabolite of methanol, and to the metabolic precursors of methanol and formaldehyde, aspartame and MTBE. In addition, epidemiological studies have associated exposure to formaldehyde with increases in the

incidence of both leukemias and lymphomas (IARC, 2004). However, the key studies, Soffritti et al. (2002a), NEDO (1985/2008b) and Apaja (1980), have associated uncertainties (see below and discussions in Sections 4.9.2 and 5.4.3) that reduce confidence in the chosen descriptor.

The statistically significant increase in the incidence of lymphoreticular tumors observed in the Soffritti et al. (2002a) drinking water study of Sprague-Dawley rats was used in the determination of the POD for estimating the methanol oral CSF. A PBPK model was developed, and several model predictions of internal dose metrics were considered for use in the dose-response analysis and derivation of the human equivalent dose. Methanol metabolized was selected as the dose metric best suited for derivation of the oral POD because of its superior fit to the response data and consistency with the hypothesis that formaldehyde may be the carcinogenic agent associated with methanol exposure. The EPA multistage cancer model was used to derive a $BMDL_{10}$ for the male rat in terms of mg methanol metabolized/day. Assuming that metabolized methanol distributes in the body according to body weight to the ¾ power, the rat $BMDL_{10}$ of 63.9 mg-day was converted to a human $BMDL_{10}$ of 3,553 mg-day. The human PBPK model was then used to convert this human mg-day value for total methanol metabolized back to a human equivalent methanol oral dose HED($BMDL_{10}$) of 51.5 mg/kg-day for lymphomas in the male rat. The oral CSF of 2E-03 $(mg/kg\text{-}day)^{-1}$ was then derived based on a linear extrapolation from this POD to estimated background levels.

Pulmonary adenomas/adenocarcinomas in male F344 rats and pheochromocytomas in female F344 rats observed in the chronic inhalation study of NEDO (1985/2008b) were considered in the determination of the POD for estimating the inhalation CSF. In this case, all dose metrics estimated by the PBPK model provided a similar acceptable fit to the tumor response data. Methanol metabolized was selected as the dose metric for derivation of the inhalation POD for consistency with the approach used for the derivation of the oral POD and with the hypothesis that formaldehyde may be the carcinogenic agent associated with methanol exposure. As for the oral POD, the EPA multistage cancer model was used to derive a $BMDL_{10}$ for the rat in terms of mg methanol metabolized/day. Assuming that metabolized methanol distributes in the body according to body weight to the ¾ power, the rat $BMDL_{10}$ of 15 mg-day was converted to a human $BMDL_{10}$ of 971 mg-day. The human PBPK model was then used to convert this human mg-day value for total methanol metabolized back to a human equivalent methanol inhalation concentration HEC($BMCL_{10}$) of 81,900 $\mu g/m^3$ for pheochromocytomas in the female rat. The inhalation cancer unit risk of 1E-06 $(\mu g/m^3)^{-1}$ was then derived based on a linear extrapolation from this POD to estimated background levels.

Section 5.4.3 of this assessment documents several uncertainties with the quantification of cancer risk. The main uncertainties can be grouped into issues related to study quality, the interpretation of study results, and the consistency of the results with other laboratories. Other uncertainties discussed in Section 5.4.3 include the choice of tumor endpoint, the choice of dose-

response model, the PBPK model and dose metric used for the animal to human extrapolations, and the human relevance of the carcinogenic responses in rats and mice.

7. REFERENCES

Abbondandolo, A; Bonatti, S; Corsi, C; et al. (1980) The use of organic solvents in mutagenicity testing. Mutat Res 79:141–150.

ACGIH (American Conference of Governmental Industrial Hygienists). (2000) Threshold Limit Values for Chemical Substances and Physical Agents and Biological Exposure Indices. American Conference of Governmental Industrial Hygienists. Cincinnati, OH.

Adanir, J; Ozkalkanti, MY; Aksun, M. (2005) Percutaneous methanol intoxication: Case report. Eur J Anaesthiol 22:560–561.

Agarwal, DP. (2001) Genetic polymorphisms of alcohol metabolizing enzymes. Pathol Biol (Paris) 49(9):703–709.

Airas, L; Paavilainen, T; Marttila, RJ; et al. (2008) Methanol intoxication-induced nigrostriatal dysfunction detected using 6-[18F]fluoro-L-dopa PET. Neurotoxicol 29:671–674.

Akaike, H. (1973) Information theory and an extension of the maximum likelihood principle. Petrov, BN; Csaki, F; eds. Second International Symposium on Information Theory, September 1971, Tsahkadsor, Armenia, USSR. Budapest, Hungary: Akademia Kiado. pp.267–281.

Albert RE, Sellakumar AR, Laskin S, Kuschner M, Nelson N, Snyder CA. 1982. Gaseous formaldehyde and hydrogen chloride induction of nasal cancer in the rat. J Natl Cancer Inst. 68(4):597-603.

Albin, RL and Greenamyre, JT. (1992) Alternative excitotoxic hypotheses. Neurology 42:733–738.

Allen, BC; Kavlock, RJ; Kimmel, CA; et al. (1994) Dose-response assessment for developmental toxicity II: comparison of generic benchmark dose estimates with no observed adverse effect levels. Fundam Appl Toxicol 23:487–495.

Andresen, H; Schmoldt, H; Matschke, J; et al. (2008) Fatal methanol intoxication with different survival times –morphological findings and postmortem methanol distribution. Forensic Sci Intl 179:206–210.

Andrews, JE; Ebron-McCoy, M; Logsdon, TR; et al. (1993) Developmental toxicity of methanol in whole embryo culture: a comparative study with mouse and rat embryos. Toxicology 81(3):205–215.

Andrews, JE; Ebron-McCoy, M; Kavlock, RJ; et al. (1995) Developmental toxicity of formate and formic acid in whole embryo culture: a comparative study with mouse and rat embryos. Teratology 51:243–251.

Andrews, JE; Ebron-McCoy, M; Schmid, JE; et al. (1998) Effects of combinations of methanol and formic acid on rat embryos in culture. Teratology 58(2):54–61.

Andrews, LS; Clary, JJ; Terrill, JB; et al. (1987) Subchronic inhalation toxicity of methanol. J Toxicol Environ Health 20:117–124.

Ang, HL; Deltour, L; Hayamizu, TF; et al. (1996) Retinoic acid synthesis in mouse embryos during gastrulation and craniofacial development linked to class IV alcohol dehydrogenase gene expression. J Biol Chem 271:9526–9534.

Antony, AC. (2007) In utero physiology: role of folic acid in nutrient delivery and fetal development. Am J Clin Nutr 85(suppl):598S– 603S.

Apaja, M. (1980) Evaluation of toxicity and carcinogenicity of malonaldehyde. Acta Universitatis Ouluensis Series D Medica 55 Anatomica, Pathologica, Microbiologica No. 8, 1–59.

Arora, V; Nijjar, IS; Thukral, H; et al. (2005) Bilateral putaminal necrosis caused by methanol intoxication- a case report. Ind J Radiol Imag 15:341–342.

Arora, V; Nijjar, IBS; Multani, AS; et al. (2007) MRI findings in methanol intoxication: a report of two cases. Brit J Radiol 80:e243–e246.

Aschner, M; Kimmelberg, HK. (1996) The Role of Glia in Neurotoxicity, Published by CRC Press, p.365.

ATSDR (Agency for Toxic Substances and Disease Registry). (1997) Toxicological review of methyl tertiary butyl ether. Agency for Toxic Substances and Disease Registry, Department of Health, Atlanta, GA.

ATSDR (Agency for Toxic Substances and Disease Registry). (1999) Toxicological review of formaldehyde. Agency for Toxic Substances and Disease Registry, Department of Health, Atlanta, GA.

Aufderheide, TP; White, SM; Brady, WJ; et al. (1993) Inhalational and percutaneous methanol toxicity in two firefighters. Ann Emergency Med 22(12):1916–1918.

Aziz, MH; Agrawal, AK; Adhami, VM; et al. (2002) Methanol-induced neurotoxicity in pups exposed during lactation through mother: role of folic acid. Neurotoxicol Teratol 24(4): 519–527.

Azmak, D. (2006) Methanol related deaths in Edirne. Legal Med 8:35–42.

Barceloux, DG; Bond, GR; Krenzelok, EP; et al. (2002) American Academy of Clinical Toxicology practice guidelines on the treatment of methanol poisoning. J Toxicol Clin Toxicol 40(4):415–446.

Battelle. (1981) Final report on a chronic inhalation toxicology study in rats and mice exposed to formaldehyde. Prepared for the Chemical Industry Institute of Toxicology. Prepared by Battelle Columbus Laboratories, Columbus, OH. CIIT Docket # 10922.

Batterman, SA; Franzblau, A. (1997) Time-resolved cutaneous absorption and permeation rates of methanol in human volunteers. Int Arch Occup Environ Health 70(5):341–351.

Batterman, SA; Franzblau, A; D'Arcy, JB; et al. (1998) Breath, urine, and blood measurements as biological exposure indices of short-term inhalation exposure to methanol. Int Arch Occup Environ Health 71:325–335.

Bearn, P; Patel, J; O’Flynn, WR. (1993) Cervical ribs: a cause of distal and cerebral embolism. Postgrad Med J 69:65–68.

Bebarta, VS; Heard, K; Dart, RC. (2006) Inhalational abuse of methanol products: elevated methanol and formate levels without vision loss. Am J Emerg Med 24:725–728.

Belpoggi F; Soffritti M; Guarino M; et al. (2002a) Results of long-term experimental studies on the carcinogenicity of Ethylene-bis-Dithiocarbamate (Mancozeb) in rats. Ann NY Acad Sci 982:123–136.

Belpoggi F; Soffritti M; Minardi F; et al. (2002b) Results of long-term carcinogenicity bioassays on tert-amyl-methyl-ether (TAME) and di-isopropyl-ether (DIPE) in rats. Ann N Y Acad Sci 982:70-86.

Belpoggi, F; Soffritti, M; Maltoni, C. (1995) Methyl-tertiary-butyl ether (MTBE) – a gasoline additive – causes testicular and lymphohaematopoietic cancers in rats. Toxicol Ind Health 11:119–149.

Belpoggi, F; Soffritti, M; Filippini, F; et al. (1997) Results of long-term experimental studies on the carcinogenicity of methyl tert-butyl ether. Ann NY Acad Sci 837:77–95.

Belpoggi, F; Soffritti, M; Maltoni, C. (1998) Pathological characterization of testicular tumours and lymphomas-leukaemias, and of their precursors observed in Sprague-Dawley rats exposed to methy-tertiary-butyl-ether (MTBE). Eur J Oncol 3(3):201–206.

Belpoggi, F; Soffritti, M; Maltoni, C. (1999) Immunoblastic lymphomas in Sprague-Dawley rats following exposure to the gasoline oxygenated additives Methyl-Tertiary-Butyl Ether (MTBE) and Ethyl-Tertiary-Butyl Ether (ETBE): early observations on their natural history. Eur J Oncol 4:563-572.

Bennett, IL, Jr; Cary, FH; Mitchell, GL, Jr; et al. (1953) Acute methyl alcohol poisoning: a review based on experiences in an outbreak of 323 cases. Medicine 32:431–463.

Benton, CD; Calhoun, FP Jr. (1952) The ocular effects of methyl alcohol poisoning: report of a catastrophe involving three hundred and twenty persons. Trans Am Acad Ophthalmol Otolaryngol 56(6):875–885.

Bessell-Browne, RJ; Bynevelt, M. (2007) Two cases of methanol poisoning: CT and MRI features. Aust Radiol 51:175–178.

Bhatia, KP; Marsden, CD. (1994) The behavioral and motor consequences of focal lesions of the basal ganglia in man. Brain 117(Pt 4): 859–876.

Black, KA; Eells, JT; Noker, PE; et al. (1985) Role of hepatic tetrahydrofolate in the species difference in methanol toxicity. Proc Natl Acad Sci 82:3854–3858.

Blancato, JN; Evans, MV; Power, FW; et al. (2007) Development and use of PBPK modeling and the impact of metabolism on variability in dose metrics for the risk assessment of methyl tertiary butyl ether (MTBE). J Environ Protect Sci 1:29–51.

Blanco, M; Casado, R; Vasquez; et al. (2006) CT and MR imaging findings in methanol intoxication. Am J Neuroradiol 27:452–454.

Bosron, WF; Li, TK. (1986) Genetic polymorphism of human liver alcohol and aldehyde dehydrogenases, and their relationship to alcohol metabolism and alcoholism. Hepatology 6(3):502–510.

Bouchard, M; Brunet, RC; Droz, PO; et al. (2001) A biologically based dynamic model for predicting the disposition of methanol and its metabolites in animals and humans. Toxicol Sci 64:169–184.

Boutwell, RK. (1964) Some biological aspects of skin carcinogenesis. Prog Exp Tumor Res 4:207–250.

Braden GL; Strayhorn CH; Germain MJ; et al. (1993) Increased osmolal gap in alcoholic acidosis. Arch Intern Med 153(20):2377–80.

Brahmi, N; Blel, Y; Abidi, N; et al. (2007) Methanol poisoning in Tunisia: report of 16 cases. Clin Toxicol 45(6):717–20.

Branch, S; Rogers, JM; Brownie, CF; et al. (1996) Supernumerary lumbar rib: manifestation of basic alterations in embryonic development of ribs. J. Appl. Toxicol. 16:115-119.

Brent, J; Lucas, M; Kulig, K; et al. (1991) Methanol poisoning in a six-week-old infant. J Pediatr 118:644–646.

Brien, JF; Clarke, DW; Richardson, B; et al. (1985) Disposition of ethanol in maternal blood, fetal blood, and amniotic fluid of third-trimester pregnant ewes. Am J Obstet Gynecol 1985 Jul 1;152(5):583–90.

Brown, RP; Delp, MD; Lindstedt, SL; et al. (1997) Physiological parameters values for physiologically based pharmacokinetic models. Toxicol Ind Health 13:407–484.

Bucher, JR. (2002) The National Toxicology Program rodent bioassay: designs, interpretations, and scientific contributions. Ann N Y Acad Sci. Dec; 982:198-207.

Burbacher, TM. (1993) Neurotoxic effects of gasoline and gasoline consituents. Environ Health Perspect 101:133–141.

Burbacher, T; Shen, D; Grant, K; et al. (1999a) Methanol disposition and reproductive toxicity in adult females. Reproductive and offspring developmental effects following maternal inhalation exposure to methanol in nonhuman primates. HEI Research Report Number 89: Part I: 9–68.

Burbacher, T; Grant, K; Shen, D; et al. (1999b) Developmental effects in infants exposed prenatally to methanol. Reproductive and offspring developmental effects following maternal inhalation exposure to methanol in nonhuman primates. HEI Research Report Number 89: Part I: 69–117.

Burbacher, TM; Grant, KS; Shen, DD; et al. (2004a) Chronic maternal methanol inhalation in nonhuman primates (*M. fascicularis*): reproductive performance and birth outcome. Neurotoxicol Teratol 26:639–650.

Burbacher, TM; Shen, DD; Lalovic, B; et al. (2004b) Chronic methanol inhalation in nonhuman primates (*M. fascicularis*): exposure and toxicokinetics prior to and during pregnancy. Neurotoxicol Teratol 26:201–221.

Burnell, JC; Li, T-K; Bosron, WF. (1989) Purification and steady-state kinetic characterization of human liver b3b3 alcohol dehydrogenase. Biochemistry 28:6810–6815.

Burwell RD, Whealin J, Gallagher M. (1992) Effects of aging on the diurnal pattern of water intake in rats. Behav Neural Biol. Nov;58(3):196-203. PubMed PMID: 1456941.

Butchko, HH; Stargel, WW; Comer, CP; et al. (2002) Aspartame: review of safety. Regul Toxicol Pharmacol 35:S1–93.

Calabrese, EJ. (2001) Assessing the default assumption that children are always at risk. Hum Ecol Risk Assess 7(1):37–59.

Caldwell, J; Jinot, J; Devoney, D; et al. (2008) Evaluation of evidence for infection as a MOA for induction of rat lymphoma. Environ Mol Mutagen 49(2):155–164.

Caldwell, J; Jinot, J; Devoney, D; et al. (2009) Author reply to comment on "Evaluation of evidence for infection as the mode of action for induction of rat lymphoma." Environ Mol Mutagen. Jan;50(1): 6-9.

Cameron, AM; Nilsen, OG; Haug, E; et al. (1984) Circulating concentrations of testosterone, luteinizing hormone and follicle stimulating hormone in male rats after inhalation of methanol. Arch Toxicol 7(Suppl):441–443.

Cameron, AM; Zahlsen, K; Haug, E; et al. (1985) Circulating steroids in male rats following inhalation of n-alcohols. Arch Toxicol 8(Suppl):422–424.

Campbell, JA; Howard, DR; Backer, LC; et al. (1991) Evidence that methanol inhalation does not induce chromosome damage in mice. Mutat Res 260:257–264.

Carson, BL; McCann, JL; Ells, JV III; et al. (1981) Methanol Health Effects. Prepared by the Midwest Research Institute. Prepared for the Office of Mobile Source Air Pollution Control, U.S. Environmental Protection Agency, Ann Arbor, MI. PB82-160797.

Caspi, R; Foerster, H; Fulcher, CA; et al. (2006) MetaCyc: a multiorganism database of metabolic pathways and enzymes. Nucleic Acids Res 34:D511–6.

CERHR (Center for the Evaluation of Risks to Human Reproduction). (2004) NTP-CERHR Expert Panel report on the reproductive and developmental toxicity of methanol. Reprod Toxicol 18:303–390.

Chemfinder. (2002) Methanol. Available at http://chemfinder.cambridgesoft.com/.

Chen, JC; Schneiderman, JF; Wortzman, G. (1991) Methanol poisoning: bilateral putaminal and cerebellar cortical lesions on CT and MR. J Comput Assist Tomogr 15(3): 522–524.

Chen-Tsi, C. (1959) Materials on the hygienic standardization of the maximally permissible concentration of methanol vapors in the atmosphere. Gig Sanit 24:7–12 (as cited in Carson, et al., 1981).

Chernoff, N; Roger, JM. (2004) Supernumerary ribs in developmental toxicity bioassays and in human populations: incidence and biological significance. J Toxicol Environ Health 7:437–449.

Chuwers, P; Osterloh, J; Kelly, T; et al. (1995) Neurobehavioral effects of low-level methanol vapor exposure in healthy human volunteers. Environ Res 71(2):141–150.

Cichoz-Lach, H; Partycka, J; Nesina, I; et al. (2007) Genetic polymorphism of alcohol dehydrogenase 3 in digestive tract alcohol damage. Hepatogastroenterology 54(76):1222–7.

Clarke, DW; Steenaart, NA; Brien, F. (1986) Disposition of ethanol and activity of hepatic and placental alcohol dehydrogenase and aldehyde dehydrogenases in the third-trimester pregnant guinea pig for single and short-term oral ethanol administration. Alcohol Clin Exp Res 10(3):330–6.

Clancy, B; Finlay, BL; Darlington, RB; et al. (2007) Extrapolating brain development from experimental species to humans. Neurotoxicology 28(5):931–7.

Clary, JJ. (2003) Methanol, is it a developmental risk to humans? Regul Toxicol Pharmacol 37:83–91.

Clewell, HJ III; Gentry, PR; Gearhart, JM; et al. (2001) Development of a physiologically based pharmacokinetic model of isopropanol and its metabolite acetone. Toxicol Sci 63:160–172.

Cogliano, VJ; Grosse, Y; Baan, RA; et al. (2005) Meeting report: summary of IAEC monographs on formaldehyde, 2-butoxyethanol, and 1-tert-butoxy-2-propanol. Environ Health Perspect 113:1205–1208.

Coleman, CN; Mason, T; Hooker, ER; et al. (1999) Developmental effects of intermittent prenatal exposure to 1,1,1-trichloroethane in the rat. Neurotoxicol Teratol 21(6):699–708.

Connell, JL; Doyle, JC; Gurry, JF. (1980) The vascular complications of cervical ribs. Aust NZ J Surg 50:125–130.

Cook, MR; Bergman, FJ; Cohen, HD; et al. (1991) Effects of methanol vapor on human neurobehavioral measures. HEI Research Report Number 42.

Cook, RJ; Champion, KM; Giometti, CS. (2001) Methanol toxicity and formate oxidation in NEUT2 mice. Arch Biochem Biophys 393:192–198.

Cooper, RL; Mole, ML; Rehnberg, GL; et al. (1992) Effect of inhaled methanol on pituitary and testicular hormones in chamber acclimated and nonacclimated rats. Toxicology 71:69–81.

Corley, RA; Barmett, GA; Ghanayem, BI. (1994) Physiologically based pharmacokinetics of 2-butoxyethanol and its major metabolite, 2-butoxyacetic acid, in rats and humans. Toxicol Appl Pharmacol 129:61–79.

Corley, RA; Mast, TJ; Carney, EW; et al. (2003) Evaluation of physiologically based models of pregnancy and lactation for their application in children's health risk assessments. Crit Rev Toxicol 33:137–211.

Crebelli, R; Conti, G; Conti, L; et al. (1989) A comparative study on ethanol and acetaldehyde as inducers of chromosome malsegregation in *Aspergillus nidulans*. Mutat Res 215:187–195.

Cronholm, T. (1987) Effect of ethanol on the redox state of the coenzyme bound to alcohol dehydrogenase studied in isolated hepatocytes. Biochem J 248:567–572.

Crump, KS. (1984) A new method for determining allowable daily intakes. Fundam Appl Toxicol 4:854–871.

Crump, KS. (1995) Calculation of benchmark doses from continuous data. Risk Anal 15:79–89.

Cruzan, G.. (2009) Assessment of the cancer potential of methanol. Critical Reviews in Toxicology, 2009; 39(4): 347–363.

Cruzan, G; Cushman, JR; Andrews, LS; Granville, GC; Johnson, KA; Hardy, CJ; Coombes, DW; Mullins, PA; Brown, WR. (1998) Chronic toxicity/oncogenicity study of styrene in CD rats by inhalation exposure for 104 weeks. *Toxicol Sci* 46:266–281.

Cumming, ME; Ong, BY; Wade, JG; et al. (1984) Maternal and fetal ethanol pharmacokinetics and cardiovascular responses in near-term pregnant sheep. Can J Physiol Pharmacol 62(12):1435–9.

Davis, VE; Brown, H; Huff, JA; et al. (1967) The alteration of serotonin metabolism to 5-hydroxytrypophol by ethanol ingestion in man. J Lab Clin Med 69:132–140.

Davoli, E; Cappellini, L; Airoldi, L; et al. (1986) Serum methanol concentrations in rats and in men after a single dose of aspartame. Food Chem Toxicol 24:187–189.

D'Alessandro, A; Osterloh, JD; Chuwers; et al. (1994) Formate in serum and urine after controlled methanol exposure at the threshold limit value. Environ Health Perspect 102:178.

De Brabander, N; Wojciechowski, M; De Decker, K; et al. (2005) Fomepizole as a therapeutic strategy in paediatric methanol poisoning. Eur J Pediatr 164:158–161.

De Flora, S; Zanacchi, P; Camoirano, A; et al. (1984) Genotoxic activity and potency of 135 compounds in the Ames reversion test and in a bacterial DNA-repair test. Mutat Res 133:161–198.

Degitz, SJ; Zucker, RM; Kawanishi, CY; et al. (2004a) Pathogenesis of methanol-induced craniofacial defects in C57BL/6J mice. Birth Defects Res. A 70:172–178.

Degitz, SJ; Rogers, JM; Zucker, RM; et al. (2004b) Developmental toxicity of methanol: pathogenesis in CD-1 and C57BL/6J mice exposed in whole embryo culture. Birth Defects Res A70:179–184.

Deltour, L; Foglio, MH; Duester, G. (1999) Metabolic deficiencies in alcohol dehydrogenase ADH1, ADH3, and ADH4 null mutant. Overlapping roles of ADH1 and ADH4 in ethanol clearance and metabolism of retinol to retinoic acid. J Biol Chem 274:16796–16801.

Dethlefs, R; Naraqi, S. (1978) Ocular manifestations and complications of acute methyl alcohol intoxication. Med J Aust 2(10):483-485.

Devore, JL. (1995) Probability and statistics for engineering and the sciences (4th ed). Belmont, CA: Duxbury.

Dicker, E; Cedebaum, AI. (1986) Inhibition of the low K_m mitachondrial aldehyde dehydrogenase by diethyl maleate and phorone in vivo and in vitro implications for formaldehyde metabolism. Biochem J 240:821–828.

Dikalova, AE; Kadiiska, MB; Mason, RP. (2001) An in vivo ESR spin-trapping study: free radical generation in rats from formate intoxication-role of the Fenton reaction. Proc Natl Acad Sci 98:13549–13553.

Dorman, DC; Moss, OR; Farris, GM; et al. (1994) Pharmacokinetics of inhaled (14_C) methanol and methanol-derived 14-C formate in normal and folate-deficient cynomolgus monkeys. Toxicol Appl Pharmacol 128(2):229–238.

Dorman, DC; Bolon, B; Struve, MF; et al. (1995) Role of formate in methanol-induced exencephaly in CD-1 mice. Teratology 52(1):30–40.

Downie, A; Khattab, TM; Malik, MI; et al. (1992) A case of percutaneous industrial methanol toxicity. Occup Med (London) 42(1): 47–49.

Dudka, J. (2006) The total antioxidant status in the brain after ethanol or 4-methyl-pyrazole administration to rats intoxicated with methanol. Exp Toxicol Pathol 57:445–448.

Dutkiewicz, B; Konczalik, J; Karwacki, W. (1980) Skin absorption and per os administration of methanol in men. Int Arch Occup Environ Health 47(1):81–88.

Eells, JT; Black, KA; Tedford, CE; et al. (1983) Methanol toxicity in the monkey: effects of nitrous oxide and methionine. J Pharmacol Exp Ther 227:349–353.

EFSA (European Food Safety Authority). (2006) Opinion of the scientific panel on food additives, flavourings, processing aids and materials in contact with food (AFC) on a request from the commission related to a new long-term carcinogenicity study on aspartame. *The EFSA Journal* 356:1–44.

EFSA (European Food Safety Authority). (2009) Updated Scientific Opinion of the Panel on Food Additives and Nutrient Sources added to Food on a request from the European Commission related to the 2nd ERF carcinogenicity study on aspartame, taking into consideration study data submitted by the Ramazzini Foundation in February 2009. *The EFSA Journal* 1015:1–18.

Ernstgàrd, L; Shibata, E; Johanson, G. (2005) Uptake and disposition of inhaled methanol vapor in humans. Toxicol Sci 88:30–38.

Ernstgàrd, L. (2005) Personal communication. E-mail correspondance from Lena Ernstgàrd to Torka Poet dated March 23, 2005 [see Section B.3.5 of Appendix B].

Estonius, M; Svensson, S; Høøg, JO. (1996) Alcohol dehydrogenase in human tissues: localization of transcripts coding for five classes of the enzyme. FEBS Lett 397:338–342.

Evans, AL. (1999) Pseudoseizures as a complication of painful cervical ribs. Dev Med Child Neurol 41:840–842.

Everitt JI, Richter CB. (1990) Infectious diseases of the upper respiratory tract: implication for toxicology studies. Environ Health Perspect 85:239–247.

Fagan, JF; Singer, LT. (1983) Infant recognition memory as a measure of intelligence. In: Advances in Infancy Research, Ed, Lipsitt, LP. Ablex, New York, NY (as cited in Burbacher et al., 1999a)

Fallang, B; Saugstad, OD; Grøgaard, J; et al. (2003) Kinematic quality of reaching movements in preterm infants. Pediatr Res 53:836–842.

Feany, MB; Anthony, DC; Frosch, MP; et al. (2001) August 2000: two cases with necrosis and hemorrhage in the putamen and white matter. Brain Pathol 11(1):121–122.

Fernandez Noda, EI; Nunez-Arguelles, J; Perez Fernandez, J; et al. (1996) Neck and brain transitory vascular compression causing neurological complications, results of surgical treatment on 1300 patients. J Cardiovasc Surg 37:155–166.

Finkelstein, Y; Vardi, J. (2002) Progressive Parkinsonism in a young, experimental physicist following long-term exposure to methanol. Neurotoxicol 23:521–525.

Fiserova-Bergerova, V; Diaz, ML. (1986) Determination and prediction of tissue-gas partition coefficients. Int Arch Occup Environ Health 58:75–87.

Fisher, JW; Dorman, DC; Medinsky, MA; et al. (2000) Analysis of respiratory exchange of methanol in the lung of the monkey using a physiological model. Toxicol Sci 53:185–193.

Fontenot, AP; Pelak, VS. (2002) Development of neurologic symptoms in a 26-year-old woman following recovery from methanol intoxication. Chest 122(4):1436–1438.

Foster, MW; Stamler, J. (2004) New insights into protein s-nitrosylation-mitochondria as a model system. 279(24):25891–25897.

Frederick, LJ; Schulte, PA; Apol, A. (1984) Investigation and control of occupational hazards associated with the use of spirit duplicators. Am Ind Hyg Assoc J 45:51–55.

Fu, SS; Sakanashi, TM; Rogers, JM; et al. (1996) Influence of dietary folic acid on the developmental toxicity of methanol and the frequency of chromosomal breakage in the CD-1 mouse. Reprod Toxicol 10:455–463.

Galter, D; Carmine, A; Buervenich, S; et al. (2003) Distribution of class I, III, and IV alcohol dehydrogenase mRNAs in the adult rat, mouse and human brain. Eur J Biochem 270:1316–1326.

Gannon KS, Smith JC, Henderson R, Hendrick P. (1992) A system for studying the microstructure of ingestive behavior in mice. Physiol Behav. Mar;51(3):515-21. PubMed PMID: 1523228.

Gaul, HP; Wallace, CJ; Auer, RN et al. (1995) MR findings in methanol intoxication. Am J Neuroradiol 16:1783–1786.

Gentry, PR; Covington, TR; Andersen, ME; et al. (2002) Application of a physiologically based pharmacokinetic model for isopropanol in the derivation of a reference dose and reference concentration. Regul Toxicol Pharmacol 36:51–68.

Gentry, PR; Covington, TR; Clewell, HJ III. (2003) Evaluation of the potential impact of pharmacokinetic differences on tissue dosimetry in offspring during pregnancy and lactation. Regul Toxicol Pharmacol 38:1–16.

Gibson, MAS; Butters, NS; Reynolds, JN; et al. (2000) Effects of chronic prenatal ethanol exposure on locomotor activity, and hippocampal weight, neurons, and nitric oxide synthase activity of the young postnatal guinea pig. Neurotoxicol Teratol 22:183–192.

Gonzalez-Quevedo, A; Obregon, F; Urbina, M; et al. (2002) Effect of chronic methanol administration on amino acids and monoamines in retina, optic nerve, and brain of the rat. Toxicol Appl Pharmacol 185(2):77–84.

Griffiths, AJF. (1981) Neurospora and environmentally induced aneuploidy. In Stich, HF; San, RHC. eds. Short-term Tests for Chemical Carcinogens. Springer-Verlag, pp. 187–199.

Guerri, C and Sanchis, R. (1985) Acetaldehyde and alcohol levels in pregnant rats and their fetuses. Alcohol 2(2):267–70.

Guggenheim, MA; Couch, JR; Weinberg, W. (1971) Motor dysfunction as a permanent complication of methanol ingestion. Arch Neurol 24:550–554.

Hailey, JR. (2004) Chairperson's report: lifetime study in rats conducted by the Ramazzini Foundation. Prepared by J.R. Hailey (pathology working group chair) NIEHS and submitted to F. Belpoggi, November 30, 2004.

Hansen, JM; Contreras, KM; Harris, C. (2005) Methanol, formaldehyde, and sodium formate exposure in rat and mouse conceptuses: a potential role of the visceral yolk sac in embryotoxicity. Birth Defects Res (Part A) 73:72–82.

Hantson, P-E. (2005) Acute methanol intoxication: physiopathology, prognosis and treatment. Bull Mem Acad R Med Belg 160:294–300.

Hantson, P; Duprez, T; Mahieu, P. (1997a) Neurotoxicity to the basal ganglia shown by magnetic resonance imaging (MRI) following poisoning by methanol and other substances. J Toxicol Clin Toxicol 35(2):151–161.

Hantson, P; Lambermont, JY; Mahieu, P. (1997b) Methanol poisoning during late pregnancy. J Toxicol Clin Toxicol 35(2):187–191.

Hanzlik, RP; Fowler, SC; Eells, JT. (2005) Absorption and elimination of formate following oral administration of calcium formate in female human subjects. Drug Metab Dispos 33:282–286.

Hassanian-Moghaddam, H; Pajoumand, A; Dadgar, SM; et al.. (2007) Prognostic factors in methanol poisoning. Human Exp Toxicol 26(7):583–6.

Harris, C; Wang, S-W; Lauchu, JJ; et al. (2003) Methanol metabolism and embryotoxicity in rat and mouse conceptuses: comparison of alcohol dehydrogenase (ADH1), formaldehyde dehydrogenase (ADH3), and CAT. Reprod Toxicol 17:349–357.

Harris, C; Dixon, M; Hansen, JM. (2004) Glutathione depletion modulates methanol, formaldehyde, and formate toxicity in cultured rat conceptuses. Cell Biol Toxicol 20:133–145.

Harris, N; Jaffe, E; Diebold, J; et al. (1999) World Health Organization classification of neoplastic diseases of the hematopoietic and lymphoid tissues: report of the clinical advisory committee meeting-Airlie house, Virginia, November 1997. J Clin Oncol 17(12):3835–3849.

Haseman JK, Hailey JR, Morris RW (1998) Spontaneous neoplasm incidences in Fischer 344 rats and B6C3F1 mice in two-year carcinogenicity studies: A National Toxicology Program update. Toxicol Pathol 26:428–441.

Hass, U; Lund, SP; Simonsen, L; et al. (1995) Effects of prenatal exposure to xylene on postnatal development and behavior in rats. Neurotoxicol Teratol 17(3):341–349.

Hauptmann, M; Lubin, JH; Stewart, PA; et al. (2003) Mortality from lymphohematopoietic malignancies among workers in formaldehyde industries. J Natl Cancer Inst 95:1615–1623.

Health Review Committee. (1999) Commentary. HEI Research Report Number 89: pp. 119–133.

Heck, H; Casanova, M. (2004) The implausibility of leukemia induction by formaldehyde: a critical review of the biological evidence on distant-site toxicity. Regul Toxicol Pharmacol 40:92–106.

Hedberg, JJ; Backlund, M; Stromberg, P; et al. (2001) Functional polymorphisms in the alcohol dehydrogenase 3 (ADH3) promoter. Pharmacogenetics 11(9):815–824.

HEI. (1987) Special Report: Automotive methanol vapors and human health: An evaluation of existing scientific information and issues for further research.

Heidelberger, C; Freeman, AE; Pienta, RJ; et al. (1983) Cell transformation by chemical agents — a review and analysis of the literature. A report of the U.S. Environmental Protection Agency Gene-Tox Program. Mutat Res 114:283–385.

Henderson, MS. (1914) Cervical rib. Report of thirty-one cases. Am J Orthop Surg 11:408–430.

Henderson, WR; Brubacher, J. (2002) Methanol and ethylene glycol poisoning: a case study and review of current literature. Can J Emerg Med 4:34–40.

Hess, DT; Matsumoto, A; Kim, SO; et al. (2005) Protein S-nitrosylation: purview and parameters. Nat Rev Mol Cell Biol 6:150–166

Hinderer, RK; Johnson, MN, Seppala, A; Jacobs, MM; Apaja, M; Patil, KD; Shubik, P. (1979) Toxicity and carcinogenicity of Agerite Resin D (ARD), trimethyldihydroquinoline polymer. Submitted for publication to J. Env. Path. Toxicol. (as cited in Apaja, 1980)

Hines, RN; McCarver, DG. (2002) The ontogeny of human drug-metabolizing enzymes: phase I oxidative enzymes. J Pharmacol Exp Ther 300:355–360.

Horton, VL; Higuchi, MA; Rickert, DE. (1992) Physiologically based pharmacokinetic model for methanol in rats, monkeys, and humans. Toxicol Appl Pharmacol 117:26–36.

Hovda, KE; Hunderi, OH; Tafjord, A-B; et al. (2005) Methanol outbreak in Norway 2002-2004; epidemiology, clinical features and prognostic signs. J Int Med 258:181–190.

Hovda, KE; Mundal, H; Urdal, P; et al. (2007) Extremely slow formate elimination in severe methanol poisoning: a fatal case report. Clin Toxicol 45:516–521.

HSDB (Hazardous Substances Data Bank). (2002) Available at http://toxnet.nlm.nih.gov/cgi-bin/sis/htmlgen?HSDB.

Hsu, HH; Chen, CY; Chen, FH et al. (1997) Optic atrophy and cerebral infarcts caused by methanol intoxication. Neuroradiol 39:192–194.

Huang, QF; Gebrewold, A; Zhang, A; et al. (1994) Role of excitatory amino acids in regulation of rat pial microvasculature. Am J Physiol 266:R158–R163.

Huff, J. (2002) Chemicals studied and evaluated in long-term carcinogenesis bioassays by both the Ramazzini Foundation and the National Toxicology Program: In tribute to Cesare Maltoni and David Rall. Ann NY Acad Sci 982208–982230.

Huff, J; LaDou, J. (2007) Aspartame bioassay findings portend human cancer hazards. Int J Occup Environ HealthOct-Dec;13(4):446-8.

Huff, J; Jacobson, MF and Davis, DL. (2009) The Limits of Two-Year Bioassay Exposure Regimens for Identifying Chemical Carcinogens. Environ Health Perspect 116: 1439-1442.

Hunderi, OH; Hovda, KE; Jacobsen, D. (2006) Use of the osmolal gap to guide the start and duration of dialysis in methanol poisoning. Scand J Urol Nephrol 40:70–74.

IARC (International Agency for Research on Cancer). (2004) Formaldehyde, 2-butoxyethanol and 1-tert-butoxy-2-propanol. Summary of data reported and evaluation. IARC Monographs on the Evaluation of Carcinogenic Risks to Humans 88:1–7.

Im, H; Mun, J; Khim, JY; et al. (2006) Evaluation of toxicological monitoring markers using proteomic analysis in rats exposed to formaldehyde. J Proteome Res 5:1354–1366.

Infurna, R; Weiss, B. (1986) Neonatal behavioral toxicity in rats following prenatal exposure to methanol. Teratology 33:259–265.

Ingemansson, SO. (1984) Clinical observations on ten cases of methanol poisoning with respect to ocular manifestations. Acta Opthalmolog (Copenh) 62(1):15–24.

IPCS (International Programme on Chemical Safety). (1997) Environmental Health Criteria 196 -- Methanol 180.

Ishii, H. (1981) Incidence of brain tumors in rats fed aspartame. Toxicol Lett 7:433–437 (as cited in EFSA, 2006).

Ishii, H; Koshimizu, T; Usami, S; et al. (1981) Toxicity of aspartame and its diketopiperazine for Wistar rats by dietary administration for 104 weeks. Toxicol Lett 21:91–94 (as cited in EFSA, 2006)

Jacobsen, D; McMartin, KE. (1986) Methanol and ethylene glycol poisonings Mechanism of toxicity, clinical course, diagnosis and treatment. Med Toxicol 1:309–334.

Jacobsen, D; Webb, R; Collins, TD; et al. (1988) Methanol and formate kinetics in late diagnosed methanol intoxication. Med Toxicol 3:418–423.

Johanson, G; Kronborg, H; Naslund, PH; et al. (1986) Toxicokinetics of inhaled 2 butoxyethanol (ethylene glycol monobutyl ether) in man. Scand J Work Environ Health 12(6): 594–602.

Johlin, FC; Fortman, CS; Nghiem, DD; et al. (1987) Studies on the role of folic acid and folate-dependent enzymes in human methanol poisoning. Mol Pharmacol 31(5):557–61.

Kahn, A; Blum, D (1979) Methyl alcohol poisoning in an 8-month-old boy: an unusual route of intoxication. J Pediatrics 94(5):841–843.

Kamata E, Nakadate M, Uchida O, Ogawa Y, Suzuki S, Kaneko T, Saito M, Kurokawa Y. 1997. Results of a 28-month chronic inhalation toxicity study of formaldehyde in male Fisher-344 rats. J Toxicol Sci. 22(3):239-54.

Kavet, R; Nauss, K. (1990) The toxicity of inhaled methanol vapors. Crit Rev Toxicol 21(1):21–50.

Kavlock, RJ; Allen, BC; Faustman, EM; et al. (1995) Dose-response assessments for developmental toxicity. IV: Benchmark doses for fetal weight changes. Fund Appl Toxicol 26: 211–222.

Kawai, T; Yasugi, T; Mizunma, K; et al. (1991) Methanol in urine as a biological indicator of occupational exposure to methanol vapor. Int Arch Occup Environ Health 63:311–318.

Keles, GT; Örgüç, S; Toprak, B; et al. (2007) Methanol poisoning with necrosis corpus callosum. Clin Toxicol 45:307–308.

Kerns, WD; Pavkov, KL; Donofrio, DJ; et al. (1983) Carcinogenicity of formaldehyde in rats and mice after long-term inhalation exposure. Cancer Res 43:4382–4392.

Kerns, W II; Tomaszewski, C; McMartin, K; et al. META Study Group. (2002) Formate kinetics in methanol poisoning. J Toxicol Clin Toxicol 40:137–143.

Keys DA, Schultz IR, Mahle DA, Fisher JW. (2004) A quantitative description of suicide inhibition of dichloroacetic acid in rats and mice. Toxicol Sci. Dec;82(2):381-93. Sep 16. PubMed PMID: 15375292.

Kim, SW; Jang, YJ; Chang, JW; et al. (2003) Degeneration of the nigrostriatal pathway and induction of motor deficit by tetrahydrobiopterin: an in vivo model relevant to Parkinson's disease. Neurobiology of Disease 13:167–176.

Knowles, K. (2008) Personal communication. E-mail correspondance from Kathryn Knowles to Jeff Gift dated June 14, 2008.

Kraut, JA; Kurtz, I. (2008) Toxic alcohol ingestions: clinical features, diagnosis, and management. Clin J Am Soc Nephrol 3(1):208–225.

Kuteifan, K; Oesterle, H; Tajahmady, T; et al., (1998) Necrosis and hemorrhage of the putamen in methanol poisoning shown on MRI. Neuroradiol 40:158–160.

Leakey JEA, Seng JE, Allaben WT. 2003. Body weight considerations in the B6C3F1 mouse and the use of dietary control to standardize background tumor incidence in chronic bioassays. Toxicol Appl Pharmacol 193:237–265.

Lee, EW; Brady, AN; Brabec, MJ; et al. (1991) Effects of methanol vapors on testosterone production and testis morphology in rats. Toxicol Ind Health 7(4):261–275.

Lee, EW; Terzo, TS; D'Arcy, JB; et al. (1992) Lack of blood formate accumulation in humans following exposure to methanol vapor at the current permissible exposure limit of 200 ppm. Am Ind Hyg Assoc J 53:99–104.

Lee, EW; Garner, CD; Terzo, TS. (1994) Animal model for the study of methanol toxicity: comparison of folate-reduced rat responses with published monkey data. J Toxicol Environ Health 41:71–82.

Lewis, RJ Jr. (1992) Sax’s dangerous properties of industrial materials. 8th edition Van Nostrand Reinhold, New York, NY.

Ley, CO; Gali, FG. (1983) Parkinsonian syndrome after methanol intoxication. Eur Neurol 22:405–409.

Lilly, MZ; Gold, KW; Rogers, RR. (1995) Integrating QA prinicples with basic elements of a research program promotes quality science in a nonGLP research laboratory. In vitro Toxicol 8:191–198.

Lindsey, JR; Davidson, MK; Schoeb, TR; Cassell, GH. (1985) *Mycoplasma pulmonis*-host relationships in a breeding colony of Sprague-Dawley rats with enzootic murine respiratory mycoplasmosis. Lab Anim Sci 35:597–608.

Liu, JJ; Daya, MR; Carrasquillo, O; et al. (1998). Prognostic factors in patients with methanol poisoning. J Toxicol Clin Toxicol 36(3):175–181.

Liu, L; Hausladen, A; Zeng, M; et al. (2001) A metabolic enzyme for S-nitrosothiol conserved from bacteria to humans. Nature 410:490–494.

Lorente, C; Cordier, S; Bergeret, A; et al. (2000) Maternal occupational risk factors for oral clefts. Scand J Work Environ Health 26(2):137–145.

Mahieu, P; Hassoun, A; Lauwerys, R; et al. (1989) Predictors of methanol intoxication with unfavorable outcome. Hum Toxicol 8(2):135–137.

Makar, AB; Tephly, TR; Mannering, GJ. (1968) Methanol metabolism in the monkey. Mol Pharmacol 4:471–483.

Maltoni, C; Lefemine, G; Cotti, G. (1986) Experimental research on trichlorothylene carcinogenesis. Princeton: Princeton Scientific Publishing Co.

Maltoni C, Ciliberti A, Cotti G, Perino G. 1988. Long-term carcinogenicity bioassays on acrylonitrile administered by inhalation and by ingestion to Sprague-Dawley rats. Ann N Y Acad Sci. 534:179-202.

Maltoni, C; Ciliberti, A; Pinto, C; et al. (1997) Results of long-term experimental carcinogenicity studies of the effects of gasoline, correlated fuels, and major gasoline aromatics on rats. Ann N Y Acad Sci 837:15–52.

Mann, WJ; Muttray, A; Schaefer, D; et al. (2002) Exposure to 200 ppm of methanol increases the concentrations of interleukin-1beta and interleukin-8 in nasal secretions of healthy volunteers. Ann Otol Rhinol Laryngol 111:633–638.

Mannering, GJ; Van Harken, DR; Makar, AB; et al. (1969) Role of the intracellular distribution of hepatic CAT in the peroxidative oxidation of methanol. Ann NY Acad Sci 168:265–280.

Maronpot, RR; Flake, G; Huff, J. (2004) Relevance of animal carcinogenesis findings to human cancer predictions and prevention. Toxicol Pathol. Mar-Apr;32 Suppl 1:40–8. Review.

McGregor, DB; Martin, R; Riach, CG; et al. (1985) Optimization of a metabolic activation system for use in the mouse lymphoma L5178Y tk^+tk^- system. Environ Mutagen 7(Suppl 3):10.

McConnell, E; Solleveld, H; Swenberg, J; et al. (1986) Guidelines for combining neoplasms for evaluation of rodent carcinogenesis studies. J Natl Cancer Inst 76(2):283–289.

McKellar, MJ; Hidajat, RR; Elder, MJ. (1997) Acute ocular toxicity: clinical and electrophysiological features Aust NZ J Opthalmol. 25(3):225–230.

Medinsky, MA; Dorman, D; Bond, J; et al. (1997) Pharmacokinetics of methanol and formate in female cynomolgus monkeys exposed to methanol vapors. HEI Research Report Number 77:1–38.

Melnick RL, Thayer KA, and Bucker JR. 2007. Conflicting views on chemical carcinogenesis arising from the design and evaluation of rodent carcinogenicity studies. Environ Health Perspect 116:130–135; doi:10.1289/ehp.9989 (available at dx.doi.org).

Meister, A; Anderson, ME. (1983) Glutathione. Ann Rev Biochem 52:711–760.

Methanol Institute. (2006) Methanol Institute Milestones. Washington, D.C. Available at http://www.methanol.org

Meyer, RJ; Beard, ME; Ardagh, MW; et al. (2000) Methanol poisoning. NZ Med J 113(1102):11–13.

Molinary, S.V. 1984. Preclinical studies of aspartame in nonprimate animals. In Aspartame: Physiology and Biochemistry (L.D. Stegink and L.J. Filer, Jr., Eds.), pp. 289-306. Marcel Dekker, Inc., New York.

Molotkov, A; Deltour, L; Foglio, MH; et al. (2002) Distinct retinoid metabolic functions for alcohol dehydrogenase genes ADH1 and ADH4 in protection against vitamin A toxicity or deficiency revealed in double null mutant mice. J Biol Chem 277:13804–13811.

Montserrat, CA; Field, MS; Perry, C; Ghandour, H; Chiang, E; Selhub, J; Shane, B; and Stover, PJ. (2006) Regulation of Folate-mediated One-carbon Metabolism by 10-Formyltetrahydrofolate Dehydrogenase. The Journal of Biological Chemistry 281(27): 18335–18342.

Mooney, SM; Miller, MW. (2001) Episodic exposure to ethanol during development differentially effects brainstem nuclei in the macaque. J Neurocytol 30:973–982.

Muthuvel, A; Rajamani, R; Senthilvelan, M; et al. (2006a) Modification of allergenicity and immunogenicity of formate dehydrogenase by conjugation with linear mono methoxy poly ethylene glycol: improvement in detoxification of formate in methanol poisoning. Clin Chim Acta 374:122–128.

Muthuvel, A; Rajamani, R; Manikandan, S; et al. (2006b) Detoxification of formate by formate dehydrogenase-loaded erythrocytes and carbicarb in folate-deficient methanol-intoxicated rats. Clin Chim Acta 367:162–169.

Nagasawa, H; Wada, M; Koyama, S; et al. (2005) A case of methanol intoxication with optic neuropathy visualized on STIR sequence of MR images. Clin Neurol 45:527–530.

Naraqi, S; Dethlefs, RF; Slobodniuk, RA; et al. (1979) An outbreak of acute methyl alcohol intoxication Aust N Z J Med 9(1):65–68.

NCI (National Cancer Institute). (2006) Prospective study of aspartame-containing beverages and risk of hematopoietic and brain cancers. Abstract No. 4010. Available from the American Association for Cancer Research (97th AACR Annual Meeting, Washington, DC) at http://www.aacr.org (as cited in EFSA, 2006).

NEDO (New Energy Development Organization). (1987) Toxicological research of methanol as a fuel for power station. Summary report on tests with monkeys, rats and mice. New Energy Development Organization, Tokyo, Japan. Unpublished report.

NEDO. (1985/2008a) Test Report: 18-month inhalation carcinogenicity study on methanol in B6C3F1 mice (Test No. 4A-223). Eight volume translation (consisting of report text, summary tables, individual animal tables and copies of pathology slides) of original report prepared by the Mitsubishi Kasei Institute of Toxicology and Environmental Sciences (currently Mitsubishi Chemical Safety Insitute, Ltd.) for the New Energy Development Organization, Tokyo, Japan. (Original report prepared in 1985; Translation submitted to the EPA IRIS hotline by the Methanol Insitute on March 28, 2008 and certified as accurate and complete by NEDO in letter dated May 12, 2008). Unpublished report.

NEDO. (1985/2008b) Test Report: 24-month inhalation carcinogenicity study on methanol in Fischer rats (Test No. 5A-268). Eight volume translation (consisting of report text, summary tables, individual animal tables and copies of pathology slides) of original report prepared by the Mitsubishi Kasei Institute of Toxicology and Environmental Sciences (currently Mitsubishi Chemical Safety Insitute, Ltd.) for the New Energy Development Organization, Tokyo, Japan. (Original report prepared in 1985; Translation submitted to the EPA IRIS hotline by the Methanol Insitute on March 28, 2008 and certified as accurate and complete by NEDO in letter dated May 12, 2008). Unpublished report.

Nelson, BK; Brightwell, WS; MacKenzie, DR; et al. (1985) Teratological assessment of methanol and ethanol at high inhalation levels in rats. Fund Appl Toxicol 5:727–736.

Nelson, J. (1967) Respiratory infections of rats and mice with emphasis on indigenous mycoplasms. In: Pathology of laboratory rats and mice. Cotchin, E; Rose, F, eds. Blackwell Scientific Publications, Oxford and Edinburgh, G.B. pp. 259–294.

Nguyen, T; Baumgartner, F; Nelems, B. (1997) Bilateral rudimentary first ribs as a cause of thoracic outlet syndrome. J Natl Med Assoc 89:69–73.

Nilsson, JA; Hedberg, JJ; Vondracek, M; et al. (2004) Alcohol dehydrogenase 3 transcription associates with proliferation of human oral keratinocytes. Cell Mol Life Sci 61:610–617.

Noker, PE; Eells, JT; Tephly, TR; et al. (1980) Methanol toxicity: treatment with folic acid and 5-formyl tetrahydrofolic acid. Alcohol Clin Exp Res 4:378–383.

NRC (National Research Council). (1994) Science and judgment in risk assessment. Prepared by the Committee on Risk Assessment of Hazardous Air Pollutants, Board on Environmental Studies and Toxicology, Commission on Life Sciences. National Academy Press, Washington, D.C.

NRC (National Research Council). (1983) Risk assessment in the federal government: managing the process. Washington, DC: National Academy Press.

NTP (National Toxicology Program). (1990) Toxicology and Carcinogenesis Studies of Toluene (CAS No.108-88-3) in F344/N Rats and B6C3F1 Mice (Inhalation Studies). Public Health Service, U.S. Department of Health and Human Services; NTP TR 371; Available from

the National Institute of Environmental Health Sciences, Research Triangle Park, NC and online at http://ntp.niehs.nih.gov/ntp/htdocs/LT_rpts/tr371.pdf.

NTP (National Toxicology Program). (1999) Toxicology Data Management System, Historical Control Tumor Incidence Summary. – Inhalation Studies of Fischer 344 Rats. Report updated 12/99. Available at http://ntp.niehs.nih.gov.

NTP (National Toxicology Program). (2000) NTP technical report on the toxicology and carcinogenesis studies of 2 butoxyethanol (CAS No. 111 76 2) in F344/N rats and B6C3F1 mice (inhalation studies). Public Health Service, U.S. Department of Health and Human Services; NTP TR 484; NIH Publ. No. 00-3974. Available from the National Institute of Environmental Health Sciences, Research Triangle Park, NC and online at http://ntp.niehs.nih.gov/ntp/htdocs/LT_rpts/tr484.pdf.

NTP (National Toxicology Program). (2003) NTP Technical Report. Toxicity studies of aspartame in FVB/N-TgN(v-Ha-ras)Led (Tg.AC) hemizygous mice and carcinogenicity studies of aspartame in B6.129-Trp53m&Brd (N5) haploinsufficient mice. NTP GMM 1, Research Triangle Park, NC (as cited in EFSA, 2006).

NTP (National Toxicology Program). (2006) Specifications for the conduct of studies to evaluate the toxic and carcinogenic potential of chemical, biological and physical agents in laboratory animals for the national toxicology program (NTP). Available at http://ntp.Niehs.Nih.Gov/files/specifications_2006oct1.Pdf.

NTP (National Toxicology Program). (2007) NTP Historical Controls Report, All Routes and Vehicles, Rats. Report prepared October, 2007. Available at http://ntp.niehs.nih.gov.

OECD (Organization for Economic Co-operation and Development). (2007) Establishment and control of archives that operate in compliance with the principles of GLP. OECD Environment, Health and Safety Publications. No. 15. OECD Environment Directorate, Paris, France.

Ohno, K; Tanaka-Azuma, Y; Yoneda, Y; et al. (2005) Genotoxicity test system based on *p53R2* gene expression in human cells: Examination with 80 chemicals. Mutat Res 588:47–57.

Onder, F; Ilker, S; Kansu, T; et al. (1999) Acute blindness and putaminal necrosis in methanol intoxication. Int Opthalmol 22:81–84.

Osterloh, JD; D'Alessandro, A; Chuwers, P; et al. (1996) Serum concentrations of methanol after inhalation at 200 ppm. J Occup Environ Med 38:571–576.

Pace, V; Perentes, E; Germann, PG. (2002) Pheochromocytomas and ganglioneuromas in the aging rats: morphological and immunohistochemical characterization. Toxicol Pathol 30(4):492–500.

Parthasarathy, NJ; Kumar, RS; Karthikeyan, P; et al. (2005a) In vitro and in vivo study of neutrophil functions after acute methanol intoxication in albino rats. Toxicol Environ Chem 87:559–566.

Parthasarathy, NJ; Kumar, RS; Devi, RS. (2005b) Effect of methanol intoxication on rat neutrophil functions. J Immunotoxicol 2:115–211.

Parthasarathy, NJ; Kumar, RS; Manikandan, S; et al. (2006a) Effect of methanol-induced oxidative stress on the neuroimmune system of experimental rats. Chemico-Biological Inter 161:14–25.

Parthasarathy, NJ; Kumar, RS; Manikandan, S; et al. (2006b) Methanol-induced oxidative stress in rat lymphoid organs. J Occup Health 48:20–27.

Parthasarathy, NJ; Kumar, RS; Manikandan, S; et al. (2007) Effect of methanol intoxication on specific immune functions of albino rats. Cell Biol Toxicol 23:177–187.

Pastino, GM; Conolly, RB. (2000) Application of a physiologically based pharmaco-kinetic model to estimate the bioavailability of ethanol in male rats: distinction between gastric and hepatic pathways of metabolic clearance. Toxicol Sci 55(2):25665.

Patankar, T; Bichile, L; Karnad, D; et al. (1999) Methanol poisoning: computed tomography scan findings in four patients. Austral Radiol 43(4):526–528.

Pelletier, JU; Habib, MH; Khalil, R; et al. (1992) Putaminal necrosis after methanol intoxication. J Neurol Neurosurg Psychiatry 55(3): 234–235.

Peng, MT; Chen, YT; Hung, SH; Yaung, CL. (1990) Circadian rhythms of feeding and drinking behavior of rats aged from 3 to 21 months. Proc Natl Sci Counc Repub China B. Apr;14(2):98-104. PubMed PMID: 2247537.

Perkins, RA; Ward, KW; Pollack, GM. (1995a) Comparative toxicokinetics of inhaled methanol in the female CD-1 mouse and Sprague-Dawley rat. Fundam Appl Toxicol 28: 245–254.

Perkins, RA; Ward, KW; Pollack, GM. (1995b) A pharmacokinetic model of inhaled methanol in humans and comparison to methanol disposition in mice and rats. Environ Health Perspect 103:726–733.

Perkins, RA; Ward, KW; Pollack, GM. (1996) Methanol inhalation: site and other factors influencing absorption, and an inhalation toxicokinetic model for the rat. Pharm Res 13:749–755.

Phang, PT; Passerini, L; Mielke, B; et al. (1988) Brain hemorrhage associated with methanol poisoning. Crit Care Med 16:137–140.

Pietruszko, R. (1980) Alcohol and aldehyde dehydrogenase isozymes from mammalian liver-their structural and functional differences. Isozymes Curr Top Biol Med Res 4:107–130.

Pikkarainen, PH; Raiha, NCR. (1967) Development of alcohol dehydrogenase activity in the human liver. Pediatr Res 1(3):165–168.

Pinkerton, LE; Hein, MJ; Stayner, LT. (2004) Mortality among a cohort of garment workers exposed to formaldehyde: an update. Occup Environ Med 61:193–200.

Pitkin, RM. (2007) Folate and neural tube defects. Am J Clin Nutr 85:285S–288S.

Plantinga, Y; Perdock, J; de Groot, L. (1997) Hand function in low-risk preterm infants: its relation to muscle power regulation. Dev Med Child Neurol 39:6–11.

Poet, TS; Teeguarden, JG; Hinderliter, PM. (2006) Final Report: Development, calibration and application of a methanol PBPK model. Prepared for the National Center for Environmental Assessment, U.S. EPA. Prepared by the Center for Biological Monitoring and Modeling, Battelle Pacific Northwest National Laboratory, Richland, WA.

Pollack, GM; Brouwer, KL. (1996) HEI Research Report Number 74: Maternal-Fetal Pharmacokinetics of Methanol. 58.

Pollack, GM; Brouwer, KL; Kawagoe, JL. (1993) Toxicokinetics of intravenous methanol in the female rat. Fundam Appl Toxicol 21:105–110.

Pollack, GM; Kawagoe, JL. (1991) Determination of methanol in whole blood by capillary gas chromatography with direct on-column injection. J Chromatogr B Biomed Appl 570:406–11.

Poon, R; Chu, IH; Bjarnason, S; et al. (1994) Inhalation toxicity study of methanol, toluene and methanol/toluene mixtures in rats: effects of 28-day exposure. Toxicol Ind Health 10(3):231–245.

Poon, R; Chu, IH; Bjarnason, S; et al. (1995) Short-term inhalation toxicity of methanol, gasoline and methanol/gasoline in the rat. Toxicol Ind Health 11(3):343–361.

Prabhakaran, V; Ettler, H; Mills, A; et al. (1993) Methanol poisoning: two cases with similar plasma methanol concentrations but different outcomes. Can Med Assoc J 148(6): 981–984.

Que, LG; Yan, Y; Whitehead, GS; et al. (2005) Protection from experimental asthma by an endogenous bronchodilator. Science 308:1618–1621.

Rajamani, R; Muthuvel, A; Senthilvelan, M; et al. (2006) Oxidative stress induced by methotrexate alone and in the presence of methanol in discrete regions of the rodent brain, retina and optic nerve. Toxicol Lett 165:265–273.

Ramazzini Foundation. 2006. European Ramazzini Foundation stands behind aspartame study results, announces ongoing research on artificial sweeteners. Available at http://www.ramzzini/it/eng/fondazione/eventidettagli.asp?id5292

Ramsey, JC; Andersen, ME. (1984) A physiologically based description of the inhaled pharmacokinetics of styrene in rats and humans. Toxicol Appl Pharmacol 73:159–175.

Rappaport, H. (1966) Tumors of the hematopoietic system. In: Atlas of Tumor Pathology, Sect III. Fasc. 9: Armed Forces Institute of Pathology. Wahsington, D.C., pp. 49-64 [as cited in Apaja, 1989]

Razin, S; Yogev, D; Naot, Y. (1998) Molecular biology and pathogenicity of mycoplasmas. Microbiol Mol Biol Rev. Dec; 62(4):1094–156. Review.

Rice, D; Barone, S Jr. (2000) Critical periods of vulnerability for the developing nervous system: evidence from humans and animal models. Environ Health Perspect 108(Suppl 3): 511–33.

Riegel, H; Wolf, G. (1966) Severe neurological deficiencies as a consequence of methyl alcohol poisoning. Fortschr Neurol Psychiat 34:346–351.

Rogers, JM; Barbee, BD; Mole, ML. (1995) Exposure concentration and time (CxT) relationships in the developmental toxicity of methanol in mice. Toxicologist 15:164.

Rogers, JM; Barbee, BD; Rhenberg, BF. (1993b) Critical periods of sensitivity for the developmental toxicity of inhaled methanol. Teratology 47:395.

Rogers, JM; Brannen, KC; Barbee, BD; et al. (2004) Methanol exposure during gastrulation causes holoprosencephaly, facial dysgenesis, and cervical vertebral malformations in C57BL/6J mice. Birth Defects Res B 71:80–88.

Rogers, JM; Mole, ML. (1997) Critical periods of sensitivity to the developmental toxicity of inhaled methanol in the CD-1 mouse. Teratology 55(6):364–372.

Rogers, JM; Mole, ML; Chernoff, N; et al. (1993a) The developmental toxicity of inhaled methanol in the CD-1 mouse, with quantitative dose-response modeling for estimation of benchmark doses. Teratology 47(3):175–88.

Rogers, VV; Wickstrom, M; Liber, K; et al. (2002) Acute and Subchronic Mammalian Toxicity of Naphthalenic Acids from Oil Sands Tailings. Toxicol Sci 66:347–355.

Rotenstreich, Y; Assia, EI; Kesler, A. (1997) Late treatment of methanol blindness. Brit J Opthalmol 81:415–420.

Rubinstein, D; Escott, E; Kelly, JP. (1995) Methanol intoxication with putaminal and white matter necrosis: MR and CT findings. Am J Neuroradiol 16(7):1492–1494.

Sakanashi, TM; Rogers, JM; Fu, SS; et al. (1996) Influence of maternal folate status on the developmental toxicity of methanol in the CD-1 mouse. Teratology 54:198–206.

Salzman, M. (2006) Methanol neurotoxicity. Clin Toxicol 44:89–90.

Saxton, EH; Miller, TQ; Collins, JD. (1999) Migraine complicated by brachial plexopathy as displayed by MRI and MRA: aberrant subclavian artery and cervical ribs. J Natl Med Assoc 91:333–341.

Sayers, RR; Yant, WP; Schrenk, HH; et al. (1944) Methanol poisoning: II. Exposure of dogs for brief periods eight times daily to high concentrations of high methanol vapor in air. J. Ind Hyg Toxicol 28:255–259.

Schaefer, PW; Grant, PE; Gonzalez, RG. (2000) Diffusion-weighted MR imaging of the brain. Radiol 217(2):331–345.

Schoeb, TR; Mcconnell, EE; Juliana, MM; Davis, JK; Davidson, MK; and Lindsey, JR. (2009) *Mycoplasma pulmonis* and Lymphoma in Bioassays in Rats. Vet Pathol 46.

Schulte, PA; Burnett, CA; Boeniger, MF; et al. (1996) Neurodegenerative diseases: occupational occurrence and potential risk factors, 1982–1991. Am J Public Health 86: 1281–1288.

Schumacher, R; Mai, A; Gutjahr, P. (1992) Association of rib abnormalities and malignancy in childhood. Eur J Pediatr 151:432–434.

Scrimgeour, EM; Dethlefs, RF; Kevau, I. (1982) Delayed recovery of vision after blindness caused by methanol poisoning. Med J Aust 2(10):481–483.

Sedivec, V; Mraz, M; Flek, J. (1981) Biological monitoring of persons exposed to methanol vapors. Int Arch Occup Environ Health 48:257–271.

Sefidbakht, S; Rasekhi, AR; Kamali, K; et al. (2007) Methanol poisoning: acute MR and CT findings in nine patients. Neuroradiol 49:427–435.

Sellakumar AR, Snyder CA, Solomon JJ, Albert RE. 1985. Carcinogenicity of formaldehyde and hydrogen chloride in rats. Toxicol Appl Pharmacol. 81(3 Pt 1):401-6.

Short, DW. 1975. The subclavian artery in 16 patients with complete cervical ribs. J Cardiovasc Surg 16:135–141.

Simintzi, I; Schulpis, KH; Angelogianni, P; et al. (2007) The effect of aspartame metabolites on the suckling rat frontal cortex acetylcholinesterase. An in vitro study. Food Chem Toxicol 45:2397–2401.

Simmon, VF; Kauhanen, K; Tardiff, RG. (1977) Mutagenic activity of chemicals identified in drinking water. Scott, D; Bridges, B; Sobel, F. eds. Progress in Genetic Toxicology. Vol 2. Elsevier/North Holland Press; pp. 249–268.

Sinkeldam, E; Kuper, C; Beems, R; et al. (1991) Combined chronic toxicity and carcinogenicity study with acesulfame-k in rats. Acesulfame-k (Mayer, D; Kemper, F, eds.). New York: Marcel Dekker; pp. 43–58.

Siragusa, RJ; Cerda, JJ; Baig, MM; et al. (1988) Methanol production from the degradation of pectin by human colonic bacteria. Am J Clin Nutr. 47:848–51

Skrzydlewska, E; Elas, M; Ostrowska, J. (2005) Protective effects of N-acetylcysteine and vitamin E derivative U83836E on proteins modifications induced by methanol intoxication. Toxicol Mechanisms Methods 15:263–270.

Smith, ME; Newman, HW. (1959) The rate of ethanol metabolism in fed and fasting animals. J Biol Chem 234:1544–1549.

Smith, M; Hopkinson, DA; Harris, H. (1971) Developmental changes and polymorphism in human alcohol dehydrogenase. Ann Hum Genet 34:251–271.

Soffritti, M; Maltoni, C; Maffei, F; et al. (1989) Formaldehyde: an experimental multipotential carcinogen. Toxicol Ind Health 5:699–730.

Soffritti, M; Belpoggi, F; Cevolani, D; et al. (2002a) Results of long-term experimental studies on the carcinogenicity of methyl alcohol and ethyl alcohol in rats. Ann NY Acad Sci 982:46–69.

Soffritti, M; Belpoggi, F; Lambertini, L; et al. (2002b) Results of long-term experimental studies on the carcinogenicity of formaldehyde. Ann NY Acad Sci 982:87–105.

Soffritti, M; Belpoggi, F; Minardi, F; et al. (2002c) Ramazzini Foundation cancer program: history and major projects, life span carcinogenicity bioassay design, chemicals studied, and results. Ann NY Acad Sci 982:26–45.

Soffritti, M; Belpoggi, F; Degli Esposti, D; et al. (2005) Aspartame induces lymphomas and leukemias in rats. Eur J Oncol 10:107–116.

Soffritti, M; Belpoggi, F; Degli Esposti, D; et al. (2006) First experimental demonstration of the multipotential carcinogenic effects of aspartame administered in the feed to Sprague-Dawley rats. Environ Health Perspect 114:379–385.

Soffritti, M; Belpoggi, F; Tibaldi, E; et al. (2007) Life span exposure to low doses of aspartame beginnig during prenatal life increases cancer effects in rats. Environ Health Perspect 115:1293–1297.

Speit, G. (2006) The implausibility of systemic genotoxic effects measured by the comet assay in rats exposed to formaldehyde. J Proteosome Res 5:2523–2524.

Spiteri NJ. (1982) Circadian patterning of feeding, drinking and activity during diurnal food access in rats. Physiol Behav. Jan;28(1):139-47. PubMed PMID:7200613.

Staab, Ca; Lander, J; Brandt, M; et al. (2008) Reduction of S-nitrosoglutathione by alcohol dehydrogenase 3 is facilitated by substrate alcohols via direct cofactor recycling and leads to GSH-controlled formation of glutathione transferase inhibitors. Biochem. J. 413: 493–504

Staats, DA; Fisher, JW; Conolly, RB. (1991) GI absorption of xenobiotics in physiologically based pharmacokinetic models: a two-compartment description. Drug Metab Disp 19(1):144–8.

Stanton, ME; Crofton, KM; Gray, LE; et al. (1995) Assessment of offspring development and behavior following gestational exposure to inhaled methanol in the rat. Fundam Appl Toxicol 28(1):100–110.

Starr, TB; Festa, JL. (2003) A proposed inhalation reference concentration for methanol. Regul Toxicol Pharmacol 38:224–231.

Stegink, LD; Brummel, MC; McMartin, KE; et al. (1981) Blood methanol concentrations in normal adult subjects administered abuse doses of aspartame. J Toxicol Environ Health 7: 281–290.

Stegink, LD; Brummel, MC; Filer, LJ; et al. (1983) Blood methanol concentrations in one-year-old infants administered graded doses of aspartame. J Nutr 113:1600–1606.

Stegink, LD; Filer, LJ Jr; Bell, EF; et al. (1989) Effect of repeated ingestion of aspartame-sweetened beverage on plasma amino acid, blood methanol, and blood formate concentrations in normal adults. Metabolism 38(4):357–63.

Steiner, EC; Rey, TD; McCroskey, PS. (1990) Reference guide for Sumusolv. Dow Chemical Co., Midland, MI.

Stern, S; Reuhl, K; Soderholm, S; et al. (1996) Perinatal methanol exposure in the rat I: Blood methanol concentration and neural cell adhesion molecules. Fundam Appl Toxicol 34: 36–46.

Sultatos, LG; Pastino, GM; Rosenfeld, CA; et al. (2004) Incorporation of the genetic control of alcohol dehydrogenase into a physiologically based pharmacokinetic model for ethanol in humans. Toxicol Sci. 2004 Mar; 78(1):20–31.

Svensson, S; Some, M; Lundsjø, A; et al. (1999) Activities of human alcohol dehydrogenase in the metabolic pathways of ethanol and serotonin. Eur J Biochem 262:324–329.

Tanner, CM. (1992) Occupational and environmental causes of Parkinsonism. Occup Med 7:503–513.

Teeguarden, JG; Deisinger, PJ; Poet, TS; et al. (2005) Derivation of a human equivalent concentration for n-butanol using a physiologically based pharmacokinetic model for n-butyl acetate and metabolites n-butanol and n-butyric acid. Toxicol Sci 85:429–446.

Teng, S; Beard, K; Pourahmad, J; et al. (2001) The formaldehyde metabolic detoxification enzyme systems and molecular cytotoxic mechanism in isolated rat hepatocytes. Chem Biol Interact 130–132:285–296.

Tephly, TR; McMartin, KE. (1984) Methanol metabolism and toxicity. Food Sci Technol 12:111–140.

Tiboni, GM; Giampietro, F; Di Giulio, C. (2003) The nitro oxide synthesis N-omega-nitro-L-arginine methyl ester (L-NAME) causes limb defects in mouse fetuses: protective effect of acute hyperoxia. Pediatr Res 54:69–76.

Til, HP; Woutersen, RA; Feron, VJ; et al. (1989) Two-year drinking water study of formaldehyde in rats. Food Chem Toxicol 27:77–87.

Thomas, DG; Breslow, N; Gart, JJ. (1997) Trend and Homogencity Analyses of Proportions and Life Table Data. Version 2.1. Computers and Biomedical Research 10:373–381.

Thrasher, JD; Kilburn, KH. (2001) Embryo toxicity and teratogenicity of formaldehyde. Arch Environ Health. 2001 Jul-Aug;56(4):300-11.

Tobe, M; Naito, K; Kurokawa, Y. (1989) Chronic toxicity study on formaldehyde administered orally to rats. Toxicology 56:79–86.

Toth, BA; Wallcave, L; Patil, K; Schmeltz, I; and Hoffmann, D. (1977) Induction of tumors in mice with the herbicide succinic acid 2,2-dimethylhydrazide. Cancer Research 37:3497–3500.

Tran, MN; Wu, AH; Hill, DW. (2007) Alcohol dehydrogenase and CAT content in perinatal infant and adult livers: potential influence on neonatal alcohol metabolism. Toxicol Lett. 30;169(3):245–52.

Trump, BF; McDowell, EM; Harris, CC. (1984) Chemical carcinogenesis in the tracheobronchial epithelium. Environ Health Perspect 55:77–84.

Tsakiris, T; Giannoulia-Karantana, A; Simintzi, I; et al. (2006) The effect of aspartame metabolites on human erythrocyte membrane acetylcholinesterase activity. Pharmacol Res 53:1–5.

Tsutsui, M; Shimokawa, H; Morishita, T; et al. (2006) Development of genetically engineered mice lacking all three nitric oxide synthases. J Pharmacol Sci 102:147–154.

Turner, C; Spanel, P; and Smith, D. (2006) A longitudinal study of methanol in the exhaled breath of 30 healthy volunteers using selected ion flow tube mass spectrometry, SIFT-MS Physiol Maes. 27:637–648.

U.S. EPA (Environmental Protection Agency). (1986a) Guidelines for the health risk assessment of chemical mixtures. Federal Register 51(185):34014–34025. Available from: http://www.epa.gov/iris/backgr-d.htm.

U.S. EPA (Environmental Protection Agency). (1986b) Guidelines for mutagenicity risk assessment. Federal Register 51(185):34006–34012. Available from: http://www.epa.gov/iris/backgr-d.htm.

U.S. EPA (Environmental Protection Agency). (1986c) Rat oral subchronic toxicity study with methanol. Conducted by Toxicity Research Laboratories, Ltd. TRL No. 032–005.

U.S. EPA (Environmental Protection Agency). (1988) Recommendations for and documentation of biological values for use in risk assessment. Prepared by the Environmental Criteria and Assessment Office, Office of Health and Environmental Assessment, Cincinnati, OH for the Office of Solid Waste and Emergency Response, Washington, DC; EPA 600/6-87/008. Available from: http://www.epa.gov/iris/backgr-d.htm.

U.S. EPA (Environmental Protection Agency). (1991) Guidelines for developmental toxicity risk assessment. Federal Register 56(234):63798–63826. Available from: http://www.epa.gov/iris/backgr-d.htm.

U.S. EPA (Environmental Protection Agency). (1994a) Interim policy for particle size and limit concentration issues in inhalation toxicity studies. Federal Register 59(206):53799. Available from: http://www.epa.gov/iris/backgr-d.htm.

U.S. EPA (Environmental Protection Agency). (1994b) Methods for derivation of inhalation reference concentrations and application of inhalation dosimetry. Office of Research and Development, Washington, DC; EPA/600/8-90/066F. Available from: http://www.epa.gov/iris/backgr-d.htm.

U.S. EPA (Environmental Protection Agency). (1995) Use of the benchmark dose approach in health risk assessment. Risk Assessment Forum, Washington, DC; EPA/630/R-94/007. Available from: http://cfpub.epa.gov/ncea/raf/recordisplay.cfm?deid=42601.

U.S. EPA (Environmental Protection Agency). (1996) Guidelines for reproductive toxicity risk assessment. Federal Register 61(212):56274–56322. Available from: http://www.epa.gov/iris/backgr-d.htm.

U.S. EPA (Environmental Protection Agency). (1997) Guidance on cumulative risk assessment, Part 1 Planning and Scoping. Science Policy Council, Washington, D.C.

U.S. EPA (Environmental Protection Agency). (1998) Guidelines for neurotoxicity risk assessment. Federal Register 63(93):26926–26954. Available from: http://www.epa.gov/iris/backgr-d.htm.

U.S. EPA (Environmental Protection Agency). (2000a) Science policy council handbook: risk characterization. Office of Science Policy, Office of Research and Development, Washington, DC; EPA 100-B-00-002. Available from: http://www.epa.gov/iris/backgr-d.htm.

U.S. EPA (Environmental Protection Agency). (2000b) Benchmark dose technical guidance document [external review draft]. Risk Assessment Forum, Washington, DC; EPA/630/R-00/001. Available from: http://www.epa.gov/iris/backgr-d.htm.

U.S. EPA (Environmental Protection Agency). (2000c) Supplementary guidance for conducting for health risk assessment of chemical mixtures. Risk Assessment Forum, Washington, DC; EPA/630/R-00/002. Available from: http://www.epa.gov/iris/backgr-d.htm.

U.S. EPA (Environmental Protection Agency) (2000d) Toxicological review of vinyl chloride. EPA.635R-00/004.

U.S. EPA (Environmental Protection Agency). (2002a) A review of the reference dose and reference concentration processes. Risk Assessment Forum, Washington, DC; EPA/630/P-02/0002F. Available from: http://www.epa.gov/iris/backgr-d.htm.

U.S. EPA (Environmental Protection Agency). (2002b) Health assessment of 1,3-butadiene. EPA/600/P-98/001F.

U.S. EPA (Enviornmental Protection Agency) (2004). Integrated risk information system: vinyl chloride. Available from www.epa.gov/iris/subst/1001.htm.

U.S. EPA (Environmental Protection Agency). (2005a) Guidelines for carcinogen risk assessment. Risk Assessment Forum, Washington, DC; EPA/630/P-03/001B. Available from: http://www.epa.gov/iris/backgr-d.htm.

U.S. EPA (Environmental Protection Agency). (2005b) Supplemental guidance for assessing susceptibility from early-life exposure to carcinogens. Risk Assessment Forum, Washington, DC; EPA/630/R-03/003F. Available from: http://www.epa.gov/iris/backgr-d.htm.

U.S. EPA (Environmental Protection Agency). (2006a) Science policy council handbook: peer review. Third edition. Office of Science Policy, Office of Research and Development, Washington, DC; EPA/100/B-06/002. Available from: http://www.epa.gov/iris/backgr-d.htm.

U.S. EPA (Environmental Protection Agency). (2006b) A Framework for Assessing Health Risk of Environmental Exposures to Children. National Center for Environmental Assessment, Washington, DC, EPA/600/R-05/093F. Available from: http://cfpub.epa.gov/ncea/cfm/recordisplay.cfm?deid=158363.

U.S. EPA (Environmental Protection Agency). (2006c) Toxic Release Inventory (TRI) On-site and Off-site Reported Disposed of or Otherwise Released (in pounds), for facilities in All Industries, for All Chemicals, U.S., 2003. Available from: http://www.epa.gov/tri. Washington, D.C.

Vara-Castrodeza, A; Peréz-Castrillón, JL; Dueñas-Laita, A. (2007) Magnetic resonance imaging in methanol poisoning. Clin Toxicol 45:429–430.

Ward, KW; Pollack, GM. (1996) Comparative toxicokinetics of methanol in pregnant and NP rodents. Drug Metab Dispos 24:1062–1070.

Ward, KW; Perkins, RA; Kawagoe, et al. (1995) Comparative toxicokinetics of methanol in the female mouse and rat. Fundam Appl Toxicol 26:258–264.

Ward, KW; Blumenthal, GM; Welsch, F; et al. (1997) Development of a physiologically based pharmacokinetic model to describe the disposition of methanol in pregnant rats and mice. Toxicol Appl Pharmacol 145:311–322.

Weiss, B; Stern, S; Soderholm, SC; et al. (1996) Developmental neurotoxicity of methanol exposure by inhalation in rats. HEI Research Report Number 73.

Wentzel, P; Rydberg, U; Eriksson, UJ. (2006) Antioxidative treatment diminishes ethanol-induced congenital malformations in the rat. Alcohol Clin Exp Res. 30(10):1752–60.

Wentzel, P; Eriksson, UJ. (2006) Ethanol-induced fetal dysmorphogenesis in the mouse is diminished by high antioxidative capacity of the mother. Toxicol Sci 2(2):416–22.

White, LR; Marthinsen, ABL; Richards, RJ; et al. (1983) Biochemical and cytological studies of rat lung after inhalation of methanol vapour. Toxicol Lett 17:1–5.

Wilson, SL; Cradock, MM. (2004) Review: Accounting for prematurity in developmental assessment and the use of age-adjusted scores. J Pediatr Pschol 29:641–649.

Wu, AH; Kelly, T; McKay, C; et al. (1995) Definitive identification of an exceptionally high methanol concentration in an intoxication of a surviving infant: methanol metabolism by first-order elimination kinetics. J Forensic Sci 40(2):315–320.

Yuan J. (1993) Modeling blood/plasma concentrations in dosed feed and dosed drinking water toxicology studies. Toxicol Appl Pharmacol. Mar;119(1):131-41. PubMed PMID: 8470117.

Zorzano, A; Herrera, E. (1989) Disposition of ethanol and acetaldehyde in late pregnant rats and their fetuses. Pediatr Res 25(1):102–6.

APPENDIX A. SUMMARY OF EXTERNAL PEER REVIEW AND PUBLIC COMMENTS AND DISPOSITION

[Page intentionally left blank]

APPENDIX B. DEVELOPMENT, CALIBRATION AND APPLICATION OF A METHANOL PBPK MODEL

This appendix is adapted from a report prepared for the U.S. EPA under contract by the Center for Biological Monitoring and Modeling, Battelle Northwest Laboratories (WA 09, Battelle Project No. 48746, January 31, 2007).

B.1. SUMMARY

This appendix describes the development, calibration, and approach for application of mouse, rat, and human PBPK models to extrapolate mouse and rat methanol inhalation-route internal dose metrics to human inhalation exposure concentrations that result in the same internal dose (HEC). The human oral methanol dose(s) yielding internal dose(s) equivalent to the mouse or rat internal dose at the (HED) is also presented.

A PBPK model was developed to describe the blood kinetics of methanol (MeOH) in mice and humans. The model includes compartments for lung/blood MeOH exchange, liver, fat, and the rest of the body. To describe blood MeOH kinetics, the model employs two saturable descriptions of MeOH metabolic clearance in mice and rats, and one first-order metabolic clearance, and a first-order description of renal clearance (from blood) in humans. Renal clearance is a minor pathway and does not appreciably affect MeOH blood kinetics.

This model is a revision of the model reported by Ward et al. (1997), reflecting significant simplifications (removal of compartments for placentae, embryo/fetus, and extraembrionic fluid) and two elaborations (addition of an intestine lumen compartment to the existing stomach lumen compartment and addition of a bladder compartment which impacts simulations for human urinary excretion.), while maintaining the ability to describe MeOH blood kinetics. The model reported here uses a single consistent set of parameters; the Ward et al. model employed a number of data-set specific parameters. Other biokinetic MeOH models that were considered as starting points for the current model also used varied parameters by dataset to achieve model fits to the data. For example, the model of Bouchard et al. (2001) used different respiratory rates and fractional inhalation absorbed for different human exposures.

The mouse model was calibrated against inhalation-route blood MeOH kinetic data and verified using intravenous-route blood MeOH kinetic data. The rat model was calibrated against low-dose intravenous data and validated with inhalation-route data. The human model was calibrated against inhalation-route MeOH kinetic data. The models accurately described the inhalation route pharmacokinetics of MeOH. Mouse model simulations of oral- and i.v.-route kinetics compare well to some but not all the experimental data.

The MeOH HECs predicted by the model (based on 1,000 ppm inhalation exposure in mice) were >1,000 ppm using either blood AUC or C_{max} as the dose metrics. The MeOH HED

derived by cross-route extrapolation of this inhalation-route HEC was 110 mg/kg-day, based on MeOH blood AUC following zero order uptake of MeOH (a constant rate of delivery). Because of the lack of human data from high-dose exposures, it was not possible to calibrate the model for inhalation exposures above 1,000 ppm or oral exposures above 110 mg/kg-day. However, because the BMD approach was used to estimate an internal experimental animal dose and UFs were applied to the internal dose, the human model can be used to back-calculate that internal dose to an RfC and an RfD below 1,000 ppm or 110 $_{mg/kg\text{-}day}$, respectively.

B.2. MODEL DEVELOPMENT

B.2.1. Model Structure

This model is a revision of the model reported by Ward et al. (1997), reflecting significant simplifications and two elaborations, while maintaining the ability to describe MeOH blood kinetics in mice, rats, and humans (Figure B-1). The kidney, pregnancy and the fetal compartment have been removed. The kidney was lumped with the body compartment because the blood:tissue partition coefficients for these tissues were similar. The elaborate time-dependent descriptions of pregnancy were removed because analysis of the available pharmacokinetic data indicates that blood MeOH kinetics in NP and pregnant mice are not different enough to warrant separate descriptions. Because the maternal blood:fetal blood partition coefficients were near 1, there was no need to explicitly model fetal kinetics; they will be equivalent to maternal blood kinetics. Further supporting data exist for ethanol, which is quite similar to MeOH in its partitioning and transport properties. In rats (Zorzano and Herrara, 1989; Guerri and Sanchis 1985), sheep (Brien et al., 1985; Cumming et al., 1984), and guinea pigs (Clarke et al., 1986), fetal and maternal blood concentrations of ethanol are virtually superimposable; maternal to fetal blood ratios are very close to 1, including during late gestation. Also, fetal brain concentrations in guinea pigs (Clarke et al., 1986) were also very similar to the mothers'.

In addition to the absolute maternal-fetal concentration similarity noted above, it is common practice to use blood concentrations as an appropriate metric for risk extrapolation via PBPK modeling for effects in various tissues, based on the reasonable expectation that any tissue:blood differences will be similar in both the test species and humans. For example, even if the brain:blood ratio was around 1.2 in the mouse or rat, the similar biochemical make-up of brain tissue and blood in rats and humans leads to the expectation that the brain:blood levels in humans (which depend on the biochemical make-up) will also be close to 1.2, and so the relative "error" that might occur by using blood instead of brain concentration in evaluating the dose-response in rats will be cancelled out by using blood instead of brain concentration in the human. The fact that measured fetal blood levels are virtually identical to maternal levels for methanol (and ethanol) tells us that the rate of metabolism in the fetus is not sufficient to significantly

reduce the fetal concentration versus maternal, and use of a PBPK model to predict maternal levels will give a *better* estimate of fetal exposure than use of the applied dose or exposure, because there *are* animal-human differences in adult PK of MeOH for which the model accounts, based on PK data from humans as well as rodents.

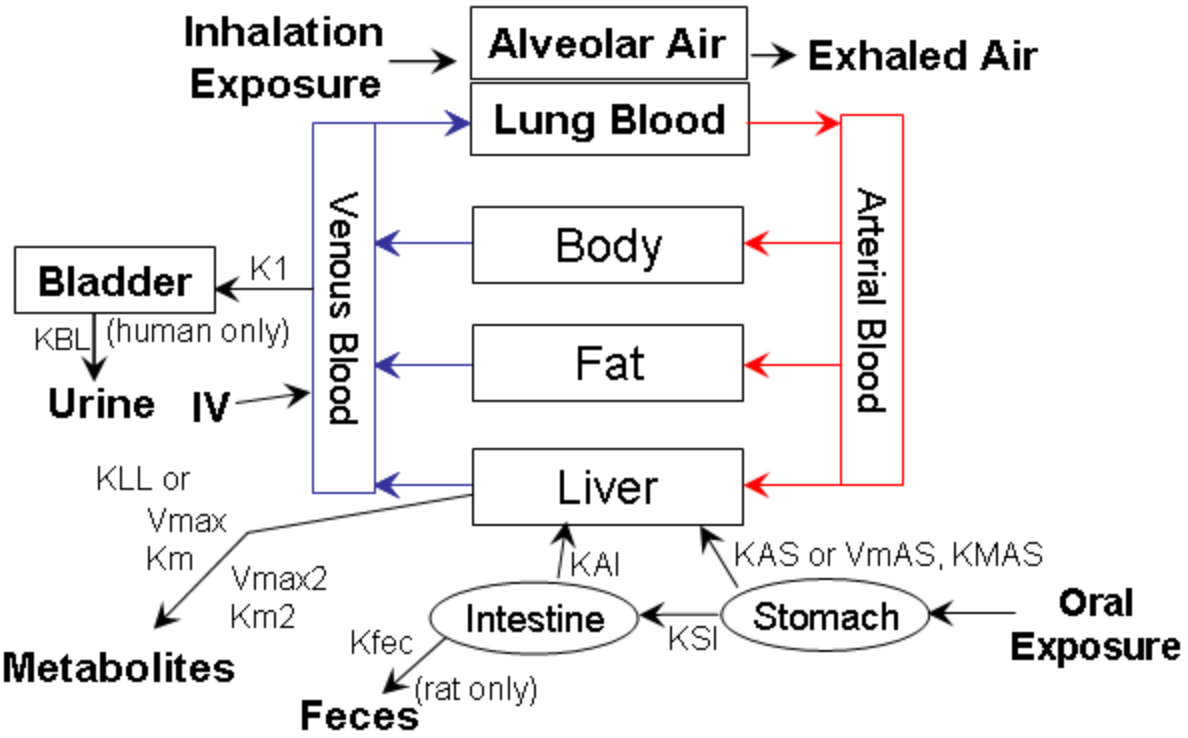

Figure B-1. Schematic of the PBPK model used to describe the inhalation, oral, and i.v. route pharmacokinetics of MeOH. KAS, first-order oral absorption rate from stomach; KAI, first-order uptake from the intestine; KSI, first-order transfer between stomach and intestine; Vmax and Km and Vmax2 and Km2, Michaelis-Menten rate constants for high affinity/low capacity and low affinity/high capacity metabolic clearance of MeOH; KLL, alternate first-order rate constant; KBL, rate constant for urinary excretion from bladder. Both metabolic pathways were used to describe MeOH clearance in the mouse and rat, while a single pathway describes metabolic clearance in the human.

A lung compartment was added to describe delivery of MeOH to blood as a function of ventilation, partitioning, and blood flow rather than the less standard approach used by Ward et al. (1997). A term was added to the gas uptake equations to describe the fractional respiratory bioavailability of MeOH. A fat compartment was included because it is the only tissue with a tissue:blood partitioning coefficient appreciably different than unity, and the liver is included because it is the primary site of metabolism. A bladder compartment was added to better describe the kinetics of human urinary data, where the drop in excretion rate is slower than the predicted decline in blood methanol and hence rate of metabolite production. Also, to best describe the observed rat dosimetry after oral exposure while maintaining metabolic parameters

fit to data from inhalation and IV exposure, a small rate of elimination from the intestine (lumen) compartment to feces. (The mouse data could be adequately fit with this rate set to zero, corresponding to 100% absorption; humans were assumed to have zero fecal elimination, like the mouse.) The final models thus include compartments for fat, liver, the rest of the body, bladder (only used for humans), and lung. The mouse and rat models describe inhalation, oral, and intravenous route dosing and the human model describes inhalation and oral route dosing and the rat model includes a non-zero rate of fecal elimination. Although there is an endogenous background level of both MeOH and formate (See Section 3.3), the model does not explicitly describe or account for background levels of MeOH or formate. In this analysis, when non-zero background levels have been measured (in blood), that background was simply subtracted from the concentrations measured during exposure. However, a zero-order rate of infusion could be added to the liver, blood, or stomach compartments to mimic background levels if that was considered necessary.

MeOH is well absorbed by the inhalation and oral routes, and is readily metabolized to formaldehyde, which is rapidly converted to formate in both rodents and humans. Although the enzymes responsible for metabolizing formaldehyde are different in rodents (CAT) and humans (ALD) the metabolite, formate, is the same, and the metabolic rates are similar (Clary, 2003). Most of the published rodent kinetic models for MeOH describe the metabolism of MeOH to formaldehyde as a saturable process but differ in the handling of formate metabolism and excretion (Bouchard et al., 2001; Fisher et al., 2000; Ward et al., 1997; Horton et al., 1992). Ward et al. (1997) used one saturable and one first-order pathway for mice, and Horton et al. (1992) applied two saturable pathways of metabolism to describe MeOH elimination in rats. Bouchard et al. (2001) employed one metabolic pathway and a second pathway described as urinary elimination in rats and humans. The need for two saturable metabolic pathways in the mouse model was confirmed through simulation and optimization. High exposure (>2,000 ppm MeOH) and low exposure (1,000 ppm MeOH) blood data could not be adequately fit either visually or by more formal optimization without the second saturable metabolic pathway. The optimization approach and results are found below and in the Additional Materials at the end of this appendix.

While the PPK model explicitly describes the concentration of methanol, it only describes the rate of metabolism or conversion of MeOH to its metabolites. Distribution and metabolism of formaldehyde is not considered by the model, and this model tracks neither formate nor formaldehyde. (The data that would be needed to parameterize or validate a specific description of either of these metabolites is not available). Since the metabolic conversion of formaldehyde to formate is rapid (< 1 minute) in all species (Kavet and Nauss, 1990), the MeOH clearance rate may approximate a formate production rate, though this has not been verified. Thus the rate of MeOH metabolism predicted by the model can be used as a dose metric for either or both of these metabolites, but scaling of that metabolic rate metric to humans would

require use of an inter-species scaling factor, $(BW_{human}/BW_{rodent})^{0.25}$, to account for the general expectation of slower clearance of the metabolites in humans.

The model was initially coded in acslXtreme v1.4 and updated in acslXtreme v 2.3 (Aegis Technologies, Huntsville, AL). Most procedures used to generate this report, except those for the optimization, may be run by executing the corresponding .m files. The model code (acslXtreme .csl file) and supporting .m files are available electronically and as text in the Additional Materials at the end of this appendix. A key identifying .m files associated with figures and tables in this report is also provided in the Additional Materials.

B.2.2. Model Parameters

Physiological parameters such as tissue volumes, blood flows, and ventilation rates were obtained from the open literature (Table B-1). Parameters for blood flow, ventilation, and metabolic capacity were scaled as a function of body weight raised to the 0.75 power, according to the methods of Ramsey and Andersen (1984).

Table B-1. Parameters used in the mouse and human PBPK models

	Mouse	Rat SD | F344		Human		Source
Body weight (kg)	0.03[a]	0.275[b]		70		Measured/estimated
Tissue volume (% body weight)						
Liver	5.5	3.7		2.6		Brown et al. 1997
Blood arterial	1.23	1.85		1.98		
venous	3.68	4.43		5.93		
Fat	7.0	7.0		21.4		
Lung	0.73	0.50		0.8		
Rest of body	72.9	73.9		58.3		Calculated[c]
Flows (L/hr/kg$^{0.75}$)						
Alveolar ventillation[d]	25.4	16.4		16.5		Perkins et al. 1995a; Brown et al. 1997; U.S. EPA, 2004
Cardiac output	25.4	16.4		24.0		
Percentage of cardiac output						
Liver	25.0	25.0		22.7		Brown et al. 1997
Fat	5.0	7.0		5.2		
Rest of body	70.0	68		72.1		Calculated
Biochemical constants[e]				**1st order**	**saturable**	
$V_{max}C$ (mg/hr/kg$^{0.75}$)	19	5.0	0	NA	33.1	Fitted
Km (mg/L)	5.2	6.3	NA	NA	23.7	
$V_{max}2C$ (mg/hr/kg$^{0.75}$)	3.2	8.4	22.3	NA		
Km2 (mg/L)	660	65	100	NA		
K1C (BW$^{0.25}$/hr)	NA	NA		0.0373	0.0342	
KLLC (BW$^{0.25}$/hr)[f]	NA	NA		95.7	NA	

Oral absorption					
VmASC (mg/hr/kg$^{0.75}$)	1830	5570	377		Mouse and rat fitted (mouse and human KMASC assumed = rat); other human values are those for ethanol from Sultatos et al. (2004), with VmASC set so that for a 70-kg person VmAS/KM = the first-order constant of Sultatos et al.
KMASC (mg/kg)	620	620	620		
KSI (hr^{-1})	2.2	7.4	3.17		
KAI (hr^{-1})	0.33	0.051	3.28		
Kfec (hr^{-1})	0	0.029	0		
Partition coefficients					
Liver:Blood	1.06	1.06	0.583[h]		Ward et al., 1997; Fiserova-Bergerova and Diaz, 1986
Fat:Blood	0.083	0.083	0.142		
Blood:Air	1350[i]	1350	1626		Horton et al., 1992; Fiserova-Bergerova and Diaz, 1986
Body:Blood	0.66	0.66	0.805		Rodent: estimated; human: Fiserova-Bergerova and Diaz, 1986 (human "body" assumed = muscle)
Lung:Blood	1	1	1.07		
Bladder time-constant (KBL, hr^{-1})[j]	NA		0.564	0.612	Fitted (human)
Inhalation fractional availability (%)	0.665	0.20	0.866[k]		Rodent: fitted; human Ernstgard et al., 2005

NA - Not applicable for that species
[a]Both sources of mouse data report body weights of approximately 30 g
[b]The midpoints of rat weights reported for each study was used and ranged from 0.22 to 0.33 kg
[c]The volume of the other tissues was subtracted from 91% (whole body minus a bone volume of approximately 9%) to get the volume of the remaining tissues
[d]Minute ventilation was measured and reported for much of the data from Perkins et al. (1996) and the average alveolar ventilation (estimated as 2/3 minute ventilation) for each exposure concentration was used in the model. When ventilation rates were not available, a mouse QPC (Alveolar Ventilation/BW$^{0.75}$) of 25.4 was used (average from Perkins et al., 1995a). The QPC used to fit the human data was obtained from U.S. EPA (2004). This QPC was somewhat higher than calculated from Brown et al. (1997) (~13 L/hr/kg$^{0.75}$)
[e]V_{max}, Km, and $V_{max}2$, Km2 represent the two saturable metabolic clearance processes assumed to occur solely in the liver. The V_{max} used in the model = $V_{max}C$ (mg/kg$^{0.75}$·hr)×BW$^{0.75}$. K1C is the first-order loss from the blood for human simulations that represents urinary elimination. Allometric scaling for first-order clearance processes was done as previously described (Teeguarden et al., 2005); The K1 used in the model= K1C / BW$^{0.25}$
[f]KLLC – alternate human first-order metabolism rate (used only when $V_{max}C = V_{max}2C = 0$)
[g]Human oral simulations used a zero order dose rate equal to the $_{mg/kg\text{-}day}$ dose
[h]Human liver:blood estimated from correlation to (measured) fat:blood, based on data from 28 other solvents
[I]Rat partition coefficient used for mice as done by Ward et al. (1997)
[j]KBL – a first-order rate constant for clearance from the bladder compartment, used to account for the difference between blood kinetics and urinary excretion data as observed in humans
[k]For human exposures, the fractional availability was from Šedivec et al. (1981), corrected for the fact that alveolar ventilation is 2/3 of total respiration rate

Mouse model partition coefficients were used as reported (liver, fat, blood:air) or estimated (lung, body). The mouse body compartment partition coefficient was set approximately equal to the measured value for muscle (Ward et al., 1997). The mouse lung partition coefficient was assumed to be 1.0, similar to the liver partition coefficient. This parameter has no numerically significant impact on modeled blood dose metrics.

Human partition coefficients were reported by Horton et al. (1992), but were in fact measured in rat tissues. The reported rat fat partition coefficient was considerably closer to unity than reported for MeOH or ethanol by other researchers (Ward et al., 1997; Pastino and Conolly,

2000) and assumed to be in error. Human partition coefficients were obtained from Fiserova-Bergerova and Diaz (1986).

B.2.3. Mouse Model Calibration

B.2.3.1. *Inhalation-Route Calibration*

For purposes of conducting interspecies extrapolations of MeOH dosimetry, the inhalation route was the most important route requiring calibration for the mouse model. The critical endpoint and NOEL, which are the basis for the HEC estimation, are from inhalation-route studies. The ability to predict blood MeOH concentrations from inhalation exposures was therefore a priority. Pharmacokinetic data from other routes, i.v. and oral, were used to verify clearance terms derived by fitting to the inhalation data or to estimate a MeOH oral uptake rate constants. Holding other parameters constant, the mouse PBPK model was calibrated against inhalation-route blood pharmacokinetic data (Figure B-2) by fitting five parameters: Michaelis-Menten constants for one high affinity/low capacity and one low-affinity high-capacity enzyme and the inhalation fractional availability term.

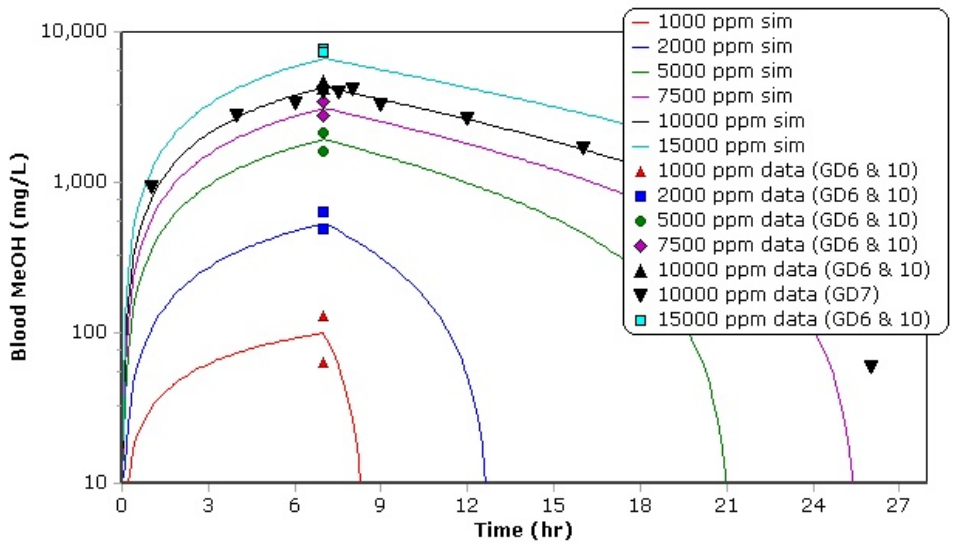

Figure B-2. Model fits to data sets from GD6, GD7, and GD10 mice for 7-hour inhalation exposures to 1,000–15,000 ppm MeOH. Maximum concentrations are from Table 2 in Rogers et al. (1993). The complete data set for GD7 mice exposed to 10,000 ppm is from Rogers et al. (1997) and personal communication (Additional Materials). Symbols are concentration means of a minimum of n = 4 mice/concentration. Default ventilation rates (Table B-1) were used to simulate these data.

For these mouse simulations, pulmonary ventilation was set to 25.4 (L/hr/kg$^{0.75}$), the average value measured by Perkins et al. (1995a), which is similar to the value of 29 (L/hr/kg$^{0.75}$) reported in Brown et al. (1997). Where ventilation rates were reported for individual exposure

concentrations by Perkins et al. (1995a), they were used directly in the model and a notation was made in the figure legend. Reported ventilation rates varied from 592 to 857 L/kg x 8 hr, depending on exposure concentration (Perkins et al., 1995a). Adjusting these values to 2/3 total (for alveolar ventilation) and allometrically scaling by $BW^{0.75}$, values used in the model for these exposures ranged from 20.5 to 29.7 ($L/hr/kg^{0.75}$) (See Table B-1). A fractional availability of 73% of alveolar ventilation was visually optimized to best describe the inhalation-route blood MeOH pharmacokinetic data. This percentage of uptake for inhalation exposures is similar to values reported for other alcohols in rodents (Teeguarden et al., 2005), but considerably lower than the value reported by Perkins et al. (1995a) of 126% of alveolar ventilation (85% of total ventilation).

The calibrated model predicted blood MeOH concentration time-course agreed well with measured values in adult mice in the inhalation studies of Rogers et al. (1997, 1993) (Figure B-2), and Perkins et al. (1995a), as well as in NP and early gestation (GD8) mice of Dorman et al. (1995) (Figure B-3). Parameter values used in the calibrated model are given in Table B-1.

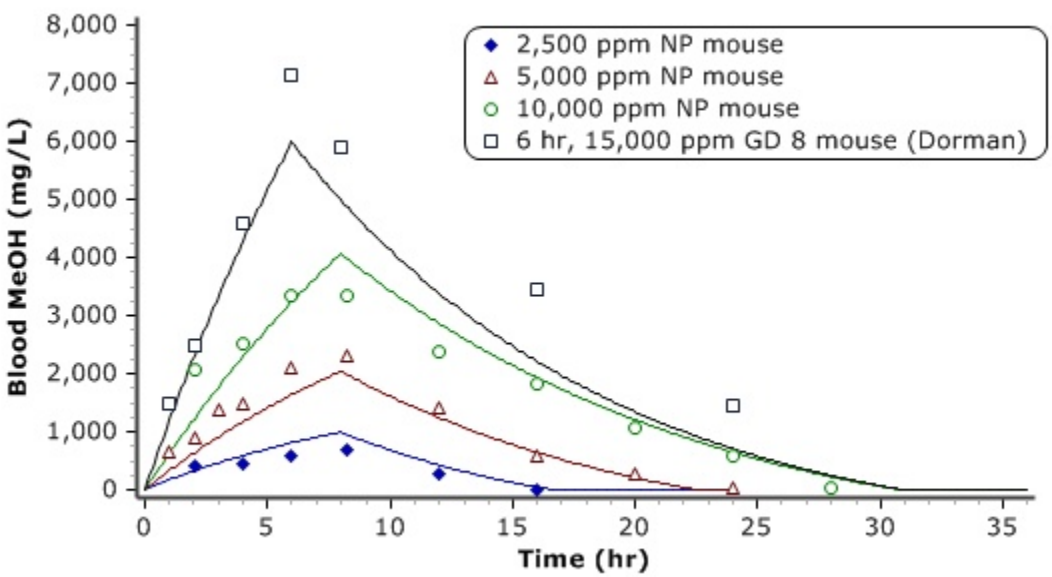

Figure B-3. Simulation of inhalation exposures to MeOH in NP mice from Perkins et al. (1995a) (8-hour exposures) and Dorman et al. (1995), (6-hour exposures). Data points represent measured blood MeOH concentrations and lines represent PBPK model simulations. Note: data was obtained using DigitizIt (SharIt! Inc. Greensburg, PA) to digitize data from Figure 2 of Perkins et al. (1995a) and Figure B-2 from Dorman et al., (1995). Default ventilation rates (Table B-1) were used to simulate the Dorman data. The alveolar ventilation rate for each data set from Perkins et al. (1995) was set equal to the measured value reported in that manuscript. For the 2,500, 5,000, and 10,000 ppm exposure groups, the alveolar ventilation rates were 29, 24, and 21 (L/hr/kg0.75), respectively. The cardiac output for these simulations was set equal to the alveolar ventilation rate.

B.2.3.1. ***(should be B.2.3.2) Oral-Route Calibration***

The mouse model was calibrated for the oral route by fitting the rate constants for oral uptake of MeOH. Calibration of the oral route was not required for interpretation of the critical toxicology studies. This exercise was undertaken to estimate the rate constants for oral uptake so it could be used to make dose-route extrapolations for calculating human oral-route exposures equivalent to mouse exposures at the NOEL.

Ward et al. (1997) described MeOH uptake as the sum of a fast and slow process (two rate constants), with a fraction of the administered dose attributed to each process. The rate constants and the fraction of the dose attributed to each process were varied to describe oral-route blood MeOH kinetics for each GD. For instance, the fraction of the total oral dose assigned to the fast absorption process varied from 54 to 71%, depending on the data set. An alternative approach with uptake attributed to stomach and intestine, which allows for greater flexibility in fitting the data (Staats et al., 1991), was compared to a simpler one utilizing a single rate of uptake. In both the current model and the model of Ward et al. (1997), orally ingested MeOH was assumed to be 100 % absorbed.

Initially, a single oral absorption rate constant (KAS, hr^{-1}) was fitted to oral-route blood MeOH kinetics reported by Ward et al. (1997, 1995). Using these data, an average KAS (0.62 hr^{-1}) was estimated that provides adequate fits to MeOH blood kinetics following 2,500 mg/kg dose in NP and GD18 mice and 1,500 mg/kg in GD8 mice up to ~8 hours. At later time points, however, a model using a single oral uptake rate constant consistently under predicts blood concentrations of MeOH (results not shown). Fits were improved by using the two compartment GI tract model (Figure B-4). However, when fitting the oral data in rats, it was found that the fits were significantly improved if the uptake from the stomach was treated as a saturable process. V_{max} (VMASC) was scaled as $BW^{0.75}$, as is done for other V_{max}s, and the Km (KMASC) was scaled as BW^{1} to reflect that the variable used is the total amount in the stomach, whose volume is expected to scale with BW^{1}. For the mouse, model fits were not significantly improved when KMASC was allowed to vary (change from the value fitted to rats, 1830 mg/kg), so it was kept at the rat value.

Using the two-compartment oral absorption model and adjusting only the absorption parameters resulted in a good fit to the lower oral dose (1,500 mg/kg) (Dorman et al., 1995), but consistently under-prediction of the 2,500 mg/kg oral dosing blood levels (Ward et al., 1997). When the metabolic constants (V_{max}C values) were decreased, the data from the higher dose were fit, but the fit of the data for the 1,500 mg/kg dose was lost (see Additional Materials, Figure B-19). Also, when using the lower clearance required to fit the data of Ward et al. (1997), the inhalation data of Rogers et al. (1993) could no longer be fit by the model (see Additional Materials, Figure B-20). The two-compartment GI tract approach (with parameters that better fit the low dose data) was retained in the model and used for all final mouse oral route simulations.

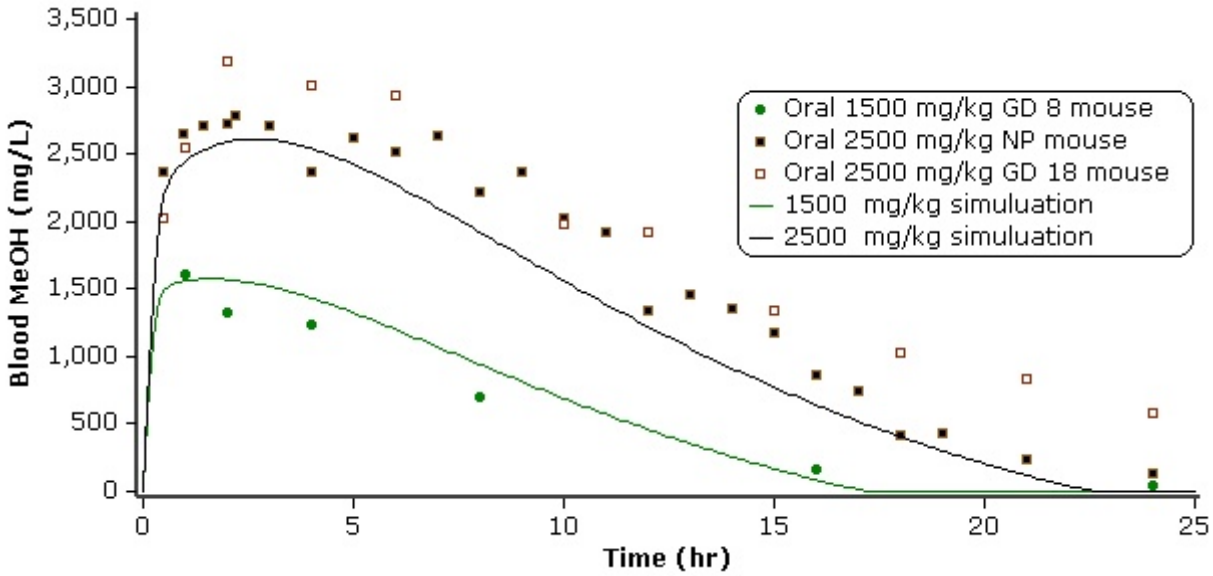

Figure B-4. Oral exposures to MeOH in pregnant mice on GD8 (Dorman et al., 1995) or NP and GD18. Data points represent measured blood concentrations and lines represent PBPK model estimations for NP mice.

Source: Ward et al., (1997).

B.2.3.1. ***(B2.3.3) Intravenous Route Simulation***

The parameterization of MeOH clearance (high-and-low affinity metabolic pathways) was verified by simulation of data sets describing the intravenous-route pharmacokinetics of MeOH. MeOH blood kinetics data in NP mice are only available for a single i.v. dose of 2,500 mg/kg (Ward et al., 1997). MeOH blood kinetics are also reported in GD18 mice following administration of a broader range of doses: 100, 500, and 2,500 mg/kg. Because MeOH kinetics appear similar for NP and pregnant mice after administration of 2,500 mg/kg prior to 20 hours, the model is expected to fit data for both pregnant and NP mice using the same set of parameters, and hence, data for both life stages were used to verify metabolic clearance of MeOH.

Initial blood concentrations of MeOH following i.v. administration were not proportional to administered dose in the data from Ward et al. (1997). Initial concentrations were approximately 1.5-fold lower in the 100 mg/kg dose group than expected if a dose-independent volume of distribution (V_D) is assumed (Figure B-5A). Initial blood concentrations were, however, proportional to administered dose between 2,500 and 500 mg/kg. Two possible explanations were then considered:

1) the V_D, which is not impacted by any other PBPK parameters and is only determined by the biochemical partitioning properties of MeOH, is twofold lower at 100 mg/kg than at the higher concentrations, while the V_D at 500 and 2,500 mg/kg are exactly as predicted by the PBPK model without adjustment; or

2) a dilution error occurred during preparation of the 100 mg/kg dosing solution used by Ward et al. (1997).

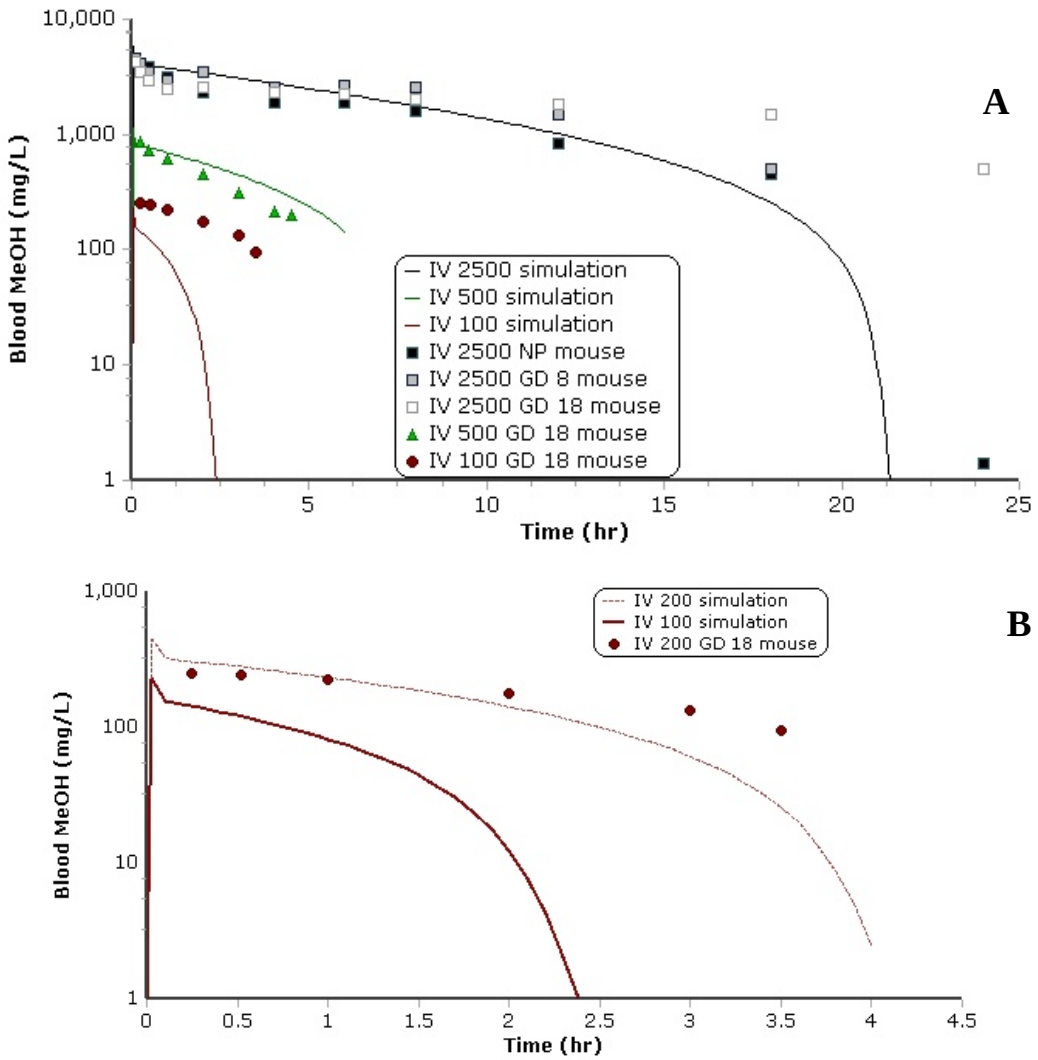

Figure B-5. Mouse intravenous route MeOH blood kinetics. A) MeOH was infused over 1.5 minutes into female CD-1 mice at target doses of 100 (circles), 500 (triangles) or 2,500 (squares) mg/kg. Mice were NP, GD9 or GD18 at the time of dosing. Data points represent measured blood concentrations and lines represent PBPK model simulations. B) Comparison of the 100 mg/kg dose data (points) and PBPK model simulations assuming a 100 mg/kg dose as reported (solid line) or to a presumed 200 mg/kg dose (dashed lines). Note: the 24-hour time point data from the 500 mg/kg NP and GD 9 mice are below the reported detection limit (2 µg/ml) and so are not shown.

Source: Adapted from Ward et al. (1997).

To account for this unexpected nonproportionality, Ward et al. (1997) used higher partition coefficients for placenta and embryonic fluid and lower V_{max} for the metabolism of

MeOH for the 100 and 500 mg/kg doses than for the 2,500 mg/kg dose. These adjustments to partition coefficients effectively change the volume of distribution. However, the PBPK model obtained with measured partition coefficients and otherwise calibrated to inhalation data, as described above, was capable of simulating both the 500 and 2,500 mg/kg data without adjustment or varying parameters between those 2 doses. Further, the data at the nominal dose of 100 mg/kg could also be adequately fit without other parameter adjustment simply by simulating a dose of 200 mg/kg (dotted line, Figure B-5B). If the relative difference in the V_D at 100 mg/kg was not a round number and/or the apparent value at 500 mg/kg was intermediate between 100 and 2,500 mg/kg, the possibility of a dose-related variation in this or other parameters would be given more weight. Also it seems unlikely that the volumes of distribution would be different in these animals solely based on differing exposure concentrations. But the far simpler and more likely explanation for the observed pattern of V_D seems to be a dosing error (2). Therefore, a single set of parameters was retained which describe the 2,500 and 500 mg/kg doses rather than adjust parameters to fit a data set (the 100 mg/kg dose group) that appeared inconsistent and may be the result of a simple experimental error rather than attributable to a dose dependence.

Thus, high- (2,500 mg/kg) and mid-dose (500 mg/kg) intravenous-route pharmacokinetic data were used to validate the parameters calibrated from the inhalation studies for the metabolic clearance of MeOH. Metabolic constants reasonably predict blood MeOH kinetics following a 2,500 mg/kg dose in NP animals until 12 hours postexposure, but under predict blood MeOH in GD9 and GD18 mice at 8 hours of exposure and beyond, and under-predict levels in both NP and pregnant mice at 15 hours and beyond. At this high-dose, where blood kinetics of MeOH were reported in NP, GD9, and GD18 mice, the data for the GD18 mice was inconsistent with the GD9 and NP animals. The GD9 data at 12 hours appears inconsistent with the NP data, but then the 2 are nearly identical again at 15 hours, so it is not clear if that difference at 12 hours is real or just due to experimental variability. Blood levels of MeOH were ~500 mg/L in GD18 mice at 24 hours, but were nondetectable after 18 hours in the other groups (detection limit 2 mg/L). Blood concentrations were accurately predicted following administration of 500 mg/kg MeOH (Figure B-5A). The model predictions did not match the 100 mg/kg data unless one assumed an error in dose preparation, as described above (Figure B-5B). The calibration of the MeOH PBPK model is consistent with both the available inhalation and oral-route data.

B.2.3.1. ***(B2.3.4)Total Methanol Metabolic Clearance***

Quantifying production of formaldehyde following MeOH exposure for use as an alternative dose metric is of particular interest because formaldehyde is also undergoing toxicity assessment. However, it is important to understand that because the model was developed to describe blood MeOH kinetics, metabolism of MeOH to neither formaldehyde nor formate is specifically described; the model tracks neither of these metabolites. While the metabolic clearance of MeOH described by the model may be presumed to equate with formaldehyde

production, this metabolic flux simply leaves the computational model system without specific attribtution. Since the metabolic conversion of formaldehyde to formate is rapid in all species (< 1 minute) (Kavet and Nauss, 1990), the MeOH clearance rate may approximate a formate production as well as a formaldehyde production rate, though this has not been verified.

Thus, production of formaldehyde or formate following exposure to MeOH can only be estimated by summing the total amount of MeOH cleared by metabolic processes. If used, this metric of formaldehyde or formate dose should be adjusted by an inter-species scaling factor ($SF = [BW_{human}/BW_{rodent}]^{0.25}$) to adjust for expected species differences in the clearance of these two metabolites (this is a default factor based on the generally accepted assumption that total metabolism scales as $BW^{0.75}$ and hence clearance per BW scales as $1/BW^{0.25}$). The rate of MeOH clearance may roughly be equated to the total amount of metabolites produced. Values of total MeOH clearance as a function of exposure in mice and humans are presented in the Additonal Materials (Tables 7-9).

B.2.3.1. ***(B.2.3.5)Formal Optimization of Mouse Model Parameters***

Formal optimization of five parameters (inhalation fractional availability and the V_{max} and Kms for high and low affinity MeOH metabolism) was attempted using optimization routines in acslXtreme v2.01.1.2. Under the best circumstances, formal optimizations offer the benefit of repeatability and confirmation that global optima have not been significantly missed by user-guided visual optimization. Incorporating judgments regarding the value of specific data sets, while possible when visually fitting, is more difficult when using optimization routines. This is an important distinction between these approaches for this modeling exercise.

The mouse inhalation route NOEL was less than 1,000 ppm MeOH. The model is calibrated against inhalation-route data because of the importance of this exposure route in the assessment. Unfortunately, the vast majority of the MeOH data came from much higher exposure concentrations. As expected, various attempts at formal optimization lead to improved fits for some but never all data sets. This is to be expected when there is significant variability in the underlying data. Various data-weighting schemes were included to improve overall optimization while maintaining a good fit to the lowest concentration (1,000 ppm) data. In the end, formal optimization provided no significant improvement over the fractional availability and metabolic parameter values obtained by visual optimization, so these were retained in the final version of the model.

Further details on the approach and results from the formal optimization are found in the Additional Materials in outline format with supporting figures. More complete documentation was not developed because the products of the optimizations were not used in the final model. The documentation is intended only to demonstrate that appropriate optimizations were conducted and what the results of those optimizations were.

B.2.4. Mouse Model Sensitivity Analysis

An evaluation of the importance of selected parameters on mouse model estimates of blood MeOH AUC was performed by conducting a sensitivity analysis using the subroutines within acslXtreme. Files for reproducing the sensitivity analysis are available in the model as described in the additional materials. The analysis was conducted by measuring the change in model output corresponding to a 1% change in a given model parameter when all other parameters were held fixed. A normalized sensitivity coefficient of 1 indicates that there is a one-to-one relationship between the fractional change in the parameter and model output; values close to zero indicate a small effect on model output. A positive value for the normalized sensitivity coefficient indicates that the output and the corresponding model parameter are directly related while a negative value indicates they are inversely related.

Sensitivity analyses were conducted for the inhalation and oral routes. The inhalation-route analysis was conducted under the exposure conditions of Rogers and Mole (1997) and Rogers et al. (1993), 7-hour inhalation exposures at the NOEL concentration of 1,000 ppm. The oral route sensitivity analysis was conducted for an oral dose of 1,000 mg/kg.

Parameters with sensitivity coefficients less than 0.1 are not reported. The parameters with the largest sensitivity coefficients for the inhalation route at 1,000 ppm were pulmonary ventilation, $V_{max}C$, and partitioning to the body compartment (Figures B-6 [metabolism] and B-7 [flows and partition coefficients]). MeOH AUC was also sensitive to KM2 and $V_{max}C$. The sensitivity coefficient for pulmonary ventilation increases from 1 to ~1.75 during the exposure period as metabolism begins to saturate. The sensitivity coefficient is 1 for concentrations 100 ppm MeOH or less or when hepatic clearance is nonlimiting.

Oral-route mouse blood MeOH AUC was sensitive to the rate constants for uptake. Blood AUC was most sensitive to the first-order rate constant for uptake from the stomach, KAS, during the first hour after exposure, becoming less important over time (Figure B-8). Blood MeOH AUC was also modestly sensitive to KAI, and KSI, the rate constants for uptake from the intestine and transfer rates between compartments, respectively.

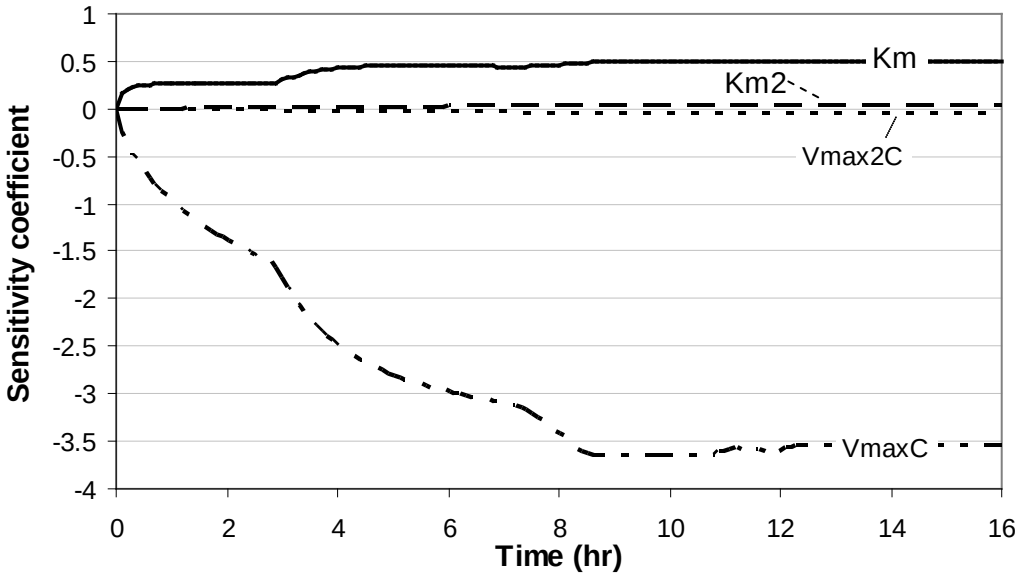

Figure B-6. Mouse model inhalation route sensitivity coefficients for metabolic parameters. Sensitivity coefficients calculated for an exposure of 1,000 ppm MeOH are reported for blood MeOH AUC. Note: Km, Vmax refer to the high-affinity, low-capacity pathway and Km2, Vmax2 refer to the low-affinity, high-capacity pathway.

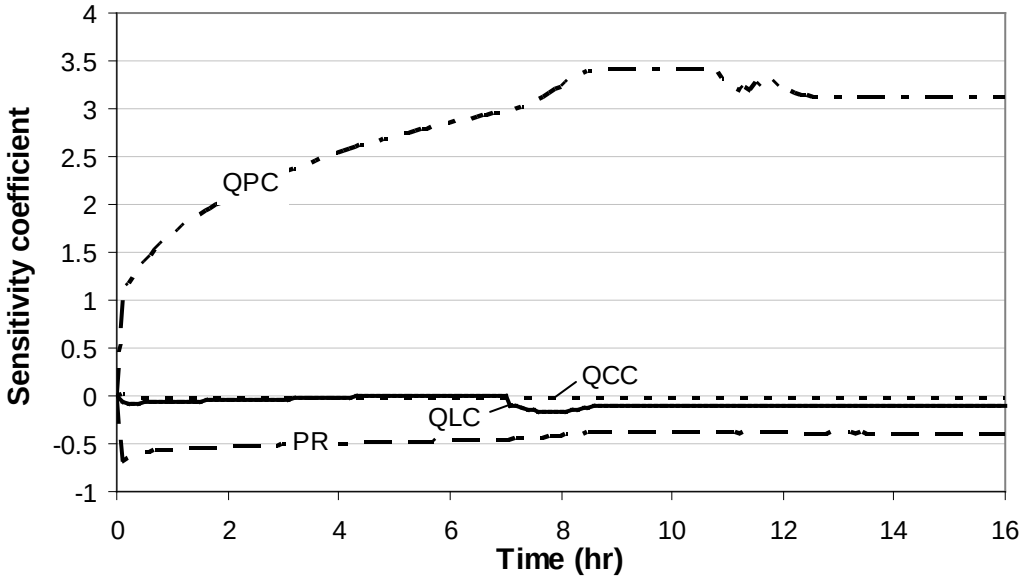

Figure B-7. Mouse model inhalation route sensitivity coefficients for flow rates (QCC: cardiac output; QPC: alveolar ventilation), and partitioning to the body (PR) compartment are reported for blood MeOH AUC. Sensitivity coefficients calculated for an exposure to 1,000 ppm MeOH.

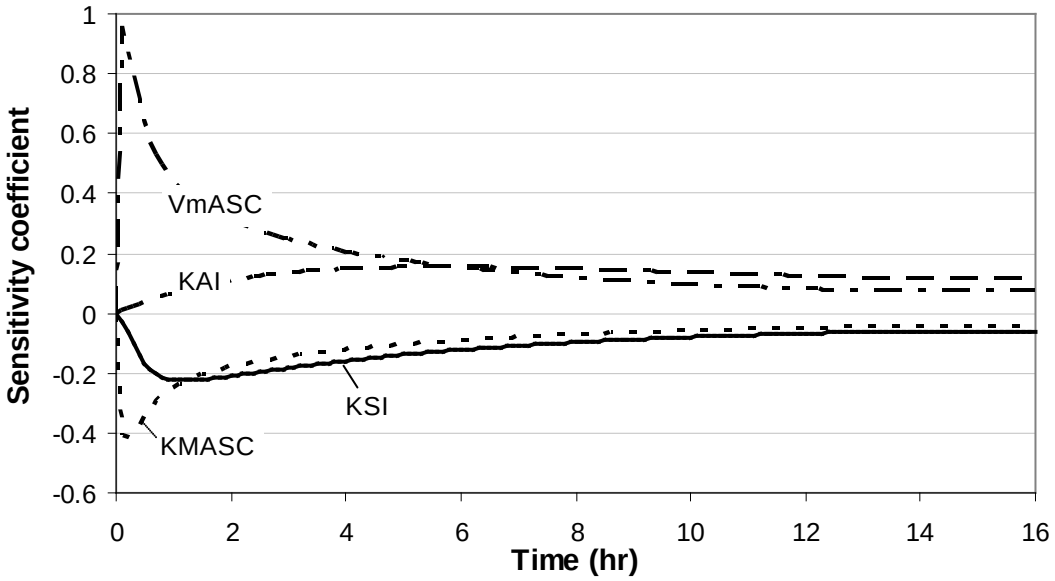

Figure B-8. Mouse model sensitivity coefficients for oral exposures to MeOH. The sensitivity of blood MeOH AUC to oral absorption rate constants (KAS: stomach; KAI: intestine; KSI: transfer between compartments) is reported.

B.2.5. Mouse Drinking Water Ingestion Pattern

To simulate exposures of mice via drinking water under bioassay conditions, an ingestion pattern first used by Keys et al. (2004) , based on data from Yuan (1993) was used. The pattern specifies a fraction of percent of total daily ingestion consumed in each half-hour interval. The first interval was shifted to correspond to the beginning of the active (dark) period, for consistency with patterns used for humans and rats. A Table function was used in acslXtreme to interpolate an instantaneous rate between the measured (30-min) values, with normalization so that the 24-hour integral equals 100%. The daily pattern is shown in Figure B-9A and the resulting blood concentration for a mouse exposed for 6 days per week (2100 mg/kg) is shown in Figure B-9B.

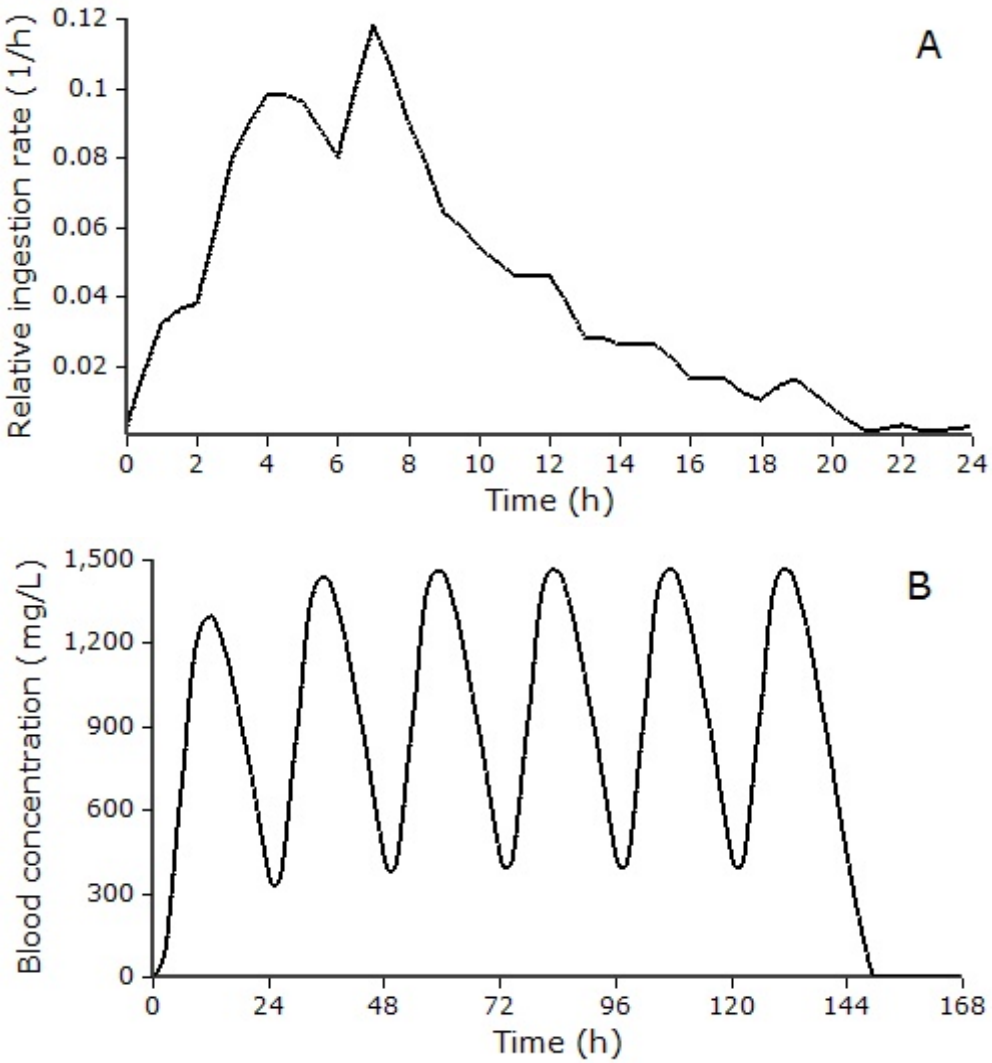

Figure B-9. Mouse daily drinking water ingestion pattern (A) and resulting predicted blood concentration for a 6 d/wk exposure (B). Mouse drinking water exposures were simulated by multiplying the fractional rate (1/h) as a function of clock time by the daily total dose ingested (mg) to obtain a rate of addition of methanol into the stomach lumen compartment (mg/h).

Source: Yuan (1993); Keys et al. (2004)

B.2.6. Rat Model Calibration

The model was initially calibrated-to-fit data from intravenous, inhalation, and oral exposures in Sprague-Dawley (SD) rats using the 100 and 2500 mg/kg intravenous (IV) data provided in the command file of Ward et al. (1997). Holding other parameters constant, the rat PBPK model was calibrated against the Ward et al. (1997) IV-route blood pharmacokinetic data (Figure B-10) by fitting Michaelis-Menten constants for one high affinity/low capacity and one low-affinity, high-capacity enzyme, using the optimization routines in acslXtreme v2.3. Also shown for comparison in Figure B-10A are the 100 mg/kg IV data of Horton et al. (1992), obtained using Fischer 344 (F344) rats (data extracted from figures using DigitizIt), with a model simulation (heavy red line) which differs from that for the SD rat only due to the predicted effect of know body weight differences. While the fit to the Ward et al. data for SD rats is excellent, especially for the lower dose, the rate of clearance is over-predicted for the F344 rat when parameters fit to SD rat data are used. The 100 mg/kg IV data, with an alternate simulation for the F344 rat obtained with distinct parameters (see below) is expanded in Figur B-10B, emphasizing the difference in clearance between the two strains.

We then attempted to fit the model to the inhalation data of Horton et al. (1992) by adjusting only the inhalation fractional uptake (FRACIN). The results, shown in Figure B-11A, are clearly poor. While the model does match the uptake portion of the inhalation data for the 1200 and 2000 ppm exposures, it under-predicts the peak concentration reached at 200 ppm. Further, the post-exposure clearance predicted by the model is much more rapid than indicated by the data, as occurred with the IV kinetics (Figure B-10). (Since the peak concentration for the 2000 ppm inhalation exposure actually occurred at 7 hr, we also simulated a 7-hr exposure, shown by the thin black line. The result indicates that the data are more consistent with and better predicted by the longer exposure duration, but clearance is still over-predicted post-exposure.) Therefore we concluded that the data show a clear strain difference in metabolism, and should support at least a partially independent set of parameters for SD and F344 rats.

We then combined the 100 mg/kg IV and inhalation data of Horton et al. (for F344 rats) and attempted to simultaneously identify the four metabolic parameters (Vmax and Km for two pathways) and FRACIN. However when this was done the resulting values for the two Km's were ~ 90 ± 50 mg/L and 70 ± 40 mg/L (Km and Km2, respectively), which are clearly indistinguishable from a statistical standpoint. If instead the Km's were fixed at the more distinct values identified from the SD rat IV data (6.3 and 65 mg/L), the optimization routine tended to set the Vmax associated with the lower Km to zero. Thus the F344 rat data of Horton et al. (1992) appear to be most consistent with a single metabolic pathway, even though the observed concentrations spanned almost 2 orders of magnitude. Therefore those data (including the 100 mg/kg IV data) were simultaneously fit by adjusting a single Vmax and Km, along with the

inhalation fraction, FRACIN, with the second metabolic pathway set to zero (Figures B-10B and B-11B).

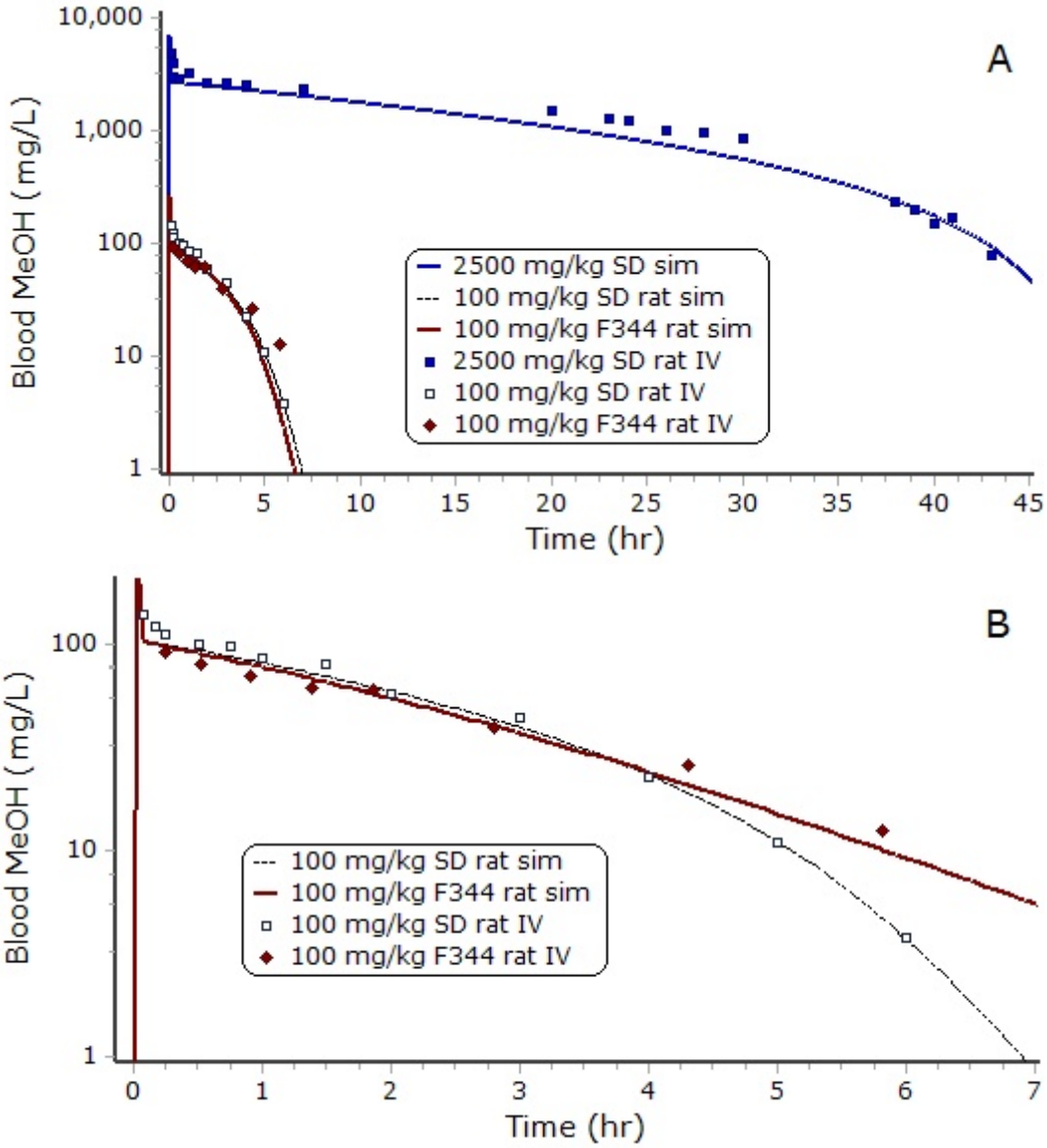

Figure B-10. NP rat i.v.-route methanol blood kinetics. MeOH was infused into: female Sprague-Dawley rats (275 g) at target doses of 100 (open squares and thin black line) or 2,500 (filled squares and heavy blue line) mg/kg; or (filled diamonds and heavy red lines) male F-344 rats (220 g) at target doses of 100 mg/kg. Data points represent measured blood concentrations and lines represent PBPK model simulations with (A) metabolic parameters fit to the Sprague-Dawley rat data or (B) metabolic parameters fit to F-344 data (see text for further details).

Source: Ward et al.(1997; squares); Horton et al. (1992; diamonds).

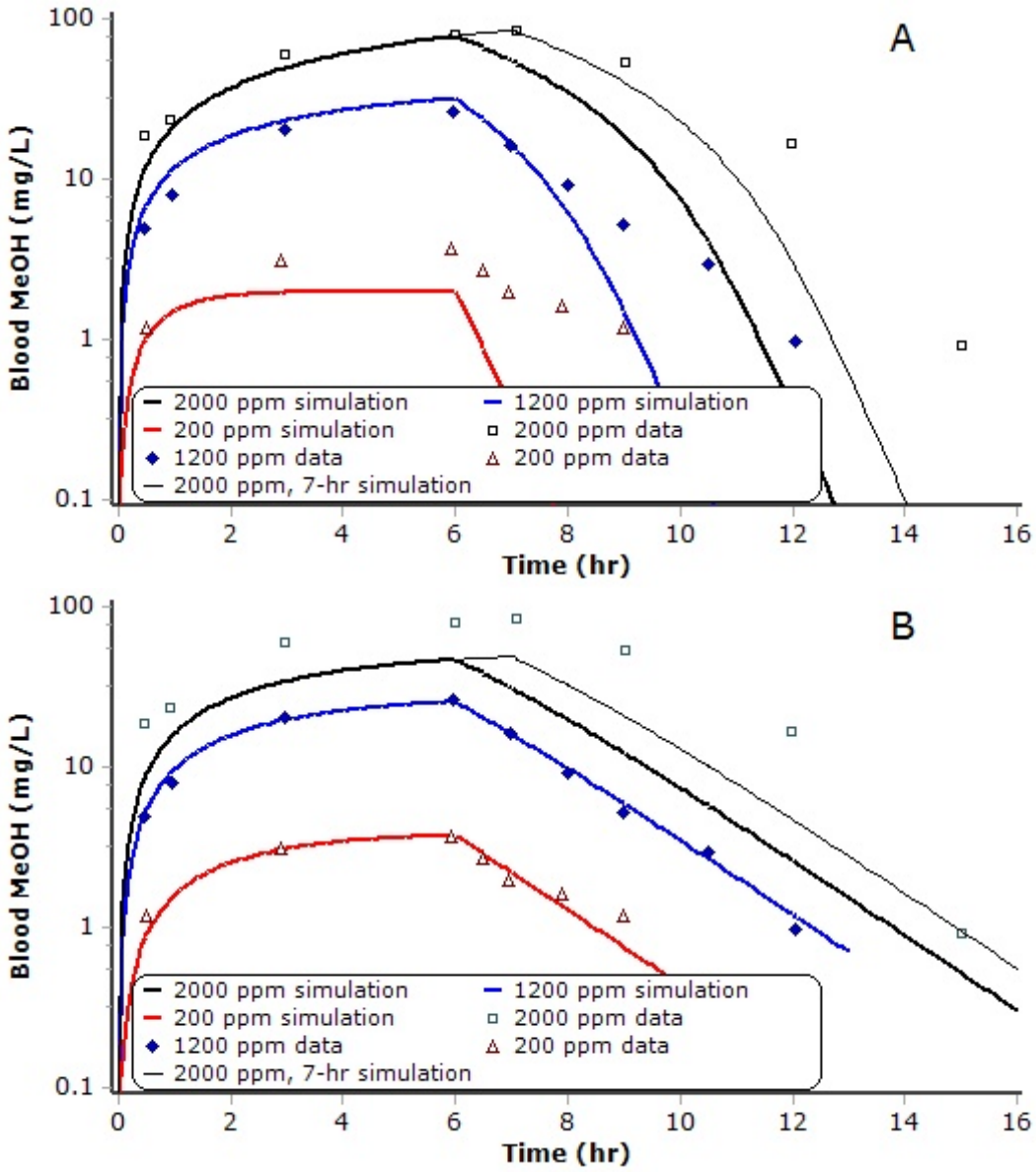

Figure B-11. Model fits to data sets from inhalation exposures to 200 (triangles), 1,200 (diamonds), or 2,000 (squares) ppm MeOH in male F-344 rats. (A) Model fits with metabolic parameters set to values obtaine from IV data for Sprague-Dawley rats, with only the inhaled fraction (FRACIN) adjusted. (B) Model fits obtained by fitting metabolic parameters (Vmax and Km) for a single pathway, along with FRACIN, to these data as well as the 100 mg/kg IV data from F-344 rats (Figure B-9B).

Symbols are concentrations obtained using DigitizIt!. Lines represent PBPK model fits. As the 7-hour data point at 2,000 ppm is higher than the 6-hour data point (more evident on a linear scale) and appears more consistent with a 7-hour exposure, a model simulation for a 7-hour exposure at 2,000 ppm is also shown (lighter line).

Source: Horton et al. (1992)

Model simulations of the F344 rat data with the F344-specific parameters are shown in Figure B-10B (heavy red line) and Figure B-11B. Unfortunately we were unable to simultaneously fit the inhalation data for all exposure levels, although a wide range of metabolic saturation (Km) values were tested. We could obtain a better fit of the high-concentration data by constraining FRACIN to a higher value, for example, but then the fits to the lower concentration data were compromised (not shown). Examining Figure 2 of Horton et al. (1992), the experimental variability (indicated by the error bars) on the 2000 ppm data was much larger than the 200 or 1200 ppm data, and as indicated by the simulations in Figure B-11 here, there is at least the appearance that the exposure was actually for 7 hr instead of 6 hr. (To be clear, the 2000 ppm data were used in the optimization with the duration of inhalation set to 6 hr, but the routine selected parameters which only poorly fit those data.) Since our greatest concern is in predicting dosimetry at lower exposure levels, near to the points of departure, we decided to retain the fits shown here. The corresponding parameters are listed in Table B-1. The fractional absorption (20%) was lower than that estimated for mice (66.5%), but Perkins et al. (1995) also found lower fractional absorption of inhaled methanol in rats vs. mice.

Finally, first-order oral absorption parameters were first fit to the lower dose (100 mg/kg) oral absorption data reported by Ward et al. (1997), using the optimization routines in acslXtreme v2.3 (Figure B-12, heavy/solid lines). (Since the animals used were SD rats, the SD-specific metabolic parameters were used.) While the fit to the low-concentration data was quite good (Figure B-12, lower panel), the fit to the 2500 mg/kg data (Figure B-12, upper panel) exhibited a much faster and higher peak than shown by the data. Even when the model was fit to both the high- and low-concentration data simultaneously, the fit to the high-concentration data could not be significantly improved without completely degrading the low-concentration fit (not shown). Also note that the 2500 mg/kg linear simulation completely over-estimates all the data points; i.e., the area-under-the-curve for this dose is higher than indicated by the data, indicating that the assumption of 100% absorption is not valid. Therefore, an alternative model using a saturable (Michaelis-Menten) equation for absorption from the stomach and fecal elimination (linear term) from the intestine was considered (thin lines) and found to significantly improve the high-concentration simulation, with a nearly identical fit the low-concentration data. While methanol absorption is not known to be regulated by transporters or other processes that would give rise to rate saturation, it is clear form the discrepancy between the linear model and the 2500 mg/kg data that uptake is slower than predicted by such a model and its use would lead to an over-prediction of internal concentrations. Therefore parameters for the saturable uptake model are reported in Table B-1 and the KMASC applied to mice and humans. Note that since the saturation constant corresponds to a fairly large dose (620 mg/kg), the model is still effectively linear at low- to moderate dose rates.

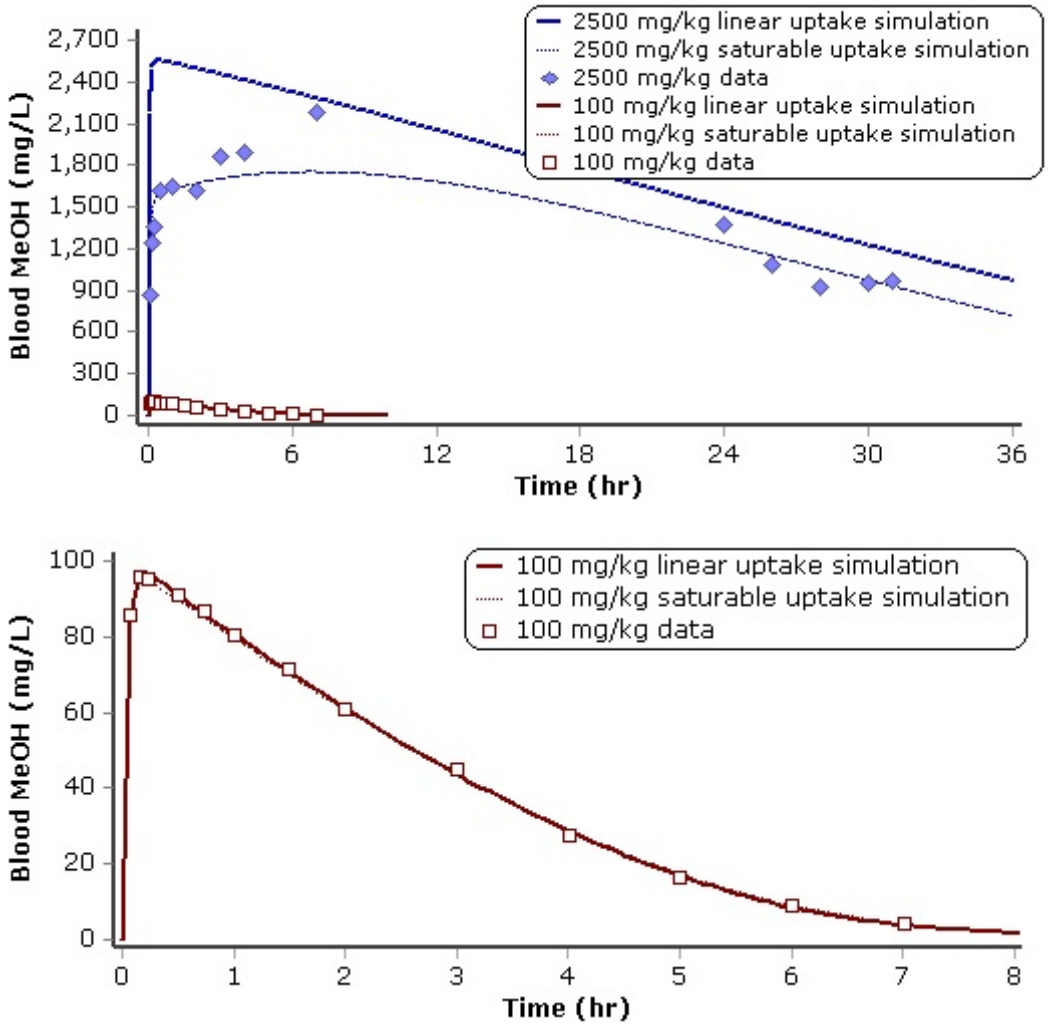

Figure B-12. Model fits to data sets from oral exposures to 100 (squares) or 2,500 (diamonds) mg/kg MeOH in female Sprague-Dawley rat (Expanded scale in lower panel). Symbols are concentrations obtained from the command file. The thick lines represent PBPK model fits using a linear (first-order) equation for absorption from the stomach compartment with no fecal elimination, while the thin lines use a Michaelis-Menton equation with a small fraction eliminated in the feces. All other GI rates, including absorption from the intestine, are first order.

Source: Ward et al.(1997).

B.2.7. *Rat Model Simulations*

A range of adverse developmental effects was noted in rat pups exposed to methanol throughout embryogenesis (NEDO, 1987). SD rats were exposed in utero over different periods of pregnancy and as neonates via inhalation or in drinking water. Inhalation exposures to methanol were carried out for 18–22 hours, depending on the exposure group. Simulations of predicted C_{max}, AUC, and total metabolized from 22-hour exposures to 500, 1,000, and 5,000 ppm MeOH are shown in Figure B-13. Simulations of oral exposures of SD rats to 65.9, 624.1, or 2,177 mg/kg-day (500, 5,000, 20,000 ppm in drinking water), daily dose estimations from the study of Soffritti et al. (2002), based on measured water consumption, kindly provided by Cynthia Van Landingham, Environ International, Ruston, Louisiana, are shown in Figure B-13. Although the exposures in these studies are to rats over long periods and in some cases exposures of the newborn pups, the model simulations are to NP adult rats only, using the dose-group specific average body weights of 0.33-0.34 kg BW from the study of Soffritti et al. (2002) and do not take into account changes is body weight or composition. These simulated values are presumed to be a better surrogate for and predictor of target-tissue concentrations in developing rats, and the corresponding estimated human concentrations a better predictor of developmental risk in humans than would be obtained using the applied concentration or dose and default extrapolations. The logic here is simply that the ratio of actual target tissue concentration (in the developing rat pup or human) to the simulated concentration in the NP adult is expected to be the same in both species and hence, that proportionality drops out in calculating a HEC.

Figure B-13 depicts simulations run to determine internal doses for 22 hours/day inhalation exposures at 500, 1,000, or 2,000 ppm. Simulation results for continuous inhalation exposures are shown for contrast. The simulations show that for all but the highest dose (2,000 ppm) steady state is reached within 22 hours, and that “periodicity,” where the concentration time course is the same for each subsequent day, is reached by the 2nd day of exposure. At 2,000 ppm, however, steady state is not reached until after 48 hours for the continous exposure. Therefore, the C_{max}, 24-hour AUC and amount metabolized per day (AMET) were by simulating 22 hours/day exposures for 5 days and calculating values of AUC and AMET over the last day (24 hours) of that period.

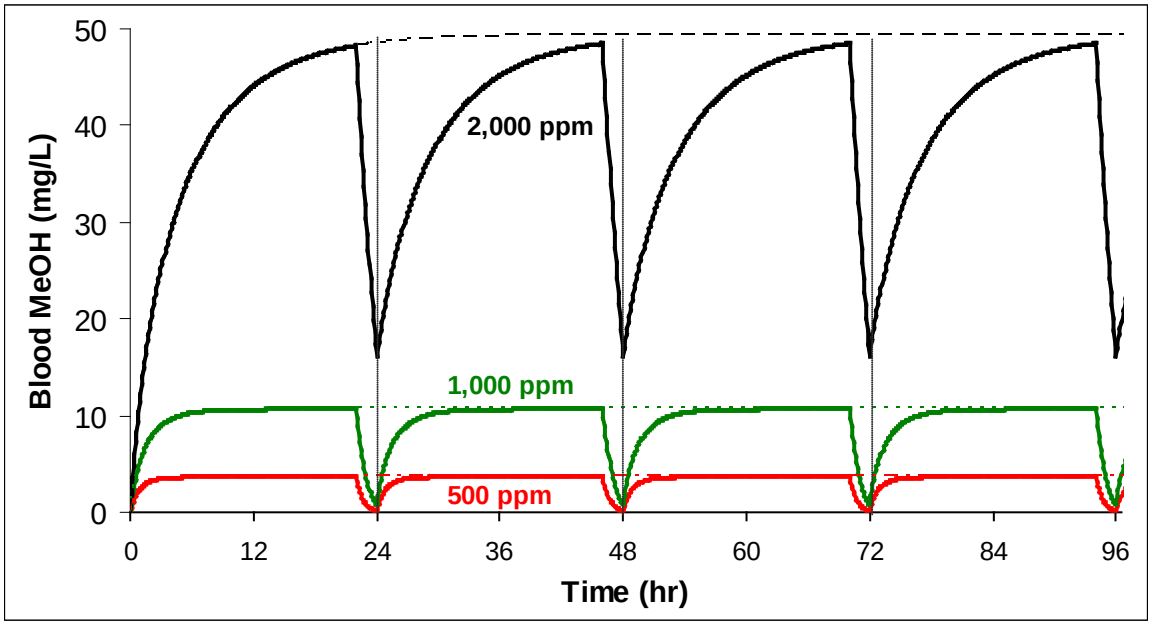

Exposure concentration (ppm)	C_{max} (mg/L)	AUC (hr·mg/L)	AMET (mgEq)
500	3.6	79	17.6
1,000	10.6	227	34.8
2000	48.5	968	67.2

Figure B-13. Simulated Sprague-Dawley rat inhalation exposures to 500, 1,000, or 2,000 ppm MeOH. Rat BW was set to 0.33 kg. Simulations are shown for both continuous (thin, dashed/dotted lines in plot) and 22 hours/day exposures (thick, solid lines in plot). Cmax, AUC, and amount metabolized (AMET) are determined from the 22 hour/day simulations, run for a total of 5 days (120 hours), with the AUC and AMET calculated for the last 24 hours of the simulation.

Figure B-14 depicts simulations run to mimic a single oral exposure, treated as a continuous infusion for 12 hours (assuming 12-hour period when rats are awake and active). Total AUC and AMET and AUC24 and AMET24 for the first 24 hours after start of exposure were calculated.

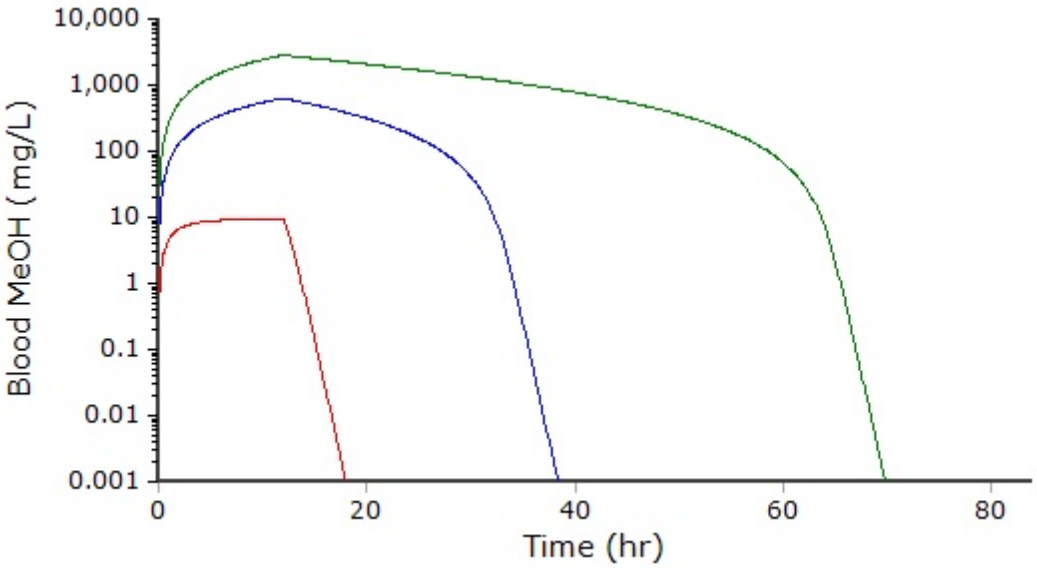

Exposure dose (mg/kg·day)	Body weight (kg)	C_{max} (mg/L)	AUC (hr·mg/L)	AUC24 (hr·mg/L)	AMET (mgEq)	AMET24 (mgEq)
66.0	0.33	9.3	104.8	104.8	21.2	21.2
624.1	0.33	631.6	9,525	8,817	155.6	122.6
2177	0.34	2,832.4	72,617	45,138	347.4	138.4

Figure B-14. Simulated rat oral exposures of Sprague-Dawley rats to 65.9, 624.2, or 2,177 mg MeOH/kg/day. Dosing was simulated as a 12-hour, zero-order infusion to the liver compartment. The AUC and total amount metabolized are given for a period sufficient for the MeOH to clear (84 hours), and the AUC24 and AMET24 values represent just the first 24 hours of exposure. (Results shown for illustrative purposes. Dosimetry used in assessment was simulated using a more realistic water ingestion pattern.)

To simulate ingestion of methanol in drinking water by rats under bioassay conditions, an ingestion pattern based on the observations of Spiteri (1982) and Peng et al. (1990). While mice ingest water in frequent, small bouts (Gannon et al., 1992) that are reasonably described as a continuous delivery to the stomach, rats exhibit clear periods of ingestion alternating with periods where no ingestion occurs (Spiteri, 1982; Peng et al., 1990). Based on those data a reasonable representation of rat water ingestion can be described as serious of pulses. During the dark/active period of each day (first 12 hr) each bout of drinking was assumed to last 45 min followed by 45 min without ingestion (total of 8 bouts). During the light/inactive period (next 12 hr) drinking bouts were assumed to last only 30 min followed by 2.5 hr (150 min) without drinking (4 bouts). An equal amount was assumed to be consumed in each bout within the dark period, likewise within each light-period bout, with the respective amounts adjusted such that 80% of the total ingestion occurs during the dark and 20% during the light (Burwell et al., 1992). The resulting absorption pattern is shown in Figure B-15A and a simulated blood concentration time-curve (for 50 mg/kg/day dosing) is shown in Figure B-15B.

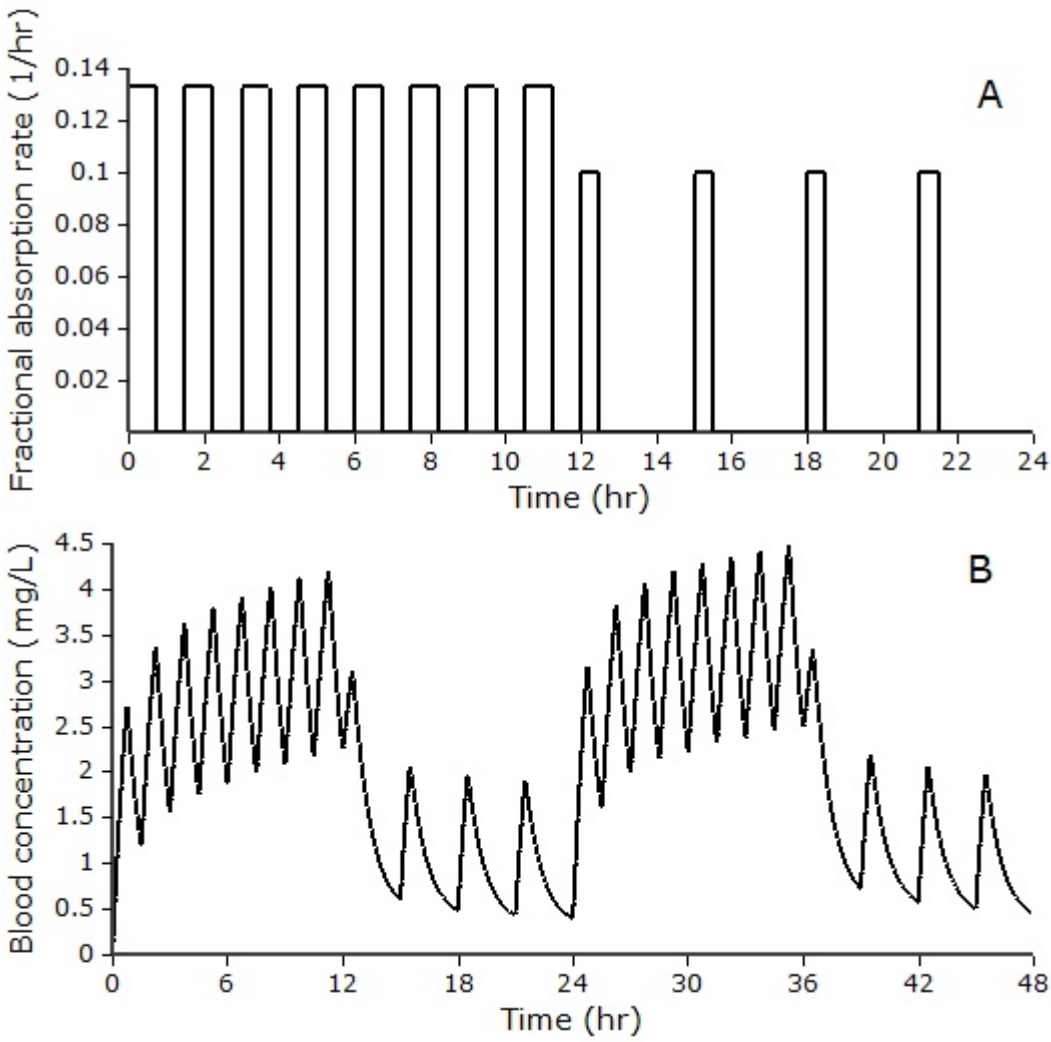

Figure B-15. Rat daily drinking water ingestion pattern (A) and resulting predicted blood concentration for a 2-day exposure (B). Rat drinking water exposures were simulated by multiplying the fractional absorption rate (1/hr) as a function of clock time by the daily total dose ingested (mg) to obtain a rate of addition of methanol into the stomach lumen compartment (mg/h).

B.2.8. Human Model Calibration

B.2.8.1. *Inhalation Route*

The mouse model was scaled to human body weight (70 kg or study-specific average), using human tissue compartment volumes and blood flows, and calibrated to fit the human inhalation-exposure data available from the open literature, which comprised data from four publications (Ernstgard et al., 2005; Batterman et al., 1998; Osterloh et al., 1996; Sedivec et al., 1981).

A first-order rate of loss of MeOH from the blood, K1C, and a first-order bladder compartment time constant, KBL, were used to provide an estimate of urinary MeOH

elimination. The inhalation-route urinary MeOH kinetic data described by Sedivec et al. (1981) (Figure B-16) were used to inform these parameters. The urine MeOH concentration data reported by the authors were converted to amount in urine by assuming 0.5 mL/hr/kg total urinary output (Horton et al., 1992). Sedivec et al. (1981) measured a fractional uptake of 57.7%, based on total amount inhaled. Since the PBPK model uses alveolar rather than total ventilation and this is typically assumed to be 2/3 of total ventilation the fractional uptake of Sedivec et al. (1981) was corrected by dividing by 2/3 to obtain a value for FRACIN of 0.8655. The resulting values of K1C and KBL, shown in Table B-1, differ somewhat depending on whether first-order or saturable liver metabolism is used. These are only calibrated against a small data set and should be considered an estimate. Urine is a minor route of MeOH clearance with little impact on blood MeOH kinetics.

Although the high-doses used in the mouse studies warrant the use of a second metabolic pathway with a high Km, the human exposure data all represent lower concentrations and may not require or allow for accurate calibration of a second metabolic pathway. Horton et al. (1992) employed two sets of metabolic rate constants to describe human MeOH disposition, similar to the description used for rats and mice, but in vitro studies using monkey tissues with non-MeOH substrates were used as justification for this approach. Although Bouchard et al. (2001) described their metabolism using Michaelis-Menten metabolism, Starr and Festa (2003) reduced that to an effective first-order equation and showed adequate fits. Perkins et al. (1995) estimated a Km of 320 ± 1273 mg/L (mean ± S.E.) by fitting a one-compartment model to data from a single oral poisoning to an estimated dose. In addition to the extremely high standard error, the large standard error for the associated V_{max} (93 ± 87 mg/kg/hr) indicates that the set of Michaelis-Menten constants was not uniquely identifiable using this data. Other Michaelis-Menten constants that have been used to describe MeOH metabolism in various models for primates are given in Table B-2. Because the Km calculated by Perkins et al. (1995) from the high-dose oral exposure is 320 mg/L, while the highest observed concentration in the data sets considered here is 14 mg/L (Batterman et al., 1998), forcing the model to use this higher Km would simply result in fits that are effectively indistinguishable from the linear model. A simple, linear model is preferred over the use of a Km value that high.

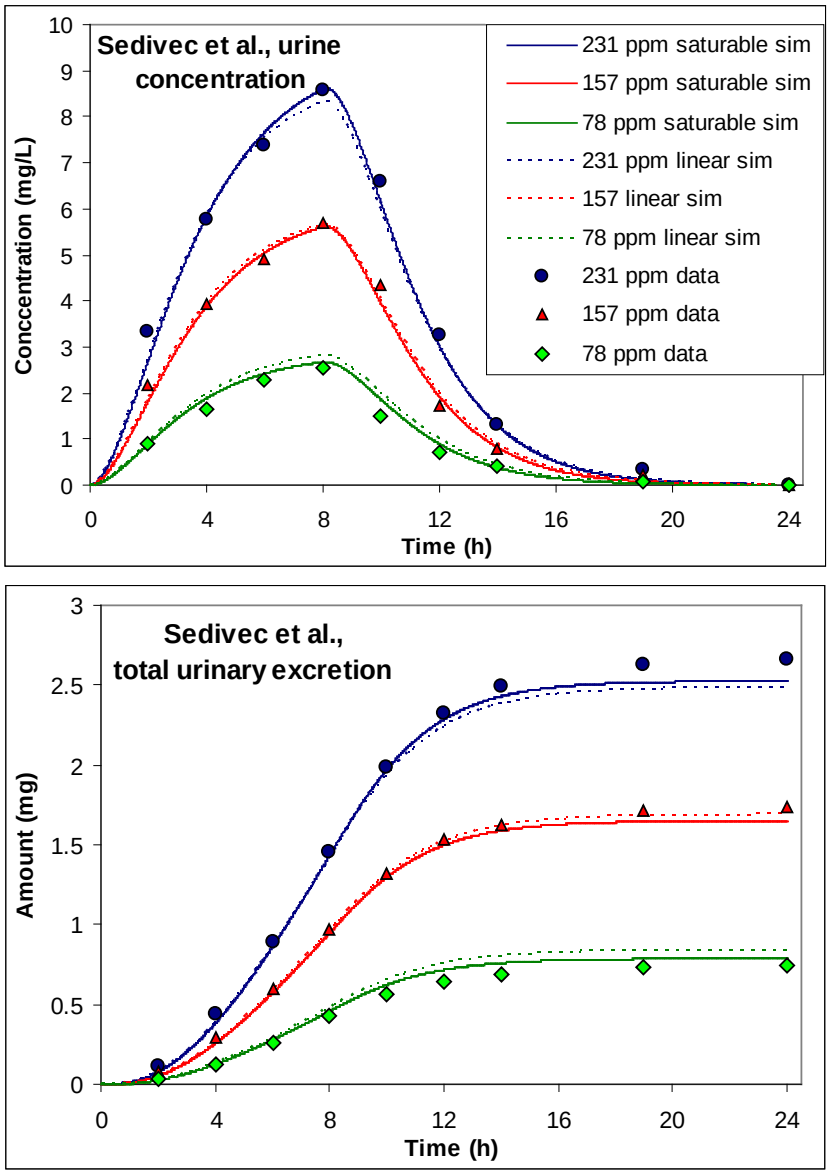

Figure B-16. Urinary MeOH elimination concentration (upper panel) and cumulative amount (lower panel), following inhalation exposures to MeOH in human volunteers. Data points in lower panel represent estimated total urinary MeOH elimination from humans exposed to 78 (diamonds), 157 (triangles), and 231 (circles) ppm MeOH for 8 hours, and lines represent PBPK model simulations. Solid lines are model results with the saturable equation for hepatic metabolism while dashed lines show results for liner metabolism. Data digitized from Sedivec et al. (1981) and provided for modeling by the EPA.

Source: Sedivec et al. (1981).

Table B-2. Primate kms reported in the literature

Km (mg/L)	Reference	Note
320 ±1273	Perkins et al., 1995	Human: oral poisoning, estimated dose
716 ± 489	Perkins et al., 1995	Cynomolgus monkey: 2 g/kg dose
278	Perkins et al., 1995	Rhesus monkey: 0.05-1 mg/kg dose
252 ± 116	Perkins et al., 1995	Cynomolgus monkey: 1 g/kg dose
33.9	Horton et al., 1992	PBPK model: adapted from rat Km
0.66	Fisher et al., 2000	PBPK model, Cynomolgus monkey:10-900 ppm
23.7 ± 8.7[a]	(This analysis.)	PBPK model, human: 100-800 ppm

Note- the values from Perkins et al. (1995b), are ± S.E.
[a]Mean ± S.D. This Km was optimized while also varying V_{max}, K1C, and KBL, from all of the at-rest human inhalation data as a part of this project. The S.D. given for this analysis is based on the Optimize function of acslXtreme, which assumes all data points are discrete and not from sets of data obtained over time and therefore a true S.D. would be a higher value. The final value reported in Table B-1 (21 mg/L) was obtained by sequentially rounding and fixing these parameters, then re-optimizing the remaining ones. For more detail, see text and Table B-3.

To estimate both the Michaelis-Menten and first-order rates, all human data under nonworking conditions (Batterman et al., 1998; Osterloh et al., 1996; Sedivec et al., 1981) were used. Before discussing the parameter estimation, however, adjustments were made to one of these data sets (Osterloh et al., 1996). Batterman et al., (1998) and Sedivec et al. (1981) both subtracted background levels before reporting their results. However, Osterloh et al. (1996) measured and reported (plotted) blood methanol in nonexposed controls (data shown in Figure B-17). The data for Osterloh et al. (1996) clearly show a time-dependent trend which is close to linear, and a linear regression is also included. However, the blood concentration (average) in the exposed group of that study was ~1.2 mg/L, whereas the data and regression in Figure B-17 indicate a value of ~ 0.9 mg/L. Therefore, the exposure data for Osterloh et al (1996) were corrected by subtracting time-zero value for the exposed group *plus* a time-dependent factor obtained by multiplying the slope of this regression (0.093 mg/L-hr) by the measurement time.

The metabolic (first-order or saturable) and urinary elimination constants were numerically fit to the nonworking human data sets while holding the value for FRACIN at 0.8655 (estimated from the results of Sedivec et al. as described above) and holding the ventilation rate constant at 16.5 L/hr/kg$^{0.75}$ and QPC at 24 L/hr/kg$^{0.75}$ (values used by EPA [2000d] for modeling the inhalation-route kinetics vinyl chloride). Other human-specific physiological parameters were set as reported in Table B-1.

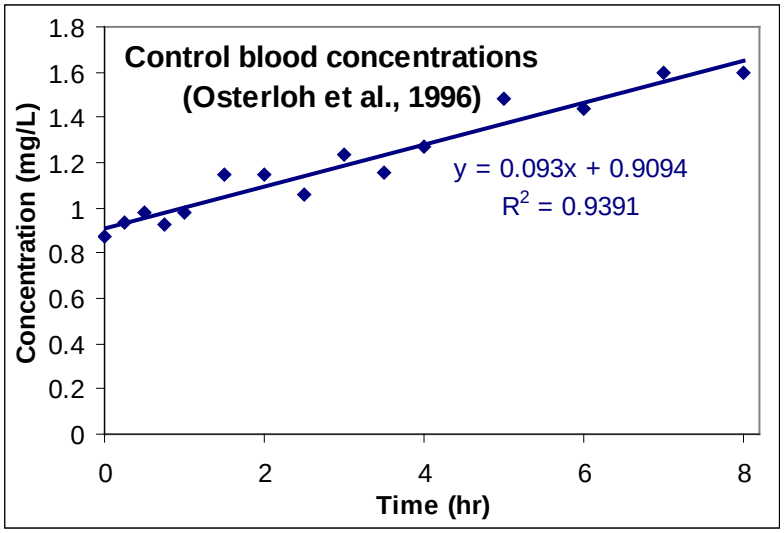

Figure B-17. Control (nonexposed) blood methanol concentrations

Source: Ernstgard et al. (2005); Osterloh et al. (1996).

Either (a) the set of $V_{max}C$, Km, K1C, and KBL were simultaneously varied while fitting the entire data set or (b) KLLC, K1C, and KBL were so varied and fit. Thus the two model fits are separated by a single degree of freedom (one additional parameter in case [a]). Statistical results given in Tables B-2 and B-3 are from these global fitting exercises. Final fitted parameters that have been used in the model for the risk assessment are given in Table B-1. The resulting fits of the two parameterizations (1st order or optimized Km/V_{max}) are shown in Figures B-16 and B-18.

Use of a first-order rate has the advantage of resulting in one fewer variable in the model and results in an adequate fit to the data, but the saturable model clearly fits some of the data better (Figures B-16 and B-18). To discriminate the goodness-of-fit resulting from the inclusion of an additional variable necessary to describe saturable metabolism versus using a single first-order rate, a likelihood ratio test was performed. Models are considered to be nested when the basic model structures are identical except for the addition of complexity, such as the added metabolic rate. Under these conditions, the likelihood ratio can be used to statistically compare the relative ability of the two different metabolism scenarios to describe the same data, as described by Collins et al. (1999). The hypothesis that one metabolic description is better than another is calculated using the likelihood functions evaluated at the maximum likelihood estimates. Since the parameters are optimized in the model using the maximum LLF, the resultant LLF is used for the statistical comparison of the models. The equation states that two times the log of the likelihood ratio follows a χ^2 distribution with *r* degrees of freedom:

$$-2[\log(\lambda(\text{model}1)/\lambda(\text{model}2))] = -2[\log\lambda(\text{model}1) - \log\lambda(\text{model}2)] \cong \chi_r^2$$

The likelihood ratio test states that if twice the difference between the maximum LLF of the two different descriptions of metabolism is greater than the χ^2 distribution, then the model fit has been improved (Devore, 1995; Collins et al., 1999; Steiner et al., 1990).

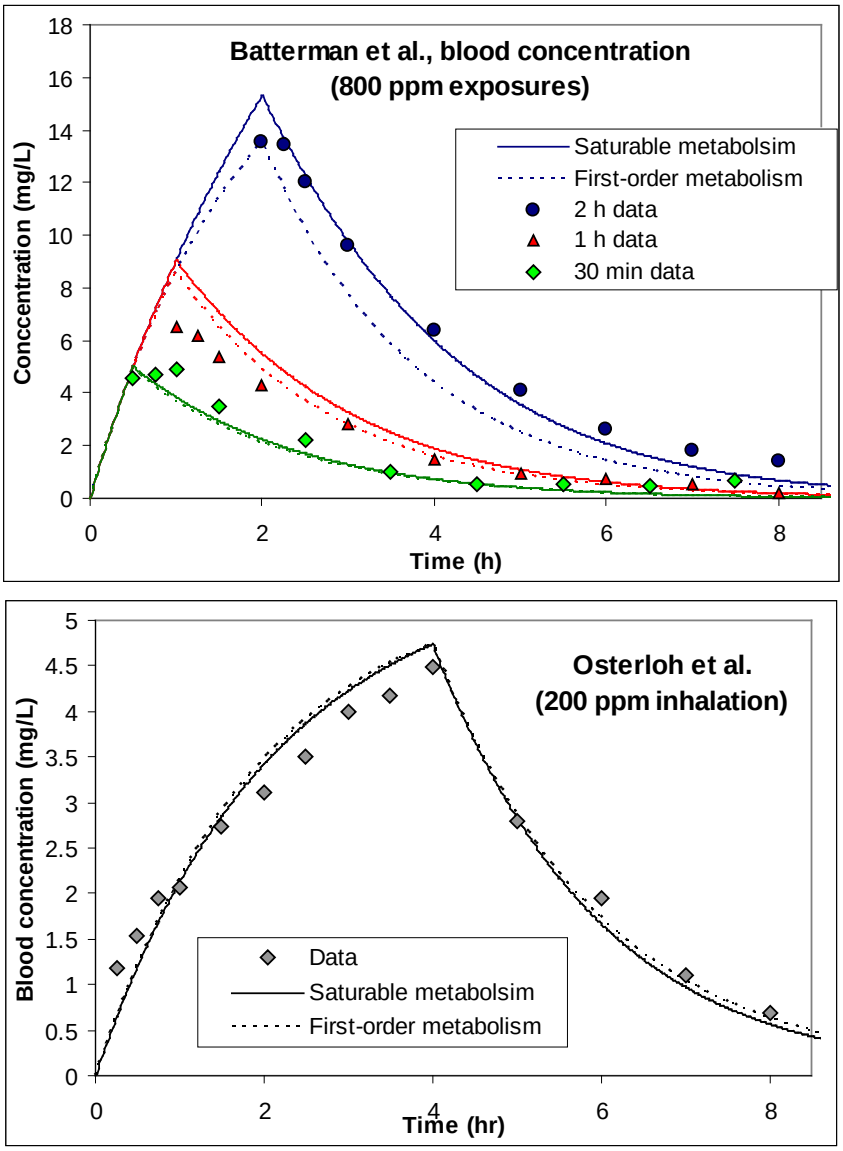

Figure B-18. Data showing the visual quality of the fit using optimized first-order or Michaelis-Menten kinetics to describe the metabolism of MeOH in humans. The rate constants used for each simulation are given in Table B-3.

Source: Batterman et al. (1998: top); Osterloh et al. (1996: bottom).

Table B-3. Parameter estimate results obtained using acslXtreme to fit all human data using either saturable or first-order metabolism

Parameters	Optimized value	S.D.	Correlation matrix	LLF
Michaelis-Menten (optimized)			-0.994	-24.1
Km	23.8	8.8		

$V_{max}C$	33.2	10.1		
First Order			NA	-31.0
KLLC	95.7	5.4		

Note: The S.D.s are based on the Optimize function of acslXtreme, which assumes all data points are discrete and not from sets of data obtained over time and therefore a true S.D. would be a higher value.

At greater than a 99.95% confidence level, using 2 metabolic rate constants (Km and $V_{max}C$) is preferred over utilizing a single rate constant (Table B-4). While the correlation coefficients (Table B-3) indicate that V_{max} and Km are highly correlated, that is not unexpected, and the S.D.s (Table B-3) indicate that each is reasonably bounded. If the data were indistinguishable from a linear system, Km in particular would not be so bounded from above, since the Michaels-Menten model becomes indistinguishable from a linear model as $V_{max}C$ and Km tend to infinity. Moreover, the internal dose candidate POD, for example the $BMDL_{10}$ for the inhalation-induced brain-weight changes from NEDO (1987), with methanol blood AUC as the metric, is 374.67 mg-hr/L, which corresponds to an average blood concentration of 15.6 mg/L. Therefore the Michaelis-Menten metabolism rate equation appears to be sufficiently supported by the existing data, and its use is expected to improve the accuracy of the HEC calculations, since those are being conducted in a concentration range in which the nonlinearity has an impact.

Table B-4. Comparison of LLF for Michaelis-Menten and first-order metabolism

LLF (logλ) for M-M	LLF (logλ) for 1st order	LLF 1st versus M-M [a]	χ_r^2 (99% confidence) [b]	χ_r^2 (99.95% confidence) [b]
-24.1	-31.0	34.1	13.8	12.22

Note: The models were optimized for all of the human data sets under non working conditions. M-M: Michaelis-Menten

[a]obtained using this equation: $-2[\log\lambda(\text{model}1) - \log\lambda(\text{model}2)]$

[b]significance level at r = 1 degree of freedom.

While the use of Michaelis-Menten kinetics might allow predictions across a wide exposure range (into the nonlinear region), extrapolation above 1,000 ppm is not suggested since the highest human exposure data are for 800 ppm. Extrapolations to higher concentrations are potentially misleading since the nonlinearity in the exposure-internal-dose relationship for humans is uncertain above this point. The use of a BMD or internally applied UFs should place the exposure concentrations within the range of the model.

The data from Ernstgard et al. (2005) was used to assess the use of the first-order metabolic rate constant to a dataset collected under conditions of light work. Historical measures of QPC (52.6 L/hr/kg$^{0.75}$) and QCC (26 L/hr/kg$^{0.75}$) for individuals exposed under conditions of 50 w of work from that laboratory (52.6 L/hr/kg$^{0.7}$) (Ernstgard, personal communication; Corley

et al., 1994; Johanson et al., 1986) were used for the 2-hour exposure period (Figure B-19). Otherwise, there were no changes in the model parameters (no fitting to these data). The results are remarkably good, given the lack of parameter adjustment to data collected in a different laboratory, using different human subjects than those to which the model was calibrated.

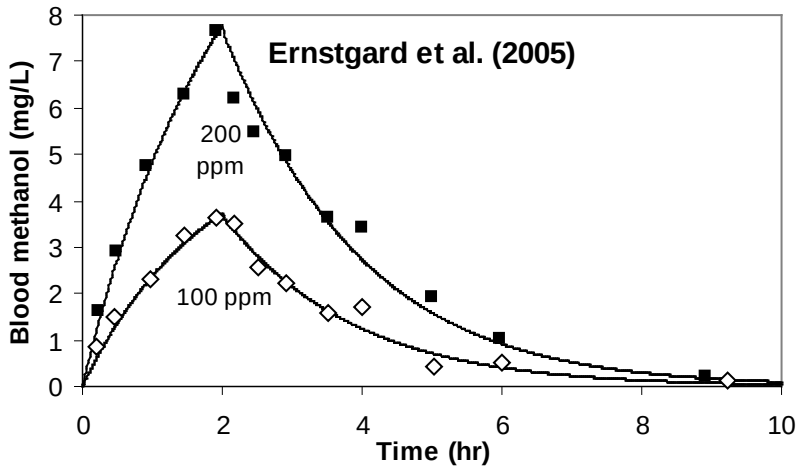

Figure B-19. Inhalation exposures to MeOH in human volunteers. Data points represent measured blood MeOH concentrations from humans (4 males and 4 females) exposed to 100 ppm (open symbols) or 200 ppm (filled symbols) for 2 hours during light physical activity. Solid lines represent PBPK model simulations with no fitting of model parameters. For the first 2 hours, a QPC of 52.6 L/hr/kg0.75 (Johansen et al. 1986), and a QCC of 26 L/hr/kg0.75 (Corley et al., 1994) were used by the model.

Source: Ernstgard et al.(2005).

B.2.8.1. ***(Should be B.2.8.2) Oral Route***

There were no human data available for calibration or validation of the oral route for the human model. In the absence of data to estimate rate constants for oral uptake, the 'humanset.m' file which sets parameters for human simulations applies the KMAS for the mouse with the other absorption parameters set to match those identified for ethanol in humans by Sultatos et al. (2004); VmASC was set such that for a 70-kg person, VMAS/KMAS matches the first-order uptake constant of Sultatos et al. (2004) (0.21 hr^{-1}). While Sultatos et al. include a term for ethanol metabolism in the stomach, no such term is included here and the rate of fecal elimination is set to zero, corresponding to 100% absorption. However zero-order ingestion, a continuous infusion at a constant rate into the stomach lumen equal to the daily dose/24 hours, was assumed for all human simulations. Since absorption was assumed to be 100% of administered MeOH, at steady state the rate of uptake from the stomach and intestine compartments (combined) must equal the rate of infusion to the stomach. Since C_{max} is driven by the oral absorption rate, which was assumed rather than fitted and verified, C_{max} was not used as a dose metric for human oral route simulations. AUC, which is less dependent on rate of uptake,

was used as the dose metric and for estimation of HEDs. Since the AUC was computed for a continuous oral exposure, its value is just 24-hours times the steady-state blood concentration at a given oral uptake rate.

B.2.8.1. ***(B.2.8.3) Inhalation Route HECs and Oral Route HEDs***

The atmospheric MeOH concentration resulting in a human daily average blood MeOH AUC (hr×mg/L) or C_{max} (mg/L) equal to that occurring in experimental animals following exposure at the POD concentration is termed the HEC. Similarly, the oral dose (rate) resulting in human daily average blood MeOH AUC (hr×mg/L) equivalent to that occurring in an experimental animal at the POD concentration is termed the HED.

To determine the HEC for specific exposures in mice, the mouse PBPK model is first used to determine the daily blood MeOH 24-hours AUC and C_{max} associated with 7 hour/day inhalation exposures. Mice were exposed each day for 10 days, so the full 10-day exposure was simulated and an average 24-hours AUC calculated over that time, so no other duration adjustment was needed. The human AUC was determined for the last 24 hours of a continuous 1,000-hour exposure, to assure steady state was achieved. The human C_{max} was determined at steady state and so is equivalent to the steady state blood MeOH concentration. Results are given in Table B-5 and for inhalation shown in Figure B-20.

For example, for a 1,000 ppm exposure this resulted in model-predicted peak blood of 133 mg/L and an AUC of 770 (hr×mg/L). The human model can then be used to determine the human MeOH exposure concentration leading to the same daily average AUC or C_{max} under continuous exposure conditions. Based on AUC, the HEC of the 1,000-ppm exposure is 684 ppm, while based on peak (human steady-state) concentration, the HEC is predicted to be 1110 ppm. The parameters used in the human model for these simulations are listed in Table B-1 for saturable kinetics.

The HED was calculated by using the human model to find the oral dose ($_{mg/kg\text{-}day}$) that gave a blood MeOH AUC equivalent to the mouse AUC following an exposure at the POD. Zero-order absorption was assumed. For example, the human oral exposure equivalent to a 1,000-ppm inhalation exposure in mice (i.e., with an AUC of 770 mg-hr/L) is 163 mg/kg-day. Since a 200 mg/kg-day oral exposure gave a human AUC of 1,320 mg-hr/L, which falls between the values predicted for inhalation exposures at 800 ppm (1,090 mg-hr/L) and 1,000 ppm (2,090 mg-hr/L), this oral exposure rate was taken to be the upper end for the model to accurately estimate an HED.

Table B-5. PBPK model predicted C_{max} and 24-hour AUC for mice and humans exposed to MeOH

Exposure concentration (ppm)	Inhalation Route				Oral Route	
	Mouse[a]		Human[b]		Human	
	AUC (mg-hr/L)	C_{max} (mg/L)	AUC (mg-hr/L)	Css (mg/L)	Dose (mg/kg-day)	AUC (mg-hr/L)
1	0.15	0.021	0.59	0.025	0.1	0.204
10	1.52	0.22	5.97	0.25	1	2.05
50	7.98	1.14	30.6	1.28	10	21.2
100	17.0	2.45	63.3	2.64	50	124
250	53.4	7.77	177	7.36	100	315
500	170	26.1	447	18.6	200	1320
1,000	770	133	2090	87.2	500	39400
2000	3310	524	31100	1300	1,000	125000
5000	17300	2000	147000	6130	2000	297000
1,0000	51200	4710	341,000	14200	5000	814000

[a]The mouse 24-hour average AUC were calculated under the conditions of the bioassay: 10 days of exposure with 7 hours of exposure during each 24 hour period.
[b]Human simulation results are considered unreliable above 1,000 ppm (inhalation) or 200 mg/kgday (oral), but are included for comparison

Again, since the available human exposure data is to, at most, 800 ppm, the model could not be calibrated for higher exposures that approximate most of the mouse and rat exposure concentrations. The AUC in humans for similar exposure levels is ~3 times greater than in the mouse, primarily because human exposure estimates are expected to result from 24-hour exposures and the mice were exposed for 7 hours.

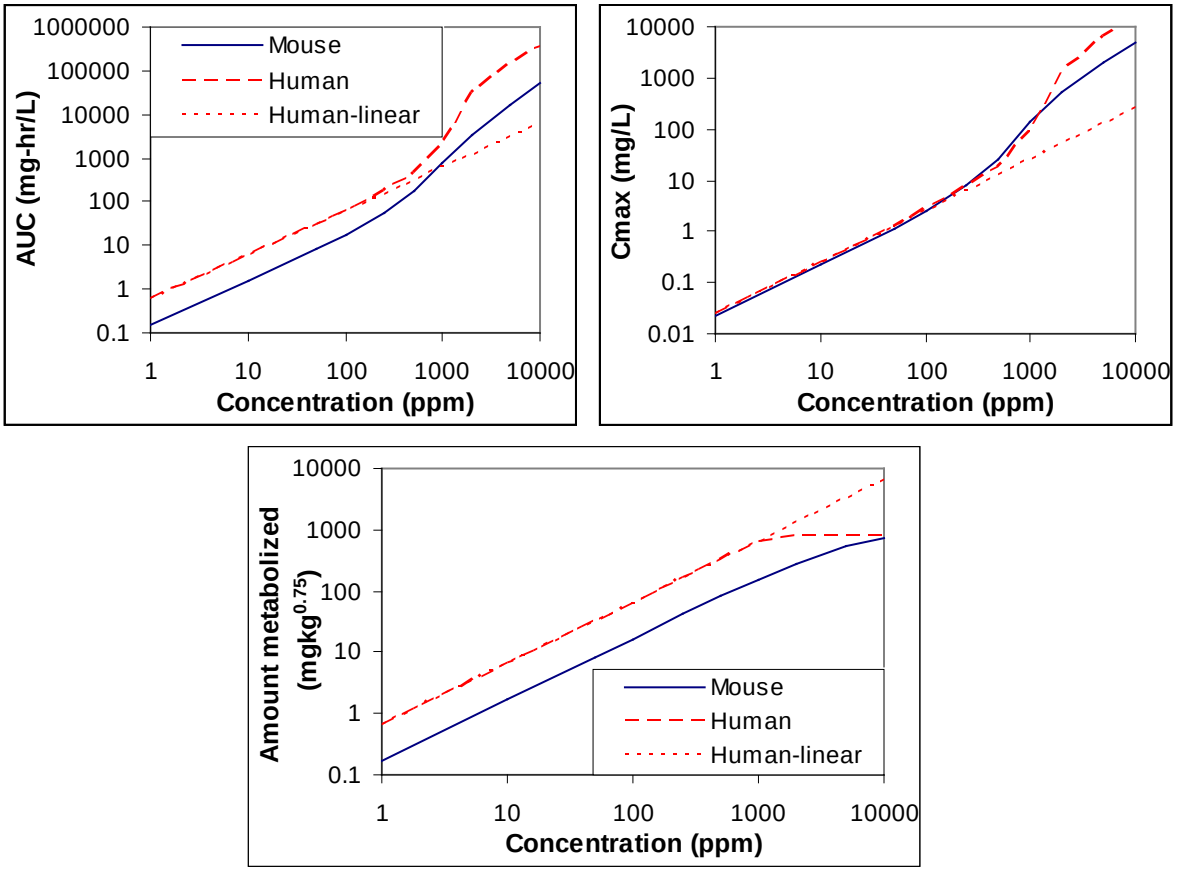

Figure B-20. Predicted 24-hour AUC (upper left), Cmax (upper right), and amount metabolized (lower) for MeOH inhalation exposures in the mouse (average over a 10-day exposure at 7 hours/day) and humans (steady-state values for a continuous exposure). C_{max} for human exposures is equal to the steady-state blood concentration. For humans, the long-dashed lines are model predictions using Michaelis-Menten metabolism (optimized Km of 23.8 mg/L) and the short-dashed lines are model predictions using first-order kinetics. Amount metabolized normalized to $BW^{0.75}$ to reflect cross-species scaling (Human simulation results above 1,000 ppm are not considered reliable but are shown for comparison).

While the PBPK computational code can be used in the future to derive HECs or HEDs for other exposures, an alternative approach was developed that allows non-PBPK model users to estimate MeOH HECs and HEDs from benchmark doses in the form of AUCs. This approach uses algebraic equations describing the relationship between predicted MeOH 24-hour AUC or total amount metabolized in the liver (MET, mg [per day]) (constant 24-hour exposure) and the inhalation exposure level (i.e., an HEC in ppm) (Equations 1, 1b, 3 or 3b) or oral exposure rate (i.e., an HED in mg/kg-day) (Equations 2, 2b, 4 or 4b). To use the equations to derive an HEC or HED, the target human AUC is applied to the appropriate equation. Since these relationships are for continuous exposures, blood concentration is constant, and hence extrapolation for a C_{max} is obtained by simply using AUC = $24*C_{max}$.

$$\text{HEC (ppm}_{<1000}) = 0.0224 \times \text{AUC} + \frac{1334 \times \text{AUC}}{794 + \text{AUC}} \qquad \text{Equation 1a}$$

$$\text{RfC (ppm)} = \left(0.0224 \times \text{AUC} + \frac{1334 \times \text{AUC}}{794 + \text{AUC}}\right) \Big/ UF \qquad \text{Equation 1b}$$

$$\text{HED (mg/kg/day}_{<200}) = 0.0058 \times \text{AUC} + \frac{275.4 \times \text{AUC}}{569 + \text{AUC}} \qquad \text{Equation 2a}$$

$$\text{RfD (mg/kg/day)} = \left(0.0058 \times \text{AUC} + \frac{275.4 \times \text{AUC}}{569 + \text{AUC}}\right) \Big/ UF \qquad \text{Equation 2b}$$

$$\text{HEC (ppm}_{<1000}) = 0.063554 \times \text{MET} + \frac{14.69 \times \text{MET}}{(19282.9 - \text{MET})} \qquad \text{Equation 3a}$$

$$\text{RfC (ppm)} = \left(0.063554 \times \text{MET} + \frac{14.69 \times \text{MET}}{(19282.9 - \text{MET})}\right) \Big/ UF \qquad \text{Equation 3b}$$

$$\text{HED (mg/kg/day}_{<200}) = 0.014287 \times \text{MET} + \frac{3.3 \times \text{MET}}{(19282.9 - \text{MET})} \qquad \text{Equation 4a}$$

$$\text{RfD (mg/kg/day)} = \left(0.014287 \times \text{MET} + \frac{3.3 \times \text{MET}}{(19282.9 - \text{MET})}\right) \Big/ UF \qquad \text{Equation 4b}$$

B.2.9. Conclusions and Discussion

Mouse, rat, and human MeOH PBPK models have been developed and calibrated to data in the open literature. The model simplifies the structure used by Ward et al. (1997) while adding specific refinements (e.g., a standard lung compartment and a two-compartment GI tract).

Although the endpoints of concern are developmental effects which occur during in utero and (to a lesser extent) lactational exposure, it is not necessary for a MeOH PBPK model to specifically describe pregnancy (i.e., specify a fetal/gestational/conceptus compartment) and lactation in order for it to provide better cross-species extrapolation of risk than default methods. Representation of the unique physiology of pregnancy and the fetus/conceptus would be necessary if MeOH pharmacokinetics differed significantly during pregnancy or if the observed partitioning of MeOH into the fetus/conceptus versus the mother showed a concentration ratio significantly greater than or less than 1. MeOH pharmacokinetics GD6–GD10 in the mouse, are not different from NP mice (Pollack and Brouwer, 1996), and the maternal blood:fetus/conceptus partition coefficient is reported to be near 1 (Ward et al., 1997; Horton et al., 1992). At GD18 in the mouse, maternal blood levels are only modestly different from those in NP animals (see Figures B-4 and B-5 for examples), and in general the PBPK model simulations for the NP animal match the pregnancy data as well as the NP data. Likewise maternal blood kinetics in monkeys differs little from those in NP animals (see Section 3.4.7). Further, in both mice and monkeys, to the extent that late-pregnancy blood levels differ from NP for a given exposure, they are higher; i.e., the difference between model predictions and actual concentrations is in the same direction. These data support the assumption that the ratio of actual target-tissue methanol concentration to (predicted) NP maternal blood concentrations will be about the same across

species, and hence that using NP maternal blood levels in place of fetal concentrations will not lead to a systematic error when extrapolating risks. Thus, a full representation of pregnancy and the fetal/conceptus compartment appears to be unnecessary.

While lactational exposure is less direct than fetal exposure and blood or target-tissue levels in the breast-feeding infant or pup are likely to differ more from maternal levels, the health-effects data indicate that most of the effects of concern are due to fetal exposure, with only a small influence due to postbirth exposures. Separating out the contribution of postbirth exposure from pre-birth exposure to a given endpoint in a way that would allow the risk to be estimated from estimates of both exposure levels would be extremely difficult, even if one had a lactation/child PBPK model that allowed for prediction of blood (or target-tissue) levels in the offspring. And one would still expect the target-tissue concentrations in the offspring to be closely related to maternal blood levels (which depend on ambient exposure and determine the amount delivered through breast milk), with the relationship between maternal levels and those in the offspring being similar across species.

Therefore, the development of a lactation/child PBPK model appears not to be supported, given the minimal change that is likely to result in risk extrapolations and use of (NP) maternal blood levels as a measure of risk in the offspring is still considered preferable over use of default extrapolation methods. In particular, the existing human data allow for accurate predictions of maternal blood levels, which depend strongly on the rate of maternal methanol clearance. Failing to use the existing data (via PBPK modeling) on human methanol clearance (versus that in other species) would be to ignore this very important determinant of exposure to breast-fed infants. And since bottle-fed infants do *not* receive methanol from their mothers, they are expected to have lower or, at most, similar overall exposures for a given ambient concentration than the breast-fed infant, so that use of maternal blood levels for risk estimation should also be adequately protective for that group.

During model development, several inconsistencies between experimental blood MeOH kinetic data embedded in the Ward et al. model (1995) and the published figures first reporting these data were discovered. Therefore, data were digitized from the published literature when a figure was available, and the digitized data was compared to the provided data. When the digitized data and the data embedded in the computational files (i.e., provided to Battelle under contract from the EPA) were within 3% of each other, the provided data was used; when the difference was greater than 3%, the digitized data was used. Often, using the published figures as a data source resulted in substantial improvements of the fit to the data in the cases where the published figures were different from the embedded data.

The final MeOH PBPK model fits well inhalation-route blood kinetic data from separate laboratories in rodents and humans. Intravenous-route blood MeOH kinetic data in NP mice were only available for a single i.v. dose of 2,500 mg/kg, but were available for GD18 mice following administration of a broader range of doses: 100, 500, and 2,500 mg/kg. Up to

20 hours postexposure, blood MeOH kinetics appear similar for NP and pregnant mice after administration of 2,500 mg/kg. The intravenous pharmacokinetic data in GD18 mice showed an unexpected dose-dependent nonlinearity in initial blood concentrations, suggesting either a dose dependence on the volume distribution, which is unlikely, or some source of experimental variability. To account for this nonlinearity, Ward et al. (1997) used dose-specific partition coefficients for placenta and embryonic fluid and V_{max} for the metabolism of MeOH. The current model uses a consistent set of parameters that are not varied by dose and therefore does not fit these 100 mg/kg dose intravenous data. The model does fit the 500 and 2,500 mg/kg doses, and if a presumed i.v. dose of 200 mg/kg (twice the reported 100 mg/kg) is employed, is able to predict initial blood concentrations for the lowest dose data, as expected. The i.v. data from the Ward et al. (1995) model does match the corresponding published figures.

The model fits to the mouse oral-route MeOH kinetic data using a consistent set of parameters (Figure B-4) are reasonably good but not as good as fits to the inhalation data. The model consistently underpredicts the amount of blood MeOH reported in two studies (Ward et al., 1997, 1995). Ward et al. (1997) utilized a different V_{max} for each oral absorption data set. In the report by Ward et al. (1997) the GD18 and the GD8 data from Dorman et al. (1995) were both fit using a V_{max} of ~80 mg/kg/hr (body weights were not listed, the model assumed that GD8 and GD18 mice were both 30 g; Ward et al. (1997) did not scaled by body weight), but lower partition coefficients for placenta (1.63 versus 3.28) and embryonic fluid (0.0037 versus 0.77). The current model adequately fits the oral pharmacokinetic data using a single set of parameters that is not varied by dose or source of data.

The fits of the rat model to the limited dataset readily available were quite good. The low-dose exposures of all routes were emphasized in model optimization since they were the doses most relevant to risk assessment. Based on a rat inhalation exposure to 500 ppm, the human HEC would be 301 ppm (by applying an AUC of 226 [Figure B-12] to Equation 1).

The mouse, rat, and human models fit multiple datasets from multiple research groups using consistent parameters that are representative of each species, but are not varied within species. Using the model, it will be possible to ascertain chronic human exposure concentrations that are likely to be without an appreciable risk of deleterious effects.

B.3. ADDITIONAL MATERIAL

- Results from Optimizations
- acslXtreme Program (.csl) File (Electronic Attachment)
- acslXtreme procedure (.cmd) file
- Key to .m files for reproducing the results in this report
- Code for .m files

- Personal communication from Lena Ernstgard regarding human exposures reported in the Ernstgard and Johanson, 2005 SOT poster
- Personal communication from Dr. Rogers regarding mouse exposures to MeOH
- Data and simulations for MeOH Metabolic Clearance/Total Metabolites Produced
- Multiple daily oral dosing for humans

B.3.1. Results From Optimizations

B.3.1.1. ***Approach for and Results of the Optimization of Metabolic Parameters and Inhalation Route Fractional Availability in Mice***

The approach and results are presented below in outline format with supporting figures. More complete documentation was not developed because the products of the optimizations were not used in the final model. The documentation here is intended only to demonstrate that appropriate optimizations were conducted and what the results of those optimizations were.

1. The V_{max} for the low affinity pathway was set to 0 and the remaining $V_{max}C$, Km, and fractional availability were optimized using inhalation data only.
    a. The optimizer was unable to find a value for Km that was greater than 0.
    b. The resulting metabolic parameters essentially represented a zero order loss process.
2. The V_{max} for the low affinity pathway was set to 0 and the remaining $V_{max}C$ and Km were optimized using all (oral, intravenous and inhalation) data.
    a. The optimized single Km, 135 mg/L, was equal to the average of the 2 original Kms.
    b. Fits to the MeOH blood levels following inhalation exposures > 2,000 ppm are slightly improved, but the model fits to the 1,000 ppm exposure concentration overpredict reported values by 20%.
3. Parameters for both metabolic pathways were optimized using all (oral, intravenous and inhalation) data.
    a. The fit to the high-dose intravenous data from Ward et al. (1997) (2,500 mg/kg) was improved (Figure B-21).
    b. The fit to the high-dose oral data, also from Ward et al. (1997), (2,500 mg/kg) was improved (Figure B-22).
    c. The fit to the mid-dose i.v. data (500 mg/kg) dose was not as good as using the visually fit parameters (Figure B-21)
    d. The fit to the low-dose oral data (1,500 mg/kg) was not as good when the visually fit parameters were used (Figure B-22). The low-dose data was from Dorman et al. (1995).

e. Neither set of parameters resulted in an adequate fit to the low-dose intravenous data (100 mg/kg; Figure B-21).

f. Fits to the inhalation data following exposures to < 5,000 ppm MeOH were substantially worse than when using the visually fit parameters (Figure B-23)

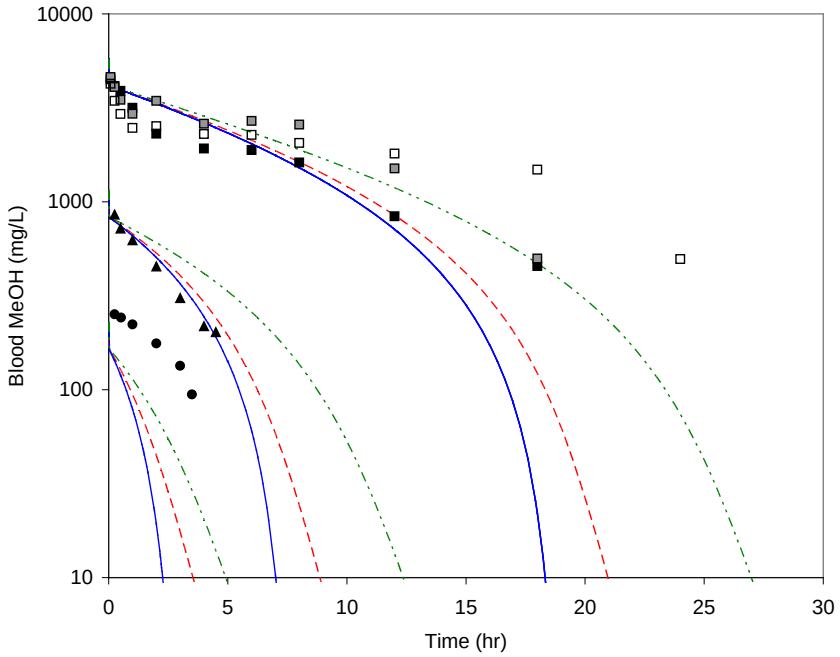

Figure B-21. Fit of the model to i.v. data using different clearance and uptake parameter optimizations. Solid blue lines - visually optimized; dashed red lines - clearance parameters (Km, Km2, VmaxC, Vmax2C) optimized using all inhalation data sets; dash/dot green lines - clearance parameters optimized using all data sets (inhalation, oral, and intravenous).

Source: Ward et al. (1997).

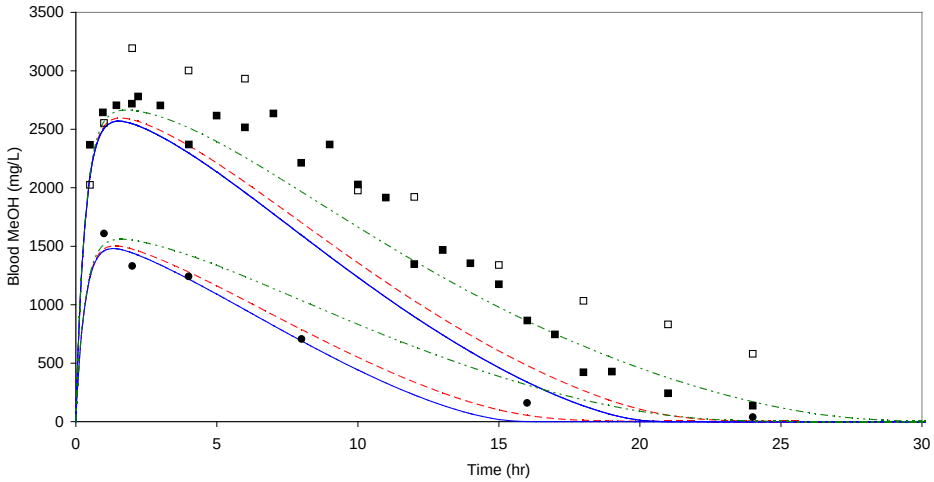

Figure B-22. Fit of the model to oral data using different clearance and uptake parameter optimizations. Solid blue lines - visually optimized; dashed red lines - clearance parameters (Km, Km2, $V_{max}C$, $V_{max}2C$) optimized using all inhalation data sets; dash/dot green lines - clearance parameters optimized using all data sets (inhalation, oral, and intravenous).

Source: Ward et al. (1997); Dorman et al. (1995).

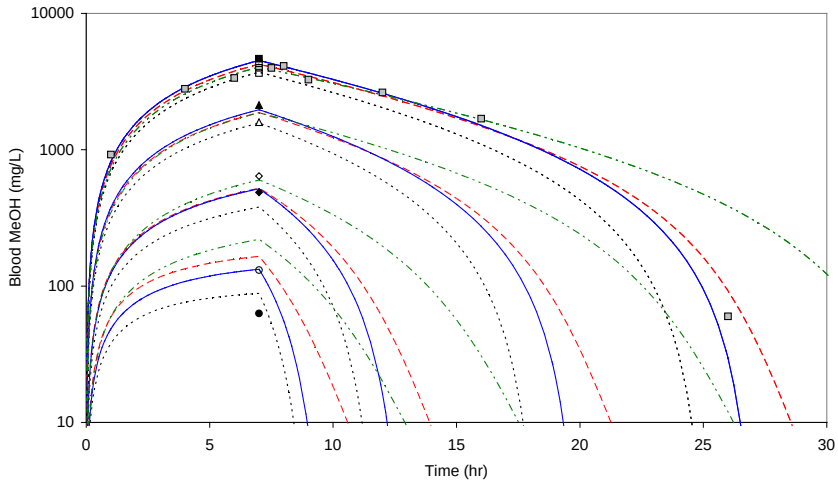

Figure B-23. Fit of the model to inhalation data using different clearance and uptake parameter optimizations. Dotted black lines - model optimized fractional inhalation, solid blue lines - visually optimized; dashed red lines - clearance parameters (Km, Km2, VmaxC, Vmax2C) optimized using all inhalation data sets; dash/dot green lines - clearance parameters optimized using all data sets (inhalation, oral, and intravenous).

Source: Rogers et al. (1997).

B.3.1.1. *[B3.1.2.] Conclusion*

Under the best circumstances, formal optimizations offer the benefit of repeatability and confirmation that global optima have not been missed by user-guided visual optimization. Incorporating judgments regarding the value of specific data sets while easy when visually fitting, is difficult at best when using optimization routines. This is an important distinction between these approaches for this modeling exercise.

The mouse NOEL was 1,000 ppm MeOH. Fitting the blood MeOH concentration data at this exposure drove our modeling exercises because of the importance of this exposure group in the risk assessment. Unfortunately, the vast majority of the blood MeOH data came from much higher exposures. As expected, our various attempts at optimization led to fits that were better for some, but never all, data sets. This is to be expected when there is clearly significant variability in the underlying data. Various data weighting schemes were included to improve overall optimization while maintaining a good fit to the 1,000 ppm data. In the end, optimization offered no significant improvement over the fractional uptake and metabolic parameter values obtained by visual optimization, so these were retained in the final version of the model.

B.3.2. acslXtreme Program (.csl) File

```
PROGRAM MeOH -- PBPK Model for Methanol
PROGRAM MeOH -- PBPK Model for Methanol
! Based on MeOH Model by Ward et al 1997 with these revisions:
! TS Poet, P Hinderliter and J Teeguarden,
! Center for Biological Monitoring and Modeling   4/16/05
! Pacific Northwest National Laboratory
! Model contains inhalation, iv, and oral (multiple patterns).
! 1) Removed fetal compartment and other tissues that could be lumped
! based on similarity of partition coefficients or did not need to be
! specified directly (Bone, mammary tissue) for the modeling purposes here.
! 2) Changed day to hr.
! 3) Flows (scaled to BW or BW**0.75), Metabolism (BW**0.75) and
! tissue volumes (BW) are scaled in the model.
! Final has somach and intestine compartments which provide fast and
! slow absorption rates, respectively.
! 4) Bladder compartment (for human simulations) added by Paul
! Schlosser, U.S. EPA, Oct. 2008
! 5) "Sipping" drinking water exposure code for rats, to match data
! from Peng et al. (1990)
! 6) Time-variable drinking pattern for mice from Keys et al. (2004)
! added by Paul Schlosser, U.S. EPA, Aug. 2009
! Version is final version used for simulations
! ************ MODEL UNITS *****************
!       Concentration, mg/L
!       Mass of Chemical, mg
!       Volume, L
!       Flow, L/hr
!       Body Weight Kg
!=========================72 Character Line=========================!
INITIAL
! Initialize some Variables before start
```

```
Integer IDS, MULTE
REAL DRT(6), DRP(6)   !store drink water times, percents in array!

CONSTANT      BW = 0.030       ! Body weight (kg)
CONSTANT      QPC = 15.        ! Alveolar ventilation (L/hr/kg**0.75)

! Blood Flows (fraction of cardiac output)
        CONSTANT      QCC = 15.0       ! Cardiac output (L/hr/kg**0.75)
        CONSTANT      QFC = 0.05       ! Fat
        CONSTANT      QLC = 0.25       ! Liver
! Blood flow to rest of body Calculated by Flow Balance!
        QRC = 1.0 - (QFC + QLC)
        QC = QCC*BW**0.75
        QP = QPC*BW**0.75

! Tissue Volumes for mice (fraction of body weight)
        CONSTANT      VAC = 0.0123   ! Arterial blood
        CONSTANT      VFC = 0.07       ! Fat
        CONSTANT      VLC = 0.055      ! Liver
        CONSTANT      VLuC = 0.0073  ! Lung tissue
        CONSTANT      VVBC = 0.0368 ! Venous blood
        VRC = 0.91 - (VAC+VFC+VLC+VLuC+VVBC)

! Partition Coefficients (Mouse values from Ward et al used as default)
        CONSTANT      PB = 1350        ! MeOH Blood:Air; Use Horton value!
        CONSTANT      PF = 0.08        ! MeOH Fat:Blood
        CONSTANT      PL = 1.1         ! MeOH Liver:Blood
        CONSTANT      PLU = 1.0        ! MeOH Lung:Blood, compartment for dosing only
        CONSTANT      PR = 0.8         ! MeOH Rest of body:Blood

! Hepatic Metabolism of MeOH
        CONSTANT      KM = 45.0        ! mg/L
        CONSTANT      VMAXC = 15.0  ! mg/hr/BW**0.75
        VMAX = VMAXC*BW**0.75       ! mg/hr
        CONSTANT      VMAX2C = 15.0! 2nd saturable pathway
        VMAX2 = VMAX2C*BW**0.75
        CONSTANT      KM2= 45.0
        CONSTANT KLLC = 0.0           ! First-order metabolism
! Set VMAXC = VMAX2C = 0, when KLLC > 0
        KLL = KLLC/BW**0.25

! MeOH Clearance from Blood!
        CONSTANT      K1C = 0.01       ! First-order clearance, BW**0.25/hr
        K1 = K1C/BW**0.25      ! Scaled blood elimination, hr-1
! This lumped term was used in the WARD model an accounted for
! renal elimination and "additional" non-hepatic metabolism of
! MeOH associated only with high dose i.v. data.
! A 1st-order term should not be used to represent two processes
! with different dose-dependencies.
! This has not been used for mouse data (set=0), but was used to
! approximate human urinary data!

! Bladder compartment added (Paul Schlosser, U.S. EPA, 10/2008)
        CONSTANT KBL=0.0    ! Bladder constant, 1/hr

! Fractional Absorption of MeOH
        CONSTANT      FRACin = 0.85  ! Inhalation, value from Perkins et al
```

```
        CONSTANT    KFEC = 0.0      ! Fecal elimination constant, 1/hr
                ! KFEC determines oral bioavailability

! Molecular Weight of MeOH
        CONSTANT    MWMe = 32.0   ! mol wt, g/mol!

! Closed Chamber Parameters
        CONSTANT    VChC = 100.0  ! Volume of closed chamber (L)
        CONSTANT    Rats = 0.0      ! Number of rats in chamber
        CONSTANT    kLoss = 0.0     ! Chamber loss rate /hr
        ! Set RATS = 0.0 and KLOSS = 0.0 for open chamber

! Blood Flows (L/hr)
        QF = QFC*QC  ! Fat
        QL = QLC*QC  ! Liver
        QR = QRC*QC  ! Rest of Body

! Tissue Volumes (mL)
        VAB = VAC*BW! Arterial blood volume
        VF = VFC*BW             ! Fat
        VL = VLC*BW             ! Liver
        VLu = VLuC*BW           ! Lung
        VR = VRC*BW             ! Rest of the body
        VVB = VVBC*BW           ! Venous blood
        VBL = VAB + VVB         ! Total blood

!----------Timing commands------------!
        CONSTANT    TCHNG = 6.0             ! End of exposure!
        CONSTANT    TSTOP = 24.0            ! End of experiment/simulation!
        CONSTANT    POINTS = 1000.0         ! No. points for simulation output!
        CONSTANT    REST = 100000.0         ! End of work period for human exercise
        CONSTANT    WORK = 100000.0         ! Start of work period for human exercise
        SCHEDULE DS1.AT.REST        ! Change from work to rest conditions
        SCHEDULE DS2.AT.WORK        ! Change from rest to work conditions
        ! Human Rest/Work (changes in blood-flow fractions to fat/liver not currently used0
        CONSTANT QPCHR=15.0, QCCHR=15.0, QLCHR=0.25, QFCHR=0.05  ! Rest
        CONSTANT QPCHW=52.0, QCCHW=26.0, QLCHW=0.16, QFCHW=0.06          ! Work

!---------Simulation Control------------!
! Exposure Conditions Based on User Defined Initial Amounts of
! Chemical (mg)
        CONSTANT CONCppm = 0.0    ! Air Concentration in ppm
        VCh = VChC-(Rats*BW)                    ! Volume of Occupied Chamber
        CONCmg = CONCppm*MWMe/24451   ! Convert ppm to mg/Liter!
        ACHO = CONCmg*VCH                       ! Init Amt in Chamber, mg!

! Oral dosing
        CONSTANT    KAS = 0.1       ! 1st order oral abs, hr-1
        CONSTANT    KMASC = 550   ! Saturable oral abs Kmasc [=] mg/kg
                KMAS = KMASC*BW
        CONSTANT    VASC   = 1740 ! Saturable oral ab VmaxC, mg/hr/kg^0.75
                VAS = VASC*BW**0.75 ! Saturable oral ab Vmax, mg/hr
        CONSTANT    KAI = 0.1       ! 1st order oral abs from intestine, hr-1
        CONSTANT    KSI = 0.5       ! 1st order transfer stom to intes hr-1
        CONSTANT    DOSE = 0.0      ! Oral dose in mg/kg BW
        CONSTANT    ODS = 0.0       ! Switch for zero order oral uptake
        ! (Set to 1 for zero order, set to 0 for first order)
```

```
        ODOSE = DOSE*BW*(1.0-ODS)          ! Convert mg/kg to mg total (oral)
        RAOZ = DOSE*BW*ODS/24.0   ! mg/hr for zero order dosing

        ! Daily dose for steady drinking water by "sipping" (by rats)
                CONSTANT DWDOSE = 0        ! mg/kg/d by periodic sipping
                CONSTANT PER1 = 1.5        ! Period between sipping episodes (hr) during dark
        ! "Between" means from the start of 1 to the start of the next episode
                CONSTANT DUR1 = 0.75       ! Duration of sipping episodes during dark (hr)
                CONSTANT PER2 = 3.0        ! Period during light (hr) between sipping episodes
                CONSTANT DUR2 = 0.5        ! Duration of sipping episodes during light (hr)
                CONSTANT FNIGHT = 0.8      ! Fraction of drinking during night
                constant days = 7.0      ! days/week of oral exposure
                constant metd = 7.0      ! number of days at end over which AUCBF and AMETF
                                         ! are averaged
                tmetf = metd*24.0
                dayon=24.0*days
        ! Night sipping rate (mg/h) during episodes
                DWRNIGHT = DWDOSE*BW*FNIGHT*PER1/(12.0*DUR1)
        ! Day sipping rate (mg/h) during episodes
                DWRDAY = DWDOSE*BW*(1-FNIGHT)*PER2/(12.0*DUR2)
        IDOSE=0
        ! Above assumes 12-hr each for day/night

! Drinking Table from Deborah Keys for mice, as used in
! A quantitative description of suicide inhibition of dichloroacetic acid in rats and mice.
! Keys DA, Schultz IR, Mahle DA, Fisher JW.
! Toxicol Sci. 2004 Dec;82(2):381-93.
! Based on data of Yuan, J. (1993). Modeling blood/plasma concentrations in dosed feed and dosed
! drinking water toxicology studies. Toxicol. Appl. Pharmacol. 119, 131-141.
constant rdrink = 1.0 ! Default for use of sipping w/ DWDOSE abopve
        ! set rdrink = 0.0 to use pattern below
table mdrinkp,1,49 / 0., .5, 1., 1.5, 2., 2.5, 3., 3.5, &
      4., 4.5, 5., 5.5, 6., 6.5, 7., 7.5, &
      8., 8.5, 9., 9.5, 10., 10.5, 11., 11.5,  &
     12., 12.5, 13., 13.5, 14., 14.5, 15., 15.5,  &
     16., 16.5, 17., 17.5, 18., 18.5, 19., 19.5,  &
     20., 20.5, 21., 21.5, 22., 22.5, 23., 23.5, 24.0,  &
      0.12 , 0.9, 1.6, 1.8, 1.9, 2.9, 4.0, 4.5, 4.9, 4.9,  &
     4.8, 4.4, 4.0, 5.0, 5.9, 5.3, 4.5, 3.9,  &
     3.2, 3.0, 2.7, 2.5, 2.3, 2.3, 2.3, 1.9,  &
     1.4, 1.4, 1.3, 1.3, 1.3, 1.1, 0.8, 0.8,  &
     0.8, 0.6, 0.5, 0.7, 0.8, 0.6, 0.4, 0.2,  &
     0.05, 0.08, 0.14, 0.07, 0.06, 0.08, 0.12 /

        ! Larger bolus dosing
                CONSTANT DRDOSE=0.0        ! Total dose by drinking water in boluses, mg/kg day
        ! Times for multiple oral drinks/day *after* 0
                ! Must be ascending, 0 <= times < 24 hr
                ! CONSTANT DRT=0, 2, 4, 6, 8, 10        ! Rat values
                Constant DRT = 0.0, 3.0, 5.0, 8.0, 11.0, 15.0       ! Human values
                ! DRTIME(1) assumed = 0 and not used
        ! Fraction consumed by drinking at those times
                CONSTANT DRP = 0.25, 0.1, 0.25, 0.1, 0.25, 0.05

        !Total oral bolus dose; initial value given at t=0 via initial condition
                TODOSE = DRP(1)*DRDOSE*BW*(1.0-ODS) + ODOSE
```

```
! IV dosing
        CONSTANT IVDOSE = 0.0       ! IV dose, mg/kg
        CONSTANT TINF = 0.025       ! Length of exposure (hrs), default = 1.5 min (bolus)
                ! 1.5 min reported by Ward and Pollack, DMD 1996
        TIV = IVDOSE*BW       ! Expected amt infused, mg
        IV1 = TIV/TINF  ! Rate of infusion, mg/hg

! For I.V. Runs, control step size if necessary by changing MaxT, not POINTs or CINT
        MAXT = 1.0      ! Maximum Step Size, Hours
        !IF (IVDOSE.GE.1.0E-4) MAXT = 1.0E-4

! Liver infusion
        CONSTANT LIVR0 = 0.0          ! Zero-order liver total, mg/kg/day
        RLIV0 = LIVR0*BW/TCHNG      ! Rate in mg/hr

!--------Dose Scheduling-----------------
        CONSTANT MULTE=0                        ! Default is *no* repeated dosing/inhalation
        CIZONE = 1.0   ! Start with inhalation on
        IVZONE = 1.0   ! Start with IV on
        SCHEDULE OFF.AT.TCHNG    ! Turn off exposure at TCHNG
        DAY = 0;
        NEWDAY = 0; IDS = 2   ! First dose given as initial condition
        IF (MULTE) SCHEDULE ORALDOSE.AT.DRT(2)
ALGORITHM IALG = 2  ! Gear algorithm
END     ! END OF INITIAL

DYNAMIC

DERIVATIVE
!************************   MeOH   *************************
        IVR = IVZONE*IV1        ! IV dosing; IVR = ate of infusion, mg/hg
! Oral Dosing
        DWING = ( (DWRNIGHT*PULSE(0.0,PER1,DUR1)*PULSE(0.0,24.0,12.0) + &
                DWRDAY*PULSE(0.0,PER2,DUR2)*(1-PULSE(0.0,24.0,12.0)) )*rdrink + &
                (1-rdrink)*mdrinkp(mod(T,24.0))*0.02*DWDOSE*BW )*PULSE(0.0,168,dayon)
        RAS = KAS*STOM + VAS*STOM/(KMAS+STOM)
        RSTOM = DWING + RAOZ - RAS - KSI*STOM   ! Change in stomach (mg/hr)
        RINT = KSI*STOM - RFEC - KAI*AINTEST        ! Change in intestines (mg/hr)
        RLZ = RLIV0*CIZONE   ! Zero-order to liver
        RAO = RAS + KAI*AINTEST + RLZ       ! Oral absorption (mg/hr)
        RFEC = KFEC*AINTEST
        FEC = INTEG(RFEC, 0.0)
        STOM = INTEG(RSTOM, TODOSE)      ! Amt in stomach (mg)
        AINTEST = INTEG(RINT, 0.0)   ! Amt in intestines (mg)
        OralDoseCheck = INTEG(RAO, 0.0)

! Arterial Blood
        RAAB = QC*(CVLU - CAB)
        AAB = INTEG(RAAB, 0.0)          ! Amount, mg
        CAB = AAB/VAB                   ! Concentration, mg/L
        AAUCB = INTEG(CAB, 0.0)         ! AUC, hr*mg/L

! Fat
        RF = QF*(CAB - CVF)
        AF = INTEG(RF, 0.0)     ! Amount, mg
        CF = AF/VF      ! Concentration, mg/L
        CVF = CF/PF     ! AUC, hr*mg/L
```

```
! Liver
        RAL = QL*(CAB - CVL) + RAO - RMETL - RMETL2 - RMETL3
        AL = INTEG(RAL, 0.0)  ! Amount, mg
        CL = AL/VL            ! Concentration, mg/L
        CVL = CL/PL           ! Concentration, mg/L
        AUCL = INTEG(CL, 0.0)! AUC, hr*mg/L

! Liver Metabolism
        RMETL = VMAX*CVL/(KM + CVL)
        METL = INTEG(RMETL, 0.0)
        RMETL2 = VMAX2*CVL/(KM2 + CVL)
        METL2 = INTEG(RMETL2, 0.0)
        RMETL3 = KLL*CVL
        METL3 = INTEG(RMETL3, 0.0)

! Total Amount Metabolized (Formate and Formaldehyde)
! Does not include K1C for human MeOH excretion estimate
        AMET = METL + METL2 + METL3
        AMET24 = AMET*24.0/TSTOP
! Total amount metabolized in last tmetf hr of exposure, averaged per day
        AMETF = INTEG((RMETL+RMETL2+RMETL3)*PULSE(TSTOP-tmetf,TSTOP,tmetf),0.0)* &
                24.0/tmetf      ! (tmetf = 24.0*metd)
! Chamber concentration (mg/L)
        RACh = (Rats*QP*CLEx) - (FRACin*Rats*QP*CCh) - (kLoss*ACh)
        ACh = INTEG(RACh, AChO)

! The following calculation yields an air concentration equal to the
! closed chamber value if a closed chamber run is in place and a
! specified constant air concentration if an open chamber run is in place
        CCh = ACh*Cizone/VCh
        CCPPM = CCh*24451/MWMe
        CLoss = INTEG(kLoss*ACh, 0.0)

! Lungs
        RALu = QP*(FRACin*CCh - CLEx) + QC*(CVB - CVLu)
        ALu = INTEG(RALu, 0.0)
        CLu = ALu/VLu ! Concentration, mg/L
        CVLu = CLu/PLu        ! Exiting Concentration, mg/L

! Amount Inhaled
        RInh = FRACin*QP*CCh
        AInh = INTEG(RInh, 0.0)        ! mg per rat
        AInhC = AInh*Rats     ! mg for a group of rats

! Amount Exhaled
        CLEx = CVB/PB         ! Concentration, mg/L
        RAEx = QP*CLEx
        AEx = INTEG(RAEx, 0.0)*PULSE(0,TCHNG,TSTOP)     ! Amount, mg per rat
        AExC = AEx*Rats       ! Amount, mg, for a group of rats
        AxF = INTEG(RAEx*PULSE(TCHNG,24,24), 0.0)       ! Amount exhaled post-exposure

! Rest of Body
        RAR = QR*(CAB - CVR)
        AR = INTEG(RAR, 0.0)  ! Amount, mg
        CR = AR/VR            ! Concentration, mg/L
        CVR = CR/PR   ! Exiting Venous Concentration, mg/L
```

```
        AUCR = INTEG(CR, 0.0)          ! AUC, hr*mg/L

! Venous Blood (mg)
        RURB = K1*CVB*VVB              ! Lumped Clearance from Blood
        RAVB = QF*CVF + QL*CVL + QR*CVR + IVR - QC*CVB - RURB
        AVB = INTEG(RAVB, 0.0)         ! Amount, mg
        CVB = AVB / VVB                ! Concentration, mg/L
        AUCB = INTEG(CVB, 0.0)         ! AUC, hr*mg/L (total over entire exposure)
        AUCBB = AUCB*24.0/TSTOP        ! Average over exposure, hr*mg/(L*day)
        AUCBF = INTEG(CVB*PULSE(TSTOP-tmetf,TSTOP,tmetf),0)*24.0/tmetf
                ! AUCBF = Last tmetf AUC averaged/day (tmetf = 24.0*metd)
                ! For "steady state" AUC in blood over a day, set exposures to
                ! several weeks to reach "periodicity", then use AUCBF w/ metd = 7

! Bladder compartment, added by PS, U.S. EPA, 10/2008
        RBL = KBL*ABL          ! Rate of clearance from bladder (mg/hr)
        ABL = INTEG((RURB-RBL),0.0) ! Amount in bladder (mg)
        RUR= RBL/(BW*0.5e-3)! Urine concentration = rate/[BW*(0.5e-3 L/h/kg BW)]
        URB = INTEG(RBL, 0.0) ! Amount cleared to urine, mg
        URBF = INTEG(RURB*PULSE(TSTOP-tmetf,TSTOP,tmetf),0)*24.0/tmetf
                ! Amount cleared to urine in last tmetf averaged/day (tmetf = 24.0*metd)

!************************  Mass Balance   *************************
        Tbody = AAB + AF + AL + ALU + AR + AVB + ABL + STOM + AINTEST
        MetabORClrd = METB + METL + METL2 + METL3 + AEX + FEC
        TMass = Tbody + MetabORClrd
        TDose = AinH + INTEG(IVR+DWING+RAOZ+RLZ,0.0) + TODOSE
        MassBal=100*(TDose-TMass)/(TMass+1e-12)
        !compare to TIV, ODOSE, or AINHC
! Check Blood Flows
        QTOT = QF + QL + QR
        QRECOV = 100.0*QTOT/QC
END     ! End of Derivative
TERMT(T.GE.TStop)

!-------Exposure Control------------
DISCRETE ORALDOSE          ! Stom is amount in stomach
        IDOSE = DRP(IDS)*DRDOSE*BW
        STOM = STOM + IDOSE          ! Drinking percent
        TODOSE = TODOSE + IDOSE
        IF (IDS.EQ.1) THEN
                STOM = STOM + ODOSE
                TODOSE = TODOSE + ODOSE
        ENDIF
        IDS = IDS+1
        IF (IDS.EQ.7) THEN      ! For 6 doses
                IDS = 1
                NEWDAY = NEWDAY + 24
                SCHEDULE ORALDOSE.AT.NEWDAY  ! Go to start of the next day
        ELSE
                SCHEDULE ORALDOSE.AT.(NEWDAY+DRT(IDS)) ! Go to next drink time
        ENDIF
END     ! OF DISCRETE ORALDOSE

DISCRETE OFF           ! Turn INHAL exposure off
        CIZONE = 0.0
        IVZONE = 0.0
```

```
        DAY=DAY+1
        IF (MULTE) SCHEDULE ON.AT.(DAY*24.0)
END     ! OF DISCRETE OFF

DISCRETE ON
        CIZONE=1.0
        SCHEDULE OFF.AT.(T+TCHNG)
END     ! OF DISCRETE ON

DISCRETE DS1            ! Human at rest
        ! Equations scheduled for change during simulation repeated here
        QC = QCCHR*BW**0.75
        QP = QPCHR*BW**0.75
        QF = QFC*QC  ! QFCHR*QC    ! Equations for alternate flow fractions
        QL = QLC*QC  ! QLCHR*QC    ! But QFC and QLC taken to be 'at rest' values
        QRC = 1.0 - (QFC + QLC)
        QR = QRC*QC
END     ! OF DISCRETE DS1

DISCRETE DS2            ! Human at work (50W)
        ! Equations scheduled for change during simulation repeated here
        QC = QCCHW*BW**0.75
        QP = QPCHW*BW**0.75
        QF = QFC*QC  ! QFCHW*QC    ! Equations for alternate flow fractions
        QL = QLC*QC  ! QLCHW*QC    ! But don't seem to work (fit data) well
        QRC = 1.0 - (QFC + QLC)
        QR = QRC*QC
END     ! OF DISCRETE DS2

END     ! End of Dynamic
END     ! End of Program
```

B.3.3. acslXtreme procedure (.cmd) file

```
! File MEOHCBMMfinal.CMD - FOR PBPK MODEL FOR METHANOL
! taken from .cmd file from Ward et al., Edited by KWW - 06/02/96
! Developed for this (CBMM) model - 4/15/15
! Final with Digitized Data - 5/25/05
! Final Version has fast and slow rates of oral absorption
! Version 4 is final version used for simulations
! Final Version 1.10.06
! Beyond this comment, this file is left "as is" for archival purposes.  But most if not all of
! the functions and data sets defined here are replicated and/or replaced in the .m files below.
! Only use these when there is no corresponding .m file.
! – Paul Schlosser, U.S. EPA, Oct. 2008
!-----------------------------------------------------------
PREPARE T,CVB,MetB

! Procedural blocks for general mouse/rat data
PROCED CDMICE    ! Anatomic/physiologic data for mice
SET BW=0.03, TSTOP=1.5
SET IVDose=0, DOSE=0, CONCppm=0
SET PL=1.06, PF=0.083, PR=0.66, PB=1350
```

```
SET QPC=25.4,QCC=25.4,fracin=0.73
SET QLC = 0.25,QFC=0.05
SET KM=12,VmaxC=14.3,KLC=0.0,KAS=2
SET Vmax2c=19,km2=210,KAI=0.22,KSI=1.1
SET VAC = 0.0123,VFC = 0.07,VLC = 0.055
SET VLuC = 0.0073, VVBC = 0.0368
!Volumes from Brown et al
!Mouse QPC avg from Brown 29, 24 used in Corley et al and others
!AVG of measured vent rates by Perkins et al 25.4 L/hr/kg^0.75
!Blood volume 4.9% total. As per Brown 25:75 split art:ven
!Metab originally from Ward et al - KldC for mice =0
END

PROCED HUMAN
SET BW=70
SET IVDose=0, DOSE=0, CONCppm=0
SET PL=1.06, PR=0.66, fracin=0.75
SET VFC=0.214, VLC=0.026,VLUC=0.008
SET VAC= 0.0198,VVBC=0.0593
SET QPC=18.5, QCC=18.5, QLC=0.227, QFC=0.052
SET KM=12,VmaxC=11,KLC=0.044,KAS=2.0
SET KAI=0.22,KSI=1.1
SET PB = 1626, PF=0.14
SET Vmax2c=0
!Volumes from Brown et al
!QPC from Brown, upper end 13.4 L/hr/kg^0.75
!Need higher for data, 15 L/hr/kg^0.75 used in several published human models
!Blood volume 7.9% total. As per Brown 25:75 split art:ven
!Frac absorbed from Ernstgard SOT poster + personal communication
!Human Partition Coef. equal to mice. Horton et al. used rat
!Except Human Partition Coef blood and fat - from Fiserova-Bergerova and Diaz, 1986
! - but rat values are inconsistent with expected fat partitioning for an alcohol like this
! - for example Pastino and Conolly EtOH model, fat PC =0.1
END

PROCED SDRAT      !Anatomic/physiologic data for rats
SET BW=0.3, TSTOP=1.5
SET IVDose=0, DOSE=0, CONCppm=0
SET PL=1.6, PF=0.1, PR=1.3
SET KM=45,VmaxC=15,KLC=0.1,KAS=5
SET VAC = 0.0185, VFC=0.07, VLC= 0.034, VLuC=0.005, VVBC=0.0555
!Volumes from Brown et al
!PC from horton et al., PF reduced to 0.1 from Horton's 1.1
!Blood volume 7.4% total. As per Brown 25:75 split art:ven
!Metab originally from Ward et al - KldC for mice =0
!Rat model not calibrated
END

PROCED PREG
```

```
!For GD 18 mice, BW increased as estimated from Roger's et al
!Increased VFC as per Corley CRT development review
!This just to give a WAG as to how data might change from BW and different volume of
distribution
!Not invoked for any PROCs below as the default
!Liver to 140% of NP
SET BW = 0.055, VFC=0.08,VLC=0.11,VVBC=0.05
END

PROCED CLEARIT
SET IVDose=0, DOSE=0, CONCppm=0
END

PROCED SHOWIT
display Vmaxc,km,klc,pb,pf,pr,pl,kas,fracin
END

!Procedural blocks for all non-pregnant mouse data
! IV
PROCED MWARDIV25
!Ward et al., TAP 1997
!Figure 2, data from Ward model cmd
!Data was checked via digitizit - within +/-5% of cmd file
CLEARIT
CDMICE
SET TSTOP=24.0
SET IVDOSE=2500., tchng=0.025
END

PROCED PMWARDIV25
PLOT /D=MWARDIV25, CVB
END

DATA MWARDIV25(T,CVB)
0.08    4481.8
0.25    4132.2
0.5     3888
1.00    3164.8
2.0     2303.5
4.00    1921.5
6       1883.8
8       1620
12      838
18      454.7
24      NaN
END

PROCED MWARD95IV25
!Ward et al., FAT 1995
```

```
!Figure 2
!Data via digitizit
CLEARIT
CDMICE
SET TSTOP=24.0
SET IVDOSE=2500., tchng=0.025
END

PROCED PMWARD95IV25
PLOT /D=MWARD95IV25, CVB
END

DATA MWARD95IV25(T,CVB)
0.53    3299.60
1.06    3244.54
1.54    3190.71
3.07    2803.13
4.07    2544.36
5.02    2237.77
6.02    2063.59
7.02    1873.10
8.02    1521.92
9.03    1670.30
10.03   1423.12
END

! Procs for pegnant IV below: MWARDGD9IV25, MWARDGD18IV25, MWARDGD18IV5,
MWARDGD18IV1
! Oral
PROCED MWARDPO25
!Ward et al., FAT 1995
!Figure 2, data from Ward model cmd
!Data was checked via digitizit - within +/-5% of cmd file
CLEARIT
CDMICE
SET TSTOP=24, DOSE=2500
END

PROCED PMWARDPO25
PLOT /D=MWARDPO25, CVB
END

DATA MWARDPO25(T,CVB)
0.504   2370
0.96    2645
1.44    2705
1.992   2719
2.208   2781
3       2704
```

```
4.008   2370
4.992   2617
6       2516
7.008   2635
7.992   2213
9       2370
10.008 2028
10.992 1916
12      1347
13.008 1467
13.992 1354
15      1175
16.008 864.3
16.992 745.2
18      422.4
19.01   428
21      243
24      136
END

!Procs for pregnant Oral below: MDORGD8PO15, MWARDGD18PO25
!Inhalation
! QPC set to measured as in Perkins et al., FAT, 1995 for each concentration

PROCED MPERKIN25
!Perkins et al., FAT, 1995
!Fig. 2 data in Ward cmd file
CLEARIT
CDMICE
SET TSTOP=24, CONCppm=2500, vchc=5000
SET QPC = 29., QCC=29.
SET TCHNG=8
END

PROCED PMPERKIN25
PLOT /D=MPERKIN25, CVB
END

!This data from DigitizIt
DATA MPERKIN25(T,CVB)
2.0     414.0
4.0     453.0
6.0     586.0
8.25    694.0
12      282.0
16      0.6
END

!This data from cmd file
```

```
!DATA MPERKIN25(T,CVB)
!1.99        386.49
!4.01        617.57
!6.00        816.22
!8.26        970.27
!12.00       393.24
!16.0        13.51
END

PROCED MPERKIN50
!Perkins et al., FAT, 1995
!Fig. 2, data in Ward cmd file
!Data in command file higher than appears in figure
CLEARIT
CDMICE
SET TSTOP=24, CONCppm=5000, vchc=5000
SET TCHNG=8, qpc=24.,qcc=24.
END

PROCED PMPERKIN50
PLOT /D=MPERKIN50, CVB
END

!this from Digitizit, Fig 2 Perkins et al
DATA MPERKIN50(T,CVB)
1     644.00
2     877.00
3     1340.00
4     1450.00
6     2040.00
8.25  2290.0
12    1410.0
16    583.0
20    271.0
24    9.7
END

!This data from cmd file
!DATA MPERKIN50(T,CVB)
!1.0   906.76
!2.0   1202.7
!3.0   1828.38
!4.0   1986.49
!6.0   2800
!8.3   3125.68
!12.0  1914.86
!16.0  806.76
!20.0  367.57
!24.0  10.81
```

```
!END

PROCED MPERKIN100
!Perkins et al., FAT, 1995
!Fig. 2 data in Ward cmd file
!Note, Table 6 in Ward paper - max value of 3260 +/- 151
CLEARIT
CDMICE
SET TCHNG=8, CONCppm=1,0000, tstop=36,vchc=5000
SET QPC=21,qcc=21
END

PROCED PMPERKIN100
PLOT /D=MPERKIN100, CVB
END

!this from Digitizit, Fig 2 Perkins et al
DATA MPERKIN100(T,CVB)
2.0     2080.0
4.0     2530.0
6.0     3350.0
8.25    3350.0
12      2370.0
16      1830.0
20      1080.0
24      591.0
28      44.6
END

!DATA MPERKIN100(T,CVB)
!This from original cmd file
!2.0     2809.46
!4.0     3405.4
!6.0     4528.38
!8.3     4524.32
!12.0    3212.16
!16.0    2456.76
!20.0    1439.19
!24.0    798.65
!28.0    55.4
!END

! Procs for Preg mouse Inhalaiton date below: MDOR8IN10,MDOR8IN15
        !and:MROGGD7IN10, MROGGD6IN1, MROGGD6IN2, MROGGD6IN5,
MROGGD6IN10

!pregnant mice
! IV
PROCED MWARDGD9IV25
```

```
!Ward et al., DMD, 1996
!Not used in the manuscript, only in cmd file
CLEARIT
CDMICE
SET TSTOP=24
SET IVDOSE=2500., TINF=0.025
END

PROCED PMWARDGD9IV25
PLOT /D=MWARDGD9IV25, CVB
END

DATA MWARDGD9IV25(T,CVB)
0.0833 4606.2
0.25   4079.5
0.5    3489.3
1      2939.6
2      3447.6
4      2605.0
6      2690.5
8      2574.9
12     1506.1
18     498.6
24.    NaN
END

PROCED PROCED MWARDGD18IV25
!Ward et al., DMD, 1996
!Note, Table 6 in Ward paper - max value of 3521+/- 492
CLEARIT
CDMICE
SET TSTOP=24
SET IVDOSE=2500., TINF=0.025
END

PROCED PMWARDGD18IV25
PLOT /D=MWARDGD18IV25, CVB
END

DATA MWARDGD18IV25(T,CVB)
0.0833 4250.0
0.25   3445.1
0.5    2936.8
1.0    2470.5
2.0    2528.1
4.0    2292.3
6.0    2269.4
8.0    2057.0
12     1805.9
```

```
18      1482.2
24.0    496.1
END

PROCED MWARDGD18IV5
!Ward et al., DMD, 1996
!Note, Table 6 in Ward paper - max value of 868.8 +/- 53.9
CLEARIT
CDMICE
SET TSTOP=6
SET IVDOSE=500., TINF=0.025
END

PROCED PMWARDGD18IV5
PLOT /D=MWARDGD18IV5, CVB
END

DATA MWARDGD18IV5(T,CVB)
0.25    854.7
0.5     720.2
1.0     624.1
2.0     453.2
3.0     307.6
4.0     217.7
4.5     202.6
END

PROCED MWARDGD18IV1
!Ward et al., DMD, 1996
!Ward Proc GD8, but must be 18 as per PBPK manuscript
!Note, Table 6 in Ward paper - max value of 252 +/- 12.9
!table matches file
CLEARIT
CDMICE
SET TSTOP=4
SET IVDOSE=100.

PROCED PMWARDGD18IV1
PLOT /D=MWARDGD18IV1, CVB
END

DATA MWARDGD18IV1(T,CVB)
0.25    252
0.52    242.2
1.0     222.7
2       176.4
3       134.2
3.5     94.41
END
```

```

! Oral

PROCED MDORGD8PO15
!Ward et al., cmd file
!Note, Table 6 in Ward paper - max value of 1610 +/- 704
!Table and file match w/in round off
!Data must be from Dorman
!Dorman Teratology, 1995, Fig. 1
!within error for Digitiz data the same
CLEARIT
CDMICE
SET TSTOP=24, DOSE=1500
END

PROCED PMDORGD8PO15
PLOT /D=MDORGD8PO15, CVB
END

DATA MDORGD8PO15(T,CVB)
1       1609.6
2       1331.2
4       1241.6
8       707.2
16      160.0
24      38.4
END

PROCED MWARDGD18PO25
!Ward et al., DMD, 1996
!Note, Table 6 in Ward paper - max value of 3205 +/- 291
CLEARIT
CDMICE
SET TSTOP=24, DOSE=2500
END

PROCED PMWARDGD18PO25
PLOT /D=MWARDGD18PO25, CVB
END

!from cmd file, replaced with digitized
!DATA MWARDGD18PO25(T,CVB)
!0.25   2770.
!0.5    3299.
!1      3336.
!2      3502.
!4      3217.
!6      2999.
!10     2036.
```

```
!12     1832.
!15     949.1
!18     403.5
!21     40.47
!24.    16.03
!END

!Digitizit data
DATA MWARDGD18PO25(T,CVB)
0.5     2024
1       2554
2       3193
4       3002
6       2933
10      1976
12      1922
15      1339
18      1033
21      832
24      580
END

!Inhalation

PROCED MDOR8IN10
! Ward et al., TAP 1997
!Note, Table 6 in Ward paper - max value of 2080 +/- 800
!Fig 7? Table 6 attributes to Dorman
!Digitizit of Dorman Fig 2 matches cmd file
!actual exposure ppm 9900
CLEARIT
CDMICE
SET TCHNG=6, CONCppm=9900, tstop=36
END

PROCED PMDOR8IN10
PLOT /D=MDOR8IN10, CVB
END

DATA MDOR8IN10(T,CVB)
1       771.2
2       1017.6
4       1788.8
6       2076.8
8       2281.6
16      1152.0
24      268.8
END
```

```
PROCED MDOR8IN15
! Ward et al., TAP 1997
!Note, Table 6 in Ward paper - max value of 7136 +/- 736
!Fig 7? Table 6 attributes to Dorman
!Digitizit of Dorman Fig 2 matches cmd file
CLEARIT
CDMICE
SET TCHNG=6, CONCppm=15000, tstop=36
SET vchc=5000000000
END

PROCED PMDOR8IN15
PLOT /D=MDOR8IN15, CVB
END

DATA MDOR8IN15(T,CVB)
1       1475.2
2       2486.4
4       4588.8
6       7123.2
8       5888.0
16      3456.0
24      1446.4
END

!Files above provided in cmd file from Ward PBPK model, TAP 1997
!Files below added for this evaluation,
!sources described in proc files and in notebook

PROCED MROGGD7IN10
! Rogers et al., Teratology, 1997
! Actual Values kindly Provided by Rogers
CLEARIT
CDMICE
SET TCHNG=7, CONCppm=1,0000, tstop=36
SET vchc=500000000,bw=0.032
END

PROCED PMROGGD7IN10
PLOT /D=MROGGD7IN10, CVB
END

DATA MROGGD7IN10(T,CVB)
1       930
4       2800
6       3360
7       3990
7.5     3980
8       4120
```

```
9        3270
12       2630
16       1690
26       60
END

PROCED MROGGD6IN1
CLEARIT
!Rogers et al., Teratology, 1993
!Rogers data from GD 6 and 10
!In Table 2
CDMICE
SET TCHNG=7, CONCppm=1,000, tstop=36,vchc=500000000,bw=0.032
END

PROCED PMROGGD6IN1
PLOT /D=MROGGD6IN1, CVB
END

DATA MROGGD6IN1(T,CVB)
7        63
7        131
END


PROCED MROGGD6IN2
! Rogers et al., Teratology, 1993
!Rogers data from GD 6 and 10
!In Table 2
CLEARIT
CDMICE
SET TCHNG=7, CONCppm=2000, tstop=36, vchc=500000000,bw=0.032
END

PROCED PMROGGD6IN2
PLOT /D=MROGGD6IN2, CVB
END

DATA MROGGD6IN2(T,CVB)
7        487
7   641
END

PROCED MROGGD6IN5
! Rogers et al., Teratology, 1993
!Rogers data from GD 6 and 10
!In Table 2
CLEARIT
CDMICE
```

```
SET TCHNG=7, CONCppm=5000, tstop=36,vchc=500000000,bw=0.032
END

PROCED PMROGGD6IN5
PLOT /D=MROGGD6IN5, CVB
END

DATA MROGGD6IN5(T,CVB)
7        2126
7   1593
END

PROCED MROGGD6IN10
! Rogers et al., Teratology, 1993
!Rogers data from GD 6, 10, 15
!In Table 2
CLEARIT
CDMICE
SET TCHNG=7, CONCppm=1,0000, tstop=36,vchc=500000000,bw=0.032
END

PROCED PMROGGD6IN10
PLOT /D=MROGGD6IN10, CVB
END

DATA MROGGD6IN10(T,CVB)
7        4653
7   4304
7   3655
END

!Human inhalation dta

PROCED HJOHIN1
!Ernstgard et al. SOT poster 200 ppm human
!Digitized from Fig 2
!Also personal communication - Ernstgard
!QPC from Johanson et al. Scand J. Work Env. 86 =52.6
!If Assume value = alveolar. similar to Astrand '83 value of 56 L/hr/kr^0.75
!Fracin - 50% of total (from poster) ~76%
!QCC from Corley et al TAP 129, 1994
CLEARIT
HUMAN
SET TCHNG=2, CONCppm=100, tstop=16
SET QPC=52.6,qcc=26,vchc=500000000
END

PROCED PHJOHIN1
PLOT /D=HJOHIN1, CVB
```

```
END

DATA HJOHIN1(T,CVB)
0.20    0.87
0.46    1.50
0.97    2.31
1.46    3.24
1.91    3.65
2.17    3.52
2.50    2.55
2.91    2.23
3.51    1.59
4.01    1.72
5.02    0.41
6.00    0.50
9.24    0.12
END

PROCED HJOHIN2
!Ernstgard et al. SOT poster 200 ppm human
!Digitized from Fig 2
!Also personal communication - Ernstgard
!QPC from Johanson et al. Scand J. Work Env. 86 =52.6
!If Assume value = alveolar. similar to Astrand '83 value of 56 L/hr/kr^0.75
!Fracin - 50% of total (from poster) ~75%
!QCC from Corley et al TAP 129, 1994
CLEARIT
HUMAN
SET TCHNG=2, CONCppm=200, tstop=16
SET QPC=52.6,qcc=26,vchc=500000000
END

PROCED PHJOHIN2
PLOT /D=HJOHIN2, CVB
END

DATA HJOHIN2(T,CVB)
0.22    1.63
0.49    2.92
0.92    4.76
1.47    6.30
1.90    7.65
2.16    6.20
2.47    5.49
2.91    4.96
3.50    3.64
4.00    3.43
4.99    1.94
5.97    1.03
```

```
8.90    0.21
END

PROCED HOSTERIN2
! Osterloh et al., JOEM 1996
! Digitized data provided by EPA
! Subtracted background from exposure blood levels
CLEARIT
HUMAN
SET TCHNG=4, CONCppm=200, tstop=16
SET vchc=500000000, BW=78.2
END

PROCED PHOSTERIN2
PLOT /D=HOSTERIN2, CVB
END

DATA HOSTERIN2(T,CVB)
0.05    0.54
0.25    1.39
0.50    1.82
0.75    2.28
1.00    2.42
1.50    2.94
2.00    3.37
2.50    3.90
3.00    4.21
3.50    4.61
4.00    4.82
5.00    2.99
6.00    2.30
7.00    1.40
7.95    1.07
END

PROCED HBATIN82
!Batterman et al., Int Arch Occ Health 1998
!Digitized Data
CLEARIT
HUMAN
SET TCHNG=2, CONCppm=800, tstop=16
SET vchc=500000000
END

PROCED PHBATIN82
PLOT /D=HBATIN82, CVB
END

DATA HBATIN82(T,CVB)
```

```
2.223   13.658
2.495   13.282
2.742   11.928
3.230   9.456
4.231   6.197
5.247   3.953
6.262   2.325
7.251   1.551
8.216   1.176
END

PROCED HBATIN81
!Batterman et al., Int Arch Occ Health 1998
!Digitized Data
CLEARIT
HUMAN
SET TCHNG=1, CONCppm=800, tstop=16
SET vchc=500000000
END

PROCED PHBATIN81
PLOT /D=HBATIN81, CVB
END

DATA HBATIN81(T,CVB)
1.096   6.477
1.398   6.136
1.644   5.345
2.143   4.270
3.178   2.661
4.188   1.307
5.199   0.732
6.266   0.552
7.292   0.356
8.209   0.093
END

PROCED HBATIN830
!Batterman et al., Int Arch Occ Health 1998
!Digitized Data
!body weight not provided
CLEARIT
HUMAN
SET TCHNG=0.5, CONCppm=800, tstop=16
SET vchc=500000000
END

PROCED PHBATIN830
PLOT /D=HBATIN830, CVB
```

```
END

DATA HBATIN830(T,CVB)
0.579   4.608
0.857   4.685
1.137   4.870
1.650   3.452
2.650   2.082
3.662   0.910
4.693   0.316
5.713   0.320
6.643   0.292
7.696   0.547
END

PROCED HSEDIN231
!Sedivec et al., Int Arch Occ Health 1981
!Digitized Data
!Note, urine volumes not given, these are estimates
!urine production of 0.75 mg/hr, this for info purposes only!!!
CLEARIT
HUMAN
SET TCHNG=8, CONCppm=231, tstop=24
SET vchc=500000000
END

PROCED PHSEDIN231
PLOT /D=HSEDIN231, Metb
END

DATA HSEDIN231(T,Metb)
0.043   0.0042
2.174   0.33
4.478   0.87
6.478   1.46
8.522   2.15
10.348 2.63
12.130 2.91
14.044 3.07
18.870 3.32
23.696 3.52
END

PROCED HSEDIN157
!Sedivec et al., Int Arch Occ Health 1981
!Digitized Data
!Note, urine volumes not given, these are estimates
!urine production of 0.75 mg/hr, this for info purposes only!!!CLEARIT
HUMAN
```

```
SET TCHNG=8, CONCppm=157, tstop=24
SET vchc=500000000
END

PROCED PHSEDIN157
PLOT /D=HSEDIN157, Metb
END

DATA HSEDIN157(T,Metb)
0.126   0.0038
2.204   0.228
4.242   0.576
6.196   0.975
8.326   1.47
10.163 1.81
12.094 2.00
14.016 2.12
18.8966         2.34
23.776 2.53
END

PROCED HSEDIN78
!Sedivec et al., Int Arch Occ Health 1981
!Digitized Data
!Note, urine volumes not given, these are estimates
!urine production of 0.75 mg/hr, this for info purposes only!!!
CLEARIT
HUMAN
SET TCHNG=8, CONCppm=78, tstop=24
SET vchc=500000000
END

PROCED PHSEDIN78
PLOT /D=HSEDIN78, Metb
END

DATA HSEDIN78(T,Metb)
0.03    0.013
2.06    0.189
3.96    0.397
6.09    0.652
8.09    0.820
10.11   0.933
11.93   1.02
13.92   1.09
18.89   1.27
END

!AUC, Cmax estimation procedures
```

```
Proced mousin
!To determine AUC for 7 hr exposure in mice
CLEARIT
CDMICE
SET TCHNG=7, tstop=24
SET vchc=50000000000
SET CONCppm=1
start /nc
d concppm,AUCB,amet,cvb
SET CONCppm=5
start /nc
d concppm,AUCB,amet,cvb
SET CONCppm=10
start /nc
d concppm,AUCB,amet,cvb
SET CONCppm=25
start /nc
d concppm,AUCB,amet,cvb
SET CONCppm=50
start /nc
d concppm,AUCB,amet,cvb
SET CONCppm=75
start /nc
d concppm,AUCB,amet,cvb
SET CONCppm=100
start /nc
d concppm,AUCB,amet,cvb
SET CONCppm=175
start /nc
d concppm,AUCB,amet,cvb
SET CONCppm=208.3
start /nc
d concppm,AUCB,amet,cvb
SET CONCppm=250
start /nc
d concppm,AUCB,amet,cvb
SET CONCppm=325
start /nc
d concppm,AUCB,amet,cvb
SET CONCppm=500
start /nc
d concppm,AUCB,amet,cvb
SET CONCppm=750
start /nc
d concppm,AUCB,amet,cvb
SET CONCppm=1,000
start /nc
d concppm,AUCB,amet,cvb
SET CONCppm=2000
```

```
start /nc
d concppm,AUCB,amet,cvb
SET CONCppm=2500
start /nc
d concppm,AUCB,amet,cvb
SET CONCppm=5000
start /nc
d concppm,AUCB,amet,cvb
SET CONCppm=1,0000
start /nc
d concppm,AUCB,amet,cvb
SET CONCppm=50000
start /nc
d concppm,AUCB,amet,cvb
END

Proced mousinC
!To determine 7 hr Cmax, note - not at SS
CLEARIT
CDMICE
SET TCHNG=7, tstop=7,VCHC=50000000000
SET CONCppm=1
start /nc
d conc ppm,cvb
SET CONCppm=10
start /nc
d concppm,CVB
SET CONCppm=50
start /nc
d concppm,CVB
SET CONCppm=100
start /nc
d concppm,CVB
SET CONCppm=250
start /nc
d concppm,CVB
SET CONCppm=500
start /nc
d concppm,CVB
SET CONCppm=1,000
start /nc
d concppm,CVB
SET CONCppm=2000
start /nc
d concppm,CVB
SET CONCppm=2500
start /nc
d concppm,CVB
SET CONCppm=5000
```

```
start /nc
d concppm,CVB
SET CONCppm=1,0000
start /nc
d concppm,CVB
SET CONCppm=50000
start /nc
d concppm,CVB
END

Proced humin
! To determine 24 hr AUC,Cmax at SS for human
CLEARIT
human
SET TCHNG=360, tstop=1,000
SET vchc=5000000000, points=48
SET Concppm=1
Start /nc
d concppm,aucBb,cvb
SET CONCppm=10
start /nc
d concppm,aucBb,cvb
SET CONCppm=50
start /nc
d concppm,aucBb,cvb
SET CONCppm=100
start /nc
d concppm,aucBb,cvb
SET CONCppm=250
start /nc
d concppm,aucBb,cvb
SET CONCppm=500
start /nc
d concppm,aucBb,cvb
SET CONCppm=625
start /nc
d concppm,aucBb,cvb
SET CONCppm=750
start /nc
d concppm,aucBb,cvb
SET CONCppm=875
start /nc
d concppm,aucBb,cvb
SET CONCppm=1,000
start /nc
d concppm,aucBb,cvb
SET CONCppm=2000
start /nc
d concppm,aucBb,cvb
```

```
SET CONCppm=2500
start /nc
d concppm,aucBb,cvb
SET CONCppm=5000
start /nc
d concppm,aucBb,cvb
SET CONCppm=1,0000
start /nc
d concppm,aucBb,cvb
SET CONCppm=50000
start /nc
d concppm,aucBb,cvb
END

Proced humor
! To determine 24 hr AUC
! Oral exposure
CLEARIT
human
SET TCHNG=1,000, tstop=1,000
SET vchc=5000000000, points=48
SET dose=0.1
SET ODS=1
start /nc
d dose,aucBb
SET dose=1
Start /nc
d dose,aucBb
SET dose=5
start /nc
d dose,aucBb
SET dose=10
start /nc
d dose,aucBb
SET dose=50
start /nc
d dose,aucBb
SET dose=100
start /nc
d dose,aucBb
SET dose=250
start /nc
d dose,aucBb
SET dose=350
start /nc
d dose,aucBb
SET dose=500
start /nc
d dose,aucBb
```

```
SET dose=750
start /nc
d dose,aucBb
SET dose=1,000
start /nc
d dose,aucBb
SET dose=2500
start /nc
d dose,aucBb
SET dose=5000
start /nc
d dose,aucBb
S ODS=0
END

!Procedural blocks for all non-pregnant rat data
!Not calibrated!!!!!!
!Procs from Ward CMD file

PROCED WARDIV25
CLEARIT
SDRAT
SET TSTOP=48.
SET IVDOSE=2500.
END

PROCED PWARDIV25
PLOT /D=WARDIV25, CVB
END

DATA WARDIV25(T,CVB)
0.072       4849
0.168       3926
0.24        2965
0.504       2836
1.008       3248
1.992       2589
3           2619
4.008       2514
7.008       2315
19.992      1495
22.992      1272
24          1214
25.992      982
28.008      957
30          860
37.992      238
39          200
40.008      150
```

```
40.992          167
43.008          77
END

PROCED WARDIV1
CLEARIT
SDRAT
SET TSTOP=8
SET IVDOSE=100., tchng=0.016
END

PROCED PWARDIV1
PLOT /D=RG0IV1, CVB
END

DATA WARDIV1 (T,CVB)
0.072           141.7
0.168           121.8
0.24            111.6
0.504           99.7
0.744           97.4
1.008           86.3
1.488           80.3
1.992           58
3               44.4
4.008           22.8
4.992           10.9
6               3.8
7.008           1.4
END

PROCED WARDPO25
CLEARIT
cdmice
SET BW=0.3
SET TSTOP=48
SET DOSE=2500
END

PROCED PWARDPO25
PLOT /D=WARDPO25, CVB
END

DATA WARDPO25(T,CVB)
0.072   862.7
0.168   1243
0.24    1356
0.504   1621
1.008   1641
```

```
1.992   1611
3       1869
4.008   1896
7.008   2181
24      1365
25.992  1081
28.008  921
30      958.4
31.008  969.8
45      42.9
46.008  27.1
46.992  16.4
48      23.9
49.008  41.9
49.992  13.1
52.008  2.3
52.992  1
END

PROCED WARDPO1
CLEARIT
cdmice
SET BW=0.3
SET DOSE=100, tstop=8
END

PROCED PWARDPO1
PLOT /D=WARDPO1, CVB
END

DATA WARDPO1(T,CVB)
0.072           85.5
0.168           95.6
0.24            95.5
0.504           91.1
0.744           86.6
1.008           80.6
1.488           71.3
1.992           61.1
3               45.1
4.008           27.4
4.992           16.4
6               8.9
7.008           4.2
END
```

B.3.4. Procedural .m files for reproducing the results in Appendix B and Chapter 3

B.3.4.1. ***Key to ACSL Extreme v2.5.0.6 .m files***

Found in the Runtime Files Folder

CDmice.m Sets parameters for (CD) mouse simulations

Rogers-mouse-inhal.m Figure B-2 - Simulations of mouse inhalation exposures from GD 6, 7, 8 and 10 mice from Rogers et al., 1993.

PerkinsDorm-mouse-inh.m Figure B-3 - Simulations of inhalation exposures to MeOH in NP mice from Perkins et al. 1995 (8 hr exposures) and GD 8 mice from Dorman et al. 1995 (6 hr exposures)

Ward_mouse_GD18.m Figure B-4 - Oral exposures to MeOH in pregnant and non-pregnant mice Data from Dorman et al., 1995 and Ward et al., 1997

Ward-mouse-iv.m Figure B-5 - Simulations of mouse IV exposures to MeOH from Ward et al., 1997

Apaja-mouse-drink.m Calculates internal doses for mice in Apaja (1980)

SDrat.m Sets parameters for Sprague-Dawley (SD) rat simulations

F344rat.m Sets parameters for F344 rat simulations

Ward-rat-iv.m Figure B-10 – Simulations rat IV exposures from Ward et al., 1997 and Horton et al., 1992

Horton-rat-inhal.m Figure B-11 – Simulations rat inhalation exposures from Horton et al., 1992

Ward-rat-oral.m Figure B-12 – Simulations rat oral exposures from Ward et al., 1997

Nedo-rat-inhal-devpmt-rat.m Figure B-13 – Simulations rat inhalation (bioassay) exposures (200, 500, 1,000, 2000, & 5000 ppm)

Nedo-rat-inhal-cancer.m Simulations for NEDO F344 rat cancer inhalation study

rat-infu-sims.m Figure B-14 – Simulations rat "oral" exposures (bioassay doses, but using liver infusion; for illustration only)

humanset.m Sets human MeOH PBPK parameters

Sedivec_human_inh.m Figure B-16 - Simulation of human urinary MeOH elimination following Inhalation exposures from Sedivec et al. 1981

Batterman_human_inh.m Figure B-17 (upper panel) - Simulations of human inhalation exposure data of Batterman et al. 1998

Osterloh_human_inh.m Figure B-17 (lower panel) - Simulations of human inhalation exposure data of Osterloh et al. 1996

Ernstgard_human_inh.m Figure B-18 - Simulations of human inhalation exposures to MeOH from Ernstgard et al. 2005

mouse_inh_sim.m Produces data for Table B-5, mouse inhalation exposures

human_inh_sim.m Produces data for Table B-5, human inhalation expsoures

human_oral_sim.m Produces data for Table B-5, human oral exposures

human_drink_compare.m Figure B-24 and Table B-9 (altenate drinking pattern comparison)

Found in the Sensitivity Analysis Files Folder

Fig_B-6 Sensitivity of the mouse model to metabolic parameters (e.g., Km and V_{max}) for the inhalation route

Fig_B-7 Sensitivity of the mouse model to flow parameters (e.g., blood flow to liver) and to the rest-of-body partition coefficient for the inhalation route

Fig_B-8 Sensitivity analysis of the rat model to oral absorption parameters for a bolus oral exposure (1,000 mg/kg)

B.3.4.1. *[B.3.4.2.] Code for .m files*

```
% File CDmice.m
% Sets parameters for mouse simulations, MeOH PBPK model
CONCPPM=10; WESITG=0; WEDITG=0; CINT-0.1;
start @nocallback
BW=0.03; TSTOP=24; TCHNG=7; REST=20000; WORK=20000;
IVDOSE=0; DOSE=0; DRDOSE=0; RATS=0; KLOSS=0; LIVR0=0;
PL=1.06; PF=0.083; PR=0.66; PLU=1; PB=1350;
QPC=25.4; QCC=25.4; FRACIN=0.73; KFEC=0;
QLC=0.25; QFC=0.05;
KM=12; VMAXC=14.3; K1C=0.0; KAS=0.0; KLLC=0;
VMAX2C=19; KM2=210; KAI=0.5; KSI=5.0;
VAC=0.0123; VFC=0.07; VLC=0.055; VLUC=0.0073; VVBC=0.0368;
CONCPPM=0.0; IVDOSE=0.0; DOSE=0.0; DWDOSE=0; MULTE=0; RDRINK=1;
% Volumes from Brown et al
% Mouse QPC avg from Brown 29; 24 used in Corley et al and others
% AVG of measured vent rates by Perkins et al 25.4 L/hr/kg^0.75
% Blood volume 4.9% total. As per Brown 25:75 split art:ven
% Metab originally from Ward et al - KldC for mice = 0

% use mouseINH_fit-params.m % File contents copied below
% Updated parameters as obtained by Paul Schlosser, U.S. EPA
% August 11, 2009 [this file updated]

% Values generated through parameter estimation script 'mouseINH_fit.m'
VMAX2C = 3.222500e+00; KM2 = 660; VMAXC = 19; KM = 5.2; FRACIN = 6.650939e-01;

% Values generated through parameter estimation script 'mouseor_fit.m'
VASC = 1.833246e+03; KSI = 2.2; KAI = 0.33; MASC = 620;
```

```
% File Rogers_mouse_inhal.m (Figure B-2)
% Produces MeOH PBPK figures for Rogers' mouse inhalation exposures
% Variables in the plot command are case sensitive
use CDmice
        % set mouse parameters
%------- DATA BLOCKS
        % These data blocks taken directly from MeOH CBMMv3.cmd
        % Data for are T (hours), CV (mg/L)
        % semicolons (";") creates a new line in a data file

% Rogers et al., Teratology, 1997
D7IN10 = [1, 930; 4, 2800; 6, 3360; 7, 3990; 7.5, 3980;
8, 4120; 9, 3270; 12, 2630; 16, 1690; 26, 60];

%Rogers et al., Teratology, 1993
D6IN1 = [7, 63; 7, 131]; D6IN2 = [7, 487; 7, 641];
D6IN5 = [7, 2126; 7, 1593]; D6IN7p5 = [7, 2801; 7, 3455];
D6IN10 = [7, 4653; 7, 4304]; D6IN15 = [7, 7720; 7, 7394];

%-----RUN MODEL
RATS=0.0; KLOSS=0.0; % -> open chamber
TCHNG=7; CONCPPM=10000; TSTOP=27.0; MULTE=0; BW=0.032;
CINT=TSTOP/1000; cs=[]; prepare @clear T CVB
```

```
for CONCPPM=[1, 2, 5, 7.5, 10, 15]*1000
        start @nocallback
        cs=[cs,_cvb];
        % Since TSTOP & CINT not changing, assume _t also the same.
end

%-----PLOT COMMANDS
        % The rogers.aps file will retain changes made using the plot
        % editor as long as the editor is called by clicking the
        % words EDIT PLOT PROPERTIES not the little icon in the
        % properties dialogue box
 plot(_t,cs(:,1), _t,cs(:,2), _t,cs(:,3), _t,cs(:,4), _t,cs(:,5), _t,cs(:,6), ...
        D6IN1(:,1),D6IN1(:,2),D6IN2(:,1),D6IN2(:,2),D6IN5(:,1),D6IN5(:,2), ...
        D6IN7p5(:,1),D6IN7p5(:,2),D6IN10(:,1),D6IN10(:,2), ...
        D7IN10(:,1),D7IN10(:,2),D6IN15(:,1),D6IN15(:,2),  'rogers.aps')

%-----WRITE OUT DATA TO A TEXT FILE FOR IMPORTING INTO EXCEL
    % Cannot save data with different # of rows to the same table.
cs=[_t,cs];
save cs @file='Rogersplotdata.csv' @format=ASCII @separator=ascii
```

```
% File: PerkinsDorm-mouse-inh.m (Figure B-3)
% Produces MeOH PBPK simulations Perkins 1995 inhalation exposures,
% and Ward 1997 (pregnant) and Dorman 1995 for comparison)
% Includes all nonpregnant and "early" GD (<GD 10) sets
% GD18 not included

%------- DATA BLOCKS
        % These data blocks taken directly from MeOH CBMMv3.cmd
        % Data for are T (hours), CV (mg/L)
% Perkins et al, FAT, 1995
        Perk25 =[2, 414; 4, 453; 6, 586;
        8.25, 694; 12, 282; 16    0.6];
%Perkins et al, FAT, 1995
        Perk50= [1, 666; 2, 905; 3, 1370;
        4, 1480; 6, 2090; 8.25, 2310;
        12, 1420; 16, 597; 20, 276; 24, 36.2];
%Perkins et al, FAT, 1995
        Perk100=[2, 2080.0; 4, 2530; 6, 3350;
        8.25, 3350; 12, 2370; 16, 1830;
        20, 1080; 24, 591; 28, 44.6];
%Ward et al., TAP 1997
        Dor815=[1, 1475.2; 2, 2486.4; 4, 4588.8;
        6, 7123.2; 8, 5888; 16, 3456; 24, 1446.4];

%table 6, TAP 1997
%estimate all Cmax at end of exposure
%this is to compare model fits to published values that may be different from cmd file
%the last value (2300) is not in table, it is estimated from figure in Perkins et al from 5000 ppm exposure
% 8      3250  - non pregnant mouse 10,000 ppm
% 6      7136  - GD 8 mouse  15,000 ppm
% 8      2300  - non preg mouse 15,000 ppm

%-----RUN MODEL
use CDmice
RATS=0; KLOSS=0; % -> open chamber
MULTE=0; TSTOP=24; CONCPPM=2500; QPC = 29; QCC=29; TCHNG=8;
```

```
start @nocallback
Cs25 = _cvb; Ts25 = _t;
CONCPPM=5000; QPC=24; QCC=24; start @nocallback
Cs50 = _cvb; Ts50 = _t;
CONCPPM=10000; TSTOP=36; QPC=21; QCC=21; start @nocallback
Cs100 = _cvb; Ts100 = _t;
use CDmice
RATS=0; KLOSS=0; % -> open chamber
TCHNG=6; CONCPPM=15000; TSTOP=36; start @nocallback

%-----PLOT COMMANDS
        % The .aps file will retain changes made using the plot
        % editor as long as the editor is called by clicking the
        % words EDIT PLOT PROPERTIES not the little icon in the
        % properties dialogue box
plot(Ts25, Cs25, Ts50, Cs50, Ts100, Cs100,_t, _cvb, ...
        Perk25(:,1), Perk25(:,2), Perk50(:,1), Perk50(:,2), ...
        Perk100(:,1), Perk100(:,2),Dor815(:,1), Dor815(:,2), 'inhalation.aps')

%-----WRITE OUT DATA TO A TEXT FILE FOR IMPORTING INTO EXCEL
    % Can't save data with different # of rows to the same table.
mytable1 = [Ts25, Cs25, Ts50, Cs50, Ts100, Cs100,_t, _cvb];
save mytable1 @file='PerkinDormanplotdata.csv' @format=ASCII @separtor=comma
```

```
% File WardGD18.m
% Creates Figure B-4, including Ward et al 1997 NP and GD 18 mouse data
% and Dorman et al 1995 GD 8 mouse data.
CDmice
TSTOP=25; DOSE=1500; CONCPPM=0; MULTE=0;
prepare @clear T CVB
start @nocallback
T1=_t;P1=_cvb;
DOSE=2500; start @nocallback
D15=[1, 1609.6; 2, 1331.2; 4, 1241.6;
8, 707.2; 16, 160; 24, 38.4];
D25a=[0.5, 2370; 0.96, 2645; 1.44, 2705; 2, 2719;
2.2, 2781; 3, 2704; 4, 2370; 5, 2617; 6, 2516;
7, 2635; 8, 2213; 9, 2370; 10, 2028; 11, 1916;
12, 1347; 13, 1467; 14, 1354; 15, 1175; 16, 864.3;
17, 745.2; 18, 422.4; 19, 428; 21, 243; 24, 136];
D25b=[0.5, 2024; 1, 2554; 2, 3193; 4, 3002; 6, 2933;
10, 1976; 12, 1922; 15, 1339; 18, 1033; 21, 832; 24, 580];

plot(D15(:,1),D15(:,2),D25a(:,1),D25a(:,2),D25b(:,1),D25b(:,2),...
        T1,P1,_t,_cvb,"wardgd18plot.aps")
% File Ward-mouse-iv.m
% M File for reproducing MeOH PBPK Figure B-5 For WARD iv mouse exposures
% (also Ward Pregnant Includes all nonpregnant and Pregnant)
```

```
%------- DATA BLOCKS
   %Taken directly from MeOH CBMMv3.cmd, values are [T (hours), CV (mg/L)]
%Ward et al, FAT 1995
NPIV25=[0.08, 4481.8; 0.25, 4132.2; 0.5, 3888; 1, 3164.8; 2, 2303.5;
        4, 1921.5; 6, 1883.8; 8, 1620; 12, 838; 18, 454.7; 24, 1.41];
%PROCED MWARDGD8IV25
GD8IV25=[0.0833, 4606.2; 0.25, 4079.5; 0.5, 3489.3; 1, 2939.6; 2, 3447.6;
        4, 2605.0; 6, 2690.5; 8, 2574.9; 12, 1506.1; 18, 498.6; 24, 0.554];
```

```
%!Ward et al., DMD, 1996
GD18IV25=[0.0833, 4250.0; 0.25, 3445.1; 0.5, 2936.8; 1, 2470.5; 2, 2528.1;
        4, 2292.3; 6, 2269.4; 8, 2057.0; 12, 1805.9; 18, 1482.2; 24.0, 496.1];
%Ward et al., DMD, 1996
GD18IV5=[0.25, 854.7; 0.5, 720.2; 1, 624.1;
        2, 453.2; 3, 307.6; 4, 217.7; 4.5, 202.6];
%Ward et al., DMD, 1996
GD18IV1=[0.25, 252; 0.52, 242.2; 1, 222.7; 2, 176.4; 3, 134.2; 3.5, 94.41];

%-----RUN MODEL
use CDMICE
TSTOP=24.0; IVDOSE=2500; TCHNG=0.025; start @nocallback
CVs25 = _cvb; Ts25 = _t; TSTOP=6; IVDOSE=500; start @nocallback
CVs5 = _cvb; Ts5 = _t; TSTOP=4; IVDOSE=100; start @nocallback
CVs1 = _cvb; Ts1 = _t; IVDOSE=200; start @nocallback

%-----PLOT COMMANDS
% The .aps file will retain changes made using the plot
% editor as long as the editor is called by clicking the
% words EDIT PLOT PROPERTIES not the little icon in the
% properties dialogue box
plot(Ts25, CVs25, Ts5, CVs5, Ts1, CVs1, NPIV25(:,1), NPIV25(:,2),...
        GD8IV25(:,1), GD8IV25(:,2), GD18IV25(:,1), GD18IV25(:,2), ...
        GD18IV5(:,1), GD18IV5(:,2), GD18IV1(:,1), GD18IV1(:,2), 'iv.aps')
plot(_t, _cvb, Ts1, CVs1, GD18IV1(:,1), GD18IV1(:,2), 'ivb.aps')

%-----WRITE OUT DATA TO A TEXT FILE FOR IMPORTING INTO EXCEL
        % Cant save data with different # of rows to the same table.
mytable1 = [Ts25, CVs25, Ts5, CVs5, _t, _cvb, Ts1, CVs1];
save mytable1 @file='WardIV.csv' @format=ASCII @separator=comma
```

```
% File Apaja-mouse-drink.m
% Calculates internal doses for mice in Apaja (1980)
use CDmice
DWDOSE=1; start @nocallback
DWDS=[0.045, 550; 0.045, 970; 0.045, 1800;
        0.040, 560; 0.040, 1000; 0.040. 2100];
% Above are BWs and doses for males, then females, from Apaja (1980)
ODS=1; TSTOP=24*3*7; MULTE=1; DAYS=6.0; simres=[]; LIVR0=0;
PER1=1.5; DUR1=0.75; PER2=3.0; DUR2=0.5; FNIGHT=0.8; CINT=0.01;
prepare @clear T CVB STOM
for RDRINK =0 %[1, 0] % 0 -> mouse drinking pattern
for i=1:length(DWDS)
        BW=DWDS(i,1); DWDOSE=DWDS(i,2); start @nocallback
        simres=[simres;[TDOSE*(24/TSTOP)/BW,BW,AUCBF,max(_cvb),AMF]];
end
plot(_t,_cvb)
end
simres=[simres(:,1)*7/6, simres];
simres/100      % Print values to screen (/100)
TDOSE*(24/TSTOP)/BW         % Check that final total dose/day is correct
save simres @file='Apaja_mouse_drink_sims.csv' @format=ascii @separator=comma
```

```
% File SDrat.m
% Sets parameters for rat simulations, MeOH PBPK model
CONCPPM=10; WESITG=0; WEDITG=0; TSTOP=24; TCHNG=6; MULTE=0;
REST=20000; WORK=20000;
```

```
start @nocallback
BW=0.275; TSTOP=24; FRACIN=0.2;
IVDOSE=0; DOSE=0; CONCPPM=0; DRDOSE=0; DWDOSE=0; ODS=0; LIVR0=0;
QCC=16.4; QPC=16.4; QFC=0.07; QLC=0.25;
PL=1.06; PF=0.083; PR=0.66; PB=1350;
KM=6.3; VMAXC=5.0; VMAX2C=8.4; KM2=65;
KLLC=0.0; K1C=0.0;
VAC=0.0185; VFC=0.07; VLC=0.037; VLUC=0.005; VVBC=0.0443;

KAS=10.9; KSI=6.8; KAI=0.039; KFEC=0.0; VASC=0;
% Just above are linear absorption params fit to 100 mg/kg
% oral data, w/ no fecal elimination

KAS=0.0; % Below are for saturable uptake model
% Values generated through parameter estimation script 'ratoral_fit.m'
KSI = 7.4; KAI = 0.051; KFEC = 0.029; VASC = 5.573125e+03; KMASC = 620;
```

```
% File F344rat.m: parameters specific to F344 rat
% Created by Paul Schlosser, U.S. EPA, Aug. 2009
use SDrat
VMAXC=0; VMAX2C=22.3; KM2=100;
```

```
% File: Ward-rat-iv.m
% Creates Figure B-9; rat MeOH PBPK model, to simulate
% Ward '97 rat iv 2500 & 100 mg/kg (BW=275, SD)
% and Horton '92 iv 100 mg/kg (BW=100, F344)
rwi25 =[0.072, 4849; 0.168, 3926; 0.24, 2965; 0.5, 2836; 1, 3248;
2, 2589; 3, 2619; 4, 2514; 7, 2315; 20, 1495; 23, 1272; 24, 1214;
26, 982; 28, 957; 30, 860; 38, 238; 39, 200; 40, 150; 41, 167; 43, 77];

% ward '97 rat iv 100 mg/kg (BW 275, SD)
rwi1=[0.072, 141.7; 0.168, 121.8; 0.24, 111.6; 0.5, 99.7; 0.744, 97.4;
1, 86.3; 1.488, 80.3; 2, 58; 3, 44.4; 4, 22.8; 5, 10.9; 6, 3.8];

% horton '92 rat iv 100 mg/kg (BW 220, F344)
rhi1=[0.24, 91.13; 0.52, 80.14; 0.90, 70.29; 1.38, 61.22;
1.86, 60.63; 2.79, 39.40; 4.30, 26.05; 5.81, 12.51];

use SDrat
prepare @clear T CVB
TSTOP=48; IVDOSE=2500; TCHNG=0.016; BW=0.275; CINT=0.1; start @nocallback
Twi25 = _t; Cwi25 = _cvb;
IVDOSE=100; start @nocallback
Twi1 = _t; Cwi1 = _cvb;
BW=0.22; start @nocallback

plot(Twi25, Cwi25, Twi1, Cwi1, _t, _cvb, rwi25(:,1), rwi25(:,2), ...
        rwi1(:,1), rwi1(:,2), rhi1(:,1), rhi1(:,2), 'rwi2500.aps')

use F344rat
IVDOSE=100; BW=0.22; TCHNG=0.016; CINT=0.1; start @nocallback
plot(Twi25, Cwi25, Twi1, Cwi1, _t, _cvb, rwi25(:,1), rwi25(:,2), ...
        rwi1(:,1), rwi1(:,2), rhi1(:,1), rhi1(:,2), 'rwi100.aps')
```

```
% File: Horton-rat-inhal.m
% MeOH PBPK model rat simulations for Horton '92 rat inhalation data
% Creates Figure B-10
```

```
hi20=[0.46, 18.70; 1, 23.76; 3, 59.73; 6, 80.12
7, 83.25; 9, 53.49; 12, 16.54; 15, 0.91];
hi12=[0.46, 4.89; 1, 8.02; 3, 20.57; 6, 26.63;
7, 16.12; 8, 9.28; 9, 5.23; 10.5, 2.93; 12, 0.98];
hi2=[0.48, 1.2; 3, 3.1; 6, 3.7; 6.47, 2.7;
7, 2.0; 8, 1.6; 9, 1.2];

use F344rat
prepare @clear T CVB
TSTOP=16; CONCPPM=2000; TCHNG=6; BW=0.22; CINT=0.1; start @nocallback
t20 = _t; c20 = _cvb;
CONCPPM=1200; TSTOP=13; start @nocallback
t12 = _t; c12 = _cvb;
CONCPPM=200; TSTOP=10; start @nocallback
t2 = _t; c2 = _cvb;
TSTOP=16; CONCPPM=2000; TCHNG=7; start @nocallback

plot(t20, c20, t12, c12, t2, c2, hi20(:,1), hi20(:,2), ...
        hi12(:,1), hi12(:,2), hi2(:,1), hi2(:,2), _t, _cvb, 'hi2000.aps')
```

```
% File: Ward-rat-oral.m
% MeOH PBPK model rat simulations for Ward '97 rat oral data
% Creates Figre B-11
use SDRat
KAS=10.9; KSI=6.8; KAI=0.039; KFEC=0.0; VASC=0;
BW=0.3; ODS=0; prepare @clear T CVB
DOSE=100; TSTOP=10; start @nocallback
t1=_t;c1=_cvb;
DOSE=2500; TSTOP=36; start @nocallback
t2=_t;c2=_cvb;

KAS=0; use ratoral_fit-params
DOSE=100; TSTOP=10; start @nocallback
t1A=_t;c1A=_cvb;
DOSE=2500; TSTOP=36; start @nocallback
t2A=_t;c2A=_cvb;

d1=[0.072, 85.5; 0.168, 95.6; 0.24, 95.5; 0.504, 91.1;
0.744, 86.6; 1.008, 80.6; 1.488, 71.3; 1.992, 61.1;
3, 45.1; 4.008, 27.4; 4.992, 16.4; 6, 8.9; 7.008, 4.2];

d25=[0.072, 862.7; 0.168, 1243; 0.24, 1356; 0.504, 1621;
1.008, 1641; 1.992, 1611; 3, 1869; 4.008, 1896; 7.008, 2181;
24, 1365; 25.992, 1081; 28.008, 921; 30, 958.4; 31.008, 969.8];

plot(t2,c2, t2A,c2A, d25(:,1),d25(:,2), ...
        t1,c1, t1A,c1A, d1(:,1),d1(:,2),"wardratoralplot.aps")
plot(t2,c2, t2A,c2A, d25(:,1),d25(:,2), ...
        t1,c1, t1A,c1A, d1(:,1),d1(:,2),"wardratoralplotb.aps")
```

```
% File: Nedo-rat-inhal-devpmt.m
% MeOH PBPK model rat simulations for rat inhalation exposures
% 200, 500, 1000, 2000, and 5000 ppm
% Internal doses for NEDO developmental inhalation exposures, Sprague-Dawley rats
% Creates Figure B-13 ('simres' is tabulated results)
use SDRat
prepare @clear T CVB
```

```
simres=[]; ts=[]; cs=[]; ts2=[]; cs2=[]; TSTOP=24*2*7; CINT=1;
for CONCPPM=[200, 500, 1000, 2000, 5000]
        TCHNG=22; MULTE=1; start @nocallback
        res=[CONCPPM,max(_cvb),AUCBF,AMF];
        ts=[ts,_t]; cs=[cs,_cvb];
        TCHNG=TSTOP; MULTE=0; %CONCPPM=22*cp/24;
start @nocallback
        simres=[simres;[res,CONCPPM,max(_cvb),AUCBF,AMF]];
        ts2=[ts2,_t]; cs2=[cs2,_cvb];
end

simres
plot(ts(:,2),cs(:,2),ts(:,3),cs(:,3),ts(:,4),cs(:,4), ...
        ts2(:,2),cs2(:,2),ts2(:,3),cs2(:,3),ts2(:,4),cs2(:,4), ...
        [24 24],[0,95], 'fig13.aps')
save simres @file='Nedo_devpomt_rat_inhal_sims.csv' @format=ascii @separator=comma
cs=[ts(:,1),cs,cs2]; save cs @file='Fig13_sims.csv' @format=ascii @separator=comma
```

```
% File Nedo-rat-inhal-cancer.m
% Simulations for NEDO F344 rat cancer inhalation study
use F344rat
TCHNG=22.7; TSTOP=5*7*24; MULTE=1;
res=[]; CONCPPM=200; prepare @clear T CVB
start @nocallback
TCHNG=19.5; ODS=1; cppm=[0,10,100,1000];
bwm=[422.1, 418.3, 417.7, 410.0];
bwf=[268.7, 270.6, 267.0, 264.9];
for sdose=[0,25.4863]
        for i=1:length(cppm)
                CONCPPM=cppm(i);
                BW=bwm(i)/1000;
                DOSE=sdose/(BW^0.25);
                start @nocallback
                res=[res;[CONCPPM,TCHNG,BW,AUCBF,max(_cvb),AMF]]
                BW=bwf(i)/1000;
                DOSE=sdose/(BW^0.25);
                start @nocallback
                res=[res;[CONCPPM,TCHNG,BW,AUCBF,max(_cvb),AMF]]
        end
end

save res @file='Nedo_rat_cancer_sims.csv' @format=ascii @separator=comma
```

```
% File: rat-infu-sims.m
% MeOH PBPK model rat simulations for zero-order liver infusions
% Creates Figre B-14
use SDRat
lv0=[0.33, 65.9; 0.33, 624.1; 0.34, 2177;
        0.49, 53.2; 0.50, 524;
0.54    1780];
% Above are BWs and doses from Soffretti et al. 2002a
prepare @clear T CVB
TCHNG=12; MULTE=0; simres=[]; ts=[]; cs=[];
for i=1:3
        BW=lv0(i,1); LIVR0=lv0(i,2); TSTOP=24; start @nocallback
        res=[LIVR0,BW,max(_cvb),0,AUCB,0,AMET];
```

```
        TSTOP=84; start @nocallback
        res(4)=AUCB; res(6)=AMET; simres=[simres;res];
        ts=[ts,_t]; cs=[cs,_cvb];
end
simres/100
plot(ts(:,1),cs(:,1),ts(:,2),cs(:,2),ts(:,3),cs(:,3),'fig14b.aps')
save simres @file='rat_liver-infusion_sims.csv' @format=ascii @separator=comma
```

```
% File: humanset.m
% Sets parameters for human simulations.  Expects the user to define
% metabf = "linear" to use 1st-order metabolism parameters; otherwise
% metabf set to "non-linear" and Michaelis-Menten parameters used.
BW = 70; FRACIN = 0.8655; IVDOSE=0; DOSE=0; CONCPPM=0; LIVR0=0;
PB = 1626; PL = 0.583; %1.06;
PF = 0.142; PR = 0.805; %0.66;
PLU=1.07; %1.0;
VFC = 0.214; VLC = 0.026; VLUC = 0.008;
VAC = 0.0198; VVBC = 0.0593;
QPC = 18.5; QCC = 18.5; QLC = 0.227; QFC = 0.052;
KM = 12.76; VMAXC = 0; %VMAXC=11.72; %low KM optimum
KM2 = 460; VMAX2C = 0; %VMAX2C=304.5; %high KM optimum
KLLC = 60.7; %linear liver metabolism optimum
K1C = 0.0397; KAI = 0.22; KSI = 1.1; KAS = 2.0;
RATS=0; KLOSS=0; % constant exposure/no chamber losses
QPC=24.0; QCC=16.5; REST=3000; WORK=3000;

% Below are optimal values for Michaelis-Menten liver metabolism
K1C = 0.0342; KLLC = 0.0; KBL=0.612;
KM = 23.7; VMAXC = 33.1;

% Mouse oral uptake KMASC; others set to match ethanol values
% for humans from Sultatos et al. (2004), with VASC set so that
% VASC/KMAS = 0.21/h, the Sultatos et al. 1st-order constant,
% and KFEC = 0 corresponding to assumed 100% absorption.
VASC = 377; KSI = 3.17; KAI = 3.28; KMASC = 620; KFEC=0;

exist metabf; % check if metabf defined
if ~ans  % If not...
        metabf = "non-linear"
end
if metabf=="linear"
        % Below are optimal values for 1st-order liver metabolism
        K1C = 0.0373; KLLC = 95.7; KBL=0.564; VMAXC=0.0;
        % Below are 'no bladder values; uncomment next line to use
        %K1C = 0.0278; KLLC = 70.3; KBL=1000.0; VMAXC=0.0;
else metabf="non-linear";
end
disp(['Simulation for ',ctot(metabf),' human kinetics']);
```

```
% File: Sedivec_human_inh.m
% Creates MeOH PBPK Figure B-16
% For human inhalation exposures, w/ data of Sedivec et al

%------- DATA BLOCKS
        % These data blocks taken directly from MeOH CBMMv3.cmd
        % Data are T (hours), CV (mg/L), cumulative urinary clearance (mg)
        % Rounded to 3-4 sig figs
```

```
% Sedivec et al., Int Arch Occ Health 1981, urine
HS231 = [2, 3.338, 0.1168; 4, 5.776, 0.4358; 6, 7.371, 0.8960;
                    8, 8.581, 1.454; 10, 6.576, 1.985; 12, 3.243, 2.328;
                    14, 1.32 , 2.488; 19, 0.333, 2.632; 24, 0, 2.661];

HS157 = [2, 2.185, 0.0765; 4, 3.941, 0.291; 6, 4.896, 0.600;
                    8, 5.708, 0.971; 10, 4.360, 1.324; 12, 1.738, 1.537;
                    14, 0.776, 1.625; 19, 0.231, 1.713; 24, 0, 1.733];

HS78 = [2, 0.881, 0.0308; 4, 1.648, 0.1193; 6, 2.285, 0.2570;
                    8, 2.551, 0.4263; 10, 1.515, 0.5686; 12, 0.708, 0.6464;
                    14, 0.430, 0.6863; 19, 0.094, 0.7321; 24, 0, 0.7403];

%-----RUN MODEL
use humanset
TCHNG=8; TSTOP=24; CONCPPM=231;
prepare @clear T RUR METB
start @nocallback
  ur1 = _metb; t1 = _t; cu1=_rur;, % Save time series for urine MeOHc
CONCPPM=157; start @nocallback
  ur2 = _metb; t2 = _t; cu2= _rur;
CONCPPM=78; start @nocallback

%-----PLOT COMMANDS
 plot(t1,ur1,t2,ur2,_t,_metb,HS231(:,1),HS231(:,3),...
    HS157(:,1),HS157(:,3),HS78(:,1),HS78(:,3), 'sedivic.aps')
 plot(t1,cu1,t2,cu2,_t,_rur,HS231(:,1),HS231(:,2),...
    HS157(:,1),HS157(:,2),HS78(:,1),HS78(:,2), 'sedivic2.aps')

%-----WRITE OUT DATA TO A TEXT FILE FOR IMPORTING INTO EXCEL
    % Cant save data with different # of rows to the same table.
 mytable1 = [t1,ur1,cu1,t2,ur2,cu2,_t,_metb,_rur];
eval(['save mytable1 @file=Sedv_fit_KLLC.',num2str(round(KLLC)),'.csv @format=ascii
@separator=comma']);
```

```
% File: Batterman_human_inh.m
% Creates MeOH PBPK Figure B-17 (upper panel)
% For human inhalation exposures of Batterman et al 1998

   %These data blocks taken directly from MeOH CBMMv3.cmd
   %Data are T (hours), CV (mg/L)
% Batterman et al., Int Arch Occ Health 1998
HB82=[2, 13.6; 2.25, 13.4; 2.5, 12; 3, 9.6;
          4, 6.4; 5, 4.1; 6, 2.6; 7, 1.8; 8, 1.4];
HB81=[1, 6.5; 1.25, 6.2; 1.5, 5.4; 2, 4.3; 3, 2.8;
4, 1.5; 5, 0.94; 6, 0.72; 7, 0.52; 8, 0.23];
HB830=[0.5, 4.6; 0.75, 4.7; 1, 4.9; 1.5, 3.5; 2.5, 2.2;
3.5, 1; 4.5, 0.52; 5.5, 0.51; 6.5, 0.47; 7.5, 0.68];

use humanset
prepare @clear T CVB
TCHNG=2; CONCPPM=800; TSTOP=16; start @nocallback
t2=_t; c2=_cvb; TCHNG=1; start @nocallback
t1=_t; c1=_cvb; TCHNG=0.5; start @nocallback
t30=_t; c30=_cvb;

%-----PLOT COMMANDS
```

```
plot(t2,c2, t1,c1, t30,c30, HB82(:,1),HB82(:,2), ...
        HB81(:,1),HB81(:,2),HB830(:,1),HB830(:,2), 'batterman.aps')

%-----WRITE OUT DATA TO A TEXT FILE FOR IMPORTING INTO EXCEL
    % Cant save data with different # of rows to the same table.
le=1:min([length(t1),length(t2),length(t30)]);
 mytable1 = [t2(le),c2(le),t1(le),c1(le),t30(le),c30(le)];
eval(['save mytable1 @file=Batter_fit_KLLC.',num2str(round(KLLC)),'.csv ' ...
        '@format=ascii @separator=comma']);
```

```
% File: Osterloh_human_inh.m
% Creates Fig B-17 (lower panel)
% Data from Osterloh et al., JOEM 1996
% Digitized data provided by EPA (dat1)
% Subtracted background from exposure blood levels
% by Paul Schlosser, U.S. EPA
use humanset
BW=78.2;
dat1=[0.05, 0.54; 0.25, 1.39; 0.50, 1.82; 0.75, 2.28; 1, 2.42;
                1.5, 2.94; 2, 3.37; 2.5, 3.90; 3, 4.21; 3.5, 4.61;
                4, 4.82; 5, 2.99; 6, 2.30; 7, 1.40; 8, 1.07];
dat=[0.25, 1.183; 0.5, 1.526; 0.75, 1.948; 1, 2.073; 1.5, 2.741;
                2, 3.118; 2.5, 3.495; 3, 3.998; 3.5, 4.181; 4, 4.48;
                5, 2.790; 6, 1.943; 7, 1.106; 8, 0.687];

prepare @clear T CVB
TCHNG=4; CONCPPM=200; TSTOP=16; start @nocallback
plot(_t,_cvb,dat(:,1),dat(:,2), 'osterloh.aps')
mytable1=[_t,_cvb];
eval(['save mytable1 @file=Oster_fit_KLLC.',num2str(round(KLLC)),'.txt @format=ascii']);
```

```
% File: Ernstgard_human_inh.m
% Creates MeOH PBPK Figure B-18, w/ data of Ernstgard et al 2005a,b
% For human inhalation exposures w/ exercise
%------- DATA BLOCKS
   %These data blocks taken directly from MeOH CBMMv3.cmd
   %Data are T (hours), CV (mg/L)
% Ernstgard et al. SOT poster, 100 ppm & 200 ppm human
ern1 =[0.20, 0.87; 0.46, 1.50; 0.97, 2.31; 1.46, 3.24;
        1.91, 3.65; 2.17, 3.52; 2.50, 2.55; 2.91, 2.23; 3.51, 1.59;
        4.01, 1.72; 5.02, 0.41; 6.00, 0.50; 9.24, 0.12];
ern2 =[0.22, 1.63; 0.49, 2.92; 0.92, 4.76; 1.47, 6.30;
        1.90, 7.65; 2.16, 6.20; 2.47, 5.49; 2.91, 4.96; 3.50, 3.64;
        4.00, 3.43; 4.99, 1.94; 5.97, 1.03; 8.90, 0.21];

%-----RUN MODEL
use humanset
QPCHR=QPC; QCCHR=QCC; REST=2.0; WORK=0.0;
TCHNG=2.0; CONCPPM=100; TSTOP=10.0; QPCHW=52.6; QCCHW=26.0;
        %FRACIN=0.9509; %FRACIN=0.9324;
prepare T CVB QP QC
start @nocallback,
cv1 = _cvb; t1 = _t; CONCPPM=200; start @nocallback

%-----PLOT COMMANDS
 plot(t1, cv1, _t, _cvb,...
        ern1(:,1),ern1(:,2),ern2(:,1),ern2(:,2), 'ernstgard.aps')
```

```
%-----WRITE OUT DATA TO A TEXT FILE FOR IMPORTING INTO EXCEL
    % Cant save data with different # of rows to the same table.
 mytable1 = [t1, cv1, _t, _cvb];
eval(['save mytable1 @file=Ernst_nofit_KLLC.',num2str(round(KLLC)),'.csv ' ...
        '@format=ascii @separator=comma']);
```

```
% File: mouse_inh_sim.m
% Runs simulations for Table B-5, mouse internal-dose calculations
% from inhalation exposure, over the concentration range specified
% in the 'for' statement below.
% Results saved to file 'MouseInhalSims.csv'.
use CDMice
BW=0.03; TCHNG=7; % 7 hr/day exposures
TSTOP=240; MULTE=1; % Run for 10 days; multi-day exposure 'on'
RATS=0.0; KLOSS=0.0; % -> open chamber
prepare @clear T CVB
CONCPPM=10000; CINT=0.02; start @nocallback
% plot(_t,_cvb)  % uncomment to see/check that periodicity reached by TSTOP
inhres=[]; CINT=0.2;
for CONCPPM=[1, 10, 50, 100, 250, 500, 1000, 2000, 5000, 10000]
        start @nocallback
        inhres=[inhres;[CONCPPM, AUCBB, max(_cvb), AMET24/(BW^0.75)]];
end
 save inhres @file=MouseInhalSims.csv @format=ASCII @separator=comma
```

```
% File: human_inh_sim.m
% Runs simulations for Table B-5, human internal-dose calculations
% from inhalation exposure, over the concentration range specified
% in the 'for' statement below.
% Results saved to file 'HumanInhSims_KLLC.#.csv', where # is
% value of KLLC used (0 if non-linear/Michaelis-Menten kinetics).
% If metab="linear", 1st order kinetics used; otherwise non-linear.
use humanset
WESITG=0; WEDITG=0; simres=[]; MULTE=0; CINT=1.0; RATS=0.0; KLOSS=0.0;
CONCPPM=0; TSTOP=1000; TCHNG=1000; DOSE=0; DWDOSE=0; ODS=1;
prepare @clear T CVB STOM
start @nocallback
for CONCPPM=[1, 10, 50, 100, 250, 500, 1000, 2000, 5000, 10000]
        start @nocallback
        simres=[simres;[CONCPPM,AUCBF,max(_cvb),AMF/(BW^0.75)]]
end
disp(['Simulation for ',ctot(metabf),' human kinetics']);
eval(['save simres @file=HumanInhSims_KLLC.',num2str(round(KLLC)), ...
                '.csv @format=ascii @separator=comma']);
```

```
% File: human_oral_sim.m
% Runs simulations for Table B-5, human internal-dose calculations from
% oral exposure, over the exposure range specified in the 'for' statement below.
% Results saved to file 'Hum_DW_Sims_KLLC.#.csv', where # is value of KLLC
% used (0 if non-linear/Michaelis-Menten kinetics).
% If metab="linear", 1st order kinetics used; otherwise non-linear.
use humanset
WESITG=0; WEDITG=0; MULTE=0; CINT=0.1; RATS=0.0; KLOSS=0.0;
CONCPPM=0; TSTOP=1000; DWDOSE=0; DOSE=1; ODS=1; DRDOSE=0;
prepare @clear T CVB STOM
start @nocallback
simres=[];
```

```
for DOSE=[0.1, 1, 10, 50, 100, 250, 500, 1000, 2000, 5000]
        start @nocallback
        simres=[simres;[DOSE,AUCBF,max(_cvb)],AMF];
end
disp(['Simulation for ',ctot(metabf),' human kinetics']);
eval(['save simres @file=Hum_DW_Sims_KLLC.',num2str(round(KLLC)),'.csv ' ...
        '@format=ascii @separator=comma']);
```

```
% file human_drink_compare.m
% creates Figure B-24 and Table B-9
% Created by Paul Schlosser, U.S. EPA, 8/26/09
use humanset
WESITG=0; WEDITG=0; MULTE=0; CINT=0.1; TSTOP=48; DOSE=0.1; ODS=1; DRDOSE=0;
prepare @clear T CVB
start @nocallback
T1=_t; C1=_cvb; DOSE=0; LIVR0=0.1; TCHNG=12; MULTE=1; start @nocallback
T2=_t; C2=_cvb; LIVR0=0; ODS=0; DOSE=0.1; start @nocallback
T3=_t; C3=_cvb; DOSE=0; DRDOSE=0.1; start @nocallback
plot(T1,C1,T2,C2,T3,C3,_t,_cvb,'humoralsim.aps')

tbl=[]; metd = 1.0;
for dse=[0.1, 1.0, 10, 100, 250, 500]
        row=[]; LIVR0=0; DOSE=0; DRDOSE=dse; start @nocallback
        row=[dse,max(_cvb),AUCBF,AMETF];
        LIVR0=dse; DOSE=0; DRDOSE=0; start @nocallback
        row=[row,max(_cvb),AUCBF,AMETF];
        LIVR0=0; DOSE=dse; DRDOSE=0; start @nocallback
        tbl=[tbl;[row,max(_cvb),AUCBF,AMETF]];
end
tbl
```

B.3.5. Personal Communication from Lena Ernstgard Regarding Human Exposures Reported in the Ernstgard and Johanson, 2005 SOT Poster

From: Lena Ernstgård [Lena.Ernstgard@imm.ki.se]
Sent: Wednesday, March 23, 2005 12:39 AM
To: Poet, Torka S
Subject: RE: Human MeOH poster

Hi,
We measured the ventilation rate and they ought to be similar to those reported by Dr. Johanson at the same workload.
Sincerly,
Lena Ernstgård

At 18:41 2005-03-22, you wrote:

> Thank you very much. Your net uptake is what we thought. Did you measure ventilation rates?

Thanks again,
Torka

Torka Poet, PhD
Center for Biological Monitoring and Modeling
Pacific Northwest National Laboratories
902 Battelle Blvd.
P.O. Box 999, MSIN P7-59

Richland, WA 99352
ph: (509)376-7740
fax: (509)376-9449
e-mail: Torka.poet@pnl.gov
(Express Mail Delivery: 790 Sixth Street, Zip Code 99354)

From: Lena Ernstgård [mailto:Lena.Ernstgard@imm.ki.se]
Sent: Sunday, March 20, 2005 11:21 PM
To: Poet, Torka S
Subject: Re: Human MeOH poster
Hi,
The manuscript has not been submitted yet, but it will be soon I hope. I will save your mail and send you a copy as soon as possible.
When I say % of net uptake, i mean the relative uptake. It is calculated as: conc in exposure chamber - (minus) exhaled conc / (divided by) conc in exposure chamber. I hope you understand how we have done.
Sincerly,
Lena Ernstgård

B.3.6. Personal Communication from Dr. Rogers Regarding Mouse Exposures

Jeff Gift, Ph.D.
National Center for Environmental Assessment EPA (B243-01) RTP, NC 27711
919-541-4828
919-541-0245 (fax)
gift.jeff@epa.gov

----- Forwarded by Jeff Gift/RTP/USEPA/US on 04/04/2005 04:31 PM -----
John Rogers
To: Jeff Gift/RTP/USEPA/US@EPA
04/04/2005 03:50 PM
Subject: Re: report(Document link: Jeff Gift)

Hi Jeff:
It's easier just to give you the numbers from that figure in tabular form:

Time (hr) (exposure ends @ 7 hr)	Blood [MeOH] (mg/ml)	SEM
1	0.93	0.05
4	2.80	0.20
6	3.36	0.08
7	3.99	0.13
7.5	3.98	0.21
8	4.12	0.07
9	3.27	0.16
12	2.63	0.21
16	1.69	0.08
26	0.06	0.02

Whew! Surprised I could find these numbers that fast, I get a little worried when someone asks for 12 year old data, I'm not as organized as I'd like to be,to say the least.

John

John M. Rogers, Ph.D.
Chief, Developmental Biology Branch (MD-67) Reproductive Toxicology Division National Health and Environmental Effects Research Laboratory Research Triangle Park, NC 27711
T: (919)541-5177
F: (919)541-4017
e-mail: rogers.john@epa.gov

B.3.7. Total MeOH Metabolic Clearance/Metabolites Produced

Table B-6. Mouse total MeOH metabolic clearance/metabolites produced following inhalation exposures[a]

Exposure concentration (ppm)	AUC (mg/L-hr)	C_{max} (mg/L)	Total MeOH metabolically cleared (mg)
1	1.51E-01	2.16E-02	1.20E-02
10	1.53E+00	2.18E-01	1.20E-01
50	8.03E+00	1.15E+00	6.01E-01
100	1.72E+01	2.46E+00	1.20E+00
250	5.38E+01	7.83E+00	2.99E+00
500	1.72E+02	2.64E+01	5.89E+00
525	1.89E+02	2.94E+01	6.17E+00
550	2.09E+02	3.26E+01	6.45E+00
575	2.29E+02	3.62E+01	6.73E+00
600	2.51E+02	3.99E+01	7.01E+00
625	2.74E+02	4.40E+01	7.28E+00
675	3.24E+02	5.30E+01	7.83E+00
750	4.09E+02	6.84E+01	8.63E+00
875	5.77E+02	9.88E+01	9.93E+00
1,000	7.76E+02	1.34E+02	1.12E+01
2000	5.12E+03	7.57E+02	2.37E+01
5000	1.73E+04	2.00E+03	3.77E+01
1,0000	4.98E+04	4.60E+03	5.50E+01

[a]Total over a 36-hour period during which mice were exposed for 7 hours to MeOH according to the conditions of the dose-response study.

Table B-7. Human total MeOH metabolic clearance/metabolites produced from inhalation exposures[a]

Exposure concentration (ppm)	AUC (mg/L-hr)	C_{max} (mg/L)	Total MeOH metabolically cleared (mg)
1	0.7142	0.0300	10.23
10	7.142	0.300	102.3
50	35.71	1.498	511.7
100	71.42	2.997	1023
250	178.6	7.491	2559
500	357.1	14.98	5117
625	446.4	18.73	6396
750	535.7	22.47	7676
875	625.0	26.22	8955
1,000	714.2	29.97	10234

[a]Total over a 24-hour period during which humans were exposed continuously to MeOH.

Table B-8. Human total MeOH metabolic clearance/metabolites produced following oral exposures[a]

Exposure concentration (mg/kg-day)	AUC (mg/L-hr)	Total MeOH metabolically cleared (mg)
0.1	0.3795	6.2152
1	3.7954	62.152
5	18.977	310.8
10	37.954	621.5
50	189.8	3108
100	379.5	6215
250	948.8	15538

[a]Total over a 24-hour period during which humans were exposed continuously to MeOH.
Note: MeOH in the model is eliminated via exhalation, metabolism, and urinary excretion (human only). Total MeOH metabolically cleared approximates total production of down stream metabolites, but as a dose metric is not equivalent to formaldehyde or formate concentration.

B.3.8. Multiple Daily Oral Dosing for Humans

Current mode simulations of oral exposures to humans use a constant rate of infusion to the stomach lumen. This approach results in a steady rate of absorption from the stomach equal to the exposure rate irregardeless of the oral uptake rate constants (assumed equal to the mouse), hence avoids the difficulty that independent values of these constants are not available for humans due to a lack of human oral PK data.. A more likely drinking scenario was tested by using additional code within the model to simulate a 6-times/day drinking schedule, over the course of 15 h (see code below). The schedule is still an approximation, as it assumes 6 episodes of drinking, each considered to be a bolus. Specifically, it was assumed that humans drank at 0, 3, 5, 8, 11, and 15 hours from the first ingestion of each day, with the respective fractions of daily consumption being 25, 10, 25, 10, 25, and 5% at those times. The predicted blood concentrations resulting from simulations of six daily boluses, once/day boluses, 12 h/d infusion (zero order), or constant (zero order) are shown in Figure B-24 for a total dose of 0.1 mg/kg. Table B-9 shows PBPK model predicted C_{max}, AUC, and Amet (for the last 24 hours of repeated exposures) for humans exposed to MeOH via six daily boluses, 12 h/d infusion, or a single daily gavage.

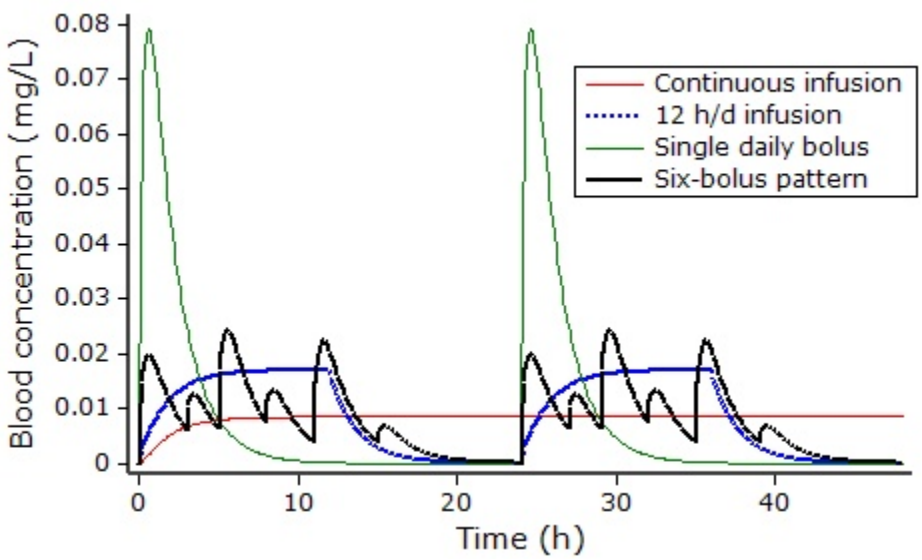

Figure B-24. Simulated human oral exposures to 0.1 mg MeOH/kg/-day comparing the first few days for four exposure scenarios: continuous (zero-order) infusion; 12 h/d infusion, a single daily bolus, and a pattern of six boluses per day (see text).

Table B-9. Repeated daily oral dosing of humans with MeOH*

Dose (mg/kg)	Six daily boluses			12 h/d infusion			Single-daily bolus		
	C_{max} (mg/L)	AUC (mg-h/L)	Amet (mg)	C_{max} (mg/L)	AUC (mg-h/L)	Amet (mg)	C_{max} (mg/L)	AUC (mg-h/L)	Amet (mg)
0.1	0.0204	0.0581	1.97	0.0170	0.0583	1.97	0.0569	0.0584	1.98
1	0.205	0.584	19.7	0.171	0.586	19.8	0.579	0.594	19.8
10	2.16	6.17	197	1.83	6.21	197	6.64	7.01	197
100	33.4	109	1,950	41.4	125	1,950	95.2	204	1,920
250	182	720	4,400	237	857	4,420	296	1,150	4,440
500	746	3,290	5,180	866	3,540	5,190	903	4,250	5,270

***AUC in blood and Amet (amount metabolized) computed from 24-48 h**

APPENDIX C. RfC DERIVATION OPTIONS

C.1. RFC DERIVATIONS USING THE NEDO METHANOL REPORT (NEDO, 1987)

The BMD approach was utilized in the derivation of potential chronic inhalation reference values. In the application of the BMD approach, continuous models in the EPA's BMDS, version 2.1, were fit to datasets for decreased brain weight in male rats exposed throughout gestation and the postnatal period to 6 weeks and male rats exposed during gestation on days 7–17 only (NEDO, 1987). Although there remains uncertainty surrounding the identification of the proximate teratogen of importance (methanol, formaldehyde, or formate), the dose metrics chosen for the derivation of RfCs were based on blood methanol levels. This decision was primarily based on evidence that the toxic moiety is not likely to be the formate metabolite of methanol (CERHR, 2004), and evidence that levels of the formaldehyde metabolite following methanol maternal and/or neonate exposure would be much lower in the fetus and neonate than in adults. While recent in vitro evidence indicates that formaldehyde is more embryotoxic than methanol and formate, the high reactivity of formaldehyde would significantly limit its transport from maternal to fetal blood, and the capacity for the metabolism of methanol to formaldehyde is lower in the fetus and neonate versus adults. Further discussions of methanol metabolism, dose metric selection and MOA issues are covered in Sections 3.3, 4.5 and 4.6.

C.1.1. Decreased Brain Weight in Male Rats Exposed throughout Gestation and into the Postnatal Period (NEDO, 1987)

The results of NEDO (1987), shown in Table 4-14, indicate that there is not a cumulative effect of ongoing exposure on brain-weight decrements in rats exposed postnatally; i.e., the dose response in terms of percent of control is about the same at 3 weeks postnatal as at 8 weeks postnatal in rats exposed throughout gestation and the F_1 generation. However, there does appear to be a greater brain-weight effect in rats exposed postnatally versus rats exposed only during organogenesis (GD7–GD17). In male rats exposed during organogenesis only, there is no statistically significant decrease in brain weight at 8 week after birth at the 1,000 ppm exposure level. Conversely, in male rats exposed to the same level of methanol throughout gestation and the F_1 generation, there was an approximately a 5% decrease in brain weights (statistically significant at the $p < 0.01$ level). The extent to which this observation is due to recovery in rats for which exposure was discontinued at birth versus a cumulative effect in rats exposed postnatally is not clear. The fact that male rats exposed to 5,000 ppm methanol only during organogenesis experienced a decrease of brain weight of 10% at 8 weeks postnatal indicates that postnatal exposure is not necessary for the observation of persistent postnatal effects. However, the fact that this decrease was less than the 13% decrease observed in male rats exposed to

2,000 ppm methanol throughout gestation, and the 8 week postnatal period indicates that the absence of postnatal exposure allows for some measure of recovery.

It appears that once methanol exposure is discontinued, continuous biological processes that are disrupted by exposure, manifesting as decreased brain weight, undergo some recovery and brain weights begin to return to normal values. This indicates that brain weight is susceptible to both the level and duration of exposure. Therefore, a dose metric that incorporates a time component would be the most appropriate metric to use. For these reasons and because it is more typically used in internal-dose-based assessments and better reflects total exposure within a given day, daily AUC (measured for 22-hour exposure/day) was chosen as the most appropriate dose metric for modeling the effects of methanol exposure on brain weights in rats exposed throughout gestation and continuing into the F_1 generation.

Application of the EPA methanol PBPK model (described in Section 3.4) to the NEDO (1987) study in which developing rats were exposed during gestation and the postnatal period presents complications that need to be discussed. The neonatal rats in this study were exposed to methanol gestationally before parturition, as well as lactationally and inhalationally after parturition. The PBPK model developed by the EPA only estimates internal dose metrics for methanol exposure in NP adult mice and rats. Experimental data indicate that inhalation-route blood methanol kinetics in NP mice and pregnant mice on GD6–GD10 are similar (Dorman et al., 1995; Perkins et al., 1995a,b; Rogers et al., 1993a,b). In addition, experimental data indicate that the maternal blood:fetal partition coefficient for mice is approximately 1 (see Section 3.4.1.2). Assuming that these findings apply for rats, they indicate that pharmacokinetic and blood dose metrics for NP rats are appropriate surrogates for fetal exposure during early gestation. However, as is discussed to a greater extent in Section 5.3, the additional routes of exposure presented to the pups in this study (lactation and inhalation) present uncertainties that make it reasonable to assume that average blood levels in pups in the NEDO report are also greater than those of the dam. However, it is also reasonable to assume that any differences seen between the pups and dams would also be seen in mothers and human offspring. Therefore, the presumed differences between pup and dam blood methanol levels are deemed relatively inconsequential, and the PBPK model-estimated adult blood methanol levels are assumed to be appropriate dose metrics for the purpose of this analysis.

The first step in the current analysis is to convert the inhalation doses, given as ppm values from the studies, to an internal dose surrogate or dose metric using the EPA PBPK model (see Section 3.4). Predicted AUC values for methanol in the blood of rats and humans are summarized in Table C-1.

Table C-1. EPA's PBPK model estimates of methanol blood levels (AUC) in rats following inhalation exposures

Exposure level (ppm)	Methanol in blood AUC (hr × mg/L)[a] in rats
500	79.2
1,000	226.7
2000	967.8

[a]AUC values were obtained by simulating 22 hour/day exposures for 5 days and calculated for the last 24 hours of that period.

The current BMD technical guidance (U.S. EPA, 2000b) suggests that in the absence of knowledge as to what level of response to consider adverse, a change in the mean equal to 1 control S.D. from the control mean can be used as a BMR for continuous endpoints. However, it has been suggested that other BMRs, such as 5% change relative to estimated control mean, are also appropriate when performing BMD analyses on fetal weight change as a developmental endpoint (Kavlock et al., 1995). Therefore, in this assessment, both a 1 control mean S.D. change and a 5% change relative to estimated control mean were considered. All models were fit using restrictions and option settings suggested in the EPA BMD technical guidance document (U.S. EPA, 2000b).

C.1.2. BMD Approach with a BMR of 1 Control Mean S.D. – Gestation and into the Postnatal Period (NEDO, 1987)

A summary of the results most relevant to the development of a POD using the BMD approach (BMD, BMDL, and model fit statistics) for decreased brain weight at 6 weeks in male rats exposed to methanol throughout gestation and continuing into the F_1 generation, with a BMR of 1 control mean S.D, is provided in Table C-2. The 6 week male brain weight responses were chosen because they resulted in lower BMD and BMDL estimates than male responses at 3 and 8 weeks and female responses at any time point (data not shown). Model fit and was determined by statistics (AIC and χ^2 residuals of individual dose groups) and visual inspection, as recommended by EPA (2000b). There is a 2.5-fold range of BMDL estimates from adequately fitting models, indicating considerable model dependence. In addition, the fit of the Hill and more complex Exponential models is better than the other models in the dose region of interest as indicated by a lower scaled residual at the dose group closest to the BMD (0.09 versus -0.67 or -0.77) and visual inspection. In accordance with EPA BMD Technical Guidance (EPA, 2000b), the BMDL from the Hill model (bolded), is selected as the most approriate basis for an RfC derivation because it results in the lowest BMDL from among a broad range of BMDLs and provides a superior fit in the low dose region nearest the BMD. The $BMDL_{1SD}$ was determined to be 90.9 hr × mg/L using the 95% lower confidence limit of the dose-response curve expressed in terms of the AUC for methanol in blood.

Table C-2. Comparison of BMD_{1SD} results for decreased brain weight in male rats at 6 weeks of age using modeled AUC of methanol as a dose metric

Model	BMD_{1SD} (AUC, hr × mg/L) [a]	$BMDL_{1SD}$ (AUC, hr × mg/L)[a]	*p*-value	AIC[c]	Scaled residual[d]
Linear	278.30	225.30	0.5376	-203.84	-0.77
2nd degree polynomial	278.30	225.30	0.5376	-203.84	-0.77
3rd degree polynomial	278.30	225.30	0.5376	-203.84	-0.77
Power	278.30	225.30	0.5376	-203.84	-0.77
Hill[b]	170.57	**90.93**	0.8366	-203.04	0.09
Exponential 2	260.94	209.10	0.612	-204.10	-0.67
Exponential 3	260.94	209.10	0.612	-204.10	-0.67
Exponential 4	172.08	96.93	0.8205	-203.10	0.09
Exponential 5	172.08	96.93	0.8205	-203.10	0.09

[a]The BMDL is the 95% lower confidence limit on the AUC estimated to decrease brain weight by 1 control mean S.D. using BMDS model options and restrictions suggested by EPA BMD technical guidance (U.S. EPA, 2000b).
[b]There is a 2.5-fold range of BMDL estimates from adequately fitting models, indicating considerable model dependence. In addition, the fit of the Hill and more complex Exponential models is better in the dose region of interest as indicated by a lower scaled residual at the dose group closest to the BMD (0.09 versus -0.67 or -0.77) and visual inspection. Thus, in accordance with EPA BMD Technical Guidance (EPA, 2000), the BMDL from the Hill model (bolded) is considered the most appropriate POD for us in an RfC derivation.
[c]AIC = Akaike Information Criterion = -2L + 2P, where L is the log-likelihood at the maximum likelihood estimates for the parameters, and P is the number of modeled degrees of freedom (usually the number of parameters estimated).
[d]χ^2d residual (measure of how model-predicted responses deviate from the actual data) for the dose group closest to the BMD scaled by an estimate of its S.D. Provides a comparative measure of model fit near the BMD. Residuals that exceed 2.0 in absolute value should cause one to question model fit in this region.

Source: NEDO (1987).

```
=====================================================================
         Hill Model. (Version: 2.14;  Date: 06/26/2008)
         Input Data File: C:\Usepa\BMDS21\Data\Methanol\NEDO\Gest-F1\hilm-6wk-brwHil-
Restrict.(d)
         Gnuplot Plotting File:  C:\Usepa\BMDS21\Data\Methanol\NEDO\Gest-F1\hilm-6wk-
brwHil-Restrict.plt
                                                Mon Aug 24 13:08:09 2009
 ====================================================================

 BMDS Model Run
~~~~~~~~~~~~~~~~~~~~~~~~~~~~~~~~~~~~~~~~~~~~~~~~~~~~~~~~~~~~~~~~~~~~~~~~

   The form of the response function is:

   Y[dose] = intercept + v*dose^n/(k^n + dose^n)


   Dependent variable = Mean
   Independent variable = Dose
   rho is set to 0
   v is set to -0.5
   Power parameter restricted to be greater than 1
   A constant variance model is fit

   Total number of dose groups = 4
   Total number of records with missing values = 0
   Maximum number of iterations = 250
   Relative Function Convergence has been set to: 1e-008
```

```
   Parameter Convergence has been set to: 1e-008



                    Default Initial Parameter Values
                            alpha =   0.00539333
                              rho =            0   Specified
                        intercept =         1.78
                                v =         -0.5   Specified
                                n =       1.2699
                                k =      924.206


             Asymptotic Correlation Matrix of Parameter Estimates

             ( *** The model parameter(s)  -rho    -v
                   have been estimated at a boundary point, or have been specified by
the user,
                   and do not appear in the correlation matrix )

                    alpha    intercept            n            k

     alpha            1     1.7e-008    -1.7e-008    -2.9e-009

 intercept     1.7e-008            1        -0.56        -0.73

         n    -1.7e-008        -0.56            1         0.15

         k    -2.9e-009        -0.73         0.15            1



                         Parameter Estimates

                                                        95.0% Wald Confidence Interval
Variable         Estimate        Std. Err.     Lower Conf. Limit   Upper Conf. Limit
alpha       0.00496114        0.0010023          0.00299667          0.00692562
intercept      1.77806        0.0193152              1.7402             1.81591
        n      1.07212         0.217805            0.645228             1.49901
        k      915.874          179.818             563.437             1268.31



     Table of Data and Estimated Values of Interest

 Dose       N    Obs Mean     Est Mean   Obs Std Dev  Est Std Dev   Scaled Res.
------     ---   --------     --------   -----------  -----------   ----------

    0    12       1.78         1.78         0.07       0.0704         0.0956
 79.2    12       1.74         1.74         0.09       0.0704          -0.21
226.7    11       1.69         1.69         0.06       0.0704          0.159
967.8    14       1.52         1.52         0.07       0.0704        -0.0355



 Model Descriptions for likelihoods calculated


 Model A1:        Yij = Mu(i) + e(ij)
            Var{e(ij)} = Sigma^2

 Model A2:        Yij = Mu(i) + e(ij)
            Var{e(ij)} = Sigma(i)^2

 Model A3:        Yij = Mu(i) + e(ij)
            Var{e(ij)} = Sigma^2
     Model A3 uses any fixed variance parameters that
```

```
     were specified by the user

 Model  R:         Yi = Mu + e(i)
            Var{e(i)} = Sigma^2


                       Likelihoods of Interest

            Model      Log(likelihood)   # Param's      AIC
             A1          105.539862            5    -201.079724
             A2          106.570724            8    -197.141449
             A3          105.539862            5    -201.079724
         fitted          105.499930            4    -202.999859
              R           77.428662            2    -150.857324


                    Explanation of Tests

 Test 1:  Do responses and/or variances differ among Dose levels?
          (A2 vs. R)
 Test 2:  Are Variances Homogeneous? (A1 vs A2)
 Test 3:  Are variances adequately modeled? (A2 vs. A3)
 Test 4:  Does the Model for the Mean Fit? (A3 vs. fitted)
 (Note:  When rho=0 the results of Test 3 and Test 2 will be the same.)

                      Tests of Interest

   Test    -2*log(Likelihood Ratio)  Test df        p-value

   Test 1              58.2841          6          <.0001
   Test 2              2.06173          3          0.5597
   Test 3              2.06173          3          0.5597
   Test 4            0.0798644          1          0.7775

The p-value for Test 1 is less than .05.  There appears to be a
difference between response and/or variances among the dose levels
It seems appropriate to model the data

The p-value for Test 2 is greater than .1.  A homogeneous variance
model appears to be appropriate here


The p-value for Test 3 is greater than .1.  The modeled variance appears
 to be appropriate here

The p-value for Test 4 is greater than .1.  The model chosen seems
to adequately describe the data


        Benchmark Dose Computation

Specified effect =             1

Risk Type        =     Estimated standard deviations from the control mean

Confidence level =           0.95

              BMD =        169.597
```

```
BMDL =        103.912
```

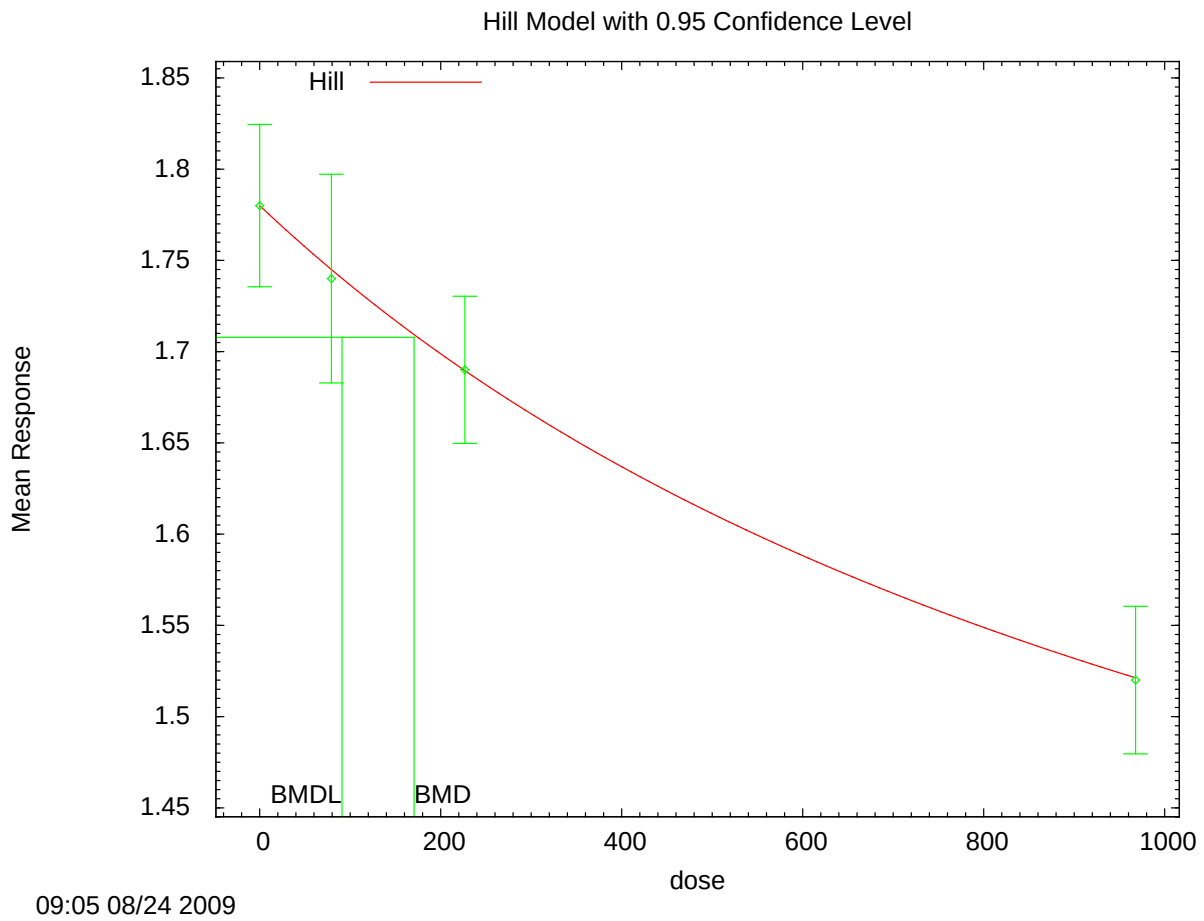

Figure C-1. Hill model, BMR of 1 Control Mean S.D. - Decreased Brain weight in male rats at 6 weeks age versus AUC, F1 Generation inhalational study

Source: NEDO (1987).

Once the $BMDL_{1SD}$ was obtained in units of hr × mg/L, it was used to derive a chronic inhalation reference value. The first step is to calculate the HEC using the PBPK model described in Appendix B. An algebraic equation is provided (Equation 1 of Appendix B) that describes the relationship between predicted methanol AUC and the human equivalent inhalation exposure concentration (HEC) in ppm.

$$BMDL_{HEC}\ (ppm) = 0.0224*BMDL_{1SD}+(1334*BMDL_{1SD})/(794+ BMDL_{1SD})$$

$$BMDL_{HEC}\ (ppm) = 0.0224*374.7+(1334*374.7)/(794+ 90.9) = 139\ ppm$$

Next, because RfCs are typically expressed in units of mg/m^3, the HEC value in ppm was converted using the conversion factor specific to methanol of 1 ppm = 1.31 mg/m^3:

$$HEC\ (mg/m^3) = 1.31 \times 139\ ppm = 182\ mg/m^3$$

Finally, this HEC value was divided by a composite 100-fold UF (3 for uncertainty associated with animal to human differences, 10 for consideration of human variability, and 3 for database deficiencies) to obtain the chronic inhalation reference value:

$$RfC\ (mg/m^3) = 182\ mg/m^3 \div 100 = 1.8\ mg/m^3$$

C.1.3. BMD Approach with a BMR of 0.05 Change Relative to Estimated Control Mean – Gestation and into the Postnatal Period (NEDO, 1987)

A summary of the results most relevant to the development of a POD using the BMD approach (BMD, BMDL, and model fit statistics) for decreased brain weight at 6 weeks in male rats exposed to methanol throughout gestation and continuing into the F_1 generation, with a BMR of 0.05 change relative to estimated control mean, is provided in Table C-3. The 6 week male brain weight responses were chosen because they resulted in lower BMD and BMDL estimates than male responses at 3 and 8 weeks and female responses at any time point (data not shown). Model fit was determined by statistics (AIC and χ^2 residuals of individual dose groups) and visual inspection, as recommended by U.S. EPA (2000b). There is a 2.4-fold range of BMDL estimates from adequately fitting models, indicating considerable model dependence. In addition, the fit of the Hill and more complex Exponential models is better than the other models in the dose region of interest as indicated by a lower scaled residual at the dose group closest to the BMD (0.09 versus -0.67 or -0.77) and visual inspection. In accordance with EPA BMD Technical Guidance (EPA, 2000b), the BMDL from the Hill model (bolded), is selected as the most approriate basis for an RfC derivation because it results in the lowest BMDL from among a broad range of BMDLs and provides a superior fit in the low dose region nearest the BMD. The $BMDL_{05}$ was determined to be 123.9 hr × mg/L, using the 95% lower confidence limit of the dose-response curve expressed in terms of the AUC for methanol in blood.

Table C-3. Comparison of BMD_{05} results for decreased brain weight in male rats at 6 weeks of age using modeled AUC of methanol as a dose metric

Model	BMD_{05} (AUC, hr × mg/L)[a]	$BMDL_{05}$ (AUC, hr × mg/L)[a]	*p*-value	AIC[c]	Scaled Residual[d]
Linear[b]	344.49	297.92	0.5376	-203.84	-0.77
2nd degree polynomial	344.49	297.92	0.5376	-203.84	-0.77
3rd degree polynomial	344.49	297.92	0.5376	-203.84	-0.77
Power	344.49	297.92	0.5376	-203.84	-0.77
Hill	223.18	123.87	0.8366	-203.04	-0.09
Exponential 2	325.82	278.26	0.612	-204.10	-0.67
Exponential 3	325.82	278.26	0.612	-204.10	-0.67
Exponential 4	223.94	129.97	0.8205	-203.10	0.09
Exponential 5	223.94	129.97	0.8205	-203.10	0.09

[a]The BMDL is the 95% lower confidence limit on the AUC estimated to decrease brain weight by 5% using BMDS model options and restrictions suggested by EPA BMD technical guidance (U.S. EPA, 2000b).
[b]There is a 2.4-fold range of BMDL estimates from adequately fitting models, indicating considerable model dependence. In addition, the fit of the Hill and more complex Exponential models is better in the dose region of interest as indicated by a lower scaled residual at the dose group closest to the BMD (0.09 versus -0.67 or -0.77) and visual inspection. Thus, in accordance with EPA BMD Technical Guidance (EPA, 2000), the BMDL from the Hill model (bolded) is considered the most appropriate POD for us in an RfC derivation.
[c]AIC = Akaike Information Criterion = -2L + 2P, where L is the log-likelihood at the maximum likelihood estimates for the parameters, and P is the number of modeled degrees of freedom (usually the number of parameters estimated).
[d]χ^2d residual (measure of how model-predicted responses deviate from the actual data) for the dose group closest to the BMD scaled by an estimate of its S.D. Provides a comparative measure of model fit near the BMD. Residuals that exceed 2.0 in absolute value should cause one to question model fit in this region.

Source: NEDO (1987).

```
=====================================================================
        Hill Model. (Version: 2.14;  Date: 06/26/2008)
        Input Data File: C:\Usepa\BMDS21\Data\Methanol\NEDO\Gest-F1\hilm-6wk-brwHil-
Restrict.(d)
        Gnuplot Plotting File:  C:\Usepa\BMDS21\Data\Methanol\NEDO\Gest-F1\hilm-6wk-
brwHil-Restrict.plt
                                                Mon Aug 24 09:40:25 2009
 ====================================================================

 BMDS Model Run
~~~~~~~~~~~~~~~~~~~~~~~~~~~~~~~~~~~~~~~~~~~~~~~~~~~~~~~~~~~~~~~~~~~~~~~~

   The form of the response function is:

   Y[dose] = intercept + v*dose^n/(k^n + dose^n)


   Dependent variable = Mean
   Independent variable = Dose
   rho is set to 0
   Power parameter restricted to be greater than 1
   A constant variance model is fit

   Total number of dose groups = 4
   Total number of records with missing values = 0
   Maximum number of iterations = 250
   Relative Function Convergence has been set to: 1e-008
   Parameter Convergence has been set to: 1e-008
```

```
                    Default Initial Parameter Values
                            alpha =   0.00539333
                              rho =            0   Specified
                        intercept =         1.78
                                v =        -0.26
                                n =      1.08282
                                k =      401.076


            Asymptotic Correlation Matrix of Parameter Estimates

            ( *** The model parameter(s)  -rho    -n
                  have been estimated at a boundary point, or have been specified by
the user,
                  and do not appear in the correlation matrix )

                   alpha    intercept            v            k

     alpha             1       4e-009    -1.2e-008     6.2e-009

 intercept       4e-009            1         0.54        -0.64

         v    -1.2e-008         0.54            1        -0.99

         k     6.2e-009        -0.64        -0.99            1



                          Parameter Estimates

                                                   95.0% Wald Confidence Interval
Variable      Estimate        Std. Err.     Lower Conf. Limit   Upper Conf. Limit
alpha         0.00495736       0.00100154          0.00299438          0.00692034
intercept     1.77823        0.0184949             1.74198             1.81448
        v    -0.600699         0.340055             -1.2672           0.0657974
        n     1               NA
        k     1284.65           1317.9            -1298.39             3867.68

NA - Indicates that this parameter has hit a bound
     implied by some inequality constraint and thus
     has no standard error.



     Table of Data and Estimated Values of Interest

 Dose       N    Obs Mean     Est Mean   Obs Std Dev  Est Std Dev   Scaled Res.
------     ---   --------     --------   -----------  -----------   ----------

    0    12       1.78         1.78         0.07       0.0704         0.0872
 79.2    12       1.74         1.74         0.09       0.0704         -0.165
226.7    11       1.69         1.69         0.06       0.0704         0.0884
967.8    14       1.52         1.52         0.07       0.0704       -0.00677



 Model Descriptions for likelihoods calculated


 Model A1:        Yij = Mu(i) + e(ij)
            Var{e(ij)} = Sigma^2

 Model A2:        Yij = Mu(i) + e(ij)
            Var{e(ij)} = Sigma(i)^2
```

```
Model A3:        Yij = Mu(i) + e(ij)
           Var{e(ij)} = Sigma^2
    Model A3 uses any fixed variance parameters that
    were specified by the user

Model  R:         Yi = Mu + e(i)
            Var{e(i)} = Sigma^2


                        Likelihoods of Interest

             Model      Log(likelihood)   # Param's      AIC
              A1          105.539862            5    -201.079724
              A2          106.570724            8    -197.141449
              A3          105.539862            5    -201.079724
          fitted          105.518584            4    -203.037168
               R           77.428662            2    -150.857324


                     Explanation of Tests

 Test 1:  Do responses and/or variances differ among Dose levels?
          (A2 vs. R)
 Test 2:  Are Variances Homogeneous? (A1 vs A2)
 Test 3:  Are variances adequately modeled? (A2 vs. A3)
 Test 4:  Does the Model for the Mean Fit? (A3 vs. fitted)
 (Note:  When rho=0 the results of Test 3 and Test 2 will be the same.)

                       Tests of Interest

   Test    -2*log(Likelihood Ratio)  Test df        p-value

   Test 1              58.2841          6          <.0001
   Test 2              2.06173          3          0.5597
   Test 3              2.06173          3          0.5597
   Test 4            0.0425562          1          0.8366

The p-value for Test 1 is less than .05.  There appears to be a
difference between response and/or variances among the dose levels
It seems appropriate to model the data

The p-value for Test 2 is greater than .1.  A homogeneous variance
model appears to be appropriate here


The p-value for Test 3 is greater than .1.  The modeled variance appears
 to be appropriate here

The p-value for Test 4 is greater than .1.  The model chosen seems
to adequately describe the data


        Benchmark Dose Computation

Specified effect =          0.05

Risk Type        =     Relative risk

Confidence level =           0.95

              BMD =        223.178
```

```
BMDL =        123.872
```

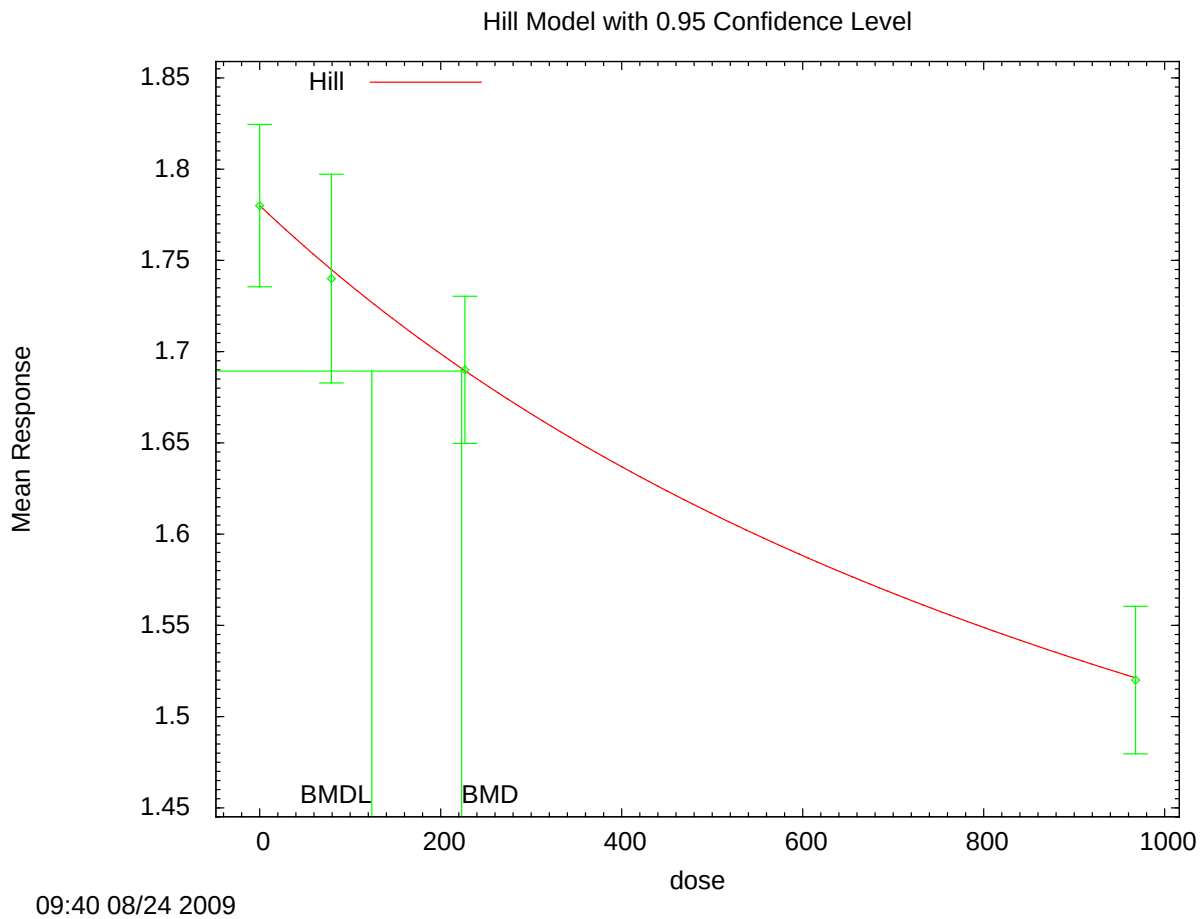

Figure C-2. Hill model, BMR of 0.05 relative risk - Decreased Brain weight in male rats at 6 weeks age versus AUC, F_1 Generation inhalational study.

Source: NEDO (1987).

Once the $BMDL_{05}$ was obtained in units of hr × mg/L, it was used to derive a chronic inhalation reference value. The first step is to calculate the HEC using the PBPK model described in Appendix B. An algebraic equation is provided (Equation 1 of Appendix B) that describes the relationship between predicted methanol AUC and the human equivalent inhalation exposure concentration (HEC) in ppm.

$$BMDL_{HEC}\ (ppm) = 0.0224*BMDL_{05} + (1334*BMDL_{05})/(794 + BMDL_{05})$$

$$BMDL_{HEC}\ (ppm) = 0.0224*503.0 + ((1334*123.9)/(794 + 123.9)) = 183\ ppm$$

Next, because RfCs are typically expressed in units of mg/m^3, the HEC value in ppm was converted using the conversion factor specific to methanol of 1 ppm = 1.31 mg/m^3:

$$HEC\ (mg/m^3) = 1.31 \times 183\ ppm = 240\ mg/m^3$$

Finally, this HEC value was divided by a composite 100-fold UF (3 for uncertainty associated with animal to human differences, 10 for consideration of human variability, and 3 for database deficiencies) to obtain the chronic inhalation reference value:

$$RfC\ (mg/m^3) = 240\ mg/m^3 \div 100 = 2.4\ mg/m^3$$

C.2. DECREASED BRAIN WEIGHT IN MALE RATS EXPOSED DURING GESTATION ONLY (GD7–GD17) (NEDO, 1987)

C_{max}, as calculated by the EPA's PBPK model, was selected as the dose metric for this exposure scenario, in concordance with the choice of this dose metric for the increased incidence of cervical rib in mice in the Rogers et al. study (1993). Exposures occurred only during the major period of organogenesis in both studies. As there is evidence that C_{max} is a better predictor of response than AUC for incidence of cervical rib (see Appendix D), it was assumed appropriate to consider C_{max} the better predictor for decreased brain weight as well.

The first step in the current analysis is to convert the inhalation doses, given as ppm values from the studies, to an internal dose surrogate or dose metric using the EPA PBPK model (see Section 3.4). Predicted C_{max} values for methanol in the blood of rats are summarized in Table C-4.

Table C-4. EPA's PBPK model estimates of methanol blood levels (C_{max}) in rats following inhalation exposures

Exposure level (ppm)	Methanol in lood C_{max} (mg /L)[a] in rats
200	1.2
1,000	10.6
5000	630.5

[a]C_{max} values were obtained by simulating 22 hr/day exposures

The current BMD technical guidance (U.S. EPA, 2000b) suggests that in the absence of knowledge as to what level of response to consider adverse, a change in the mean equal to 1 control S.D. from the control mean can be used as a BMR for continuous endpoints. However, it has been suggested that other BMRs, such as 5% change relative to estimated control mean, are also appropriate when performing BMD analyses on fetal weight change as a developmental endpoint (Kavlock et al., 1995). Therefore, in this assessment, both a 1 control mean S.D. change and a 5% change relative to estimated control mean were considered. All models were fit using restrictions and option settings suggested in the EPA's BMD technical guidance document (U.S. EPA, 2000b).

C.2.1. BMD Approach with a BMR of 1 Control Mean S.D. (GD7–GD17) (NEDO, 1987)

A summary of the results most relevant to the development of a POD using the BMD approach (BMD, BMDL, and model fit statistics) for decreased brain weight at 8 weeks in male rats exposed to methanol during gestation from days 7–17, with a BMR of 1 control mean S.D, is provided in Table C-5. Male brain weight responses were chosen because they resulted in lower BMD and BMDL estimates than female responses (data not shown). Model fit was determined by statistics (AIC and χ^2 residuals of individual dose groups) and visual inspection, as recommended by EPA (2000b). The polynomial and power models reduced to linear form and returned identical modeling results. In contrast, the more complex Hill and Exponential4 models, which estimate a response "plateau" or asymptote, returned similar, markedly nonlinear results. This is because these models approximated the response "plateau" to be near the maximum drop in brain weight observed in the study (approximately 10% at the high dose), resulting in a distinctly "L" shaped dose-response curve.[89] In this case, the only PBPK model estimated C_{max} dose that is associated with a significant response over controls, the high-dose, is 60-fold higher than the mid-dose C_{max} estimate. Thus, there are many plausible curve shapes and,consequently, a wide range of BMDL estimates. Per EPA (2000b) guidance and to err on the side of public health protection, the lowest $BMDL_{1SD}$ of 10.26 mg methanol/L in blood estimated from adequate and plausible models was chosen for use in the RfC derivation. However, it should be noted that there is a great deal of uncertainty and model dependence associated with these dose-response data.

Table C-5. Comparison of BMD_{1SD} results for decreased brain weight in male rats at 8 weeks of age using modeled C_{max} of methanol as a dose metric

Model	BMD_{1SD} (C_{max}, mg/L)[a]	$BMDL_{1SD}$ (C_{max}, mg/L)[a]	*p*-value	AIC[c]	Scaled residual[d]
Linear	207.18	135.22	0.7881	-173.12	-0.43
2nd degree polynomial	207.18	135.22	0.7881	-173.12	-0.43
3rd degree polynomial	207.18	135.22	0.7881	-173.12	-0.43
Power	207.18	135.22	0.7881	-173.12	-0.43
Hill[b]	43.08	**10.26**	0.9602	-171.59	-0.10
Exponential 2	199.98	127.55	0.9494	-173.13	-0.42
Exponential 3	199.98	127.55	0.9494	-173.13	-0.42
Exponential 4[b]	39.53	**10.26**	Not reported	-171.59	0.10

[89] The extent of the "L" shape is dependent on the asymptote term, or "plateau" level, estimated for the data. If the asymptote term (v) in the Hill model is set to -.4 (representing a 20% drop from the control brain weight of 2 grams), the model result is more linear and the BMD and BMDL estimates are approximately 4-fold higher.

[a]The BMDL is the 95% lower confidence limit on the C_{max} estimated to decrease brain weight by 1 control mean S.D. using BMDS model options and restrictions suggested by EPA BMD technical guidance (U.S. EPA, 2000b).
[b]Per EPA (2000b) guidance and to err on the side of public health protection, the lowest $BMDL_{1SD}$ of 10.26 mg methanol/L in blood estimated from adequate and plausible models was chosen for use in the RfC derivation
[c]AIC = Akaike Information Criterion = -2L + 2P, where L is the log-likelihood at the maximum likelihood estimates for the parameters, and P is the number of modeled degrees of freedom (usually the number of parameters estimated).
[d]χ^2d residual (measure of how model-predicted responses deviate from the actual data) for the dose group closest to the BMD scaled by an estimate of its S.D. Provides a comparative measure of model fit near the BMD. Residuals that exceed 2.0 in absolute value should cause one to question model fit in this region.

Source: NEDO (1987)

```
=====================================================================
        Hill Model. (Version: 2.14;  Date: 06/26/2008)
        Input Data File: C:\Usepa\BMDS21\Data\Methanol\NEDO\Gest-only\hilm-8wk-
brwHil-Restrict.(d)
        Gnuplot Plotting File:  C:\Usepa\BMDS21\Data\Methanol\NEDO\Gest-only\hilm-
8wk-brwHil-Restrict.plt
                                                Tue Aug 25 12:40:30 2009
 ====================================================================

 BMDS Model Run
~~~~~~~~~~~~~~~~~~~~~~~~~~~~~~~~~~~~~~~~~~~~~~~~~~~~~~~~~~~~~~~~~~~~~~~~~

   The form of the response function is:

   Y[dose] = intercept + v*dose^n/(k^n + dose^n)


   Dependent variable = Mean
   Independent variable = Dose
   Power parameter restricted to be greater than 1
   The variance is to be modeled as Var(i) = exp(lalpha  + rho * ln(mean(i)))

   Total number of dose groups = 4
   Total number of records with missing values = 0
   Maximum number of iterations = 250
   Relative Function Convergence has been set to: 1e-008
   Parameter Convergence has been set to: 1e-008



                    Default Initial Parameter Values
                           lalpha =     -4.68678
                              rho =            0
                        intercept =            2
                                v =        -0.19
                                n =     0.861776
                                k =      303.331


          Asymptotic Correlation Matrix of Parameter Estimates

     ( *** The model parameter(s)  -n
           have been estimated at a boundary point, or have been specified by the user,
           and do not appear in the correlation matrix )

                  lalpha          rho    intercept            v            k

     lalpha            1           -1       -0.083          0.6        -0.18

        rho           -1            1        0.096         -0.6         0.18
```

```
 intercept       -0.083        0.096            1         0.19        -0.55

         v          0.6         -0.6         0.19            1        -0.73

         k        -0.18         0.18        -0.55        -0.73            1



                            Parameter Estimates

                                                        95.0% Wald Confidence Interval
Variable         Estimate        Std. Err.     Lower Conf. Limit   Upper Conf. Limit
lalpha          7.03732          4.98399            -2.73112             16.8058
rho            -18.1432          7.32604             -32.502            -3.78448
intercept        2.0068        0.0134454             1.98045             2.03316
        v     -0.232906        0.0881494           -0.405676          -0.0601362
        n             1               NA
        k       121.949          194.687            -259.631             503.529

NA - Indicates that this parameter has hit a bound
     implied by some inequality constraint and thus
     has no standard error.



     Table of Data and Estimated Values of Interest

 Dose       N    Obs Mean     Est Mean   Obs Std Dev  Est Std Dev   Scaled Res.
------     ---   --------     --------   -----------  -----------   ----------

    0    11          2         2.01        0.047       0.0608         -0.371
  1.2    11       2.01            2        0.075       0.0614          0.295
 10.6    12       1.99         1.99        0.072       0.0662         0.0954
630.5    10       1.81         1.81        0.161        0.154        -0.0338



 Model Descriptions for likelihoods calculated


 Model A1:        Yij = Mu(i) + e(ij)
           Var{e(ij)} = Sigma^2

 Model A2:        Yij = Mu(i) + e(ij)
           Var{e(ij)} = Sigma(i)^2

 Model A3:        Yij = Mu(i) + e(ij)
           Var{e(ij)} = exp(lalpha + rho*ln(Mu(i)))
     Model A3 uses any fixed variance parameters that
     were specified by the user

 Model  R:         Yi = Mu + e(i)
            Var{e(i)} = Sigma^2


                        Likelihoods of Interest

            Model      Log(likelihood)   # Param's      AIC
             A1           83.205960            5    -156.411920
             A2           92.060485            8    -168.120970
             A3           90.797178            6    -169.594356
         fitted           90.795933            5    -171.591867
              R           70.761857            2    -137.523714


                    Explanation of Tests

```

```
 Test 1:  Do responses and/or variances differ among Dose levels?
          (A2 vs. R)
 Test 2:  Are Variances Homogeneous? (A1 vs A2)
 Test 3:  Are variances adequately modeled? (A2 vs. A3)
 Test 4:  Does the Model for the Mean Fit? (A3 vs. fitted)
 (Note:  When rho=0 the results of Test 3 and Test 2 will be the same.)

                     Tests of Interest

   Test    -2*log(Likelihood Ratio)  Test df        p-value

   Test 1              42.5973          6          <.0001
   Test 2              17.7091          3        0.000505
   Test 3              2.52661          2          0.2827
   Test 4           0.00248896          1          0.9602

The p-value for Test 1 is less than .05.  There appears to be a
difference between response and/or variances among the dose levels
It seems appropriate to model the data

The p-value for Test 2 is less than .1.  A non-homogeneous variance
model appears to be appropriate

The p-value for Test 3 is greater than .1.  The modeled variance appears
 to be appropriate here

The p-value for Test 4 is greater than .1.  The model chosen seems
to adequately describe the data


        Benchmark Dose Computation

Specified effect =             1

Risk Type        =     Estimated standard deviations from the control mean

Confidence level =           0.95

              BMD =        43.0842

             BMDL =       10.2551
```

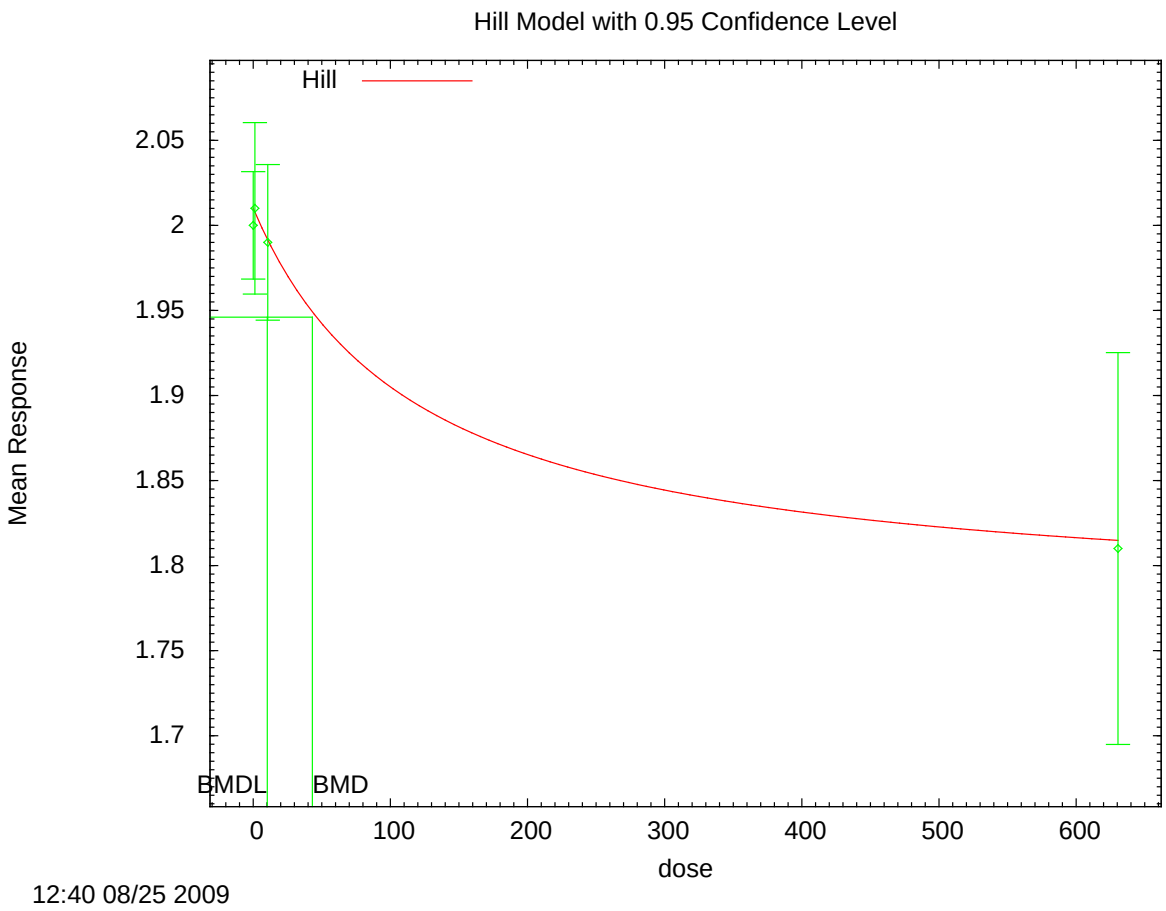

Figure C-3. Hill model, BMR of 1 Control Mean S.D. - Decreased Brain weight in male rats at 8 weeks age versus C_{max}, Gestation only inhalational study.

Source: NEDO (1987).

Once the $BMDL_{1SD}$ was obtained in units of mg/L, it was used to derive a chronic inhalation reference value. The first step is to calculate the HEC using the PBPK model described in Appendix B. An algebraic equation is provided (Equation 1 of Appendix B) that describes the relationship between predicted methanol AUC and the human equivalent inhalation exposure concentration (HEC) in ppm. This equation can also be used to estimate model predictions for HECs from C_{max} values because C_{max} values and AUC values, were estimated at steady-state for constant 24-hour exposures (i.e., AUC = 24 x C_{max}).

$$BMDL_{HEC}\ (ppm) = 0.0224*BMDL_{1SD}*24+(1334*BMDL_{1SD}*24)/(794+ BMDL_{1SD}*24)$$

$$BMDL_{HEC}\ (ppm) = 0.0224*10.3*24 + ((1334*10.3*24)/(794+ 10.3*24)) = 322\ ppm$$

Next, because RfCs are typically expressed in units of mg/m^3, the HEC value in ppm was converted using the conversion factor specific to methanol of 1 ppm = 1.31 mg/m^3:

$$HEC\ (mg/m^3) = 1.31 \times 322\ ppm = 422\ mg/m^3$$

Finally, this HEC value was divided by a composite 100-fold UF (3 for uncertainty associated with animal to human differences, 10 for consideration of human variability, and 3 for database deficiencies) to obtain the chronic inhalation reference value:

$$RfC\ (mg/m^3) = 422\ mg/m^3 \div 100 = 4.2\ mg/m^3$$

C.2.2. BMD Approach with a BMR of 0.05 Change Relative to Control Mean (GD7–GD17) (NEDO, 1987)

A summary of the results most relevant to the development of a POD using the BMD approach (BMD, BMDL, and model fit statistics) for decreased brain weight at 8 weeks in male rats exposed to methanol during gestation from days 7 to 17, with a BMR of 0.05 change relative to estimated control mean, is provided in Table C-6. Model fit was determined by statistics (AIC and χ^2 residuals of individual dose groups) and visual inspection, as recommended by EPA (2000b). Modeling considerations and uncertainties for this dataset were discussed in C.2.1 and, as was done for the BMR of 1 S.D., the lowest $BMDL_{05}$ of 21.07 mg methanol/L in blood estimated from adequate and plausible models was chosen for use in the RfC derivation.

Table C-6. Comparison of BMD_{05} modeling results for decreased brain weight in male rats at 8 weeks of age using modeled C_{max} of methanol as a common dose metric

Model	BMD_{05} (C_{max}, mg/L)[a]	$BMDL_{05}$ (C_{max}, mg/L)[a]	*p*-value	AIC[c]	Scaled residual[d]
Linear[b]	328.84	226.08	0.7881	-173.12	0.02
2nd degree polynomial	328.84	226.08	0.7881	-173.12	0.02
3rd degree polynomial	328.84	226.08	0.7881	-173.12	0.02
Power	328.84	226.08	0.9446	-173.12	0.02
Hill[b]	92.30	Not reported	0.9602	-171.59	0.10
Exponential 2	320.62	215.13	0.9494	-173.13	0.02
Exponential 3	320.62	215.13	0.9494	-173.13	0.02
Exponential 4[b]	76.36	**21.07**	Not reported	-171.59	0.10

[a]The BMDL is the 95% lower confidence limit on the C_{max} estimated to decrease brain weight by 5% using BMDS model options and restrictions suggested by EPA BMD technical guidance (U.S. EPA, 2000b).
[b]Per EPA (2000b) guidance and to err on the side of public health protection, the lowest $BMDL_{05}$ of 21.07 mg methanol/L in blood estimated from adequate and plausible models was chosen for use in the RfC derivation.
[c]AIC = Akaike Information Criterion = -2L + 2P, where L is the log-likelihood at the maximum likelihood estimates for the parameters, and P is the number of modeled degrees of freedom (usually the number of parameters estimated).
[d]χ^2d residual (measure of how model-predicted responses deviate from the actual data) for the dose group closest to the BMD scaled by an estimate of its S.D. Provides a comparative measure of model fit near the BMD. Residuals that exceed 2.0 in absolute value should cause one to question model fit in this region.

Source: NEDO (1987).

```
=====================================================================
         Exponential Model. (Version: 1.61;  Date: 7/24/2009)
         Input Data File: C:\Usepa\BMDS21\Data\Methanol\NEDO\Gest-only\expm-8wk-
brwSetting.(d)
         Gnuplot Plotting File:
                                                Tue Aug 25 14:15:15 2009
 ====================================================================

 BMDS Model Run
~~~~~~~~~~~~~~~~~~~~~~~~~~~~~~~~~~~~~~~~~~~~~~~~~~~~~~~~~~~~~~~~~~~~~~~~

   The form of the response function by Model:
      Model 2:     Y[dose] = a * exp{sign * b * dose}
      Model 3:     Y[dose] = a * exp{sign * (b * dose)^d}
      Model 4:     Y[dose] = a * [c-(c-1) * exp{-b * dose}]
      Model 5:     Y[dose] = a * [c-(c-1) * exp{-(b * dose)^d}]

    Note: Y[dose] is the median response for exposure = dose;
          sign = +1 for increasing trend in data;
          sign = -1 for decreasing trend.

      Model 2 is nested within Models 3 and 4.
      Model 3 is nested within Model 5.
      Model 4 is nested within Model 5.


   Dependent variable = Mean
   Independent variable = Dose
   Data are assumed to be distributed: normally
   Variance Model: exp(lnalpha +rho *ln(Y[dose]))
   The variance is to be modeled as Var(i) = exp(lalpha + log(mean(i)) * rho)
```

```
Total number of dose groups = 4
Total number of records with missing values = 0
Maximum number of iterations = 250
Relative Function Convergence has been set to: 1e-008
Parameter Convergence has been set to: 1e-008

MLE solution provided: Exact


                              Initial Parameter Values

  Variable          Model 2           Model 3           Model 4           Model 5
  --------          -------           -------           -------           -------
   lnalpha               NC                NC            7.32457                NC
       rho               NC                NC           -18.5236                NC
         a               NC                NC             2.1105                NC
         b               NC                NC         0.00239093                NC
         c               NC                NC           0.816778                NC
         d               NC                NC                 --                NC



                            Parameter Estimates by Model

  Variable          Model 2           Model 3           Model 4           Model 5
  --------          -------           -------           -------           -------
   lnalpha               NC                NC            7.03418                NC
       rho               NC                NC           -18.1386                NC
         a               NC                NC            2.00677                NC
         b               NC                NC         0.00941775                NC
         c               NC                NC           0.902498                NC
         d               NC                NC                 --                NC

  NC = No Convergence


         Table of Stats From Input Data

  Dose      N         Obs Mean     Obs Std Dev
  -----    ---       ----------   -------------
      0     11            2        0.047
    1.2     11         2.01        0.075
   10.6     12         1.99        0.072
  630.5     10         1.81        0.161


                     Estimated Values of Interest

   Model      Dose      Est Mean      Est Std     Scaled Residual
  -------    ------    ----------    ---------    ----------------
       4         0         2.007      0.06082          -0.3692
               1.2         2.005      0.06142           0.2932
              10.6         1.988      0.06617          0.09527
             630.5         1.812       0.1538         -0.03335



Other models for which likelihoods are calculated:

  Model A1:        Yij = Mu(i) + e(ij)
             Var{e(ij)} = Sigma^2

  Model A2:        Yij = Mu(i) + e(ij)
             Var{e(ij)} = Sigma(i)^2

  Model A3:        Yij = Mu(i) + e(ij)
```

```
                Var{e(ij)} = exp(lalpha + log(mean(i)) * rho)

  Model  R:        Yij = Mu + e(i)
                Var{e(ij)} = Sigma^2


                              Likelihoods of Interest

                    Model      Log(likelihood)      DF         AIC
                   -------    -----------------    ----   ------------
                      A1        83.20596            5     -156.4119
                      A2        92.06049            8      -168.121
                      A3        90.61606            6     -169.2321
                       R        70.76186            2     -137.5237
                       4        90.79579            5     -171.5916


Additive constant for all log-likelihoods =     -40.43.  This constant added to the
above values gives the log-likelihood including the term that does not
depend on the model parameters.


                               Explanation of Tests

Test 1:  Does response and/or variances differ among Dose levels? (A2 vs. R)
Test 2:  Are Variances Homogeneous? (A2 vs. A1)
Test 3:  Are variances adequately modeled? (A2 vs. A3)

Test 6a: Does Model 4 fit the data? (A3 vs 4)


                          Tests of Interest

  Test          -2*log(Likelihood Ratio)       D. F.         p-value
--------        ------------------------      ------     --------------
  Test 1                          42.6           6            < 0.0001
  Test 2                         17.71           3            0.000505
  Test 3                         2.889           2              0.2359
 Test 6a                        -0.3595           1                 N/A


  The p-value for Test 1 is less than .05.  There appears to be a
  difference between response and/or variances among the dose
  levels, it seems appropriate to model the data.

  The p-value for Test 2 is less than .1.  A non-homogeneous
  variance model appears to be appropriate.

  The p-value for Test 3 is greater than .1.  The modeled
  variance appears to be appropriate here.

  The p-value for Test 6a is less than .1.  Model 4 may not adequately
  describe the data; you may want to consider another model.


Benchmark Dose Computations:

  Specified Effect = 0.050000

         Risk Type = Relative deviation

  Confidence Level = 0.950000


                BMD and BMDL by Model

   Model             BMD                BMDL
```

```
-------        ------------        ----------
   2                  0                  0        Not computed
   3                  0                  0        Not computed
   4            76.3561            21.0664
   5                  0                  0        Not computed
```

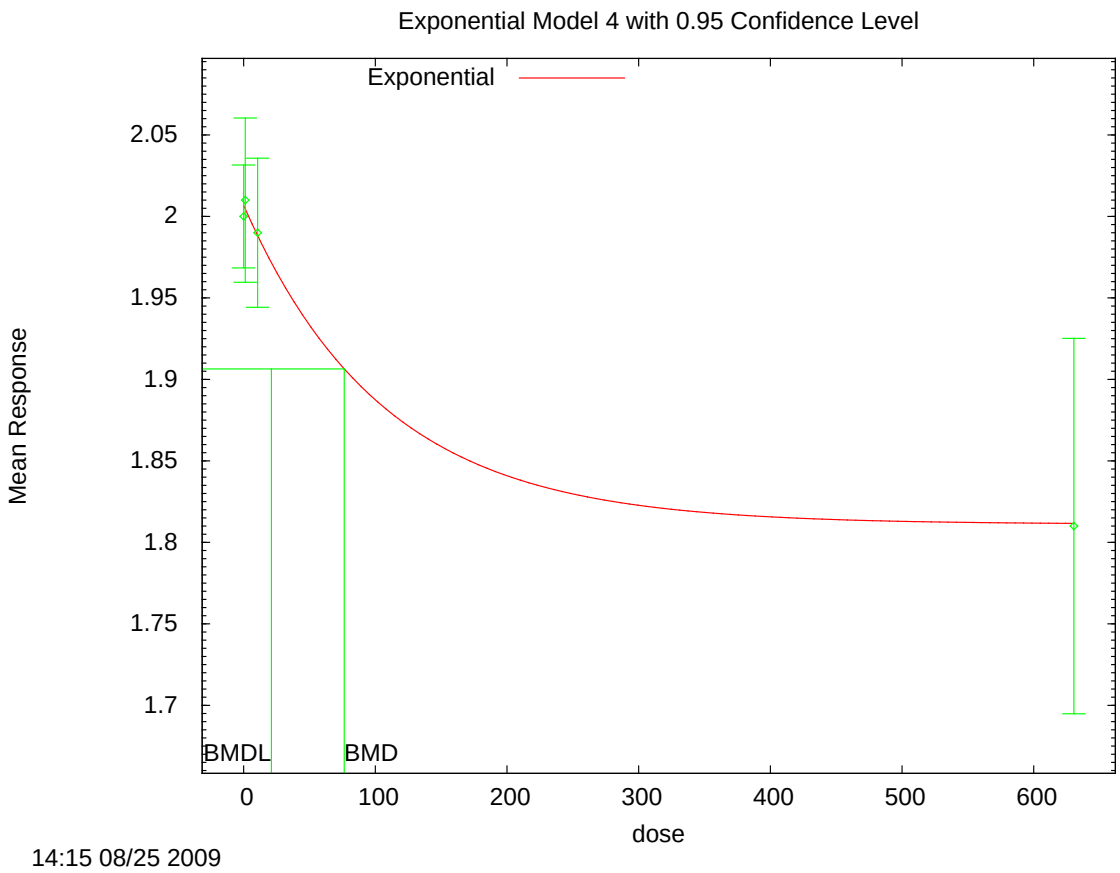

Figure C-4. Exponential4 model, BMR of 0.05 relative risk - Decreased Brain weight in male rats at 8 weeks age versus C_{max}, Gestation only inhalational study.

Source: NEDO (1987).

Once the $BMDL_{05}$ was obtained in units of mg/L, it was used to derive a chronic inhalation reference value. The first step is to calculate the HEC using the PBPK model described in Appendix B. An algebraic equation is provided (Equation 1 of Appendix B) that describes the relationship between predicted methanol AUC and the human equivalent inhalation exposure concentration (HEC) in ppm. This equation can also be used to estimate model predictions for HECs from C_{max} values because C_{max} values, and AUC values were estimated at steady-state for constant 24-hour exposures (i.e., AUC = 24 x C_{max}).

$$BMDL_{HEC}\ (ppm) = 0.0224*BMDL_{05}*24+(1334*BMDL_{05}*24)/(794+ BMDL_{05}*24)$$

$$BMDL_{HEC}\ (ppm) = 0.0224*21.07*24 + ((1334*21.07*24)/(794+ 21.07*24)) = 530\ ppm$$

Next, because RfCs are typically expressed in units of mg/m^3, the HEC value in ppm was converted using the conversion factor specific to methanol of 1 ppm = 1.31 mg/m^3:

$$HEC\ (mg/m^3) = 1.31 \times 530\ ppm = 695\ mg/m^3$$

Finally, this HEC value was divided by a composite 100-fold UF (3 for uncertainty associated with animal to human differences, 10 for consideration of human variability, and 3 for database deficiencies) to obtain the chronic inhalation reference value:

$$RfC\ (mg/m^3) = 695\ mg/m^3 \div 100 = 7.0\ mg/m^3$$

C.3. RfC DERIVATIONS USING ROGERS ET AL. (1993)

For the purposes of deriving an RfC for methanol from developmental endpoints using the BMD method and mouse data, cervical rib incidence data were evaluated from Rogers et al. (1993). In this paper, Rogers et al. (1993) also utilized a BMD methodology, examining the dosimetric threshold for cervical ribs and other developmental impacts by applying a log-logistic maximum likelihood model to the dose-response data. Using air exposure concentrations (ppm) as their dose metric, a value for the lower 95% confidence limit on the benchmark dose for 5% additional risk in mice was 305 ppm (400 mg/m^3), using the log-logistic model. Although the teratology portion of the NEDO study (1987) also reported increases in cervical rib incidence in Sprague-Dawley rats, the Rogers et al. (1993) study was chosen for dose-response modeling because effects were seen at lower doses, it was peer-reviewed and published in the open literature, and data on individual animals were available for a more statistically robust analysis utilizing nested models available in BMDS.

The first step in the current BMD analysis is to convert the inhalation doses, given as ppm values from the studies, to an internal dose surrogate or dose metric using the EPA's PBPK model (see Section 3.4). For cervical rib malformations, C_{max} of methanol in blood (mg/L) is chosen as the appropriate internal dose metric metric (see Appendix D for further explanation). Predicted C_{max} values for methanol in the blood of mice are summarized in Table C-7.

Table C-7. EPA's PBPK model estimates of methanol blood levels (C_{max}) in mice following inhalation exposures

Exposure concentration (ppm)	Methanol in blood C_{max} (mg/L)[a] in mice
1	0.0216
10	0.218
50	1.14
100	2.46
250	7.83

Exposure concentration (ppm)	Methanol in blood C_{max} (mg/L)[a] in mice
500	26.4
1,000	134

[a]Rounded to three significant figures.

These C_{max} values are then used as the dose metric for the BMD analysis of cervical rib incidence.

A 10% BMR level is the value typically calculated for comparisons across chemicals and endpoints for dichotomous responses because this level is near the low end of the observable range for many types of toxicity studies. However, reproductive and developmental studies having a nested design often have a greater sensitivity, and a 5% BMR is typically appropriate for determination of a POD (U.S. EPA, 2000b; Allen et al., 1994). Rogers et al. (1993) utilized a 5% added risk for the BMR in the original study. This assessment utilizes both a 10% and 5% extra risk level as a BMR for the determination of a POD.[90] The nested suite of models available in BMDS was used to model the cervical rib data. In general, data from developmental toxicity studies are best modeled using nested models, as these models account for any intralitter correlation (i.e., the tendency of littermates to respond similarly to one another relative to other litters in a dose group). All models were fit using restrictions and option settings suggested in the EPA's BMD technical guidance document (U.S. EPA, 2000b).

C.3.1. BMD Approach with a BMR of 0.10 Extra Risk (Rogers et al., 1993)

A summary of the results most relevant to the development of a POD using the BMD approach (BMD, BMDL, and model fit statistics) for increased incidence of cervical rib in mice exposed to methanol during gestation from days 6 to 15, with a BMR of 0.10 extra risk, is provided in Table C-8. Model fit was determined by statistics (AIC and χ^2 residuals of individual dose groups) and visual inspection, as recommended by U.S. EPA (2000b). The best model fit to these data (from visual inspection and comparison of AIC values) was obtained using the Nested Logistic (NLogistic) model. The $BMDL_{10}$ was determined to be 94.3 mg/L using the 95% lower confidence limit of the dose-response curve expressed in terms of the C_{max} for methanol in blood.

Table C-8. Comparison of BMD modeling results for cervical rib incidence in mice using modeled C_{max} of methanol as a common dose metric

Model	BMD_{10} (C_{max}, mg/L)[a]	$BMDL_{10}$ (C_{max}, mg/L)[a]	*p*-value	AIC[c]	Scaled residual[d]
NLogistic[b]	141.492	94.264	0.293	1046.84	0.649
NCTR	207.945	103.972	0.241	1048.92	0.662

[90] Starr and Festa (2003) have argued that the Rogers et al. (1993) study's experimental design lacked the statistical power to detect a 5% risk and that a 5% level lay below the observable response data. However, EPA's BMD guidance (U.S. EPA, 2000b) does not preclude the use of a BMR that is below observable response data and EPA has deemed that the Rogers et al. (1993) is adequate for the consideration of a 5% BMR.

Model	BMD_{10} (C_{max}, mg/L)[a]	$BMDL_{10}$ (C_{max}, mg/L)[a]	*p*-value	AIC[c]	Scaled residual[d]
Rai and Van Ryzin	221.509	110.754	0.163	1051.65	0.661

[a]Daily C_{max} was estimated using a mouse PBPK model as described in section 3.4 of the methanol toxicological review; the BMDL is the 95% lower confidence limit on the C_{max} for a 10% extra risk (dichotomous endpoints) estimated by the model using the likelihood profile method (U.S. EPA, 2000b).
[b]Model choice based on adequate *p* value (> 0.1), visual inspection, low AIC, and low (absolute) scaled residual.
[c]AIC = Akaike Information Criterion = -2L + 2P, where L is the log-likelihood at the maximum likelihood estimates for the parameters, and P is the number of modeled degrees of freedom (usually the number of parameters estimated).
[d]χ^2d residual (measure of how model-predicted responses deviate from the actual data) for the dose group closest to the BMD scaled by an estimate of its S.D. Provides a comparative measure of model fit near the BMD. Residuals exceeding 2.0 in absolute value should cause one to question model fit in this region.

Source: Rogers et al. (1993).

```
=====================================================================
NLogistic Model.
(Version: 2.13; Date: 02/20/2007)
Input Data File: U:\Methanol\BMDS\CervicalRib\Cmax\NLog_Cmax_10_default.(d)
Wed Nov 07 15:45:40 2007
=====================================================================

BMD Method for RfC: Incidence of Cervical Rib in Mice versus Cmax Methanol, GD 6-15
inhalational study (Rogers,et al., 1993)
~~~~~~~~~~~~~~~~~~~~~~~~~~~~~~~~~~~~~~~~~~~~~~~~~~~~~~~~~~~~~~~~~~~~~~~~~~~~
  The probability function is:

 Prob. = alpha + theta1*Rij + [1 - alpha - theta1*Rij]/

                      [1+exp(-beta-theta2*Rij-rho*log(Dose))],

          where Rij is the litter specific covariate.

 Restrict Power rho >= 1.

 Total number of observations = 166
 Total number of records with missing values = 0
 Total number of parameters in model = 9
 Total number of specified parameters = 0

 Maximum number of iterations = 250
 Relative Function Convergence has been set to: 1e-008
 Parameter Convergence has been set to: 1e-008

                  Default Initial Parameter Values
                          alpha =     0.297863
                           beta =     -7.94313
                         theta1 =            0
                         theta2 =            0
                            rho =      1.09876
                           phi1 =     0.213134
                           phi2 =     0.309556
                           phi3 =     0.220142
                           phi4 =     0.370587

                                Parameter Estimates

        Variable           Estimate             Std. Err.
           alpha            0.102434             *
            beta            -4.80338             *
          theta1           0.0325457             *
          theta2           -0.436115             *
```

```
             rho                  1            *
            phi1           0.200733            *
            phi2           0.307656            *
            phi3           0.212754            *
            phi4           0.368426            *

* - Indicates that this value is not calculated.

 Log-likelihood: -515.422   AIC: 1046.84

                              Litter Data

            Lit.-Spec.              Litter                            Scaled
   Dose        Cov.     Est._Prob.   Size    Expected   Observed   Residual
-----------------------------------------------------------------------------
   0.0000    1.0000      0.135         1       0.135         0     -0.3950
   0.0000    1.0000      0.135         1       0.135         0     -0.3950
   0.0000    2.0000      0.168         2       0.335         0     -0.5790
   0.0000    2.0000      0.168         2       0.335         1      1.1490
   0.0000    2.0000      0.168         2       0.335         0     -0.5790
   0.0000    2.0000      0.168         2       0.335         2      2.8770
   0.0000    2.0000      0.168         2       0.335         0     -0.5790
   0.0000    3.0000      0.200         3       0.600         0     -0.7317
   0.0000    3.0000      0.200         3       0.600         0     -0.7317
   0.0000    3.0000      0.200         3       0.600         1      0.4874
   0.0000    3.0000      0.200         3       0.600         1      0.4874
   0.0000    4.0000      0.233         4       0.930         0     -0.8699
   0.0000    4.0000      0.233         4       0.930         1      0.0650
   0.0000    4.0000      0.233         4       0.930         0     -0.8699
   0.0000    4.0000      0.233         4       0.930         1      0.0650
   0.0000    5.0000      0.265         5       1.326         0     -1.0004
   0.0000    5.0000      0.265         5       1.326         1     -0.2458
   0.0000    5.0000      0.265         5       1.326         3      1.2632
   0.0000    5.0000      0.265         5       1.326         1     -0.2458
   0.0000    5.0000      0.265         5       1.326         0     -1.0004
   0.0000    5.0000      0.265         5       1.326         1     -0.2458
   0.0000    5.0000      0.265         5       1.326         1     -0.2458
   0.0000    5.0000      0.265         5       1.326         0     -1.0004
   0.0000    5.0000      0.265         5       1.326         0     -1.0004
   0.0000    5.0000      0.265         5       1.326         1     -0.2458
   0.0000    6.0000      0.298         6       1.786         3      0.7656
   0.0000    6.0000      0.298         6       1.786         6      2.6578
   0.0000    6.0000      0.298         6       1.786         1     -0.4959
   0.0000    6.0000      0.298         6       1.786         0     -1.1267
   0.0000    6.0000      0.298         6       1.786         0     -1.1267
   0.0000    6.0000      0.298         6       1.786         1     -0.4959
   0.0000    6.0000      0.298         6       1.786         2      0.1348
   0.0000    6.0000      0.298         6       1.786         0     -1.1267
   0.0000    6.0000      0.298         6       1.786         2      0.1348
   0.0000    6.0000      0.298         6       1.786         3      0.7656
   0.0000    6.0000      0.298         6       1.786         5      2.0271
   0.0000    6.0000      0.298         6       1.786         0     -1.1267
   0.0000    6.0000      0.298         6       1.786         3      0.7656
   0.0000    6.0000      0.298         6       1.786         3      0.7656
   0.0000    6.0000      0.298         6       1.786         3      0.7656
   0.0000    6.0000      0.298         6       1.786         5      2.0271
   0.0000    7.0000      0.330         7       2.312         0     -1.2513
   0.0000    7.0000      0.330         7       2.312         1     -0.7100
   0.0000    7.0000      0.330         7       2.312         2     -0.1688
   0.0000    7.0000      0.330         7       2.312         3      0.3725
   0.0000    7.0000      0.330         7       2.312         2     -0.1688
   0.0000    7.0000      0.330         7       2.312         3      0.3725
   0.0000    7.0000      0.330         7       2.312         5      1.4551
   0.0000    7.0000      0.330         7       2.312         0     -1.2513
   0.0000    7.0000      0.330         7       2.312         2     -0.1688
   0.0000    7.0000      0.330         7       2.312         5      1.4551
   0.0000    7.0000      0.330         7       2.312         1     -0.7100
```

0.0000	7.0000	0.330	7	2.312	2	-0.1688
0.0000	7.0000	0.330	7	2.312	1	-0.7100
0.0000	8.0000	0.363	8	2.902	1	-0.9020
0.0000	8.0000	0.363	8	2.902	4	0.5204
0.0000	8.0000	0.363	8	2.902	3	0.0463
0.0000	8.0000	0.363	8	2.902	8	2.4170
0.0000	8.0000	0.363	8	2.902	2	-0.4279
134.0000	1.0000	0.494	1	0.494	0	-0.9887
134.0000	1.0000	0.494	1	0.494	0	-0.9887
134.0000	2.0000	0.430	2	0.859	0	-1.0732
134.0000	2.0000	0.430	2	0.859	2	1.4251
134.0000	3.0000	0.383	3	1.150	3	1.7287
134.0000	3.0000	0.383	3	1.150	1	-0.1400
134.0000	3.0000	0.383	3	1.150	2	0.7944
134.0000	3.0000	0.383	3	1.150	1	-0.1400
134.0000	4.0000	0.356	4	1.425	3	1.1858
134.0000	4.0000	0.356	4	1.425	0	-1.0729
134.0000	5.0000	0.346	5	1.732	0	-1.0898
134.0000	5.0000	0.346	5	1.732	4	1.4275
134.0000	5.0000	0.346	5	1.732	0	-1.0898
134.0000	5.0000	0.346	5	1.732	1	-0.4604
134.0000	5.0000	0.346	5	1.732	0	-1.0898
134.0000	6.0000	0.350	6	2.099	3	0.4839
134.0000	6.0000	0.350	6	2.099	2	-0.0534
134.0000	7.0000	0.363	7	2.543	3	0.2128
134.0000	7.0000	0.363	7	2.543	2	-0.2530
134.0000	7.0000	0.363	7	2.543	2	-0.2530
134.0000	7.0000	0.363	7	2.543	2	-0.2530
134.0000	7.0000	0.363	7	2.543	2	-0.2530
134.0000	7.0000	0.363	7	2.543	0	-1.1847
134.0000	8.0000	0.383	8	3.068	2	-0.4373
134.0000	8.0000	0.383	8	3.068	0	-1.2562
134.0000	8.0000	0.383	8	3.068	8	2.0195
526.0000	2.0000	0.703	2	1.406	2	0.8346
526.0000	3.0000	0.631	3	1.892	3	1.1101
526.0000	4.0000	0.562	4	2.250	2	-0.1967
526.0000	4.0000	0.562	4	2.250	1	-0.9842
526.0000	5.0000	0.506	5	2.530	3	0.3091
526.0000	5.0000	0.506	5	2.530	5	1.6241
526.0000	5.0000	0.506	5	2.530	3	0.3091
526.0000	5.0000	0.506	5	2.530	1	-1.0058
526.0000	6.0000	0.466	6	2.796	3	0.1162
526.0000	6.0000	0.466	6	2.796	3	0.1162
526.0000	6.0000	0.466	6	2.796	3	0.1162
526.0000	6.0000	0.466	6	2.796	5	1.2556
526.0000	6.0000	0.466	6	2.796	6	1.8253
526.0000	6.0000	0.466	6	2.796	5	1.2556
526.0000	6.0000	0.466	6	2.796	2	-0.4534
526.0000	6.0000	0.466	6	2.796	0	-1.5928
526.0000	6.0000	0.466	6	2.796	2	-0.4534
526.0000	6.0000	0.466	6	2.796	0	-1.5928
526.0000	6.0000	0.466	6	2.796	5	1.2556
526.0000	6.0000	0.466	6	2.796	4	0.6859
526.0000	6.0000	0.466	6	2.796	3	0.1162
526.0000	6.0000	0.466	6	2.796	2	-0.4534
526.0000	6.0000	0.466	6	2.796	4	0.6859
526.0000	6.0000	0.466	6	2.796	2	-0.4534
526.0000	7.0000	0.444	7	3.105	0	-1.5658
526.0000	7.0000	0.444	7	3.105	4	0.4511
526.0000	7.0000	0.444	7	3.105	5	0.9554
526.0000	7.0000	0.444	7	3.105	1	-1.0615
526.0000	7.0000	0.444	7	3.105	4	0.4511
526.0000	7.0000	0.444	7	3.105	1	-1.0615
526.0000	7.0000	0.444	7	3.105	5	0.9554
526.0000	7.0000	0.444	7	3.105	3	-0.0531

```
  526.0000    7.0000      0.444         7       3.105         4      0.4511
  526.0000    7.0000      0.444         7       3.105         1     -1.0615
  526.0000    7.0000      0.444         7       3.105         3     -0.0531
  526.0000    7.0000      0.444         7       3.105         3     -0.0531
  526.0000    8.0000      0.437         8       3.496         0     -1.5793
  526.0000    8.0000      0.437         8       3.496         7      1.5832
  526.0000    8.0000      0.437         8       3.496         5      0.6796
  526.0000    9.0000      0.443         9       3.985         0     -1.6270
  526.0000    9.0000      0.443         9       3.985         6      0.8225

 2005.0000    1.0000      0.926         1       0.926         1      0.2834
 2005.0000    1.0000      0.926         1       0.926         1      0.2834
 2005.0000    1.0000      0.926         1       0.926         1      0.2834
 2005.0000    2.0000      0.894         2       1.789         1     -1.5502
 2005.0000    2.0000      0.894         2       1.789         2      0.4157
 2005.0000    3.0000      0.853         3       2.559         3      0.5454
 2005.0000    3.0000      0.853         3       2.559         1     -1.9294
 2005.0000    3.0000      0.853         3       2.559         1     -1.9294
 2005.0000    3.0000      0.853         3       2.559         3      0.5454
 2005.0000    4.0000      0.802         4       3.208         4      0.6851
 2005.0000    4.0000      0.802         4       3.208         4      0.6851
 2005.0000    4.0000      0.802         4       3.208         4      0.6851
 2005.0000    4.0000      0.802         4       3.208         2     -1.0440
 2005.0000    4.0000      0.802         4       3.208         3     -0.1795
 2005.0000    4.0000      0.802         4       3.208         4      0.6851
 2005.0000    4.0000      0.802         4       3.208         4      0.6851
 2005.0000    5.0000      0.743         5       3.714         1     -1.7660
 2005.0000    5.0000      0.743         5       3.714         3     -0.4648
 2005.0000    5.0000      0.743         5       3.714         5      0.8364
 2005.0000    5.0000      0.743         5       3.714         5      0.8364
 2005.0000    5.0000      0.743         5       3.714         4      0.1858
 2005.0000    5.0000      0.743         5       3.714         4      0.1858
 2005.0000    6.0000      0.681         6       4.086         6      0.9945
 2005.0000    6.0000      0.681         6       4.086         2     -1.0836
 2005.0000    6.0000      0.681         6       4.086         4     -0.0445
 2005.0000    6.0000      0.681         6       4.086         5      0.4750
 2005.0000    6.0000      0.681         6       4.086         6      0.9945
 2005.0000    6.0000      0.681         6       4.086         5      0.4750
 2005.0000    6.0000      0.681         6       4.086         4     -0.0445
 2005.0000    6.0000      0.681         6       4.086         5      0.4750
 2005.0000    6.0000      0.681         6       4.086         3     -0.5641
 2005.0000    6.0000      0.681         6       4.086         6      0.9945
 2005.0000    6.0000      0.681         6       4.086         0     -2.1227
 2005.0000    6.0000      0.681         6       4.086         0     -2.1227
 2005.0000    7.0000      0.623         7       4.361         7      1.1486
 2005.0000    7.0000      0.623         7       4.361         5      0.2781
 2005.0000    7.0000      0.623         7       4.361         5      0.2781
 2005.0000    7.0000      0.623         7       4.361         7      1.1486
 2005.0000    7.0000      0.623         7       4.361         6      0.7133
 2005.0000    8.0000      0.576         8       4.606         0     -1.7419

Combine litters with adjacent levels of the litter-specific covariate
within dose groups until the expected count exceeds 3.0, to help improve
the fit of the X^2 statistic to chi-square.

Grouped Data
                    Mean                                    Scaled
      Dose   Lit.-Spec. Cov.     Expected  Observed    Residual
   -------------------------------------------------------------
    0.0000        1.0000            0.270         0     -0.5586
    0.0000        2.0000            1.675         3      1.0237
    0.0000        3.0000            2.401         2     -0.2443
    0.0000        4.0000            3.722         2     -0.8049
    0.0000        5.0000            3.977         4      0.0098
    0.0000        5.0000            3.977         2     -0.8614
    0.0000        5.0000            3.977         1     -1.2970
    0.0000        5.0000            1.326         1     -0.2458
```

0.0000	6.0000	3.573	9	2.4207
0.0000	6.0000	3.573	1	-1.1474
0.0000	6.0000	3.573	1	-1.1474
0.0000	6.0000	3.573	2	-0.7013
0.0000	6.0000	3.573	5	0.6367
0.0000	6.0000	3.573	5	0.6367
0.0000	6.0000	3.573	6	1.0827
0.0000	6.0000	3.573	8	1.9747
0.0000	7.0000	4.624	1	-1.3869
0.0000	7.0000	4.624	5	0.1441
0.0000	7.0000	4.624	5	0.1441
0.0000	7.0000	4.624	5	0.1441
0.0000	7.0000	4.624	7	0.9096
0.0000	7.0000	4.624	3	-0.6214
0.0000	7.0000	2.312	1	-0.7100
0.0000	8.0000	5.805	5	-0.2698
0.0000	8.0000	5.805	11	1.7418
0.0000	8.0000	2.902	2	-0.4279
134.0000	1.0000	0.989	0	-1.3982
134.0000	2.0000	1.718	2	0.2488
134.0000	3.0000	3.449	6	1.3759
134.0000	3.0000	1.150	1	-0.1400
134.0000	4.0000	2.850	3	0.0799
134.0000	5.0000	3.463	4	0.2388
134.0000	5.0000	3.463	1	-1.0962
134.0000	5.0000	1.732	0	-1.0898
134.0000	6.0000	4.199	5	0.3044
134.0000	7.0000	5.086	5	-0.0284
134.0000	7.0000	5.086	4	-0.3578
134.0000	7.0000	5.086	2	-1.0166
134.0000	8.0000	3.068	2	-0.4373
134.0000	8.0000	3.068	0	-1.2562
134.0000	8.0000	3.068	8	2.0195
526.0000	2.0000	1.406	2	0.8346
526.0000	3.0000	1.892	3	1.1101
526.0000	4.0000	4.500	3	-0.8351
526.0000	5.0000	5.060	8	1.3670
526.0000	5.0000	5.060	4	-0.4926
526.0000	6.0000	5.592	6	0.1644
526.0000	6.0000	5.592	8	0.9700
526.0000	6.0000	5.592	11	2.1785
526.0000	6.0000	5.592	2	-1.4469
526.0000	6.0000	5.592	2	-1.4469
526.0000	6.0000	5.592	9	1.3729
526.0000	6.0000	5.592	5	-0.2384
526.0000	6.0000	5.592	6	0.1644
526.0000	7.0000	3.105	0	-1.5658
526.0000	7.0000	3.105	4	0.4511
526.0000	7.0000	3.105	5	0.9554
526.0000	7.0000	3.105	1	-1.0615
526.0000	7.0000	3.105	4	0.4511
526.0000	7.0000	3.105	1	-1.0615
526.0000	7.0000	3.105	5	0.9554
526.0000	7.0000	3.105	3	-0.0531
526.0000	7.0000	3.105	4	0.4511
526.0000	7.0000	3.105	1	-1.0615
526.0000	7.0000	3.105	3	-0.0531
526.0000	7.0000	3.105	3	-0.0531
526.0000	8.0000	3.496	0	-1.5793
526.0000	8.0000	3.496	7	1.5832
526.0000	8.0000	3.496	5	0.6796
526.0000	9.0000	3.985	0	-1.6270
526.0000	9.0000	3.985	6	0.8225
2005.0000	1.0000	2.777	3	0.4909

```
2005.0000        2.0000            3.577         3     -0.8022
2005.0000        3.0000            5.118         4     -0.9786
2005.0000        3.0000            5.118         4     -0.9786
2005.0000        4.0000            3.208         4      0.6851
2005.0000        4.0000            3.208         4      0.6851
2005.0000        4.0000            3.208         4      0.6851
2005.0000        4.0000            3.208         2     -1.0440
2005.0000        4.0000            3.208         3     -0.1795
2005.0000        4.0000            3.208         4      0.6851
2005.0000        4.0000            3.208         4      0.6851
2005.0000        5.0000            3.714         1     -1.7660
2005.0000        5.0000            3.714         3     -0.4648
2005.0000        5.0000            3.714         5      0.8364
2005.0000        5.0000            3.714         5      0.8364
2005.0000        5.0000            3.714         4      0.1858
2005.0000        5.0000            3.714         4      0.1858
2005.0000        6.0000            4.086         6      0.9945
2005.0000        6.0000            4.086         2     -1.0836
2005.0000        6.0000            4.086         4     -0.0445
2005.0000        6.0000            4.086         5      0.4750
2005.0000        6.0000            4.086         6      0.9945
2005.0000        6.0000            4.086         5      0.4750
2005.0000        6.0000            4.086         4     -0.0445
2005.0000        6.0000            4.086         5      0.4750
2005.0000        6.0000            4.086         3     -0.5641
2005.0000        6.0000            4.086         6      0.9945
2005.0000        6.0000            4.086         0     -2.1227
2005.0000        6.0000            4.086         0     -2.1227
2005.0000        7.0000            4.361         7      1.1486
2005.0000        7.0000            4.361         5      0.2781
2005.0000        7.0000            4.361         5      0.2781
2005.0000        7.0000            4.361         7      1.1486
2005.0000        7.0000            4.361         6      0.7133
2005.0000        8.0000            4.606         0     -1.7419

 Chi-square =     105.13   DF = 98    P-value = 0.2930

To calculate the BMD and BMDL, the litter specific covariate is fixed
 at the mean litter specific covariate of all the data: 5.379518
====================================================================
```

```
Specified effect =            0.1
Risk Type        =      Extra risk
Confidence level =           0.95
             BMD =        141.492
            BMDL =        94.264
```

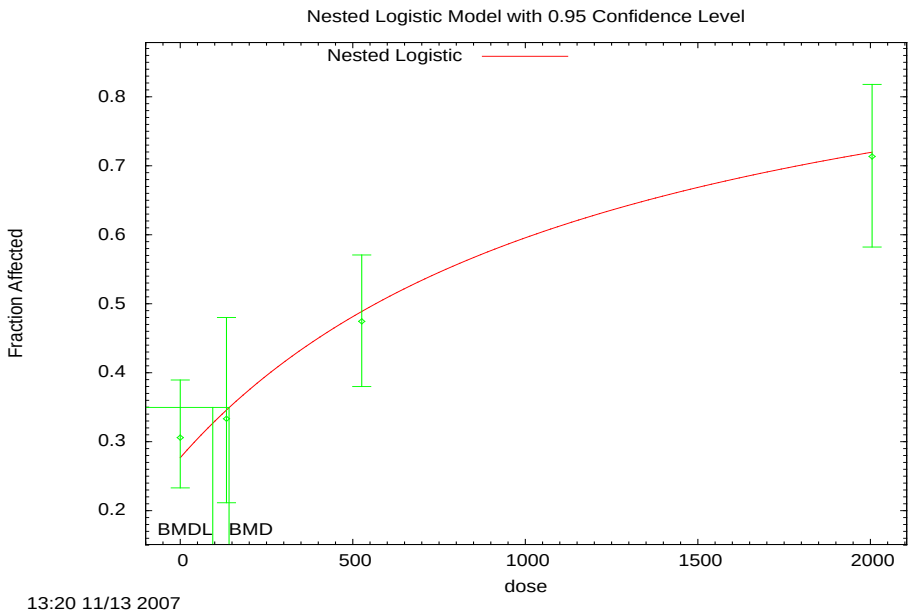

Figure C-5. Nested Logistic Model, 0.1 Extra Risk - Incidence of Cervical Rib in Mice versus C_{max} Methanol, GD 6-15 inhalational study.

Source: Rogers et al. (1993).

Once the $BMDL_{10}$ was obtained in units of mg/L, it was used to derive a chronic inhalation reference value. The first step is to calculate the HEC using the PBPK model described in Appendix B. An algebraic equation is provided (Equation 1 of Appendix B) that describes the relationship between predicted methanol AUC and the human equivalent inhalation exposure concentration (HEC) in ppm. This equation can also be used to estimate model predictions for HECs from C_{max} values because C_{max} values and AUC values were estimated at steady-state for constant 24-hour exposures (i.e., AUC = 24 x C_{max}).

$$BMDL_{HEC}\ (ppm) = 0.0224*BMDL_{10}*24+(1334*BMDL_{10}*24)/(794+ BMDL_{10}*24)$$

$$BMDL_{HEC}\ (ppm) = 0.0224*94.3*24 + ((1334*94.3*24)/(794+ 94.3*24)) = 1038\ ppm$$

Next, because RfCs are typically expressed in units of mg/m^3, the HEC value in ppm was converted using the conversion factor specific to methanol of 1 ppm = 1.31 mg/m^3:

$$HEC\ (mg/m^3) = 1.31 \times 1038\ ppm = 1360\ mg/m^3$$

Finally, this HEC value was divided by a composite 100-fold UF (3 for uncertainty associated with animal to human differences, 10 for consideration of human variability, and 3 for database deficiencies) to obtain the chronic inhalation reference value:

$$\text{RfC (mg/m}^3\text{)} = 1360 \text{ mg/m}^3 \div 100 = 13.6 \text{ mg/m}^3$$

C.3.2. BMD Approach with a BMR of 0.05 Extra Risk (Rogers et al., 1993)

A summary of the results most relevant to the development of a POD using the BMD approach (BMD, BMDL, and model fit statistics) for increased incidence of cervical rib in mice exposed to methanol during gestation from days 6 to 15, with a BMR of 0.05 extra risk, is provided in Table C-9. Model fit was determined by statistics (AIC and χ^2 residuals of individual dose groups) and visual inspection, as recommended by U.S. EPA (2000b). The best model fit to these data (from visual inspection and comparison of AIC values) was obtained using the NLogistic model. The $BMDL_{05}$ was determined to be 44.7 mg/L using the 95% lower confidence limit of the dose-response curve expressed in terms of the C_{max} for methanol in blood.

Table C-9. Comparison of BMD modeling results for cervical rib incidence in mice using modeled C_{max} of methanol as a common dose metric

Model	BMD_{05} (C_{max}, mg/L)[a]	$BMDL_{05}$ (C_{max}, mg/L)[a]	*p*-value	AIC[c]	Scaled residual[d]
NLogistic[b]	67.022	44.651	0.293	1046.84	0.649
NCTR	101.235	50.618	0.241	1048.92	0.662
Rai and Van Ryzin	107.838	53.919	0.163	1051.65	0.661

[a]Daily C_{max} was estimated using a mouse PBPK model as described in section 3.4 of the methanol toxicological review; the BMDL is the 95% lower confidence limit on the C_{max} for a 5% extra risk (dichotomous endpoints) estimated by the model using the likelihood profile method (U.S. EPA, 2000b).
[b]Model choice based on adequate *p* value (> 0.1), visual inspection, low AIC, and low (absolute) scaled residual.
[c]AIC = Akaike Information Criterion = -2L + 2P, where L is the log-likelihood at the maximum likelihood estimates for the parameters, and P is the number of modeled degrees of freedom (usually the number of parameters estimated).
[d]χ^2d residual (measure of how model-predicted responses deviate from the actual data) for the dose group closest to the BMD scaled by an estimate of its S.D. Provides a comparative measure of model fit near the BMD. Residuals exceeding 2.0 in absolute value should cause one to question model fit in this region.

Source: Rogers et al. (1993).

```
=====================================================================
NLogistic Model.
(Version: 2.13; Date: 02/20/2007)
Input Data File: U:\Methanol\BMDS\CervicalRib\Cmax\NLog_Cmax_10_default.(d)
Wed Nov 07 15:45:40 2007
=====================================================================
```

BMD Method for RfC: Incidence of Cervical Rib in Mice versus C_{max} Methanol, GD 6-15 inhalational study (Rogers, et al., 1993)

```
~~~~~~~~~~~~~~~~~~~~~~~~~~~~~~~~~~~~~~~~~~~~~~~~~~~~~~~~~~~~~~~~~~~~~~~~~~~~
  The probability function is:

 Prob. = alpha + theta1*Rij + [1 - alpha - theta1*Rij]/

                        [1+exp(-beta-theta2*Rij-rho*log(Dose))],

           where Rij is the litter specific covariate.

 Restrict Power rho >= 1.

 Total number of observations = 166
 Total number of records with missing values = 0
 Total number of parameters in model = 9
 Total number of specified parameters = 0

 Maximum number of iterations = 250
 Relative Function Convergence has been set to: 1e-008
 Parameter Convergence has been set to: 1e-008

                  Default Initial Parameter Values
                          alpha =     0.297863
                           beta =     -7.94313
                         theta1 =            0
                         theta2 =            0
                            rho =      1.09876
                           phi1 =     0.213134
                           phi2 =     0.309556
                           phi3 =     0.220142
                           phi4 =     0.370587

                                Parameter Estimates

        Variable           Estimate             Std. Err.
           alpha            0.102434             *
            beta            -4.80338             *
          theta1           0.0325457             *
          theta2           -0.436115             *
             rho                   1             *
            phi1            0.200733             *
            phi2            0.307656             *
            phi3            0.212754             *
            phi4            0.368426             *

* - Indicates that this value is not calculated.

 Log-likelihood: -515.422   AIC: 1046.84
                               Litter Data

            Lit.-Spec.              Litter                           Scaled
   Dose       Cov.     Est._Prob.   Size    Expected   Observed   Residual
-----------------------------------------------------------------------------
   0.0000    1.0000      0.135         1       0.135         0     -0.3950
   0.0000    1.0000      0.135         1       0.135         0     -0.3950
   0.0000    2.0000      0.168         2       0.335         0     -0.5790
   0.0000    2.0000      0.168         2       0.335         1      1.1490
   0.0000    2.0000      0.168         2       0.335         0     -0.5790
   0.0000    2.0000      0.168         2       0.335         2      2.8770
   0.0000    2.0000      0.168         2       0.335         0     -0.5790
   0.0000    3.0000      0.200         3       0.600         0     -0.7317
   0.0000    3.0000      0.200         3       0.600         0     -0.7317
   0.0000    3.0000      0.200         3       0.600         1      0.4874
   0.0000    3.0000      0.200         3       0.600         1      0.4874
   0.0000    4.0000      0.233         4       0.930         0     -0.8699
```

0.0000	4.0000	0.233	4	0.930	1	0.0650
0.0000	4.0000	0.233	4	0.930	0	-0.8699
0.0000	4.0000	0.233	4	0.930	1	0.0650
0.0000	5.0000	0.265	5	1.326	0	-1.0004
0.0000	5.0000	0.265	5	1.326	1	-0.2458
0.0000	5.0000	0.265	5	1.326	3	1.2632
0.0000	5.0000	0.265	5	1.326	1	-0.2458
0.0000	5.0000	0.265	5	1.326	0	-1.0004
0.0000	5.0000	0.265	5	1.326	1	-0.2458
0.0000	5.0000	0.265	5	1.326	1	-0.2458
0.0000	5.0000	0.265	5	1.326	0	-1.0004
0.0000	5.0000	0.265	5	1.326	0	-1.0004
0.0000	5.0000	0.265	5	1.326	1	-0.2458
0.0000	6.0000	0.298	6	1.786	3	0.7656
0.0000	6.0000	0.298	6	1.786	6	2.6578
0.0000	6.0000	0.298	6	1.786	1	-0.4959
0.0000	6.0000	0.298	6	1.786	0	-1.1267
0.0000	6.0000	0.298	6	1.786	0	-1.1267
0.0000	6.0000	0.298	6	1.786	1	-0.4959
0.0000	6.0000	0.298	6	1.786	2	0.1348
0.0000	6.0000	0.298	6	1.786	0	-1.1267
0.0000	6.0000	0.298	6	1.786	2	0.1348
0.0000	6.0000	0.298	6	1.786	3	0.7656
0.0000	6.0000	0.298	6	1.786	5	2.0271
0.0000	6.0000	0.298	6	1.786	0	-1.1267
0.0000	6.0000	0.298	6	1.786	3	0.7656
0.0000	6.0000	0.298	6	1.786	3	0.7656
0.0000	6.0000	0.298	6	1.786	3	0.7656
0.0000	6.0000	0.298	6	1.786	5	2.0271
0.0000	7.0000	0.330	7	2.312	0	-1.2513
0.0000	7.0000	0.330	7	2.312	1	-0.7100
0.0000	7.0000	0.330	7	2.312	2	-0.1688
0.0000	7.0000	0.330	7	2.312	3	0.3725
0.0000	7.0000	0.330	7	2.312	2	-0.1688
0.0000	7.0000	0.330	7	2.312	3	0.3725
0.0000	7.0000	0.330	7	2.312	5	1.4551
0.0000	7.0000	0.330	7	2.312	0	-1.2513
0.0000	7.0000	0.330	7	2.312	2	-0.1688
0.0000	7.0000	0.330	7	2.312	5	1.4551
0.0000	7.0000	0.330	7	2.312	1	-0.7100
0.0000	7.0000	0.330	7	2.312	2	-0.1688
0.0000	7.0000	0.330	7	2.312	1	-0.7100
0.0000	8.0000	0.363	8	2.902	1	-0.9020
0.0000	8.0000	0.363	8	2.902	4	0.5204
0.0000	8.0000	0.363	8	2.902	3	0.0463
0.0000	8.0000	0.363	8	2.902	8	2.4170
0.0000	8.0000	0.363	8	2.902	2	-0.4279
134.0000	1.0000	0.494	1	0.494	0	-0.9887
134.0000	1.0000	0.494	1	0.494	0	-0.9887
134.0000	2.0000	0.430	2	0.859	0	-1.0732
134.0000	2.0000	0.430	2	0.859	2	1.4251
134.0000	3.0000	0.383	3	1.150	3	1.7287
134.0000	3.0000	0.383	3	1.150	1	-0.1400
134.0000	3.0000	0.383	3	1.150	2	0.7944
134.0000	3.0000	0.383	3	1.150	1	-0.1400
134.0000	4.0000	0.356	4	1.425	3	1.1858
134.0000	4.0000	0.356	4	1.425	0	-1.0729
134.0000	5.0000	0.346	5	1.732	0	-1.0898
134.0000	5.0000	0.346	5	1.732	4	1.4275
134.0000	5.0000	0.346	5	1.732	0	-1.0898
134.0000	5.0000	0.346	5	1.732	1	-0.4604
134.0000	5.0000	0.346	5	1.732	0	-1.0898
134.0000	6.0000	0.350	6	2.099	3	0.4839
134.0000	6.0000	0.350	6	2.099	2	-0.0534
134.0000	7.0000	0.363	7	2.543	3	0.2128
134.0000	7.0000	0.363	7	2.543	2	-0.2530

134.0000	7.0000	0.363	7	2.543	2	-0.2530
134.0000	7.0000	0.363	7	2.543	2	-0.2530
134.0000	7.0000	0.363	7	2.543	2	-0.2530
134.0000	7.0000	0.363	7	2.543	0	-1.1847
134.0000	8.0000	0.383	8	3.068	2	-0.4373
134.0000	8.0000	0.383	8	3.068	0	-1.2562
134.0000	8.0000	0.383	8	3.068	8	2.0195
526.0000	2.0000	0.703	2	1.406	2	0.8346
526.0000	3.0000	0.631	3	1.892	3	1.1101
526.0000	4.0000	0.562	4	2.250	2	-0.1967
526.0000	4.0000	0.562	4	2.250	1	-0.9842
526.0000	5.0000	0.506	5	2.530	3	0.3091
526.0000	5.0000	0.506	5	2.530	5	1.6241
526.0000	5.0000	0.506	5	2.530	3	0.3091
526.0000	5.0000	0.506	5	2.530	1	-1.0058
526.0000	6.0000	0.466	6	2.796	3	0.1162
526.0000	6.0000	0.466	6	2.796	3	0.1162
526.0000	6.0000	0.466	6	2.796	3	0.1162
526.0000	6.0000	0.466	6	2.796	5	1.2556
526.0000	6.0000	0.466	6	2.796	6	1.8253
526.0000	6.0000	0.466	6	2.796	5	1.2556
526.0000	6.0000	0.466	6	2.796	2	-0.4534
526.0000	6.0000	0.466	6	2.796	0	-1.5928
526.0000	6.0000	0.466	6	2.796	2	-0.4534
526.0000	6.0000	0.466	6	2.796	0	-1.5928
526.0000	6.0000	0.466	6	2.796	5	1.2556
526.0000	6.0000	0.466	6	2.796	4	0.6859
526.0000	6.0000	0.466	6	2.796	3	0.1162
526.0000	6.0000	0.466	6	2.796	2	-0.4534
526.0000	6.0000	0.466	6	2.796	4	0.6859
526.0000	6.0000	0.466	6	2.796	2	-0.4534
526.0000	7.0000	0.444	7	3.105	0	-1.5658
526.0000	7.0000	0.444	7	3.105	4	0.4511
526.0000	7.0000	0.444	7	3.105	5	0.9554
526.0000	7.0000	0.444	7	3.105	1	-1.0615
526.0000	7.0000	0.444	7	3.105	4	0.4511
526.0000	7.0000	0.444	7	3.105	1	-1.0615
526.0000	7.0000	0.444	7	3.105	5	0.9554
526.0000	7.0000	0.444	7	3.105	3	-0.0531
526.0000	7.0000	0.444	7	3.105	4	0.4511
526.0000	7.0000	0.444	7	3.105	1	-1.0615
526.0000	7.0000	0.444	7	3.105	3	-0.0531
526.0000	7.0000	0.444	7	3.105	3	-0.0531
526.0000	8.0000	0.437	8	3.496	0	-1.5793
526.0000	8.0000	0.437	8	3.496	7	1.5832
526.0000	8.0000	0.437	8	3.496	5	0.6796
526.0000	9.0000	0.443	9	3.985	0	-1.6270
526.0000	9.0000	0.443	9	3.985	6	0.8225
2005.0000	1.0000	0.926	1	0.926	1	0.2834
2005.0000	1.0000	0.926	1	0.926	1	0.2834
2005.0000	1.0000	0.926	1	0.926	1	0.2834
2005.0000	2.0000	0.894	2	1.789	1	-1.5502
2005.0000	2.0000	0.894	2	1.789	2	0.4157
2005.0000	3.0000	0.853	3	2.559	3	0.5454
2005.0000	3.0000	0.853	3	2.559	1	-1.9294
2005.0000	3.0000	0.853	3	2.559	1	-1.9294
2005.0000	3.0000	0.853	3	2.559	3	0.5454
2005.0000	4.0000	0.802	4	3.208	4	0.6851
2005.0000	4.0000	0.802	4	3.208	4	0.6851
2005.0000	4.0000	0.802	4	3.208	4	0.6851
2005.0000	4.0000	0.802	4	3.208	2	-1.0440
2005.0000	4.0000	0.802	4	3.208	3	-0.1795
2005.0000	4.0000	0.802	4	3.208	4	0.6851
2005.0000	4.0000	0.802	4	3.208	4	0.6851
2005.0000	5.0000	0.743	5	3.714	1	-1.7660

```
2005.0000    5.0000      0.743         5       3.714         3     -0.4648
2005.0000    5.0000      0.743         5       3.714         5      0.8364
2005.0000    5.0000      0.743         5       3.714         5      0.8364
2005.0000    5.0000      0.743         5       3.714         4      0.1858
2005.0000    5.0000      0.743         5       3.714         4      0.1858
2005.0000    6.0000      0.681         6       4.086         6      0.9945
2005.0000    6.0000      0.681         6       4.086         2     -1.0836
2005.0000    6.0000      0.681         6       4.086         4     -0.0445
2005.0000    6.0000      0.681         6       4.086         5      0.4750
2005.0000    6.0000      0.681         6       4.086         6      0.9945
2005.0000    6.0000      0.681         6       4.086         5      0.4750
2005.0000    6.0000      0.681         6       4.086         4     -0.0445
2005.0000    6.0000      0.681         6       4.086         5      0.4750
2005.0000    6.0000      0.681         6       4.086         3     -0.5641
2005.0000    6.0000      0.681         6       4.086         6      0.9945
2005.0000    6.0000      0.681         6       4.086         0     -2.1227
2005.0000    6.0000      0.681         6       4.086         0     -2.1227
2005.0000    7.0000      0.623         7       4.361         7      1.1486
2005.0000    7.0000      0.623         7       4.361         5      0.2781
2005.0000    7.0000      0.623         7       4.361         5      0.2781
2005.0000    7.0000      0.623         7       4.361         7      1.1486
2005.0000    7.0000      0.623         7       4.361         6      0.7133
2005.0000    8.0000      0.576         8       4.606         0     -1.7419

Combine litters with adjacent levels of the litter-specific covariate
within dose groups until the expected count exceeds 3.0, to help improve
the fit of the X^2 statistic to chi-square.

Grouped Data
                    Mean                                      Scaled
      Dose   Lit.-Spec. Cov.     Expected  Observed    Residual
  -----------------------------------------------------------
    0.0000        1.0000            0.270         0     -0.5586
    0.0000        2.0000            1.675         3      1.0237
    0.0000        3.0000            2.401         2     -0.2443
    0.0000        4.0000            3.722         2     -0.8049
    0.0000        5.0000            3.977         4      0.0098
    0.0000        5.0000            3.977         2     -0.8614
    0.0000        5.0000            3.977         1     -1.2970
    0.0000        5.0000            1.326         1     -0.2458
    0.0000        6.0000            3.573         9      2.4207
    0.0000        6.0000            3.573         1     -1.1474
    0.0000        6.0000            3.573         1     -1.1474
    0.0000        6.0000            3.573         2     -0.7013
    0.0000        6.0000            3.573         5      0.6367
    0.0000        6.0000            3.573         5      0.6367
    0.0000        6.0000            3.573         6      1.0827
    0.0000        6.0000            3.573         8      1.9747
    0.0000        7.0000            4.624         1     -1.3869
    0.0000        7.0000            4.624         5      0.1441
    0.0000        7.0000            4.624         5      0.1441
    0.0000        7.0000            4.624         5      0.1441
    0.0000        7.0000            4.624         7      0.9096
    0.0000        7.0000            4.624         3     -0.6214
    0.0000        7.0000            2.312         1     -0.7100
    0.0000        8.0000            5.805         5     -0.2698
    0.0000        8.0000            5.805        11      1.7418
    0.0000        8.0000            2.902         2     -0.4279

  134.0000        1.0000            0.989         0     -1.3982
  134.0000        2.0000            1.718         2      0.2488
  134.0000        3.0000            3.449         6      1.3759
  134.0000        3.0000            1.150         1     -0.1400
  134.0000        4.0000            2.850         3      0.0799
  134.0000        5.0000            3.463         4      0.2388
  134.0000        5.0000            3.463         1     -1.0962
  134.0000        5.0000            1.732         0     -1.0898
```

134.0000	6.0000	4.199	5	0.3044
134.0000	7.0000	5.086	5	-0.0284
134.0000	7.0000	5.086	4	-0.3578
134.0000	7.0000	5.086	2	-1.0166
134.0000	8.0000	3.068	2	-0.4373
134.0000	8.0000	3.068	0	-1.2562
134.0000	8.0000	3.068	8	2.0195
526.0000	2.0000	1.406	2	0.8346
526.0000	3.0000	1.892	3	1.1101
526.0000	4.0000	4.500	3	-0.8351
526.0000	5.0000	5.060	8	1.3670
526.0000	5.0000	5.060	4	-0.4926
526.0000	6.0000	5.592	6	0.1644
526.0000	6.0000	5.592	8	0.9700
526.0000	6.0000	5.592	11	2.1785
526.0000	6.0000	5.592	2	-1.4469
526.0000	6.0000	5.592	2	-1.4469
526.0000	6.0000	5.592	9	1.3729
526.0000	6.0000	5.592	5	-0.2384
526.0000	6.0000	5.592	6	0.1644
526.0000	7.0000	3.105	0	-1.5658
526.0000	7.0000	3.105	4	0.4511
526.0000	7.0000	3.105	5	0.9554
526.0000	7.0000	3.105	1	-1.0615
526.0000	7.0000	3.105	4	0.4511
526.0000	7.0000	3.105	1	-1.0615
526.0000	7.0000	3.105	5	0.9554
526.0000	7.0000	3.105	3	-0.0531
526.0000	7.0000	3.105	4	0.4511
526.0000	7.0000	3.105	1	-1.0615
526.0000	7.0000	3.105	3	-0.0531
526.0000	7.0000	3.105	3	-0.0531
526.0000	8.0000	3.496	0	-1.5793
526.0000	8.0000	3.496	7	1.5832
526.0000	8.0000	3.496	5	0.6796
526.0000	9.0000	3.985	0	-1.6270
526.0000	9.0000	3.985	6	0.8225
2005.0000	1.0000	2.777	3	0.4909
2005.0000	2.0000	3.577	3	-0.8022
2005.0000	3.0000	5.118	4	-0.9786
2005.0000	3.0000	5.118	4	-0.9786
2005.0000	4.0000	3.208	4	0.6851
2005.0000	4.0000	3.208	4	0.6851
2005.0000	4.0000	3.208	4	0.6851
2005.0000	4.0000	3.208	2	-1.0440
2005.0000	4.0000	3.208	3	-0.1795
2005.0000	4.0000	3.208	4	0.6851
2005.0000	4.0000	3.208	4	0.6851
2005.0000	5.0000	3.714	1	-1.7660
2005.0000	5.0000	3.714	3	-0.4648
2005.0000	5.0000	3.714	5	0.8364
2005.0000	5.0000	3.714	5	0.8364
2005.0000	5.0000	3.714	4	0.1858
2005.0000	5.0000	3.714	4	0.1858
2005.0000	6.0000	4.086	6	0.9945
2005.0000	6.0000	4.086	2	-1.0836
2005.0000	6.0000	4.086	4	-0.0445
2005.0000	6.0000	4.086	5	0.4750
2005.0000	6.0000	4.086	6	0.9945
2005.0000	6.0000	4.086	5	0.4750
2005.0000	6.0000	4.086	4	-0.0445
2005.0000	6.0000	4.086	5	0.4750
2005.0000	6.0000	4.086	3	-0.5641
2005.0000	6.0000	4.086	6	0.9945
2005.0000	6.0000	4.086	0	-2.1227

```
2005.0000        6.0000            4.086         0     -2.1227
2005.0000        7.0000            4.361         7      1.1486
2005.0000        7.0000            4.361         5      0.2781
2005.0000        7.0000            4.361         5      0.2781
2005.0000        7.0000            4.361         7      1.1486
2005.0000        7.0000            4.361         6      0.7133
2005.0000        8.0000            4.606         0     -1.7419

 Chi-square =     105.13   DF = 98    P-value = 0.2930

To calculate the BMD and BMDL, the litter specific covariate is fixed
 at the mean litter specific covariate of all the data: 5.379518
====================================================================
Specified effect =           0.05
Risk Type        =      Extra risk
Confidence level =           0.95
             BMD =        67.0227
            BMDL =       44.6514
```

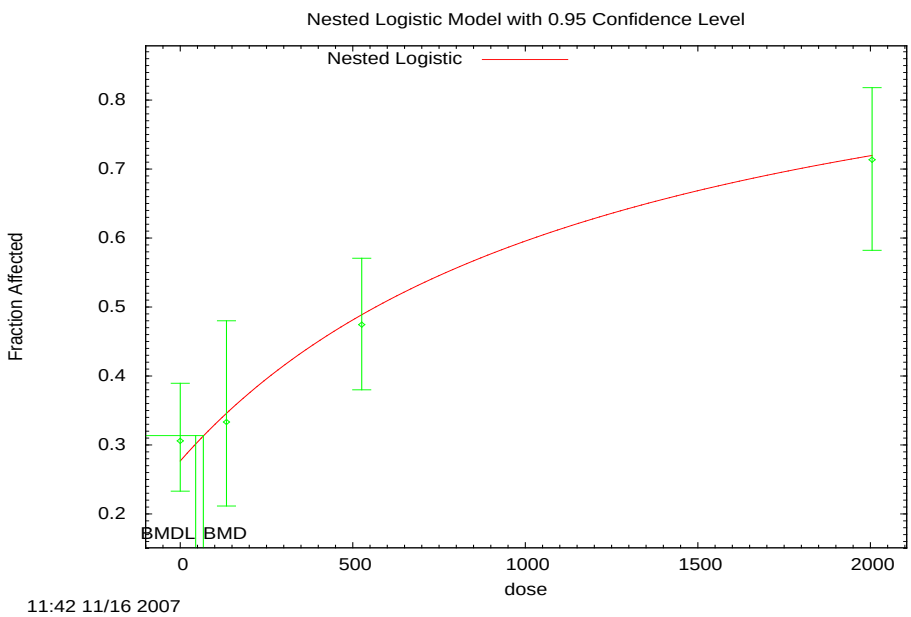

Figure C-6. Nested Logistic Model, 0.05 Extra Risk - Incidence of Cervical Rib in Mice versus C_{max} Methanol, GD 6-15 inhalational study.

Source: Rogers et al. (1993).

Once the $BMDL_{05}$ was obtained in units of mg/L, it was used to derive a chronic inhalation reference value. The first step is to calculate the HEC using the PBPK model described in Appendix B. An algebraic equation is provided (Equation 1 of Appendix B) that describes the relationship between predicted methanol AUC and the human equivalent inhalation exposure concentration (HEC) in ppm. This equation can also be used to estimate model predictions for HECs from C_{max} values because C_{max} values and AUC values were estimated at steady-state for constant 24-hour exposures (i.e., AUC = 24 x C_{max}).

$$BMDL_{HEC}\ (ppm) = 0.0224*BMDL_{05}*24+(1334*BMDL_{05}*24)/(794+ BMDL_{05}*24)$$

$$BMDL_{HEC}\ (ppm) = 0.0224*44.7*24 + ((1334*44.7*24)/(794+ 44.7*24)) = 791\ ppm$$

Next, because RfCs are typically expressed in units of mg/m^3, the HEC value in ppm was converted using the conversion factor specific to methanol of 1 ppm = 1.31 mg/m^3:

$$HEC\ (mg/m^3) = 1.31 \times 791\ ppm = 1036\ mg/m^3$$

Finally, this HEC value was divided by a composite 100-fold UF (3 for uncertainty associated with animal to human differences, 10 for consideration of human variability, and 3 for database deficiencies) to obtain the chronic inhalation reference value:

$$RfC\ (mg/m^3) = 1036\ mg/m^3 \div 100 = 10.4\ mg/m^3$$

C.4. RFC DERIVATIONS USING BURBACHER ET AL. (1999A,B)

The BMD approach was utilized in the derivation of potential chronic inhalation reference values from effects seen in monkeys due to prenatal methanol exposure. Deficits in VDR were evaluated from Burbacher et al. (1999a,1999b). In the application of the BMD approach, continuous models in the EPA's BMDS, version 1.4.1c, were fit to the dataset for increased latency in VDR in neonatal monkeys. As the EPA's PBPK model was not parameterized for monkeys, external concentration (ppm) was used as the dose metric.

The VDR test, which assesses time (from birth) it takes for an infant to grasp for a brightly colored object containing an applesauce-covered nipple, is a measure of sensorimotor development. Beginning at 2 weeks after birth, infants were tested 5 times/day, 4 days/week. Performance on that test, measured as age from birth at achievement of test criterion (successful object retrieval on 8/10 consecutive trials over 2 testing sessions), was reduced in all treated male infants. The times (days after birth) to achieve the criteria for the VDR test were 23.7 ± 4.8 (n = 3), 32.4 ± 4.1 (n = 5), 42.7 ± 8.0 (n = 3), and 40.5 ± 12.5 (n = 2) days for males and 34.2 ± 1.8 (n = 5), 33.0 ± 2.9 (n = 4), 27.6 ± 2.7 (n = 5), and 40.0 ± 4.0 (n = 7) days for females in the control to 1800 ppm groups, respectively. As discussed in Section 4.3.2, this type of response data is sometimes adjusted to account for premature births by subtracting time (days) premature from the time (days from birth) needed to meet the test criteria (Wilson and Cradock, 2004). When this type of adjustment is applied, the times (days after birth or, if shorter, days after control mean gestation length) to achieve the criteria for VDR test were 22.0 ± 9.54 (n = 3), 26.2 ± 8.61 (n = 5), 33.3 ± 10.0 (n = 3), and 39.5 ± 16.3 (n = 2) days for males and 32.0 ± 4.3 (n = 5), 21.8 ± 5.6 (n = 4), 24.0 ± 5.7 (n = 5), and 32.0 ± 14.8 (n = 7) days for females in the control to 1800 ppm groups, respectively. When these data were modeled within BMDS (version 2.1), there was no significant difference between unadjusted responses and/or variances among the dose levels for males and females combined (p = 0.244), for males only (p = 0.321)

and for males only with the high-dose group excluded ($p = 0.182$), or for adjusted responses of males and females combined ($p = 0.12$), males only ($p = 0.448$) and males only with the high-dose group excluded ($p = 0.586$).[91] The only data that offered a significant dose-response trend was that for unadjusted ($p = 0.0265$) and adjusted ($p = 0.009$) female responses, but the model fits for the adjusted female response data were unacceptable. Only the unadjusted female VDR response data offered both a dose-response trend and acceptable model fits. The modeling results for this data set are presented in Table C-10.

The current BMD technical guidance (U.S. EPA, 2000b) suggests that in the absence of knowledge as to what level of response to consider adverse, a change in the mean equal to 1 control S.D. from the control mean can be used as a BMR for continuous endpoints. A summary of the results most relevant to the development of a POD using the BMD approach (BMD, BMDL, and model fit statistics) for increased latency of VDR in female neonatal monkeys exposed to methanol with a BMR of 1 control mean S.D. is provided in Table C-10. Model fit was determined by statistics (AIC and χ^2 residuals of individual dose groups) and visual inspection, as recommended by EPA (2000b). The 3rd degree polynomial model returned a lower AIC than the other models.[92] The $BMDL_{1SD}$ was determined to be 81.7 hr×mg/L, using the 95% lower confidence limit of the dose-response curve expressed in terms of the ppm of external methanol concentration.

[91] BMDS continuous models contain a test for dose-response trend, test 1, which compares a model that fits a distinct mean and variance for each dose group to a model that contains a single mean and variance. The dose response is considered to be significant if this comparison returns a p value < 0.05.

[92] A detailed analysis of this dose response revealed that modeling results, particularly the BMDL estimation, are very sensitive to the high-dose response. There is no data to inform the shape of the curve between the mid- and high-exposure levels, making the derivation of a BMDL very uncertain. The data were analyzed without the high dose to determine if the downward trend in the low- and mid-exposure groups is significant. It was not, so nonnegative restriction on the β coefficients of the poly models was retained.

Table C-10. Comparison of BMD modeling results for VDR in female monkeys using AUC blood methanol as the dose metric

Model	BMD_{1SD} (AUC, hr × mg/L)[a]	$BMDL_{1SD}$ (AUC, hr × mg/L)[a]	p-value	AIC[c]	Scaled residual[d]
Linear	119.058	51.9876	0.1440	110.4492	0.5380
2nd degree polynomial	114.094	59.6412	0.2388	109.43782	0.0994
3rd degree polynomial	120.176	81.6513	0.2718	109.17894	0.0199
Power[b]	133.517	63.0615	0.1112	111.11010	0.0000
Hill	132.283	--	NA	113.11010	0.0000

[a]AUC was estimated using a rat PBPK model as described in section 3.4 of the methanol toxicological review; the BMDL is the 95% lower confidence limit on the AUC of a decrease of 1 control mean S.D. estimated by the model using the likelihood profile method (U.S. EPA, 2000b).
[b]Model choice based on adequate *p* value (> 0.1), visual inspection, low AIC, and low (absolute) scaled residual.
[c]AIC = Akaike Information Criterion = -2L + 2P, where L is the log-likelihood at the maximum likelihood estimates for the parameters, and P is the number of modeled degrees of freedom (usually the number of parameters estimated).
[d]χ^2d residual (measure of how model-predicted responses deviate from the actual data) for the dose group closest to the BMD scaled by an estimate of its S.D. Provides a comparative measure of model fit near the BMD. Residuals that exceed 2.0 in absolute value should cause one to question model fit in this region.

Source: Burbacher et al. (1999a).

```
 ====================================================================
 Polynomial Model.
 (Version: 2.13;  Date: 04/08/2008)
 Input Data File: C:\USEPA\BMDS2\Data\Burbacher\PolfemSet.(d)
 Gnuplot Plotting File:  C:\USEPA\BMDS2\Data\Burbacher\PolfemSet.plt
                                                Fri Dec 12 15:30:29 2008
 ====================================================================
 VDR in female monkeys using AUC blood methanol as the dose metric
~~~~~~~~~~~~~~~~~~~~~~~~~~~~~~~~~~~~~~~~~~~~~~~~~~~~~~~~~~~~~~~~~~~~~~~
    The form of the response function is:

   Y[dose] = beta_0 + beta_1*dose + beta_2*dose^2 + ...

   Dependent variable = F_VDR
   Independent variable = F_Dose
   The polynomial coefficients are restricted to be positive
   The variance is to be modeled as Var(i) = exp(lalpha + log(mean(i)) * rho)

   Total number of dose groups = 4
   Total number of records with missing values = 0
   Maximum number of iterations = 250
   Relative Function Convergence has been set to: 1e-008
   Parameter Convergence has been set to: 1e-008

                  Default Initial Parameter Values
                         lalpha =      4.07254
                            rho =            0
                         beta_0 =         34.2
                         beta_1 =            0
                         beta_2 =            0
                         beta_3 =            0

            Asymptotic Correlation Matrix of Parameter Estimates

            ( *** The model parameter(s)  -beta_1    -beta_2
```

```
                  have been estimated at a boundary point, or have been specified by
the user,
                  and do not appear in the correlation matrix )

                  lalpha          rho       beta_0       beta_3

    lalpha            1           -1      -0.0076        0.018
       rho           -1            1       0.0076       -0.018
    beta_0      -0.0076       0.0076            1        -0.37
    beta_3        0.018       -0.018        -0.37            1

                                 Parameter Estimates
                                                          95.0% Wald CI
       Variable         Estimate        Std. Err.     Lower Conf. Limit   Upper Conf.
Limit
         lalpha         -13.5062          9.81148            -32.7363
5.72395
            rho          4.90831          2.77841           -0.537284
10.3539
         beta_0          31.5013          1.49057             28.5798
34.4228
         beta_1     8.36431e-025               NA
         beta_2                0               NA
         beta_3     3.19775e-006     1.53534e-006        1.88544e-007        6.20695e-
006

NA - Indicates that this parameter has hit a bound
     implied by some inequality constraint and thus
     has no standard error.

     Table of Data and Estimated Values of Interest

 Dose       N    Obs Mean     Est Mean   Obs Std Dev  Est Std Dev   Scaled Res.
------     ---   --------     --------   -----------  -----------   ----------

    0     5       34.2         31.5         4.09         5.55           1.09
 6.73     4         33         31.5         5.83         5.55           0.54
28.28     5       27.6         31.6         5.94         5.58          -1.59
138.1     7         40         39.9         10.7         9.93         0.0199

 Model Descriptions for likelihoods calculated

 Model A1:        Yij = Mu(i) + e(ij)
           Var{e(ij)} = Sigma^2
 Model A2:        Yij = Mu(i) + e(ij)
           Var{e(ij)} = Sigma(i)^2
 Model A3:        Yij = Mu(i) + e(ij)
           Var{e(ij)} = exp(lalpha + rho*ln(Mu(i)))
     Model A3 uses any fixed variance parameters that
     were specified by the user

 Model  R:         Yi = Mu + e(i)
            Var{e(i)} = Sigma^2

                       Likelihoods of Interest

            Model      Log(likelihood)   # Param's      AIC
             A1          -51.042924            5     112.085848
             A2          -47.867444            8     111.734888
             A3          -49.286738            6     110.573475
         fitted          -50.589469            4     109.178938
              R          -55.013527            2     114.027055

                     Explanation of Tests

 Test 1:  Do responses and/or variances differ among Dose levels?
          (A2 versus R)
```

```
 Test 2:  Are Variances Homogeneous? (A1 vs A2)
 Test 3:  Are variances adequately modeled? (A2 versus A3)
 Test 4:  Does the Model for the Mean Fit? (A3 versus fitted)
 (Note:  When rho=0 the results of Test 3 and Test 2 will be the same.)

                     Tests of Interest

   Test    -2*log(Likelihood Ratio)  Test df        p-value

   Test 1              14.2922          6         0.02654
   Test 2              6.35096          3         0.09573
   Test 3              2.83859          2          0.2419
   Test 4              2.60546          2          0.2718

The p-value for Test 1 is less than .05.  There appears to be a
difference between response and/or variances among the dose levels
It seems appropriate to model the data

The p-value for Test 2 is less than .1.  A non-homogeneous variance
model appears to be appropriate

The p-value for Test 3 is greater than .1.  The modeled variance appears
 to be appropriate here

The p-value for Test 4 is greater than .1.  The model chosen seems
to adequately describe the data



Specified effect =             1
Risk Type        =     Estimated S.D.s from the control mean
Confidence level =          0.95
             BMD =        120.176
            BMDL =        81.6513
```

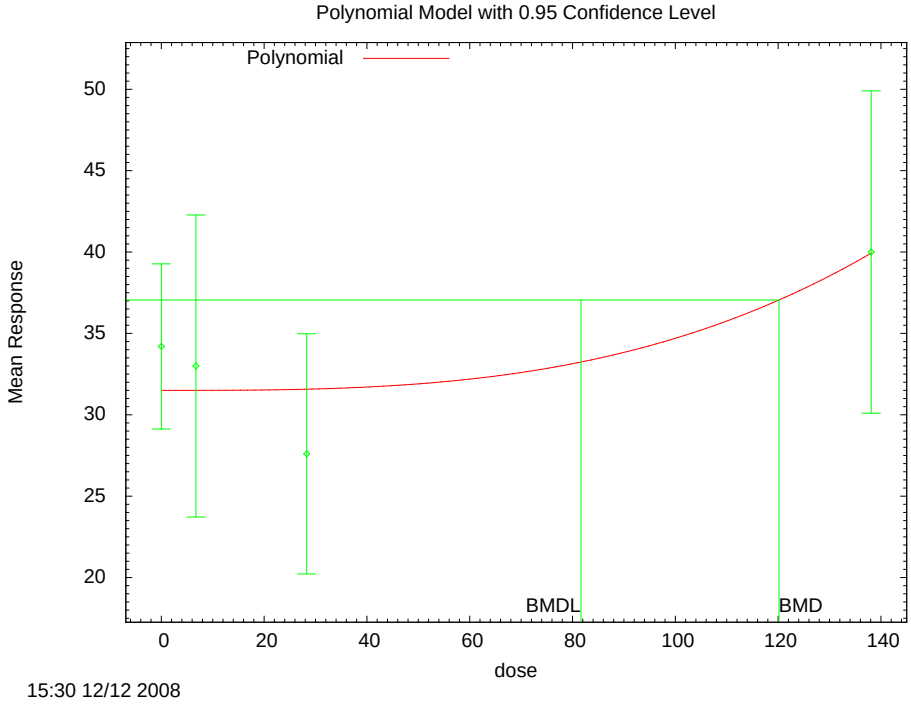

Figure C-7. 3rd Degree Polynomial Model, BMR of 1 Control Mean S.D. - VDR in female monkeys using AUC blood methanol as the dose metric.

Source: Burbacher et al. (1999a, 1999b)

Once the $BMDL_{1SD}$ was obtained in units of ppm, it was used to derive a chronic inhalation reference value. The first step is to calculate the HEC using the PBPK model described in Appendix B. An algebraic equation is provided (Equation 1 of Appendix B) that describes the relationship between predicted methanol AUC and the human equivalent inhalation exposure concentration (HEC) in ppm.

$$BMDL_{HEC}\ (ppm) = 0.0224*BMDL_{1SD}+(1334*BMDL_{1SD})/(794+ BMDL_{1SD})$$

$$BMDL_{HEC}\ (ppm) = 0.0224*81.7+(1334*81.7)/(794+ 81.7) = 126.3\ ppm$$

Next, because RfCs are typically expressed in units of mg/m^3, the HEC value in ppm was converted using the conversion factor specific to methanol of 1 ppm = 1.31 mg/m^3:

$$HEC\ (mg/m^3) = 1.31 \times 126.3\ ppm = 165\ mg/m^3$$

Finally, this HEC value was divided by a composite 100-fold UF (3 for uncertainty associated with animal to human differences, 10 for consideration of human variability, and 3 for database deficiencies) to obtain the chronic inhalation reference value:

$$RfC\ (mg/m^3) = 165\ mg/m^3 \div 100 = 1.7\ mg/m^3$$

APPENDIX D. RfC DERIVATION – COMPARISON OF DOSE METRICS

D.1. METHODS

D.1.1. Dose Metric Comparisons

Three potential dose metrics were evaluated for possible use in risk extrapolation of methanol-induced developmental effects: AUC of methanol in the blood; C_{max} of methanol in the blood; and total metabolism of methanol. The latter metric was considered because developmental effects may be caused by metabolites of methanol, particularly formaldehyde, and formate. These three metrics were evaluated by determining how well they were able to explain the variation in response for incidence of cervical ribs (CR) and supernumerary ribs (SNR) in a concentration-time bioassay by Rogers et al. (1995, raw data obtained from personal communication). In particular, pregnant CD-1 mice were exposed to 2,000, 5,000, 10,000, or 15,000 ppm methanol for 1, 2, 3, 5, or 7 hours on GD7 and developmental effects evaluated at GD17. This endpoint was selected because it was the most sensitive of those examined and gave a reasonable dose-response relationship overall.

Initially, the fraction of pups within each litter carrying either or both CR and SNR was calculated, and then the average across all litters in each concentration-time combination was computed. However, as shown in Figure D-1, the resulting data appear to be nonmonotonic, with the responses from 5-hour exposures exceeding those from 7-hour exposures, and the responses from 2-hour exposures exceeding those from 3-hour exposures. It was noted that the study was done with a block-design, where the dams/litters for some concentration-time combination were divided between multiple blocks and the average CR + SNR incidence in controls varied from 30–52% among the 8 blocks. Therefore block-control response (percent) was subtracted from each exposed litter's response (percent) *before* calculating an average response among litters in a given concentration-time combination. The resulting data are presented in Figure D-1.

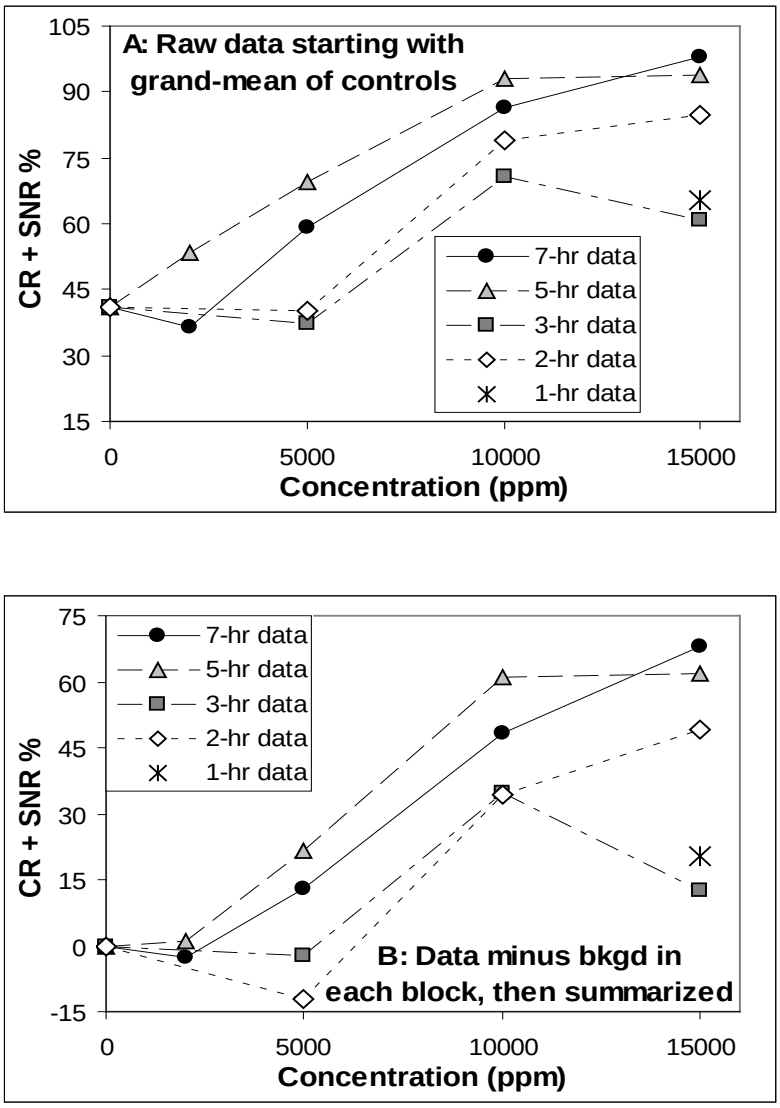

Figure D-1. Exposure-response data for methanol-induced CR plus SNR malformations in mice at various concentration-time combinations. The percent response in each litter was first calculated, with direct averages shown in the first panel relative to the grand-mean for the controls. In the second panel, the percent response in controls for each block of exposures in the study was first subtracted from each litter's response in that block before taking averages across litters.

Source: Rogers et al. (1995).

While the correction for background differences does not completely correct the apparent nonmonotonic dose, the 2-hour response is now less than or below the 3-hour response at 5,000 and 10,000 ppm, and the strong disparity that appeared between the 5- and 7-hour data at 2,000 ppm is eliminated. Overall, the data show a more consistent dependence on duration of exposure, except for the response to 3 hours of 15,000 ppm methanol. Therefore these

background-corrected response measures will be used to evaluate the 3 dose metrics, with the exception that the 3-hour 15,000 ppm data point will be dropped as an outlier. In particular, the dose-response relationship based on these data will be plotted against each of the dose metrics to determine which provides the most consistent overall dose-response relationship.

D.2. RESULTS

D.2.1. Dose Metric Comparisons

The average incidence of CR plus SNR from the concentration-time developmental bioassay of Rogers et al. (1995), with block-specific control values subtracted from each litter average before calculating overall average responses, is plotted in Figure D-2 against three dose metrics: AUC, C_{max}, and total amount metabolized of methanol (The volume units for C_{max} and AUC were adjusted to put all three data sets on approximately the same scale for comparison).

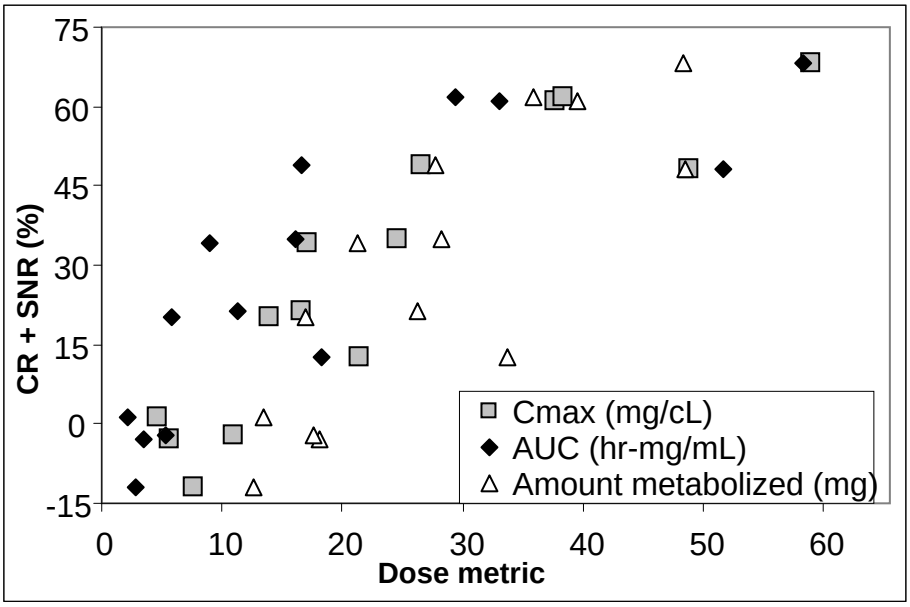

Figure D-2. Internal dose-response relationships for methanol-induced CR plus SNR malformations in mice at various concentration-time combinations for three dose metrics. The percent response in controls for each block of exposures in the study was first subtracted from each litter's response in that block before taking averages across litters. The set of response values plotted for each metric is the same, only the metric associated with those responses changes.

Source: Rogers et al. (1995).

While none of the metrics results are in complete alignment of the dose-response data, the scatter for the C_{max} dose-response (i.e., the range of response values associated with a given small range of the dose metric – scatter in the y-direction) is quite a bit less than either of the

other two metrics. Thus, C_{max} appears to be a better predictor of response than AUC or amount metabolized. Looking at the exposure-response data in Figure D-1, one can see that 2- and 3-hour exposures at 5,000 ppm elicit no increase over control, while 5- and 7-hour exposures at this level do.

If AUC or amount metabolized were true measures of risk, then one would expect a graded response, where the 2- and 3-hour exposures were intermediate between controls and 5–7-hour exposures. But the lack of response at those shorter times indicates that the concentration (C_{max}) has not risen high enough in such a short exposure to cause a response, while it has at the longer durations. From Figure D-2, it appears that a C_{max} of 11 mg/cL (1,100 mg/L) is a NOAEL, with a linear increase in CR + SNR from that level to 38 mg/cL, after which the response begins to plateau. Note that while the plot is of response above background, the plateau is effectively at 100% total incidence: the highest points in Figure D-1 are from the 7-hour exposures at 15,000 ppm, where actual incidence was 98% (30% in controls); and the next highest points are from the 5-hour 15,000 and 10,000 ppm exposures, where the incidences were 94% and 93%, respectively (32% in controls; both from the same block).

APPENDIX E. EVALUATION OF THE CANCER POTENCY OF METHANOL

E.1. INTRODUCTION

Two studies were selected for the evaluation of the cancer potency of methanol (Soffritti et al., 2002a, 2000b, 2002c; NEDO, 1987, 1987/2008b). The Soffritti et al. (2002a) study is the only oral study available with effects that show a statistically significant increase in incidence of any cancer endpoints in the treated groups versus the concurrent control group (pair-wise comparison) and is used to derive the POD for deriving an oral cancer slope factor. The NEDO (1987, 1987/2008b) 24-month rat study is the only inhalation study available with effects that show a statistically significant increase in incidence of any cancer endpoints and was used to derive the POD for the inhalation cancer unit risk. A third study, Apaja (1980), reported statistically significant increases in malignant lymphomas in Eppley Swiss Webster mice over historical controls (pair-wise comparison) following drinking water exposure to methanol. Because this study did not involve a concurrent control group it is not used for the derivation of a cancer oral slope factor, but its dose-response is evaluated here for comparative purposes.

E.1.1. Oral CSF POD

The Soffritti et al. (2002a) study, conducted by the Ramazzini Foundation, presents a number of challenges if these data are to be used in dose-response modeling to assess the carcinogenic potency of methanol. One challenge, determining the appropriate HED, is best addressed using a PBPK model to derive an HED dose that considers the kinetic differences in humans and the animal model, i.e., species extrapolation. Such a model was developed by the EPA and is not addressed in this appendix; however, the dose metrics derived from that PBPK model are used in the modeling of the data.

The other major challenge, which is addressed in this appendix, is how to model the nonstandard protocol by which methanol was tested, as reported in Soffritti et al. (2002a). In most oncogenicity studies, typified by those conducted by the NTP, animals are dosed for 104 weeks, with a scheduled sacrifice of all surviving animals at the end of treatment. In the study for methanol reported by Soffritti et al. (2002a), while the animals were treated with methanol for 104 weeks, animals were not euthanized and examined on a specified schedule but were followed until their natural death. It is well known that the incidence of background tumors in a number of organs is different between that seen at a scheduled sacrifice at 104 or 105 weeks and in the same sex/strain that is followed for a lifetime. A higher background incidence can increase the difficulty of detecting chemically related responses (Melnick et al., 2007). Further, performing pathological examinations on tissues collected after natural death can create

difficulties associated with cell autolysis.[93] At the same time, the shorter duration of the 2-year bioassays used at the NTP misses about two thirds of the life span of the rodent, potentially missing late stage or late appearing chemically related tumor responses (Melnick et al., 2007). ERF believes that "cutting short an experiment after two years may mask a possible carcinogenic response," but ERF further suggests that all chronic cancer studies "should continue until spontaneous animal death" (Soffritti et al., 2002a). Soffritti et al. (2002a) cite ERF studies of benzene, xylenes, mancozeb, and vinyl acetate monomer as examples for which carcinogenic responses were observed after the 2-year treatment period.

These data were evaluated using three different approaches and two different dose-response models (EPA's multistage cancer and a multistage Weibull time-to-tumor model). These approaches involved using the administered dose and models that would rely upon the published data (Option 1), while another would rely on unpublished information that would be provided by the Ramazzini Foundation (Options 1 and 2), while a third option (Option 3) would also rely upon this unpublished information but would also incorporate results from PBPK modeling for methanol developed by the EPA.

E.1.2. Selection of the Data Modeled and HED

The individual animal data from the Ramazzini Foundation study was provided to EPA in the standard NTP format in which the number of days on study, the tissues examined and the tumor types found were given for each animal. The tumors with incidences that were statistically significantly increased or were considered to be rare tumors and considered for dose-response modeling were the incidence of hepatocellular carcinoma in male rats and the incidence of hemolymphoreticular neoplasms in both male and female rats. The incidence of lympho-immunoblastic lymphomas was modeled separately, and the combined incidence of all the lymphomas was considered for dose-response modeling. Table E-2 provides the incidence of these neoplasms reported in each dose group. The incidence of histiocytic sarcomas and myeloid leukemias were not significantly increased in either sex. The incidence of these tumors was not combined with the lymphoblastic lymphomas because they are of a different cell line and the combination is not typically evaluated either for statistical significance or dose-response modeling (McConnell et al., 1986).

The drinking water concentrations provided in the Soffritti et al. (2002a) study were converted to doses in mg/kg-day. Initially, an attempt was made to estimate the dose of methanol to individual animals for development of an average dose; however, water consumption information was available only on a cage-by-cage basis. Based on the available information, the average water consumption for each treatment group was calculated using the available data

[93] Autolysis may develop in carcasses of animals if they are not processed immediately after death or if the animals become severely moribund prior to death. These types of changes can compromise pathological diagnosis and subclassification of neoplasms.

reported for weeks 1–104. Although individual body weights were available, the corresponding intake was not available. The average body weight over the period of dosing for the experiment (using measurements taken on day 1–day 736) was calculated for each dosed group. A weighted average was calculated for the body weights using the number of animals for which body weights were recorded at each time point. The average body weight and the average water consumption in (mL/day) were used to calculate the mg/kg-day doses. The equation used for this calculation is:

$$\text{Dose}(\text{mg}/\text{kg}-\text{day}) = \frac{\text{Dose}(\text{ppm}) \times \text{WaterConsumption}(\text{mL}/\text{day})}{1000 \times \text{BodyWeight}(\text{kg})}.$$

Table E-1 provides the values used to obtain the mg/kg-day doses, as well as the resulting mg/kg-day doses. In addition, the average and median times of death were calculated for each group (both dosed and control), for the only the dosed groups combined (excluding the controls), and for all the groups in the study combined (including control). These values were obtained using the reported weeks on study for each animal. One male rat (ID # 129) in the 20,000 ppm group was not examined microscopically and was excluded from the time of death calculations and all modeling. If this animal was included in the calculations for the average and median times of death, the median time of death for all male rat dosed groups would increase from 97–98 weeks; all of the other average and median times of death that include the 20,000 ppm group do not change.

In the absence of a kinetic model, extrapolation from animal to human was based on the default assumption of body weight$^{3/4}$. This extrapolation was applied to the animal POD estimates to obtain the HEDs reported in Table E-1. This extrapolation was calculated using the average body weight of the dosed animals excluding controls (0.33 kg for the female rats and 0.51 kg for the male rats) over the dosing period of the study (through day 736) and 70 kg for the human body weight. The equation used for the body weight^{¾} extrapolation is

$$\left(\frac{Animal\ Body\ Weight\ (kg)}{Human\ Body\ Weight\ (kg)}\right)^{1/4}$$

and results in a value of 0.26 for the female rats and 0.29 for the male rats.

E.1.2.1. ***Dose-Response Modeling***

Option 1 – Quantal Dose-Response Modeling. Under this option, the standard default modeling approach outlined in the Cancer Guidelines (U.S. EPA, 2005a) was applied. The cancer bioassay data were fit using a multistage model, which is the current model preferred by EPA's IRIS program for cancer dose-response modeling. The PODs for use in the derivation of

CSFs were calculated using the multistage-cancer model available in the BMDS program (http://www.epa.gov/NCEA/bmds).

BMDS was used to estimate BMDs and 95% lower bounds on the BMDs or BMDLs associated with a 10% extra risk ($BMDL_{10}$). For this assessment, the multistage model was determinded to be an appropriate model for characterization of the dose-response curve in the observable range. At this time, the MOA for the tumors observed following exposure to methanol is not known; therefore, linear extrapolation was conducted to estimate a CSF.

Option 2 – Time-to-Tumor Dose-Response Modeling. This option is similar to Option 1; however, rather than the use of quantal models, a time-to-tumor model was applied to the selected datasets. Data for this analysis was provided by the Ramazzini Foundation and can be obtained from their web site (http://www.ramazzini.it/fondazione/study.asp). The same assumptions regarding the HED and low-dose extrapolation were applied. Because BMDS does not include time-to-tumor modeling, the QRISK portion of Statox was relied upon for dose-response modeling. Statox is an internal EPA program that is used for gathering and analyzing animal bioassay data and contains the QRISK component for dose-response modeling. The QRISK component of Statox Version 5.5 fits a multistage Weibull model to the data. The multistage Weibull model is multistage in dose and Weibull in time and essentially assesses the probability that a tumor would have been identified at time t. The multistage Weibull model has the form:

$$p(d,t) = 1 - e^{-(q_0 + q_1 \times d + q_2 \times d^2 \cdots + q_k \times d^k) \times (t - t_0)^c}$$

with dose (d) and time (t) as the variables. The parameters estimated by fitting the model to the data are the dose parameters q_0 through q_k, the induction time (t_0) and the power term for time (c).

If t_0 is interpreted as the time (assumed to be the same for all animals) from when a tumor is observable (i.e., capable of being detected if the animal were to be sacrificed and a necropsy performed) to the time the tumor causes the death of the animal, then these models can be applied to data on incidental and fatal tumors simultaneously. Note that t and t_0 only appear in the model in the form of t-t_0. To make this explicit, we write $P(d,t) = F(d,t-t_0)$. The probability of an incidental tumor by time t is taken to be $F(d,t)$ ($t_0 = 0$) and the probability of a fatal tumor by time t is taken to be $F(d,t-t_0)$. There are three possible types of incidence contexts for each animal which contribute separately to the likelihood function for this model. These are:

- Censored response – animal died without having the tumor(s) being modeled
- Incidental response – the animal died with the tumor(s) but the death was not caused by the tumor(s) (i.e., the time to death from those tumors would have been later than the actual death time); and

- Fatal incidence – the tumor(s) being modeled was the cause of death.

The contribution of each animal to the likelihood is then defined for its time of death *(t)*. The complete likelihood is defined as:

$$\prod_{j=1}^{g}\left\{\left[\coprod_{\text{Incidence}(i,j)=\text{Censored}}(1-F(d_j,t)\right]\times\left[\prod_{\text{Incidence}(i,j)=\text{Incidental}}(F(d_j,t)-F(d_j,t-t_0)\right]\times\left[\prod_{\text{Incidence}(i,j)=\text{Fatal}}\left(\frac{\partial F(d_j,t-t_0)}{\partial t}\right)\right]\right\}$$

where *g* is the number of dose groups in the study, including the control group, and *i* varies from 1 to the total number of animals in the study examined for the tumor type(s) being modeled.

As with the quantal modeling, the lower bound on a dose at an extra risk of 10% was estimated. Goodness-of-fit was determined by visually inspecting graphical output of the modeling. AIC values were also calculated for the time-to-tumor model fit.

This option was proposed because time-to-tumor modeling is typically applied to account for differences in survival among treated and control groups. However, in this case there were no differences detected in the survival times. Figures E-1 and E-2 are graphs of the proportion surviving versus the weeks on study for the female rats and male rats, respectively. In addition, the Life Table program (Thomas et al., 1997) was run on the data. None of the statistical tests in this program indicated a difference in survival between the control and the dosed groups.

The protocol used by the Ramazzini Foundation was different from that typically employed in chronic rat bioassays. In typical rodent bioassays, a compound is administered to the animals for approximately 104 weeks, and the animals sacrificed within a short period (days) following the end of treatment. In the Ramazzini Foundation bioassays (i.e., for methanol, formaldehyde, MTBE, and aspartame), the animals were administered compounds for 104 weeks but were allowed to live until a natural death, which, in some animals, occurred months after the completion of chemical administration. This can have an impact on the tumor incidence and therefore, the potential risk of tumor development associated with administration of a given compound. Time-to-tumor modeling was used in this case to attempt to adjust for the extended life span of the some of the animals in this study.

For time-to-tumor modeling, the POD must consider a specific time as well as a specific risk level. Since this study was not a standard study with a fixed study length, several assumptions can be made with regard to the time to be used. For this modeling exercise, Two different possible approaches were considered.

For the first approach, the model was fit to animal data using all the times reported up to the last death time or 153 weeks for the female rats and 148 weeks for the male rats. Every tumor observed was assumed to be a fatal tumor or the cause of death in the animal. While the animals lived longer than 104 or 105 weeks, the POD was calculated at 105 weeks, since it was assumed that an animal life span of 148–153 weeks would not correspond to the average 70-year human life span.

For the second approach, an attempt was made to simulate what might have occurred if the study had been a standard 2-year protocol that was terminated at 105 weeks, with all surviving animals sacrificed at 105 weeks. It was assumed that the tumors discovered in the animals that survived longer than 105 weeks would have been present and found at necropsy. Therefore, all tumors in animals that died in weeks 105 and earlier were assumed to be fatal or the cause of death in the animals, and all tumors that would have been discovered at the necropsy of animals were assumed to be incidental or not the cause of death. The life span assumed for this analysis was 105 weeks in the rat and the POD was calculated for a 10% risk to a human at 105 weeks. This approach was conducted mainly for comparative purposes to evaluate the potential impact on the POD if the study duration was shortened and for a more direct comparison to the quantal PODs and serves only as bounding exercise for the risk.

Option 3 – Dose-Response Modeling using PK Dose Metrics. For the third approach, PK dose metrics obtained from the PBPK model (Section 3.4) were used as the doses. Both time-to-tumor modeling and quantal modeling was done. The Statox program was used to estimate MLEs and lower bounds on dose associated with a 10% extra risk (LED10s), and BMDS multistage model was used to estimate BMDs and 95% lower bounds on the BMDs or BMDLs associated with a 10% extra risk (BMDL10). Each of the dose metrics, provided in Table E-5, were used in this option of the dose-response modeling.

E.1.2.1. ***Results for Oral Slope Factor POD***

Quantal Dose-Response Modeling (Option 1). Quantal dose-response modeling was conducted using estimated mg/kg-day doses and the incidence of lympho-immunoblastic neoplasms and the combined lymphomas for the female rat and the hepatocellular carcinomas, the lympho-immunoblastic neoplasms, and the combined lymphomas for the male rat. The results of the quantal modeling for this option are given in Table E-3. The multistage model gave an adequate fit (p value > 0.05) and was able to derive $BMDL_{10}$ values for all of the lymphoma data. However, for the male rat hepatocellular carcinomas, the multistage model failed to estimate a $BMDL_{10}$. Human equivalent $BMDL_{10}$ values[94] and CSF are also provided in Table E-3.

The POD values calculated from the female rat data ranged from 259–405 mg/kg-day for the lympho-immunoblastic neoplasms and 251–400 mg/kg-day for the combined lymphomas. For the HED POD values calculated from the male rat data, the range of values for the liver hepatocellular carcinomas was 537–567 mg/kg-day; however, for 3 of the models (Multistage, Quantal Linear and Log-Probit), the BMDS program failed to estimate a $BMDL_{10}$. The lympho-immunoblastic endpoint in the male rats produced POD values that ranged from 110–223 mg/kg-day, and the all lymphomas incidence data gave POD values of 113–227 mg/kg-day. Figures E-3

[94] Computed from the animal values by multiplying by the body weight$^{3/4}$ animal-to-human extrapolation value (0.26 for females and 0.29 for males)

through E-7 show graphs of the quantal models that give the lowest POD for each of the endpoints modeled.

Time-to-Tumor Dose-Response Modeling (Option 2). Results of the time-to-tumor modeling using estimated mg/kg-day doses with POD and CSF values for each approach described above are given in Table E-4. Approach 2 gives smaller POD estimates than Approach 1. With Approach 2, an artificial end of the study is assumed of 105 weeks and the designation of approximately half of the total tumors changed from fatal to incidental. This approach evaluates the potential impact on the POD of terminating the study at 105 weeks, rather than allowing the animals to live until their natural death, assuming that the same animals bearing tumors would be "observed" at 105 weeks, rather than at later time points. For Approach 1, the model was fit to the actual observed weeks-on-study, and a time of 105 weeks was used in calculating the POD. For the female rat, the PODs based on the lympho-immunoblastic neoplasms were 349 mg/kg-day for approach 1 and 179 mg/kg-day forApproach 2. The PODs for the combined lymphomas ranged were 321 and 198 mg/kg-day for the 2 appraoches. For the PODs calculated from the male rat data, the values were 783 and 612 mg/kg-day for the hepatocellular carcinomas, 174 and 91 mg/kg-day for the lympho-immunoblastic neoplasms, and 192 and 92 mg/kg-day for the combined lymphomas. Figures E-3 through E-7 show the modeling results for the time-to-tumor modeling using Approache 1 where the time is fixed at 105 weeks and the doses are allowed to vary. Figures E-8 and E-9 show Kaplan-Meier curves versus the model fit to the combined lymphoma data for the females and males, respectively. In these graphs each line corresponds to a specific dose, and time is allowed to vary up to the study end of 153 or 148 weeks. For the male rat combined lymphomas (Figure E-9), the multistage Weibull predicted values more closely match the Kaplan-Meier at 105 weeks than at the average life span (94 weeks) or the end of study (148 weeks). For the female rat combined lymphomas, the closest match of the Kaplan-Meier curves to the model predicted values appears to be around the average life span of 96 weeks.

The AIC values for the time-to-tumor modeling are all higher than those for the quantal modeling. However, since the LLFs on which the AIC are based are different for time-to-tumor versus quantal models, the AIC values from time-to-tumor models cannot be compared to those from quantal models.

Dose-Response Modeling using PBPK Dose Metrics (Option 3). Both time-to-tumor and quantal dose-response modeling were conducted using the incidence of lympho-immunoblastic neoplasms and the combined lymphomas for the female rat and the hepatocellular carcinomas, the lympho-immunoblastic neoplasms, and the combined lymphomas for the male rat and the three PBPK dose metrics (blood methanol AUC, peak blood concentration, and the total metabolized per day) obtained from the EPA's PBPK model (Table E-5).

Only Approach 1 was used for the time-to-tumor dose-response modeling using PBPK dose metrics, and results are given in Table E-6a; HEDs are provided in Table E-6b.

The results of the multistage quantal modeling are given in Table E-7. Most model runs gave an adequate fit to the data by the χ^2 Goodness of Fit p-value (e.g., p-values > 0.05), although for male rat hepatocellular carcinomas, the calculations using the AUC or amount metabolized dose metric were unable to converge for the model fit or the derivation of a BMDL. A plot of the model fit for male rat combined lymphomas using total methanol metabolized per day as the dose metric (the endpoint and dose metric used in the derivation of the oral CSF) is shown in Figure E-10; HEDs are provided in Table E-8 where the BMDL was calculated.

E.2. INHALATION ORAL CANCER UNIT RISK POD

The NEDO (1987, 1987/2008b) study was conducted using a standard protocol with exposure for 104 weeks, followed by sacrifice of all animals surviving to 104 weeks. As with the Soffretti (2002a) study, pharmacokinetic dose metrics for use in the dose-response assessment were determined for the inhalation exposures using the EPA's PBPK model.

E.2.1. Selection of the Data Modeled and HED

The individual animal data from the NEDO (1987/2008b) study were provided in a 2008 translation of the study from Japanese to English. Although the translation provided the number of days on study and the neoplastic responses seen in each animal, the translation did not provide results if a tissue was examined histopathologically with no neoplastic responses. This makes it difficult to determine which of the individual animals were not examined, although the tables did indicate that, for some of the animals, selected organs (specifically a few lungs in males and a few adrenal glands in females) were not examined. Therefore, time-to-tumor analysis could not be conducted with results from the inhalation data as was done with the oral data. However, survival analysis of all the data from the NEDO (1987/2008b) study did not indicate that there were any survival problems (Figures E-11 and E-12). This suggests that a time-to-tumor analysis is not necessary.

The tumors with significantly increased incidence that were considered for dose-response modeling were the female rat adrenal gland pheochromocytomas and the male rat lung tumors (papillary adenomas and adenocarcinomas combined or papillary adenomas, adenocarcinomas and adenomatosis combined); Table E-9 gives the incidence of these tumors.

E.2.1.1. ***Dose-Response Modeling***

Quantal Dose-Response Modeling using Pharmacokinetic Dose Metrics. For the selected endpoints from the NEDO (1987) study, only quantal dose-response modeling using pharmacokinetic internal dose metrics estimated by the PBPK model (described in Section 3.4 and Appendix B) was conducted. Each of the dose metrics provided in Table E-10 was used in the BMDS software with the incidence data in Table E-9 to estimate the BMDs and 95% lower confidence limits (BMDLs) associated with a 10% extra risk ($BMDL_{10}$).

E.2.2. Results for the IUR POD

Quantal dose-response modeling was conducted using the incidence of adrenal gland phoechromocytomas in female rats and the combined incidence of lung adenomas and adenocarcinomas or lung adenomas, adenocarcinomas and adenomatosis in male rats using the pharmacokinetics dose metrics derived from the EPA's PBPK model. The results of this modeling are given in Table E-11. The multistage model gave an adequate fit to the data in all instances as determined by the χ^2 goodness-of-fit *p*-value (e.g., *p*-values > 0.05). A plot of the model fit for female rat pheochromocytomas using total methanol metabolized per day as the dose metric (the endpoint and dose metric used in the derivation of the IUR) is shown in Figure E-13. HECs are provided in Table E-12.

E.3. ANALYSIS OF APAJA (1980) DRINKING WATER STUDY

The Apaja (1980) study was similar to the Soffritti et al. (2002a) study in that it was a life span drinking water study. The primary differences are that Apaja (1980) used Eppley Swiss Webster mice, did not stop exposure at 104 weeks and did not employ an untreated concurrent control group. Methanol exposure groups of this study served as controls for malonaldehyde exposed mice. As with the Soffretti (2002a) study, pharmacokinetic dose metrics for use in the dose-response assessment were determined for the oral exposures using the EPA's PBPK mouse model.

E.3.1. Selection of the Data Modeled and HED

Individual animal data from the Apaja (1980) study were not available. Therefore, time-to-tumor analysis could not be conducted. The tumors with significantly increased incidence that were considered for dose-response modeling were malignant lymphomas in male and female mice; Table E-13 gives the incidence of these tumors.

E.3.1.1. ***Dose-Response Modeling***

Quantal Dose-Response Modeling using Pharmacokinetic Dose Metrics. A 1st degree multisage model was used to evaluate the malignant lymphoma response from the Apaja (1980) study versus pharmacokinetic dose metrics without background[95] was conducted. Each of the dose metrics provided in Table E-14 was used in the BMDS software with the incidence data in Table E-13 to estimate the BMDs and 95% lower confidence limits (BMDLs) associated with a 10% extra risk ($BMDL_{10}$).

[95] The assumption of zero background dose is consistent with what was done for the derivation of the oral CSF and EPA practice.

E.3.2. Results for the IUR POD

Quantal dose-response modeling was conducted using the incidence of malignant lymphoma in male and female Eppley Swiss Webster mice using the pharmacokinetics dose metrics derived from the EPA's PBPK model. The results of this modeling are given in Table E-15. The 1st degree multistage model gave an adequate fit to the data in all instances as determined by the χ^2 goodness-of-fit *p*-value (e.g., *p*-values > 0.05). A plot of the model fits for male and female mice using total methanol metabolized per day as the dose metric is shown in Figure E-14. $BMDL_{10}$ HECs associated with each dose metric are provided in Table E-16.

E.4. BACKGROUND DOSE ANALYSES

The primary purpose of this cancer analysis is for the determination of cancer risk associated with increases in the levels of methanol or its metabolites (e.g., formate, formaldehyde) over background. Thus, the PBPK model estimates of internal dose used in the dose-response analyses described above do not describe or account for background levels of methanol or its metabolites. However, background levels of methanol may have contributed to the response levels reported for some of the tumors associated with methanol. If this contribution is large, it could significantly impact cancer risk estimates.

Of the Soffritti et al. (2002a), NEDO (1985/2008b) and Apaja (1989) studies, only the NEDO study reported methanol blood levels in test animals. Based on background levels of methanol in the blood of F344 rats reported by NEDO (1987; 1985/2008b) PBPK model estimates of AUC methanol (mg-h/L), Cmax methanol (mg/L) and total metabolites (mg/day) in control animals were obtained. AUC methanol, Cmax methanol and methanol metabolite background levels were estimated to be 97.16 mg-h/L, 4.05 mg/L and 7.79 mg/day for female F344 rats and 96.02, 4.00 and 10.81 mg/day for male F344 rats, respectively.

Available bioassays do not allow for the quantification of the relationship between background levels and background responses, but the "background dose" Multistage-cancer model contained in version 2.1 of EPA's BMDS software can be used to estimate what background dose would be necessary to explain the dose-response data evaluated in this assessment if all of the background response were due to background levels of methanol or its metabolites. The results of dose-response modeling of cancer endpoints evaluated in this assessment using the Multistage-cancer "background dose" model are shown in Table E-17.

As can be seen from Table E-17, the Multistage-cancer-bgdose model predicts that AUC methanol, Cmax methanol and methanol metabolite background doses necessary to explain the dose-response data if all of the background response were due to background levels of methanol or its metabolites are well above the actual background levels for these metrics predicted by the PBPK model. In the case of lymphoma responses in Sprague-Dawley rats, the background doses for all metrics predicted by the Multistage-cancer-bgdose model are 20-2,000 fold higher than

the actual background doses predicted in F344 rats by the PBPK model. In the case of female pheochromocytoma and male lung responses in F344 rats, the background doses predicted by the Multistage-cancer-bgdose model are 3-5 fold higher than the actual background doses predicted by the PBPK model. The fact that background dose estimates from the Multistage-cancer-bgdose model are several-fold and sometimes more than 1,000-fold higher than the PBPK model predictions suggests that the contribution of background levels of methanol or its metabolites to the background responses of these tumors is relatively small.

Table E-1. Calculation of mg/kg-day doses

	Female Sprague-Dawley Rats					Male Sprague-Dawley Rats				
Dose (ppm)	Body weight (kg)	Water consump. (g/day or mL/day)	Dose (mg/kg -day)	Average time of death (wk)	Median time of death (wk)	Body weight (kg)	Water consump. (g/day or mL/day)	Dose (mg/kg - day)	Average time of death (wk)	Median time of death (wk)
0	0.33	42.55	0	98	102	0.50	52.57	0	91	91
500	0.33	43.05	66.0	96	99	0.49	52.06	53.2	97	98
5000	0.33	41.11	624.1	94	97	0.50	52.58	524	93	93
20000	0.34	37.26	2177	98	101	0.54	48.32	1780	93	100
Averaged over all dosed groups (excluding control)	0.33			96	99	0.51			94	97
Averaged over all groups (including control)	0.33			97	100	0.51			93	96

Source: Soffretti et al. (2002a).

Table E-2. Incidence for neoplasms considered for dose-response modeling

Dose (ppm)	Dose (mg/kg-day)	Number of animals examined	Heptocellular carcinomas	Histiocytic sarcoma	Leukemia monocytic	Leukemia myloid	Lymphoma lymphoblastic	Lymphoma lympocytic	Lymphoma lympho-immunoblastic	All lymphomas combined
Female Sprague-Dawley rats										
0	0	100		1		3	0	0	9	9
500	66.0	100		2		3	1	1	17	19[a]
5000	624.1	100		2		3	1	0	19[a]	20[a]
20000	2177	100		3		3	1	0	21[a]	22[b]
Cochran Armitage Trend Test				0.19		0.5	0.3	0.8	0.04	0.04
Male Sprague-Dawley rats										
0	0	100	0	2	1	8	1		16	17
500	53.2	100	2	4	0	4	3		24	27
5000	524	100	2	1	0	6	1		28[a]	29[a]
20000	1780	99	3	1	0	1	1		37[b]	38[b]
Cochran Armitage Trend Test			0.10	0.9	0.8	0.98	0.7		0.0007	0.001

[a]Fisher's Exact *p*-value < 0.05; [b]Fisher's Exact p-value < 0.01

Source: Soffretti et al. (2002a).

Table E-3. Results from multistage (1º) quantal modeling rat data using mg/kg-day exposures and default HED derivation method

		AIC	*p*-value	Scaled residual at observed dose closest to BMD	Animal values		Human values	
					BMD_{10}	$BMDL_{10}$	Human equivalent $BMDL_{10}$[a]	CSF[b]
Female Sprague-Dawley rat	All organs lympho-immunoblastic	359.16	0.19	-0.07	2179.51	1058.99	277.5	3.6E-4
	All organs - all lymphomas	371.95	0.11	-0.07	2141.88	1033.69	270.9	3.7E-4
Male Sprague-Dawley rat	Hepatocellular carcinoma	72.84	0.38	Failed[a]				
	All organs lympho-immunoblastic	455.67	0.34	0.14	714.26	448.43	131.0	7.6E-4
	All organs – all lymphomas	468.79	0.24	0.11	744.35	456.11	133.3	7.5E-4

[a]Model failed to optimize.
[b]Calculated as CSF = 0.1/Human $BMDL_{10}$.

Source: Soffretti et al. (2002a).

Table E-4. Results from time-to-tumor modeling data using mg/kg-day exposures and default HED derivation method

				Human values[b]		
		AIC	Prediction time (weeks)	MLE (mg/kg-day)	LED_{10} (mg/kg-day)	CSF[c]
Approach 1 - Model fit to actual death times, dose estimates computed at 105 weeeks[a]						
Female Sprague-Dawley rat	All organs lympho-immunoblastic	831.42	105	729.0	348.6	2.9E-4
	All organs all lymphomas	900.46	105	679.1	320.9	3.1E-4
Male Sprague-Dawley rat	Hepatocellular carcinoma	105.45	105	4250.7	783.3	1.3E-04
	All organs lympho-immunoblastic	1254.58	105	302.0	173.8	5.8E-4
	All organs all lymphomas	1309.86	105	356.7	191.8	5.2E-4
Approach 2 - Truncating study at 105 Weeks[a]						
Female Sprague-Dawley rat	All organs lympho-immunoblastic	631.81	105	370.7	178.5	5.6E-4
	All organs all lymphomas	664.43	105	431.9	198.0	5.1E-4
Male Sprague-Dawley rat	Hepatocellular carcinoma	1.16E+05[d]	105	1013.7	612.2	1.6E-4
	All organs lympho-immunoblastic	914.42	105	150.8	91.2	1.1E-3
	All organs – all lymphomas	935.29	105	157.1	92.2	1.1E-3

[a]Individual animal pathology data needed for the modeling reported in this table can be obtained from the Ramazzini Foundation web site (http://www.ramazzini.it/fondazione/study.asp).
[b]Human values are computed by converting the animal doses to HED before modeling by multiplying by the body weight$^{3/4}$ animal-to-human extrapolation value (0.26 for females and 0.29 for males).
[c]Calculated as CSF = 0.1/Human LED_{10}.
[d]Model failed to optimize.

Source: Soffretti et al. (2002a).

Table E-5. PBPK model estimated dose-metrics for doses

Sex	Dose (mg/kg-day)	Body weight (kg)	AUC (mg-h/L)	Peak (mg/L)	Amount metabolized (mg/day)
Female Sprague-Dawley	66	0.33	66.84	5.96	18.39
	624.1	0.33	9543.63	500.59	126.68
	2177	0.34	91262.27	4157.98	141.60
Male Sprague-Dawley	53.2	0.49	55.76	4.81	21.82
	524	0.50	7500.14	395.56	168.85
	1780	0.54	80420.25	3629.08	200.03

Source: Soffretti et al. (2002a).

Table E-6a. Results from time-to-tumor modeling of data using PBPK dose metrics

Approach 1 - Model fit to actual death times, dose estimates computed at 105 weeeks		Prediction Time (wk)	AUC (mg-h/L)			Peak (mg/L)			Amount Metabolized (mg/d)		
			AIC	MLE	LED_{10}	AIC	MLE	LED_{10}	AIC	MLE	LED_{10}
Female Sprague-Dawley rat	All organs lympho-immunoblastic	105	832.43	152281	64486	832.35	6763.4	2895.3	829.24	160.45	90.7
	All organs all lymphomas	105	901.43	143138	59574	901.36	6356.1	2675.3	898.24	145.53	82.2
Male Sprague-Dawley rat	Hepatocellular carcinoma	105	110.47	undefined	119186	110.45	undefined	5385.9	109.60	undefined	300.4
	All organs lympho-immunoblastic	105	1242.72	55409	30059	1244.61	2460.2	1341.3	1242.66	141.63	77.3
	All organs – all lymphomas	105	1297.74	66211	33315	1297.66	2939.5	1487.2	1295.95	143.14	82.7

Source: Soffretti et al. (2002a)

Table E-6b. HEDs from time-to-tumor modeling of data using PBPK dose metrics

Approach 1 - Model fit to actual death times, dose estimates computed at 105 weeeks		AUC (mg-h/L)	Peak (mg/L)	Amount Metabolized (mg)
		LED_{10} (mg/kg-day)	LED_{10} (mg/kg-day)	LED_{10} (mg/kg-day)
Female Sprague-Dawley rat	All organs lympho-immunoblastic	647.0	676.2	87.7
	All organs all lymphomas	618.3	645.4	79.4
Male Sprague-Dawley rat	Hepatocellular carcinoma	965.4	1023.9	260.0
	All organs lympho-immunoblastic	594.0	457.3	62.4
	All organs – all lymphomas	657.1	478.1	66.7

Source: Soffretti et al. (2002a)

Table E-7. Results of Multistage (1º) quantal modeling of data using PBPK dose metrics

AUC (mg-h/L)					Peak (mg/L)					Amount Metabolized (mg/d)				
AIC	*p*-value	Scaled residual at dose nearest to BMD	BMD_{10}	$BMDL_{10}$	AIC	*p*-value	Scaled residual at dose nearest to BMD	BMD_{10}	$BMDL_{10}$	AIC	*p*-value	Scaled residual at dose nearest to BMD	BMD_{10}	$BMDL_{10}$
Female Sprague-Dawley rats														
All organs lympho-immunoblastic														
357.9	0.13	-0.132	112790	49771	359.9	0.13	-1.56	5034.3	2240.3	357.9	0.34	-0.913	139.8	77.2
All organs – all lymphomas														
372.78	0.075	-0.128	111621	48789.6	372.17	0.077	-0.145	4982.2	2196.3	370.57	0.18	-0. 002	134.4	74.5
Male Sprague-Dawley rats														
Hepatocellular carcinoma														
73.21	0.37	Failed[a]			73.19	0.37	Failed[a]			72.55	0.36	Failed[a]		
All organs lympho-immunoblastic														
457.45	0.14	1.214	36865	21989	457.3	0.15	1.173	1639.0	981.7	455.46	0.36	-0.750	94.4	61.6
All organs – all lymphomas														
468.09	0.15	0.878	37822	22195	467.98	0.15	0.838	1686.5	993.1	467.35	0.20	-0.901	101.7	63.9

[a]BMD computation failed. BMD is larger than three times maximum input doses.

Source: Soffretti et al. (2002a).

Table E-8. Application of human PBPK model to derive HEDs from results of multistage (1º) quantal modeling of data using PBPK dose metrics

		AUC (mg-h/L)	Peak (mg/L)	Amount metabolized (mg/d)[a]
		HED $BMDL_{10}$ (mg/kg-day)	HED $BMDL_{10}$ (mg/kg-day)	HED $BMDL_{10}$ (mg/kg-day)
Female Sprague-Dawley rat	All organs lympho-immunoblastic	560.96	584.37	74.54
	All organs – all lymphomas	555.20	578.18	71.92
Male Sprague-Dawley rat	Hepatocellular carcinoma	N/A	N/A	N/A
	All organs lympho-immunoblastic	395.99	405.56	49.65
	All organs – all lymphomas	397.25	407.22	51.50[b]

[a]Total metabolized methanol was selected as the preferred dose metric (see discussion in section 5.4.1.3). Before applying human PBPK model to obtain these HED $BMDL_{10}$ estimates, Table E-7 mg/d values were converted to human mg/d by multiplying by either: $(BW_{human})^{¾}/(BW_{rat})^{¾}=(70\ kg)^{¾}/(0.33\ kg)^{¾}=55.6$ for male rats or, $(BW_{human})^{¾}/(BW_{rat})^{¾} = (70\ kg)^{¾}/(0.26\ kg)^{¾} = 66.5$ for female rats.
[b]This value was used in the derivation of the methanol oral cancer slope factor.

Source: Soffretti et al. (2002a).

Table E-9. Incidence for neoplasms considered for dose-response modeling

Dose (ppm)	Examined	Adrenal gland phoechromocytoma	Lung adenoma and adenocarcinoma	Lung adenoma, adenocarcinoma, adenomatosis
Female F344 rats				
0	50	2		
10	51	3		
100	49	2		
1,000	51	7		
Male F344 rats				
0	52		1	5
10	50		5	6
100	52		2	7
1,000	52		7[a]	11
Cochran Armitage Trend Test p_values		0.015	0.0259	0.0415

[a]Fisher's Exact *p*-values < 0.05

Source: NEDO (1987, 1987/2008b).

Table E-10. PBPK dose metrics for doses

Dose (ppm)	AUC (mg-h/L)	Peak (mg/L)	Amount metabolized (mg)
Female F344 rats			
0	0.00	0.00	0.00
10	3.70	0.19	0.30
100	37.53	1.93	2.94
1,000	434.29	22.69	28.96
Male F344 rats			
0	0	0	0
10	3.70	0.19	0.41
100	37.53	1.93	4.11
1,000	433.61	22.68	40.19

Source: NEDO (1987, 1987/2008b).

Table E-11. Benchmark results from multistage quantal dose-response modeling data using PBPK dose-metrics

Model	AUC (mg-h/L)					Peak (mg/L)					Amount metabolized (mg/d)				
	AIC	*p*-value	Scaled residual at dose nearest to BMD	BMD_{10}	$BMDL_{10}$	AIC	*p*-value	Scaled residual at dose nearest to BMD	BMD_{10}	$BMDL_{10}$	AIC	*p*-value	Scaled residual at dose nearest to BMD	BMD_{10}	$BMDL_{10}$
Female F344 rats															
Adrenal glands – pheochromocytoma															
Multistage (3º)	101.37	0.88	0.000	442.1	217.0	101.37	0.88	0.000	23.1	11.3	101.37	0.88	0.000	29.5	14.6
Male F344 rats															
Lung – adenomas and adenocarcinomas															
Multistage (3º)	107.99	0.16	0.000	454.9	230.7	107.99	0.16	0.000	23.8	12.1	107.99	0.16	0.001	42.2	21.6
Lung – adenomas, adenocarcinomas and adenomatosis															
Multistage (1º)	168.61	0.89	-0.035	378.9	168.8	168.61	0.89	-0.035	19.8	8.83	168.59	0.90	-0.038	34.8	15.6

Source: NEDO (1987, 1987/2008b).

Table E-12. Application of human PBPK model to derive HECs from $BMDL_{10}$ estimates in Table E-11 using multistage quantal modeling

		AUC (mg-h/L)	Peak (mg/L)	Amount metabolized (mg/d)[a]
		HEC $BMCL_{10}$ (mg/m^3)	HEC $BMCL_{10}$ (mg/m^3)	HEC $BMCL_{10}$ (mg/m^3)
Female F344 rat	**Adrenal glands - phoechromocytoma**	384.2262	464.79844	81.85[b]
Male F344 rat	**Lung - adenomas and adenocarcinomas**	401.96305	485.15995	101.27
	Lung - adenomas, adenocarcinomas and adenomatosis	316.20336	386.70859	73.12

[a] Total metabolized methanol was selected as the preferred dose metric (see discussion in section 5.4.2.3). Before applying human PBPK model to obtain these HEC $BMCL_{10}$ estimates, Table E-7 mg/d values were converted to human mg/d by multiplying by either: $(BW_{human})^{3/4}/(BW_{rat})^{3/4}=(70\ kg)^{3/4}/(0.33\ kg)^{3/4}=55.6$ for male rats or, $(BW_{human})^{3/4}/(BW_{rat})^{3/4}=(70\ kg)^{3/4}/(0.26\ kg)^{3/4}=66.5$ for female rats.
[b] This value was used in the derivation of the methanol inhalation unit risk.

Source: NEDO (1985/2008b)

Table E-13. Incidence for malignant lymphoma (Apaja, 1980)

Dose (ppm)	Examined	Malignant Lymphoma
Female Swiss Webster mice		
Historical untreated controls [a,b]	200	38
10	25	4
100	25	9[c]
1,000	25	10[d]

Dose (ppm)	Examined	Malignant Lymphoma
Male Swiss Webster mice		
Historical untreated controls [a]	100	8
10	25	1
100	25	6[d]
1,000	25	4

[a]Toth et al. (1977); [b]Hinderer et al. (1979); [c]*p*-value = 0.06; [d] *p*-values < 0.05

Source: Apaja (1980)

Table E-14. PBPK dose metrics for doses in Apaja (1980)

Daily Dose (mg/kg-d)	Weekly Avg. Dose (mg/kg-d)	Body Weight (kg)	AUC (mg-h/L)	Peak (mg/L)	Amount metabolized (mg)
Female Swiss Webster mice					
0	0	0.040	0	0	0
560.01	479.99	0.040	484.86	88.40	18.38
1000.00	857.13	0.040	3466.74	383.10	28.45
2099.98	1800.00	0.040	19503.87	1462.07	39.18
Male Swiss Webster mice					
0	0	0.045	0	0	0
550.00	471.42	0.045	500.63	89.77	20.29
970.00	831.39	0.045	3405.26	373.72	31.15
1800.00	1542.86	0.045	14998.60	1162.69	41.86

Source: Apaja (1980).

Table E-15. Benchmark results from Multistage-cancer dose-response modeling data for malignant lymphoma in Swiss Webster mice (Apaja, 1980) using PBPK dose-metrics

Gender	AUC (mg-h/L)					Peak (mg/L)					Amount metabolized (mg/d)				
	AIC	*p*-value	Scaled residual at dose nearest to BMD	BMD_{10}	$BMDL_{10}$	AIC	*p*-value	Scaled residual at dose nearest to BMD	BMD_{10}	$BMDL_{10}$	AIC	*p*-value	Scaled residual at dose nearest to BMD	BMD_{10}	$BMDL_{10}$
Female mice[a]	288.91	0.32	1.354	5808.3	2957.6	288.42	0.43	1.090	428.5	225.1	288.07	0.55	-0.937	22.7	10.1
Male mice[a]	122.09	0.083	-0.883	11164.2	4343.04	121.58	0.12	-0.641	798.3	338.9	120.97	0.21	1.309	35.8	18.3

[a]Multistage-cancer (1º) used for AUC and Peak metrics; Multistage-cancer (2º) used for Amount metabolized metric

Source: Apaja (1980).

1

Table E-16. Application of human PBPK model to derive HEDs from $BMDL_{10}$ estimates of Table E-15, Multistage (1º) modeling of malignant lymphoma in Swiss mice (Apaja, 1980) using PBPK dose metrics

	AUC (mg-h/L)	Peak (mg/L)	Amount metabolized (mg/d)[a]
	HED $BMDL_{10}$ (mg/kg-day)	HED $BMDL_{10}$ (mg/kg-day)	HED $BMDL_{10}$ (mg/kg-day)
Female mice	248	281	9.7
Male mice	269	305	14.7

[a]Before applying human PBPK model Table 11 mg/day values were converted to human mg/day by multiplying by either: $(BW_{human})^{¾}/(BW_{rat})^{¾}=(70\ kg)^{¾}/(0.33\ kg)^{¾}=55.6$ for male rats or, $(BW_{human})^{¾}/(BW_{rat})^{¾} = (70\ kg)^{¾}/(0.26\ kg)^{¾} = 66.5$ for female rats.

Table E-17. Benchmark results for all tumor types using BMDS 2.1 multistage "background dose" models and PBPK dose-metrics

Model	AUC (mg-h/L)					Peak (mg/L)					Amount metabolized (mg/d)				
	AIC	*p*-value	Background Dose	BMD_{10}	$BMDL_{10}$	AIC	*p*-value	Background Dose	BMD_{10}	$BMDL_{10}$	AIC	*p*-value	Background Dose	BMD_{10}	$BMDL_{10}$
Female Sprague-Dawley rats (Soffritti et al., 2002a)															
All organs lympho-immunoblastic															
Multistage (1º)	361.99	0.045	168476	112790	49771	359.93	0.14	7480.0	5034.3	2240.3	357.87	0.34	169.0	139.8	77.2
All organs – all lymphomas															
Multistage (1º)	372.78	0.075	179247	111621	48790	372.72	0.077	7961.1	4982.2	2196.3	370.57	0.18	175.1	134.4	74.1
Male Sprague-Dawley rats (Soffritti et al., 2002a)															
Hepatocellular carcinoma															
Multistage (1º)	97.52	0.00	Failed[a]			73.19	0.37	Failed[a]			72.55	0.36	Failed[a]		
All organs lympho-immunoblastic															
Multistage (1º)	455.11	0.18	85497.6	36501	21901	454.97	0.20	3781.3	1625.7	979.1	453.98	0.30	190.2	97.8	63.2
All organs – all lymphomas															
Multistage (1º)	468.09	0.15	96684.3	37822	22195	467.98	0.15	4285.6	1686.5	993.1	467.35	0.20	221.2	101.7	63.9
Female F344 rats (NEDO, 1985/2008b)															
Adrenal glands – pheochromocytoma															
Multistage (2º)	101.46	0.84	553.1	450.9	214.8	103.45	0.56	28.9	23.6	11.2	101.47	0.83	36.7	30.1	14.4
Male F344 rats (NEDO, 1985/2008b)															
Lung – adenomas and adenocarcinomas															
Multistage (1º)	108.15	0.14	248.16	507.9	226.0	108.15	0.14	13.0	26.6	11.8	108.19	0.14	23.0	47.3	21.0
Lung – adenomas, adenocarcinomas amd adenomatosis															
Multistage (1º)	168.61	0.89	430.38	378.9	168.8	168.61	0.89	22.5	19.8	8.8	168.59	0.90	39.3	34.8	15.6
Female Swiss Webster mice (Apaja, 1989)															
Malignant lymphomas															
Multistage (1º)	288.91	0.32	11933.3	5808	2958	288.42	0.43	863.1	428.5	225.1	289.00	0.37	32.8	16.8	9.1
Male Swiss Webster mice (Apaja, 1989)															
Multistage (1º)	122.09	0.083	9573.9	11164	4343.0	121.58	0.12	646.9	798.3	338.9	121.30	0.20	28.6	38.1	17.6

[a]BMD computation failed. BMD is larger than three times maximum input doses.
Source: NEDO (1987, 1987/2008b).

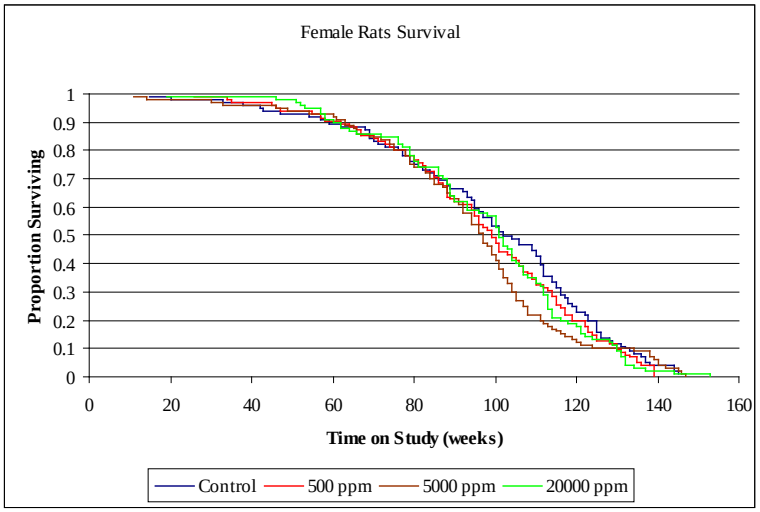

Figure E-1. Female rat survival.

Source: Soffretti et al. (2002a).

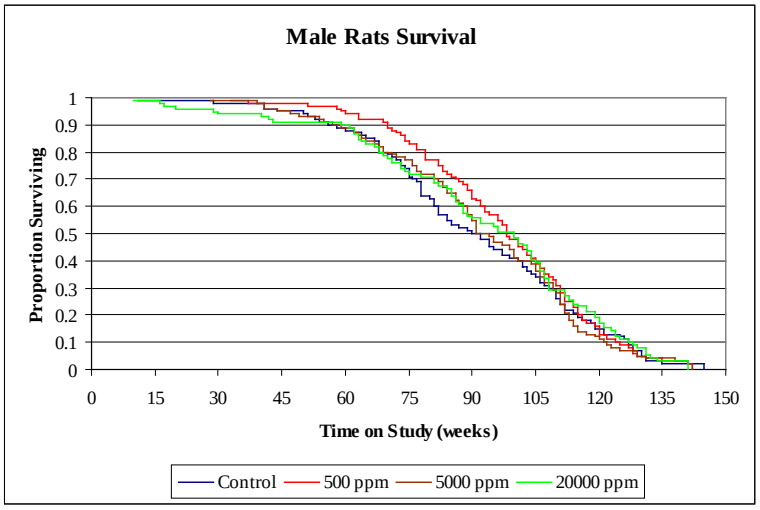

Figure E-2. Male rats survival.

Source: Soffretti et al. (2002a).

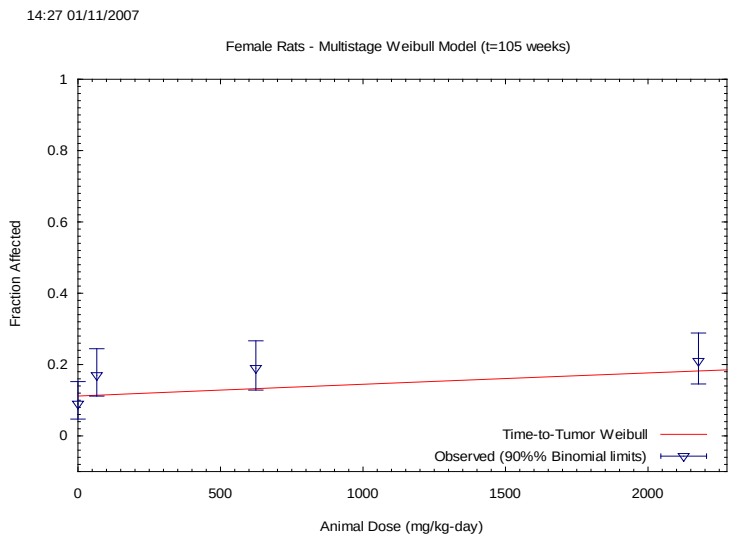

Figure E-3. Female – Lymphomas lympho-immunoblastic – Multistage Weibull Model – Approach 1.

Source: Soffretti et al. (2002a).

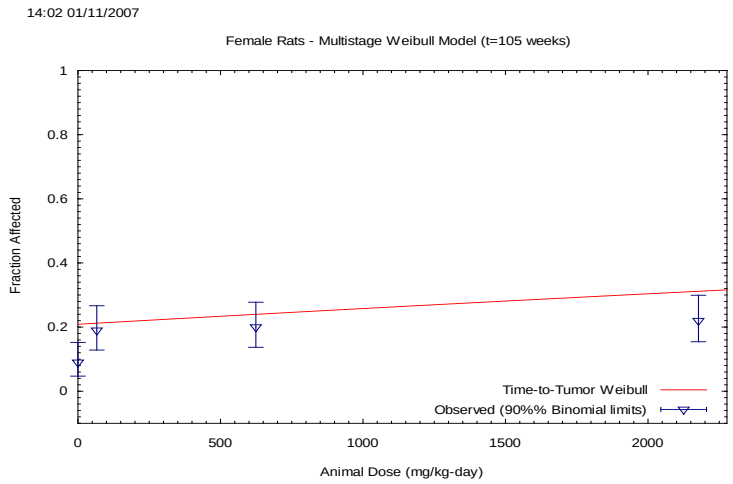

Figure E-4. Female – All lymphomas – Multistage Weibull Model – Approach 1.

Source: Soffretti et al. (2002a).

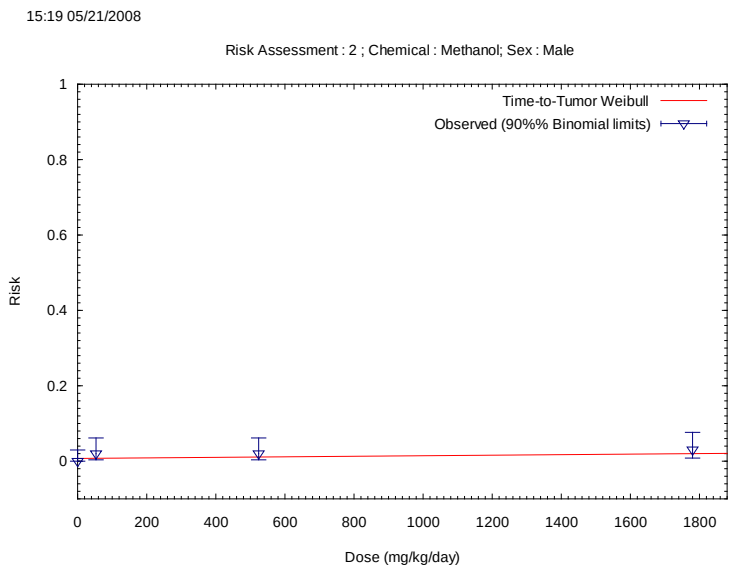

Figure E-5. Male – Hepatocellular carcinoma – Multistage Weibull Model – Approach 1.

Source: Soffretti et al. (2002a).

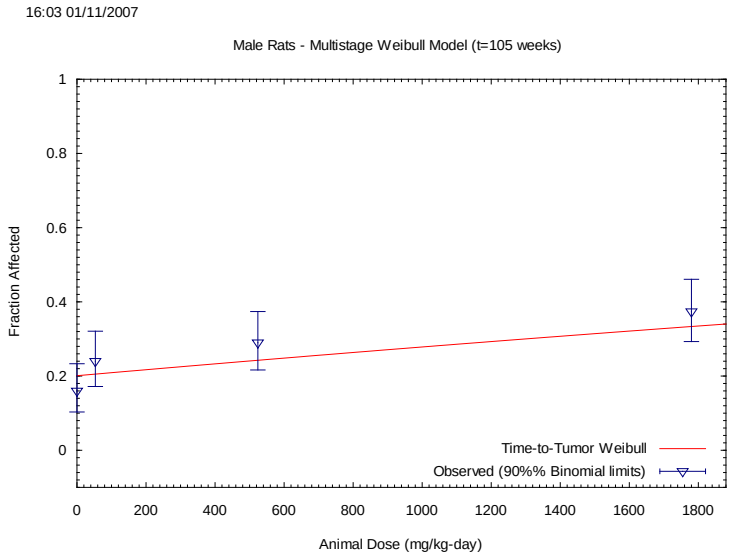

Figure E-6. Male – Lymphomas lympho-immunoblastic – Multistage Weibull Model – Approach 1.

Source: Soffretti et al. (2002a).

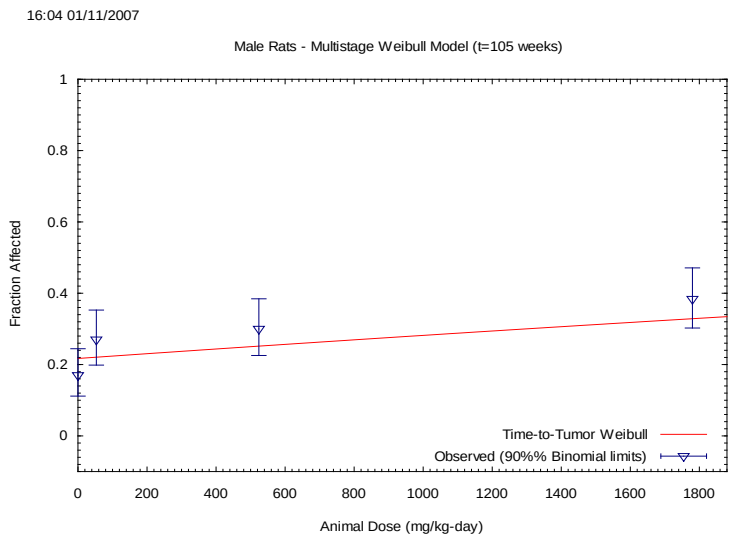

Figure E-7. Male – All lymphomas – Multistage Weibull Model – Approach 1.

Source: Soffretti et al. (2002a).

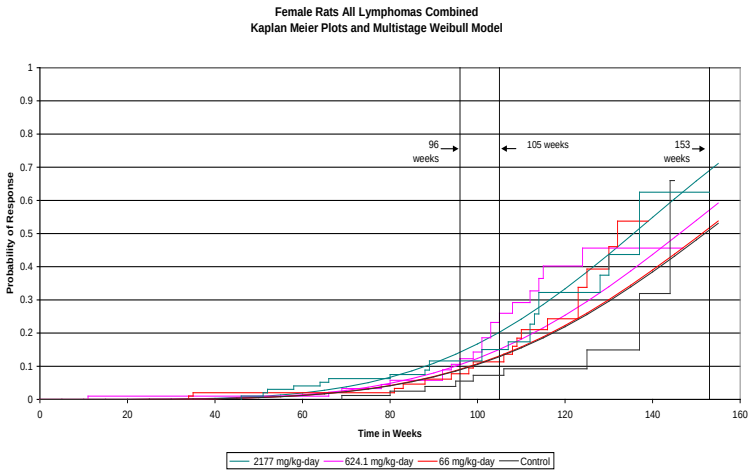

Figure E-8. Female rats –All lymphomas time-to-tumor model fit and Kaplan Meier curves.

Source: Soffretti et al. (2002a).

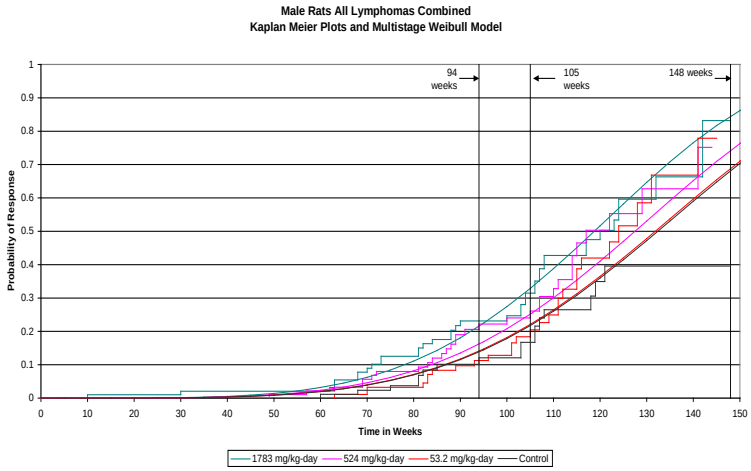

Figure E-9. Male rats –All lymphomas time-to-tumor model fit and Kaplan Meier curves.

Source: Soffretti et al. (2002a).

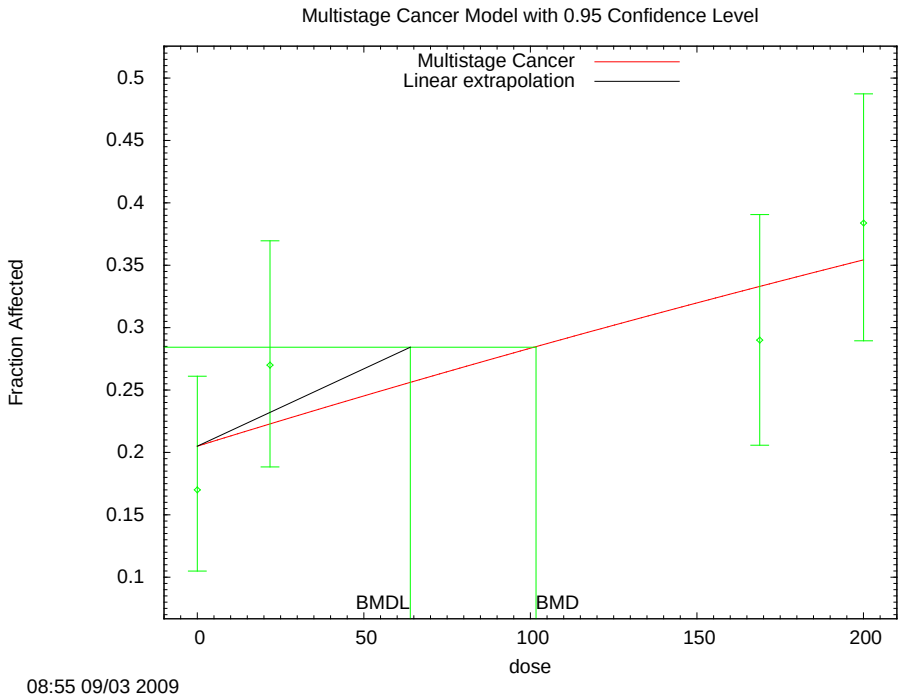

Figure E-10. Male rats- All lymphomas; dose = amount metabolized (mg/day); 1º multistage model.

Source: Soffretti et al. (2002a).

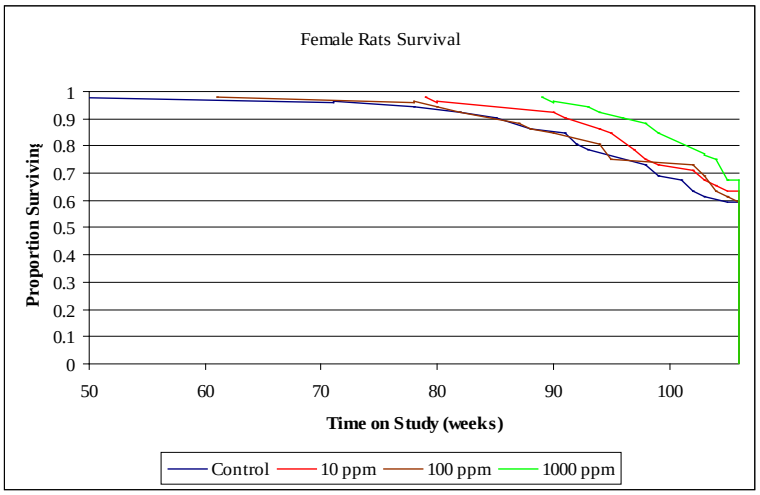

Figure E-11. Female rat survival.

Source: NEDO (1987, 1987/2008b).

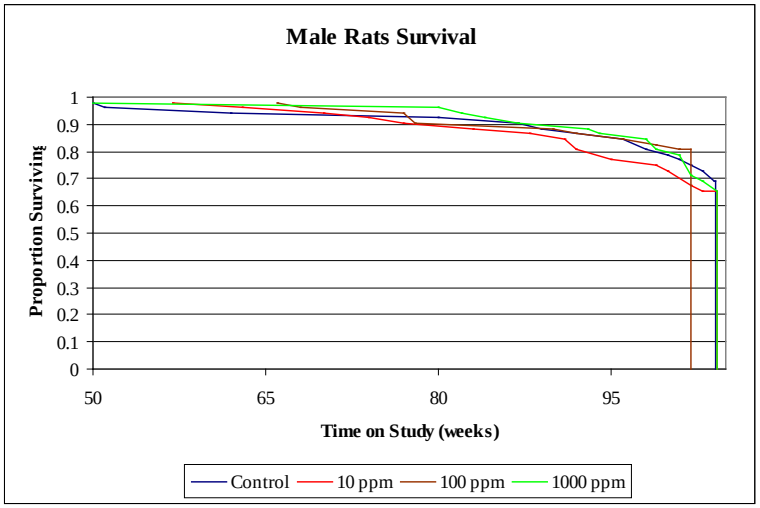

Figure E-12. Male rat survival.

Source: NEDO (1987, 1987/2008b).

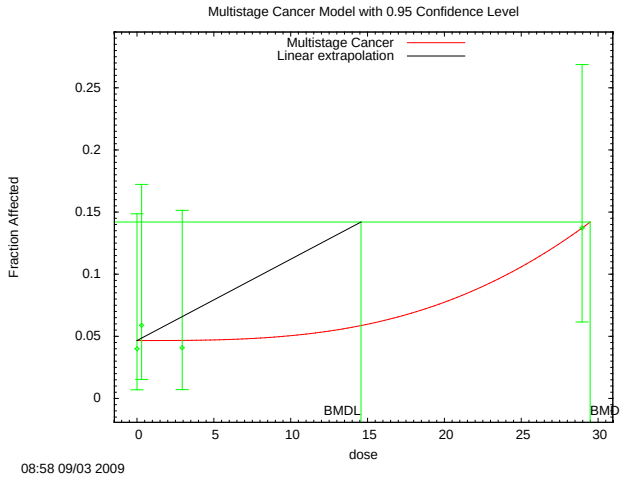

Figure E-13. Female rats- pheochromocytomas; dose = amount metabolized (mg/d); 3º multistage model.

Source: NEDO (1987, 1987/2008b)

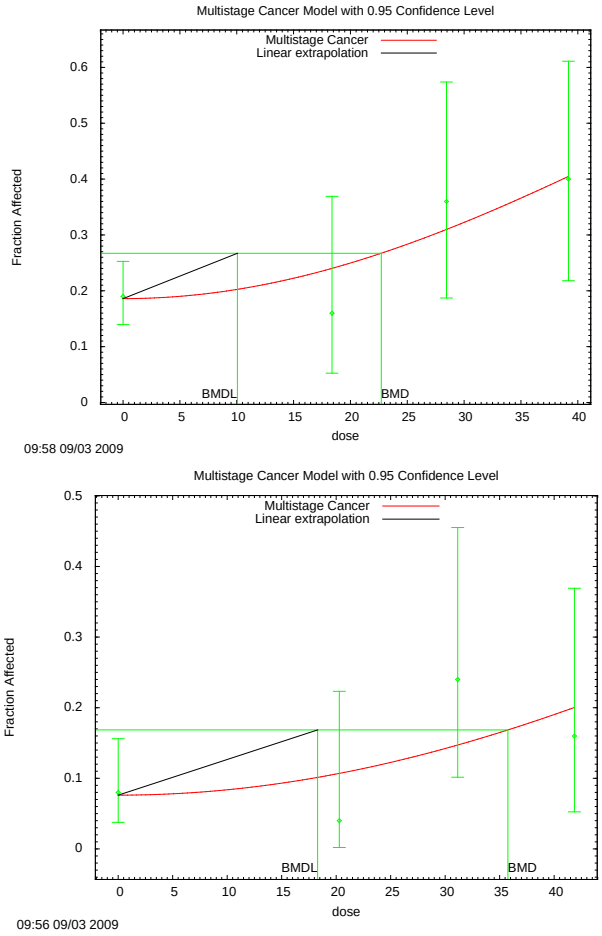

Figure E-14. Plots for female (top; p= 0.55) and male (bottom; p= 0.21) mice – malignant lymphoma; dose=amount metabolized (mg/d); 2º multistage model.

Source: Apaja (1980)